https://doi.org/10.15388/vu.thesis.948
https://orcid.org/0000-0003-4682-4964

VILNIAUS UNIVERSITETAS

Audrius Zakšauskas

Karboanhidrazių izofermentų selektyvių slopiklių kūrimas ir sintezė

DAKTARO DISERTACIJA

Technologijos mokslai,
Chemijos inžinierija (T 005)

VILNIUS 2026

Disertacija rengta 2013–2026 metais Vilniaus universiteto Biotechnologijos institute.

Disertacija ginama eksternu.

Mokslinis konsultantas – prof. dr. Daumantas Matulis (Vilniaus universitetas, technologijos mokslai, chemijos inžinerija, T 005).

Gynimo taryba:
Pirmininkas – prof. dr. Rolandas Meškys (Vilniaus universitetas, technologijos mokslai, chemijos inžinerija – T 005).
Nariai:
prof. dr. Eglė Arbačiauskienė (Kauno technikos universitetas, gamtos mokslai, chemija – N 003),
doc. dr. Rima Budvytytė (Vilniaus Universitetas, gamtos mokslai, biochemija – N 004),
dr. Jonas Šarlauskas (Vilniaus Universitetas, technologijos mokslai, chemijos inžinerija – T 005),
dr. Saulius Šumanas (Pietų Floridos universitetas, JAV, gamtos mokslai, biochemija – N 004).

Disertacija ginama viešame Gynimo tarybos posėdyje 2026 m. liepos mėn. 2 d. 13 val. Vilniaus universiteto Gyvybės mokslų centro R401 auditorijoje. Adresas: Saulėtekio al. 7, Vilnius, Lietuva, tel. +370 5 2234419 ; el. paštas info@gmc.vu.lt

https://doi.org/10.15388/vu.thesis.948
https://orcid.org/0000-0003-4682-4964

VILNIUS UNIVERSITY

Audrius Zakšauskas

Design and Synthesis of Isozyme-Selective Carbonic Anhydrase Inhibitors

DOCTORAL DISSERTATION

Technological Sciences,
Chemical Engineering (T 005)

VILNIUS 2026

The dissertation was prepared between 2013 and 2026 at the Institute of Biotechnology, Life Sciences Center of Vilnius University.

The dissertation is defended on an external basis

Academic consultant – Prof. Dr. Daumantas Matulis (Vilnius University, Technological Sciences, Chemical Engineering, T 005).

This doctoral dissertation will be defended in a public meeting of the Dissertation Defence Panel:

Chairman – Prof. Dr. Rolandas Meškys (Vilnius University, Technological Sciences, Chemical Engineering, T 005).
Members:
Prof. Dr. Eglė Arbačiauskienė (Kaunas University of Technology, Natural Sciences, Chemistry, N 003),
Assoc. Prof. Dr. Rima Budvytytė (Vilnius University, Natural Sciences, Biochemisty, N 004),
Dr. Jonas Šarlauskas (Vilnius University, Technological Sciences, Chemical engineering, T 005),
Dr. Saulius Šumanas (University of South Florida, USA, Natural Sciences, Biochemisty, N 004).

The dissertation shall be defended at a public meeting of the Dissertation Defence Panel at 13:00 on 2 July 2026 in Room R401 of the Life Sciences Centre (Vilnius University).
Address: Saulėtekio av. 7, Room No. R401, Vilnius, Lithuania
Tel. +370 5 2234419 ; e-mail: info@gmc.vu.lt

TURINYS

SANTRUMPOS

BMR	Branduolių magnetinis rezonansas
CA	Karboanhidrazė
CARP	Į karboanhidrazę panašus baltymas (CA related protein)
DFT	Tankio funkcionalo teorija (density functional theory)
DMF	Dimetilformamidas
DMSO	Dimetilsulfoksidas
HPLC	Didelio efektyvumo skysčių chromatografija
MeOH	Metanolis
NaOAc	Natrio acetatas
TEA	Trietilaminas
THF	Tetrahidrofuranas
ZBG	Su cinko jonu besijungianti grupė (angl. zinc binding group)

ĮVADAS

Mažamolekulinių cheminių vaistų kūrimas yra ilgas ir brangus procesas, kuris pastaraisiais dešimtmečiais tampa vis sudėtingesnis dėl padidėjusių reikalavimų veiksmingumui ir saugumui. Pirmasis etapas šiame procese yra potencialaus, galinčio būti naudingu gydant konkrečią ligą ar būklę, kandidato į vaistus nustatymas, organinė sintezė ir optimizavimas. Norint tai sėkmingai atlikti reikia suprasti kokiais būdais vaistai sąveikauja su biologinių sistemų tikslinėmis struktūromis (receptoriais, fermentais, medžiagų transporteriais ir pan.) ir kaip keičiant struktūrą pasiekti norimas vaistų savybes.

Siekiant suprasti bendrus vaistų kūrimo principus vieni iš patraukliausių tiriamųjų taikinių yra fermentai. Jie dažniausiai pasižymi selektyviu veikimu, t.y. dideliu specifiškumu substratams, todėl galima tikėtis sukurti tik konkretų procesą veikiančius vaistus. Be to, yra žinoma daug ligų, kurios siejamos su fermentų ekspresijos, ir tuo pačiu jų atliekamų funkcijų, pokyčiais. Taip pat, didelis fermentų katalizinis aktyvumas leidžia tikėtis, kad net nedidelis slopiklio kiekis stipriai paveiks aktyvumą ir sukels didelį terapinį efektą. Ir be viso to, tokie ryškūs aktyvumo pokyčiai dažniausiai palengvina laboratorinius tyrimus ir pagreitina patį tyrimų procesą. Todėl šioje disertacijoje pasirinkta viena tokių tiriamųjų taikinių šeima – karboanhidrazės.

Karboanhidrazės yra fermentai randami visuose gyvuose organizmuose, nuo bakterijų iki žinduolių, katalizuojantys plačiai sutinkamą anglies dioksido hidratacijos reakciją:

$$CO_2 + H_2O \rightleftharpoons H^+ + HCO_3^-$$

Kodėl gi tos karboanhidrazės tokios svarbios? Žiūrint į gazuotame gėrime kylančius burbuliukus sunku įsivaizduoti kam tos CA aplamai reikalingos. Pasirodo anglies dioksido hidratacijos reakcija yra ganėtinai lėta[1] (k-0,039 s^{-1}), o karboanhidrazės pagreitina ją iki ~10^6 s^{-1} ir tokiu būdu gali žymiai įtakoti įvairiausius organizme vykstančius procesus.

Vien žmogaus organizme aptinkama 12 katalitiškai aktyvių alfa šeimos karboanhidrazių, kurios pasižymi dideliu struktūriniu panašumu, bet skiriasi savo lokalizacija ląstelėje ir organuose, funkcija ir kataliziniu aktyvumu.

Karboanhidrazės žmogaus organizme atlieka skirtingas fiziologines funkcijas dalyvaudamos tokiuose procesuose kaip CO_2 pernaša, pH reguliacija, elektrolitų apykaita, kaulų rezobcija, vėžinių navikų susidarymas ir t.t. Tam tikrų karboanhidrazių veiklos pokyčiai (padidėjęs aktyvumas, ekspresija) yra siejami su įvairiomis ligomis, kurios gydomos CA slopikliais (glaukoma, epilepsija, idiopatinė intrakranijinė hipertenzija, aukštumos liga, migrena ir pan). Daugumos medicinoje naudojamų CA slopiklių trūkumas yra

šalutiniai poveikiai, kurie pirmiausia siejami su mažu atrankumu tikslinėms karboanhidrazėms. Todėl CA izofermentams atrankių slopiklių sukūrimas visą laiką išlieka aktualia užduotimi.

Ne mažiau svarbūs kiti CA slopiklių panaudojimo būdai, kai foto-, radioaktyviomis ir pan. grupėmis modifikuotas slopiklis atlieka vaizdinimo arba citotoksinę funkciją. Šios taikymo sritys tapo ypač aktualios pastaraisiais dešimtmečiais ir siejamos pagrinde su CA IX padidėjusia ekspresija vėžiniuose navikuose. Tokiu atveju CA aktyvumo pakeitimas nebūna svarbiausia užduotis, tačiau atrankus jungimasis prie tikslinių CA izofermentų yra dar svarbesnis.

Šiame **darbe iškeltas tikslas** sukurti ir susintetinti selektyvius CA izofermentams slopiklius, atskleisti selektyvumą nulemiančius faktorius ir panaudoti juos naujų junginių kūrimui.

Tikslui pasiekti iškelti šie **uždaviniai**:

- Susintetinti 3,4-dipakeistus-2-halobenzensulfonamidus ir atskleisti pakaitų įtaką slopiklių afiniškumui ir selektyvumui.
- Siekiant įvertinti kuo arčiau CA kofaktoriaus esančių inhibitorių pakaitų įtaką susintetinti 2-pakeistus-benzensulfonamidus.
- Nustatyti ir įvertinti pakaitų padėties, dydžio ir lankstumo įtaką CA slopiklių afiniškumui ir selektyvumui.
- Sukurti naujus su vėžiniais susirgimais siejamos CA IX didelio afiniškumo bei selektyvumo inhibitorius.

MOKSLINIS NAUJUMAS

Disertacijoje susintetintos ir palygintos dvi grupės benzensulfonamidinių slopiklių turinčių masyvius pakaitus 4,5- ir 2,5- padėtyse. Abiejose grupėse surasta slopiklių pasižyminčių išskirtinai geru sub-nanomoliniu afiniškumu atskiriems CA izofermentams.

Susintetinti junginiai įgalino nustatyti slopiklio–CA kompleksų kristalines struktūras. Tai padėjo suprasti slopiklių struktūros–biologinio aktyvumo sąryšius ir davė bendrą teigiamą tyrimų poslinkį, ypač su vėžiniais susirgimais siejamo karboanhidrazės IX izofermento slopiklių paieškoje.

Ištirtas 2,4-dihalo-5-sulfamoilbenzoatų turinčių identiškus halogenus nukleofilinio pakeitimo reakcijų regioelektyvumas ir surastas naujas būdas 2,5-dipakeistų-4-halo-benzensulfonamidų sintezei.

Nustatyta, kad 2,5-dipakeistų benzensulfonamidinių slopiklių grupėje ypač didelę įtaką slopiklio savybėms turi 2-padėtyje esantys pakaitai. 2- amino ir 2-sulfanilpakaitai pasižymi dideliu afiniškumu ir selektyvumu CA IX izofermentui. Tuo tarpu 2-sulfonilpakaitai sąlygoja labai didelį afiniškumo sumažėjimą visiems CA izofermentams. Taip pat parodyta, kad 2-pakeisti benzensulfonamidai gali būti perspektyvūs ir geresni CA IX slopikliai nei ligšioliniai panašios struktūros vaistai, tokie kaip bumetanidas ir piretanidas.

GINAMIEJI TEIGINIAI

1. Benzensulfonamidinių CA slopiklių pakaitų esančių *para*-padėtyje lankstumas įtakoja slopiklių selektyvumą atskiriems CA izofermentams.
2. Benzensulfonamidų *para*- sulfanil- ir sulfonilgrupės sąlygoja skirtingas pakaitų pozicijas CA aktyviajame centre, bei įtakoja didesnį slopiklio afiniškumą nei amino pakaitai.
3. Slopikliai sukurti į 5-[2-(benzimidazol-1-il)acetil]-2-chlor-benzensulfonamidą įvedant papildomus pakaitus, pasižymi didesniu afiniškumu visoms karboanhidrazėms, bet stipriai sumažina selektyvumą tikslinei CA VA.
4. Sulfonamidinių slopiklių *orto*-padėtyje esantys sulfanil- ir sulfonilpakaitai stipriai įtakoja afiniškumą ir selektyvumą tikslinei CA IX (sulfanil – didina, sulfonil – mažina).

1. LITERATŪROS APŽVALGA

1.1 CA paplitimas ir struktūra, konservatyvus centras

Karboanhidrazės (EC 4.2.1.1), tai metalo fermentai katalizuojantys vieną iš paprasčiausių reakcijų:

$$CO_2 + H_2O \rightleftharpoons H_2CO_3 \overset{\text{labai greita}}{\rightleftharpoons} H^+ + HCO_3^- \quad (1)$$

$$CO_2 + H_2O \rightleftharpoons H^+ + HCO_3^- \quad (2)$$

$$CO_2 + OH^- \rightleftharpoons HCO_3^- \quad (3)$$

Karboanhidrazės šią ganėtinai lėtą reakciją gali pagreitinti nuo 0,039 s^{-1} iki ~10^6 s^{-1} ir tokiu būdu žymiai įtakoti įvairiausius organizme vykstančius procesus[1,2].

Dar neseniai buvo žinomos penkios CA šeimos: alfa, beta, gama, delta, zeta[3,4]. Šiuo metu jau žinomos septynios CA šeimos (prisidėjo eta ir theta[5,6]) Dauguma šių metalo fermentų aktyviajame centre turi Zn^{2+} joną, tačiau yra sutinkamos ir CA su Cd^{2+}, Fe^{2+}, Co^{2+} jonais[7–10]. Iš visų šeimų reikia išskirti gyvūnuose sutinkamą alfa-CA šeimą. Tuo pačiu tai vienintelė žmogaus organizme sutinkama CA šeima. Pastarąją šeimą sudaro 15 karboanhidrazių (1 lentelė), iš kurių 12 pasižymi kataliziniu aktyvumu, o 3 yra katalizinio aktyvumo neturintys į karboanhidrazes panašūs baltymai (angl. carbonic anhydrase related protein, CARP).

1 lentelė. Žmogaus CA izofermentų katalitinis aktyvumas, lokalizacija ir siejamumas su ligomis[7].

Izofermentas	CO_2 hidratacijos aktyvumas	Lokalizacija	Sąsajos
CA I	Mažas	Citozolyje	Hemolizinė anemija
CA II	Didelis	Citozolyje	Glaukoma, edema, aukštikalnių liga
CA III	Labai mažas	Citozolyje	-
CA IV	Didelis	Membraninis-neaišk.	Glaukoma
CA VA	Vidutinis-didelis	Mitochondrijose	Nutukimas
CA VB	Vidutinis	Mitochondrijose	-
CA VI	Vidutinis	Sekrecijoje	Kariesas
CA VII	Didelis	Citozolyje	Epilepsija, neuropatinis skausmas
CARP VIII	Neaktyvus	Citozolyje	-
CA IX	Didelis	Transmembraninis	Vėžys
CARP X	Neaktyvus	Citozolyje	-
CARP XI	Neaktyvus	Citozolyje	-
CA XII	Vidutinis-mažas	Transmembraninis	Glaukoma, vėžys
CA XIII	Mažas	Citozolyje	Nevaisingumas
CA XIV	Vidutinis	Transmembraninis	-

Visi 13 aktyvių α-CA izofermentų skiriasi savo lokalizacija ląstelėje ir organuose, katalitinių domenų skaičiumi (CAVI, CA IX ir CA XII turi 2 domenus), funkcija ir kataliziniu aktyvumu (1 pav.)[7,11].

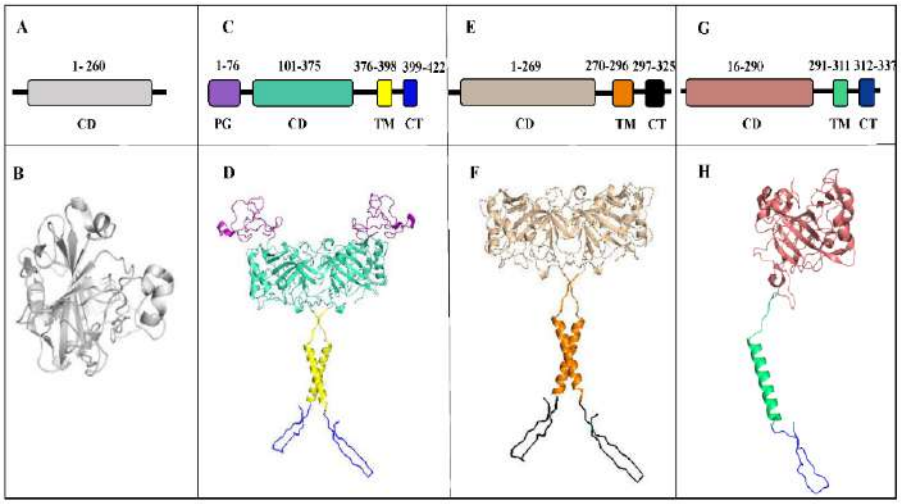

1 pav. CA izofermentų schemos ir struktūros. Viršutinė panelė, domenų schema: (A) CA II: katalitinis domenas (CD, pilka); (C) CA IX: proteoglikaninis domenas (PG, violetinė), katalitinis domenas (cianas), transmembraninis domenas (TM, geltona) ir C-galinis domenas (CT, mėlyna); (E) CA XII: katalitinis domenas (rusva), transmembraninis domenas (oranžinė) ir C-galinis domenas (juoda); (G) CA XIV: katalitinis domenas (varinė), transmembraninis domenas (žalia) ir C-galinis domenas (mėlyna). Apatinė panelė: (B) CA II, (D) CA IX, (F) CA XII ir (H) CA XIV piešinys[12].

Tačiau nepaisant skirtumų CA pasižymi tuo, kad jų katalitiniai domenai yra labai panašūs (konservatyvūs), ypač aktyvaus centro srityje. Visuose domenuose aktyvaus centro gilumoje yra cinko atomas koordinuotas tarp trijų histidino fragmentų (2 pav., His 19, 94, ir 96). Šonuose yra hidrofobinių fragmentų sritis, kuri palengvina substrato (CO_2) prisijungimą, ir hidrofilinė sritis, kuri dalyvaujant protonų šaudyklei His64 palaiko protonų perdavimą per tvarkingą vandens molekulių tinklą[13,14].

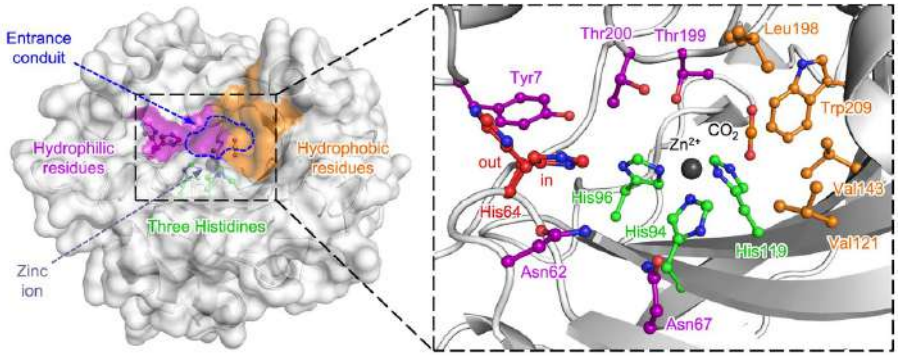

2 pav. Bendra katalitinio domeno forma (CAII). Hidrofobinė sritis (oranžinė), palengvinanti substrato (CO_2) prisijungimą, ir hidrofilinė sritis (violetinė), kurioje palaikomas protonų perdavimas per tvarkingą vandens molekulių tinklą[13].

Literatūroje išskiriamos 1-3 sritys (kišenės) esančios prie Zn-jono kurių aminorūgščių skirtumai yra svarbūs (3 pav., 2 lentelė)[15].

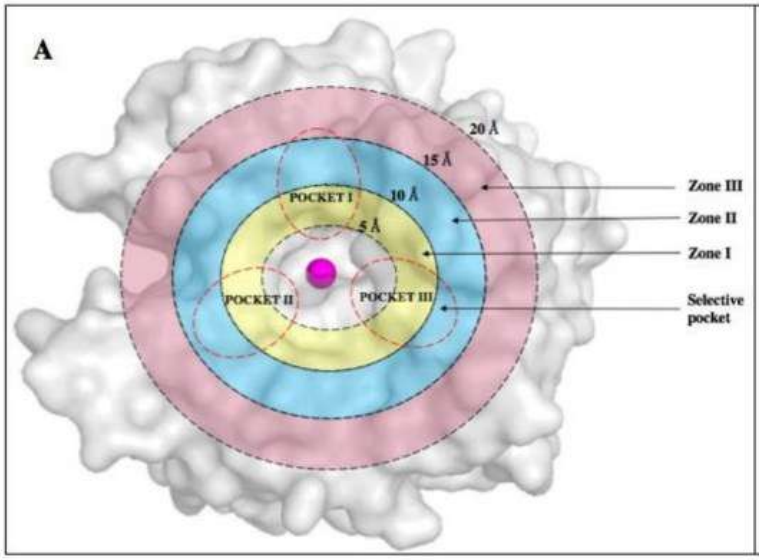

3 pav. CA II paviršiaus atvaizdavimas zonomis ir kišenėmis. Aktyviosios srities cinkas pavaizduotas raudona sfera. Įvairios zonos aktyviojoje srityje (atstumas nuo cinko): I zona (5–10 Å) – geltona, II zona (10–15 Å) – žydra, o III zona (15–20 Å) – rožinė. Trys kišenės aktyviojoje srityje ir aplink ją, apibrėžtos raudonais brūkšneliais[12].

2 lentelė. CA izofermentų skirtumai(CA II numeracija)[12].

Eil. Nr *	Atstumas iki cinko (Å)	CA I	CA II	CA IX	CA XII
5-10 Å					
62	9.1	Val	Asn	Asn	Asn
65	6.9	Ser	Ala	Ser	Ser
67	7.3	His	Asn	Gln	Lys
10-15 Å					
60	13.7	Ile	Leu	Arg	Thr
69	13.8	Asn	Glu	Thr	Asn
91	11.1	Phe	Ile	Leu	Thr
131	10.4	Leu	Phe	Val	Ala
135	12.2	Ala	Val	Leu	Ser
204	13.7	Tyr	Leu	Ala	Asn
15-20 Å					
19	19.1	Leu	Asp	Val	Lys
20	15.2	Tyr	Phe	Ser	Tyr
57	19.6	Lys	Leu	Leu	Phe
58	16.3	Glu	Arg	Arg	Leu
71	21.1	Glu	Asp	Pro	Pro
72	15.9	Asp	Asp	Pro	Ser
123	15.4	Trp	Trp	Leu	Tyr
130	19.1	Ser	Asp	Arg	Asp
132	17.3	Ala	Gly	Asp	Ser
136	17.6	Ser	Gln	Gly	Asn
170	18.9	Lys	Lys	Ser	Lys
173	19.6	Arg	Ser	Glu	Glu

*CA II numeracija

1.2 Klasikiniai CA slopikliai.

CA slopikliai pagal veikimo mechanizmą gali būti skirstomi į dvi grupes: a) su metalo jonu kompleksą sudarantys junginiai; b) nesudarantys tiesioginio ryšio su metalo jonu junginiai[7]. Pirmai grupei priklauso klasikiniai slopikliai – sulfonamidai ir jų dariniai (sulfamatai, sulfamidai ir pan.) (1 schema), bei kiti su metalais kompleksuojantys anijonai. Kitai grupei priklausantys slopikliai įvairiais būdais[16] jungiasi prie cinko jono koordinuotos vandens molekulės vandeniliniais ryšiais (fenoliai, poliaminai ir kt.) arba kitų CA aktyvaus centro vietų užkimšdami priėjimą prie aktyvaus centro.

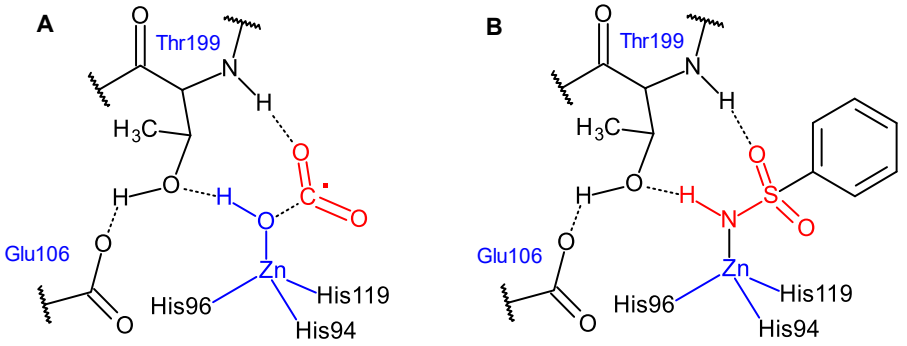

1 schema. Pirmos grupės CA inhibitorių veikimo mechanizmas. CA aktyvaus centro schemos: (A) CO_2 hidratacijos/dehidratacijos reakcijos pereinamoji būsena; (B) arilsulfonamido prisijungimas (Pagal[17])

Pirmi slopikliai buvo surasti netrukus po karboanhidrazių atradimo – buvo nustatyta, kad pirminiai benzensulfonamidai (sulfanilamidas ir kt.) inhibuoja CA aktyvumą, tuo tarpu antriniai benzensulfonamidai ir benzensulfonrūgštys „netrukdo“ CA veiklai [18]. Kiek vėliau buvo surasti CA slopikliai heterocikliniai sulfonamidai, tokie kaip acetozolamidas [19].

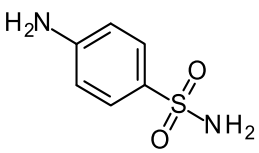

sulfanilamidas

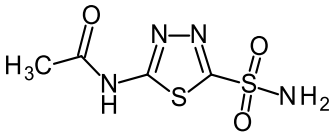

acetozolamidas

Vėliau buvo surasta dar ne viena nauja CA slopinančių junginių klasė[20–24], bet sulfonamidai taip ir liko plačiausiai naudojamais tiek tyrimuose, tiek farmacijoje. Vaistiniai sulfonamidiniai preparatai (4 ir 5 pav.) netgi priskiriami CA slopiklių klasei, nepriklausomai nuo to kokioms ligoms skiriami gydyti (https://go.drugbank.com/categories/DBCAT000727).

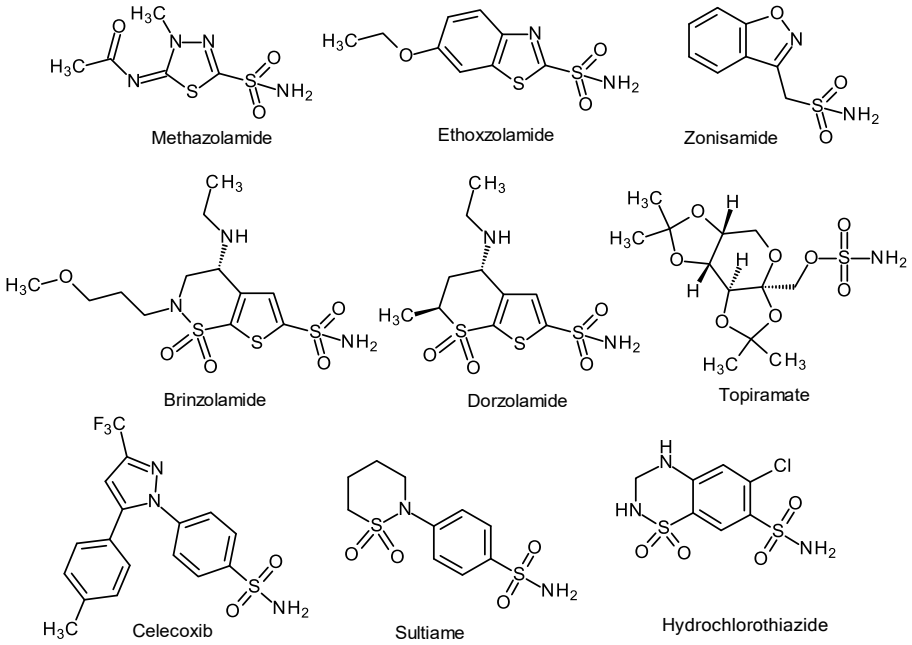

4 pav. Vaistų pasižyminčių CA slopinimu pavyzdžiai.

Taipogi reikia išskirti vieną grupę vaistinių junginių, pasižyminčių CA slopinimu, tai *orto*-pakeisti benzensulfonamidai (5 pav.). Šie junginiai *orto*-padėtyje dažniausiai turi nedidelius chloro- ar trifluorometilpakaitus, arba didesnius fenoksipakaitus bumetanido ir piretanido atveju. Jie buvo sugrupuoti ir aprašyti dar 2008 metais, bet autoriai, panašu nesuprato arba neįvertino pakaito svarbos[25]. Netgi ir 2025 metais parašytoje apžvalgoje prie pat sulfonamido esančioms grupėms neskirta dėmesio[26].

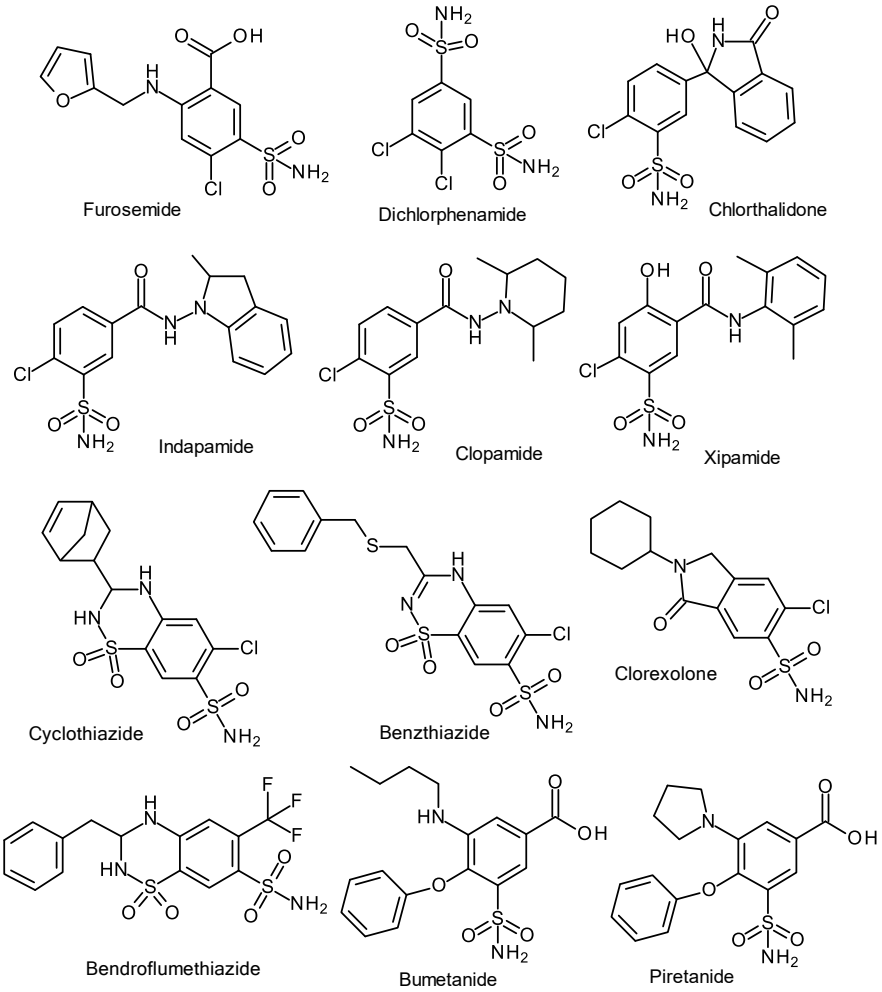

5 pav. *Orto*-pakeistų benzensulfonamidų pavyzdžiai.

Bendra selektyvių slopiklių kūrimo strategija pavaizduota 2 schemoje. Ji yra pagrįsta slopiklio jungimusi prie CA centre esančio metalo jono, bei prie griaučių (dažniausiai tai aromatinės ar heteroaromatinės sistemos) prijungtų įvairių grupių sąveikomis su CA aktyvaus centro paviršiuje esančiais aminorūgščių fragmentais. Schemoje pavaizduoti du pakaitai, kurie dėka individualių savybių gali sąveikauti su įvairiu atstumu esančiais hidrofobiniais arba hidrofiliniais paviršių fragmentais. Atskirai išskirtas pakaitas R, kuris yra arčiau aktyvaus centro nei kiti pakaitai ir dažniausiai įvardijamas kaip sąveikaujantis su konkrečiai hidrofobinėje dalyje esančia kišene. Pakaitas R gali būti riboto dydžio, dažniausia tai chloro atomas, nors yra išimčių (CF_3 ir fenoksigrupės 5 paveiksle ir kitur[27,28]).

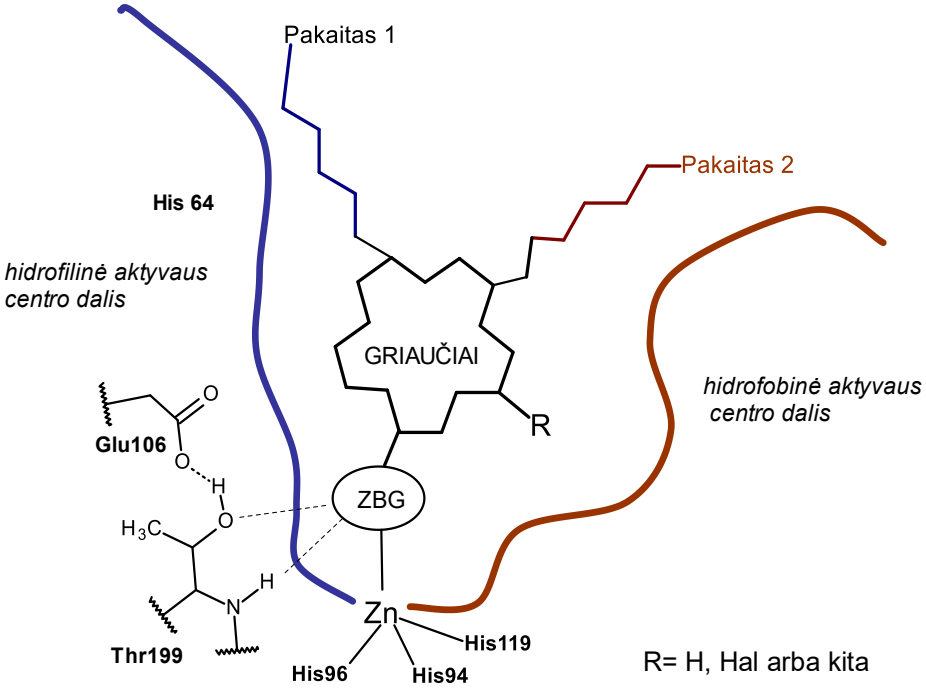

2 schema. Schema apibūdinanti bendrą CA slopiklių kūrybos strategiją. ZBG (zinc binding group) – su cinko jonu besijungianti grupė, R – prie ZBG esanti grupė, dažniausiai chloro atomas.

2. MEDŽIAGOS IR METODAI

Tyrimuose naudotos pradinės medžiagos ir reagentai įsigyti iš specializuotų tiekėjų ir naudoti be papildomo gryninimo. Lydymosi temperatūros nustatytos atviruose kapiliaruose IA9100 (*Electrothermal*) prietaisu. Reakcijų eiga sekta plonasluoksnės chromatografijos metodu naudojant TLC Silica gel 60 F_{254} (*Merck*) plokšteles, detektuojant 254/365 nm UV spinduliuote UV-6 S/L (*Herolab*) prietaisu. Chromatografiniam gryninimui naudotas Silica gel 60 (0,040-0,063 mm, *Merck*). Junginių ^{1}H, ^{13}C-BMR spektrai užrašyti spektrometru Ascend 400 (*Brucker*) (400 MHz ir 100 MHz), vidiniu standartu naudojant likutinius tirpiklių signalus. Aukštos skiriamosios gebos masių spektrai užrašyti Agilent TOF 6230 (*Agilent Technologies*) spektrometru ir Agilent Infinity 1260 HPLC sistema (*Agilent Technologies*).

3. REZULTATAI

Šiame darbe susintetinta eilė benzensulfonamidinių CA slopiklių turinčių įvairius pakaitus 2-, 4- ir 5-padėtyse. Rezultatai pateikti 5 straipsniuose (**I-V**). Pirmi trys straipsniai skirti 2-halo-4,5-dipakeistiems benzensulfonamidiniams slopikliams. Ketvirtas straipsnis skirtas 2-halo-4-pakeistų ir 4-halo-2-pakeistų sulfamoilbenzoatų saveikų su karboanhidrazėmis palyginimui. Penktame straipsnyje ištirta prie sulfonamido grupės *orto*-padėtyje esančių pakaitų įtaka CA slopinimui.

Tyrimai pradėti nuo 4-aminopakeistų benzensulfonamidų 5-oje padėtyje turinčių karbonilamino grupes (**I str.**). Slopiklių sintezės pradėtos nuo 2,4-dichlor- ir 2,4-dibrom-5-sulfamoilbenzoinių rūgščių (**1**, **2**).

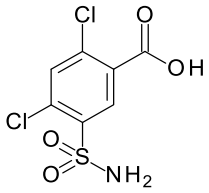

1

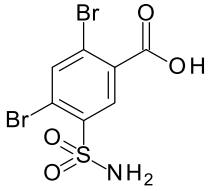

2

Iš šių dviejų benzoinių rūgščių per tarpinius chloranhidridus susintetinta eilė 2,4-dihalobenzamidų (**3-15**) su įvairaus ilgio amidopakaitais (3 schema). Gryninant 3-hidroksipropilbenzamidą **5** buvo pastebėtas pašalinio junginio susidarymas – etilacetatate vyko peresterifikavimo reakcija. Identifikuotas *O*-acetil benzamidas **14**, kuris vėliau resintetintas su 78 proc. išeiga, virinant etilacetate esant sieros rūgšties. Tuo tarpu su 2-hidroksietilbenzamidu **4** tokia reakcija nestebima.

Antras pakaitas įvestas pakeičiant halogeną įvairiais aminais. Reakcijos atliktos kaitinant 2,4-dichlorbenzamidus **3-7**, **11**, **15** alifatinių aminų pertekliuje 110-130 °C temperatūroje, be metalų katalizės [29]. Dibrombenzamido **13** reakcijos su aminais atliktos virinant dioksane ilgesnį laiką, taip išvengiant pašalinių produktų susidarymo (4 schema). Dalis junginių susintetinti hidrolizuojant (**1c**, **15**) arba modifikuojant amidus (**8a**)[30].

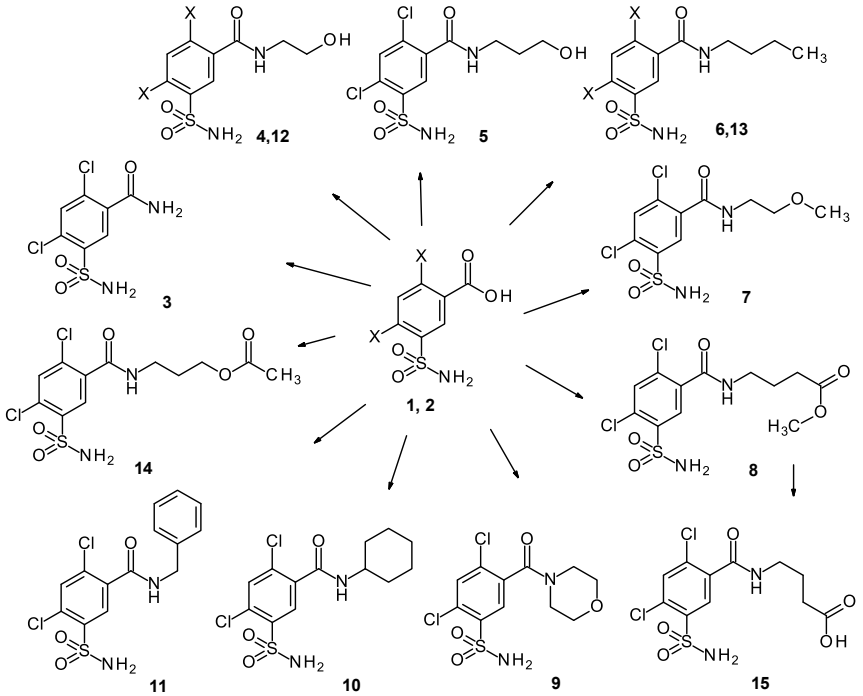

X: Cl (**1, 3-11, 14-15**), Br (**2, 12-13**)
R: NH_2 (**3**) $NH(CH_2)_2OH$ (**4,12**), $NH(CH_2)_3OH$ (**5**), $NH(CH_2)_3CH_3$ (**6,13**), $NH(CH_2)_2OCH_3$ (**7**), $NH(CH_2)_3CO_2CH_3$ (**8**), N-morfolinil- (**9**), NH-cikloheksil-(**10**), NH-benzil- (**11**), $NH(CH_2)_3OAc$ (**14**), $NH(CH_2)_3CO_2H$ (**15**).

3 schema. 2,4-dihalobenzamidų **3-15** sintezė.

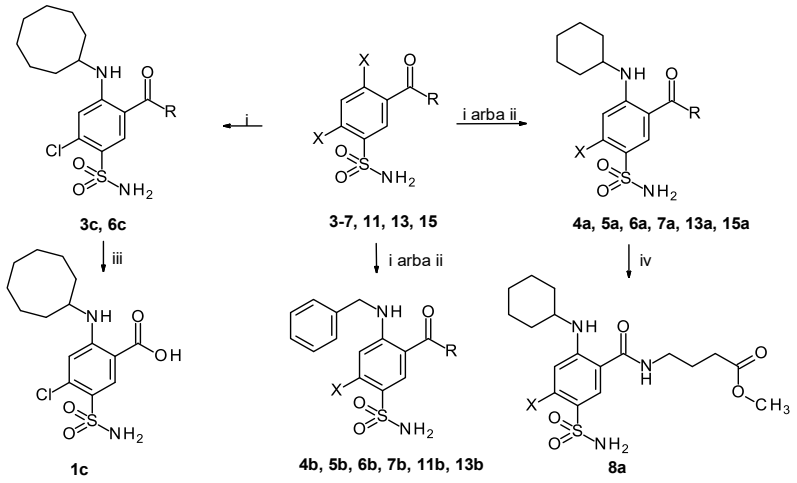

X: Cl (**3-8, 11, 15**), Br (**13**)
R: NH_2(**3**) $NH(CH_2)_2OH$ (**4**), $NH(CH_2)_3OH$ (**5**), $NH(CH_2)_3CH_3$ (**6, 13**), $NH(CH_2)_2OCH_3$ (**7**), $NH(CH_2)_3CO_2CH_3$ (**8**), NH-benzil- (**11**), $NH(CH_2)_3CO_2H$ (**15**),

4 schema. 4-aminopakeistų benzensulfonamidų sintezė.

Sekanti junginių serija (**II, IV str.**) turi per sieros atomą prijungtus įvairaus ilgio pakaitus. 2,4-Dihalosulfamoilbenzoinių rūgščių darinių reakcijos su tioliais literatūroje praktiškai neaprašytos, todėl tikėtasi, kad reakcijos vyks panašiai kaip su aminais, pakeičiant tolimesnį nuo sulfonamido halogeno atomą. Tokiu būdu iš atitinkamų benzamidų (**3-14**) susintetinta eilė junginių su įvairiais sulfanilpakaitais (5 schema).

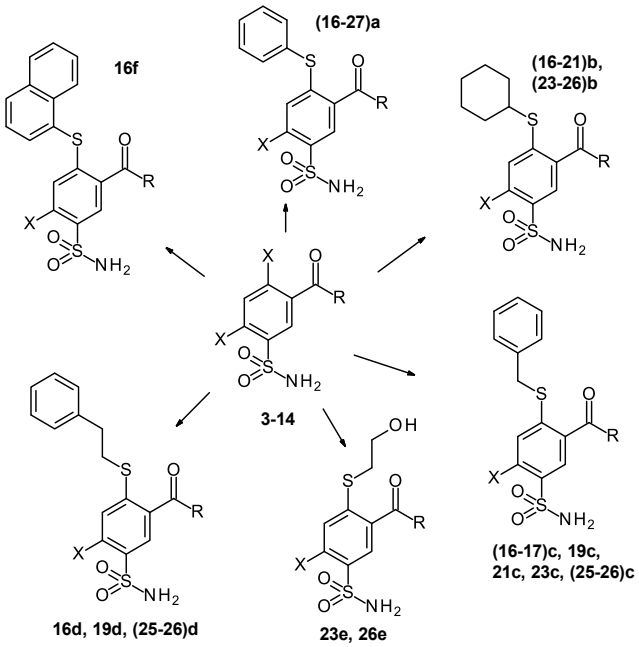

X: Cl (**3-11, 14-24, 27-28**), Br (**12-13, 25-26**)
R: NH_2 (**3, 16**), $NH(CH_2)_2OH$ (**4, 12, 17, 25**), $NH(CH_2)_3OH$ (**5, 18**), $NH(CH_2)_3CH_3$ (**6, 13, 19, 26**), $NH(CH_2)_2OCH_3$ (**7, 20**), $NH(CH_2)_3CO_2CH_3$ (**8, 21**), N-morfolinil- (**9, 22**), NH-cikloheksil- (**10, 23**), NH-benzil- (**11, 24**), $NH(CH_2)_3OAc$ (**14, 27**), $NH(CH_2)_3CO_2H$ (**15, 28**).

5 schema. 2-sulfanilbenzamidų sintezė.

Reakcijų sąlygų pasirinkimą įtakojo nukleofilo pobūdis. Junginių **3-8, 10-14** reakcijos su tiofenoliu arba 1-tionaftoliu vyko lengviausiai, virinant MeOH esant trietilamino. Su cikloheksantioliu šiomis reakcijos sąlygomis reakcijos vyko labai lėtai, todėl polinis protoninis tirpiklis buvo pakeistas į polinį aprotoninį DMSO, o trietilaminas – į bevandenį K_2CO_3. Tai leido atlikti junginių **3-8, 10-13** reakcijas per 2-6 valandas vietoje dienų ar savaičių, esant tai pačiai temperatūrai.

Naudojant kitus, vidutinio reaktingumo nukleofilus (pirminius alkiltiolius ir pan.) reakcijos atliktos poliniame aprotoniniame tirpiklyje (DMSO) esant TEA.

Vienintelė išimtis buvo morfolinildarinio **9** reakcija su tioliais, kai net su tiofenoliu reikėjo reakciją atlikti 120 °C temperatūroje, poliniame aprotoniniame tirpiklyje (DMSO) su Cs_2CO_3.

Susintetinti sulfanildariniai buvo toliau oksiduoti iki sulfonildarinių. Oksidacijos reakcijos atliktos geromis išeigomis (69-92 %), acto rūgštyje su vandenilio peroksidu *in situ* generuojant peracto rūgštį (6 schema). Oksiduojant hidroksilo grupę turinčius amidus buvo stebimas *O*-acetatų susidarymas ir siekiant to išvengti reakcijos produktų mišinys buvo papildomai veikiamas praskiesta druskos rūgštimi.

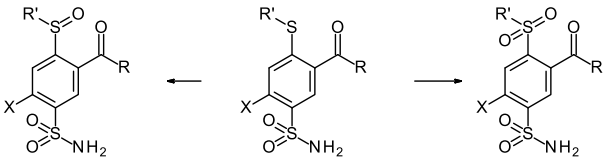

40a,c — **16d, 17a-c, 18a-b, 19a-b, 20a-b, 21b-c, 23a-c,e, 24a-b, 25a-c, 26a-b** — **30d, 31a-c, 32a-b, 33a-b, 34a-b, 35b-c, 36a-c,e, 37a-b, 38b-c, 39a-b.**

X: Cl (**16-24, 30-37, 40c**), Br (**25-26, 38-39, 40a**)
R: NH_2 (**16, 30**), $NH(CH_2)_2OH$ (**17, 25, 31, 38, 40a**), $NH(CH_2)_3OH$ (**18, 32**), $NH(CH_2)_3CH_3$ (**19, 26, 33, 39**), $NH(CH_2)_2OCH_3$ (**20, 34**), $NH(CH_2)_3CO_2CH_3$ (**21, 35**), NH-cikloheksil- (**23, 36, 40c**), NH-benzil- (**24, 37**)
R': a) fenil-, b) cikloheksil-, c) benzil-, d) 2-feniletil-, e) 2-hidroksietil-

6 schema. 4-sulfonil- ir 4-sulfinilbenzensulfonamidų sintezė.

Benzoinės rūgštys **29b, d** susintetintos iš atitinkamų benzamidų **16b, d** rūgštinės hidrolizės sąlygomis. Tačiau panašiai atlikus esterių **21b, 35c** hidrolizę (7 schema) buvo stebimas dviejų produktų susidarymas. Todėl tolimesnė esterių **21a-c** hidrolizė atlikta šarminėje terpėje, kambario temperatūroje, susidarant tik tiksliniams produktams.

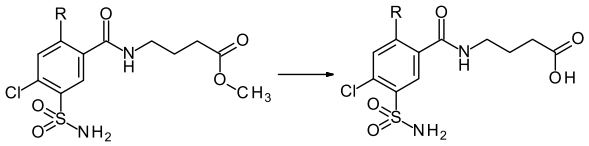

21a-c, 35c — **28a-c, 41c**

R: (**21a, 28a**), (**21b, 28b**), (**21c, 28c**), (**35c, 41c**).

7 schema. 4-aminobutaninių rūgščių darinių sintezė

Sekanti junginių serija (**III str**.) buvo sukurta remiantis žiniomis[31] apie CA VA izofermentui selektyvius slopiklius. Susintetinti junginiai 2-chlor- ir 2,4-dichlorbenzensulfonamidų pagrindu, 5-oje padėtyje turintys įvairius heterociklus.

Junginiai **42a-h** ir **43a-c** susintetinti tikslinius heterociklus alkilinant (bromoacetil)-2-chlorobenzenesulfonamidu **42** arba 5-(bromoacetil)-2,4-dichlorobenzenesulfonamidu **43**. *N*-alkilinimai atlikti THF esant NaOAc kambario temperatūroje. Siekiant išvengti benzimidazolų dialkilinimo naudotas nedidelis heterociklo perteklius. Junginiai **42g** ir **42h** susintetinti naudojant 1,2,3,4-tetrahidrochinolino ir indolino perteklių, be bazės (8 schema).

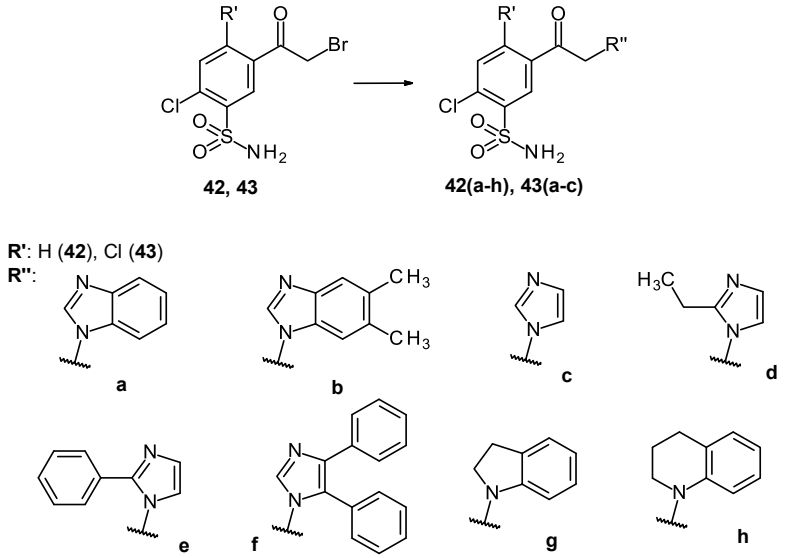

8 schema. Junginių **42a-h** and **43a-c** sintezė.

Junginio **46** nepavyko susintetinti tiesiogiai acilinant 1-aminobenzimidazolą 2,4-dichlor-5-sulfamoilbenzoilchloridu įvairiomis salygomis. Bet apsaugojus sulfonamido grupę *N,N'*-dimetilaminometiliden-grupe (9 schema, junginys **44**) pavyko išvengti pašalinių produktų susidarymo ir acilinimo reakcijos metu susintetintas junginys **45,** kurį deblokavus gautas tikslinis benzensulfonamidas **46**.

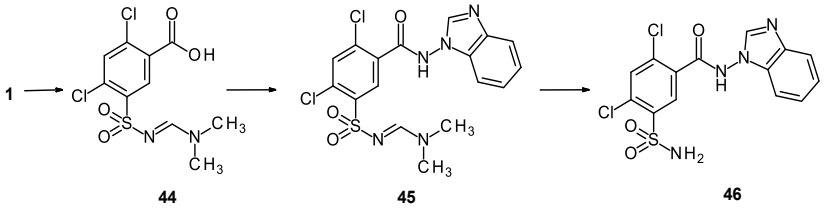

9 schema. Junginio **46** sintezė.

Dalis 2,4-dichlorjunginių (**43a,b, 46**) modifikuoti įvedant sieros tiltelį turinčius fragmentus pagal aprašytas (**II str**.) metodikas (10 schema). Taip susintetinti junginiai **47-50**.

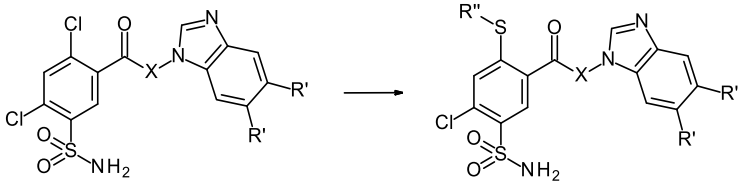

43a: X=CH_2, R'=H
43b: X=CH_2, R'=CH_3
46: X=NH, R'=H

47: X=CH_2, R'=H, R''=2-feniletil-
48: X=CH_2, R'=CH_3, R''=fenil-
49: X=NH, R'=H, R''=fenil-
50: X=NH, R'=H, R''=cikloheksil-

10 schema. 2-chlor-4,5-dipakeistų benzensulfonamidų **47-50** sintezė.

Straipsnyje **IV** aprašyta sekanti pakeistų halogenintų benzensulfonamidų grupė. Iš pradinių metil 2,4-dihalo-5-sulfamoilbenzoatų **51**, **52** susintetinti metil 2-halo-4-pakeisti ir 4-halo-2-pakeisti-5-sulfamoilbenzoatai (11 schema). Reakcijos sąlygos buvo parinktos remiantis ankstesniais darbais (**II** str.) kuriuose aprašytos 2,4-dihalo-5-sulfamoilbenzamidų reakcijos su sierą turinčiais nukleofilais. Atliekant reakcijas metanolyje aromatiniai tioliai (tiofenolis ir 1-tionaftolis) lengvai keitė halogeno atomą sudarydami *para*-pakeistus benzensulfonamidus **55a,f** ir **56a**. Tuo tarpu reakcijos su tioliais turinčiais CH_2 ar CH grupę tokiomis sąlygomis vyksta labai lėtai ar visai nevyksta. Siekiant paspartinti reakcijas polinis protoninis tirpiklis pakeistas į polinį aprotoninį DMSO ir susintetinti *orto*-pakeisti benzensulfonamidai **53b-e, 54b** (11 schema). Reakcijose taip pat stebėtas *para*- ir dipakeistų benzensulfonamidų susidarymas.

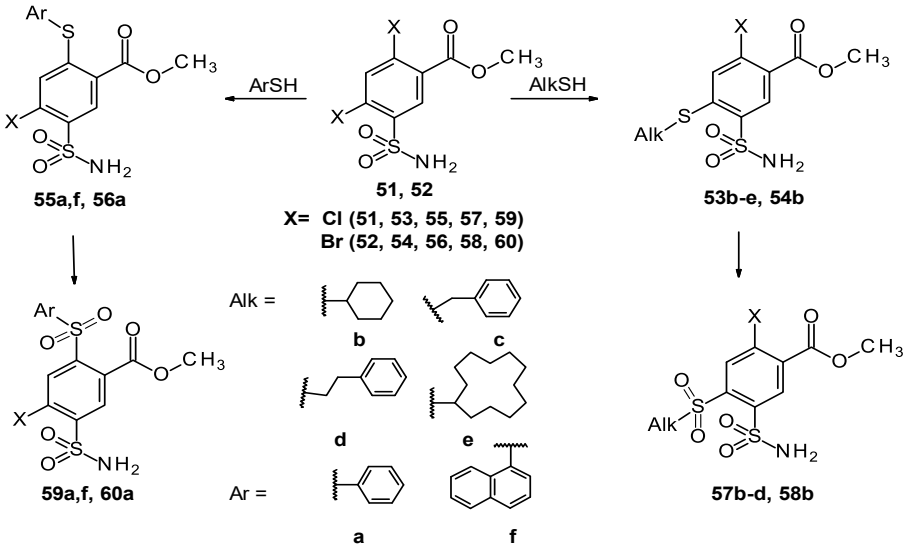

11 schema. Metil halo-2- ir 4-pakeistų-5-sulfamoilbenzoatų sintezė.

Buvo ištirtas 2,4-dihalo-5-sulfamoil-benzoatų **51, 52** nukleofilinio aromatinio pakeitimo reakcijų regioselektyvumas (3 lentelė). Visos reakcijos atliktos DMSO su tioliu ir trietilaminu, 60 °C temperatūroje 72h. Reakcijos konversija, produktų santykis ir struktūrų identifikavimas atliktas BMR ir HPLC/UV/MS pagalba.

2 lentelė. 2,4-dihalo-5-sulfamoilbenzoatų **51**, **52** reakcijos su tioliais išeigos ir produktų santykiais nustatyti pagal ^{1}H-BMR spektroskopijos ir HPLC/UV/MS tyrimų duomenis (*italic*). * 2- ir 4-pakeistų izomerų susidariusių junginių **51** ir **52** reakcijose su tiofenoliu atskirti HPLC būdu nepavyko.

Pradinis junginys	Tiolis	Konversija (%)	2-pakeistas (%)	4-pakeistas (%)	2,4-dipakeisti (%)
51		30.07 *28.77*	18.70 *17.38*	81.30 *82.62*	-
52		15.71 *13.92*	9.09 *14.11*	90.91 *85.89*	-
51		89.47 *96.67*	58.82 *88.78**	35.29	5.88 *11.22*
52		95.07 *96.92*	51.81 *85.55**	40.42	7.77 *14.45*
51		72.73 *71.55*	23.53 *22.91*	73.53 *72.79*	2.94 *4.30*
51		72.15 *73.60*	12.28 *12.05*	87.72 *87.95*	-

Pradinis junginys	Tiolis	Konversija (%)	2-pakeistas (%)	4-pakeistas (%)	2,4-dipakeisti (%)
51		90.97 *95.25*	76.34 *78.84*	19.08 *15.72*	4.58 *5.44*
51		13.70 *18.19*	-	100.00 *100.00*	-

Tiolių reaktingumo mažėjimo seka yra tokia: fenil->naftil->benzil-≥2-etilfenil->cikloheksil-≥ciklododecil-. Dipakeistų produktų susidarymas stebimas reakcijose su fenil-, naftil- ir benziltioliais. 2-pakeistų produktų daugiau susidaro reakcijose su aromatiniais tioliais, kitais atvejais dominuoja 4-pakeisti produktai. Ciklododeciltiolio atveju stebimas tik vieno 2-pakeisto izomero susidarymas.

Trūkstami 2-pakeisti metilo esteriai **55a-d, f** susintetinti iš jau aprašytų 2-pakeistų benzamidų **16a-d, f** (12 schema). Amido grupė pakeista į esterio grupę vienos stadijos reakcijoje kaitinant metanolyje su tionilo chloridu.

Sulfanildarinių **53**(**b-d**), **54b**, **55**(**a-d**, **f**), **56a** oksidacija iki sulfonil darinių **57**(**b-d**), **58b, 59**(**a-d**,**f**), **60a** atlikta *in situ* generuojant peracto rūgštį (11 ir 12 schemos).

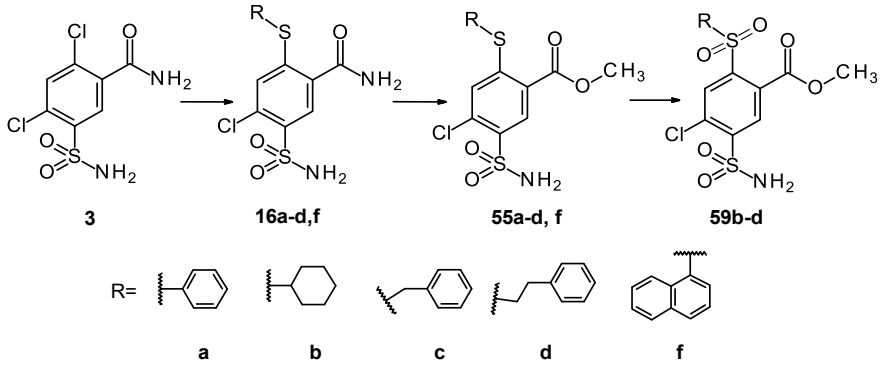

12 schema. Metil 4-chlor-2-pakeistų-5-sulfamoilbenzoatų sintezė.

Straipsnyje **V** siekiama ištirti arti sulfonamido grupės esančių pakaitų įtaką jungimuisi su karboanhidrazėmis. Tam susintetinti *orto*-pakeisti benzensulfonamidai su amino-, sulfanil-, sulfinil- ir sulfonilpakaitais.

Kadangi 2,4-dihalodarinių reakcijose susidaro įvairūs produktai, buvo pasirinktas pradinis junginys su labiau nuspėjama elgsena – 4-chlor-3-sulfamoilbenzoinė rūgštis (**62**). Iš jos remiantis jau išbandytomis metodikomis susintetinti pradiniai junginiai – metilo esteris (**63**) ir eilė amidų (**64-66**) (13 schema).

Iš 4-chlor-3-sulfamoilbenzoinės rūgšties esterio **63** nukleofilinio aromatinio pakeitimo reakcijose susintetinti 4-sulfanilpakeisti junginiai **67a-d,f-m** (13 schema). Reakcijos atliktos šildant su įvairiais tioliais dimetilformamide, esant K_2CO_3. Tomis pačiomis reakcijos sąlygomis susintetinti 4-sulfanilpakeisti sulfamoilbenzamidai **68a-d, f, g, j-m**.

4-amino-pakeisti junginiai **69b, c** sintetinti benzamidą **64** kaitinant atitinkamo amino pertekliuje 130 °C. Junginys **69e** susintetintas virinant tolueno ir ciklooktilamino mišinyje.

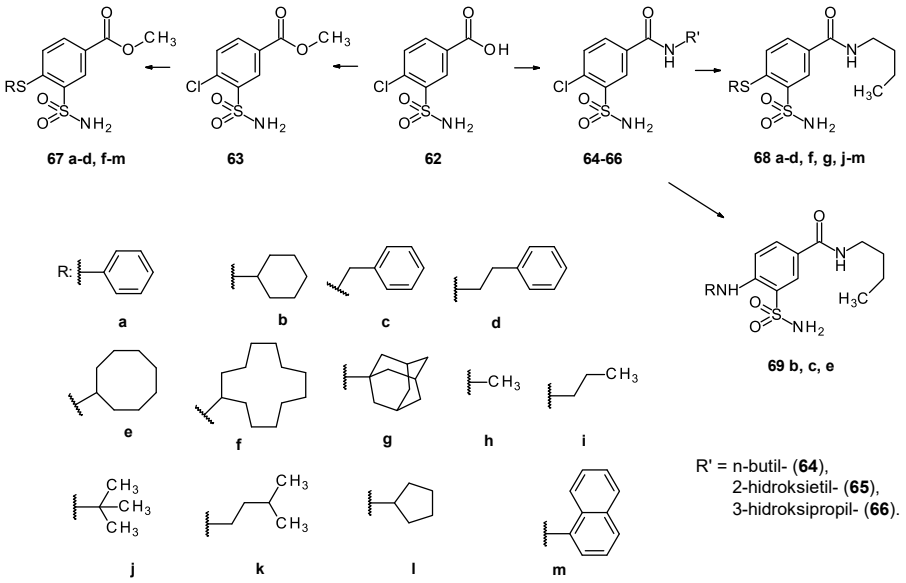

13 schema. Metil 4-sulfanil-pakeistų-3-sulfamoil-benzoatų **67a-d, f-m**, 4-sulfanilpakeistų-3-sulfamoilbenzamidų **68 a-d, f, g, j-m** ir 4-amino-pakeistų-3-sulfamoilbenzamidų **69 b, c, e** sintezė.

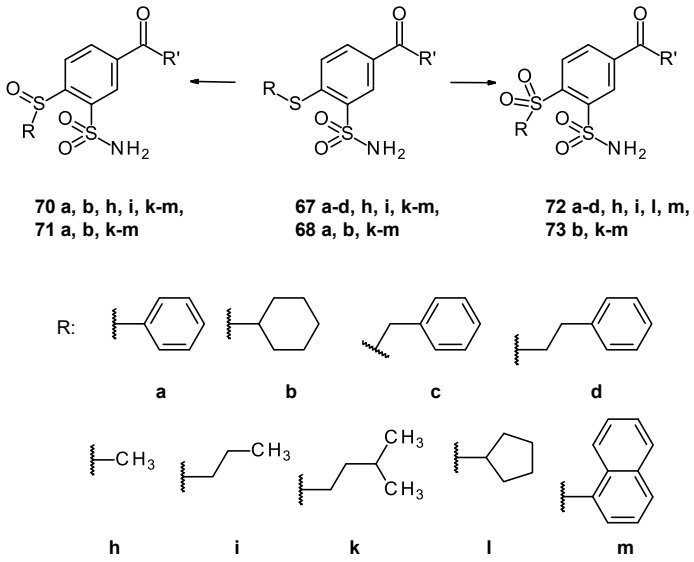

14 schema. Metil 4-sulfinilpakeistų-3-sulfamoilbenzoatų **70a, b, h, i, k-m**, *N*-butil-4- sulfinilpakeistų-3-sulfamoilbenzamidų **71a, b, k-m**, metil 4-sulfonilpakeistų-3-sulfamoilbenzoatų **72a-d, h, i, l, m ir** *N*-butil-4-sulfonilpakeistų-3-sulfamoilbenzamidų **73b, k-m** sintezė.

Esterių **67a-d, h, i, k-m** ir benzamidų **68a**, **b**, **k-m** oksidacijos iki sulfinil- ir sulfonil- junginių atliktos naudojant *in situ* generuotą peracto rūgštį (14 schema). Atliekant reakciją kambario temperatūroje susintetinti sulfinil-junginiai **70a, b, h, i, k-m**, **71a, b, k-m**, o kaitinant reakcijos mišinį 70 °C temperatūroje susintetinti sulfonil- junginiai **72a-d, h, i, l, m, 73b, k-m**.

4. REZULTATŲ APTARIMAS

Pirmame straipsnyje atlikta susintetintų junginių jungimosi su 12 α-CA izofermentų duomenų analizė. Pirma atlikus vieną pakaitą turinčių junginių (*N*-pakeistų 2,4-dihalo-5-sulfamoilbenzamidų **3-15**) afiniškumo ir selektyvumo analizę nustatyta, kad jie stipriausiai jungiasi su CA VII. Įvedus antrą pakaitą (2-aminopakeisti-4-halo-5-sulfamoilbenzamidai, 4 schema) daugumoje atvejų stebimas padidėjęs afiniškumas ir selektyvumas CA IX ir CA XIV izofermentams. Selektyvumas šioms CA priklauso nuo antrojo pakaito dydžio. Benzilamino grupė dėl savo lankstumo lengviau saveikauja su visų izofermentų aktyvaus centro fragmentais ir taip padidina afiniškumą, tačiau sumažina selektyvumą lyginant su mažiau lanksčia cikloheksilamino grupe. Kelios junginių ir karboanhidrazių kompleksų kristalografinės struktūros parodė kontaktus tarp slopiklio pakaitų ir baltymo aminorūgščių ir padidino supratimą apie tiriamų sistemų struktūros-aktyvumo sąryšius.

Antrame straipsnyje aprašyti susintetinti CA slopikliai turintys du pakaitus, vienas iš kurių prijungtas per sieros atomą turintį jungtuką (2-sulfanil- arba 2-sulfonilpakeisti-4-halo-5-sulfamoilbenzamidai). Šių junginių cheminių struktūrų ir jungimosi parametrų analizė parodė dviejų pakaitų svarbą ir įtaką afiniškumui bei selektyvumui konkretiems CA izofermentams. Kristalinės baltymo-slopiklio kompleksų struktūros (6 pav.) parodė struktūriškai panašių slopiklio pakaitų išsidėstymo karboanhidrazės izofermentų aktyviuosiuose centruose skirtumus bei galimas pakaitų ir aktyvių centrų sąveikos vietas.

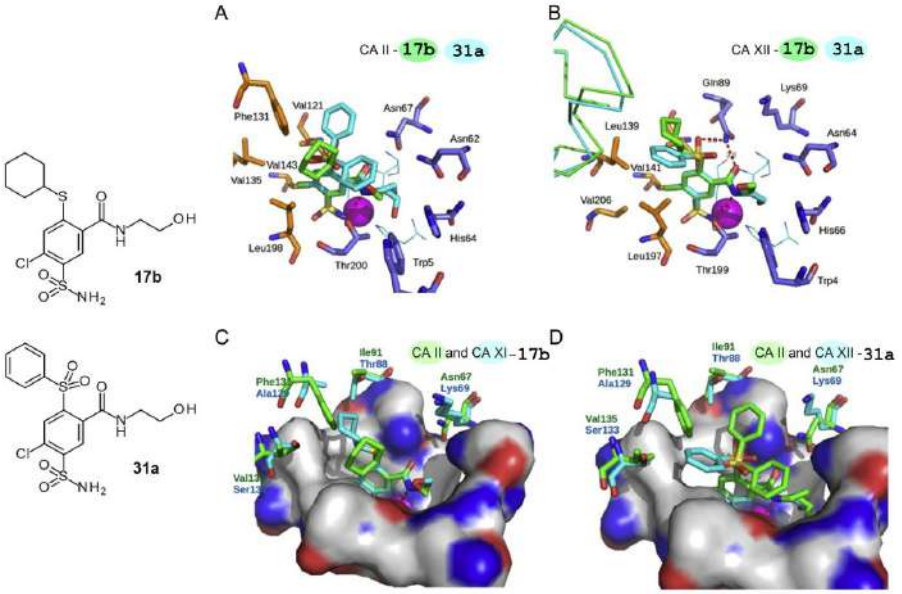

6 pav. Junginių **17b** ir **31a** kristalografinės struktūros CA II ir CA XII aktyviuosiuose centruose. A ir B paveiksluose lyginamas dviejų panašios cheminės struktūros junginių (**17b** (žalia) ir **31a**(žydra)) prisijungimas prie CA II (A; junginys **17b** (PDB ID: 6R6F) ir **31a** (PDB ID: 6R6J)) ir CA XII (B; junginys **17b** (PDB ID: 6R6Y) ir **31a** (PDB ID: 6R71)). CA aktyviųjų centrų hidrofobinių aminorūgščių šoninės grandinės yra oranžinės, hidrofilinių – mėlynos spalvos. Cinko jonas pavaizduotas kaip violetinė sfera. C ir D paveikslėliuose lyginamas junginių **17b** ir **31a** prisijungimas prie CA II (žalia) ir CA XII (žydra). Panašios CA II ir CA XII aktyviųjų centrų aminorūgščių šoninės grandinės pavaizduotos kaip paviršiai.

Taip pat reikia pažymėti, kad lyginant su pirmame straipsnyje aprašytais aminopakeistais junginiais pastarosios serijos junginiai pasižymi didesniu afiniškumu, o jungimosi su CA VII, CA IX, CA XII arba CA XIV atvejais stebimos subnanomolinės vertės.

Trečiame straipsnyje susintetinta selektyvių CA VA inhibitorių serija, pagrįsta anksčiau aprašytu junginiu 5-[2-(benzimidazol-1-il)acetil]-2-chlor-benzensulfonamidu (**42a**). Pirma ištirti 2-halo- ir 2,4-dihalobenzensulfonamidai su pakaitais 5-oje padėtyje ir jų afiniškumo priklausomybė nuo pakaite esančių heterociklų prigimties ir dydžio (7 pav.).

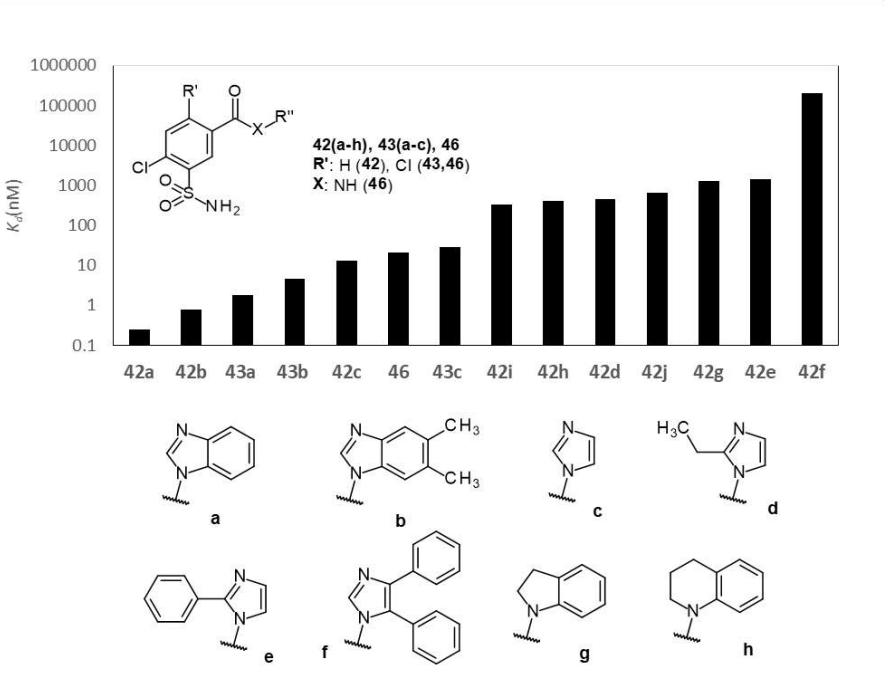

7 pav. Jungimosi su CA VA izofermentu stebimųjų disociacijos konstantų palyginimas. Junginiai išdėstyti mažėjančio afiniškumo tvarka.

Nustatyta, kad benzimidazolo žiedas yra palankesnis nei imidazolo dėl aromatinės-aromatinės sąveikos su CA VA Tyr64. Benzimidazolo/imidazolo žiedo antras azoto atomas taip pat yra svarbus ir sudaro vandenilinius ryšius tarp azoto atomo ir Thr62 hidroksilo CA VA. Kai antro azoto atomo nėra, pavyzdžiui, indolino arba 3,4-dihidro-2H-chinolino pakaitų atveju (junginiai **42g, 42h**), selektyvumas CA VA atžvilgiu išnyksta. Gi antro pakaito įvedimas į benzensulfonamido *para*-padėtį padidina junginių afiniškumą visiems CA izofermentams ir stipriai sumažina selektyvumą tiksliniam CA VA (8 pav.).

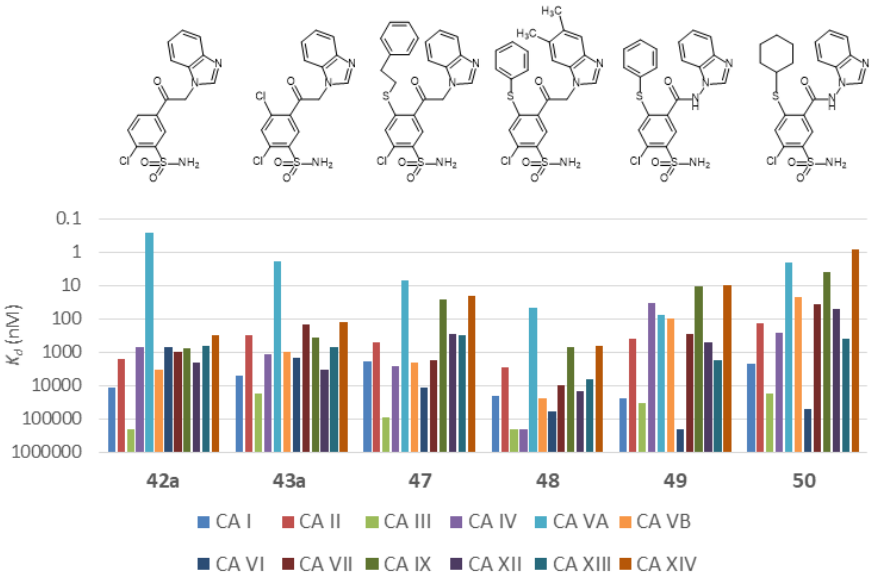

8 pav. Junginių **42a**, **43a** ir **47-50** sąveikos su 12 CA izofermentų K_d vertės selektyvumo CA VA izofermentui palyginimui.

Ketvirtame straipsnyje sukurtos kelios junginių serijos ir ištirta pakaitų bei jų padėčių poveikis metil- 2- arba 4-pakeistų-5-sulfamoilbenzoatų jungimuisi prie žmogaus CA izofermentų. Išsamiai išnagrinėti skirtingo dydžio sulfanilo (-S-) ir sulfonilo (-SO_2-) pakaitai, pateiktos šių dviejų junginių grupių prisijungusių prie CA aktyviųjų centrų kristalinės struktūros (9 pav.). *Para*-pakeisti 2-halobenzensulfonamidai, tiek sulfanil- (**55-56** grupės), tiek sulfonil- pakeisti (**59-60** grupės), jungėsi panašiai su įvairiomis CA izofermentų grupėmis ir nedemonstravo selektyvumo. Tuo tarpu *orto*-sulfanilpakeisti 4-halobenzensulfonamidai pasižymėjo itin geru afiniškumu ir selektyvumu su vėžiu siejamam CA IX izofermentui (junginių **53b, e** ir **54b** K_d artėjo prie 0,1 nM). Gi analogiški *orto*-sulfonilpakeisti 4-halobenzensulfonamidai (**57** ir **58** grupės) su visais CA izofermentais jungėsi silpnai (10 pav.).

Toks netikėtai didelis afiniškumo kritimas buvo priimtas kaip požymis, kad pasiekta ta riba, kuomet atlikus nedidelius pakitimus benzensulfonamido struktūroje *orto*-padėtyje, galima tikėtis esminių pokyčių slopiklio-baltymo saveikoje. Kas ir buvo atlikta sekančiame darbe.

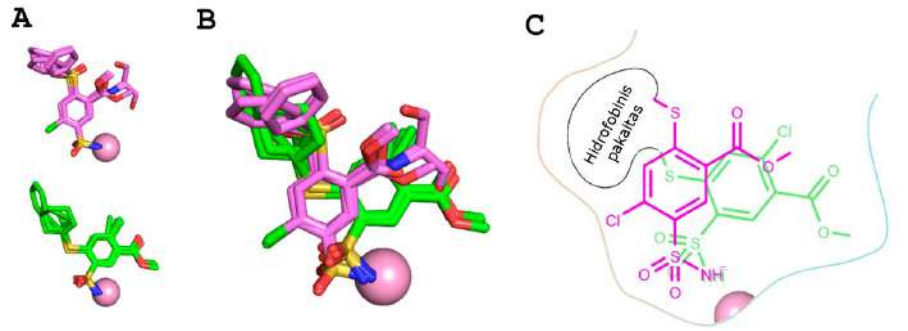

9 pav. Junginių cheminių struktūrų koreliacija ir CA izofermentų kristalinių struktūrų palyginimas. (A) Perkloti kristalinių struktūrų ligandai: *para*-pakeisti ligandai yra rausvos spalvos (PDB ID: 7PP9, 7PUW, 7POM, 7Q0C), *orto*-pakeisti ligandai yra žalios spalvos (PDB ID: 6R6F, 6R71, 7PUU, 7PUV, 7Q0E). (B) Palyginimui parodytos aukščiau paminėtos perklotos struktūros. (C) Schema, vaizduojanti B panelėje parodytų junginių padėtis, oranžinė linija žymi hidrofobiškesnę aktyviosios vietos pusę.

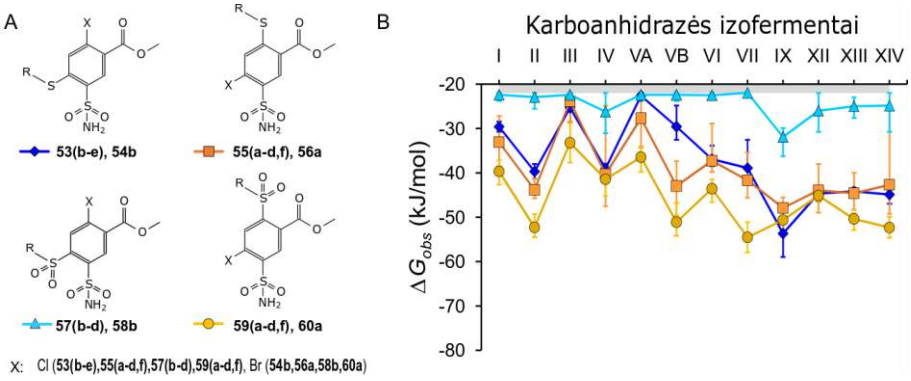

10 pav. (A) Keturių junginių grupių – metil halo- 2- arba 4-pakeistų 5-sulfamoilbenzoatų cheminės struktūros. (B) Vidutinis stebimos standartinės Gibso energijos pokytis junginiams, priklausantiems vienai iš keturių grupių. Stulpeliai rodo skirtumą tarp stipriausio ir silpniausio tos grupės junginių afiniškumo nurodytam CA izofermentui. Pirmos grupės (mėlyni rombai) junginiai pasižymi didžiausiu afiniškumu ir selektyvumu CA IX izofermentui.

Penktame straipsnyje tyrimams pasirinkta išsamiai išnagrinėti *orto*-padėtyje esančių benzensulfonamido pakaitų įtaką. Pasirinkti junginiai panašūs į geriausius ankstesnio straipsnio junginius, tik sąmoningai praleisti halogeno atomai, kad būtų lengviau susintetinti daugiau ir įvairesnių *orto*-pakeistų junginių. Buvo susintetintos serijos benzensulfonamidų su linijiniais

ir cikliniais pakaitais nuo metil- iki adamantanil-, prijungtais per sulfanil- (-S-), sulfinil- (-SO-) ir sulfonil-jungtukus (-SO_2-). Keičiant jungtuko oksidacijos laipsnį siekta dėl elektronų akceptorinių savybių sumažinti slopiklių sulfonamido grupės pK_a ir sustiprinti jungimąsi su CA. Deja, junginiai su -SO- arba -SO_2- jungtuku nepaisant sumažėjusio vienetu pK_a daug silpniau jungėsi su visomis CA nei junginiai su -S- jungtimi (11 pav.). Pakaitų mažinimo strategija nedavė norimų rezultatų – nors ir sulfinil- bei sulfonil-pakeistų slopiklių afiniškumas padidėjo, bet net junginiai su mažiausiu metilo pakaitu (**70h, 72h**) nepasiekė sulfanilo junginio **67h** afiniškumo. Pagrindinė to priežastis buvo leistinos junginių konformacijos, kurios buvo apskaičiuotos naudojant kvantinio tankio funkcionalo teoriją (DFT, atliko V. Kairys). Deguonies atomai junginiuose su –SO- ir –SO_2- riboja molekulės lankstumą randant optimalią padėtį aktyviajame baltymo centre ir veikia kaip sterinis trukdis.

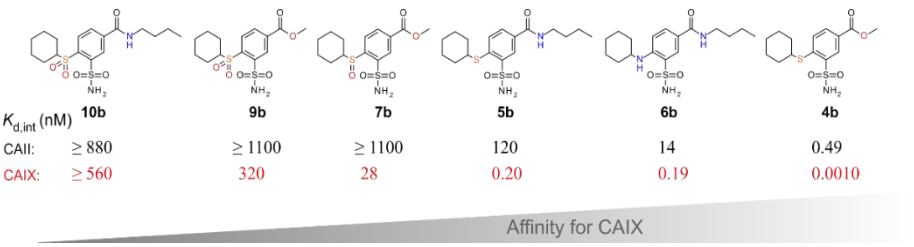

11 pav. Junginiai išdėstyti didėjančio afiniškumo CA IX tvarka (**V** straipsnio numeracija).

Didžiausią afiniškumą CA IX šiame tyrime parodė metil 4-sulfanil-pakeisti-3-sulfamoilbenzoatai, ypač **67b**. Tuo tarpu *N*-butil-4-sulfanil-pakeisti-3-sulfamoilbenzamidai (**68-69** serijos) su visomis karboanhidrazėmis jungėsi silpniau, bet išlaikydami panašų selektyvumą CA IX. Bet didžiausiu afiniškumu CAIX pasižymėjo anksčiau (**IV** str.) sukurti panašūs junginiai, turintys 2-chlor- arba 2-brompakaitus (**53b, e** ir **54b)**.

IŠVADOS

1. 2-halo-benzensulfonamidų 4- ir 5- padėties pakaitai, dėl įvairioms sąveikoms palankios didelės aktyvaus centro erdvės, teigiamai įtakoja slopiklių afiniškumą daugumai CA-izofermentų. Kombinuotas pakaitų lankstumo sumažinimas sukeliant sterinius trukdžius įgalina pagerinti selektyvumą atskiriems izofermentams.
2. Norint pasiekti didžiausią slopiklio afiniškumą ir selektyvumą CA VA ir CA VII, uženka vieno masyvaus pakaito 5-oje 2,4- dihalobenzensulfonamido padėtyje.
3. Metil 2,4-dihalo-5-sulfamoil-benzoatų reakcijose su ariltioliais dominuoja 2-padėties halogeno atomo pakeitimas, o reakcijose su alkiltioliais – 4-os padėties halogeno atomo pakeitimas.
4. 2,5-dipakeisti benzensulfonamidai dėka masyvių 2-os padėties amino ir sulfanilpakaitų pasižymi dideliu afiniškumu ir selektyvumu CA IX izofermentui. Halogeno atomo įvedimas į 4-ą padėtį padidina afiniškumą CA IX neįtakodamas selektyvumo.
5. Sulfinil- ir ypač sulfonilpakaitams 2-oje padėtyje sąveikaujant su gretima sulfonamido grupe sudaromi steriniai trukdžiai stipriai sumažina slopiklių afiniškumą visiems CA izofermentams. Šiems junginiams 2-os padėties pakaito dydžio ir lankstumo įtaka CA izofermentų slopinimui yra nereikšminga.

LITERATŪROS SĄRAŠAS

(1) Khalifah, R. G. The Carbon Dioxide Hydration Activity of Carbonic Anhydrase. I. Stop-Flow Kinetic Studies on the Native Human Isoenzymes B and C. *J. Biol. Chem.* **1971**, *246* (8), 2561–2573. https://doi.org/10.1016/S0021-9258(18)62326-9.

(2) Gibbons, B. H.; Edsall, J. T. Rate of Hydration of Carbon Dioxide and Dehydration of Carbonic Acid at 25°. *J. Biol. Chem.* **1963**, *238* (10), 3502–3507. https://doi.org/10.1016/S0021-9258(18)48696-6.

(3) *Drug Design of Zinc-Enzyme Inhibitors: Functional, Structural, and Disease Applications*; Supuran, C. T., Winum, J.-Y., Eds.; Wiley series in drug discovery and development; Wiley: Hoboken, NJ, 2009.

(4) Tripp, B. C.; Smith, K.; Ferry, J. G. Carbonic Anhydrase: New Insights for an Ancient Enzyme. *J. Biol. Chem.* **2001**, *276* (52), 48615–48618. https://doi.org/doi.org/10.1074/jbc.r100045200.

(5) Del Prete, S.; Vullo, D.; Fisher, G. M.; Andrews, K. T.; Poulsen, S.-A.; Capasso, C.; Supuran, C. T. Discovery of a New Family of Carbonic Anhydrases in the Malaria Pathogen Plasmodium Falciparum—The η-Carbonic Anhydrases. *Bioorg. Med. Chem. Lett.* **2014**, *24* (18), 4389–4396. https://doi.org/10.1016/j.bmcl.2014.08.015.

(6) Kikutani, S.; Nakajima, K.; Nagasato, C.; Tsuji, Y.; Miyatake, A.; Matsuda, Y. Thylakoid Luminal θ-Carbonic Anhydrase Critical for Growth and Photosynthesis in the Marine Diatom Phaeodactylum Tricornutum. *PNAS* **2016**, *113* (35), 9828–9833. https://doi.org/10.1073/pnas.1603112113.

(7) Baranauskienė, L.; Matulis, D. Overview of Human Carbonic Anhydrases. In *Carbonic Anhydrase as Drug Target: Thermodynamics and Structure of Inhibitor Binding*; Matulis, D., Ed.; Springer International Publishing: Cham, 2019; pp 3–14. https://doi.org/10.1007/978-3-030-12780-0_1.

(8) Jensen, E. L.; Clement, R.; Kosta, A.; Maberly, S. C.; Gontero, B. A New Widespread Subclass of Carbonic Anhydrase in Marine Phytoplankton. *ISME J* **2019**, *13* (8), 2094–2106. https://doi.org/10.1038/s41396-019-0426-8.

(9) Lane, T. W.; Saito, M. A.; George, G. N.; Pickering, I. J.; Prince, R. C.; Morel, F. M. M. A Cadmium Enzyme from a Marine Diatom. *Nature* **2005**, *435* (7038), 42–42. https://doi.org/10.1038/435042a.

(10) Macauley, S. R.; Zimmerman, S. A.; Apolinario, E. E.; Evilia, C.; Hou, Y.-M.; Ferry, J. G.; Sowers, K. R. The Archetype Gamma-Class

Carbonic Anhydrase (Cam) Contains Iron When Synthesized in Vivo. *Biochem.* **2009**, *48* (5), 817–819. https://doi.org/10.1021/bi802246s.

(11) Hilvo, M.; Baranauskiene, L.; Salzano, A. M.; Scaloni, A.; Matulis, D.; Innocenti, A.; Scozzafava, A.; Monti, S. M.; Di Fiore, A.; De Simone, G.; Lindfors, M.; Janis, J.; Valjakka, J.; Pastorekova, S.; Pastorek, J.; Kulomaa, M. S.; Nordlund, H. R.; Supuran, C. T.; Parkkila, S. Biochemical Characterization of CA IX, One of the Most Active Carbonic Anhydrase Isozymes. *J. Biol. Chem.* **2008**, *283* (41), 27799–27809. https://doi.org/10.1074/jbc.M800938200.

(12) Singh, S.; Lomelino, C.; Mboge, M.; Frost, S.; McKenna, R. Cancer Drug Development of Carbonic Anhydrase Inhibitors beyond the Active Site. *Molecules* **2018**, *23* (5), 1045. https://doi.org/10.3390/molecules23051045.

(13) Kim, J. K.; Lim, S. W.; Jeong, H.; Lee, C.; Kim, S.; Son, D. W.; Kumar, R.; Andring, J. T.; Lomelino, C.; Wierman, J. L.; Cohen, A. E.; Shin, T. J.; Ghim, C.-M.; McKenna, R.; Jo, B. H.; Min, D.; Choi, J.-M.; Kim, C. U. Fast Product Release Requires Active-Site Water Dynamics in Carbonic Anhydrase. *Nat. Commun.* **2025**, *16* (1), 4404. https://doi.org/10.1038/s41467-025-59645-x.

(14) Silverman, D. N.; Lindskog, S. The Catalytic Mechanism of Carbonic Anhydrase: Implications of a Rate-Limiting Proteolysis of Water. *Acc. Chem. Res.* **1988**, *21*, 30–36. https://doi.org/doi.org/10.1021/ar00145a005.

(15) Pinard, M. A.; Mahon, B.; McKenna, R. Probing the Surface of Human Carbonic Anhydrase for Clues towards the Design of Isoform Specific Inhibitors. *Biomed. Res. Int.* **2015**, *2015*, e453543. https://doi.org/10.1155/2015/453543.

(16) Supuran, C. T. How Many Carbonic Anhydrase Inhibition Mechanisms Exist? *J. Enzyme Inhib. Med. Chem.* **2016**, *31* (3), 345–360. https://doi.org/10.3109/14756366.2015.1122001.

(17) Sato, Y.; Hoshino, H.; Iki, N. Thermodynamics of Binding of a Sulfonamide Inhibitor to Metal-Mutated Carbonic Anhydrase as Studied by Affinity Capillary Electrophoresis. *J. Inorg. Biochem.* **2015**, *150*, 133–138. https://doi.org/10.1016/j.jinorgbio.2015.06.011.

(18) Mann, T.; Keilin, D. Sulphanilamide as a Specific Inhibitor of Carbonic Anhydrase. *Nature* **1940**, *146* (3692), 164–165. https://doi.org/10.1038/146164a0.

(19) Roblin, R. O. Jr.; Clapp, J. W. The Preparation of Heterocyclic Sulfonamides1. *J. Am. Chem. Soc.* **1950**, *72* (11), 4890–4892. https://doi.org/10.1021/ja01167a011.

(20) Angeli, A.; Tanini, D.; Viglianisi, C.; Panzella, L.; Capperucci, A.; Menichetti, S.; Supuran, C. T. Evaluation of Selenide, Diselenide and

Selenoheterocycle Derivatives as Carbonic Anhydrase I, II, IV, VII and IX Inhibitors. *Bioorg. Med. Chem.* **2017**, *25* (8), 2518–2523. https://doi.org/10.1016/j.bmc.2017.03.013.

(21) Maresca, A.; Temperini, C.; Vu, H.; Pham, N. B.; Poulsen, S.-A.; Scozzafava, A.; Quinn, R. J.; Supuran, C. T. Non-Zinc Mediated Inhibition of Carbonic Anhydrases: Coumarins Are a New Class of Suicide Inhibitors. *J. Am. Chem. Soc.* **2009**, *131* (8), 3057–3062. https://doi.org/10.1021/ja809683v.

(22) Parr, J. S.; Khalifah, R. G. Inhibition of Carbonic Anhydrases I and II by N-Unsubstituted Carbamate Esters. *J. Biol. Chem.* **1992**, *267* (35), 25044–25050. https://doi.org/10.1016/S0021-9258(19)74003-4.

(23) Scolnick, L. R.; Clements, A. M.; Liao, J.; Crenshaw, L.; Hellberg, M.; May, J.; Dean, T. R.; Christianson, D. W. Novel Binding Mode of Hydroxamate Inhibitors to Human Carbonic Anhydrase II. *J. Am. Chem. Soc.* **1997**, *119* (4), 850–851. https://doi.org/doi.org/10.1021/ja963832z.

(24) Winum, J.-Y.; Innocenti, A.; Scozzafava, A.; Montero, J.-L.; Supuran, C. T. Carbonic Anhydrase Inhibitors. Inhibition of the Human Cytosolic Isoforms I and II and Transmembrane, Tumor-Associated Isoforms IX and XII with Boronic Acids. *Bioorg. Med. Chem.* **2009**, *17* (10), 3649–3652. https://doi.org/10.1016/j.bmc.2009.03.058.

(25) Temperini, C.; Cecchi, A.; Scozzafava, A.; Supuran, C. T. Carbonic Anhydrase Inhibitors. Interaction of Indapamide and Related Diuretics with 12 Mammalian Isozymes and X-Ray Crystallographic Studies for the Indapamide-Isozyme II Adduct. *Bioorg. Med. Chem. Lett.* **2008**, *18* (8), 2567–2573. https://doi.org/10.1016/j.bmcl.2008.03.051.

(26) D'Ambrosio, K.; Di Fiore, A.; Alterio, V.; Langella, E.; Monti, S. M.; Supuran, C. T.; De Simone, G. Multiple Binding Modes of Inhibitors to Human Carbonic Anhydrases: An Update on the Design of Isoform-Specific Modulators of Activity. *Chem. Rev.* **2025**, *125* (1), 150–222. https://doi.org/10.1021/acs.chemrev.4c00278.

(27) Čapkauskaitė, E.; Zubrienė, A.; Baranauskienė, L.; Tamulaitienė, G.; Manakova, E.; Kairys, V.; Gražulis, S.; Tumkevičius, S.; Matulis, D. Design of [(2-Pyrimidinylthio)Acetyl]Benzenesulfonamides as Inhibitors of Human Carbonic Anhydrases. *Eur. J. Med. Chem.* **2012**, *51*, 259–270. https://doi.org/10.1016/j.ejmech.2012.02.050.

(28) Smirnov, A.; Zubrienė, A.; Manakova, E.; Gražulis, S.; Matulis, D. Crystal Structure Correlations with the Intrinsic Thermodynamics of Human Carbonic Anhydrase Inhibitor Binding. *PeerJ* **2018**, *6*, e4412. https://doi.org/10.7717/peerj.4412.

(29) Sturm, K.; Siedel, W.; Weyer, R.; Ruschig, H. Zur Chemie Des Furosemids, I. Synthesen von 5-Sulfamoyl-anthranilsäure-Derivaten. *Chem. Ber.* **1966**, *99* (1), 328–344. https://doi.org/10.1002/cber.19660990150.

(30) Smirnovienė, J.; Smirnov, A.; Zakšauskas, A.; Zubrienė, A.; Petrauskas, V.; Mickevičiūtė, A.; Michailovienė, V.; Čapkauskaitė, E.; Manakova, E.; Gražulis, S.; Baranauskienė, L.; Chen, W.-Y.; Ladbury, J. E.; Matulis, D. Switching the Inhibitor-Enzyme Recognition Profile via Chimeric Carbonic Anhydrase XII. *ChemistryOpen* **2021**, *10* (5), 567–580. https://doi.org/10.1002/open.202100042.

(31) Čapkauskaitė, E.; Linkuvienė, V.; Smirnov, A.; Milinavičiūtė, G.; Timm, D. D.; Kasiliauskaitė, A.; Manakova, E.; Gražulis, S.; Matulis, D. Combinatorial Design of Isoform-Selective N-Alkylated Benzimidazole-Based Inhibitors of Carbonic Anhydrases. *ChemistrySelect* **2017**, *2* (19), 5360–5371. https://doi.org/10.1002/slct.201700531.

SUMMARY

INTRODUCTION

The development of small-molecule chemical drugs is a long and costly process that has become increasingly complex in recent decades due to higher requirements for efficacy and safety. The first stage of this process involves the identification, organic synthesis, and optimization of a potential drug candidate capable of being useful in the treatment of a specific disease or condition. Achievement of this stage requires an understanding of how drugs interact with target structures of biological systems (receptors, enzymes, transporters, etc.) and how desired drug properties can be obtained through structural modification.

In order to understand general principles of drug development, enzymes are among the most attractive research targets. They usually exhibit selective activity, i.e., high substrate specificity, which makes it possible to develop drugs that affect only a specific biological process. In addition, many diseases are known to be associated with changes in enzyme expression and, consequently, in the functions they perform. Furthermore, the high catalytic activity of enzymes allows even small amounts of an inhibitor to significantly affect enzyme activity and produce a strong therapeutic effect. Moreover, such pronounced changes in activity often facilitate laboratory studies and accelerate the research process itself. Therefore, in this dissertation, one such family of research targets—carbonic anhydrases—was selected.

Carbonic anhydrases are enzymes found in all living organisms, from bacteria to mammals, that catalyze the widely occurring carbon dioxide hydration reaction:

$$CO_2 + H_2O \rightleftharpoons H^+ + HCO_3^-$$

Why are carbonic anhydrases so important? When observing bubbles rising in a carbonated beverage, it is difficult to imagine why CAs are needed at all. However, the carbon dioxide hydration reaction is relatively slow ($k = 0.039\ s^{-1}$ (Khalifah, 1971)), and carbonic anhydrases accelerate it to approximately $10^6\ s^{-1}$, thereby significantly influencing a wide range of physiological processes.

In the human body alone, 12 catalytically active alpha-family carbonic anhydrases have been identified. These enzymes exhibit high structural similarity but differ in their cellular and organ localization, physiological function, and catalytic activity.

Carbonic anhydrases perform diverse physiological functions in the human body, participating in processes such as CO_2 transport, pH regulation,

electrolyte balance, bone resorption, and tumor development, among others. Changes in the activity of certain carbonic anhydrases (increased activity or expression) are associated with various diseases that are treated using CA inhibitors, including glaucoma, epilepsy, idiopathic intracranial hypertension, high-altitude sickness, migraine, and others. A major problem of most CA inhibitors used in medicine is their side effects, which are primarily associated with poor selectivity toward the target carbonic anhydrase isozymes. Therefore, the development of isozyme-selective CA inhibitors remains a continuously relevant challenge.

Equally important are other applications of CA inhibitors, in which inhibitors modified with photo-, radioactive, or similar groups are used for imaging or cytotoxic purposes. These applications have become particularly relevant in recent decades and are mainly associated with the overexpression of CA IX in cancerous tumors. In such cases, inhibition of CA activity itself is not the primary objective; however, selective binding to the target CA isozymes becomes even more critical.

The **aim of this work** was to design and synthesize selective inhibitors of CA isozymes, to identify the factors determining selectivity, and to apply this knowledge to the development of new compounds.

To achieve this aim, the following **objectives** were set:

- To synthesize 3,4-disubstituted-2-halobenzenesulfonamides and elucidate the influence of substituents on inhibitor affinity and selectivity.
- To synthesize 2-substituted benzenesulfonamides to evaluate the influence of inhibitor substituents located close to the CA cofactor.
- To determine and evaluate the influence of substituent position, size, and flexibility on the affinity and selectivity of CA inhibitors.
- To develop new high-affinity and selective inhibitors of the cancer-associated CA IX isozyme.

SCIENTIFIC NOVELTY

In this dissertation, two groups of benzenesulfonamide inhibitors bearing bulky substituents at the 4,5- and 2,5-positions were synthesized and compared. In both groups, inhibitors exhibiting exceptionally high subnanomolar affinity toward individual CA isozymes were identified.

The synthesized compounds enabled the determination of crystal structures of inhibitor–CA complexes. This facilitated understanding of structure–biological activity relationships and provided an overall positive advance in the research, particularly in the search for inhibitors of the cancer-associated carbonic anhydrase IX isozyme.

The regioselectivity of nucleophilic substitution reactions of 2,4-dihalo-5-sulfamoylbenzoates bearing identical halogens was investigated, and a new synthetic approach for 2,5-disubstituted-4-halobenzenesulfonamides was developed.

It was determined that, within the group of 2,5-disubstituted benzenesulfonamide inhibitors, substituents at the 2-position have a particularly strong influence on inhibitor properties. 2-Amino and 2-sulfanyl substituents exhibited high affinity and selectivity toward the CA IX isozyme. In contrast, 2-sulfonyl substituents resulted in a pronounced decrease in affinity toward all CA isozymes. It was also demonstrated that 2-substituted benzenesulfonamides may represent promising and superior CA IX inhibitors compared to previously used drugs of similar structure, such as bumetanide and piretanide.

DEFENDING STATEMENTS

1. The flexibility of *para*-position substituents in benzenesulfonamide CA inhibitors influences their selectivity toward individual CA isozymes.
2. *Para*-sulfanyl and sulfonyl groups in benzenesulfonamides lead to different substituent orientations in the CA active site and result in higher inhibitor affinity than amino substituents.
3. Inhibitors developed by introducing additional substituents into 5-[2-(benzimidazol-1-yl)acetyl]-2-chlorobenzenesulfonamide exhibit higher affinity for all carbonic anhydrases, but significantly reduce selectivity toward the target CA VA.
4. Sulfanyl and sulfonyl substituents at the *ortho* position of sulfonamide inhibitors strongly influence affinity and selectivity toward the target CA IX (sulfanyl positively, sulfonyl negatively).

SUMMARY OF RESULTS

In this work, a series of benzenesulfonamide carbonic anhydrase (CA) inhibitors bearing various substituents at the 2-, 4-, and 5-positions were synthesized. The results are presented in five publications (**I**–**V**). The first three papers focus on 2-halo-4,5-disubstituted benzenesulfonamide inhibitors. The fourth paper compares the interactions of 2-halo-4-substituted and 4-halo-2-substituted sulfamoyl benzoates with carbonic anhydrases. The fifth paper investigates the influence of *ortho*-substituents on the sulfonamide group on CA inhibition.

The studies were initiated with 4-amino-substituted benzenesulfonamides bearing carbonylamino groups at the 5-position (**I**). The synthesis of inhibitors was started from 2,4-dichloro- and 2,4-dibromo-5-sulfamoylbenzoic acids (**1**, **2**).

From these two benzoic acids, a series of 2,4-dihalobenzamides (**3**–**15**) with amide substituents of various lengths was synthesized via intermediate acid chlorides (Scheme 3). During the purification of 3-hydroxypropylbenzamide **5**, the formation of a side product was observed - transesterification occurred in ethyl acetate. *O*-acetyl benzamide **14** was identified and later resynthesized with a 78% yield by refluxing in ethyl acetate in the presence of acid. In contrast, such a reaction was not observed with 2-hydroxyethylbenzamide **4**.

The second substituent was introduced by replacing the halogen with various amines. Reactions were carried out by heating 2,4-dichlorobenzamides **3**–**7**, **11**, and **15** in excess aliphatic amines at 110–130 °C without metal catalysis [29]. Reactions of dibromobenzamide **13** with amines were performed by prolonged reflux in dioxane, thereby avoiding the formation of side products (Scheme 4).

The next series of compounds (**II**, **IV**) contains substituents of various lengths attached via a sulfur atom. Reactions of 2,4-dihalosulfamoylbenzoic acid derivatives with thiols are practically not described in the literature; therefore, it was expected that these reactions would proceed similarly to those with amines, substituting the halogen atom farther from the sulfonamide group. In this way, a series of compounds with various thioaryl substituents was synthesized from the corresponding benzamides (**3**–**14**) (Scheme 5).

Reaction conditions varied depending on the nucleophile. Reactions of compounds **3**–**8** and **10**–**14** with thiophenol or 1-thionaphthol proceeded most easily by refluxing in methanol in the presence of triethylamine. With cyclohexanethiol, reactions under these conditions were very slow; therefore, the polar protic solvent was replaced with polar aprotic DMSO, and triethylamine was replaced with anhydrous K_2CO_3. This allowed reactions of compounds **3**–**8** and **10**–**13** to be completed within 2–6 hours instead of days or weeks at the same temperature.

When other moderately reactive nucleophiles (primary alkyl thiols, etc.) were used, reactions were carried out in polar aprotic solvent (DMSO) in the presence of triethylamine.

The only exception was the morpholine derivative **9**, whose reactions with thiols required heating to 120 °C in DMSO with Cs_2CO_3, even with thiophenol.

The synthesized thioaryl derivatives were further oxidized to sulfonyl derivatives. Oxidation reactions were carried out with good yields (69–92%) in acetic acid using hydrogen peroxide, generating peracetic acid *in situ* (Scheme 6). During the oxidation of amides containing hydroxyl groups, the formation of *O*-acetates was observed; to avoid this, the reaction product mixture was additionally treated with dilute hydrochloric acid.

Benzoic acids **29b, d** were synthesized from the corresponding benzamides **16b, d** under acidic hydrolysis conditions. However, when ester hydrolysis of **21b** and **35c** was carried out under similar conditions (Scheme 7), the formation of two products was observed. Therefore, further hydrolysis of esters **21a**–**c** was performed under basic conditions at room temperature, yielding only the desired products.

The next series of compounds (**III**) was designed based on previous knowledge [31] about inhibitors selective for the CA VA isozyme. Compounds were synthesized based on 2-chloro- and 2,4-dichlorobenzenesulfonamides bearing various heterocycles at the 5-position.

In Scheme 8, compounds **42a–h** and **43a–c** were synthesized by alkylation of target heterocycles with (bromoacetyl)-2-chlorobenzenesulfonamide **42** or 5-(bromoacetyl)-2,4-dichlorobenzenesulfonamide **43**. *N*-alkylations were performed in THF with NaOAc at room temperature. Compounds **42g** and **42h** were synthesized using an excess of 1,2,3,4-tetrahydroquinoline and indoline without base.

Compound **46** could not be synthesized directly by acylation of 1-aminobenzimidazole with 2,4-dichloro-5-sulfamoylbenzoyl chloride under various conditions. However, protection of the sulfonamide group with an *N,N'*-dimethylaminomethylidene group (Scheme 9, compound **45**) prevented side reactions, allowing synthesis of compound **45** via acylation; deprotection yielded the target benzenesulfonamide **46**.

Some 2,4-dichloro compounds (**43a, b, 46**) were modified by introducing sulfur-bridged fragments according to methods described in paper **II** (Scheme 10), yielding compounds **47–50**.

Paper **IV** describes the next group of substituted halogenated benzenesulfonamides. From initial methyl 2,4-dihalo-5-sulfamoylbenzoates **51** and **52**, methyl 2-halo-4-substituted and 4-halo-2-substituted-5-sulfamoylbenzoates were synthesized (Scheme 11). Reaction conditions were selected based on previous work (paper **II**) describing reactions of 2,4-dihalo-5-sulfamoylbenzamides with sulfur-containing nucleophiles.

When reactions were carried out in methanol, aromatic thiols (thiophenol and 1-thionaphthol) readily substituted the halogen atom, forming *para*-substituted benzenesulfonamides **55a, f**, and **56a**. In contrast, reactions with

thiols containing CH_2 or CH groups proceeded very slowly or did not occur at all under these conditions. To accelerate reactions, the polar protic solvent was replaced with polar aprotic DMSO, yielding *ortho*-substituted benzenesulfonamides **53b–e** and **54b** (Scheme 11). *Para*- and disubstituted benzenesulfonamides were also observed.

The regioselectivity of nucleophilic aromatic substitution reactions of 2,4-dihalo-5-sulfamoylbenzoates **51** and **52** was investigated (Table 3). All reactions were performed in DMSO with thiol and triethylamine at 60 °C for 72 h. Reaction conversion, product ratios, and structure identification were determined by NMR and HPLC/UV/MS.

Table 3. Yields and product ratios of reactions of 2,4-dihalo-5-sulfamoylbenzoates 51 and 52 with thiols determined by ^{1}H NMR spectroscopy and HPLC/UV/MS data (italic). *The 2- and 4-substituted isomers formed in reactions of compounds **51** and **52** with thiophenol could not be separated by HPLC.

Starting compound	Thiol	Conversion (%)	2-substituted (%)	4-substituted (%)	2,4-disubstituted
51		30.07 *28.77*	18.70 *17.38*	81.30 *82.62*	-
52		15.71 *13.92*	9.09 *14.11*	90.91 *85.89*	-
51		89.47 *96.67*	58.82 *88.78**	35.29	5.88 *11.22*
52		95.07 *96.92*	51.81 *85.55**	40.42	7.77 *14.45*
51		72.73 *71.55*	23.53 *22.91*	73.53 *72.79*	2.94 *4.30*
51		72.15 *73.60*	12.28 *12.05*	87.72 *87.95*	-
51		90.97 *95.25*	76.34 *78.84*	19.08 *15.72*	4.58 *5.44*
51		13.70 *18.19*	-	100.00 *100.00*	-

The reactivity of thiols decreases in the following order: phenyl > naphthyl > benzyl ≥ 2-ethylphenyl > cyclohexyl ≥ cyclododecyl. Formation

of disubstituted products was observed in reactions with phenyl-, naphthyl-, and benzyl thiols. A higher proportion of 2-substituted products was obtained with aromatic thiols, whereas in other cases 4-substituted products predominated. In the case of cyclododecyl thiol, only one 2-substituted isomer was observed.

Missing 2-substituted methyl esters **55a–d, f** were synthesized from previously described 2-substituted benzamides **16a–d, f** (Scheme 12). The amide group was converted into an ester in a one-step reaction by heating in methanol with thionyl chloride.

Oxidation of sulfanyl derivatives **53**(**b–d**), **54b, 55**(**a–d, f**), and **56a** to sulfonyl derivatives **57**(**b–d**), **58b, 59**(**a–d, f**), and **60a** was performed by *in situ* generation of peracetic acid (Schemes 11 and 12).

Paper **V** aimed to investigate the influence of substituents located near the sulfonamide group on binding to carbonic anhydrases. For this purpose, *ortho*-substituted benzenesulfonamides with amino-, sulfanyl-, sulfinyl-, and sulfonyl substituents were synthesized.

Since reactions of 2,4-dihalo derivatives yield various products, a starting compound with more predictable behavior — 4-chloro-3-sulfamoylbenzoic acid (**62**) — was selected. Using previously established methods, initial compounds were synthesized from it: the methyl ester (**63**) and a series of amides (**64–66**) (Scheme 13).

From ester **63** of 4-chloro-3-sulfamoylbenzoic acid, nucleophilic aromatic substitution reactions yielded 4-sulfanyl-substituted compounds **67a–d, f–m** (Scheme 13). Reactions were performed by heating with various thiols in dimethylformamide in the presence of K_2CO_3. Under the same conditions, 4-sulfanyl-substituted sulfamoylbenzamides **68a–d, f, g, j–m** were synthesized.

4-Amino-substituted compounds **69b, c** were synthesized by heating benzamide **64** in an excess of the corresponding amine at 130 °C. Compound **69e** was synthesized by refluxing in a mixture of toluene and cyclooctylamine.

Oxidation of esters **67a–d, h, i, k–m** and benzamides **68a, b, k–m** to sulfinyl and sulfonyl compounds was performed using *in situ* generated peracetic acid (Scheme 14). Reactions at room temperature yielded sulfinyl compounds **70a, b, h, i, k–m** and **71a, b, k–m**, whereas heating the reaction mixture to 70 °C yielded sulfonyl compounds **72a–d, h, i, l, m** and **73b, k–m**.

DISCUSSION

In the first article, an analysis of binding data of synthesized compounds with 12 α-carbonic anhydrase (α-CA) isozymes was performed. Initially, affinity and selectivity studies of monosubstituted compounds (*N*-substituted 2,4-dihalo-5-sulfamoylbenzamides **3–15**) revealed that they bind most strongly to CA VII. Upon introduction of a second substituent (2-amino-substituted-4-halo-5-sulfamoylbenzamides, Scheme 4), increased affinity and selectivity toward CA IX and CA XIV isozymes were observed in most cases. Selectivity toward these CA isozymes depended on the size of the second substituent. Due to its flexibility, the benzylamino group interacts more readily with active-site fragments across all isozymes, thereby increasing affinity but reducing selectivity compared to the less flexible cyclohexylamino group. Several crystallographic structures of compound–carbonic anhydrase complexes revealed contacts between inhibitor substituents and protein amino acids, providing deeper insight into the structure–activity relationships of the studied systems.

In the second article, CA inhibitors bearing two substituents were synthesized, one of which was attached via a sulfur-containing linker (2-sulfanyl- or 2-sulfonyl-substituted-4-halo-5-sulfamoylbenzamides). Analysis of the chemical structures and binding parameters of these compounds demonstrated the importance and influence of both substituents on affinity and selectivity toward specific CA isozymes. Crystal structures of protein–inhibitor complexes revealed possible interaction sites between substituents and the active site, as well as pronounced differences in the positioning of sulfanyl and sulfonyl substituents within the CA active site (Figure 6).

It should also be noted that, compared to the amino-substituted compounds described in the first article, compounds from the latter series exhibited higher affinity, with subnanomolar binding values observed for CA VII, CA IX, CA XII, or CA XIV.

In the third article, a series of selective CA VA inhibitors was synthesized based on the previously described compound 5-[2-(benzimidazol-1-yl)acetyl]-2-chlorobenzenesulfonamide (**42a**). Initially, 2-halo- and 2,4-dihalobenzenesulfonamides bearing substituents at the 5-position were investigated, and the dependence of affinity on the nature and size of heterocycles present in the substituent was evaluated (Figure 7). It was determined that the benzimidazole ring is more favorable than imidazole due to aromatic–aromatic interactions with CA VA Tyr64. The nitrogen atom of the benzimidazole/imidazole ring was also shown to be important, forming hydrogen bonds with the Thr62 hydroxyl group of CA VA. In the absence of

this nitrogen atom, as in the case of indoline or 3,4-dihydro-2H-quinoline substituents (compounds **42g** and **42h**), selectivity toward CA VA was lost. Introduction of a second substituent into the *para* position of the benzenesulfonamide increased affinity toward all CA isozymes but markedly reduced selectivity for the target CA VA (Figure 8).

In the fourth article, several compound series were developed and the effects of substituents and their positions on the binding of methyl-2- or 4-substituted-5-sulfamoylbenzoates to human CA isozymes were investigated. Sulfanyl (-S-) and sulfonyl (-SO_2-) substituents of varying size were studied in detail, and crystal structures of these two compound classes bound to CA active sites were determined (Figure 9). *Para*-substituted 2-halobenzenesulfonamides, both sulfanyl-substituted (groups **55–56**) and sulfonyl-substituted (groups **59–60**), bound similarly to various CA isozymes and did not demonstrate selectivity. In contrast, *ortho*-sulfanyl-substituted 4-halobenzenesulfonamides exhibited exceptionally high affinity and selectivity toward the cancer-associated CA IX isozyme (K_d values of compounds **53b**, e, and **54b** approached 0.1 nM). Conversely, the analogous *ortho*-sulfonyl-substituted 4-halobenzenesulfonamides (groups **57** and **58**) bound weakly to all CA isozymes (Figure 10). This unexpectedly large decrease in affinity was interpreted as evidence that a threshold had been reached where small structural modifications at the *ortho* position of benzenesulfonamides can induce major changes in inhibitor–protein interactions. This hypothesis was further explored in subsequent work.

In the fifth article, the influence of *ortho*-substituents on benzenesulfonamides was investigated in greater detail. Compounds similar to the most potent inhibitors from article **IV** were selected, but halogen atoms were deliberately omitted to facilitate the synthesis of a larger and more diverse set of *ortho*-substituted compounds. A series of benzenesulfonamides bearing linear and cyclic substituents ranging from methyl to adamantyl, attached via sulfanyl (-S-), sulfinyl (-SO-), and sulfonyl (-SO_2-) linkers, were synthesized. By varying the oxidation state of the linker, the aim was to reduce the pK_a of the sulfonamide group through increased electron-accepting properties and thereby enhance CA binding. Unfortunately, despite a one-unit decrease in pK_a, compounds with -SO- or –SO_2- linkers bound much more weakly to all CA isozymes than those containing an -S- linker (Figure 11). The strategy of reducing substituent size did not yield the desired outcome: although affinity increased for sulfinyl- and sulfonyl-substituted inhibitors, even compounds with the smallest methyl substituent (**70h** and **72h**) did not reach the affinity of the corresponding sulfanyl compound **67h**. The primary reason for this was attributed to the accessible conformations of the

compounds, which were calculated using density functional theory (DFT; performed by V. Kairys). Oxygen atoms in compounds with -SO- and $–SO_2$- linkers restrict molecular flexibility in achieving an optimal orientation within the protein active site and act as a steric hindrance.

CONCLUSIONS

1. Substituents at the 4- and 5-positions of 2-halo-benzenesulfonamides positively influence inhibitor affinity toward most CA isozymes due to the large active-site space that is favorable for various interactions. Combined reduction of substituent flexibility by introducing steric hindrance enables improved selectivity toward individual isozymes.
2. For binding to CA VA and CA VII, a single bulky substituent at the 5-position of 2,4-dihalobenzenesulfonamides is sufficient to achieve the highest affinity and selectivity.
3. In reactions of methyl 2,4-dihalo-5-sulfamoylbenzoates with aryl thiols, substitution of the halogen atom at the 2-position predominates, whereas in reactions with alkyl thiols, substitution of the halogen atom at the 4-position predominates.
4. 2,5-Disubstituted benzenesulfonamides exhibit high affinity and selectivity toward the CA IX isozyme due to bulky amino and sulfanyl substituents at the 2-position. Introduction of a halogen atom at the 4-position increases affinity toward CA IX without affecting selectivity.
5. Steric hindrance formed by interactions between sulfinyl and especially sulfonyl substituents at the 2-position and the adjacent sulfonamide group strongly reduces inhibitor affinity toward all CA isozymes. For these compounds, the influence of the size and flexibility of the 2-position substituent on CA isozyme inhibition is negligible.

PADĖKA

Prof. Daumantui Matuliui už patarimus, palaikymą ir kryptingą vadovavimą – visa tai leido pasiekti ilgai atidėliotą tikslą.

Biotermodinamikos ir vaistų tyrimo skyriaus darbuotojams bei studentams, kurių darbų ir tyrimų dėka susintetinti junginiai įgydavo naujų, papildomai motyvuojančių prasmių.

Organinės sintezės laboratorijoje C308 kartu vargusiems kolegoms ir studentams dėkoju už visokeriopą pagalbą, tiek sintezės darbuose, tiek kuriant puikią darbinę atmosferą.

Dr. Editai Čapkauskaitei dėkoju už pakvietimą į šią laboratoriją ir kantrybę sprendžiant uždavinius, atsiradusius šio neapdairaus veiksmo pasekoje.

Už kristalografinius tyrimus GMC kolegoms dr. A. Smirnov, dr. E. Manakovai ir dr. S. Gražuliui, bei dr. K. Tars grupei iš Rygos.

Dr. V. Kairiui už pakeistą požiūrį į molekulinio modeliavimo tyrimų svarbą.

A. Rukšėnaitei, dr. A. Sakalauskui ir M. Malikėnui už masių spektrometrijos eksperimentus.

Pabaigoje norėčiau padėkoti savo pirmam dėstytojui Petrui Kadziauskui atvėrusiam duris į Organinės chemijos pasaulį ir Skystųjų kristalų laboratorijos bendradarbiams – Onutei ir Povilui Adomėnams suteikusiems neįkainojamos patirties, bei iš esmės pakeitusiems supratimą apie organinės sintezės galimybes.

PUBLIKACIJŲ ĮTRAUKTŲ Į DISERTACIJĄ SĄRAŠAS

1. **Zakšauskas, A.**, Čapkauskaitė, E., Jezepčikas, L., Linkuvienė, V., Kišonaitė, M., Smirnov, A., Manakova, E., Gražulis, S., Matulis, D. Design of two-tail compounds with rotationally fixed benzenesulfonamide ring as inhibitors of carbonic anhydrases. *European Journal of Medicinal Chemistry,* 2018, 156, 61-78. DOI: 10.1016/j.ejmech.2018.06.059

   Autorių indėlis: Idėja-koncepcija, **A.Z**. ir E.Č.; metodika, **A.Z**. ir E.Č.; tyrimai, **A.Z**., E.Č.; L.J., V.L., M.K., A.S., E.M.; rašymas - darbinio projekto rengimas, E.Č., V.L.; rašymas - peržiūra ir redagavimas, **A.Z**.; priežiūra, D.M.; projekto administracija, D. M.; finansavimo įsigijimas, S.G. ir D.M.

2. **Zakšauskas, A**., Čapkauskaitė, E., Jezepčikas, L., Linkuvienė, V., Paketurytė, V., Smirnov, A., Leitans, J., Kazaks, A., Dvinskis, E., Manakova, E., Gražulis, S., Tars, K., Matulis, D. Halogenated and Di-Substituted Benzenesulfonamides as Selective Inhibitors of Carbonic Anhydrase Isoforms. *European Journal of Medicinal Chemistry*, 2020, 185, 111825. doi.org/10.1016/j.ejmech.2019.111825.

   Autorių indėlis: Idėja-koncepcija, **A.Z**. ir E.Č.; metodika, **A.Z**. ir E.Č.; tyrimai, **A.Z**., E.Č.; L.J., V.L., V.P., A.S., J.L., A.K., E.D., E.M.; rašymas - darbinio projekto rengimas, E.Č., V.L.; rašymas - peržiūra ir redagavimas, **A.Z**.; priežiūra, K.T., D.M.; projekto administracija, D. M.; finansavimo įsigijimas, J.L., S.G. ir D.M.

3. Čapkauskaitė, E., **Zakšauskas, A**., Ruibys, V., Linkuvienė, V., Paketurytė, V., Gedgaudas, M., Kairys, V., Matulis. D. Benzimidazole design, synthesis, and docking to build selective carbonic anhydrase VA inhibitors. *Bioorganic & Medicinal Chemistry*. 2018, 26(3), 675-687. DOI: 10.1016/j.bmc.2017.12.035.

   Autorių indėlis: Idėja-koncepcija, E.Č ir **A.Z**.; metodika, **A.Z**. ir E.Č.; tyrimai, E.Č., **A.Z**., V.R., V.L., V.P., M.G., V.K.; rašymas - darbinio projekto rengimas, E.Č.; rašymas - peržiūra ir redagavimas, **A.Z**.; projekto administracija, finansavimo įsigijimas, D.M.

4. **Zakšauskas, A.,** Čapkauskaitė, E., Paketurytė-Latvė, V., Smirnov, A., Leitans, J., Kazaks, A., Dvinskis, E., Stančaitis, L., Mickevičiūtė, A., Jachno, J., Jezepčikas, L., Linkuvienė, V., Sakalauskas, A., Manakova, E., Gražulis, S., Matulienė, J., Tars, K., Matulis, D. Methyl 2-Halo-4-Substituted-5-Sulfamoyl-Benzoates as High Affinity and Selective Inhibitors of Carbonic Anhydrase IX. *Int. J. Mol. Sci*. 2022, 23, 130. doi.org/10.3390/ijms23010130

   Autorių indėlis: Idėja-koncepcija, **A.Z**. ir E.Č.; metodika, **A.Z**. ir E.Č.; tyrimai, **A.Z**., V.P.-L., A.S. (A. Smirnovas), J.L., A.K., E.D., L.S., A.M.,

J.J., L.J., V.L., A.S. (A. Sakalauskas), E. M., ir J.M.; rašymas - darbinio projekto rengimas, V.P.-L.; rašymas - peržiūra ir redagavimas, **A.Z**.; priežiūra, K.T., D.M.; projekto administracija, S.G., D. M.; finansavimo įsigijimas, J.L., J.M. ir D.M.

5. **Zakšauskas, A.,** Paketurytė-Latvė, V., Jankūnaitė, A., Čapkauskaitė, E., Becart, Y., Smirnov, A., Pospíšilová, K., Leitans, J., Brynda, J., Kazaks, A., Baranauskiene, L., Manakova, E., Gražulis, S., Kairys, V., Tars, K., Rezacova, P., Matulis, D. Affinity and Selectivity of Protein–Ligand Recognition: A Minor Chemical Modification Changes Carbonic Anhydrase Binding Profile. *Journal of Medicinal Chemistry*. 2025, 68(16), 17752-17773. doi: 10.1021/acs.jmedchem.5c01421

Autorių indėlis: Idėja-koncepcija, **A.Z**. ir E.Č.; metodika, **A.Z**. ir E.Č.; tyrimai, **A.Z**., V.P.-L., J.A., E.Č., Y.B., A.S., E. M., K.P., J.B., J.L., L.B. ir V.K.; rašymas - darbinio projekto rengimas, V.P.-L.; rašymas - peržiūra ir redagavimas, **A.Z**.; priežiūra, S.G., K.T., P.R. ir D.M.; projekto administracija, finansavimo įsigijimas, D.M.

NEĮTRAUKTOS Į DISERTACIJĄ PUBLIKACIJOS

1. Dudutienė, V., Matulienė, J., Smirnov, A., Timm, D., Zubrienė, A., Baranauskienė, L., Morkūnaitė, V., Smirnovienė, J., Michailovienė, V., Juozapaitienė, V., Mickevičiūtė, A., Kazokaitė, J., Bakšytė, S., Kasiliauskaitė, A., Jachno, J., Revuckienė, J., Kišonaitė, M., Pilipuitytė, V., Ivanauskaitė, E., Milinavičiūtė, G., Smirnovas, V., Petrikaitė, V., Kairys, V., Petrauskas, V., Norvaišas, P., Lingė, D., Gibieža, P., Čapkauskaitė, E., **Zakšauskas, A**., Kazlauskas, E., Manakova, E., Gražulis, S., Ladbury, J., Matulis, D. Discovery and characterization of novel selective inhibitors of carbonic anhydrase IX. *Journal of Medicinal Chemistry,* 2014, 57 (22), 9435–9446. DOI: 10.1021/jm501003k

2. V. Dudutienė, A. Zubrienė, A. Smirnov, D. D. Timm, J. Smirnovienė, J. Kazokaitė, V. Michailovienė, **A. Zakšauskas**, E. Manakova, S. Gražulis and D. Matulis. Functionalization of Fluorinated Benzenesulfonamides and Their Inhibitory Properties toward Carbonic Anhydrases. *ChemMedChem*, 2015, 10 (4), 662–687. DOI: 10.1002/cmdc.201402490

3. Juozapaitienė, V., Bartkutė, B., Michailovienė, V., **Zakšauskas, A**., Baranauskienė, L., Satkūnė, S., Matulis, D. 2016. Purification, enzymatic activity and inhibitor discovery for recombinant human carbonic anhydrase XIV. *Journal of Biotechnology*. 2016, 240, 31-42. DOI: 10.1016/j.jbiotec.2016.10.018

4. Zubrienė, A., Smirnov, A., Dudutienė, V., Timm, D. D., Matulienė, J., Michailovienė, V., **Zakšauskas, A**., Manakova, E., Gražulis, S., Matulis, D. Intrinsic Thermodynamics and Structures of 2,4- and 3,4-Substituted Fluorinated Benzenesulfonamides Binding to Carbonic Anhydrases. *ChemMedChem*, 2017, 12 (2), 161-176. DOI: 10.1002/cmdc.201600509.

5. Linkuvienė, V., Zubrienė, A., Manakova, E., Petrauskas, V., Baranauskienė, L., **Zakšauskas, A**., Smirnov, A., Gražulis, S., Ladbury, J.E., Matulis, D. Thermodynamic, kinetic, and structural parameterization of human carbonic anhydrase interactions toward enhanced inhibitor design. *Q Rev Biophys*., Published online: 26 November 2018, e10. DOI: 10.1017/S0033583518000082

6. Smirnovienė, J., Smirnov, A., **Zakšauskas, A**., Zubrienė, A., Petrauskas, V., Mickevičiūtė, A., Michailovienė, V., Čapkauskaitė, E., et al. Switching the Inhibitor-Enzyme Recognition Profile via Chimeric Carbonic Anhydrase XII. *ChemistryOpen*, 2021, 10(5), 567-580. doi:10.1002/open.202100042

7. Matulienė, J., Žvinys, G., Petrauskas, V., Kvietkauskaitė, A., **Zakšauskas, A**., et al. Picomolar fluorescent probes for compound affinity determination to carbonic anhydrase IX expressed in live cancer cells. *Scientific Reports,* 2022**,** 12, 17644. doi.org/10.1038/s41598-022-22436-1

8. Lingė, D., Gedgaudas, M., Merkys, A., Petrauskas, V., Vaitkus, A., Grybauskas, A., Paketurytė, V., Zubrienė, A., **Zakšauskas, A**., et al. PLBD: protein–ligand binding database of thermodynamic and kinetic intrinsic parameters, *Database*, Volume 2023, 2023, baad040.doi.org/10.1093/database/baad040

9. Žvinys, G., Petrosiute, A., **Zakšauskas, A**., Zubrienė, A., et al. High-Affinity NIR-Fluorescent Inhibitors for Tumor Imaging via Carbonic Anhydrase IX. *Bioconjugate Chem*, 2024, 35, 6, 790–803. doi.org/10.1021/acs.bioconjchem.4c00144

10. Paketurytė-Latvė, V., Smirnov, A., Manakova,E., Baranauskiene, L., Petrauskas, V., Zubrienė, A., Matulienė, J., Dudutienė, V., Čapkauskaitė, E., **Zakšauskas, A**., et al. From X-ray crystallographic structure to intrinsic thermodynamics of protein–ligand binding using carbonic anhydrase isozymes as a model system. *IUCrJ*, 2024, 11|, 4, 556-569. doi.org/10.1107/S2052252524004627

11. Petrosiute, A., **Zakšauskas, A**., Lučiūnaitė, A., Petrauskas, V., Baranauskienė, L., Kvietkauskaitė, A., et al. Carbonic anhydrase IX inhibition as a path to treat neuroblastoma. *British Journal of Pharmacology*, 2025, 182(7), 1610-1629. doi.org/10.1111/bph.17429

.

KONFERENCIJŲ SĄRAŠAS

1. E. Čapkauskaitė, **A. Zakšauskas**, L. Jezepčikas, V. Linkuvienė, D. Matulis. Carbonic Anhydrase Inhibitors: 2-Halogeno-4,5-disubstituted Benzenesufonamides. Balticum Organicum Syntheticum – BOS **2016**, Riga, Latvia.
2. **A. Zakšauskas**, E. Čapkauskaitė, V. Linkuvienė, V. Ruibys, D. Matulis. Benzenesulfonamides with N-imidazolyl Fragments as Inhibitors of Carbonic Anhydrase VA. Balticum Organicum Syntheticum – BOS **2016**, Riga, Latvia.
3. A.Jankūnaitė, V. Paketurytė, **A. Zakšauskas,** D. Matulis. Synthesis and Analysis of 2,5-substituted Benzenesulfonamides as Inhibitors of Carbonic Anhydrases. 25th Young Research Fellows meeting – SCT **2018**, Orleans, France.
4. A.Jankūnaitė, V. Paketurytė, **A. Zakšauskas,** E. Čapkauskaitė, D. Matulis. Synthesis and Binding Analysis of 2,5-disubstituted Benzenesulfonamides as Inhibitors of Carbonic Anhydrases. Balticum Organicum Syntheticum – BOS **2018**, Tallinn, Estonia.
5. A.Jankūnaitė, V. Paketurytė, **A. Zakšauskas,** E. Čapkauskaitė. Synthesis and Binding Analysis of Carbonic Anhydrases Inhibitors – 1,2-disubstituted 6-chlorobenzimidazole-5-sulfonamides. Chemistry and Chemical Technology, **2019,** Vilnius, Lithuania.
6. L. Stančaitis, E. Čapkauskaitė, **A. Zakšauskas**, V. Paketurytė-Latvė, D. Matulis. Methyl 2-halo-4-substituted-5-sulfamoyl-benzoates as high affinity and selective Inhibitors of Carbonic Anhydrase IX. Balticum Organicum Syntheticum – BOS **2022**, Vilnius, Lithuania.

PUBLIKACIJŲ KOPIJOS

European Journal of Medicinal Chemistry 156 (2018) 61–78

Contents lists available at ScienceDirect

European Journal of Medicinal Chemistry

journal homepage: http://www.elsevier.com/locate/ejmech

Research paper

Design of two-tail compounds with rotationally fixed benzenesulfonamide ring as inhibitors of carbonic anhydrases

Audrius Zakšauskas [a], Edita Čapkauskaitė [a], Linas Jezepčikas [a], Vaida Linkuvienė [a], Miglė Kišonaitė [a], Alexey Smirnov [b], Elena Manakova [b], Saulius Gražulis [b], Daumantas Matulis [a, *]

[a] Department of Biothermodynamics and Drug Design, Institute of Biotechnology, Vilnius University, Saulėtekio al. 7, Vilnius LT-10257, Lithuania
[b] Department of Protein – DNA Interactions, Institute of Biotechnology, Vilnius University, Saulėtekio al. 7, Vilnius LT-10257, Lithuania

ARTICLE INFO

Article history:
Received 24 April 2018
Received in revised form
11 June 2018
Accepted 23 June 2018
Available online 27 June 2018

Keywords:
Fluorescent thermal shift assay
Benzenesulfonamide
Carbonic anhydrase
Inhibitor
Structure-thermodynamics relationships
X-ray crystallography

ABSTRACT

Rational design of compounds that would bind specific pockets of the target proteins is a difficult task in drug design. The 12 isoforms of catalytically active human carbonic anhydrases (CAs) have highly similar active sites that make it difficult to design inhibitors selective for one or several CA isoforms. A series of CA inhibitors based on 2-chloro/bromo-benzenesulfonamide that is largely fixed in the CA active site together with one or two tails yielded compounds that were synthesized and evaluated as inhibitors of CA isoforms. Introduction of a second tail had significant influence on the binding affinity and two-tailed compounds in most cases provided high affinity and selectivity for CA IX and CA XIV. The contacts between several compounds and CA amino acids were determined by X-ray crystallography. Together with the intrinsic enthalpy and entropy of binding they provided the structure-thermodynamics correlations for this series of compounds with the insight how to rationally build compounds with desired CA isoform as a target.

1. Introduction

Rational design of small molecular weight compounds that would tightly and specifically bind a desired binding site on a disease-related target protein is still an elusive task despite efforts of scientists to find a common path to design pharmaceutical compounds. This is because the correlations between compound chemical structures and the energetics of their interaction with protein molecules are still poorly understood.

Here we describe a novel group of substituted aromatic sulfonamides in the attempts to understand the structure–thermodynamics relationships of their binding to Carbonic anhydrases (CA, EC 4.2.1.1), therapeutically-relevant protein targets which are zinc-containing metalloenzymes and catalyze the reversible reaction of carbon dioxide hydration into bicarbonate and proton [1]. CAs participate in various physiological processes related to respiration, bicarbonate transport between lungs and metabolizing tissues, pH and CO_2 homeostasis, electrolyte secretion in many tissues, etc. [2,3]. The family of human CAs comprises 15 isoforms (isozymes) – 12 of them are catalytically active, while the remaining isoforms CA VIII, CA X, and CA XI are inactive. Twelve active human CA isoforms possess different catalytic activity and cellular localization – five are cytosolic (CA I, CA II, CA III, CA VII and CA XIII), four are membrane bound (CA IV, CA IX, CA XII, and CA XIV), two are mitochondrial (CA VA and CA VB) and CA VI is secreted [4–6].

Numerous diseases are associated with the changes in expression and activity of CAs resulting in dis-balance of the interconversion between carbonic dioxide and bicarbonate causing pH alteration, disorder of ion transport, fluid secretion, and other processes. Application of selective CA inhibitors to regulate catalytic activity resulted in numerous approved drugs and still proposes therapeutic perspectives for numerous ailments.

A large number of different CA inhibitors have been synthesized to date, and used or investigated for treatment of diseases such as epilepsy [7], glaucoma [8], obesity [9,10], and sterility [11], to mention a few. Furthermore, inhibitors of CA IX and CA XII are thought to have potential to be developed as anticancer drugs [5,12]. However, most clinically used CA inhibiting drugs are insufficiently selective and inhibit not only the target CA isoforms,

* Corresponding author.
E-mail address: matulis@ibt.lt (D. Matulis).

https://doi.org/10.1016/j.ejmech.2018.06.059
0223-5234/

but also others causing undesired side effects. Therefore, it is important to build and understand how to build inhibitors that would selectively inhibit one or more target CAs.

The X-ray crystallographic structures have been solved of all isoforms except CA VA and CA VB. The binding pocket of all CA isoforms is highly similar. It contains the Zn(II) cation held by three conserved His residues. The fourth coordinated ligand of the Zn(II), a hydroxide anion or a water molecule depending on pH, catalyzes the hydration reaction of CO_2. The mechanism and the structure of the catalytic site is highly similar among isoforms, making it difficult to design isoform-selective inhibitors [13]. However, some amino acids are different among isoforms that make it possible to rationally design highly selective inhibitors.

Despite the numerous recently proposed novel classes of CAs inhibitors, among them coumarins, phenols, diols, polyamines, carboxylic acids, borols, boronic acids, and other structurally related compounds, the classical primary sulfonamides have important advantages. First, the sulfonamide group binds in the active site of CAs in a highly conserved manner making it possible to predict the tendency of the binding of the remaining part of the sulfonamide-containing molecule [1,14]. Second, the aromatic sulfonamides usually demonstrate higher binding affinity toward CAs than other inhibitors that bind to the metal ion e.g. many inorganic anions, dithio-/monothiocarbamates and xanthates, carboxylates and hydroxamates, boronic acids and borols, diols, etc. [15,16].

Many aromatic sulfonamide-based CA inhibitors are designed using the "ring" and "tail" approach [1,17]. The "ring" represents hetero/aromatic ring bearing sulfonamide group, which binds to the zinc ion, and the electron acceptor substituent, which increases the acidity of the sulfonamide group and subsequently the binding affinity. The "tail" is a flexible fragment that participates in additional interaction with the protein parts located further from the zinc ion and may also be designed to improve aqueous solubility.

In some CA isoforms, the amino acids in the active site cavity are arranged so that there are hydrophobic and hydrophilic sides situated against each other. The tail interaction with the Phe131 in CA II, located in the secondary hydrophobic binding site enhances the binding to CA [18,19]. The hydrophilic wall which is situated opposite to the Phe131 [20] is useful as a target for inhibitors bearing a hydrophilic tail [21]. A number of compounds have been designed as CA inhibitors based on this approach [13,22–24].

A number of compounds bearing two tails attached to the benzene ring have been designed. William Vernier et al. [25] attempted to make good CA II and CA IV inhibitors by balancing between lipophilicity, which improved the affinity and hydrophilicity, which improved solubility in water. Congiu et al. [26] have synthesized *N,N* - disubstituted sulfanilamide derivatives which were selective for CA IX/XII (over CA I/II). Tanpure et al. [27] have introduced new approach to employ hydrophobic and hydrophilic halves simultaneously. Authors modified CA inhibitor acetazolamide by attaching two tails to the same amino substituent. This approach resulted in compounds with good CA II/CA I selectivity. Vaškevičienė et al. [28] applied this dual-tail approach to design *para*-aminobenzenesulfonamides bearing two distinct tails at *N* atom, *beta*-alanine derivatives and thiazole derivatives. Zhuang Hou et al. [29] have proposed an interesting "two in one" improvement by designing benzenesulfonamide bearing an amino glucosamine fragment as the hydrophilic part with directly attached a cinnamamide fragment as the hydrophobic part. These compounds showed 1000-fold increased inhibitory affinity against CA II and CA IX as compared to initial benzenesulfonamide compound. Related 2-aryl-imidazoline compounds have been synthesized [30], but authors have expressed doubts about participation of polar 2-imidazoline in the interaction with the protein target.

The work of Dudutienė et al. [31] revealed that the introduction of second tail into *para*-substituted fluorinated benzenesulfonamides enhanced the binding to CA IX and significantly improved the selectivity to CA IX. It can be explained by steric clashes in CA II - the deeper CA IX cavity is more suitable for massive cyclooctyl substituent than a narrow CA II pocket with bulky Phe131, based on comparison of X-ray crystallographic structures of compound complexes with CA II and chimeric CA IX.

Here we extend an idea to make inhibitors that have their sulfonamide-bearing ring fixed in position by the 2-Cl group [32–35]. Such compounds, bearing two tails, could interact with the sides of CA active site, one being predominantly hydrophobic and another – hydrophilic. This approach could help design inhibitors that interact strongly with the target CAs and weakly – with non-target CAs. For the synthesis, the 2-chloro/bromo-benzenesulfonamide scaffold was selected due to the 2-Cl group's ability to restrain the benzene ring of the inhibitor molecule in one known position. One of the tails is made more hydrophobic (alkyl-, aryl-substituents attached through an amino group) while another as more hydrophilic (substituents containing hydroxyl, carbonyl, carboxyl, ether groups, and hydrophilic amide linkage).

2. Results and discussion

2.1. Chemistry

The synthesis of designed compounds was achieved using key intermediates 2,4-dihalo-5-sulfamoylbenzoic acids **1** and **2**. Dichloro acid **1** is commercially available, while the synthesis of dibromo acid **2** is shown in Scheme 1.

Starting from commercially available 3-methylaniline (**3**) the brominated product **4** was obtained as reported previously [36], subsequently transformed into sulfonamide **5** using the same reaction conditions described in Ref. [37]. Subsequent oxidation of methyl-group according to the procedure [38] yielded the acid **2**.

The synthesis of dihalosulfamoylbenzamides **6**–**17** is reported in Scheme 2. The heating of acid **1** and **2** with thionyl chloride at reflux afforded the corresponding acid chlorides, which were amidated with the appropriate amine using as the base the excess of amine or triethylamine.

The isolation of propanolamide **8** by concentrating ethyl acetate extract was accompanied by the formation of appreciable amounts of *O*-acetylated derivative **17**. In addition, the compound **17** was synthesized in high yield boiling the compound **8** in ethyl acetate with an acidic catalyst [39]. Interestingly, in case of ethanolamide **7**, the purification formed only traces of *O*-acetylated compound.

Dichlorobenzamides **6**–**10**, **14** were subsequently subjected to direct amination at 120 °C without solvent using excess of amine according to the procedure previously reported in Ref. [40]. Under the same reaction conditions, a large amount of byproducts resulted in dibromobenzamides **15** and **16**. The formation of byproducts was avoided by performing the reaction in boiling dioxane for 7 days.

Benzoic acid **1c** was synthesized from the corresponding benzamide **6c**. In order to avoid chloro substitution, the hydrolysis was performed by boiling in an acidic medium. However, hydrolysis of ester **11** under these conditions led to the formation of two products (**18** and **1**) as observed by TLC, perhaps due to simultaneous hydrolysis of the amide.

2.2. Compound binding to CAs

The synthesized compounds were tested as binders and inhibitors of the twelve catalytically active human CA isoforms using the fluorescent thermal shift assay (FTSA) and isothermal titration calorimetry (ITC) (Fig. 1). Since all compounds are primary

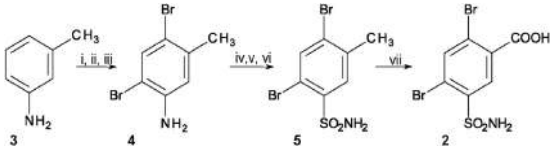

Scheme 1. The synthesis of 2,4-dibromo-5-sulfamoylbenzoic acid **2**. i) Ac_2O, AcOH; ii) Br_2, 1,2-dichloroethane; iii) conc.HCl(aq), MeOH, Δ; iv) $NaNO_2$, conc.HCl(aq), AcOH, 0 °C; v) SO_2, AcOH, Cu^+, −15 °C; vi) NH_3(aq); vii) $KMnO_4$, H_2O, 90 °C.

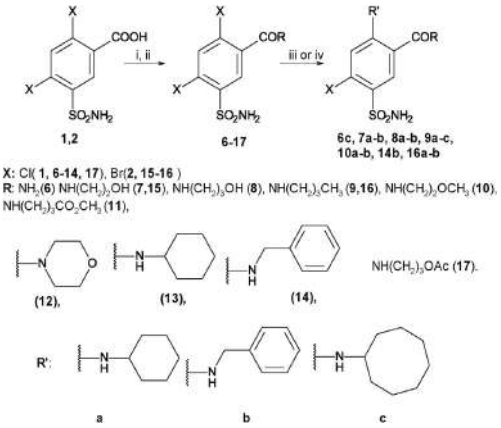

Scheme 2. The synthesis of 2-halo-4,5-disubstitutedbenzenesulfonamides. i) $SOCl_2$, toluene, Δ; ii) appropriate amine RH, THF, 0–20 °C; iii) excess appropriate amine R'H, Δ; iv) appropriate amine R'H, dioxane, Δ.

sulfonamides expected to bind to the Zn(II) and were demonstrated to interact with the CAs with a stoichiometry of 1:1, it seemed unnecessary to perform the enzymatic inhibition assay for all compounds. The observed affinities by FTSA and ITC were in good agreement (Fig. 2). However, there was some discrepancy reaching almost 10 fold for several compounds. Since FTSA has fewer limitations, than ITC, the binding constants determined calorimetrically by ITC were not used in the analysis. The primary limitation of ITC is that it does not accurately determine the affinities greater than approximately 10 nM. There were several cases when compounds bound CAs with K_{d_obs} < 10 nM and the Wiseman *c* factor was higher than 500, too high for accurate determination of the affinity. To avoid the discrepancies only FTSA affinities were used for the thermodynamic analysis. However, there were cases when FTSA yielded unreliable melting transitions and therefore ITC affinities were used. For example, compound **7a** interaction to CA XII, **8a** to CA XIII, and **10a** to CA XII and CA XIII could not be determined by FTSA and thus values obtained by ITC were used in the analysis. The observed affinities of all compounds to all tested CAs are listed in Table S1.

Sulfonamide − CA binding reaction is linked to several protonation events. First, the sulfonamide amino group must deprotonate and become negatively charged and second, the Zn(II)-bound hydroxide must bind proton and become an electrostatically neutral water molecule in order to be replaced by the sulfonamide. These linked reactions occur simultaneously with the binding reaction and are hard to observe experimentally. However, they influence the binding energetics and significantly alter the binding affinities. Therefore, it is important to distinguish the *observed* binding affinities that include the linked reactions and the *intrinsic* affinities that are calculated by subtracting the linked reactions from the observed parameters.

This proton linkage can significantly influence the binding affinity and mislead when comparing compounds or CA isoforms with different pK_as. In such cases, the structure-thermodynamics correlations may lead to incorrectly assigned reasons for the change in affinity. Therefore, when compounds with desired affinities are being designed, it is important to show the intrinsic parameters. They are listed in Table 1. However, despite the advantage in compound design to have the intrinsic parameters, it is also handy to compare the observed parameters, listed in Table S1.

The pK_as of compound sulfonamide group were determined spectrophotometrically as described in the methods section and are listed in Table 2. In addition, the protonation enthalpies were also determined and used to calculate the intrinsic enthalpies of binding. The pK_as and protonation enthalpies of CA hydroxide group were published previously.

Single-tailed benzenesulfonamides **7**–**14**, **17**–**18** have similar pK_a values, equal to 8.78 ± 0.04. The pK_as of two-tailed benzenesulfonamides **7**–**8**(**a**, **b**) differed due to the substituents in *para*-position: benzylamino substituted compounds **7b, 8b** have the highest pK_a values (10.1–10.2), while pK_as of cyclohexylamino substituted benzensulfonamides **7a, 8a** are equal to 9.7–9.8. An example of pK_a determination by spectrophotometric method is shown in Fig. 3.

However, the pK_as of cyclooctylamino substituted compounds **6c**, **1c**, and **9c** were not determined due to low solubility of the compounds. For the calculation of intrinsic parameters we used the same pK_as as for cyclohexylamino-substituted benzenesulfonamides (pK_a of compound **6c** and **9c** were equal to 9.7 and pK_a of **1c** equal to 10.4).

The enthalpies of sulfonamide amino group protonation were determined by ITC titration of alkaline inhibitor solution with the nitric acid (HNO_3) (Fig. 3, Table 2). The enthalpy of the first transition of the titration curve represents the enthalpy of the reaction between H^+ and excess OH^-, while the enthalpy of the second stage represents the enthalpy of sulfonamide protonation. The protonation enthalpies of two-tailed compounds **7**–**8**(**a**, **b**) were in the range from −36.8 kJ/mol to −39.7 kJ/mol, while ΔH_{prot} of single-tailed compounds **7**–**14**, **17**–**18** were in the range from −27.6 kJ/mol to −31.4 kJ/mol.

The structure-thermodynamics maps of compound intrinsic affinities to 12 CA isoforms are shown in Figs. 4–7. Values next to structures show the intrinsic Gibbs energies of binding to every CA isoform and the values next to arrows show the differences between the Gibbs energies of binding for compounds linked by the arrow. The difference shows the gain or loss in intrinsic affinity upon the change of the chemical structure of the compound. The error margin of the determinations is approximately 1 kJ/mol. The K_d value of 1 nM corresponds to Gibbs energy of binding of −53.4 kJ/mol. The 10-fold increase of binding affinity corresponds to the difference in Gibbs energy $\Delta\Delta G = -5.93$ kJ/mol.

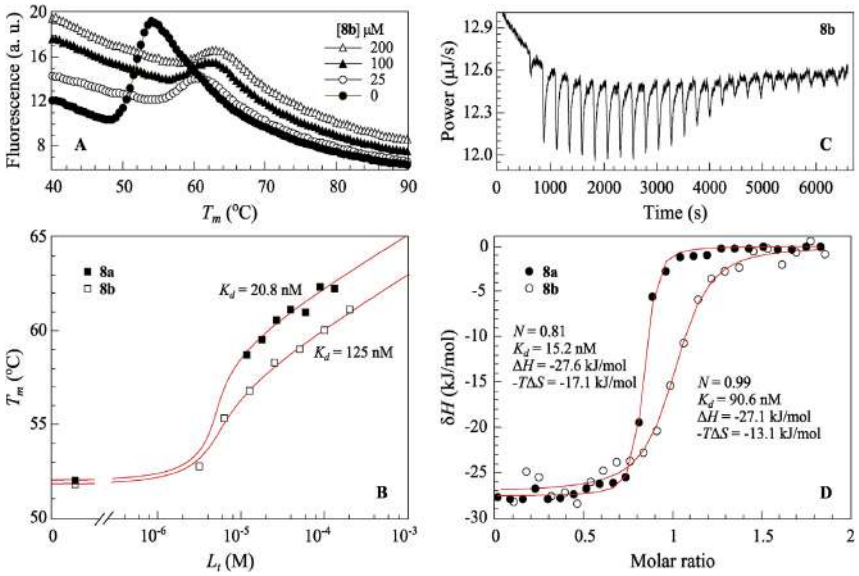

Fig. 1. The data of compound **8a** and **8b** binding to CA XII performed by FTSA (**A** and **B**) and ITC (**C** and **D**). **A**, shows the shift of fluorescence curves of CA XII unfolding as a function of temperature at various **8b** concentrations. **B**, Shows the protein melting temperature dependence on the concentration of **8a** (filled squares) and **8b** (open squares). **C**, Shows the raw ITC data of **8b** binding with CA XII, while **D** Shows the integrated ITC curves (filled circles – compound **8a**, open circles – compound **8b**). ITC and FTSA experiments were performed at 37 °C in 50 mM sodium phosphate buffer, pH 7.0, containing 100 mM NaCl and 2% DMSO.

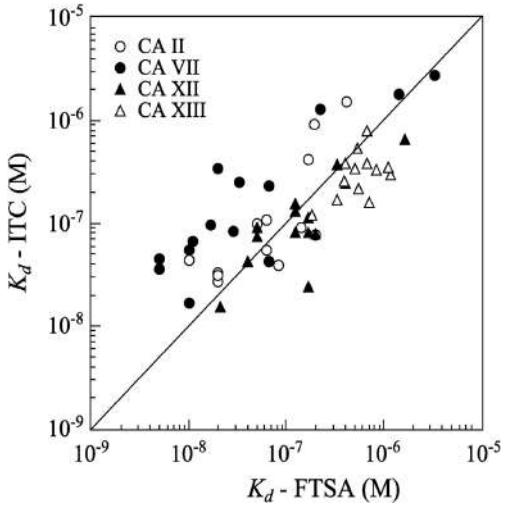

Fig. 2. Correlation between dissociation constants determined by FTSA (x-axis) and ITC (y-axis). Data was taken from Table S1.

Compound **1** bound to CAs with nanomolar affinity. After the change of carboxy group to amido moiety (**1** → **6**) the binding affinity remained essentially the same to all CAs. The lengthening of the *meta* tail (in Fig. 4 clockwise **6** → **7**, **10**, **18**, **12**, **13**, and **14**) was analyzed. The aliphatic tails of compounds **7**, **10**, and **18** interacting with CA I, CA VA, and CA VB diminished the binding affinity compared to **6**. The binding of **12** to CA VA and CA VB became much weaker, while **13** showed weaker binding affinity to CA III and CA XII. The greatest increase was found for **10** binding to CA IV (ΔG = −61.1 kJ/mol and the difference of Gibbs energies between **6** and **10** interaction with CA IV was ΔΔG = −8.1 kJ/mol). Compound **14** showed the increase in binding affinity to all CAs compared to **6**, except CA I and CA XII, where Gibbs energies remained the same, and the greatest influence was found for CA IV and CA VB (ΔΔG = −6.4 kJ/mol and −6.3 kJ/mol respectively) (Fig. 4). It was surprising that minor structural change, an addition of a methyl group far away from the sulfonamide group (**7** vs **10** to CA IV and **18** vs **11** to CA VB), significantly improved the binding affinities.

Comparing chloro **1, 6**–**7, 9**–**14, 17**–**18** and bromo **2, 15**–**16** substituted benzenesulfonamides shows a minor influence to the binding with all CAs (Fig. 4). For example, the difference between dissociation constants of compounds **1** and **2** is 1.3–3.5 times, while for **7** and **15** the maximum difference between K_ds is 2.6 times, except for their interaction with CA IV, where the difference is 5.8 fold. The difference between binding parameters for compounds **9** and **16** varies from 0.1 times (for CA VII) to 6.6 (for CA VB) times. These differences are small and show that Cl and Br substitutes have a similar effect on the binding affinity. However, since **16a** and **16b** exhibit low aqueous solubility, their binding affinity to CAs could not be determined accurately, and therefore the comparison with chlorinated analogs **9a** and **9b** was not done.

Overall, single-tailed compounds (**1**–**2, 6**–**7, 9**–**18**) are more effective CA VII inhibitors than other 11 CA isoforms. Compounds **7** and **15** are selective CA VII inhibitors showing nanomolar binding affinity (K_d = 0.06 nM, Δ_bG = −60.5 kJ/mol).

To understand the energetic contributions of small functional groups, compounds **7**, **8**, and **9** which differ in a single methylene group and a presence oh hydroxy group, were put in a triangle

Table 1
Intrinsic dissociation constants (K_{d_intr} (nM)) of the compound binding to CA isoforms. Values were calculated from data, listed in the Supplementary material Table S1.

Intrinsic dissociation constants K_{d_intr} (nM)												
Compound	CA I	CA II	CA III	CA IV	CA VA	CA VB	CA VI	CA VII	CA IX	CA XII	CA XIII	CA XIV
1(*EA1-1*)	150	0.47	8.4	1.3	42	3.9	1.1	0.14	0.60	0.76	0.96	0.54
1c(*EA1-9*)	0.41	0.45	19	0.38	ND	40	2.8	1.0	0.019	0.31	0.33	0.077
2(*LJ14-3*)	84	0.92	17	1.7	90	1.1	3.5	0.24	0.89	1.2	1.3	0.984
6(*EA1A-1*)	330	0.53	44	1.2	19	0.70	0.71	0.12	0.59	0.66	5.8	0.30
6c(*EA1A-9*)	31.0	3.1	9.6	ND	ND	200	36	19	ND	ND	ND	ND
7 (*EA3-1*)	1500	0.58	31	1.8	52	3.1	0.89	0.060	0.74	0.75	7.9	0.40
7a(*EA3-7*)	26	0.37	240	ND	66	50	6.0	2.6	0.011	*0.019*	1.2	ND
7b(*EA3-8*)	3.7	0.022	30	ND	ND	0.63	0.38	0.055	0.007	0.041	0.23	0.005
8(*EA4-1*)	2900	0.069	94	0.032	87	6.0	1.4	0.060	0.22	1.0	8.9	0.38
8a(*EA4-7*)	49	0.14	60	ND	170	20	3.6	0.88	0.004	0.013	*0.77*	0.047
8b(*EA4-8*)	15	0.006	7.6	ND	20	2.4	0.72	0.016	0.006	0.031	0.64	0.012
9(*EA5-1*)	540	0.16	30	0.42	58	0.73	0.27	0.03	0.25	0.34	6.3	0.34
9a(*EA5-7*)	370	0.80	96	ND	130	1.2	3.0	13	0.011	7.7	ND	0.11
9b(*EA5-8*)	20	0.035	30	ND	84	2.4	1.2	0.12	0.007	0.081	1.2	0.035
9c(*EA5-9*)	370	0.11	96	ND	270	6.6	3.6	1.5	0.0057	0.51	ND	0.0094
10(*EA8-1*)	810	0.48	51	0.050	40	2.2	0.93	0.075	0.36	1.4	11	0.27
10a(*EA8-7*)	37	0.29	48	ND	130	12	1.8	2.2	ND	*0.014*	*0.69*	0.051
10b(*EA8-8*)	15	0.018	38	ND	7.6	1.4	0.40	0.038	0.008	0.077	0.72	0.01
11(*EA11-1*)	1600	0.39	210	0.55	15	0.58	1.6	0.14	0.69	0.85	7.9	0.4
12(*EA7-1*)	3200	1.6	420	1.7	2300	35	2.3	0.23	0.77	2.7	19	1.1
13(*EA9-1*)	1000	1.2	750	0.74	26	0.60	2.0	0.17	1.1	10	2.6	0.40
14(*EA10-1*)	360	0.14	7.5	0.099	6.9	0.06	0.20	0.03	0.40	0.75	4.7	0.081
14b(*EA10-8*)	2.34	0.011	30.3	ND	42	0.37	0.19	0.031	0.004	0.081	1.2	0.004
15(*LJ14-5*)	1800	0.44	40	0.31	39	1.2	1.1	0.064	0.43	0.51	4.7	0.30
16(*LJ14-6*)	1300	0.14	37	0.18	33	0.11	0.32	0.032	0.10	0.21	4.2	0.10
16a(*LJ15-35*)	370	0.56	96	2.2	270	ND	36	150	0.025	0.023	4.5	0.27
16b(*LJ15-36*)	370	0.37	96	ND	270	ND	36	150	ND	0.99	110	0.37
17(*EA4-1-2*)	1700	0.52	220	0.26	200	6.1	2.0	0.12	0.65	2.4	14	0.71
18(*EA12-1*)	2500	0.84	150	1.1	18	16	1.7	0.34	1.1	0.21	8.1	0.45

(Fig. 5). Consider their interaction with CA IV. The addition of a methylene group increased the affinity for CA IV by nearly 100-fold, making the compound **8** slightly selective for this isoform. Such significant increase cannot be explained by simple hydrophobic effect and most likely involves a hydrogen bond that can be formed for compound **8** but cannot be formed for **7**. This is also confirmed by the fact that the removal of hydroxy group in **9** caused the affinity for CA IV to drop by over 10-fold. These energetic contributions are in line with the previous observations for aliphatic compounds [41–43].

The addition of cyclohexylamino tail in *para* position (Fig. 6) highly increases the binding affinity to CA I, CA IX, CA XII, CA XIII, and CA XIV, except for **9**, where addition of a tail decreased binding affinity to most CAs (except CA I, CA IX, and CA XIV, where affinity increased). This could be explained by the presence of the hydrophobic tail in the *meta* position.

Longer benzyl group resulted in greater affinity for almost all CAs comparing with analogs bearing cyclohexyl group in *para* position. However, benzyl group diminished compound selectivity for CA IX and CA XII. For example, the K_d of single tailed **8** binding to CA II was 0.07 nM, but the compound is weaker binder to CA IX and CA XII. The addition of cyclohexyl group diminished the binding affinity to CA II two times, but highly increased the affinity to CA IX and CA XII making compound **8a** selective to these two isoforms. Compound **8b** bearing benzyl group bound CA II and CA IX with the same affinity, decreased the affinity for CA XII and diminished the selectivity to cancer related CA IX and CA XII. The same tendency was observed comparing single tailed compounds **7**, **9**, and **10** with their analogs bearing cyclohexyl group (**7a**, **9a**, and **10a**) as well as benzyl group (**7b**, **9b**, and **10b**).

The influence of the changes of *meta* tail in double-tailed compounds, bearing cyclooctylamino group in *para* position, are shown in Fig. 7. Compound **1c** showed greater binding affinity to CA I, CA II, CA III, CA VB, CA VI, and CA VII than **6c**. Gibbs energies of compound **6c** binding to other CA isoforms could not be determined using FTSA due to low solubility.

The analysis of studied compounds show that two-tailed compounds could be designed as more potent binders compared with analogs bearing only a single tail in the *meta* position and modifications of tails could contribute to the selectivity. The analyzed two-tailed compounds showed the strongest affinities to CA IX and CA XIV.

In addition to the Gibbs energies (affinities), we studied the enthalpies and entropies of binding. The observed enthalpies were determined by ITC and then the intrinsic enthalpies were calculated as explained in the methods part. These intrinsic thermodynamic parameters of binding are listed in Table 2 and Fig. 8, where the ΔG is shown in bold, enthalpy ΔH in normal font, and the entropy $-T\Delta S$ is shown in italic. As in previous structural maps, the energies of binding are shown near the structures and differences of these values between compounds connected by the arrow are shown on the arrow.

Compounds exhibited enthalpy-driven binding to CA XII (with the partial exception) and CA XIII, while contribution arising from both enthalpic and entropic reasons was for CA II and CA VII. Interaction of CA II with the analyzed compounds showed large contributions of both enthalpy and entropy. The comparison of single-tailed compound **7** with structurally similar **8** showed that ΔHs were very similar, equal to −32.7 kJ/mol and −30.4 kJ/mol, respectively. However, $-T\Delta S$ of compound bearing longer and more flexible tail in *meta* position **8** was −29.9 kJ/mol, while $-T\Delta S$ of **7** was −22.2 kJ/mol and due to this greater entropic contribution **8** bound to CA II with higher affinity.

It was interesting to compare how enthalpic and entropic contribution to the Gibbs energy changed upon adding and modifying the tails in *para* position. The addition and modification of a tail to **7** showed that **7a** had the greater entropic than enthalpic influence to ΔG_{b_intr} while compound **7b** had greater enthalpic than

Table 2
Experimentally determined compound pK_a and protonation enthalpy Δ_pH (listed in the first column below compound name), calculated intrinsic Gibbs energies, enthalpies and entropies of the compound binding to four isoforms of recombinant human CAs at 37 °C.

Compound		CA II	CA VII	CA XII	CAXIII
7	Δ_bG_{intr}, kJ mol^{-1}	−54.8	−60.6	−54.1	−48.1
pK_a = 8.8	Δ_bH_{intr}, kJ mol^{-1}	−32.7	−37.6	−47.9	−45.3
Δ_pH = −29.7 kJ/mol	$-T\,\Delta_bS_{intr}$, kJ mol^{-1}	−22.1	−23.0	−6.2	−6.2
7a	Δ_bG_{intr}, kJ mol^{-1}	−56.0	−51.0	−63.5	−52.9
pK_a = 9.7	Δ_bH_{intr}, kJ mol^{-1}	−22.3	−19.4	−53.1	−44.9
Δ_pH = −39.3 kJ/mol	$-T\,\Delta_bS_{intr}$, kJ mol^{-1}	−33.7	−31.6	−10.4	−8.0
7b	Δ_bG_{intr}, kJ mol^{-1}	−63.3	−60.9	−61.7	−57.2
pK_a = 10.2	Δ_bH_{intr}, kJ mol^{-1}	−35.6	−35.1	−53.5	−49.7
Δ_pH = −38.1 kJ/mol	$-T\,\Delta_bS_{intr}$, kJ mol^{-1}	−27.7	−25.8	−8.2	−7.5
8	Δ_bG_{intr}, kJ mol^{-1}	−60.3	−60.6	−53.4	−47.8
pK_a = 8.8	Δ_bH_{intr}, kJ mol^{-1}	−30.4	−23.1	−39.7	−43.0
Δ_pH = −29.3 kJ/mol	$-T\,\Delta_bS_{intr}$, kJ mol^{-1}	−29.9	−37.5	−13.7	−4.8
8a	Δ_bG_{intr}, kJ mol^{-1}	−58.6	−53.8	−64.7	−54.1
pK_a = 9.8	Δ_bH_{intr}, kJ mol^{-1}	−23.9	−16.8	−33.6	−48.4
Δ_pH = −39.7 kJ/mol	$-T\,\Delta_bS_{intr}$, kJ mol^{-1}	−34.7	−37.0	−31.1	−5.7
8b	Δ_bG_{intr}, kJ mol^{-1}	−66.8	−64.0	−62.4	−54.6
pK_a = 9.7	Δ_bH_{intr}, kJ mol^{-1}	−39.3	−28.0	−47.1	−38.4
Δ_pH = −36.8 kJ/mol	$-T\,\Delta_bS_{intr}$, kJ mol^{-1}	−27.5	−36.0	−15.3	−16.2
9	Δ_bG_{intr}, kJ mol^{-1}	−58.2	−62.1	−56.2	−48.7
pK_a = 8.8	Δ_bH_{intr}, kJ mol^{-1}	−35.2	−22.1	−33.2	−32.5
Δ_pH = −31.4 kJ/mol	$-T\,\Delta_bS_{intr}$, kJ mol^{-1}	−23.0	−40.0	−23.0	−16.2
10	Δ_bG_{intr}, kJ mol^{-1}	−55.3	−60.1	−52.6	−47.2
pK_a = 8.8	Δ_bH_{intr}, kJ mol^{-1}	−33.3	−30.6	−39.8	−38.8
Δ_pH = −29.7 kJ/mol	$-T\,\Delta_bS_{intr}$, kJ mol^{-1}	−22.0	−29.5	−12.8	−8.4
11	Δ_bG_{intr}, kJ mol^{-1}	−55.9	−58.6	−53.8	−48.1
pK_a = 8.8	Δ_bH_{intr}, kJ mol^{-1}	−30.0	−26.4	−40.8	−52.7
Δ_pH = −31.4 kJ/mol	$-T\,\Delta_bS_{intr}$, kJ mol^{-1}	−25.9	−32.2	−13.0	4.6
12	Δ_bG_{intr}, kJ mol^{-1}	−52.3	−57.3	−50.8	−45.9
pK_a = 8.8	Δ_bH_{intr}, kJ mol^{-1}	−12.8	−23.8	−34.2	−43.9
Δ_pH = −31.0 kJ/mol	$-T\,\Delta_bS_{intr}$, kJ mol^{-1}	−39.5	−33.5	−16.6	−2.0
13	Δ_bG_{intr}, kJ mol^{-1}	−53.0	−57.9	−47.5	−51.0
pK_a = 8.8	Δ_bH_{intr}, kJ mol^{-1}	−31.9	−8.9	−27.1	−48.7
Δ_pH = −29.7 kJ/mol	$-T\,\Delta_bS_{intr}$, kJ mol^{-1}	−21.1	−49.0	−20.4	−2.3
14	Δ_bG_{intr}, kJ mol^{-1}	−58.5	−62.4	−54.1	−49.4
pK_a = 8.8	Δ_bH_{intr}, kJ mol^{-1}	−27.4	−26.1	−39.5	−42.8
Δ_pH = −27.6 kJ/mol	$-T\,\Delta_bS_{intr}$, kJ mol^{-1}	−31.1	−36.3	−14.6	−6.6
17	Δ_bG_{intr}, kJ mol^{-1}	−55.2	−58.9	−51.2	−46.6
pK_a = 8.7	Δ_bH_{intr}, kJ mol^{-1}	−27.8	−26.8	−24.5	−37.2
Δ_pH = −27.6 kJ/mol	$-T\,\Delta_bS_{intr}$, kJ mol^{-1}	−27.4	−32.1	−26.7	−9.4
18	Δ_bG_{intr}, kJ mol^{-1}	−53.9	−56.2	−57.5	−48.0
pK_a = 8.9	Δ_bH_{intr}, kJ mol^{-1}	−37.5	−21.4	−48.2	−59.0
Δ_pH = −29.3 kJ/mol	$-T\,\Delta_bS_{intr}$, kJ mol^{-1}	−16.4	−34.8	−9.3	11.0

entropic contribution. However, the longer *meta* tail had minor influence to thermodynamic parameters when the substituent to *para* position was added. Moreover, the addition of cyclohexylamino moiety (**7a** and **7b**) in *para*-position to compounds **7** and **8** induced similar changes of binding thermodynamics: 1) the unfavorable changes of enthalpic and favorable changes of entropic gain upon binding to CA II and CA VII, and 2) favorable changes of enthalpic and entropic gain upon binding to CA XII and CA XIII.

Binding of all studied single-tailed chloro-substituted benzenesulfonamides **7**–**14, 17**–**18** to CA VII was entropy driven, except **10**, where the contribution arising from enthalpic and entropic reasons was equal, and **7**, where enthalpic contribution was greater than entropic. However, enthalpic influence became smaller when the second tail in *para* position was added to compound **7**.

Comparing two-tailed compounds **7b** vs **8b**, it was clear that longer *meta* tail by one carbon atom made protein-ligand interaction entropically driven. However, this tail had minor influence to thermodynamic parameters of binding to all tested CAs when benzylamino group was added in *para* position.

CAs II and VII are structurally close [44], showing also in the tendencies in thermodynamic parameters that can be seen after adding *para* tail to compounds **7** and **8**. Thermodynamic parameters of compound binding to CA II change in the same manner as to CA VII. Modification of **7a** to **7b** increased the binding affinity by −7.3 kJ/mol to CA II and −9.9 kJ/mol to CA VII. The $\Delta\Delta H_{b_intr}$s of CA II and CA VII binding were −13.3 kJ/mol and −20.2 kJ/mol, respectively. The $-T\Delta\Delta S_{b\_intr}$ were similar as well (6.0 kJ/mol for CA II and 10.3 kJ/mol for CA VII). Similar differences in thermodynamic parameters were found comparing the changes of compounds **7b** vs **8b** and **8a** vs **8b** binding with CA II and CA VII.

The binding of CA XII to all *meta*-substituted dichlorobenzenesulfonamides (**7**–**14, 17**–**18**) was enthalpy driven, except **17**, where the contribution arising from enthalpic and entropic reasons was almost equal. Compounds **11** and **18**, bearing quite similar tails, had dominant enthalpic contribution to the binding affinity. Binding of these compounds and compound **7** to CA XII was the most enthalpy driven compound when comparing with other studied single-tailed benzenesulfonamides. The addition of a second tail to the *para* position increased the binding affinity to CA VII. The best CA XII binder **7a** ($\Delta G_{b\_intr} = -68.3$ kJ/mol) had dominant enthalpic ($\Delta H_{b\_intr} = -53.1$ kJ/mol) contribution.

Interaction of CA XIII with single-tailed chlorinated compounds (**7**–**14, 17**–**18**) was enthalpy driven. Binding of **11** and **18** to CA XIII had an unfavorable entropic contribution. It was interesting that changes of binding thermodynamics demonstrated distinct effect of enthalpy-entropy compensation in two pairs of compounds (**9** vs **11** and **9** vs **18**) in binding to CA XIII. After the addition of a tail in *para* position (compounds **7a,b** and **8a,b**) binding to CA XIII became stronger and entropic contribution slightly increased. Compound **7b** was the strongest binder of CA XIII compared with all studied benzenesulfonamides and had the greater enthalpic contribution than other two-tailed compounds.

Fig. 9 shows the enthalpy-entropy compensation graph for all studied compound binding to four CA isoforms. Squares represent the two-tailed benzenesulfonamides and triangles represent the benzenesulfonamides bearing a single tail in *meta* position. Different colors show different CA isoforms. Binding affinities span a relatively narrow range, while the range of enthalpies and entropies are significantly larger. The enthalpies of single-tailed compound interaction with CA II varied from −12.8 kJ/mol to −37.5 kJ/mol, while the range of entropies was between −16.4 kJ/mol and −39.5 kJ/mol. The range of enthalpies for CA VII was between −8.9 kJ/mol and −37.6 kJ/mol, entropies from −23.0 kJ/mol to −49.0 kJ/mol. The enthalpies for CA XII spanned between −24.5 kJ/mol and −48.2 kJ/mol, entropies from −6.2 kJ/mol and −26.7 kJ/mol. The range of enthalpies of single-tailed compounds interacting with CA XIII varied from −32.5 kJ/mol to −59.0 kJ/mol, while entropies span between 11 kJ/mol and −16.2 kJ/mol. The enthalpies of two-tailed compound interaction with CA II varied from −22.3 kJ/mol to −39.3 kJ/mol, while the range of entropies was between −27.5 kJ/mol and −34.7 kJ/mol. The range of enthalpies for CA VII was between −16.8 kJ/mol and −35.1 kJ/mol, for entropies from −25.8 kJ/mol to −37 kJ/mol. The enthalpies for CA XII spanned between −33.6 kJ/mol and −53.5 kJ/mol, entropies from −8.2 kJ/mol to −31.1 kJ/mol. The range of enthalpies of single-tailed compound interaction with CA XIII varied from −38.4 kJ/mol to −49.7 kJ/mol, while entropies spanned between −5.7 kJ/mol and −16.2 kJ/mol. Thermodynamic properties of CA II and CA VII binding was very similar-enthalpies and entropies spanned equally and thus black and red squares overlaped in the figure. Equal contribution arising from enthalpic

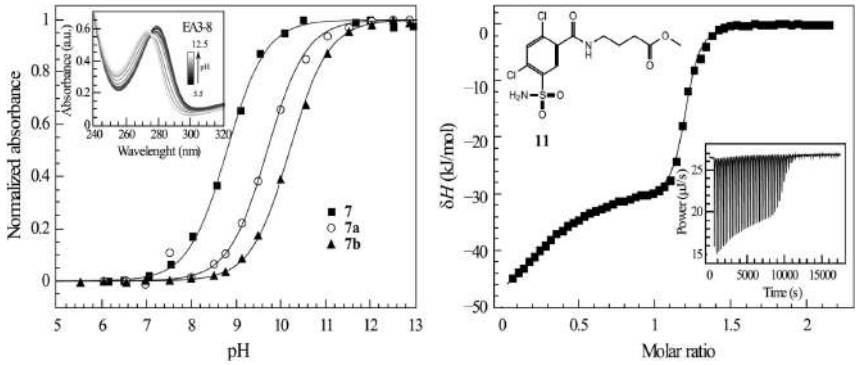

Fig. 3. Determination of the compound sulfonamide group protonation pK_a and enthalpy of protonation. The left panel shows spectrophotometrically determined pK_a values of 8.8 for compound **7** (black squares), 9.7 for **7a** (open circles), and 10.2 for **7b** (black triangles), all determined isothermally at 37 °C. The inset shows the absorbance spectra of 30 μM **7b** at pH ranging from 5.5 (black) to 12.5 (white). The right panel shows direct ITC measurement of the compound's **11** protonation enthalpy at 37 °C. The inset shows the raw ITC data.

and entropic reasons to CA XII binding affinity also overlaped red and black datapoints, however part of CA XII datapoints were shifted due to enthalpically driven interaction. Blue datapoints were the most apart, because CA XIII binding with these compounds was exclusively enthalpy driven with two compounds exhibiting unfavorable binding entropy.

2.3. X-ray crystallographic structures of CA-inhibitor complexes

In search of correlations between the binding thermodynamics and 3D structures of the bound complexes, four crystal structures of human CAs containing compounds in the active site were solved by X-Ray crystallography, compound **9** bound to CA II and CA XIII, and CA XII with **7a** and **7b**. All complexes were obtained by soaking of CA crystals with solution of the corresponding compound in the crystallization buffer. The crystal structure CA II-**9** contains one protein chain in the asymmetric unit, CA XIII-**9** – two, and the crystal structures of CA XII – four protein chains. Data collection and the refinement statistics of four datasets are presented in Table 3. The electron densities of ligands in the crystal structures are shown in Fig. 10.

The compound **9** binds to CA II 39 times more strongly than to CA XIII (K_d 0.16 (CA II) vs 6.3 (CA XIII) nM). In the crystal structures, the compound **9** binds to CA II and CA XIII in the nearly identical positions (Fig. 11AB). The chlorine atom interacts in both crystal structures with the residues that are conservative between two isoforms. The chlorobenzene ring is anchored by the chlorine in the position that was described previously [33,34,45,46]. The deeper parts of active sites of CA II and CA XIII are very similar and differ by only three amino acids: Ile91, Asn62 and Thr200 in CA II are replaced in CA XIII by Arg93, Ser64 and Val202, respectively. Thus, in CA II the hydroxyl group of Thr200 makes the hydrogen bond with the nitrogen atom of the *meta*-substituent of **9**. Such binding mode is impossible in CA XIII, since the threonine side chain is replaced there by the valine. Details of interaction of *meta*-substituent with CA XIII and CA II are depicted in Fig. 11B. In particular, Thr200 (CA II) makes a direct hydrogen bond with *meta*-substituent of ligand, whereas in CA XIII there is a water-mediated interaction. These differences in interaction of **9** with CA II and CA XIII could explain better binding of compound **9** to CA II.

The binding thermodynamics of compound **9** to CA II and CA XIII exhibit changes of both thermodynamic parameters that are favorable over CA II:

(CA II): $\Delta G = -58.2$, $\Delta H = -35.2$, $-T\Delta S = -23.0$ kJ/mol;

(CA XIII): $\Delta G = -48.7$, $\Delta H = -32.5$, $-T\Delta S = -16.2$ kJ/mol;

(CA II vs CA XIII): $\Delta\Delta G = -9.5$, $\Delta\Delta H = -2.7$, $\Delta(T\Delta S) = -6.8$ kJ/mol

Favorable changes in binding enthalpy could be associated with the direct hydrogen bond between Thr202 and ligand in CA II-**9** complex. The favorable changes in entropy are more difficult to explain.

Compound **7a** and **7b** binding mode to CA XII is presented in Fig. 11CD. Both ligands are located in the active site of CA XII in a similar way and demonstrate very similar binding affinities (K_d of **7a** 0.019 nM vs 0.041 nM of **7b**). The main differences in the binding modes of **7a** and **7b** were detected in the positions of the tail of the *meta*-substituent. In crystal structure of the complex CA XII-**7b** the tail of the *meta*-substituent in all protein subunits was found in the same well-defined conformation in the electron density. The tail of *meta*-substituent of **7b** is located deeper in the active site cavity than **7a**.The tail of *meta*-substituent of the compound **7a** in two protein chains of CA XII was found in two alternate conformations. One of the alternate conformations is similar to the position of meta-tail of the **7b** in the complex CA XII – **7b.** Other four conformations are directed towards the entrance of the active site cavity. The slight displacement in the position of the benzene ring of **7a** compared to **7b** is caused by the larger *para*-substituent of **7b** (Fig. 11D).

The binding affinities of compounds **7a** and **7b** demonstrate that compound **7a** binds to CA XII ~20 times stronger than to CA II (0.019 nM for CA XII and 0.37 nM for CA II), whereas the binding affinities of compound **7b** to CA II and CA XII are similar (0.022 nM vs 0.041 nM, Table 1). Interestingly, similar behavior of binding affinities is observed for compounds **10a** and **8a** which contain the cyclohexylamino substituent in the *para*-position. In this respect these ligands are like compound **7a** and bind to CA XII significantly stronger than to CA II (**10a** – 21 times, **8a** – 11, Table 1). Compound **7b** could be compared with compounds **10b**, **8b**, and **9b** which also contain the benzylamino substituent in the *para*-position and have similar binding affinities to CA XII and CA II, although all compounds show slightly better binding affinities to CA XII: **10b**–4 times, **7b**–2 times, **8b**–5 times, and **9b**–2 times, Table 1.

The binding of **7a** and **7b** in CA II and CA XII cannot be directly compared due to the absence of crystal structures of complexes CA

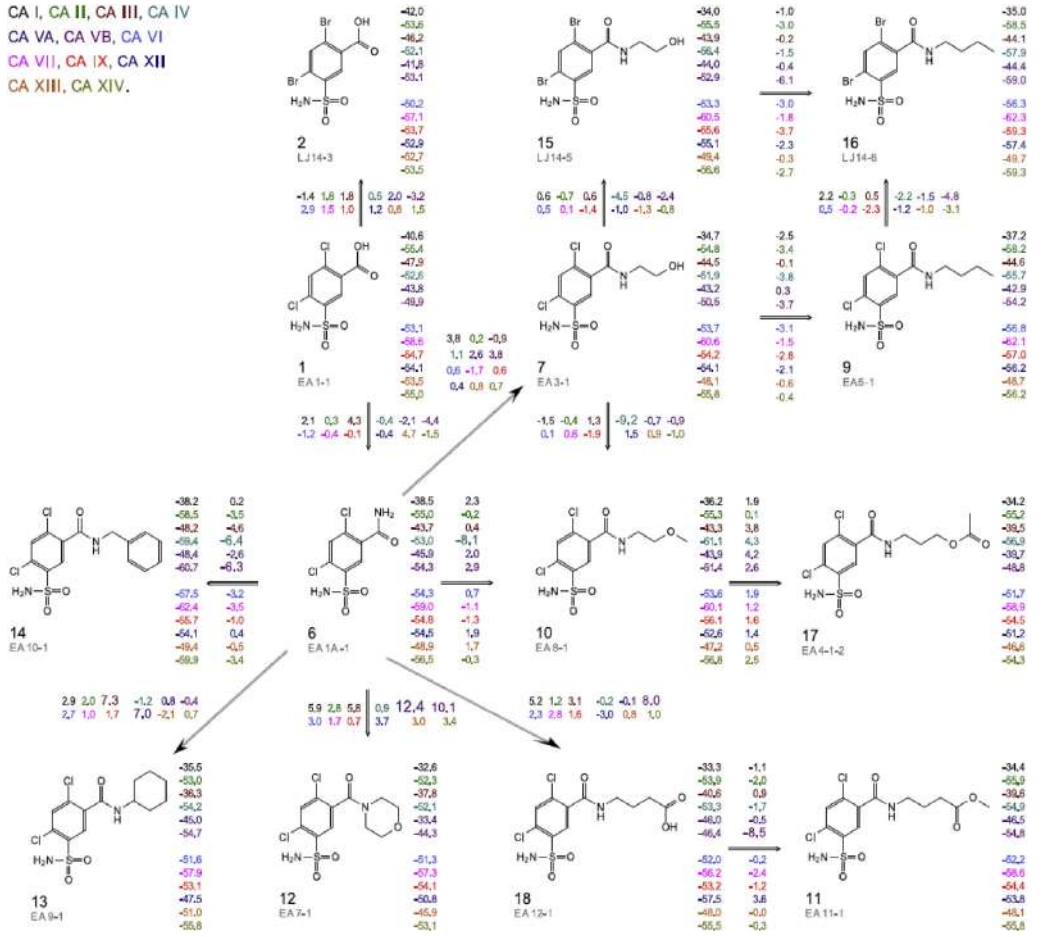

Fig. 4. Correlation map of the inhibitor chemical structures **1**–**2, 6**–**7, 9**–**18** with the intrinsic Gibbs energies of binding to all catalytically active CA isoforms. The intrinsic ΔG_{b_intr} values are shown next to the chemical structures. Differences in the binding affinities between neighboring compounds are listed on the connecting arrows. Colors show different CA isoforms. The observed Gibbs energies of binding are provided in the Supplementary material. (For interpretation of the references to color in this figure legend, the reader is referred to the Web version of this article.)

II-**7a** and CA II-**7b**. However, it is known from the crystallographic studies of chlorinated benzensulfonamides, that the binding mode of chlorinated ring in the active sites of CA II, CA XII, and CA XIII are the same due to conserved residues in these CA isoforms. The subunits from crystal structures of CA XII-**7a** and CA II-**9** can be superimposed to analyze the possible binding mode of **7a** in CA II active site. If the binding mode of the ligand in CA XII would be retained in CA II, there could be a steric clash between the cyclohexylamino group of **7a**, which is taken from the active site of CA XII, and the side chain of Phe131 in CA II (Fig. 11E, pink arrow). Therefore, the positions of **7a** and **7b** in CA II should differ from those in CA XII. The benzylamino substituent is more flexible and longer than cyclohexylamino and possibly could adopt a different conformation in the binding to hydrophobic cavity (CA II) near the Phe131 (blue arrow). We speculate that the longer and more flexible substituent could escape the collisions with Phe131 in CA II and adopt an optimal conformation for interaction with the hydrophobic part of active site. Higher conformational adaptability of this fragment possibly improves the binding affinities to CA II, but seems to have opposite effect on the selectivity of binding.

3. Conclusions

A series of mono- and di-substituted 2-chloro/bromo-benzenesulfonamides were synthesized and their binding analysis to all 12 catalytically active human CAs was performed to determine intrinsic affinities, enthalpies, and entropies of binding. The length and hydrophobicity of the *meta*-substituent affected the binding affinity toward each CAs. Single tailed compounds showed nanomolar affinity and selectivity towards CA VII. However, the introduction of a second tail had significant increase to the binding affinity and two-tailed compounds in most cases provided selectivity for CA IX and CA XIV as was designed. This selectivity depended on the length of the substituent in *para* position, where

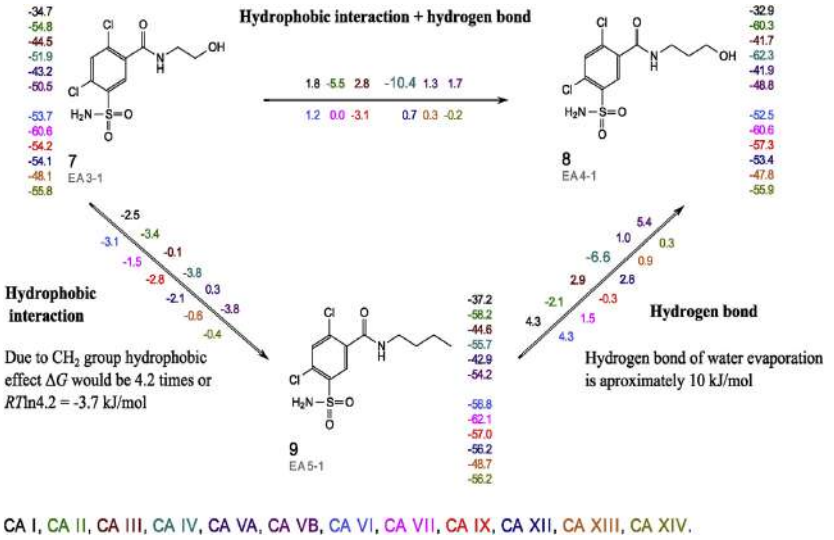

Fig. 5. Binding affinities of structurally related compounds **7**–**9** interacting with 12 CA isoforms and the explanation of binding affinities based on the hydrophobic interaction and hydrogen bond formation of model compounds.

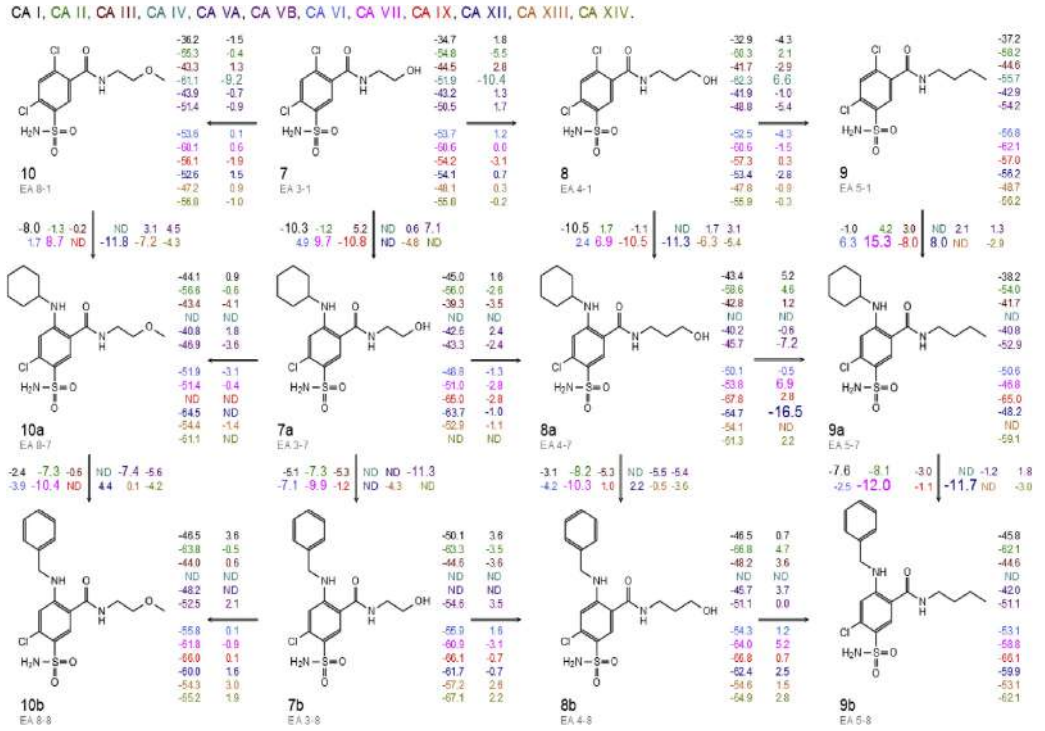

Fig. 6. Correlation map between the inhibitor chemical structures **7**–**10, 7**–**10(a**–**b)** and the intrinsic Gibbs energies of binding to CAs. Intrinsic ΔG_{b_intr} values are shown next to the chemical structures while the differences in the binding affinity between neighboring compounds are listed on the connecting arrows. Colors show different CA isoforms. (For interpretation of the references to color in this figure legend, the reader is referred to the Web version of this article.)

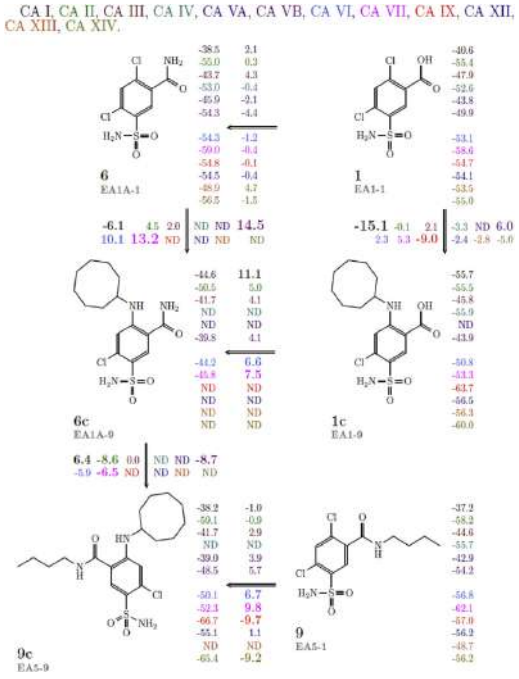

Fig. 7. Correlation map of the inhibitor chemical structures **1, 6, 9, (1, 6, 9)c** with the intrinsic Gibbs energies of binding to CAs. The intrinsic ΔG_{b_intr} values are shown next to the chemical structures while the differences in the binding affinity between neighboring compounds are listed on the connecting arrows. Colors show different CA isoforms. (For interpretation of the references to color in this figure legend, the reader is referred to the Web version of this article.)

longer benzyl group becomes more flexible and suitable for the active sites of all CA isoforms, making benzylamino substituted dual-tailed sulfonamides high affinity, but not so selective CA inhibitors as cyclohexylamino substituted analogs. X-ray crystallographic structures of several compound-CA complexes showed the contacts between the tails and amino acids providing insights into structure-thermodynamics correlations.

4. Experimental

4.1. Chemistry

All starting materials and reagents were commercial products and were used without further purification. Melting points of the compounds were determined in open capillaries on a Thermo Scientific 9100 Series and are uncorrected. ^{1}H and ^{13}C NMR spectra were recorded on a (400 and 100 MHz, respectively) spectrometer in DMSO-d_6 using residual DMSO signals (2.52 ppm and 40.21 ppm for ^{1}H and ^{13}C NMR spectra, respectively) as the internal standard. TLC was performed with silica gel 60 F254 aluminum plates (Merck) and visualized with UV light. Column chromatography was performed using silica gel 60 (0.040–0.063 mm, Merck). High-resolution mass spectra (HRMS) were recorded on a Dual-ESI Q-TOF 6520 mass spectrometer (Agilent Technologies). The purity of final compounds was verified by HPLC to be >95% using the Agilent 1290 Infinity instrument with a Poroshell 120 SB-C18 (2.1 mm × 100 mm, 2.7 μm) reversed-phase column. Analytes were eluted using a linear gradient of water/methanol (20 mM ammonium formate in both phases) from 60:40 to 30:70 over 12 min, then from 30:70 to 20:80 over 1 min, and then 20:80 over 5 min at a flow rate of 0.2 mL/min. UV detection was at 254 nm.

4.1.1. 2,4-Dibromo-5-methylaniline hydrochloride (**4**)

N-(3-tolyl)acetamide was synthesized by the known procedure [47]. Bromine (4.65 mL, 90 mmol) was added dropwise to the solution of N-(3-tolyl)acetamide (6.12 g, 41.0 mmol) in two portions. The first part was added at room temperature, the other at 60–70 °C. The reaction mixture was stirred for 15 h at 70 °C, cooled and washed with 10% Na_2SO_3. After removal of the solvent, the residue was crystallized from H_2O:MeOH (1:1) to obtain N-(2,4-dibromo-5-methyl-phenyl)acetamide. Yield 11.6 g, 92%, mp 168–169 °C(lit. 170–171 °C [48]).

N-(2,4-dibromo-5-methyl-phenyl)acetamide (11.6 g, 37.8 mmol) was refluxed in methanol (12 mL) and concentrated HCl (aq) (3 mL) solution for 10 h. After removal of the solvents, the residue was separated by filtration and washed with ice-cold water. Yield: 7.19 g, 63%, mp 165–167 °C (dec.). ^{1}H NMR δ ppm: 2.20 (3H, s, CH_3), 6.81 (3H, br s, NH_3^+), 6.91 (1H, s, C_6-H), 7.57 (1H, s, C_3-H). ^{13}C NMR δ ppm: 22.5, 106.9, 111.7, 118.9, 134.7, 137.6, 143.7.

4.1.2. 2,4-Dibromo-5-methyl-benzenesulfonamide (**5**)

A solution of $NaNO_2$ (2.77 g, 40.1 mmol) in water (7 mL) was added dropwise to a suspension of **4** (7.11 g, 22.8 mmol) in a mixture of acetic acid (35 mL) and conc. HCl(aq) (14 mL) at 0–5 °C. The reaction mixture was stirred at 5 °C for 1 h, then a cold mixture of sulfur dioxide (8.06 g, 126 mmol) and cooper (II) chloride dihydrate(1.34 g, 7.86 mmol) in acetic acid (20 mL) at −15 °C was rapidly added. The reaction mixture was stirred for 24 h at 0 °C, and then the reaction mixture was diluted with water (40 mL) and extracted with toluene (3x30 mL). The extracts were washed with water and dried over anhydrous $MgSO_4$. After removal of the solvent, the oily residue was dissolved in 30 ml of THF and conc. ammonia (53 mL) was added dropwise at 0–5 °C. The mixture was allowed to stand 24 h at room temperature. The precipitated solid was separated by filtration and purified by recrystallization from H_2O:MeOH (1:1). Yield: 5.98 g, 77%, mp 219–221 °C. ^{1}H NMR δ ppm: 2.38 (3H, s, CH_3), 7.64 (2H, s, SO_2NH_2), 7.96 (1H, s, C_6-H), 8.08 (1H, s, C_3-H). ^{13}C NMR δ ppm: 22.4, 116.9, 128.6, 131.2, 137.6, 138.2, 142.4. HRMS calcd. for $C_7H_7Br_2NO_2S$ [$(M + H)^+$]: 329.8616 (100%), found: 329.8619 (100%).

4.1.3. 2,4-Dibromo-5-sulfamoyl-benzoic acid (**2**)

The solution of $KMnO_4$ (4.74 g, 30.0 mmol) in water (80 mL) was added dropwise to the suspension of **5** (2.21 g, 6.72 mmol) in water (60 mL) over a period of 5 h at 95 °C. The reaction mixture was stirred for 12 h at 95 °C, cooled and filtered to remove the MnO_2. The excess of $KMnO_4$ is removed by treatment with oxalic acid and the solution was acidified with hydrochloric acid to pH 1. The resulting precipitate was filtered off, washed with water and crystallized from H_2O:MeOH (4:1). Yield: 1.57 g, 65%, mp 237–239 °C.

^{1}H NMR δ ppm: 7.83 (2H, s, SO_2NH_2), 8.27 (1H, s, C_6-H), 8.33 (1H, s, C_3-H), 13,96 (1H, br s, COOH). ^{13}C NMR δ ppm: 122.9, 125.0, 131.3, 133.0, 140.0, 142.7, 166.1. HRMS calcd. for $C_7H_5Br_2NO_4S$ [$(M + H)^+$]: 359.8358 (100%), found: 359.8360 (100%).

4.1.4. General procedure for the syntheses of **6**–**16**

The mixture of 2,4-dihalo-5-sulfamoylbenzoic acid (**1** or **2**) (10.0 mmol), $SOCl_2$ (2–3 eq), and 1 drop DMF in toluene (5 mL) was refluxed for 4 h. Excess $SOCl_2$ and toluene were removed by

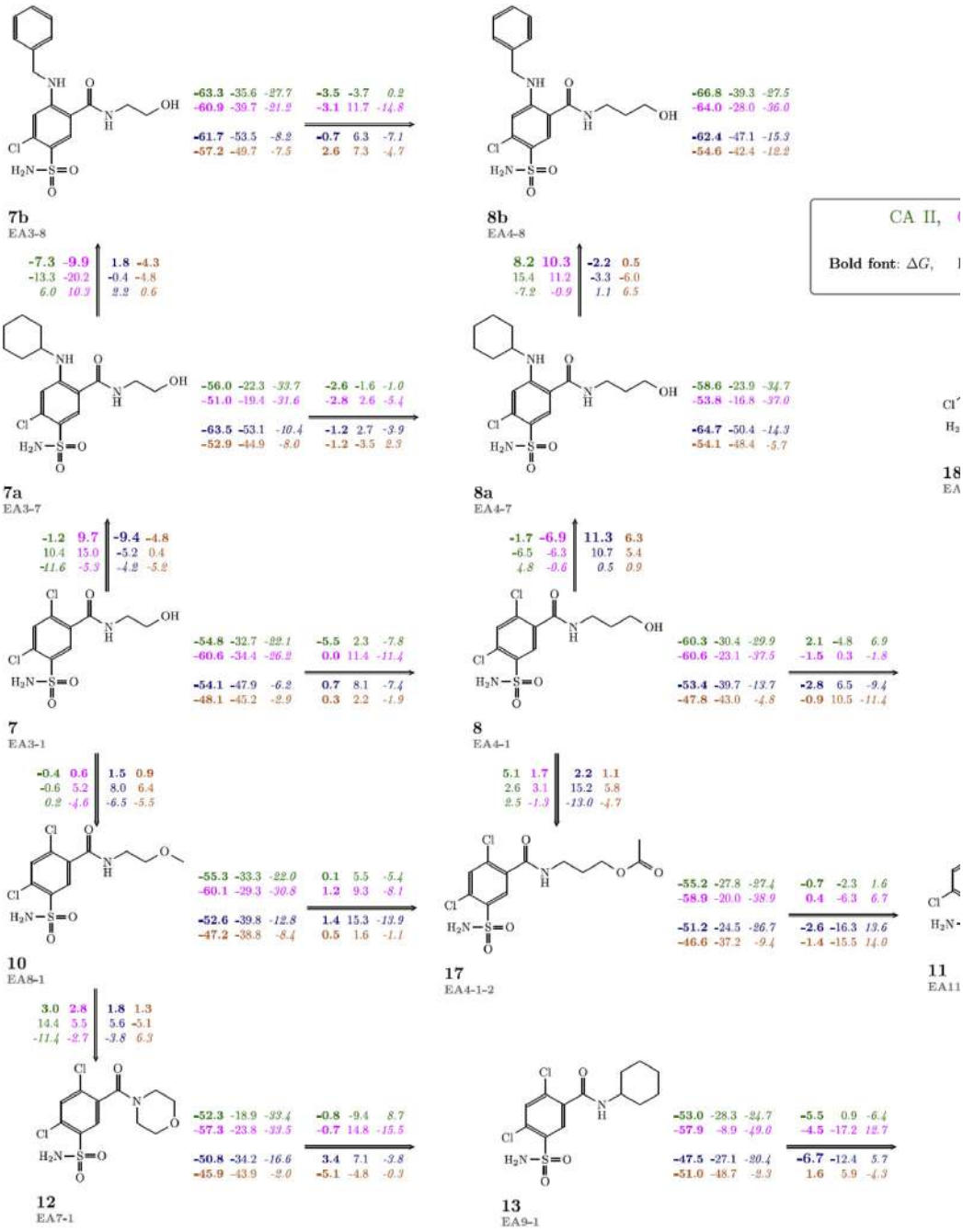

Fig. 8. Correlation map of the inhibitor chemical structures **7**–**14, 17**–**18, 7**–**8(a,b)** with the intrinsic thermodynamic parameters of bin (regular), and $-T\Delta S_{intr}$ (italic) values are shown next to the chemical structures. Differences in the binding thermodynamics between connecting arrows. Colors show different CA isoforms. (For interpretation of the references to color in this figure legend, the reader is

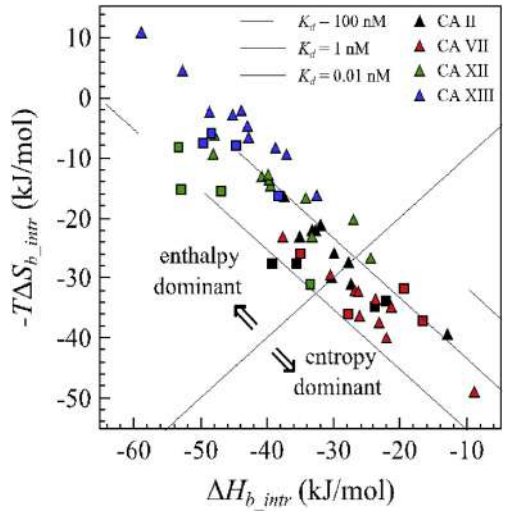

Fig. 9. The intrinsic enthalpy-entropy compensation graph. Colors represent CA isozymes (black - CA II, red - CA VII, green - CA XII, and blue - CA XIII). Squares correspond the two-tailed benzenesulfonamides, while triangles – benzenesulfonamides bearing the tail in *meta* position. Diagonal lines represent the K_ds (solid line - 0.01 nM, dashed is 1 nM, and dotted is 100 nM). (For interpretation of the references to color in this figure legend, the reader is referred to the Web version of this article.)

*4.1.4.3. 2,4-Dichloro-N-(3-hydroxypropyl)-5-sulfamoyl-benzamide (**8**, EA4-1).* [39].

*4.1.4.4. N-butyl-2,4-dichloro-5-sulfamoyl-benzamide (**9**, EA5-1).* Recrystallization was accomplished from toluene:MeOH (5:1). Yield: 3.03 g, 93%, mp 184–186 °C(lit. 180 °C [40]). ^{1}H NMR δ ppm: 0.91 (3H, t, J = 7.2 Hz, CH_3), 1.36 (2H, sext, J = 7.2 Hz, CH_2), 1.50 (2H, quint, J = 7.2 Hz, CH_2), 3.24 (2H, q, J = 6.8 Hz, $NH\underline{CH_2}$), 7.81 (2H, s, SO_2NH_2), 7.90 (1H, s, C_3-H), 7.94 (1H, s, C_6-H), 8.62 (1H, t, J = 5.6 Hz, NH). ^{13}C NMR δ ppm: 14.1, 20.0, 31.4, 39.2, 129.1, 132.1, 132.5, 134.4, 136.5, 140.4, 164.8. HRMS calcd. for $C_{11}H_{14}Cl_2N_2O_3S$ [(M + H)$^+$]: 325.0175, found: 325.0174.

*4.1.4.5. 2,4-Dichloro-N-(2-methoxyethyl)-5-sulfamoyl-benzamide (**10**, EA8-1).* Recrystallization was accomplished from toluene:-MeOH (5:1). Yield: 2.13 g, 65%, mp 137–139 °C. ^{1}H NMR δ ppm: 3.29 (3H, s, CH_3), 3.38–3.43 (2H, m, $NH\underline{CH_2}$), 3.45–3.48 (2H, m, OCH_2), 7.80 (2H, s, SO_2NH_2), 7.91 (1H, s, C_3-H), 7.93 (1H, s, C_6-H), 8.74 (1H, t, J = 5.6 Hz, NH). ^{13}C NMR δ ppm: 39.4, 58.4, 70.7, 129.2, 132.2, 132.5, 134.5, 136.3, 140.3, 165.1. HRMS calcd. for $C_{10}H_{12}Cl_2N_2O_4S$ [(M + H)$^+$]: 326.9968, found: 326.9967.

*4.1.4.6. Methyl 4-[(2,4-dichloro-5-sulfamoyl-benzoyl)amino]butanoate (**11**, EA11-1).* The product was purified by chromatography on a column of silica gel with EtOAc, R_f = 0.80. Yield: 2.03 g, 55%, mp 138–140 °C. ^{1}H NMR δ ppm: 1.77 (2H, quint, J = 7.2 Hz, CH_2), 2.41 (2H, t, J = 7.6 Hz, $COCH_2$), 3.27 (2H, q, J = 6.8 Hz, $NH\underline{CH_2}$), 3.61 (3H, m, CH_3), 7.82 (2H, s, SO_2NH_2), 7.92 (1H, s, C_3-H), 7.95 (1H, s, C_6-H), 8.69 (1H, t, J = 5.6 Hz, NH). ^{13}C NMR δ ppm: 24.7, 31.1, 38.9, 51.8, 129.2, 132.2, 132.5, 134.4, 136.3, 140.4, 165.0, 173.5. HRMS calcd. for $C_{12}H_{14}Cl_2N_2O_5S$[(M + H)$^+$]: 369.0073, found: 369.0074.

*4.1.4.7. 2,4-Dichloro-5-(morpholine-4-carbonyl)benzenesulfonamide (**12**, EA7-1).* Recrystallization was accomplished from EtOAc. Yield: 2.34 g, 69%, mp 235–236 °C. ^{1}H NMR δ ppm: 3.17–3.20 (2H, m, CH_2), 3.54–3.57 (2H, m, CH_2), 3.58–3.74 (4H, m, $2CH_2$), 7.82 (2H, s, SO_2NH_2), 7.93 (1H, s, C_3-H), 7.98 (1H, s, C_6-H). ^{13}C NMR δ ppm: 42.2, 47.1, 66.3, 66.6, 128.6, 132.2, 132.5, 133.8, 134.9, 141.0, 164.3. HRMS calcd. for $C_{11}H_{12}Cl_2N_2O_4S$[(M + H)$^+$]: 338.9968, found: 338.9966.

*4.1.4.8. 2,4-Dichloro-N-cyclohexyl-5-sulfamoyl-benzamide (**13**, EA9-1).* Recrystallization was accomplished from H_2O:MeOH (1:1) and then from toluene:MeOH (5:1). Yield: 2.21 g, 63%, mp 214–215 °C. ^{1}H NMR δ ppm: 1.17–1.34 (5H, m, Cy-H), 1.57–1.59 (1H, m, Cy-H), 1.71 (2H, br s, Cy-H), 1.84–1.86 (2H, m, Cy-H), 3.73 (1H, br s, Cy-H), 7.82 (2H, s, SO_2NH_2), 7.88 (1H, s, C_3-H), 7.93 (1H, s, C_6-H), 8.56 (1H, d, J = 7.2 Hz, NH). ^{13}C NMR δ ppm: 24.9, 25.6, 32.5, 48.8, 129.0, 132.0, 132.4, 134.5, 136.7, 140.3, 164.0. HRMS calcd. for $C_{13}H_{16}Cl_2N_2O_3S$[(M + H)$^+$]: 351.0331, found: 351.0335.

*4.1.4.9. N-benzyl-2,4-dichloro-5-sulfamoyl-benzamide (**14**, EA10-1).* Recrystallization was accomplished from H_2O:MeOH (1:1) and then from toluene:MeOH (5:1). Yield: 3.05 g, 85%, mp 179–181 °C. ^{1}H NMR δ ppm: 4.49 (2H, d, J = 6.0 Hz, CH_2), 7.26–7.33 (1H, m, Ph-H), 7.35–7.40 (4H, m, Ph-H), 7.84 (2H, s, SO_2NH_2), 7.96 (1H, s, C_3-H), 7.97 (1H, s, C_6-H), 9.21 (1H, t, J = 6.0 Hz, NH). ^{13}C NMR δ ppm: 43.1, 127.5, 127.8, 128.9, 129.3, 132.3, 132.6, 134.5, 136.1, 139.2, 140.4, 165.0. HRMS calcd. for $C_{14}H_{12}Cl_2N_2O_3S$[(M + H)$^+$]: 359.0018, found: 359.0017.

*4.1.4.10. 2,4-Dibromo-N-(2-hydroxyethyl)-5-sulfamoyl-benzamide (**15**, LJ14-5).* Recrystallization was accomplished from MeOH. Yield: 1.41 g, 35%, mp 196–198 °C. ^{1}H NMR δ ppm: 3.30 (2H, q, J = 6.0 Hz, $NH\underline{CH_2}$), 3.51 (2H, br s, $\underline{CH_2}OH$), 4.77 (1H, s, OH), 7.74 (2H, s, SO_2NH_2), 7.91 (1H, s, C_6-H), 8.19 (1H, s, C_3-H), 8.64 (1H, t, J = 6.0 Hz, NH). ^{13}C NMR δ ppm: 42.5, 59.9, 120.4, 123.6, 129.0, 138.5, 139.1, 142.5, 166.2. HRMS calcd. for $C_9H_{10}Br_2N_2O_4S$[(M + H)$^+$]: 402.8780 (100%), found: 402.8782 (100%).

*4.1.4.11. 2,4-Dibromo-N-butyl-5-sulfamoyl-benzamide (**16**, LJ14-6).* Recrystallization was accomplished from MeOH:H_2O (1:1). Yield: 1.33 g, 31%, mp 218–220 °C. ^{1}H NMR δ ppm: 0.91 (3H, t, J = 7.2 Hz, CH_3), 1.36 (2H, sext, J = 7.2 Hz, CH_2), 1.50 (2H, quint, J = 7.2 Hz, CH_2), 3.23 (2H, q, J = 6.8 Hz, $NH\underline{CH_2}$), 7.79 (2H, s, SO_2NH_2), 7.86 (1H, s, C_6-H), 8.20 (1H, s, C_3-H), 8.61 (1H, t, J = 5.6 Hz, NH). ^{13}C NMR δ ppm: 14.1, 20.0, 31.4, 39.2, 120.3, 123.5, 128.8, 138.5, 139.3, 142.6, 165.9. HRMS calcd. for $C_{12}H_{16}Br_2N_2O_3S$[(M + H)$^+$]: 428.9301 (100%), found: 428.9297 (100%).

*4.1.5. 3-[(2,4-Dichloro-5-sulfamoyl-benzoyl)amino]propyl acetate (**17**, EA4-1-2)*
[39].

*4.1.6. General procedure for the syntheses of (**7**–**10**)**a**, (**7**–**10**, **14**)**b**, (**6**, **9**)**c***

The mixture of appropriate 2,4-dichloro-*N*-substituted-5-sulfamoylbenzamide (compounds **6**–**10, 14**) (1.00 mmol) was heated in appropriate amine (6 mmol) at 120 °C for 3–4 h. The mixture was cooled to room temperature and 2N HCl(aq) (2 mL) was added. The resultant precipitate was washed with H_2O.

*4.1.6.1. 4-Chloro-2-(cyclooctylamino)-5-sulfamoyl-benzamide (**6c**, EA1A-9).* Recrystallization was accomplished twice from H_2O:2-PrOH (2:1). Yield: 216 mg, 60%, mp 242–244 °C. ^{1}H NMR δ ppm: 1.44–1.72 (12H, m, cyclooctyl-H), 1.75–1.86 (2H, m, cyclooctyl-H), 3.67 (1H, br s, cyclooctyl-H), 6.75 (1H, s, C_3-H), 7.17 (2H, s, SO_2NH_2), 7.37 (1H, brs, $CONH_2$), 8.08 (1H, brs, $CONH_2$), 8.14 (1H, s,

Table 3
Data collection and refinement statistics of human CA complexes with inhibitors **7a**, **7b**, and **9**. All datasets were collected at 100 K, test set size was 10%. Crystallization conditions of each preparation are shown in the Supplementary material.

Isoform-ligand	CA II - 9 *(EA5-1)*	CA XIII - 9 *(EA5-1)*	CA XII - 7a *(EA3-7)*	CA XII – 7b *(EA3-8)*
PDB ID	6G6T	6G5U	6G5L	6G7A
Data-collection statistics				
Space group	$P12_11$	$P2_12_12_1$	$P12_11$	$P12_11$
Unit-cell parameters (Å)	a = 42.1, b = 41.2, c = 72.1, β = 104.2°	a = 55.8, b = 58.3, c = 160.8	a = 77.1, b = 74.2, c = 91.5, β = 108.6°	a = 77.3, b = 73.9, c = 91.2, β = 108.9°
Resolution range (Å)	1.1–41.2	1.7–58.3	1.2–73.1	1.4–86.3
Wavelength (Å)	0.975522	1.54178	0.975522	1.0332
Radiation source	EMBL, P14	Rigaku MicroMax™-007 HF	EMBL, P14	EMBL, P13
Unique reflections number	86201	57444	284311	173178
R_{merge}, overall (outer shell)	0.052(0.064)	0.121 (0.444)	0.043 (0.421)	0.036 (0.186)
I/σ overall (outer shell)	28.4(15.4)	6.6 (2.8)	20.2 (4.6)	24.8 (7.0)
Multiplicity overall (outer shell)	6.4 (5.0)	4.6 (5.1)	7.0 (6.6)	6.8 (6.0)
Completeness (%) overall (outer shell)	94.3 (73.4)	98.2 (100.0)	95.9 (92.9)	94.9 (77.2)
Wilson B-factor	8.1	16.2	12.4	13.1
Refinement statistics:				
R_{work}	0.143	0.192	0.136	0.153
R_{free}	0.177	0.229	0.174	0.186
RMSD bond lengths, (Å)	0.030	0.020	0.029	0.025
RMSD bond angles (°)	2.837	1.952	2.544	2.332
Average B factors (Å²):				
all	16.1	16.6	20.2	17.0
main-chain	12.3	13.7	16.5	13.7
side-chain	16.1	16.6	20.9	17.0
inhibitors	15.8	20.3	16.0	17.2
waters	28.5	25.1	30.4	27.3
zinc	6.1	9.2	9.9	7.9
other molecules	26.9	31.5	40.2	29.9
Number of atoms:				
all	2521	4837	9751	10216
protein	2158	4165	8501	8683
inhibitor	19	38	144	125
water	328	607	1036	1356
zinc	1	2	4	4
other molecules	15	25	66	48
Ramachandran statistics (%):				
most favored regions	96	97	97	97
additionally allowed regions	4	3	3	3
outliers	0	0	0	0

C_6-H), 8.77 (1H, d, J = 8.0 Hz, cyclooctyl-NH). ^{13}C NMR δ ppm: 23.4, 25.4, 27.3, 31.5, 51.4, 111.8, 113.4, 125.7, 131.3, 135.2, 151.4, 170.8. HRMS calcd. for $C_{15}H_{22}ClN_3O_3S$ [(M + H)$^+$]: 360.1143, found: 360.1139.

*4.1.6.2. 4-Chloro-2-(cyclohexylamino)-N-(2-hydroxyethyl)-5-sulfamoyl-benzamide (**7a**, EA3-7).* The product was purified by chromatography on a column of silica gel with EtOAc, R_f = 0.65 and then the recrystallization was accomplished from toluene:2-PrOH (5:1). Yield: 90.2 mg, 24%, mp 210–212 °C. ^{1}H NMR δ ppm: 1.20–1.30 (3H, m, Cy-H), 1.38–1.46 (2H, m, Cy-H), 1.55–1.58 (1H, m, Cy-H), 1.64–1.68 (2H, m, Cy-H), 1.86–1.89 (2H, m, Cy-H), 3.29 (2H, q, J = 6.0 Hz, NH<u>CH$_2$</u>), 3.48–3.54 (3H, m, <u>CH$_2$</u>OH, Cy-H), 4.72 (1H, t, J = 5.6 Hz, OH), 6.86 (1H, s, C_3-H), 7.17 (2H, s, SO_2NH_2), 8.11 (1H, s, C_6-H), 8.51 (1H, d, J = 8.0 Hz, CyNH), 8.56 (1H, t, J = 5.6 Hz, CONH). ^{13}C NMR δ ppm: 24.3, 25.7, 32.4, 40.6, 49.9, 60.0, 112.4, 113.1, 125.8, 130.7, 135.0, 151.3, 168.4. HRMS calcd. for $C_{15}H_{22}ClN_3O_4S$ [(M + H)$^+$]: 376.1092, found: 376.1092.

*4.1.6.3. 2-(Benzylamino)-4-chloro-N-(2-hydroxyethyl)-5-sulfamoyl-benzamide (**7b**, EA3-8).* Recrystallization was accomplished three times from toluene:2-PrOH (8:1). Yield: 61.4 mg, 16%, mp 225–228 °C. ^{1}H NMR δ ppm: 3.31 (2H, q, J = 6.0 Hz, NH<u>CH$_2$</u>), 3.51 (2H, t, J = 6.0 Hz, <u>CH$_2$</u>OH), 4.49 (2H, d, J = 5.6 Hz, NH<u>CH$_2$</u>Ph), 4.73 (1H, br s, OH), 6.76 (1H, s, C_3-H), 7.19 (2H, s, SO_2NH_2), 7.25–7.39 (5H, m, Ph-H), 8.12 (1H, s, C_6-H), 8.62 (1H, t, J = 5.6 Hz, <u>NH</u>Bn), 8.75 (1H, t, J = 5.6 Hz, CONH). ^{13}C NMR δ ppm: 42.4, 46.2, 60.0, 113.4, 113.5, 126.6, 127.5, 127.6, 129.1, 130.4, 134.7, 138.9, 151.9, 168.2. HRMS calcd. for $C_{16}H_{18}ClN_3O_4S$ [(M + H)$^+$]: 384.0779, found: 384.0781.

*4.1.6.4. 4-Chloro-2-(cyclohexylamino)-N-(3-hydroxypropyl)-5-sulfamoyl-benzamide (**8a**, EA4-7).* Recrystallization was accomplished from: toluene:2-PrOH (1:1). Yield: 179 mg, 46%, mp 192–194 °C. ^{1}H NMR δ ppm: 1.20–1.30 (3H, m, Cy-H), 1.37–1.49 (2H, m, Cy-H), 1.56–1.58 (1H, m, Cy-H), 1.63–1.68 (4H, m, Cy-H, CH_2), 1.87–1.89 (2H, m, Cy-H), 3.27 (2H, q, J = 6.4 Hz, NH<u>CH$_2$</u>), 3.46 (2H, t, J = 6.4 Hz, <u>CH$_2$</u>OH), 3.51 (1H, br s, Cy-H), 4.41 (1H, br s, OH), 6.85 (1H, s, C_3-H), 7.17 (2H, s, SO_2NH_2), 8.09 (1H, s, C_6-H), 8.49 (1H, d, J = 7.6 Hz, CyNH), 8.61 (1H, t, J = 5.2 Hz, CONH). ^{13}C NMR δ ppm: 24.3, 25.7, 32.4, 32.7, 39.4, 49.9, 59.1, 112.5, 113.1, 125.8, 130.6, 135.0, 151.3, 168.3. HRMS calcd. for $C_{16}H_{24}ClN_3O_4S$ [(M + H)$^+$]: 390.1249, found: 390.1252.

*4.1.6.5. 2-(Benzylamino)-4-chloro-N-(3-hydroxypropyl)-5-sulfamoyl-benzamide (**8b**, EA4-8).* The product was purified by chromatography on a column of silica gel with EtOAc:$CHCl_3$ (2:1), R_f = 0.25. Yield: 171 mg, 43%, mp 179–182 °C. ^{1}H NMR δ ppm: 1.68 (2H, quint, J = 6.8 Hz, CH_2), 3.29 (2H, q, J = 6.4 Hz, NH<u>CH$_2$</u>),

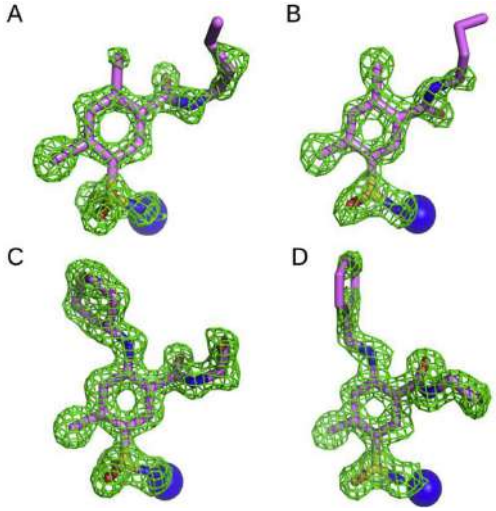

Fig. 10. Crystal structures described in this study. The electron density |F(o)-F(c)| of the ligands is calculated in the absence of ligand and contoured at 3σ as green mesh. Zinc ion is shown as a blue sphere. **A**, Compound **9** (EA5-1) bound to CA II (PDB ID 6G6T); **B**, Compound **9** (EA5-1) bound to CA XIII (subunit A, PDB ID 6G5U); **C**, Compound **7a** (EA3-7) bound to CA XII (subunit D, PDB ID 6G5L); **D**, Compound **7b** (EA3-8) bound to CA XII (subunit A, PDB ID 6G7A). (For interpretation of the references to color in this figure legend, the reader is referred to the Web version of this article.)

3.45–3.49 (2H, m, $\underline{CH_2}OH$), 4.48 (3H, d, $J = 6.0$ Hz, NH$\underline{CH_2}$Ph, OH), 6.76 (1H, s, C_3-H), 7.20 (2H, s, SO_2NH_2), 7.26–7.39 (5H, m, Ph-H), 8.10 (1H, s, C_6-H), 8.68 (1H, t, $J = 5.6$ Hz, $\underline{NH}$Bn), 8.74 (1H, t, $J = 5.6$ Hz, CONH). ^{13}C NMR δ ppm: 32.7, 39.6, 46.2, 59.1, 113.4, 113.7, 126.6, 127.5, 127.6, 129.1, 130.3, 134.7, 138.9, 151.9, 168.0. HRMS calcd. for $C_{17}H_{20}ClN_3O_4S$ [$(M + H)^+$]: 398.0936, found: 398.0936.

*4.1.6.6. N-butyl-4-chloro-2-(cyclohexylamino)-5-sulfamoyl-benzamide (**9a**, EA5-7).* The product was purified by chromatography on a column of silica gel with $CHCl_3$:EtOAc (5:1), $R_f = 0.33$. Yield: 167 mg, 43%, mp 182–184 °C. ^{1}H NMR δ ppm: 0.90 (3H, t, $J = 7.2$ Hz, CH_3), 1.20–1.58 (10H, m, Cy-H, CH_2CH_2), 1.64–1.67 (2H, m, Cy-H), 1.87–1.89 (2H, m, Cy-H), 3.21 (2H, q, $J = 6.4$ Hz, NH$\underline{CH_2}$), 3.50 (1H, br s, Cy-H), 6.85 (1H, s, C_3-H), 7.17 (2H, s, SO_2NH_2), 8.09 (1H, s, C_6-H), 8.47 (1H, d, $J = 7.6$ Hz, CyNH), 8.62 (1H, t, $J = 5.2$ Hz, CONH). ^{13}C NMR δ ppm: 14.2, 20.1, 24.2, 25.7, 31.5, 32.4, 39.4, 49.9, 112.7, 113.0, 125.8, 130.6, 134.9, 151.3, 168.2. HRMS calcd. for $C_{17}H_{26}ClN_3O_3S$ [$(M + H)^+$]: 388.1456, found: 388.1456.

*4.1.6.7. 2-(Benzylamino)-N-butyl-4-chloro-5-sulfamoyl-benzamide (**9b**, EA5-8).* Recrystallization was accomplished from toluene:2-PrOH (8:1). Yield: 91.1 mg, 23%, mp 204–206 °C. ^{1}H NMR δ ppm: 0.91 (3H, t, $J = 7.2$ Hz, CH_3), 1.33 (2H, sext, $J = 7.2$ Hz, CH_2),1.50 (2H, quint, $J = 7.2$ Hz, CH_2), 3.23 (2H, q, $J = 6.8$ Hz, CONH$\underline{CH_2}$), 4.48 (2H, d, $J = 5.6$ Hz, NH$\underline{CH_2}$Ph), 6.76 (1H, s, C_3-H), 7.19 (2H, s, SO_2NH_2), 7.25–7.39 (5H, m, Ph-H), 8.10 (1H, s, C_6-H), 8.68 (1H, t, $J = 5.6$ Hz, $\underline{NH}$Bn), 8.72 (1H, t, $J = 6.0$ Hz, CONH). ^{13}C NMR δ ppm: 14.2, 20.1, 31.5, 39.1, 46.2, 113.4, 113.8, 126.6, 127.5, 127.6, 129.1, 130.3, 134.6, 138.9, 151.9, 167.9. HRMS calcd. for $C_{18}H_{22}ClN_3O_3S$ [$(M + H)^+$]: 396.1143, found: 396.1145.

*4.1.6.8. N-butyl-4-chloro-2-(cyclooctylamino)-5-sulfamoyl-benzamide (**9c**, EA5-9).* The product was purified by chromatography on a column of silica gel with $CHCl_3$:EtOAc (5:1), $R_f = 0.35$. Yield: 112 mg, 27%, mp 172–174 °C. ^{1}H NMR δ ppm: 0.90 (3H, t, $J = 7.2$ Hz, CH_3), 1.32 (2H, sext, $J = 7.2$ Hz, CH_2), 1.45–1.65 (14H, m, cyclooctyl-H, CH_2), 1.78–1.83 (2H, m, cyclooctyl-H), 3.19–3.23 (2H, m, NH$\underline{CH_2}$), 3.66 (1H, br s, cyclooctyl-H), 6.75 (1H, s, C_3-H), 7.17 (2H, s, SO_2NH_2), 8.10 (1H, s, C_6-H), 8.52 (1H, d, $J = 7.6$ Hz, cyclooctyl-NH), 8.62 (1H, br s, CONH). ^{13}C NMR δ ppm: 14.2, 20.1, 23.4, 25.4, 27.3, 31.4, 31.5, 39.1, 51.4, 112.8, 113.3, 125.8, 130.6, 134.9, 151.1, 168.2. HRMS calcd. for $C_{19}H_{30}ClN_3O_3S$ [$(M + H)^+$]: 416.1769, found: 416.1770.

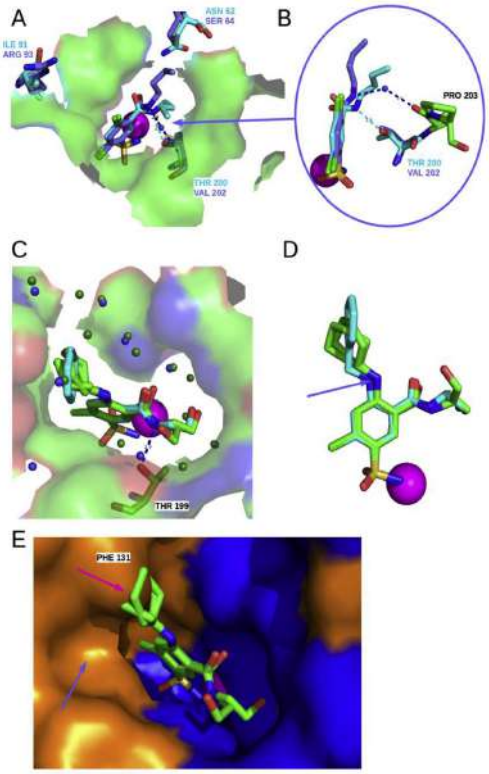

Fig. 11. The binding of **7a**, **7b**, and **9** to CA isoforms as determined by X-Ray crystallography. Zinc ion is shown as a pink sphere. **A**, The comparison of compound **9** binding in the active site of CA II (PDB ID 6G6T) and CA XIII (PDB ID 6G5U, subunit A). Residues conserved between CA II and CA XIII is shown as a green surface. Residues, different between isoforms that contact with the ligand are shown as stick model (CA II - cyan and CA XIII - blue). **B**, Detailed view of the interaction between *meta*-substituent of compound **9** and active site residues of CA II and CA XIII. **C**, The comparison of the binding mode of compounds **7a** (green, subunit A, PDB ID 6G5L) and **7b** (cyan, subunit A, PDB ID 6G7A) in the active site of CA XII. The surface is colored by CPK color scheme. Water molecules found in the crystal structures are shown as small spheres (green in CA XII-**7a**, and blue in CA XII-**7b**). **D**, A closer view showing slightly different positions of benzene ring of **7a** and **7b** and varied conformations of *meta*- and *para*-substituents. **E**, Superposition of subunits A from the crystal structures CA XII-**7a** and CA II-**9**. The surface of CA II and the compound **7a** are presented. The steric clash between Phe131 (CA II) and the *para*-substituent of compound **7a** is marked as a pink arrow. The surface of the hydrophobic residues (Val, Ile, Leu, Phe, Met, Ala, Gly, and Pro) is colored orange in the active site of CA II, whereas the charged and polar side chains (Arg, Asp, Asn, Glu, Gln, His, Lys, Ser, Thr, Tyr, Trp, and Cys) are colored blue. The blue arrow points to the hydrophobic cavity, which is presumably the binding site for the hydrophobic moiety of *para*-substituent in active site of CA II. (For interpretation of the references to color in this figure legend, the reader is referred to the Web version of this article.)

*4.1.6.9. 4-Chloro-2-(cyclohexylamino)-N-(2-methoxyethyl)-5-sulfamoyl-benzamide (**10a**, EA8-7).* The product was purified by chromatography on a column of silica gel with $CHCl_3$:EtOAc (3:1), $R_f = 0.21$. Yield: 129 mg, 33%, mp 214–216 °C. ^{1}H NMR δ ppm: 1.16–1.30 (3H, m, Cy-H), 1.37–1.47 (2H, m, Cy-H), 1.55–1.58 (1H, m, Cy-H), 1.64–1.68 (2H, m, Cy-H), 1.86–1.92 (2H, m, Cy-H), 3.27 (3H, m, CH_3), 3.35–3.40 (2H, m, $NHCH_2$), 3.43–3.46 (2H, m, OCH_2), 3.47–3.60 (1H, m, Cy-H), 6.87 (1H, s, C_3-H), 7.19 (2H, s, SO_2NH_2), 8.11 (1H, s, C_6-H), 8.50 (1H, d, $J = 8.0$ Hz, CyNH),8.68 (1H, t, $J = 5.6$ Hz, CONH). ^{13}C NMR δ ppm: 24.3, 25.7, 32.4, 39.2, 49.9, 58.4, 70.7, 112.2, 113.1, 125.8, 130.7, 135.1, 151.3, 168.4. HRMS calcd. for $C_{16}H_{24}ClN_3O_4S$ [$(M + H)^+$]: 390.1249, found: 390.1247.

*4.1.6.10. 2-(Benzylamino)-4-chloro-N-(2-methoxyethyl)-5-sulfamoyl-benzamide (**10b**, EA8-8).* The product was purified by chromatography on a column of silica gel with $CHCl_3$:EtOAc (1:1), $R_f = 0.25$. Yield: 163 mg, 41%, mp 194–197 °C. ^{1}H NMR δ ppm: 3.28 (3H, s, CH_3), 3.38–3.42 (2H, m, $CONHCH_2$), 3.45–3.47 (2H, m, OCH_2), 4.49 (2H, d, $J = 5.6$ Hz, $NHCH_2Ph$), 6.77 (1H, s, C_3-H), 7.21 (2H, s, SO_2NH_2), 7.25–7.39 (5H, m, Ph-H), 8.12 (1H, s, C_6-H), 8.75 (2H, br s, BnNH, CONH). ^{13}C NMR δ ppm: 39.2, 46.2, 58.4, 70.7, 113.3, 113.4, 126.6, 127.5, 127.6, 129.1, 130.4, 134.8, 138.8, 151.9, 168.2. HRMS calcd. for $C_{17}H_{20}ClN_3O_4S$ [$(M + H)^+$]: 398.0936, found: 398.0932.

*4.1.6.11. N-benzyl-2-(benzylamino)-4-chloro-5-sulfamoyl-benzamide (**14b**, EA10-8).* The product was purified by chromatography on a column of silica gel with $CHCl_3$:EtOAc (10:1), $R_f = 0.13$. Yield: 116 mg, 27%, mp 213–216 °C. ^{1}H NMR δ ppm: 4.45 (2H, d, $J = 6.0$ Hz, $CONHCH_2$), 4.50 (2H, d, $J = 6.0$ Hz, $NHCH_2$), 6.80 (1H, s, C_3-H), 7.22 (2H, s, SO_2NH_2), 7.26–7.39 (10H, m, Ph-H), 8.22 (1H, s, C_6-H), 8.82 (1H, t, $J = 6.0$ Hz, BnNH), 9.30 (1H, t, $J = 6.0$ Hz, $CONH_2$). ^{13}C NMR δ ppm: 42.9, 46.2, 113.1, 113.6, 126.6, 127.3, 127.5, 127.6, 127.7, 128.8, 129.1, 130.4, 134.9, 138.8, 139.9, 152.1, 168.1. HRMS calcd. for $C_{21}H_{20}ClN_3O_3S$ [$(M + H)^+$]: 430.0987, found: 430.0987.

*4.1.7. Procedure for the syntheses of **16**(**a**,**b**)*

The mixture of 2,4-dibromo-*N*-butyl-5-sulfamoyl-benzamide (**16**) (1.00 mmol), appropriate amine (2.50 mmol), and 1,4-dioxane was refluxed for 7 days. The solvent was removed under reduced pressure and 2N HCl(aq) (2 mL) was added. The resultant precipitate was washed with H_2O.

*4.1.7.1. 4-Bromo-N-butyl-2-(cyclohexylamino)-5-sulfamoyl-benzamide (**16a**, LJ15-35).* The product was purified by chromatography on a column of silica gel with EtOAc:$CHCl_3$(5:1), $R_f = 0.30$. Yield: 151 mg, 35%, mp 203–205 °C. ^{1}H NMR δ ppm: 0.90 (3H, t, $J = 7.2$, Hz, CH_3), 1.16–1.57 (10H, m, CH_3CH_2, $CH_3CH_2CH_2$, Cy-H), 1.64–1.67 (2H, m, Cy-H), 1.86–1.88 (2H, m, Cy-H), 3.20 (2H, q, $J = 6.8$ Hz, $NHCH_2$), 3.49–3.51 (1H, m, Cy-H), 7.02 (1H, s, C_3-H), 7.13 (2H, s, SO_2NH_2), 8.11 (1H, s, C_6-H), 8.41 (1H, d, $J = 7.6$ Hz, NHCy), 8.61 (1H, t, $J = 5.6$ Hz, $NHCH_2$). ^{13}C NMR δ ppm: 14.2, 20.1, 24.2, 25.7, 31.5, 32.4, 39.1, 49.8, 113.1, 116.6, 123.8, 127.4, 130.6, 151.0, 168.3. HRMS calcd. for $C_{17}H_{26}BrN_3O_3S$[$(M + H)^+$]: 434.0932 (100%), found: 434.0933 (100%).

*4.1.7.2. 2-(Benzylamino)-4-bromo-N-butyl-5-sulfamoyl-benzamide (**16b**, LJ15-36).* The product was purified by chromatography on a column of silica gel with EtOAc:$CHCl_3$(5:1), $R_f = 0.34$. Yield: 176 mg, 40%, mp 207–209 °C. ^{1}H NMR δ ppm: 0.90 (3H, t, $J = 7.2$, Hz, CH_3), 1.32 (2H, sext, $J = 7.2$ Hz, CH_3CH_2), 1.50 (2H, quint, $J = 7.2$ Hz, $CH_3CH_2CH_2$), 3.21 (2H, q, $J = 6.8$ Hz, $NHCH_2CH_2$), 4.48 (2H, d, $J = 5.6$ Hz, $NHCH_2Ph$), 6.95 (1H, s, C_3-H), 7.15 (2H, s, SO_2NH_2), 7.26–7.39 (5H, m, Ph-H), 8.11 (1H, s, C_6-H), 8.64–8.66 (2H, m, $NHCH_2Ph$, $NHCH_2$). ^{13}C NMR δ ppm: 14.2, 20.1, 31.5, 39.1, 46.2, 114.2, 117.0, 123.5, 127.5, 127.6, 128.2, 129.1, 130.3, 138.9, 151.6, 168.0. HRMS calcd. for $C_{18}H_{22}BrN_3O_3S$[$(M + H)^+$]: 442.0619 (100%), found: 442.0623 (100%).

*4.1.8. Procedure for the syntheses of **1c**, **18***

Appropriate compound (**6c, 11**) (0.500 mmol) was refluxed in methanol (2 mL), H_2O (1 mL), and concentrated HCl (aq) (1 mL) solution for 12–24 h. The progress of reaction was monitored by TLC. The reaction mixture was concentrated under reduced pressure.

*4.1.8.1. 4-Chloro-2-(cyclooctylamino)-5-sulfamoyl-benzoic acid (**1c**, EA1-9).* Recrystallization was accomplished from H_2O:MeOH (5:1). Yield: 115 mg, 64%, mp 255–257 °C. ^{1}H NMR δ ppm: 1.44–1.73 (12H, m, cyclooctyl-H), 1.77–1.89 (2H, m, cyclooctyl-H), 3.76 (1H, br s, cyclooctyl-H), 6.86 (1H, s, C_3-H), 7.31 (2H, s, SO_2NH_2), 8.39 (1H, s, C_6-H), 8.43 (1H, d, $J = 7.6$ Hz, cyclooctyl-NH), 13.26 (1H, br s, COOH). ^{13}C NMR δ ppm: 23.4, 25.4, 27.2, 31.5, 51.5, 107.8, 113.9, 126.3, 134.1, 136.9, 152.1, 169.4. HRMS calcd. for $C_{15}H_{21}ClN_2O_4S$ [$(M + H)^+$]: 361.0983, found 361.0987.

*4.1.8.2. 4-[(2,4-Dichloro-5-sulfamoyl-benzoyl)amino]butanoic acid (**18**, EA12-1).* Recrystallization was accomplished from NaOAc (20.6 mg, 0.251 mmol) solution in H_2O. Yield: 107 mg, 60%, mp 136–139 °C. ^{1}H NMR δ ppm: 1.74 (2H, quint, $J = 7.2$ Hz, CH_2), 2.31 (2H, t, $J = 7.2$ Hz, $COCH_2$), 3.27 (2H, q, $J = 6.8$ Hz, $NHCH_2$), 7.82 (2H, s, SO_2NH_2), 7.92 (1H, s, C_3-H), 7.95 (1H, s, C_6-H), 8.69 (1H, t, $J = 5.6$ Hz, NH), 12.11 (1H, br s, CO_2H). ^{13}C NMR δ ppm: 24.8, 31.4, 39.0, 129.1, 132.2, 132.5, 134.4, 136.4, 140.4, 164.9, 174.6. HRMS calcd. for $C_{11}H_{12}Cl_2N_2O_5S$ [$(M + H)^+$]: 354.9917, found: 354.9918.

Patent application has been submitted for the synthesized compounds as CA inhibitors (WO2017017505 (A1)).

4.2. Protein preparation

All recombinant human CA isoforms used in this study were expressed and purified as previously described: CA I [43], CA II [49], CA III, CA IV, CA VA, CA VB, CA VI, CA IX and CA XIV [31], CA VII and CAXIII [50], CA XII [51]. CAs were expressed in *Escherichia coli*, except CA IX, which was expressed in mammalian cells, and purified using chromatography. Their purity, as determined by electrophoretic analysis SDS-PAGE, was >95%. Protein MW was confirmed by MS to a precision of 1 Da and the concentrations before experiments were measured spectrophotometrically.

4.3. Determination of compound binding to CAs

4.3.1. Fluorescent thermal shift assay

Fluorescent thermal shift assay experiments were performed in a Corbett Rotor-Gene 6000 (Qiagen Rotor-Gene Q) instrument using the blue channel (excitation $\lambda = 365 \pm 20$ nm, detection $\lambda = 460 \pm 15$ nm). Protein samples containing various concentrations of inhibitor were heated from 25 °C to 99 °C while recording extrinsic fluorescence and determining the protein melting temperatures at each inhibitor concentration. Samples contained 5–10 μM protein, 0–200 μM ligand, 50 mM solvatochromic dye ANS and 50–100 mM sodium phosphate buffer containing 100 mM NaCl at pH 7.0, with a final DMSO concentration of 2%. The applied heating rate was 1 °C/min. Binding constants were determined as previously described in Ref. [52].

4.3.2. Isothermal titration calorimetry

ITC experiments were performed by using VP-ITC instrument (Microcal, Inc., part of Malvern, Northampton, MA, USA). For the

binding reactions the calorimeter cell contained 4–10 μM protein, 2% DMSO, 50–100 mM sodium phosphate buffer (pH 7.0) and 100 mM sodium chloride. Syringe contained 40–100 μM ligand, 2% DMSO, 50–100 mM phosphate buffer (pH 7.0) and 100 mM sodium chloride. Experiments consisted of 25 injections, volume of the first injection was 1–5 μL, while others were 10 μL, added at 200 s intervals, at 37 °C.

ITC data was analyzed using MicroCal Origin software. The first point in the integrated data graph was omitted. The binding constants, enthalpies, and entropies of binding were estimated after fitting the data with the single binding site model.

4.3.3. Protonation enthalpy of the compound

The enthalpy of inhibitor protonation was measured by titrating with 5 mM HNO_3 the cell solution containing the inhibitor (0.25 mM) and 1.5 equivalent (0.375 mM) of NaOH. The experiment consisted of 56 injections. The volume of each injection was 5 μL, added at 200 s intervals. DMSO concentrations in the syringe and the sample cell were equal (2.5%). Experiments were performed at 37 °C.

4.3.4. Spectrophotometric measurements

To determine the pK_a of the ligands, the spectrofotometer model "Agilent 89090A" was used. The constant concentration of DMSO dissolved ligand solution was added to a buffer solution (100 mM or 200 mM, ranging from pH 5.5 to 12.5 at every half pH unit) and a UV–VIS spectra were recorded at 37 °C, peltier-controlled isothermal conditions. The normalized ratio of absorbances (typically 10 nm above and below the isosbestic point) was plotted as a function of pH.

4.3.5. Calculation of intrinsic parameters

The contribution of protonation reactions was subtracted in the calculation of the intrinsic thermodynamic parameters.

The intrinsic binding constant K_{b_intr} is equal to the observed binding constant K_{b_obs} divided by the fractions of the reactive species of deprotonated inhibitor and protonated Zn(II)-hydroxide anion:

$$K_{b\_intr} = \frac{K_{b\_obs}}{f_{CA\_Zn\_H_2O} f_{RSO_2NH^-}} \quad (1)$$

K_{d_intr} can be calculated by inverting the K_{b_intr}.

$$K_{d\_intr} = \frac{1}{K_{b\_intr}} \quad (2)$$

Fractions of deprotonated compound (and protonated Zn(II)-bound water molecule can be calculated if both pK_a values are known:

$$f_{RSO_2NH^-} = \frac{10^{pH-pK_{a\_sulf}}}{1+10^{pH-pK_{a\_sulf}}} \quad (3)$$

$$f_{CAZnH_2O} = 1 - \frac{10^{pH-pK_{a\_ZnH_2O}}}{1+10^{pH-pK_{a\_ZnH_2O}}} \quad (4)$$

The intrinsic enthalpy of binding has contributions from the observed binding enthalpy (ΔH_{b_obs}), protonation enthalpies of inhibitor ($\Delta H_{p\_RSO2NH2}$), CA (ΔH_{p_CA}) and the buffer (ΔH_{p_buf}):

$$\Delta H_{b\_intr} = \Delta H_{b\_obs} - n_{RSO_2NH_2}\Delta Hp_{\_RSO_2NH_2} - n_{CA}\Delta H_{p\_CA} + n_{buf}\Delta H_{p\_buf} \quad (5)$$

where $n_{RSO_2NH_2} = f_{RSO_2NH^-} - 1$ is the number of protons binding to the inhibitor, $n_{CA} = 1 - f_{CAZnH_2O}$ is the number of protons bound to Zn(II)-hydroxide, and $n = -(n_{CA} + n_{RSO_2NH_2})$ is the sum of uptaken or released protons.

p$K_{a_CAZnH_2O}$ values of CA isoforms were previously described: CA I and CA II in Ref. [53], CA III, CA IV in Ref. [39], CA VA, CA VB in Ref. [54], CA VI in Ref. [55], CA VII in Ref. [56], CA IX in Ref. [57], CA XII in Ref. [51], CA XIII in Ref. [58], and CA XIV in Ref. [59]. The experimental values were observed at pH 25 °C, and recalculated to 37 °C by using van't Hoff equation.

4.4. Crystallography

4.4.1. Crystallization

The proteins were concentrated by ultrafiltration to 20–50 mg/mL. Crystallization conditions (buffers) are listed in Table S2. The ligand solutions for crystal soaking were made by mixing of 50 μL of corresponding reservoir solution and 0.5–1 μL of 50 mM ligand solution (in DMSO).

4.4.2. Data collection and structure determination

Three datasets of X-ray diffraction (CA II–**9**, CA XII–**7a**, and CA XII–**7b**) were collected at the EMBL beamlines P13 and P14. The CA XIII-**9** dataset was collected using Rigaku MicroMax™-007 HF X-ray generator. The datasets of CA II–**9**, CA XII–**7a**, and CA XII–**7b** were processed using XDS [60] program, whereas dataset CA XIII–**9** – by MOSFLM [61]. The molecular replacement was made by MOLREP [62] program using the following initial models: 3HLJ for CA II, 1JD0 for CA XII, and 2NNO for CA XIII. The 3D models of compounds were built using AVOGADRO [63] program. The library files which contain complete chemical and geometric descriptions of compounds were created using LIBCHECK program [64,65]. The models were prepared using COOT [66] and refined by REFMAC [67].

All represented graphics were made using Pymol programs (PyMOL, version 1.8). Coordinates and structure factors have been deposited to the RCSB Protein Data Bank (PDB). The PDB access codes are listed in Table 3.

Acknowledgments

This research was supported by the grant S-MIP-17-87 from the Research Council of Lithuania.

Appendix A. Supplementary data

Supplementary data related to this article can be found at https://doi.org/10.1016/j.ejmech.2018.06.059.

Abbreviations

CA	carbonic anhydrase
FTSA	fluorescent thermal shift assay
ITC	isothermal titration calorimetry

References

[1] V.M. Krishnamurthy, G.K. Kaufman, A.R. Urbach, I. Gitlin, K.L. Gudiksen, D.B. Weibel, G.M. Whitesides, Carbonic anhydrase as a model for biophysical and physical-organic studies of proteins and Protein–Ligand binding, Chem. Rev. 108 (2008) 946–1051.
[2] J.M. Purkerson, G.J. Schwartz, The role of carbonic anhydrases in renal physiology, Kidney Int. 71 (2007) 103–115.
[3] C.T. Supuran, Carbonic anhydrases–an overview, Curr. Pharmaceut. Des. 14 (2008) 603–614.
[4] M. Aggarwal, C.D. Boone, B. Kondeti, R. McKenna, Structural annotation of human carbonic anhydrases, J. Enzym. Inhib. Med. Chem. 28 (2013) 267–277.
[5] M. Aggarwal, R. McKenna, Update on carbonic anhydrase inhibitors: a patent review (2008-2011), Expert Opin. Ther. Pat. 22 (2012) 903–915.
[6] C.T. Supuran, A. Scozzafava, Carbonic anhydrases as targets for medicinal chemistry, Bioorg. Med. Chem. 15 (2007) 4336–4350.

[7] N. Hen, M. Bialer, B. Yagen, A. Maresca, M. Aggarwal, A.H. Robbins, R. McKenna, A. Scozzafava, C.T. Supuran, Anticonvulsant 4-aminobenzenesulfonamide derivatives with branched-alkylamide moieties: X-ray crystallography and inhibition studies of human carbonic anhydrase isoforms I, ii, vii, and XIV, J. Med. Chem. 54 (2011) 3977–3981.
[8] B.-B. Gao, A. Clermont, S. Rook, S.J. Fonda, V.J. Srinivasan, M. Wojtkowski, J.G. Fujimoto, R.L. Avery, P.G. Arrigg, S.-E. Bursell, L.P. Aiello, E.P. Feener, Extracellular carbonic anhydrase mediates hemorrhagic retinal and cerebral vascular permeability through prekallikrein activation, Nat. Med. 13 (2007) 181–188.
[9] A. Scozzafava, C.T. Supuran, F. Carta, Antiobesity carbonic anhydrase inhibitors: a literature and patent review, Expert Opin. Ther. Pat. 23 (2013) 725–735.
[10] G. De Simone, A. Di Fiore, C.T. Supuran, Are carbonic anhydrase inhibitors suitable for obtaining antiobesity drugs? Curr. Pharmaceut. Des. 14 (2008) 655–660.
[11] J. Lehtonen, B. Shen, M. Vihinen, A. Casini, A. Scozzafava, C.T. Supuran, A.K. Parkkila, J. Saarnio, A.J. Kivela, A. Waheed, W.S. Sly, S. Parkkila, Characterization of CA XIII, a novel member of the carbonic anhydrase isozyme family, J. Biol. Chem. 279 (2004) 2719–2727.
[12] O. Ozensoy Guler, G. De Simone, C.T. Supuran, Drug design studies of the novel antitumor targets carbonic anhydrase IX and XII, Curr. Med. Chem. 17 (2010) 1516–1526.
[13] V. Alterio, A. Di Fiore, K. D'Ambrosio, C.T. Supuran, G. De Simone, Multiple binding modes of inhibitors to carbonic anhydrases: how to design specific drugs targeting 15 different isoforms? Chem. Rev. 112 (2012) 4421–4468.
[14] C.T. Supuran, A. Scozzafava, J. Conway, Carbonic Anhydrase: its Inhibitors and Activators, CRC Press, 2004.
[15] C.T. Supuran, Advances in structure-based drug discovery of carbonic anhydrase inhibitors, Expet Opin. Drug Discov. 12 (2017) 61–88.
[16] C.T. Supuran, How many carbonic anhydrase inhibition mechanisms exist? J. Enzym. Inhib. Med. Chem. 31 (2016) 345–360.
[17] C.T. Supuran, A. Scozzafava, A. Casini, Carbonic anhydrase inhibitors, Med. Res. Rev. 23 (2003) 146–189.
[18] P.A. Boriack, D.W. Christianson, J. Kingery-Wood, G.M. Whitesides, Secondary interactions significantly removed from the sulfonamide binding pocket of carbonic anhydrase II influence inhibitor binding constants, J. Med. Chem. 38 (1995) 2286–2291.
[19] F. Pacchiano, M. Aggarwal, B.S. Avvaru, A.H. Robbins, A. Scozzafava, R. McKenna, C.T. Supuran, Selective hydrophobic pocket binding observed within the carbonic anhydrase II active site accommodate different 4-substituted-ureido-benzenesulfonamides and correlate to inhibitor potency, Chem Commun Camb 46 (2010) 8371–8373.
[20] J.F. Domsic, B.S. Avvaru, C.U. Kim, S.M. Gruner, M. Agbandje-McKenna, D.N. Silverman, Robert McKenna, Entrapment of carbon dioxide in the active site of carbonic anhydrase II, J. Biol. Chem. 283 (2008) 30766–30771.
[21] K.M. Jude, A.L. Banerjee, M.K. Haldar, S. Manokaran, B. Roy, S. Mallik, D.K. Srivastava, D.W. Christianson, Ultrahigh resolution crystal structures of human carbonic anhydrases I and ii complexed with "Two-Prong" inhibitors reveal the molecular basis of high affinity, J. Am. Chem. Soc. 128 (2006) 3011–3018.
[22] M. Aggarwal, B. Kondeti, R. McKenna, Insights towards sulfonamide drug specificity in α-carbonic anhydrases, Bioorg. Med. Chem. 21 (2013) 1526–1533.
[23] G. De Simone, V. Alterio, C.T. Supuran, Exploiting the hydrophobic and hydrophilic binding sites for designing carbonic anhydrase inhibitors, Expet Opin. Drug Discov. 8 (2013) 793–810.
[24] C.T. Supuran, Carbonic anhydrases: novel therapeutic applications for inhibitors and activators, Nat. Rev. Drug Discov. 7 (2008) 168–181.
[25] W. Vernier, W. Chong, D. Rewolinski, S. Greasley, T. Pauly, M. Shaw, D. Dinh, R.A. Ferre, S. Nukui, M. Ornelas, E. Reyner, Thioether benzenesulfonamide inhibitors of carbonic anhydrases II and IV: structure-based drug design, synthesis, and biological evaluation, Bioorg. Med. Chem. 18 (2010) 3307–3319.
[26] C. Congiu, V. Onnis, G. Balboni, C.T. Supuran, Synthesis and carbonic anhydrase I, II, IX and XII inhibition studies of 4-N,N-disubstituted sulfanilamides incorporating 4,4,4-trifluoro-3-oxo-but-1-enyl, phenacylthiourea and imidazole-2(3H)-one/thione moieties, Bioorg. Med. Chem. Lett 24 (2014) 1776–1779.
[27] R.P. Tanpure, B. Ren, T.S. Peat, L.F. Bornaghi, D. Vullo, C.T. Supuran, S.-A. Poulsen, Carbonic anhydrase inhibitors with dual-tail moieties to match the hydrophobic and hydrophilic halves of the carbonic anhydrase active site, J. Med. Chem. 58 (2015) 1494–1501.
[28] I. Vaškevičienė, V. Paketurytė, A. Zubrienė, K. Kantminienė, V. Mickevičius, D. Matulis, N-Sulfamoylphenyl- and N-sulfamoylphenyl-N-thiazolyl-β-alanines and their derivatives as inhibitors of human carbonic anhydrases, Bioorg. Chem. 75 (2017) 16–29.
[29] Z. Hou, B. Lin, Y. Bao, H. Yan, M. Zhang, X. Chang, X. Zhang, Z. Wang, G. Wei, M. Cheng, Y. Liu, C. Guo, Dual-tail approach to discovery of novel carbonic anhydrase IX inhibitors by simultaneously matching the hydrophobic and hydrophilic halves of the active site, Eur. J. Med. Chem. 132 (2017) 1–10.
[30] C.T. Supuran, S. Kalinin, M. Tanç, P. Sarnpitak, P. Mujumdar, S.-A. Poulsen, M. Krasavin, Isoform-selective inhibitory profile of 2-imidazoline-substituted benzene sulfonamides against a panel of human carbonic anhydrases, J. Enzym. Inhib. Med. Chem. 31 (2016) 197–202.
[31] V. Dudutienė, J. Matulienė, A. Smirnov, D.D. Timm, A. Zubrienė, L. Baranauskienė, V. Morkūnaitė, J. Smirnovienė, V. Michailovienė, V. Juozapaitienė, A. Mickevičiūtė, J. Kazokaitė, S. Bakšytė, A. Kasiliauskaitė, J. Jachno, J. Revuckienė, M. Kišonaitė, V. Pilipuitytė, E. Ivanauskaitė, G. Milinavičiūtė, V. Smirnovas, V. Petrikaitė, V. Kairys, V. Petrauskas, P. Norvaišas, D. Lingė, P. Gibieža, E. Čapkauskaitė, A. Zakšauskas, E. Kazlauskas, E. Manakova, S. Gražulis, J.E. Ladbury, D. Matulis, Discovery and characterization of novel selective inhibitors of carbonic anhydrase IX, J. Med. Chem. 57 (2014) 9435–9446.
[32] A.D. Scott, C. Phillips, A. Alex, M. Flocco, A. Bent, A. Randall, R. O'Brien, L. Damian, L.H. Jones, Thermodynamic optimisation in drug discovery: a case study using carbonic anhydrase inhibitors, ChemMedChem 4 (2009) 1985–1989.
[33] E. Čapkauskaitė, V. Linkuvienė, A. Smirnov, G. Milinavičiūtė, D.D. Timm, A. Kasiliauskaitė, E. Manakova, S. Gražulis, D. Matulis, Combinatorial design of isoform-selective N-Alkylated benzimidazole-based inhibitors of carbonic anhydrases, Chemistry 2 (2017) 5360–5371.
[34] E. Čapkauskaitė, A. Zubrienė, A. Smirnov, J. Torresan, M. Kišonaitė, J. Kazokaitė, J. Gylytė, V. Michailovienė, V. Jogaitė, E. Manakova, S. Gražulis, S. Tumkevičius, D. Matulis, Benzenesulfonamides with pyrimidine moiety as inhibitors of human carbonic anhydrases I, II, VI, VII, XII, and XIII, Bioorg. Med. Chem. 21 (2013) 6937–6947.
[35] E. Čapkauskaitė, L. Baranauskienė, D. Golovenko, E. Manakova, S. Gražulis, S. Tumkevičius, D. Matulis, Indapamide-like benzenesulfonamides as inhibitors of carbonic anhydrases I, II, VII, and XIII, Bioorg. Med. Chem. 18 (2010) 7357–7364.
[36] G.D. Parkes, E. d'. Burney, 385. Derivatives of 6-bromo- and 4: 6-dibromo-m-toluidine, J. Chem. Soc. (1935) 1619–1621.
[37] T. Fujikura, K. Miigata, S. Hashimoto, K. Imai, T. Takenaka, Studies on benzenesulfonamide derivatives with alpha- and beta-adrenergic antagonistic and antihypertensive activities, Chem Pharm Bull Tokyo 30 (1982) 4092–4101.
[38] P. Francotte, T.P. De, B. Pirotte, L. Danober, P. Lestage, D.-H. Caignard, Cycloalkylated Benzothiadiazines, a Process for Their Preparation and Pharmaceutical Compostions Containing Them, US2010009974 (A1), 2010.
[39] A. Mickevičiūtė, D.D. Timm, M. Gedgaudas, V. Linkuvienė, Z. Chen, A. Waheed, V. Michailovienė, A. Zubrienė, A. Smirnov, E. Čapkauskaitė, L. Baranauskienė, J. Jachno, J. Revuckienė, E. Manakova, S. Gražulis, J. Matulienė, E.D. Cera, W.S. Sly, D. Matulis, Intrinsic thermodynamics of high affinity inhibitor binding to recombinant human carbonic anhydrase IV, Eur. Biophys. J. 47 (2018) 271–290.
[40] K. Sturm, W. Siedel, R. Weyer, H. Ruschig, Zur Chemie des Furosemids, I. Synthesen von 5-Sulfamoyl-anthranilsäure-Derivaten, Eur. J. Inorg. Chem. 99 (1966) 328–344.
[41] D. Matulis, V.A. Bloomfield, Thermodynamics of the hydrophobic effect. I. Coupling of aggregation and pKa shifts in solutions of aliphatic amines, Biophys. Chem. 93 (2001) 37–51.
[42] D. Matulis, V.A. Bloomfield, Thermodynamics of the hydrophobic effect. II. Calorimetric measurement of enthalpy, entropy, and heat capacity of aggregation of alkylamines and long aliphatic chains, Biophys. Chem. 93 (2001) 53–65.
[43] D. Matulis, Thermodynamics of the hydrophobic effect. III. Condensation and aggregation of alkanes, alcohols, and alkylamines, Biophys. Chem. 93 (2001) 67–82.
[44] M.A. Pinard, B. Mahon, R. McKenna, Probing the surface of human carbonic anhydrase for clues towards the design of isoform specific inhibitors, BioMed Res. Int. 2015 (2015) 1–15.
[45] E. Čapkauskaitė, A. Zubrienė, L. Baranauskienė, G. Tamulaitienė, E. Manakova, V. Kairys, S. Gražulis, S. Tumkevičius, D. Matulis, Design of [(2-pyrimidinylthio)acetyl]benzenesulfonamides as inhibitors of human carbonic anhydrases, Eur. J. Med. Chem. 51 (2012) 259–270.
[46] C. Temperini, A. Cecchi, A. Scozzafava, C.T. Supuran, Carbonic anhydrase inhibitors. Comparison of chlorthalidone and indapamide X-ray crystal structures in adducts with isozyme II: when three water molecules and the keto-enol tautomerism make the difference, J. Med. Chem. 52 (2009) 322–328.
[47] L.H. Mckendry, M.W. Zettler, Process for the Preparation of 2-chloro and 2,6-dichloroanilines, US5068392 (A), 1991.
[48] T.R. Williams, D.J. Cram, Stereochemistry of sulfur compounds. IV. New ring system of carbon, nitrogen, and chiral sulfur, J. Org. Chem. 38 (1973) 20–26.
[49] P. Cimmperman, L. Baranauskienė, S. Jachimovičiūtė, J. Jachno, J. Torresan, V. Michailovienė, J. Matulienė, J. Sereikaitė, V. Bumelis, D. Matulis, A quantitative model of thermal stabilization and destabilization of proteins by ligands, Biophys. J. 95 (2008) 3222–3231.
[50] J. Sūdžius, L. Baranauskienė, D. Golovenko, J. Matulienė, V. Michailovienė, J. Torresan, J. Jachno, R. Sukackaitė, E. Manakova, S. Gražulis, S. Tumkevičius, D. Matulis, 4-[N-(Substituted 4-pyrimidinyl)amino]benzenesulfonamides as inhibitors of carbonic anhydrase isozymes I, II, VII, and XIII, Bioorg. Med. Chem. 18 (2010) 7413–7421.
[51] V. Jogaitė, A. Zubrienė, V. Michailovienė, J. Gylytė, V. Morkūnaitė, D. Matulis, Characterization of human carbonic anhydrase XII stability and inhibitor binding, Bioorg. Med. Chem. 21 (2013) 1431–1436.
[52] L. Baranauskienė, M. Hilvo, J. Matulienė, D. Golovenko, E. Manakova, V. Dudutienė, V. Michailovienė, J. Torresan, J. Jachno, S. Parkkila, A. Maresca, C.T. Supuran, S. Gražulis, D. Matulis, Inhibition and binding studies of carbonic anhydrase isozymes I, II and IX with benzimidazo[1,2-c][1,2,3]thiadiazole-7-sulphonamides, J. Enzym. Inhib. Med. Chem. 25 (2010) 863–870.

[53] V. Morkūnaitė, J. Gylytė, A. Zubrienė, L. Baranauskienė, M. Kišonaitė, V. Michailovienė, V. Juozapaitienė, M.J. Todd, D. Matulis, Intrinsic thermodynamics of sulfonamide inhibitor binding to human carbonic anhydrases I and II, J. Enzym. Inhib. Med. Chem. 30 (2015) 204–211.
[54] A. Kasiliauskaitė, V. Časaitė, V. Juozapaitienė, A. Zubrienė, V. Michailovienė, J. Revuckienė, L. Baranauskienė, R. Meškys, D. Matulis, Thermodynamic characterization of human carbonic anhydrase VB stability and intrinsic binding of compounds, J. Therm. Anal. Calorim. 123 (2016) 2191–2200.
[55] J. Kazokaitė, G. Milinavičiūtė, J. Smirnovienė, J. Matulienė, D. Matulis, Intrinsic binding of 4-substituted-2,3,5,6-tetrafluorobenezenesulfonamides to native and recombinant human carbonic anhydrase VI, FEBS J. 282 (2015) 972–983.
[56] V. Pilipuitytė, D. Matulis, Intrinsic thermodynamics of trifluoromethanesulfonamide and ethoxzolamide binding to human carbonic anhydrase VII: thermodynamics of TFS and EZA binding to CA VII, J. Mol. Recogn. 28 (2015) 166–172.
[57] V. Linkuvienė, J. Matulienė, V. Juozapaitienė, V. Michailovienė, J. Jachno, D. Matulis, Intrinsic thermodynamics of inhibitor binding to human carbonic anhydrase IX, Biochim. Biophys. Acta BBA - Gen. Subj 1860 (2016) 708–718.
[58] L. Baranauskienė, D. Matulis, Intrinsic thermodynamics of ethoxzolamide inhibitor binding to human carbonic anhydrase XIII, BMC Biophys. 5 (2012) 12.
[59] V. Juozapaitienė, B. Bartkutė, V. Michailovienė, A. Zakšauskas, L. Baranauskienė, S. Satkūnė, D. Matulis, Purification, enzymatic activity and inhibitor discovery for recombinant human carbonic anhydrase XIV, J. Biotechnol. 240 (2016) 31–42.
[60] W. Kabsch, XDS, Acta Crystallogr. D D66 (2010) 125–132.
[61] T.G.G. Battye, L. Kontogiannis, O. Johnson, H.R. Powell, A.G.W. Leslie, iMOSFLM: a new graphical interface for diffraction-image processing with MOSFLM, Acta Crystallogr. D Biol. Crystallogr. 67 (2011) 271–281.
[62] A. Vagin, A. Teplyakov, MOLREP: an automated program for molecular replacement, J. Appl. Crystallogr. 30 (1997) 1022–1025.
[63] M.D. Hanwell, D.E. Curtis, D.C. Lonie, T. Vandermeersch, E. Zurek, G.R. Hutchison, Avogadro: an advanced semantic chemical editor, visualization, and analysis platform, J. Cheminf. 4 (2012) 17.
[64] A.A. Vagin, R.A. Steiner, A.A. Lebedev, L. Potterton, S. McNicholas, F. Long, G.N. Murshudov, REFMAC5 dictionary: organization of prior chemical knowledge and guidelines for its use, Acta Crystallogr Biol Crystallogr 60 (2004) 2184–2195.
[65] M.D. Winn, C.C. Ballard, K.D. Cowtan, E.J. Dodson, P. Emsley, P.R. Evans, R.M. Keegan, E.B. Krissinel, A.G.W. Leslie, A. McCoy, S.J. McNicholas, G.N. Murshudov, N.S. Pannu, E.A. Potterton, H.R. Powell, R.J. Read, A. Vagin, K.S. Wilson, Overview of the CCP4 suite and current developments, Acta Crystallogr. D Biol. Crystallogr 67 (2011) 235–242.
[66] P. Emsley, B. Lohkamp, W.G. Scott, K. Cowtan, Features and development of ıt coot, Acta Crystallogr. D 66 (2010) 486–501.
[67] G.N. Murshudov, A.A. Vagin, E.J. Dodson, Refinement of macromolecular structures by the maximum-likelihood method, Acta Crystallogr Biol Crystallogr. 53 (1997) 240–255.

European Journal of Medicinal Chemistry 185 (2020) 111825

Contents lists available at ScienceDirect

European Journal of Medicinal Chemistry

journal homepage: http://www.elsevier.com/locate/ejmech

Research paper

Halogenated and di-substituted benzenesulfonamides as selective inhibitors of carbonic anhydrase isoforms

Audrius Zakšauskas [a], Edita Čapkauskaitė [a], Linas Jezepčikas [a], Vaida Linkuvienė [a], Vaida Paketurytė [a], Alexey Smirnov [a], Janis Leitans [b], Andris Kazaks [b], Elviss Dvinskis [b], Elena Manakova [c], Saulius Gražulis [c], Kaspars Tars [b], Daumantas Matulis [a, *]

[a] Department of Biothermodynamics and Drug Design, Institute of Biotechnology, Life Sciences Center, Vilnius University, Saulėtekio al. 7, Vilnius, LT, 10257, Lithuania
[b] Latvian Biomedical Research and Study Centre, Ratsupites 1 k-1, Riga, LV, 1067, Latvia
[c] Department of Protein – DNA Interactions, Institute of Biotechnology, Life Sciences Center, Vilnius University, Saulėtekio al. 7, Vilnius, LT, 10257, Lithuania

ARTICLE INFO

Article history:
Received 26 September 2019
Received in revised form
25 October 2019
Accepted 25 October 2019
Available online 31 October 2019

Keywords:
Benzenesulfonamide
Human carbonic anhydrase
Intrinsic binding thermodynamics
Carbonic anhydrase inhibitor

ABSTRACT

By applying an approach of a "ring with two tails", a series of novel inhibitors possessing high-affinity and significant selectivity towards selected carbonic anhydrase (CA) isoforms has been designed. The "ring" consists of 2-chloro/bromo-benzenesulfonamide, where the sulfonamide group is as an anchor coordinating the Zn(II) in the active site of CAs, and halogen atom orients the ring affecting the affinity and selectivity. First "tail" is a substituent containing carbonyl, carboxyl, hydroxyl, ether groups or hydrophilic amide linkage. The second "tail" contains aryl- or alkyl-substituents attached through a sulfanyl or sulfonyl group. Both "tails" are connected to the benzene ring and play a crucial role in selectivity. Varying the substituents, we designed compounds selective for CA VII, CA IX, CA XII, or CA XIV.

Since due to binding-linked protonation reactions the binding-ready fractions of the compound and protein are much lower than one, the "intrinsic" affinities were calculated that should be used to study correlations between crystal structures and the thermodynamics of binding for rational drug design. The "intrinsic" affinities together with the intrinsic enthalpies and entropies of binding together with co-crystal structures were used demonstrate structural factors determining major contributions for compound affinity and selectivity.

1. Introduction

Small-molecule compounds could serve as pharmaceuticals to treat numerous diseases, but the physical principles governing non-covalent binding between the compounds and proteins in aqueous solution are not fully understood even for relatively simple proteins such as carbonic anhydrases (CA). Despite a relative wealth of structural and thermodynamic information and a large series of compounds designed as inhibitors of catalytic activity by binding to the Zn(II) in the active site, the exact arrangement and recognition of the protein surface by the compound is not well understood thus hindering the rational design of compounds for pharmaceutical applications.

The CAs (EC 4.2.1.1) are Zn(II)-containing metalloenzymes that catalyze reversible hydration of carbon dioxide to bicarbonate anion and a proton, play an important role in pH regulation processes [1,2] and are involved in numerous physiological processes. Out of 15 CA isoforms present in human body, twelve are catalytically active possessing different cellular/tissue localization and activity [3,4]. Remaining three do not contain Zn(II) and thus are catalytically inactive. CAs play a role in various disorders such as glaucoma, obesity, cancer, epilepsy, etc. [5–8]. CAs were started to be exploited as targets for treatment since 1940s [9]. However, most CA inhibitors that are clinical drugs have low selectivity primarily due to high similarity between the active sites of the isoforms [10].

Aromatic sulfonamides are the largest class of CA inhibitors [11]. The most commonly used approach to design CA inhibitors is the "ring and tail" approach [2], where the "ring" consists of hetero/aromatic fragment containing sulfonamide group which is essential for binding zinc. Electron acceptor substituents are helpful due to

* Corresponding author. Saulėtekio al. 7, Vilnius, LT, 10257, Lithuania.
E-mail address: daumantas.matulis@bti.vu.lt (D. Matulis).

https://doi.org/10.1016/j.ejmech.2019.111825
0223-5234/

Abbreviations

CA	carbonic anhydrase
FTSA	fluorescent thermal shift assay (differential scanning fluorimetry, DSF)
intr	intrinsic
ITC	isothermal titration calorimetry
obs	observed
Variables	
ΔG_{intr}	change of the intrinsic standard Gibbs energy upon binding
ΔG_{obs}	change of the observed standard Gibbs energy upon binding
ΔH_{intr}	change of the intrinsic standard enthalpy upon binding
K_{d_intr}	intrinsic equilibrium dissociation constant
K_{d_obs}	observed equilibrium dissociation constant
T_m	melting temperature (midpoint of the unfolding transition)
$T\Delta S_{intr}$	change of the intrinsic standard entropy upon binding multiplied by absolute temperature

their ability to increase the acidity of the sulfonamide group thus increasing the binding affinity. The "tail" is a flexible fragment connected to the aromatic ring and participates in additional binding to the CA active site or improves the aqueous solubility of the compound. Doubly-tailed CA inhibitors have also been designed in attempts to exploit the hydrophobic and hydrophilic walls of the CA active site [12–18].

We have extended this approach by designing inhibitors which would be half fixed in active site of CAs was fruitful and inspired us to continue our investigation in this direction. We have designed and synthesized a series of 2-chloro/bromo-benzenesulfonamides bearing two “tails” which one is more hydrophilic due to substituents containing carbonyl, carboxyl, hydroxyl, ether groups and hydrophilic amide linkage and second one is more hydrophobic due to aryl-, alkyl-substituents attached through an amino group. An introduction of the second “tail” together with the fixed position of the benzene ring in most cases provides excellent selectivity for CA IX and CA XIV due to restricted ability of “tail” to move freely in search of energetically favorable position [19].

We decided to extend this set by changing the linkage to sulfur instead of amino group. The sulfur atom exhibits higher electron-withdrawing properties than the nitrogen atom, enhancing the acidity of the sulfonamide group thus increasing the observed binding affinity to CAs. The sulfur atom forms different bond length, and angles as compared to NH containing linker. Additionally, the sulfur atom does not tend to form hydrogen bonds as the nitrogen atom. The sulfanyl group containing compounds can be oxidized to sulfinyl, sulfonyl derivatives offering a new type of linkage, and also providing electron-withdrawing properties that improve the affinity. The change of the nitrogen atom to sulfur expanded the potential to build selective CAs inhibitors.

2. Results and discussion

A series of 80 benzenesulfonamides (Fig. 1) were designed as CA inhibitors and synthesized. Dihalosulfamoylbenzamides **1**-**14**, **27** contain chlorine or bromine atoms. All other compounds contain aryl- or alkyl-substituents (phenyl (all compounds -**a**), cyclohexyl (-**b**), benzyl (-**c**), and 2-phenylethyl (-**d**) or hydroxyethyl (-**e**)) attached through a sulfanyl (-S-), sulfinyl (-SO-) or sulfonyl (-SO_2-) group. Another substituent is carboxyl, amide or substituted amide.

2.1. Chemistry

The synthesis of desired compounds was achieved using key intermediates 2,4-dihalo-5-sulfamoylbenzoic acids **1** and **2** [19]. The synthesis of dihalosulfamoylbenzamides **3**–**14** has been reported in Ref. [19]. The reactions of 2,4-dihalo-5-sulfamoylbenzoic acid derivatives **3** to **14** with thiols have not been described in the literature. Instead, we followed an example of similar reactions with nitrogen-containing nucleophiles [20,21]. As expected, the nucleophilic substitution occurred in the 4-position to the sulfonamide group (Scheme 1).

The reactions of the dihalobenzamides **3**–**8, 10**–**14** with thiophenol were carried out in boiling methanol with triethylamine and resulted in 4-sulfanyl-substituted sulfonamides with good yield (60–90%). However, using the same reaction condition was unsuccessful for morpholinyl derivative **9**, which required harsher conditions (DMSO, 120 °C, Cs_2CO_3).

We have noticed that the reaction of **3-8, 10**–**13** with cyclohexylthiol under the same conditions was very slow as compared to thiophenol. The replacement of a polar protic solvent MeOH with a polar aprotic solvent DMSO and a base triethylamine with potassium carbonate allowed to perform the reaction at 60 °C for 2–4 h instead of for 12 h to a week at the same temperature. The reaction of dihalobenzamides **3**–**8, 10**–**13** with benzyl- and 2-phenylethylthiols was performed under similar conditions (DMSO, TEA, 60 °C).

Oxidation of sulfanyl derivatives (Scheme 2) was performed using *in situ* generated peracetic acid in good yields (69–92%). The formation of *O*-acetates was observed by oxidation of hydroxyl group containing compounds (**4a-c**, **5a-b**, **10e**, **12b-c**). Reaction product mixture subsequently was subjected to deacetylation by boiling in diluted HCl.

Several sulfinyl derivatives **25c**, **26e** were synthesized performing the reaction at 50 °C with a slight excess of peracetic acid**,** with intent to avoid the formation of sulfonyl-compounds. The geminal coupling constant between the non-equivalent protons of the benzylic methylene group was observed in compound **25c** (4.05 ($1H_A$, d, $J = 12.4$ Hz, $\underline{CH_2}$Ph), 4.51 ($1H_B$, d, $J = 12.4$ Hz, $\underline{CH_2}$Ph)) as in similar compounds [22].

Benzoic acids **1b**, **d** were synthesized from the corresponding benzamides **3b, d**. In order to avoid chloro substitution, hydrolysis was performed by boiling in an acidic medium. However, hydrolysis of esters **8, 8b, 20c** (Scheme 3) under these conditions led to the formation of two products as observed by TLC, perhaps due to simultaneous hydrolysis of the amide. Therefore, hydrolysis of **8a-c** was performed in the alkaline medium at room temperature with only one reaction product formed.

2.2. Compound binding to CAs

2.2.1. Affinity-selectivity profiles

To learn the full affinity-selectivity profile, we determined the affinities of all compounds, listed in Fig. 1, towards all twelve catalytically active human CA isoforms. It is important to determine the affinities towards a full set of CAs to see if a compound is truly selective and distinguishes a single CA isoform among them all as would be in human body. All of the compounds bound to CAs in the micromolar to sub-nanomolar K_d affinity range and demonstrated significant selectivities towards one or another CA isoform. Several selected cases are shown in Fig. 2 and are listed in Table 1. For example, compound **4a** demonstrated selectivity towards CA IV (Fig. 4, panel B). The affinity for CA IV was 1.4 nM, while for CA II it

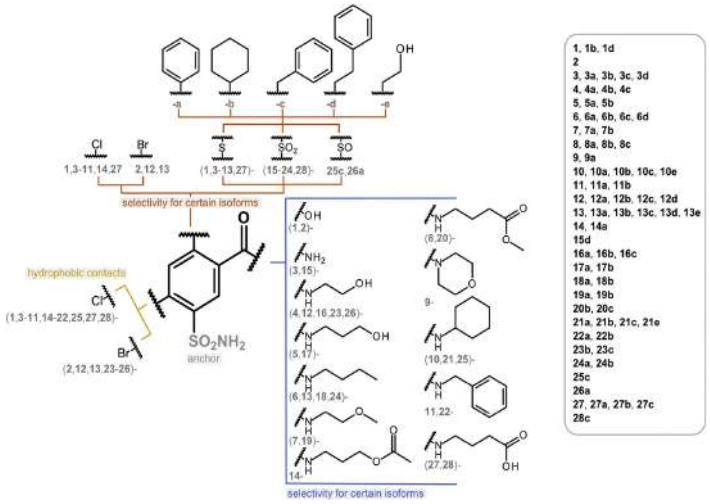

Fig. 1. Compound chemical structures used in this study. List of all compound numbers is shown on right side.

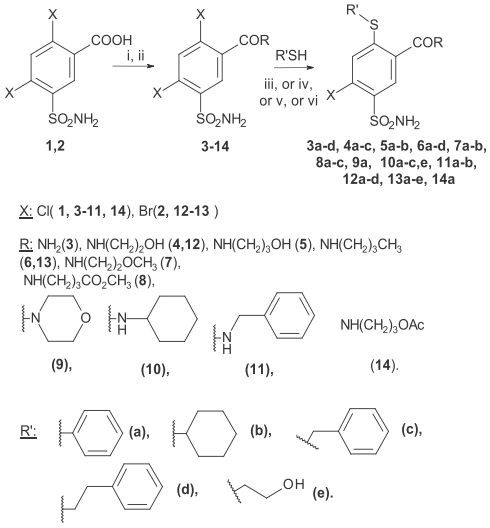

Scheme 1. Synthesis of 2-halo-4,5-disubstitutedbenzenesulfonamides: i) $SOCl_2$, toluene, Δ; ii) appropriate amine RH, THF, 0–20 °C; iii) TEA, MeOH, Δ; iv) Cs_2CO_3, DMSO, 120 °C; v) K_2CO_3, DMSO, 60 °C; vi) TEA, DMSO, 60 °C.

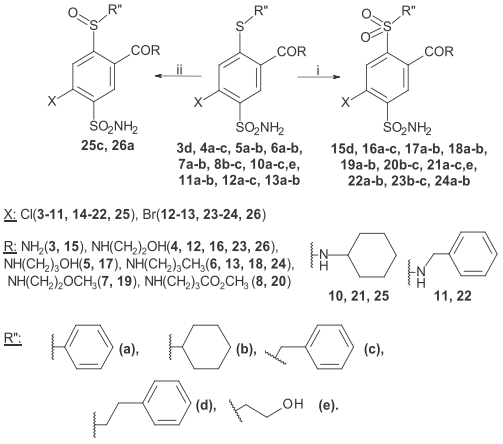

Scheme 2. The synthesis of 2-halo-4,5-disubstitutedbenzenesulfonamides: i) H_2O_2, AcOH, 75 °C; ii) PAA, AcOH, 50 °C.

was 31 nM and for CA I it was 10000 nM. Therefore, the compound exhibited some 7000-fold selectivity over the most abundant CA isoform, CA I, and some 20-fold selectivity over CA II. Fig. 2 shows the observed affinities expressed in the binding constant K_b which is an inverse of the dissociation constant K_d ($K_b = 1/K_d$).

Binding affinities were determined by the fluorescent thermal shift assay (FTSA) [23–25]. This technique is based on protein thermal stability and is universal to detect both strong and weak protein-ligand interactions [26]. Affinities were also confirmed for several selected compounds by isothermal titration calorimetry (ITC) [27,28], which in addition allows to directly determine the change in the binding enthalpy (Table S2).

It is important to recall that sulfonamide compounds bind to the Zn(II) of CA by forming a coordination bond and it is necessary for the sulfonamide group to be deprotonated in order to bind while the Zn(II) must have a water molecule bound that can be displaced by the negatively charged sulfonamide. However, both the sulfonamide and the CA at most pH values exist in the protonation form that is unable to bind and must undergo a protonation-deprotonation reaction in order to bind. These binding-linked reactions significantly diminish sulfonamide affinity for CAs and exhibits pH-dependent affinity profiles. Therefore, it is important to state that the affinities shown in Fig. 2 are determined at pH 7.0 and they would be different at other pH values. However, in drug

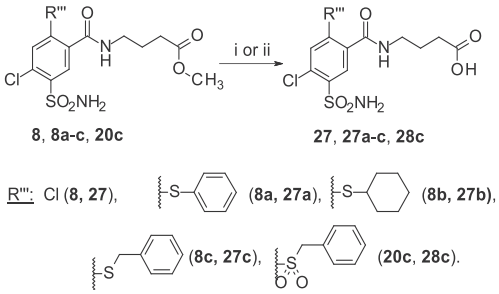

Scheme 3. The synthesis of 4-[(2,4-disubstituted-5-sulfamoyl-benzoyl)amino]butanoic acids **27, 27 a-c**, **28c**: i) conc. HCl (aq), MeOH, Δ; ii) 10% NaOH (aq), MeOH, r.t.

design, we need to investigate affinities that are independent of pH and such linked reactions. To achieve this, we calculate "intrinsic" affinities that would be observed if both the sulfonamide and the CA existed in a binding-ready form as described in the experimental part [29]. Both the *intrinsic* and *observed* affinities for all compounds towards all 12 CA isoforms are listed in Table S1. The pK_ds and the fractions of binding-ready sulfonamide and CA are also listed to help explain the calculation procedure between the observed and intrinsic values. The dissociation constants of compounds **3**–**14, 27** toward CAs have been determined previously [19] and were used here for comparison. The intrinsic enthalpy changes are listed in Table 2. It is important to note that listing the observed enthalpies is essentially useless for drug design because the values are highly buffer-dependent, while the observed affinities help the reader to see what the affinity would be at pH 7.0, a physiologically useful information. However, only the intrinsic values should be used for decisions on the compound structure alterations and possible effect on binding-selectivity profile. Therefore, the structure-thermodynamics correlation should be performed only based on intrinsic affinities.

The studied compounds were most selective for CA VII, CA IX, CA XII, and CA XIV, the intrinsic affinity was almost always stronger than 1 nM and in most cases was around 1 pM, while the observed affinity was mostly nanomolar. Some compounds were also selective for CA II, CA IV or CA VB. However, the affinity of the compounds was the lowest towards CA I, CA III, CA VA, CA VI, and CA XIII. Compounds **17a**, **18a**, **22a**, **24a** exhibited the highest observed affinity for CA VII (K_{d_obs} in the range of 0.22 nM–0.33 nM), while **24b** had the highest observed affinity for CA IX (K_{d_obs} was 0.25 nM) at pH = 7.0. However, these affinities between CA VII, CA IX, CA XII, and CA XIV differed only several fold, although the affinity for CA I was a thousand times smaller.

It is clear that even small differences between the chemical structures of compounds may have unpredictable effect on binding affinity. Nevertheless, the goal of this study is to try to find trends

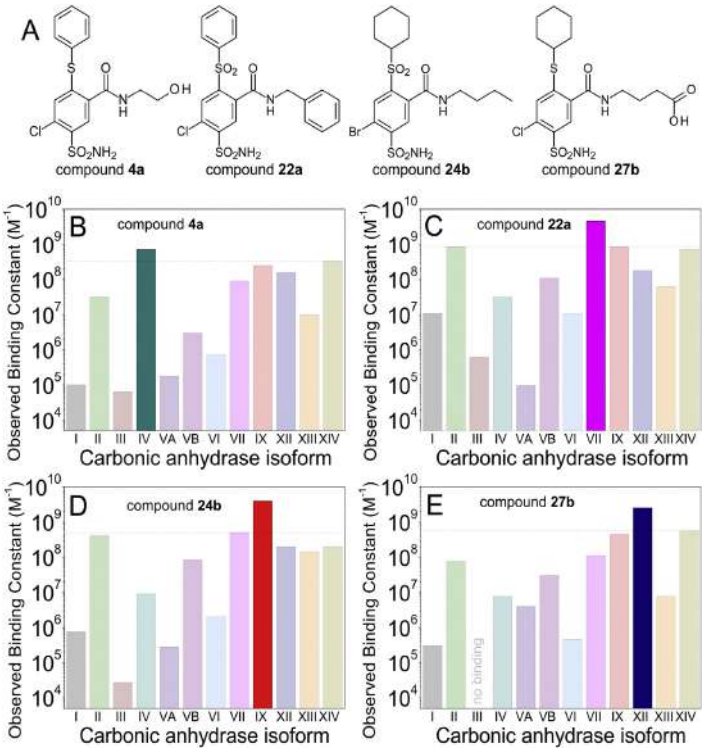

Fig. 2. Chemical structures (**A**) of several compounds that exhibited significant selectivity toward CA IV, CA VII, CA IX, or CA XII. (**B-E**) - bar charts of their observed binding constants towards all active human carbonic anhydrases at pH 7.0.

Table 1
Affinities of all synthesized compounds were determined towards all 12 catalytically active CA isoforms. The representative affinities are listed in this table while the remaining values are in Supplementary Table S1. The *observed* dissociation constants (K_{d_obs}, nM, in 50 mM sodium phosphate buffer containing 100 mM sodium chloride at pH 7.0) are listed above the *intrinsic* affinities (K_{d_intr}, nM) of compound binding to recombinant human CAs. The affinities (K_{d_obs}) were determined by the fluorescent thermal shift assay for 37 °C. The standard deviation is ±2-fold in K_d. Intrinsic affinities were calculated as described in the methods sections.

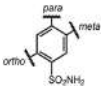

Compound					K_ds	CA I	CA II	CA III	CA IV	CA VA	CA VB	CA VI	CA VII	CA IX	CA XII	CA XIII	CA XIV
Name		Substituent															
		ortho	*meta*	*para*													
4a	*(EA3-2)*	Cl			K_{d_obs}	10000	31	15000	1.4	5600	330	1400	11	4.0	6.3	100	3.0
					K_{d_intr}	92	0.14	37	0.0040	37	1.6	1.3	0.040	0.010	0.020	0.90	0.010
17a	*(EA4-2o)*	Cl			K_{d_obs}	1400	3.3	17000	28	5600	19	1400	0.33	1.5	3.1	67	4.0
					K_{d_intr}	69	0.080	210	0.41	200	0.50	6.8	0.0070	0.020	0.060	3.2	0.080
18a	*(EA5-2o)*	Cl			K_{d_obs}	670	3.3	3300	17	4500	3.7	240	0.25	0.67	2.9	11	1.1
					K_{d_intr}	33	0.080	42	0.25	160	0.10	1.2	0.0050	0.010	0.060	0.53	0.020
22a	*(EA10-2o)*	Cl			K_{d_obs}	91	1.2	1600	32	11000	9.1	91	0.22	1.2	5.6	16	1.4
					K_{d_intr}	4.5	0.030	20	0.47	370	0.24	0.44	0.0040	0.020	0.12	0.77	0.030
24a	*(IJ15-31o)*	Br			K_{d_obs}	630	6.7	4200	10	7100	53	360	0.29	0.50	2.9	17	1.4
					K_{d_intr}	35	0.18	60	0.16	280	1.6	1.9	0.0060	0.0090	0.070	0.92	0.030
24b	*(IJ15-32o)*	Br			K_{d_obs}	1300	2.5	37000	110	3600	12	500	2.0	0.25	5.0	7.1	5.0
					K_{d_intr}	64	0.060	470	1.6	130	0.32	2.4	0.040	0.0040	0.10	0.34	0.10
Acetazolamide		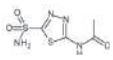			K_{d_obs}	2400	46	40000	87	840	140	220	13	21	130	79	63
					K_{d_intr}	1100	9.8	4600	12	270	34	9.8	2.4	2.9	24	35	12

K_ds of acetazolamide, commonly used as a control for binding to CAs, were taken from Ref. [37].

Table 2
Intrinsic enthalpy changes are listed for several compound binding to CAs, ΔH_{intr}, (kJ/mol) at 37 °C. These *intrinsic* enthalpy values were calculated as described in the methods section from the *observed* values determined by ITC and listed in Table S2. The protonation enthalpy change values of water molecule bound to Zn^{2+} in the active site of CAs were taken from Ref. [37] and of sulfonamide group of compounds were determined experimentally as described in section 3.5.1. The *intrinsic* values listed here take into account binding-linked protonation reactions and thus are buffer-independent while the *observed* ones depend on buffer and pH and thus should not be used in drug design.

Compound			CA II	CA VII	CA XII	CA XIII
		$\Delta_p H$ (kJ/mol)	**−23.5**	**−30.5**	**−25.5**	**−41.5**
4a	*(EA3-2)*	**−31.8**	−38.6	−28.7	−62.4	−40.7
4b	*(EA3-3)*	**−32.6**	−32.9	−21.8	−52.5	−40.2
4c	*(EA3-4)*	**−31.4**	−41.0	−33.8	−60.4	−41.6
5a	*(EA4-2)*	**−29.3**	−33.7	−32.4	−52.1	−42.1
5b	*(EA4-3)*	**−31.8**	−30.1	−25.3	−52.4	−44.9
16a	*(EA3-2o)*	**−26.8**	−30.2	−31.0	−52.1	−38.6
16b	*(EA3-3o)*	**−26.4**	−25.1	−38.1	−41.9	−37.7
16c	*(EA3-4o)*	**−25.9**	−31.2	−24.2	−31.2	−35.1
17a	*(EA4-2o)*	**−24.3**	−28.2	−22.9	−25.8	−38.7
17b	*(EA4-3o)*	**−24.3**	−20.5	−15.4	−29.6	−34.7
14a	*(EA4-2c)*	**−28.5**	−25.1	−17.7	−38.5	−35.2

how some substituents of benzenesulfonamides influence the binding affinity to human CAs. To do this, we have investigated a large group of chemically similar compounds and considered their structure-affinity relationship.

2.2.2. Compound structure determines the affinity-selectivity profile

General conclusions of each substituent contribution to *intrinsic* affinity of binding could be visualized as in Fig. 3 where compounds are arranged in pairs that differ only in a depicted chemical group.

Starting compounds (halo-substituent). The starting dihalo-compounds (**1**-**14**, **27**) bound to CAs in a similar way with few exceptions (Table S1). The highest affinity was for CA VII ($K_{d\_itnr} < 0.4$ nM), and the lowest for CA I ($K_{d\_itnr} > 80$ nM) except that compound **2** and **9** bound to CA VA as weakly as to CA I. Most compounds had a relatively high affinity for CA II, CA IX, and CA XIV ($K_{d\_itnr} < 1.5$ nM) and some compounds bound to CA IV (**5**-**8**, **10**-**14**, **27**) and CA XII (**1**, **3**-**4**, **6**, **8**, **11**-**13**, **27**) with $K_{d\_itnr} < 1.0$ nM. However,

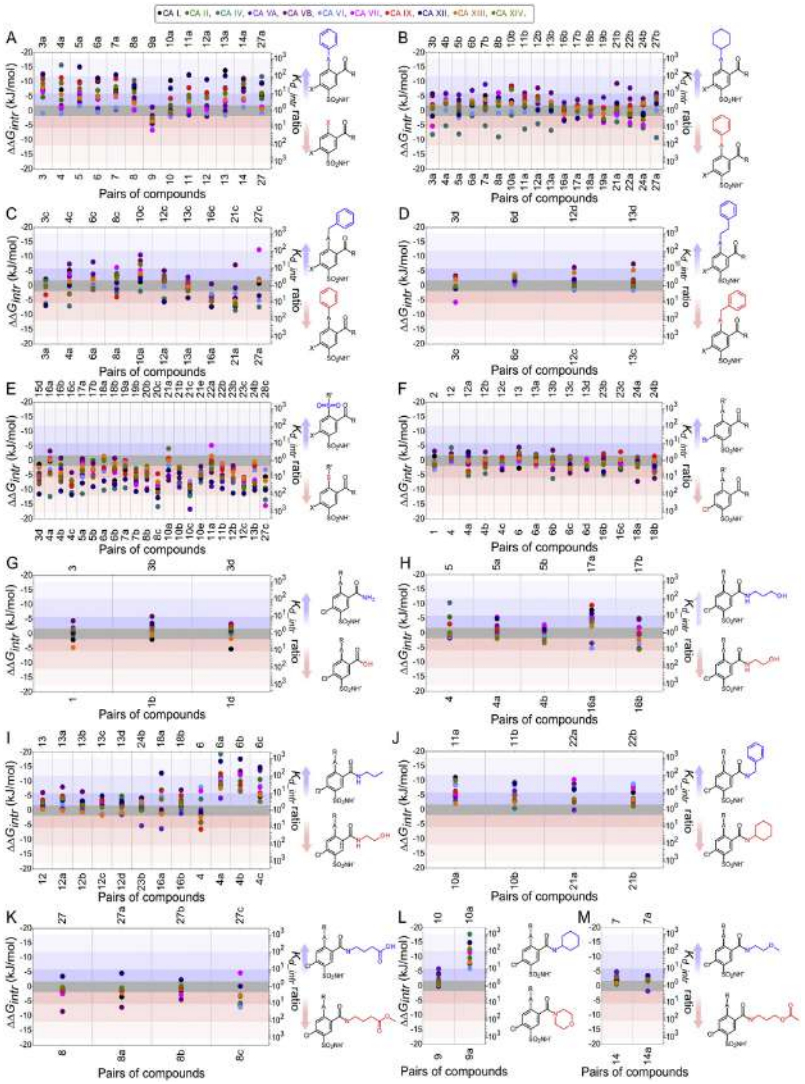

Fig. 3. Comparison of affinities of homologous compounds to CA (except to CA III) isoforms (listed in different colors, shown on top). Compounds are arranged in pairs that differ by a single substituent that is depicted. Datapoints above the zero line show that the compound bearing the shown substituent binds stronger than the compound bearing the substituent shown on the lower part of each plot. If the datapoint is below the zero line, it means that the compound bearing the lower substituent binds stronger. The differences in affinities are shown in kJ/mol units for $\Delta\Delta G_{intr}$ or the corresponding K_{d_intr} ratio shown on the right side of each plot. The darkest shaded area near the zero line shows the margin of the standard deviation of affinity determinations. **A**, benzene-bearing compounds in the *para* position bind significantly stronger than Cl or Br-containing compounds to most CAs; **B**, cyclohexyl group is preferred over the benzene except most notably CA IV; **C**, **D**, insertion of one or two methylene groups for the benzene had mixed effect; **E**, essentially all compounds bearing the S linker bound with 10 or even 100× greater affinity to nearly all CAs than the compounds bearing the SO_2 linker; **F**, comparison between Cl and Br shows a minor effect of their substitution; **G-M**, various substituents in the *meta* position had mixed effect on the affinity of compounds to CAs. It can be seen that there are some notable exceptions that hold for only one CA isoform making such compounds selective. (For interpretation of the references to color in this figure legend, the reader is referred to the Web version of this article.)

compounds **1, 2** (dichloro and dibromo benzoic acids) had the highest comparative selectivity for CA VII.

Phenyl, cyclohexyl, benzyl, and 2-phenylethyl substituents. Comparing all of the above described starting compounds with their analogous pairs - phenylsulfanyl substituted compounds ((**3**–**14, 27**)**a**), we saw a tendency that affinity for CA I, CA II, CA IV, CA VB, CA VII (not always), CA IX, CA XII, CA XIII, and CA XIV increased and for CA VA and CA VI remained similar (Fig. 3A). Only the pair of compounds **9**-**9a** contradicted this rule and this substituent slightly weakened or did not change the binding affinity.

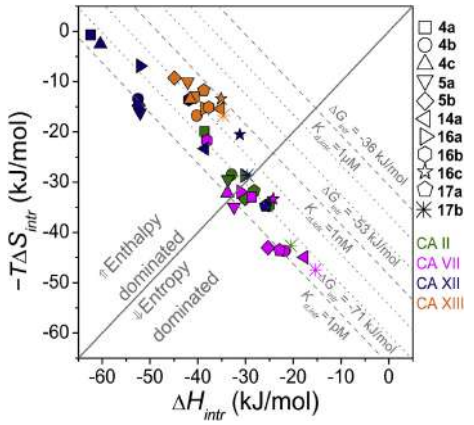

Fig. 4. The plot showing the enthalpy-entropy compensation. Intrinsic enthalpy changes upon binding for each ligand-CA pair are on the x-axis while the intrinsic entropy ($-T\Delta S_{intr}$) changes are on the y-axis of the plot. Different colors represent the four tested CA isoforms: CA II – green, CA VII – magenta, CA XII – dark blue, CA XIII – orange, while the symbols represent compounds, whose numbers are given on the right of the plot. Dashed and dotted lines indicate the intrinsic standard Gibbs energy changes or the dissociation constants and diagonal solid line indicates the situation where $-T\Delta S_{intr}$ and ΔH_{intr} contributions to the affinity (ΔG_{intr}) are equal. In all cases, both the enthalpy and entropy changes contributed favorably to the binding reaction. However, binding to CA XII and to CA XIII was almost always enthalpy driven, while to CA VII – entropy driven. (For interpretation of the references to color in this figure legend, the reader is referred to the Web version of this article.)

Compounds bearing cyclohexylsulfanyl ((**3**–**8, 10**–**13**)**b**), benzylsulfanyl ((**3**–**4, 6, 8, 10, 12**–**13**)**c**), and 2-phenylethylsulfanyl ((**3, 6, 12**–**13**)**d**) substituents had similar effect.

Fig. 3B shows the comparison of the binding affinity of phenyl- and cyclohexyl-substituted compounds, but in this case the binding also depended on sulfanyl (-S-) (**3a-3b**, **4a-4b**, **5a-5b**, **6a-6b**, **7a-7b**, **8a-8b**, **10a-10b**, **11a-11b**, **12a-12b**, **13a-13b**, **27a-27b**) and sulfonyl (-SO_2-) (**16a-16b**, **17a-17b**, **18a-18b**, **19a-19b**, **21a-21b**, **22a-22b**, **24a-24b**) linker. Phenylsulfanyl-substituted compounds had 10 or more times higher affinity for CA IV, approximately 10 times lower for CA VA and in some cases for several other CAs, while the affinity differences between compounds bearing phenylsulfanyl and cyclohexylsulfanyl substituents to remaining CAs were lower than the error margin of the measurements. Phenylsulfonyl (-SO_2-) substituted compounds, in contrast to phenylsulfanyl (-S-) substituted, did not have such high affinity for CA IV (except compounds **21a**, **22a**, **24a**), but were somewhat higher for CA VII. Similar to cyclohexylsulfanyl substituted compounds, cyclohexylsulfonyl substituent was more favorable for binding to CA VA and CA VB.

The differences in the Gibbs energy changes upon binding between phenyl substituted compounds ((**3**–**4, 6, 8, 10, 12**–**13, 16, 21, 27**)**a**) and benzyl substituted compounds ((**3**–**4, 6, 8, 10, 12**–**13, 16, 21, 27**)**c**) are shown in Fig. 3C. The replacement of these substituents had no clear dependence for the investigated compounds. However, compound **27c** had 100-fold higher affinity for CA VII than **27a**.

The benzyl substituted compounds ((**3**, **6**, **12**, **13**)**c**) are compared with the phenylethyl-substituted compounds ((**3**, **6**, **12**, **13**)**d**) in Fig. 3D. In all cases, the phenylethyl-substituted compounds **3d**, **6d**, **12d**, **13d** bound stronger to all CAs than their matching pairs, except compound **3d** bound 10 times weaker to CA VII.

Sulfanyl-, sulfinyl-, and sulfonyl-substituents. The analogous pairs of sulfanyl- and sulfonyl-substituted compounds, **3d** vs. **15d**, **4a** vs. **16a**, **4b** vs. **16b**, **4c** vs. **16c**, **5a** vs. **17a**, **5b** vs. **17b**, **6a** vs. **18a**, **6b** vs. **18b**, **7a** vs. **19a**, **7b** vs. **19b**, **8b** vs. **20b**, **8c** vs. **20c**, **10a** vs. **21a**, **10b** vs. **21b**, **10c** vs. **21c**, **10e** vs. **21e**, **11a** vs. **22a**, **11b** vs. **22b**, **12b** vs. **23b**, **12c** vs. **23c**, **13b** vs. **24b**, and **27c** vs. **28c** are compared in Fig. 3E. Almost all oxidized compounds had reduced binding affinity for all CAs as compared to their non-oxidized sulfanyl-analogue, except **16a** binding to CA VA, **21a** to CA XIV, and **22a** to CA VII. There is a general tendency that the most negative effect is on binding to CA IV, CA IV, and CA XII.

Two sulfinyl-substituted compounds (**25c, 26a)** were also investigated. Compound **25c** had its analogous pairs of sulfanyl- (**10c**) and sulfonyl- (**21c**) substituted compounds. Based on the intrinsic data (Table S1) of **10c**, **25c**, and **21c** binding, the oxidation of sulfanyl derivative decreased the binding affinity at least ten times and did not increase selectivity. However, comparing compounds **12a** and **26a**, the decrease in affinity was not very significant (except for several CAs).

Chloro and bromo substituents. We also investigated how the binding of compounds to CAs depended on the halogen substituent. Analogous pairs containing chloro and bromo substitutents, **1** vs. **2**, **4** vs. **12**, **4a** vs. **12a**, **4b** vs. **12b**, **4c** vs. **12c**, **6** vs. **13**, **6a** vs. **13a**, **6b** vs. **13b**, **6c** vs. **13c**, **6d** vs. **13d**, **16a** vs. **23b**, **16c** vs. **23c**,**18a** vs. **24a**, and **18b** vs. **24b**, bound to the same CA with the largest difference in the K_{d_intr} (several times in many cases, Fig. 3F). Based on the fact that standard deviation of the FTSA measurements is 2-fold in K_{d_obs} (or 2.8 kJ/mol in ΔG_{obs}) and there is no general tendency for compounds containing chloro or bromo substituents affinity to CAs, it can be stated that Cl or Br did not have a significant effect on the binding to CAs in this series of compounds.

Carboxamide substituents. Compounds **3**, **3b**, and **3d** had an affinity for CA VB up to 10 times greater than compounds **1**, **1b**, and **1d**, and the differences for other CAs were insignificant (Fig. 3G). It is also interesting that in many cases 3-hydroxypropyl substituent (**5, 5a-b**, **17a-b**) led to stronger interaction than the 2-hydroxyethyl substituent (**4, 4a-b**, **16a-b**) (Fig. 3H). When comparing 2-hydroxyethyl (**4**, **4a-c**, **12, 12a-d**, **16a-b**, **23b**) and *n*-butyl (**6**, **6a-c**, **13, 13a-d**, **18a-b**, **24b**) substituents, the butyl substituents appear to be more favorable in most cases (Fig. 3I). However, the influence of this group is distinguished by what other substituents were and the variability was quite high. Nevertheless, it was interesting that in the compounds **6a**, **6b** and **6c**, the butyl substituent was more than 1000 times more favorable for binding to CA XII than the 2-hydroxyethyl substituent in compounds **4a**, **4b**, and **4c**. Benzyl substituted compounds (**11a-b**, **22a-b**) bound up to 100 times stronger to all CAs than compounds with cyclohexyl substituent (**10a-b**, **21a-b**) (Fig. 3J). However, the cyclohexyl substituent was more favorable for stronger binding than morpholinyl derivative by comparing the pairs of compounds **9**-**10** and **9a**-**10a** (Fig. 3L). Compound bearing a carboxylic group (**27**, **27a**, **27b**) bound approximately 10 times stronger to CA XII and 10 times weaker to CA VB than compound having an ester group (**8**, **8a**, **8b**) (Fig. 3K). Comparing the pair of compounds **8c**-**27c**, the ester was more favorable to all CAs, except to CA VII. Compounds **7** and **7a** bound slightly stronger than compounds **14** and **14a**, but this difference was less than 10 times in K_{d_intr} (Fig. 3M).

2.2.3. Enthalpy-entropy compensation

The Gibbs energy change of binding is the sum of a number of processes occurring during the protein-ligand binding. The main Gibbs energy contributors are enthalpy (ΔH) and entropy (ΔS). Enthalpy-entropy compensation (Fig. 4 and Fig. S1) provides additional information about recognition, although this phenomenon is not fully understood. It was clear that all investigated compounds bound rather similarly to CA XIII and the affinity was

always driven by enthalpy (Fig. 4). The enthalpy contribution was also usually higher in the interaction with CA XII, but here the dispersion was greater. On the other hand, the binding of these compounds to CA II and CA VII was driven by entropy or enthalpy-entropy contribution was similar and the comparison of compounds showed that **17b** binding to CAs was more driven by entropy than for other compounds.

Looking at the enthalpy-entropy compensation plot (Fig. 4) it is clear that the investigated group of compounds bound to studied CAs with a rather wide range of binding enthalpies (−60 to −20 kJ/mol) and entropies (-$T\Delta S$ ranged from 0 to 50 kJ/mol). These ranges were significantly greater than the range of affinities (ΔG_{intr}) from −53 to −73 kJ/mol. The spread was primarily dependent on the CA isoform and less on the compound structure.

2.3. X-Ray crystallographic structures of CA-inhibitor complexes and intrinsic binding thermodynamics

2.3.1. Comparison between two compounds bound to CA II and CA XII

Four co-crystal structures of complexes between two CAs and two compounds, namely, CA II − **4b**, CA XII − **4b**, CA II − **16a**, and CA XII − **16a**, are presented in this work. The crystal structures of CA II and CA XII complexes contained 1 and 4 protein subunits in the asymmetric unit, respectively. The electron density maps of ligands bound in the active site of CAs are shown in Fig. S2. The data collection and refinement statistics are presented in Table S3. Compounds **4b** and **16a** differ by *para*-substituents: compound **4b** contains cyclohexylsulfanyl moiety (−S-C_6H_{11}) while **16a** − benzenesulfonyl (−SO_2-Ph).

Ortho-chlorobenzenesulfonamide moiety of both compounds was positioned similarly within the active site of CA II (Fig. 5A, the chlorine was fixed in the hydrophobic environment) and showed similar interactions with the protein. Positions of *para*-and *meta*-substituents of both compounds differed (Fig. 5A). The benzene ring of *para*-substituent of compound **16a** had two alternative positions, whereas cyclohexyl group of **4b** had only one conformation. The tail of *meta*-substituent of **4b** was directed toward the bulk solvent, away from the hydrophilic part of CA II active site, whereas *meta*-substituent of **16a** was located in the hydrophilic part of the active site.

Availability of both the co-crystal structures and the intrinsic energies of binding enabled the full analysis of the structure - thermodynamics correlations. The binding energies of compounds **4b** and **16a** to CA II were similar despite of different substituent in the *para*-position of these compounds, that interact with different parts of the active site ((Fig. 5E) **4b** vs. **16a**: ΔG_{intr} ((−61.5 vs. −59.0) kJ/mol), ΔH_{intr} ((−32.9 vs. −30.2) kJ/mol) and $-T\Delta S_{intr}$ ((−28.6 vs. −28.7) kJ/mol). Compounds differed only in the *para*-groups and probably the same interactions between same chemical structure of compounds (*ortho*-chlorobenzenesulfonamide moiety and amide linker of *meta*-substituent) and CA II caused the similarity of the binding energies.

Meta-substituents containing amide group in both crystal structures with CA XII were fixed by hydrogen bonds with Thr199 and Gln89 (Fig. 5B, red dashed lines). The differences were found in the position of tails of *meta*-groups: in case of **4b** the tail was directed away from the active site, whereas for **16a** the tail was located in the hydrophilic cavity. The *para*-substituents of both compounds interacted with the same part of active site in CA XII. The enthalpies of compound **4b** and **16a** binding to CA XII were identical and both compounds were enthalpy-driven (**4b**: ΔG_{intr} − −66.0 kJ/mol, ΔH_{intr} − −52.5 kJ/mol; **16a**: ΔG_{intr} − −59.0 kJ/mol, ΔH_{intr} − −52.1 kJ/mol). The binding entropies ($T\Delta S$) differed by 6.6 kJ/mol that improved the binding affinity of compound **4b** toward CA XII by about 10 fold. A similar enthalpic gain of both compound binding to CA XII could be caused by the same interaction of *ortho*-chlorobenzenesulfonamide moiety and amide linker of *meta*-substituent with the active site of CA XII. The loop (Gly138, Tyr121) that participates in the formation of protein active site was shifted in the crystal structure of CA XII-**4b** (Fig. 5B) compared with the structure of CA XII-**16a** due to a few changes in the protein packing (the unit cell of CA XII-**16a** was 2 times smaller).

Enthalpies of binding of both compounds **4b** and **16a** were similar for the same CA isoform but significantly differed between isoforms (~−30 kJ/mol for CA II and ~ −52 kJ/mol for CA XII). Binding modes of compound **4b** bound in CA II and CA XII are shown in Fig. 5C. The **4b** exhibited higher affinity for CA XII (ΔG_{intr}: −66.0 to CA XII kJ/mol vs. −61.5 kJ/mol to CA II) due to the enthalpic term (−52.5 kJ/mol in CA XII vs. −32.9 kJ/mol in CA II) and entropy term (−13.5 kJ/mol in CA XII vs. −28.6 kJ/mol in CA II). The cyclohexyl ring of **4b** in both isoforms was located in the hydrophobic part of the active site. The *ortho*-chlorobenzenesulfonamide moiety and *meta*-substituent were positioned identically because these moieties interacted with both isoforms in the relatively conservative part of active site.

Binding modes of compound **16a** in the active site of CA II and CA XII are compared in Fig. 5D. The binding affinities of the compound to CA II and CA XII were very similar ((−59.0 vs. −59.0) kJ/mol), while the binding entropies and enthalpies differed significantly. The binding energetics of **16a** to CA II and CA XII demonstrated enthalpy-entropy compensation effect. The *para*-group of compound had two conformations in the active site of CA II due to the presence of Phe131. In the active site of CA XII, the *para*-group of **16a** was found in a single conformation: benzene ring of benzenesulfonyl moiety was located in the hydrophobic environment, while the hydrophilic sulfonyl moiety − near the hydrophilic residues. It seems that the binding affinity of **16a** to CA II and XII depended only on the interactions of *ortho*-chlorobenzenesulfonamide moiety and *meta*-substituent with the conservative residues in both active sites. The changes of entropy and enthalpy likely were induced by the differences in binding thermodynamics of *para*-groups.

It seems that the binding energies of these compounds to CA II or CA XII did not significantly depend on the structural differences between compounds in *para*-position. On the other hand, compounds **16a** and **4b** had similar changes of binding energies to CA II and CA XII: **16a** ($\Delta\Delta G_{intr} = 0$ kJ/mol, $\Delta\Delta H_{intr} = -21.9$ kJ/mol and $\Delta(-T\Delta S_{intr}) = 21.8$ kJ/mol) and **4b** ($\Delta\Delta G_{intr} = -4.5$ kJ/mol, $\Delta\Delta H_{intr} = -19.6$ kJ/mol and $\Delta(-T\Delta S_{intr}) = 15.1$ kJ/mol). It is likely that the main cause of the changes in binding thermodynamics between compounds (**16a** or **4b**) to CA II and CA XII was caused by the changes in the release of water molecules during ligand-protein association process.

2.3.2. Compound orientation in CA IX and CA XII

Crystal structures of compounds **6d**, **5a** and **8b** with CA IX and **6d**, and **8b** in complex with CA XII (Fig. 6) yielded good overall electron density of the ligands (Fig. S3), being weaker for the flexible, hydrophilic tail moieties of some compounds. Ortho-chlorobenzenesulfonamide moiety in all compounds was found in a nearly identical position both in CA IX and CA XII where the chlorine atom was exposed to the hydrophobic part of active site, formed by two valine (121 and 143) and two leucine (141 and 198) residues, conserved in most CA isoforms. Therefore, the benzenesulfonamide part was fixed in all solved structures and it can be used as a rigid template for positioning of further tail moieties, consistent with our previous findings [19].

Compounds **6d** and **8b** had similar intrinsic binding affinities to CA IX and CA XII (K_{d_intr} in the range of 0.002−0.006 nM, Table S1).

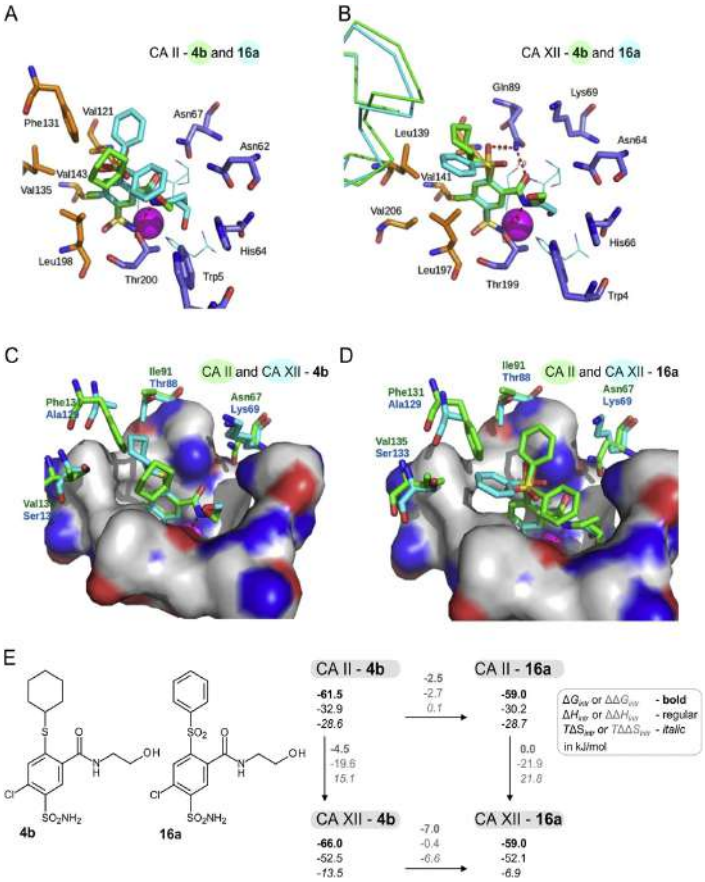

Fig. 5. X-ray crystallographic structures of compounds **4b** and **16a** in the active sites of CA II and CA XII. Panels **A** and **B** compare the binding of two compounds of similar chemical structures (**4b** (green) and **16a** (cyan)) to CA II (**A**; compound **4b** (PDB ID: 6R6F) and **16a**, PDB ID: 6R6J)) and CA XII (**B**; compound **4b** (PDB ID: 6R6Y) and **16a** (PDB ID: 6R71)). Hydrophobic residues of CA active sites are colored orange, hydrophilic – blue. Zinc ion is shown as pink sphere. Dashed red lines represent hydrogen bonds (the classical sulfonamide-CA hydrogen bonds are not shown). CA XII loop (Gly138, Tyr121) is shown as trace (green for complex CA XII-**4b** and cyan – CA XII-**16a**). Panels **C** and **D** compare compounds **4b** (**C**) and **16a** (**D**) binding to CA II (green) and CA XII (cyan). The residues that differ between CA II and CA XII active sites are shown as stick models. Similar residues of CA II and CA XII active sites are shown as the surface mode. The green and blue labels belong to CA II and CA XII models respectively. Electron densities of compounds bound to the active sites of CA II and CA XII are shown in Fig. S2. Panel **E** shows chemical structure of compounds **4b** and **16a** and the thermodynamic binding parameters to CA II and CA XII. (For interpretation of the references to color in this figure legend, the reader is referred to the Web version of this article.)

Thus, the structural differences between compounds did not influence the binding affinity to the same isoform (CA IX or CA XII). The binding modes of compound **6d** to CA IX and CA XII differed only in the position of the tail of the *para*-substituent (Fig. 6A). The differences in the binding mode of compound **8b** to CA IX and CA XII were located in the position of the tails of *meta*- and *para*-substituents (Fig. 6B). The tail of *meta*-substituent of compound **8b** stuck to the different parts of the active site of CA IX and CA XII, and was directed to solvent and was accessible for water molecules that weakened the interactions of compound with the protein surface. Thus, the same interactions between identical moieties, *ortho*-chlorobenzenesulfonamide and amide linker of *meta*-substituent, and similar molecular surface of both CAs caused the same binding affinity (Fig. 6A and B).

Compounds **8b** and **4b** structurally differed only in the *meta*-substituent, longer for **8b** (see Fig. 6C, orange circle). This difference did not have an effect on the binding affinities to CA XII (K_{d_intr}, 0.005 nM (**8b**) and 0.008 nM (**4b**)). The tails of *meta*-substituents of both compounds were directed toward the solvent. Differences in the position of cyclohexyl of *para*-substituent reflected the flexibility of this group and seemed to be not important for binding affinities to CA.

Compounds **5a**, **6d** and **8b** exhibited strong binding affinities for CA IX (0.006, 0.002, and 0.006 nM, respectively, Table S1). The tail of *meta*-substituent of the compound **5a** pushed water molecules out of the hydrophilic part of the active site and established hydrogen bonds with the protein surface (Fig. 6D, orange arrow), that, however, did not change the binding affinity. The structurally similar compound **6a** has a methyl group instead of hydroxy on the tail of *meta*-substituent. This structural change (-OH (**5a**) → $-CH_3$ (**6a**)) disabled the possibility of formation of the additional hydrogen bond. Despite this difference, both compounds had

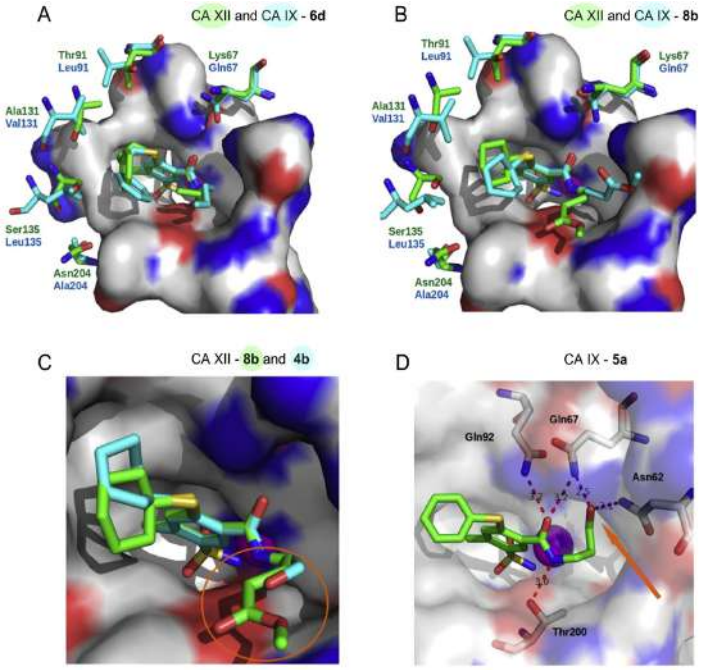

Fig. 6. X-ray crystallographic structures of compounds **6d**, **8b**, **4b** and **5a** in the active sites of CA IX and CA XII. Residues that differ between CA IX and CA XII active sites are shown as stick models. Similar residues of CA IX and CA XII active sites are shown as the surface mode. The green and blue labels belong to CA XII and CA IX models, respectively. **A**, Compound **6d** bound to active site of CA IX (cyan, PDB ID: 6QN6) and CA XII (green, PDB ID: 6QN0). **B**, Compound **8b** bound to active site of CA IX (cyan, PDB ID: 6QN2) and CA XII (green, PDB ID: 6QNL). **C**, Compounds **8b** (green, PDB ID: 6QNL) and **4b** (cyan, PDB ID: 3M5E) bound to active sites of CA XII. The structural differences between compounds **8b** and **4b** are shown in orange circle. **D**, Compounds **5a** bound to active site of CA IX (PDB ID: 6QN5). Dashed violet and red lines represent hydrogen bonds (the classical sulfonamide-CA hydrogen bonds are not shown). The orange arrow points to flexible tail of *meta*-substituent fixed by additional hydrogen bonds (violet). The hydrogen bonds shown as red dashed lines are the same between amide linker of *meta*-substituent and protein in the active site of CA II, CA IX, and XII for considered *ortho*-chlorobenzenesulfonamides. All electron densities of compounds are shown in Fig. S3. (For interpretation of the references to color in this figure legend, the reader is referred to the Web version of this article.)

similar binding affinities to CA IX (0.006 nM vs. 0.004 nM). The additional hydrogen bonds did not have impact on the binding affinity. Flexible *meta*-substituents interacted with the hydrophilic part of CA IX and CA XII active sites in all described crystal structures. Likely due to this flexibility, water molecules can efficiently compete with the compounds for the interactions with the hydrophilic part of the active sites.

Interestingly, compound **5a** exhibited an additional binding site in CA IX. There were a total of 6 inhibitor molecules bound per 4 monomers of CA IX crystal structure (Fig. S4). There were two additional molecules bound at the interface between CA IX molecules C and D. The two **5a** compound molecules even made a hydrophobic contact between their benzene rings. It seems that the formation of these two binding sites is an artifact of crystallization and the affinity could be in the micromolar to millimolar range. Therefore, it is not expected that these binding sites would have any physiological relevance.

3. Experimental

3.1. Organic synthesis

All starting materials and reagents were commercial products and were used without further purification. Melting points of the compounds were determined in open capillaries on a Thermo Scientific 9100 Series and are uncorrected. ^{1}H and ^{13}C NMR spectra were recorded on a (400 and 100 MHz, respectively) spectrometer in DMSO-d_6 using residual DMSO signals (2.52 ppm and 40.21 ppm for ^{1}H and ^{13}C NMR spectra, respectively) as the internal standard. TLC was performed with silica gel 60 F254 aluminum plates (Merck) and visualized with UV light. Column chromatography was performed using silica gel 60 (0.040–0.063 mm, Merck). High-resolution mass spectra (HRMS) were recorded on a Dual-ESI Q-TOF 6520 mass spectrometer (Agilent Technologies). The purity of final compounds was verified by HPLC to be >95% using the Agilent 1290 Infinity instrument with a Poroshell 120 SB-C18 (2.1 mm × 100 mm, 2.7 μm) reversed-phase column. Analytes were eluted using a linear gradient of water/methanol (20 mM ammonium formate in both phases) from 60:40 to 30:70 over 12 min, then from 30:70 to 20:80 over 1 min, and then 20:80 over 5 min at a flow rate of 0.2 mL/min. UV detection was at 254 nm.

2,4-dibromo-5-sulfamoyl-benzoic acid **2** and dihalosulfamoylbenzamides **3**–**14** were synthesized according to Ref. [19].

3.1.1. General procedure for the syntheses of (3–8, 10–14)a

The mixture of appropriate 2,4-dihalo-*N*-substituted-5-sulfamoylbenzamide (compounds **3**–**8, 10**–**14**) (1.00 mmol), MeOH (5 mL), thiophenol (121 mg, 1.10 mmol) and Et_3N (121 mg, 1.20 mmol) was refluxed for 2–6 h. Solvent was evaporated under reduced pressure and the resultant precipitate washed with H_2O.

*3.1.1.1. 4-Chloro-2-phenylsulfanyl-5-sulfamoyl-benzamide (**3a**, EA1A-2).* Recrystallization was accomplished from toluene: EtOH (6:1).Yield: 247 mg, 72%, mp 235–238 °C. ^{1}H NMR δ ppm: 6.76 (1H, s, C_3-H), 7.55–7.61 (5H, m, Ph-H), 7.64 (2H, s, SO_2NH_2), 7.76 (1H, s, $CONH_2$), 8.07 (1H, s, C_6-H), 8.23 (1H, s, $CONH_2$). ^{13}C NMR δ ppm: 128.7, 129.3, 130.4, 130.9, 131.6, 132.4, 133.0, 135.3, 137.7, 145.2, 167.9. HRMS calcd. for $C_{13}H_{11}ClN_2O_3S_2$ [(M + H)$^+$]: 342.9972, found: 342.9966.

*3.1.1.2. 4-Chloro-N-(2-hydroxyethyl)-2-phenylsulfanyl-5-sulfamoyl-benzamide (**4a**, EA3-2).* The product was purified by chromatography on a column of silica gel with EtOAc, R_f = 0.34. Yield: 255 mg, 66%, mp 192–193 °C. ^{1}H NMR δ ppm: 3.32–3.36 (2H, m, NHC<u>H</u>$_2$), 3.55 (2H, q, *J* = 6.0 Hz, C<u>H</u>$_2$OH), 4.79 (1H, t, *J* = 5.6 Hz, OH), 6.80 (1H, s, C_3-H), 7.53–7.57 (5H, m, Ph-H), 7.63 (2H, s, SO_2NH_2), 8.05 (1H, s, C_6-H), 8.74 (1H, t, *J* = 5.2 Hz, NH).^{13}C NMR δ ppm: 42.6, 60.0, 128.8, 129.4, 130.4, 130.8, 131.5, 132.3, 133.4, 135.2, 137.8, 144.9, 166.1. HRMS calcd. for $C_{15}H_{15}ClN_2O_4S_2$ [(M + H)$^+$]: 387.0235, found: 387.0233.

*3.1.1.3. 4-Chloro-N-(3-hydroxypropyl)-2-phenylsulfanyl-5-sulfamoyl-benzamide (**5a**, EA4-2).* Recrystallization was accomplished from toluene:2-PrOH (8:1). Yield: 257 mg, 64%, mp 146–148 °C. ^{1}H NMR δ ppm: 1.71 (2H, quint, *J* = 6.4 Hz, CH_2), 3.30–3.35 (2H, m, NHC<u>H</u>$_2$), 3.51 (2H, q, *J* = 6.0 Hz, C<u>H</u>$_2$OH), 4.50 (1H, t, *J* = 5.2 Hz, OH), 6.81 (1H, s, C_3-H), 7.54–7.57 (5H, m, Ph-H), 7.64 (2H, s, SO_2NH_2), 8.00 (1H, s, C_6-H), 8.73 (1H, t, *J* = 5.2 Hz, NH).^{13}C NMR δ ppm: 32.7, 37.0, 59.0, 128.6, 129.5, 130.4, 130.8, 131.4, 132.2, 133.8, 135.2, 137.9, 144.6, 166.0. HRMS calcd. for $C_{16}H_{17}ClN_2O_4S_2$ [(M + H)$^+$]: 401.0391, found: 401.0386.

*3.1.1.4. N-butyl-4-chloro-2-phenylsulfanyl-5-sulfamoyl-benzamide (**6a**, EA5-2).* Recrystallization was accomplished from toluene. Yield: 168 mg, 42%, mp 184–186 °C. ^{1}H NMR δ ppm: 0.92 (3H, t, *J* = 7.0 Hz, CH_3), 1.38 (2H, sext, *J* = 7.6 Hz, CH_2), 1.53 (2H, quint, *J* = 6.8 Hz, CH_2), 3.26 (2H, q, *J* = 6.4 Hz, NHC<u>H</u>$_2$), 6.82 (1H, s, C_3-H), 7.55 (5H, s, Ph-H), 7.64 (2H, s, SO_2NH_2), 7.99 (1H, s, C_6-H), 8.72 (1H, br s, NH).^{13}C NMR δ ppm: 14.2, 20.1, 31.5, 39.3, 128.6, 129.6, 130.3, 130.8, 131.5, 132.2, 133.9, 135.1, 137.9, 144.4, 165.9. HRMS calcd. for $C_{17}H_{19}ClN_2O_3S_2$ [(M + H)$^+$]: 399.0598, found: 399.0596.

*3.1.1.5. 4-Chloro-N-(2-methoxyethyl)-2-phenylsulfanyl-5-sulfamoyl-benzamide (**7a**, EA8-2).* Recrystallization was accomplished from toluene:2-PrOH (8:1). Yield: 249 mg, 62%, mp 170–172 °C. ^{1}H NMR δ ppm: 3.30 (3H, s, CH_3), 3.43 (2H, q, *J* = 5.2 Hz, NHC<u>H</u>$_2$), 3.49 (2H, t, *J* = 5.2 Hz, OCH_2), 6.81 (1H, s, C_3-H), 7.54–7.57 (5H, m, Ph-H), 7.63 (2H, s, SO_2NH_2), 8.01 (1H, s, C_6-H), 8.84 (1H, t, *J* = 5.2 Hz, NH).^{13}C NMR δ ppm: 39.5, 58.4, 70.7, 128.8, 129.5, 130.4, 130.8, 131.5, 132.4, 133.4, 135.2, 137.8, 144.8, 166.1. HRMS calcd. for $C_{16}H_{17}ClN_2O_4S_2$ [(M + H)$^+$]: 401.0391, found: 401.0390.

*3.1.1.6. Methyl 4-[(4-chloro-2-phenylsulfanyl-5-sulfamoyl-benzoyl) amino]butanoate (**8a**, VR16-3).* Recrystallization was accomplished from EtOAc:heptane (1:1). Yield: 343 mg, 77%, mp 136–137 °C. ^{1}H NMR δ ppm: 1,80 (2H, p, *J* = 7,2 Hz, NHCH$_2$C<u>H</u>$_2$), 2,42 (2H, t, *J* = 7,2 Hz, C<u>H</u>$_2$CO), 3,28 (2H, q, *J* = 6,8 Hz, NHC<u>H</u>$_2$), 3,60 (3H, s, CH_3), 6,81 (1H, s, C_3-H), 7,53-7,65 (5H, m, C_{Ar}-H), 7,65 (2H, s, NH_2), 7,99 (1H, s, C_6-H), 8,79 (1H, t, *J* = 5,6 Hz, NH).^{13}C NMR δ ppm: 24.8, 31.2, 39.0, 51.7, 128.6, 129.6, 130.3, 130.8, 131.5, 132.3, 133.7, 135.1, 138.0, 144.4, 166.0, 173.5. HRMS calcd. for $C_{18}H_{19}ClN_2O_5S_2$[(M + H)$^+$]: 443.0497, found: 443.0501.

*3.1.1.7. 4-Chloro-N-cyclohexyl-2-phenylsulfanyl-5-sulfamoyl-benzamide (**10a**, EA9-2).* Recrystallization was accomplished from toluene:2-PrOH (8:1). Yield: 344 mg, 81%, mp 236–238 °C. ^{1}H NMR δ ppm: 1.14–1.19 (1H, m, Cy-H), 1.26–1.37 (4H, m, Cy-H), 1.58–1.61 (1H, m, Cy-H), 1.73–1.75 (2H, m, Cy-H), 1.85–1.87 (2H, m, Cy-H), 3.75 (1H, br s, Cy-H), 6.82 (1H, s, C_3-H), 7.53–7.58 (5H, m, Ph-H), 7.65 (2H, s, SO_2NH_2), 7.95 (1H, s, C_6-H), 8.62 (1H, d, *J* = 8.0 Hz, NH).^{13}C NMR δ ppm: 25.1, 25.7, 32.7, 48.9, 128.6, 129.6, 130.3, 130.8, 131.5, 132.1, 134.4, 135.0, 138.0, 144.1, 165.1. HRMS calcd. for $C_{19}H_{21}ClN_2O_3S_2$ [(M + H)$^+$]: 425.0755, found: 425.0752.

*3.1.1.8. N-benzyl-4-chloro-2-phenylsulfanyl-5-sulfamoyl-benzamide (**11a**, EA10-2).* The product was purified by chromatography on a column of silica gel with $CHCl_3$:EtOAc (3:1), R_f = 0.35. Yield: 377 mg, 87%, mp 208–211 °C. ^{1}H NMR δ ppm: 4.49 (2H, d, *J* = 6.0 Hz, CH_2), 6.82 (1H, s, C_3-H), 7.25–7.30 (1H, m, Ph-H), 7.37–7.40 (4H, m, Ph-H), 7.54–7.60 (5H, m, Ph-H), 7.66 (2H, s, SO_2NH_2), 8.07 (1H, s, C_6-H), 9.34 (1H, t, *J* = 6.0 Hz, NH_2).^{13}C NMR δ ppm: 43.2, 127.4, 127.8, 128.7, 128.8, 129.6, 130.4, 130.9, 131.5, 132.5, 133.2, 135.2, 137.9, 139.4, 144.9, 166.0. HRMS calcd. for $C_{20}H_{17}ClN_2O_3S_2$ [(M + H)$^+$]: 433.0442, found: 433.0443.

*3.1.1.9. 4-Bromo-N-(2-hydroxyethyl)-2-phenylsulfanyl-5-sulfamoyl-benzamide compound (**12a**, LJ14-7).* Theproduct was purified by chromatography on a column of silica gel with EtOAc, R_f = 0.34. Yield: 362 mg, 84%, mp 191–193 °C. ^{1}H NMR δ ppm: 3.32 (2H, q, *J* = 6.0 Hz, NHC<u>H</u>$_2$), 3.54 (2H, q, *J* = 5.6 Hz, C<u>H</u>$_2$OH), 4.80 (1H, t, *J* = 5.2 Hz, OH), 6.79 (1H, s, C_3-H), 7.55 (5H, br s, Ph-H), 7.61 (2H, s, SO_2NH_2), 8.05 (1H, s, C_6-H), 8.74 (1H, br s, NH).^{13}C NMR δ ppm: 42.6, 60.0, 121.0, 128.8, 130.4, 130.8, 131.5, 132.9, 134.0, 135.2, 139.5, 144.5, 166.2. HRMS calcd. for $C_{15}H_{15}BrN_2O_4S_2$[(M + H)$^+$]: 432.9709 (100%), found: 432.9713 (100%).

*3.1.1.10. 4-Bromo-N-butyl-2-phenylsulfanyl-5-sulfamoyl-benzamide (**13a**, LJ14-9).* Recrystallization was accomplished from toluene. Yield: 244 mg, 55%, mp 184–186 °C. ^{1}H NMR δ ppm: 0.91 (3H, t, *J* = 7.2, Hz, CH_3), 1.37 (2H, sext, *J* = 7.6 Hz, CH_2), 1.52 (2H, quint, *J* = 7.2 Hz, CH_2), 3.25 (2H, q, *J* = 6.8 Hz, NHC<u>H</u>$_2$), 6.99 (1H, s, C_3-H), 7.53–7.58 (5H, m, Ph-H), 7.62 (2H, s, SO_2NH_2), 7.99 (1H, s, C_6-H), 8.72 (1H, t, *J* = 5.6 Hz, NH).^{13}C NMR δ ppm: 14.2, 20.1, 31.5, 39.3, 120.8, 128.6, 130.3, 130.8, 131.5, 133.1, 134.6, 135.1, 139.7, 144.1, 166.0. HRMS calcd. for $C_{17}H_{19}BrN_2O_3S_2$[(M + H)$^+$]: 445.0073 (100%), found: 445.0071 (100%).

*3.1.1.11. 3-[(4-Chloro-2-phenylsulfanyl-5-sulfamoyl-benzoyl)amino] propyl acetate (**14a**. EA4-2c).* [30].

*3.1.1.12. 2-Chloro-5-(morpholine-4-carbonyl)-4-phenylsulfanyl-benzenesulfonamide (**9a**, EA7-2).* The mixture of 2,4-dichloro-5-(morpholine-4-carbonyl)benzenesulfonamide (**12**) (339 mg, 1.00 mmol), DMSO (2 mL), thiophenol (121 mg, 1.10 mmol) and Cs_2CO_3 (652 mg, 2.00 mmol) was heated at 120 °C temperature for 8 h. The mixture was cooled to room temperature and brine was added. The product was extracted with EtOAc (3 × 7 mL). The organic layer was washed with H_2O, dried over anhydrous $MgSO_4$, filtered and concentrated.Recrystallization was accomplished from toluene:2-PrOH (8:1). Yield: 103 mg, 25%, mp 152–154 °C. ^{1}H NMR δ ppm: 3.17 (2H, br s, CH_2), 3.54 (2H, br s, CH_2), 3.62-3,69 (4H, m, $2CH_2$), 6.83 (1H, s, C_3-H), 7.56–7.58 (3H, m, Ph-H), 7.62–7.64 (2H, m, Ph-H), 7.75 (2H, s, SO_2NH_2), 7.86 (1H, s, C_6-H).^{13}C NMR δ ppm: 42.2, 47.2, 66.3, 66.6, 128.1, 129.0, 130.6, 130.9, 131.0, 132.7, 133.3, 135.5, 140.1, 140.6, 164.6. HRMS calcd. for $C_{17}H_{17}ClN_2O_4S_2$ [(M + H)$^+$]: 413.0391, found: 413.0393.

*3.1.2. General procedure for the syntheses of **(3–8, 9–13)b***

The mixture of appropriate 2,4-dihalo-*N*-substituted-5-sulfamoylbenzamide (compounds **3–8, 9–13**) (1.00 mmol), DMSO (2 mL), cyclohexanethiol(128 mg, 1.10 mmol) and K_2CO_3 (553 mg,

4.00 mmol) was heated at 60 °C temperature for 2–4 h. The mixture was cooled to room temperature and brine was added. The product was extracted with EtOAc (3 × 7 mL). The organic layer was washed with H_2O, dried over anhydrous $MgSO_4$, filtered and concentrated.

*3.1.2.1. 4-Chloro-2-cyclohexylsulfanyl-5-sulfamoyl-benzamide (**3b**, EA1A-3).* Recrystallization was accomplished from toluene:EtOAc (6:1) and then from toluene:acetone (5:1). Yield: 241 mg, 69%, mp 127–129 °C. ^{1}H NMR δ ppm: 1.20–1.47 (5H, m, Cy-H), 1.56–1.63 (1H, m, Cy-H), 1.67–1.72 (2H, m, Cy-H), 1.88–1.97 (2H, m, Cy-H), 3.52–3.61 (1H, m, S-Cy-H), 7.58–7.65 (4H, m, SO_2NH_2, C_3-H, $CONH_2$), 7.87 (1H, s, C_6-H), 7.97 (1H, s, $CONH_2$).^{13}C NMR δ ppm: 25.6, 31.2, 32.7, 44.1, 128.2, 130.3, 131.8, 136.3, 137.5, 141.6, 168.3. HRMS calcd. for $C_{13}H_{17}ClN_2O_3S_2$ [$(M + H)^+$]: 349.0442, found: 349.0449.

*3.1.2.2. 4-Chloro-2-cyclohexylsulfanyl-N-(2-hydroxyethyl)-5-sulfamoyl-benzamide (**4b**, EA3-3).* The product was purified by chromatography on a column of silica gel with $CHCl_3$:EtOAc (1:2), $R_f = 0.23$. Yield: 307 mg, 78%, mp 136–140 °C.^{1}H NMR δ ppm: 1.23–1.45 (5H, m, Cy-H), 1.58–1.61 (1H, m, Cy-H), 1.69–1.72 (2H, m, Cy-H), 1.90–1.93 (2H, m, Cy-H), 3.29 (2H, q, $J = 6.0$ Hz, NH$\underline{CH_2}$), 3.49–3.58 (3H, m, $\underline{CH_2}$OH, Cy-H), 4.73 (1H, t, $J = 5.6$ Hz, OH), 7.62 (1H, s, C_3-H), 7.63 (2H, s, SO_2NH_2), 7.86 (1H, s, C_6-H), 8.50 (1H, t, $J = 5.6$ Hz, NH).^{13}C NMR δ ppm: 25.6, 25.7, 32.8, 42.5, 44.2, 60.1, 128.4, 130.4, 131.8, 136.4, 137.6, 141.6, 166.5. HRMS calcd. for $C_{15}H_{21}ClN_2O_4S_2$[$(M + H)^+$]: 393.0704, found: 393.0707.

*3.1.2.3. 4-Chloro-2-cyclohexylsulfanyl-N-(3-hydroxypropyl)-5-sulfamoyl-benzamide (**5b**, EA4-3).* The product was purified by chromatography on a column of silica gel with $CHCl_3$:EtOAc (1:2), $R_f = 0.23$. Yield: 366 mg, 90%, mp 157–159 °C. ^{1}H NMR δ ppm: 1.24–1.47 (5H, m, Cy-H), 1.58–1.61 (1H, m, Cy-H), 1.63–1.72 (4H, m, Cy-H, CH_2), 1.90–1.93 (2H, m, Cy-H), 3.27 (2H, q, $J = 6.4$ Hz, NH$\underline{CH_2}$), 3.49 (2H, q, $J = 6.0$ Hz, $\underline{CH_2}$OH), 3.52–3.58 (1H, m, Cy-H), 4.47 (1H, t, $J = 5.2$ Hz, OH), 7.63 (1H, s, C_3-H), 7.64 (2H, s, SO_2NH_2), 7.81 (1H, s, C_6-H), 8.49 (1H, t, $J = 5.2$ Hz, NH).^{13}C NMR δ ppm: 25.6, 25.7, 32.7, 32.8, 36.9, 44.3, 59.0, 128.2, 130.6, 131.7, 136.7, 137.7, 141.4, 166.4. HRMS calcd. for $C_{16}H_{23}ClN_2O_4S_2$[$(M + H)^+$]: 407.0861, found 407.0856.

*3.1.2.4. N-butyl-4-chloro-2-cyclohexylsulfanyl-5-sulfamoyl-benzamide (**6b**, EA5-3).* The product was purified by chromatography on a column of silica gel with:$CHCl_3$:EtOAc (3:1), $R_f = 0.35$.Yield: 340 mg, 84%, mp 153–154 °C. ^{1}H NMR δ ppm: 0.91 (3H, t, $J = 7.2$ Hz, CH_3), 1.24–1.41 (7H, m, Cy-H, CH_2), 1.49 (2H, quint, $J = 6.8$ Hz, CH_2),1.57 (1H, br s, Cy-H), 1.69 (2H, br s, Cy-H), 1.90–1.93 (2H, m, Cy-H), 3.22 (2H, q, $J = 6.0$ Hz, NH$\underline{CH_2}$), 3.55 (1H, br s, Cy-H), 7.64 (3H, s, C_3-H, SO_2NH_2), 7.80 (1H, s, C_6-H), 8.48 (1H, br s, NH).^{13}C NMR δ ppm: 14.1, 20.0, 25.5, 25.7, 31.5, 32.7, 39.1, 44.2, 128.2, 130.6, 131.7, 136.9, 137.8, 141.3, 166.3. HRMS calcd. for $C_{17}H_{25}ClN_2O_3S_2$[$(M + H)^+$]: 405.1068, found: 405.1064.

*3.1.2.5. 4-Chloro-2-cyclohexylsulfanyl-N-(2-methoxyethyl)-5-sulfamoyl-benzamide (**7b**, EA8-3).* The product was purified by chromatography on a column of silica gel with $CHCl_3$:EtOAc (1:1), $R_f = 0.30$. Yield: 285 mg, 70%, mp 130–133 °C. ^{1}H NMR δ ppm: 1.24–1.42 (5H, m, Cy-H), 1.58–1.61 (1H, m, Cy-H), 1.69–1.71 (2H, m, Cy-H), 1.91–1.93 (2H, m, Cy-H), 3.29 (3H, m, CH_3), 3.36–3.39 (2H, m, NH$\underline{CH_2}$), 3.44–3.46 (2H, m, OCH_2), 3.55 (1H, br s, Cy-H), 7.64 (3H, s, C_3-H, SO_2NH_2), 7.83 (1H, s, C_6-H), 8.61 (1H, br s, NH).^{13}C NMR δ ppm: 25.6, 25.7, 32.8, 39.4, 44.2, 58.4, 70.8, 128.4, 130.6, 131.8, 136.4, 137.7, 141.5, 166.5. HRMS calcd. for $C_{16}H_{23}ClN_2O_4S_2$[$(M + H)^+$]: 407.0861, found: 407.0862.

*3.1.2.6. Methyl 4-[(4-chloro-2-cyclohexylsulfanyl-5-sulfamoyl-benzoyl)amino]butanoate (**8b**, EA11-3).* Recrystallization was accomplished from toluene:EtOAc (5:1). Yield: 418 mg, 93%, mp 165–167 °C. ^{1}H NMR δ ppm: 1.15–1.44 (5H, m, Cy-H), 1.57–1.60 (1H, m, Cy-H), 1.68–1.73 (2H, m, Cy-H), 1.77 (2H, quint, $J = 7.2$ Hz, CH_2), 1.89–1.92 (2H, m, Cy-H), 2.43 (2H, t, $J = 7.2$ Hz, $COCH_2$), 3.24 (2H, q, $J = 6.4$ Hz, NH$\underline{CH_2}$), 3.53–3.58 (1H, m, Cy-H), 3.61 (3H, s, CH_3), 7.65 (3H, s, C_3-H, SO_2NH_2), 7.81 (1H, s, C_6-H), 8.55 (1H, t, $J = 5.6$ Hz, NH).^{13}C NMR δ ppm: 24.8, 25.5, 25.7, 31.1, 32.7, 38.7, 40.6, 51.8, 128.1, 130.8, 131.7, 136.9, 137.9, 141.2, 166.5, 173.6. HRMS calcd. for $C_{18}H_{25}ClN_2O_5S_2$[$(M + H)^+$]: 449.0966, found: 449.0962.

*3.1.2.7. 4-Chloro-N-cyclohexyl-2-cyclohexylsulfanyl-5-sulfamoyl-benzamide (**10b**, EA9-3).* The product was purified by chromatography on a column of silica gel with $CHCl_3$:EtOAc (5:1), $R_f = 0.20$. Yield: 410 mg, 95%, mp 92–94 °C. ^{1}H NMR δ ppm: 1.10–1.38 (10H, m, Cy-H), 1.57–1.60 (2H, m, Cy-H), 1.69–1.73 (4H, m, Cy-H), 1.82–1.84 (2H, m, Cy-H), 1.90–1.92 (2H, m, Cy-H), 3.51–3.57 (1H, m, Cy-H), 3.67–3.75 (1H, m, Cy-H), 7.63 (1H, s, C_3-H), 7.64 (2H, s, SO_2NH_2), 7.77 (1H, s, C_6-H), 8.40 (1H, d, $J = 7.6$ Hz, NH).^{13}C NMR δ ppm: 25.0, 25.6 (2C), 25.7, 32.6, 32.8, 40.4, 48.7, 128.2, 130.8, 131.5, 137.2, 137.8, 141.1, 165.5.HRMS calcd. for $C_{19}H_{27}ClN_2O_3S_2$[$(M + H)^+$]: 431.1224, found: 431.1227.

*3.1.2.8. N-benzyl-4-chloro-2-cyclohexylsulfanyl-5-sulfamoyl-benzamide (**11b**, EA10-3).* The product was purified by chromatography on a column of silica gel with $CHCl_3$:EtOAc (3:1), $R_f = 0.24$. Yield: 378 mg, 86%, mp 160–162 °C. ^{1}H NMR δ ppm: 1.21–1.43 (5H, m, Cy-H), 1.56–1.59 (1H, m, Cy-H), 1.68–1.71 (2H, m, Cy-H), 1.89–1.92 (2H, m, Cy-H), 3.54–3.60 (1H, m, Cy-H), 4.45 (2H, d, $J = 6.0$ Hz, CH_2), 7.25–7.29 (1H, m, Ph-H), 7.33–7.40 (4H, m, Ph-H), 7.67 (3H, s, C_3-H, SO_2NH_2), 7.87 (1H, s, C_6-H), 9.09 (1H, t, $J = 6.0$ Hz, NH_2).^{13}C NMR δ ppm: 25.4, 25.7, 32.7, 43.0, 44.3, 127.4, 127.8, 128.3, 128.7, 130.8, 131.9, 136.5, 137.8, 139.5, 141.5, 166.5. HRMS calcd. for $C_{20}H_{23}ClN_2O_3S_2$[$(M + H)^+$]: 439.0911, found: 439.0914.

*3.1.2.9. 4-Bromo-2-cyclohexylsulfanyl-N-(2-hydroxyethyl)-5-sulfamoyl-benzamide (**12b**, LJ15-22).* The product was purified by chromatography on a column of silica gel with EtOAc, $R_f = 0.46$. Yield: 367 mg, 84%, mp 118–120 °C. ^{1}H NMR δ ppm: 1.23–1.44 (5H, m, Cy-H), 1.57–1.60 (1H, m, Cy-H), 1.69–1.72 (2H, m, Cy-H), 1,89-1,92 (2H, m, Cy-H), 3.29 (2H, q, $J = 6.4$ Hz, NH$\underline{CH_2}$), 3.48–3.56 (3H, m, HO$\underline{CH_2}$, Cy-H), 4.72 (1H, t, $J = 5.6$ Hz, OH), 7.60 (2H, s, SO_2NH_2), 7.77 (1H, s, C_3-H), 7.88 (1H, s, C_6-H), 8.48 (1H, t, $J = 5.6$ Hz, NH).^{13}C NMR δ ppm: 25.6, 25.7, 32.8, 42.4, 44.4, 60.1, 120.3, 128.4, 134.1, 137.2, 139.5, 141.2, 166.6. HRMS calcd. for $C_{15}H_{21}BrN_2O_4S_2$ [$(M + H)^+$]: 439.0178 (100%), found: 439.0177 (100%).

*3.1.2.10. 4-Bromo-N-butyl-2-cyclohexylsulfanyl-5-sulfamoyl-benzamide (**13b**, LJ15-32).* The product was purified by chromatography on a column of silica gel with $CHCl_3$:EtOAc (4:1), $R_f = 0.31$. Yield: 166 mg, 37%, mp 127–129 °C. ^{1}H NMR δ ppm: 0.90 (3H, t, $J = 7.2$, Hz, CH_3), 1.21–1.40 (7H, m, $CH_3\underline{CH_2}$, Cy-H), 1.43–1.52 (2H, m, $CH_3CH_2\underline{CH_2}$), 1.57–1.60 (1H, m, Cy-H), 1.68–1.72 (2H, m, Cy-H), 1.89–1.92 (2H, m, Cy-H), 3.20 (2H, q, $J = 6.4$ Hz, NH$\underline{CH_2}$), 3.52–3.57 (1H, m, Cy-H), 7.62 (2H, s, SO_2NH_2), 7.78 (1H, s, C_3-H), 7.82 (1H, s, C_6-H), 8.48 (1H, t, $J = 5.6$ Hz, NH).^{13}C NMR δ ppm: 14.1, 20.0, 25.5, 25.7, 31.5, 32.7, 39.1, 44.4, 120.1, 128.2, 134.2, 137.7, 139.7, 140.9, 166.4. HRMS calcd. for $C_{17}H_{25}BrN_2O_3S_2$[$(M + H)^+$]: 451.0542 (100%), found: 451.0546 (100%).

*3.1.3. General procedure for the syntheses of **(3–4, 6, 8, 10, 12–13) c, (3, 6, 12–13)d, 10e, 13e***

The mixture of appropriate 2,4-dihalo-*N*-substituted-5-sulfamoylbenzamide(compounds **3–4, 6, 8, 10, 12–13**)

(1.00 mmol), DMSO (2 mL), appropriate phenylmethanethiol, 2-phenylethanethiol, or 2-mercaptoethanol(1.10 mmol) and Et_3N (121 mg, 1.20 mmol) was heated at 60 °C temperature for 6–12 h. The progress of reaction was monitored by TLC. The mixture was cooled to room temperature and brine was added. The product was extracted with EtOAc (3 × 7 mL). The organic layer was washed with H_2O, dried over anhydrous $MgSO_4$, filtered and concentrated.

*3.1.3.1. 2-Benzylsulfanyl-4-chloro-5-sulfamoyl-benzamide (**3c**, EA1A-4).* Recrystallization was accomplished from toluene:EtOH (6:1). Yield: 305 mg, 85%, mp 203–204 °C. ^{1}H NMR δ ppm: 4.36 (2H, s, $\underline{CH_2}$Ph), 7.26–7.45 (5H, m, Ph-H), 7.61 (2H, s, C_3-H, $CONH_2$),7.63 (2H, s, SO_2NH_2), 7.95 (1H, s, C_6-H), 8.06 (1H, s, $CONH_2$).^{13}C NMR δ ppm: 36.2, 127.8, 128.3, 128.7, 129.0, 129.5, 132.3, 133.5, 136.6, 137.0, 145.0, 168.1. HRMS calcd. for $C_{14}H_{13}ClN_2O_3S_2$ [(M + H)$^+$]: 357.0129, found: 357.0127.

*3.1.3.2. 4-Chloro-2-(2-phenylethylsulfanyl)-5-sulfamoyl-benzamide (**3d**, EA1A-5).* Recrystallization was accomplished from toluene:acetone (5:1). Yield: 327 mg, 88%, mp 159–161 °C. ^{1}H NMR δ ppm: 2.91 (2H, t, J = 7.6 Hz, $\underline{CH_2}$Ph), 3.32 (2H, t, J = 7.6 Hz, CH_2S), 7.21–7.35 (5H, m, Ph-H), 7.59 (1H, s, C_3-H), 7.62 (3H, s, SO_2NH_2, $CONH_2$), 7.92 (1H, s, C_6-H), 8.02 (1H, s, $CONH_2$).^{13}C NMR δ ppm: 33.2, 34.3, 126.9, 128.2, 128.6, 128.8, 129.0, 132.6, 134.4, 137.0, 140.2, 143.6, 168.2. HRMS calcd. for $C_{15}H_{15}ClN_2O_3S_2$ [(M + H)$^+$]: 371.0285, found: 371.0281.

*3.1.3.3. 2-Benzylsulfanyl-4-chloro-N-(2-hydroxyethyl)-5-sulfamoyl-benzamide (**4c**, EA3-4).* Recrystallization was accomplished from H_2O:MeOH (5:1) and then from toluene:MeOH (5:1). Yield: 241 mg, 60%, mp 193–195 °C. ^{1}H NMR δ ppm: 3.28 (2H, q, J = 6.0 Hz, NH$\underline{CH_2}$), 3.50 (2H, q, J = 6.0 Hz, $\underline{CH_2}$OH), 4.35 (2H, s, $\underline{CH_2}$Ph), 4.73 (1H, t, J = 5.6 Hz, OH), 7.26–7.44 (5H, m, Ph-H), 7.59 (2H, s, SO_2NH_2), 7,62 (1H, s, C_3-H), 7,92 (1H, s, C_6-H), 8.56 (1H, t, J = 5.6 Hz, NH).^{13}C NMR δ ppm: 36.2, 42.5, 60.0, 127.9, 128.3, 128.7, 129.0, 129.5, 132.2, 133.9, 136.6, 137.0, 134.8, 166.3. HRMS calcd. for $C_{16}H_{17}ClN_2O_4S_2$ [(M + H)$^+$]: 401.0391, found: 401.0393.

*3.1.3.4. 2-Benzylsulfanyl-N-butyl-4-chloro-5-sulfamoyl-benzamide (**6c**, EA5-4).* The product was purified by chromatography on a column of silica gel with $CHCl_3$:EtOAc (3:1), R_f = 0.40. Yield: 153 mg, 37%, mp 148–150 °C. ^{1}H NMR δ ppm: 0.89 (3H, t, J = 7.2 Hz, CH_3), 1.33 (2H, sext, J = 7.2 Hz, CH_2),1.48 (2H, quint, J = 7.2 Hz, CH_2), 3.20 (2H, q, J = 6.8 Hz, NH$\underline{CH_2}$), 4.36 (2H, s, $\underline{CH_2}$Ph), 7.25–7.36 (3H, m, Ph-H), 7.41–7.43 (2H, m, Ph-H), 7.61 (2H, s, SO_2NH_2), 7,63 (1H, s, C_3-H), 7.85 (1H, s, C_6-H), 8.56 (1H, t, J = 5.6 Hz, NH).^{13}C NMR δ ppm: 14.1, 20.0, 31.4, 36.2, 39.2, 127.8, 128.1, 128.8, 129.0, 129.5, 132.1, 134.4, 136.6, 137.2, 143.4, 166.1. HRMS calcd. for $C_{18}H_{21}ClN_2O_3S_2$ [(M + H)$^+$]: 413.0755, found: 413.0757.

*3.1.3.5. N-butyl-4-chloro-2-phenethylsulfanyl-5-sulfamoyl-benzamide (**6d**, EA5-5).* The product was purified by chromatography on a column of silica gel with $CHCl_3$:EtOAc (3:1), R_f = 0.45. Yield: 265 mg, 62%, mp 87–88 °C. ^{1}H NMR δ ppm: 0.90 (3H, t, J = 7.2 Hz, CH_3), 1.34 (2H, sext, J = 7.2 Hz, CH_2),1.48 (2H, quint, J = 7.2 Hz, CH_2), 2.89 (2H, t, J = 7.6 Hz, $\underline{CH_2}$Ph), 3.20 (2H, q, J = 6.8 Hz, NH$\underline{CH_2}$), 3.32–3.35 (2H, m, CH_2S), 7.21–7.25 (1H, m, Ph-H), 7.28–7.33 (4H, m, Ph-H), 7.60 (1H, s, C_3-H), 7.62 (2H, s, SO_2NH_2), 7.83 (1H, s, C_6-H), 8.53 (1H, t, J = 5.6 Hz, NH).^{13}C NMR δ ppm: 14.1, 20.1, 31.5, 33.2, 34.3, 39.2, 126.9, 128.1, 128.7, 128.8, 129.1, 132.1, 135.1, 137.2, 140.1, 143.2, 166.2. HRMS calcd. for $C_{19}H_{23}ClN_2O_3S_2$ [(M + H)$^+$]: 427.0911, found: 427.0907.

*3.1.3.6. Methyl 4-[(2-benzylsulfanyl-4-chloro-5-sulfamoyl-benzoyl) amino]butanoate (**8c**, EA11-4).* The product was purified by chromatography on a column of silica gel with EtOAc:$CHCl_3$ (1:1), R_f = 0.42, and then recrystallization was accomplished from H_2O:MeOH (5:1). Yield: 306 mg, 67%, mp 115–118 °C. ^{1}H NMR δ ppm: 1.75 (2H, quint, J = 7.2 Hz, CH_2), 2.38 (2H, t, J = 7.6 Hz, $COCH_2$), 3.22 (2H, q, J = 6.8 Hz, NH$\underline{CH_2}$), 3.59 (3H, s, CH_3), 4.37 (2H, s, $\underline{CH_2}$Ph), 7.25–7.36 (3H, m, Ph-H), 7.40–7.43 (2H, m, Ph-H), 7.62 (2H, s, SO_2NH_2), 7.64 (1H, s, C_3-H), 7.86 (1H, s, C_6-H), 8.64 (1H, t, J = 6.0 Hz, NH).^{13}C NMR δ ppm: 24.7, 31.1, 36.2, 38.8, 51.8, 127.9, 128.1, 128.8, 129.0, 129.5, 132.2, 134.2, 136.6, 137.2, 143.4, 166.2, 173.5. HRMS calcd. for $C_{19}H_{21}ClN_2O_5S_2$ [(M + H)$^+$]: 457.0653, found: 457.0652.

*3.1.3.7. 2-Benzylsulfanyl-4-chloro-N-cyclohexyl-5-sulfamoyl-benzamide (**10c**, EA9-4).* Recrystallization was accomplished from H_2O:MeOH (5:1) and then from toluene:MeOH (5:1). Yield: 329 mg, 75%, mp 194–196 °C. ^{1}H NMR δ ppm: 1.07–1.13 (1H, m, Cy-H), 1.22–1.33 (4H, m, Cy-H), 1.56–1.59 (1H, m, Cy-H), 1.66–1.72 (2H, m, Cy-H), 1.79–1.85 (2H, m, Cy-H), 3.63–3.72 (1H, m, Cy-H), 4.36 (2H, s, $\underline{CH_2}$Ph), 7.25–7.31 (1H, m, Ph-H), 7.33–7.36 (2H, m, Ph-H), 7.41–7.43 (2H, m, Ph-H), 7.61 (2H, s, SO_2NH_2), 7.62 (1H, s, C_3-H), 7.81 (1H, s, C_6-H), 8.47 (1H, d, J = 7.6 Hz, NH).^{13}C NMR δ ppm: 25.1, 25.6, 32.6, 36.2, 48.8, 127.9, 128.1, 128.8, 128.9, 129.0, 129.5, 129.9, 131.9, 136.7, 143.2, 165.3. HRMS calcd. for $C_{20}H_{23}ClN_2O_3S_2$ [(M + H)$^+$]: 439.0911, found: 439.0911.

*3.1.3.8. 4-Chloro-N-cyclohexyl-2-(2-hydroxyethylsulfanyl)-5-sulfamoyl-benzamide (**10e**, EA9-11).* The product was purified by chromatography on a column of silica gel with EtOAc:$CHCl_3$ (1:1), R_f = 0.18, and then recrystallization was accomplished from H_2O:MeOH (5:1). Yield: 185 mg, 47%, mp 180–181 °C. ^{1}H NMR δ ppm: 1.09–1.18 (1H, m, Cy-H), 1.20–1.35 (4H, m, Cy-H), 1.57–1.60 (1H, m, Cy-H), 1.70–1.74 (2H, m, Cy-H), 1.82–1.84 (2H, m, Cy-H), 3.13 (2H, t, J = 6.4 Hz, SCH_2), 3.61 (2H, q, J = 6.0 Hz, $\underline{CH_2}$OH), 3.66–3.74 (1H, m, Cy-H), 5.05 (1H, t, J = 5.6 Hz, OH), 7.61 (1H, s, C_3-H), 7.62 (2H, s, SO_2NH_2), 7.78 (1H, s, C_6-H), 8.44 (1H, d, J = 7.6 Hz, NH).^{13}C NMR δ ppm: 25.1, 25.7, 32.6, 35.1, 48.7, 59.9, 128.1, 128.7, 131.9, 135.5, 137.2, 143.2, 165.5. HRMS calcd. for $C_{15}H_{21}ClN_2O_4S_2$ [(M + H)$^+$]: 393.0704, found: 393.0706.

*3.1.3.9. 2-Benzylsulfanyl-4-bromo-N-(2-hydroxyethyl)-5-sulfamoyl-benzamide (**12c**, LJ15-23).* The product was purified by chromatography on a column of silica gel with EtOAc, R_f = 0.50. Yield: 352 mg, 79%, mp 147–149 °C. ^{1}H NMR δ ppm: 3.28 (2H, q, J = 6.0 Hz, NH$\underline{CH_2}$), 3.50 (2H, q, J = 6.4 Hz, HO$\underline{CH_2}$), 4.35 (2H, s, S$\underline{CH_2}$), 4.74 (1H, t, J = 5.2 Hz, OH), 7.26-7,45 (5H, m, Ph-H), 7.56 (2H, s, SO_2NH_2), 7.77 (1H, s, C_3-H), 7.94 (1H, s, C_6-H), 8.55 (1H, t, J = 5.6 Hz, NH).^{13}C NMR δ ppm: 36.2, 42.5, 60.0, 120.9, 127.9, 128.3, 129.0, 129.5, 132.2, 134.6, 136.6, 138.9, 143.4, 166.4. HRMS calcd. for $C_{16}H_{17}BrN_2O_4S_2$[(M + H)$^+$]: 446.9865 (100%), found: 446.9870 (100%).

*3.1.3.10. 4-Bromo-N-(2-hydroxyethyl)-2-phenethylsulfanyl-5-sulfamoyl-benzamide (**12d**, LJ15-24).* The product was purified by chromatography on a column of silica gel with EtOAc, R_f = 0.42. Yield: 193 mg, 42%, mp 154–156 °C. ^{1}H NMR δ ppm: 2.89 (2H, t, J = 7.6 Hz, $SCH_2\underline{CH_2}$), 3.26-3,32 (4H, m, NH$\underline{CH_2}$, S$\underline{CH_2}$), 3.50 (2H, q, J = 6.0 Hz, HO$\underline{CH_2}$), 4.74 (1H, t, J = 5.2 Hz, OH), 7.21–7.34 (5H, m, Ph-H), 7.58 (2H, s, SO_2NH_2), 7.74 (1H, s, C_3-H), 7.92 (1H, s, C_6-H), 8.53 (1H, t, J = 5.6 Hz, NH).^{13}C NMR δ ppm: 33.3, 34.3, 42.5, 60.1, 120.9, 126.9, 128.3, 128.9, 129.0, 132.1, 135.3, 138.9, 140.2, 143.1, 166.5. HRMS calcd. for $C_{17}H_{19}BrN_2O_4S_2$[(M + H)$^+$]: 461.0022 (100%), found: 461.0016 (100%).

*3.1.3.11. 2-Benzylsulfanyl-4-bromo-N-butyl-5-sulfamoyl-benzamide (**13c**, LJ15-33).* The product was purified by chromatography on a

column of silica gel with EtOAc:$CHCl_3$ (4:1), $R_f = 0.24$. Yield: 165 mg, 36%, mp 155–157 °C. ^{1}H NMR δ ppm: 0.89 (3H, t, $J = 7.2$, Hz, CH_3), 1.34 (2H, sext, $J = 7.2$ Hz, $CH_3\underline{CH_2}$), 1.48 (2H, quint, $J = 6.8$ Hz, $CH_3CH_2\underline{CH_2}$), 3.20 (2H, q, $J = 6.8$ Hz, $NH\underline{CH_2}$), 4.36 (2H, s, $S\underline{CH_2}$), 7.25–7.43 (5H, m, Ph-H), 7.57 (2H, s, $SO_2\underline{NH_2}$), 7.78 (1H, s, C_3-H), 7.87 (1H, s, C_6-H), 8.54 (1H, t, $J = 5.6$ Hz, NH).^{13}C NMR δ ppm: 14.1, 20.0, 31.4, 36.2, 39.2, 120.7, 127.8, 128.1, 129.0, 129.5, 132.3, 135.1 136.7, 139.0, 143.0, 166.2. HRMS calcd. for $C_{18}H_{21}BrN_2O_3S_2$[(M + H)$^+$]: 459.0230 (100%), found: 459.0231 (100%).

*3.1.3.12. 4-Bromo-N-butyl-2-phenethylsulfanyl-5-sulfamoyl-benzamide (**13d**, LJ15-34).* The product was purified by chromatography on a column of silica gel with $CHCl_3$:EtOAc (4:1), $R_f = 0.28$. Yield: 259 mg, 55%, mp 157–159 °C. ^{1}H NMR δ ppm: 0.91 (3H, t, $J = 7.2$, Hz, CH_3), 1.35 (2H, sext, $J = 7.2$ Hz, $CH_3\underline{CH_2}$), 1.49 (2H, quint, $J = 6.8$ Hz, $CH_3CH_2\underline{CH_2}$), 2.90 (2H, t, $J = 7.2$ Hz, $S\underline{CH_2}CH_2$), 3.21 (2H, q, $J = 6.4$ Hz, $NH\underline{CH_2}$), 3.33 (2H, t, $J = 7.6$ Hz, $S\underline{CH_2}$), 7.21–7.33 (5H, m, Ph-H), 7.53 (2H, s, $SO_2\underline{NH_2}$), 7.74 (1H, s, C_3-H), 7.87 (1H, s, C_6-H), 8.44 (1H, t, $J = 5.2$ Hz, NH).^{13}C NMR δ ppm: 14.1, 20.0, 31.5, 33.3, 34.4, 39.2, 120.7, 126.9, 128.2, 128.8, 129.0, 132.1 135.9, 139.0 140.1, 142.8, 166.3. HRMS calcd. for $C_{19}H_{23}BrN_2O_3S_2$[(M + H)$^+$]: 473.0386 (100%), found: 473.0385 (100%).

*3.1.3.13. 4-Bromo-N-butyl-2-(2-hydroxyethylsulfanyl)-5-sulfamoyl-benzamide (**13e**, LJ15-37).* The product was purified by chromatography on a column of silica gel with EtOAc:$CHCl_3$ (3:1), $R_f = 0.32$. Yield: 144 mg, 35%, mp 153–155 °C. ^{1}H NMR δ ppm: 0.91 (3H, t, $J = 7.2$, Hz, CH_3), 1.35 (2H, sext, $J = 7.2$ Hz, $CH_3\underline{CH_2}$), 1.49 (2H, quint, $J = 7.2$ Hz, $CH_3CH_2\underline{CH_2}$), 3.13 (2H, t, $J = 6.4$ Hz, $S\underline{CH_2}$), 3.21 (2H, q, $J = 6.8$ Hz, $NH\underline{CH_2}$), 3.61 (2H, q, $J = 6.0$ Hz, $SCH_2\underline{CH_2}$), 5.05 (1H, t, $J = 5.6$ Hz, OH), 7.58 (2H, s, $SO_2\underline{NH_2}$), 7.77 (1H, s, C_3-H), 7.84 (1H, s, C_6-H), 8.51 (1H, t, $J = 5.6$ Hz, NH).^{13}C NMR δ ppm: 18.9, 24.8, 36.2, 39.8, 43.9, 64.7, 125.4, 132.9, 136.8, 140.6, 143.7, 147.8, 171.1. HRMS calcd. for $C_{13}H_{19}BrN_2O_4S_2$[(M + H)$^+$]: 413.0022 (100%), found: 413.0018 (100%).

*3.1.4. General procedure for the syntheses of **16(a-c), 17(a-b), 21e, 23(b-c)***

The 30% H_2O_2(aq) (1.50 mmol, 0.148 mL) was added to a solution of appropriate sulfanyl-compound (**4(a-c), 5(a-b), 10e, 12(b-c)**) (0.500 mmol) in AcOH (2 mL) at 70 °C and allowed stirring for 2–3h. The solvent was removed under reduced pressure, then methanol (2 mL), H_2O (1 mL) and concentrated HCl (aq) (1 mL) was added and solution was refluxed for 1 h. The solvents were removed at a reduced pressure and the resultant precipitate was washed with H_2O.

*3.1.4.1. 2-(benzenesulfonyl)-4-chloro-N-(2-hydroxyethyl)-5-sulfamoyl-benzamide (**16a**, EA3-2o).* Yield: 182 mg, 87%, mp 168–170 °C. ^{1}H NMR δ ppm: 3.31–3.36 (2H, m, $NH\underline{CH_2}$), 3.57 (2H, t, $J = 6.0$ Hz, $\underline{CH_2}OH$), 4.62 (1H, br s, OH), 7.64 (2H, t, $J = 7.2$ Hz, $C_{3',5'}$-H), 7.74 (1H, t, $J = 7.6$ Hz, $C_{4'}$-H), 7.94 (1H, s, C_3-H), 7.96 (2H, s, SO_2NH_2), 8.11 (2H, d, $J = 7.6$ Hz, $C_{2',6'}$-H), 8.35 (1H, s, C_6-H), 8.73 (1H, br s, NH).^{13}C NMR δ ppm: 42.7, 59.9, 129.0, 129.8 (2C), 132.1, 132.7, 134.8, 136.9, 140.4, 142.1, 145.4, 165.9. HRMS calcd. for $C_{15}H_{15}ClN_2O_6S_2$ [(M + H)$^+$]: 419.0133, found: 419.0135.

*3.1.4.2. 4-Chloro-2-cyclohexylsulfonyl-N-(2-hydroxyethyl)-5-sulfamoyl-benzamide (**16b**, EA3-3o).* Yield: 170 mg, 80%, mp 246–248 °C. ^{1}H NMR δ ppm: 1.17–1.24 (3H, m, Cy-H), 1.38–1.46 (2H, m, Cy-H), 1.64 (1H, br s, Cy-H), 1.80–1.83 (4H, m, Cy-H), 3.31 (2H, q, $J = 5.6$ Hz, $NH\underline{CH_2}$), 3.52 (2H, t, $J = 6.0$ Hz, $\underline{CH_2}OH$), 3.80 (1H, t, $J = 12.0$ Hz, Cy-H), 4.69 (1H, br s, OH), 7.99 (2H, s, $SO_2\underline{NH_2}$), 8.00 (1H, s, C_3-H), 8.06 (1H, s, C_6-H), 8.83 (1H, t, $J = 5.6$ Hz, NH).^{13}C NMR δ ppm: 24.9 (2C), 25.2, 42.6, 59.8, 63.0, 130.1, 131.8, 133.5, 137.6, 139.4, 145.4, 166.2. HRMS calcd. for $C_{15}H_{21}ClN_2O_6S_2$ [(M + H)$^+$]: 425.0602, found: 425.0600.

*3.1.4.3. 2-Benzylsulfonyl-4-chloro-N-(2-hydroxyethyl)-5-sulfamoyl-benzamide (**16c**, EA3-4o).* Yield: 165 mg, 76%, mp 118–120 °C. ^{1}H NMR δ ppm: 3.37 (2H, s, $NH\underline{CH_2}$,superposed with H_2O), 3.56 (2H, br s, $\underline{CH_2}OH$), 4.78 (1H, br s, OH), 4.98 (2H, br s, $\underline{CH_2}Ph$), 7.24 (2H, br s, Ph-H), 7.34 (3H, br s, Ph-H), 7.59 (1H, s, C_3-H), 8.00 (2H, s, SO_2NH_2), 8.07 (1H, s, C_6-H), 8.95 (1H, br s, NH).^{13}C NMR δ ppm: 42.7, 59.9,62.2, 128.2,129.0,129.3, 129.7,131.5 (2C),133.3,137.2, 140.1, 145.5, 166.5. HRMS calcd. for $C_{16}H_{17}ClN_2O_6S_2$ [(M + H)$^+$]: 433.0289, found: 433.0293.

*3.1.4.4. 2-(benzenesulfonyl)-4-chloro-N-(3-hydroxypropyl)-5-sulfamoyl-benzamide (**17a**, EA4-2o).* Yield: 188 mg, 87%, mp 142–144 °C. ^{1}H NMR δ ppm: 1.72 (2H, quint, $J = 6.8$ Hz, CH_2), 3.31 (2H, q, $J = 6.8$ Hz, $NH\underline{CH_2}$), 3.52 (2H, t, $J = 6.0$ Hz, $\underline{CH_2}OH$), 4.50 (1H, br s, OH), 7.64 (2H, t, $J = 7.6$ Hz, $C_{3',5'}$-H), 7.74 (1H, t, $J = 7.2$ Hz, $C_{4'}$-H), 7.89 (1H, s, C_3-H), 7.97 (2H, s, SO_2NH_2), 8.11 (2H, d, $J = 7.6$ Hz, $C_{2',6'}$-H), 8.35 (1H, s, C_6-H), 8.69 (1H, t, $J = 5.6$ Hz, NH).^{13}C NMR δ ppm: 32.4, 37.1, 58.9, 129.0, 129.7, 129.8, 132.1, 132.7, 134.8, 136.9, 140.4, 142.1, 145.4, 165.7. HRMS calcd. for $C_{16}H_{17}ClN_2O_6S_2$ [(M + H)$^+$]: 433.0289, found: 433.0288.

*3.1.4.5. 4-Chloro-2-cyclohexylsulfonyl-N-(3-hydroxypropyl)-5-sulfamoyl-benzamide (**17b**, EA4-3o).* Yield: 189 mg, 86%, mp 153–155 °C. ^{1}H NMR δ ppm: 1.14–1.24 (3H, m, Cy-H), 1.38–1.46 (2H, m, Cy-H), 1.64–1.71 (3H, m, Cy-H, CH_2), 1.81–1.83 (4H, m, Cy-H), 3.29 (2H, q, $J = 6.8$ Hz, $NH\underline{CH_2}$), 3.49 (2H, t, $J = 6.4$ Hz, $\underline{CH_2}OH$), 3.79 (1H, t, $J = 11.6$ Hz, Cy-H), 4.47 (1H, br s, OH), 8.00 (2H, s, $C_{3,6}$-H), 8.01 (2H, s, SO_2NH_2), 8.90 (1H, t, $J = 5.2$ Hz, NH).^{13}C NMR δ ppm: 24.9 (2C), 25.2, 32.4, 37.1, 58.9, 63.1, 130.0, 131.8, 133.6, 137.7, 139.4, 145.5, 166.0. HRMS calcd. for $C_{16}H_{23}ClN_2O_6S_2$ [(M + H)$^+$]: 439.0759, found: 439.0760.

*3.1.4.6. 4-Chloro-N-cyclohexyl-2-(2-hydroxyethylsulfonyl)-5-sulfamoyl-benzamide (**21e**, EA9-11o).* Yield: 95.6 mg, 45%, mp 257–260 °C. ^{1}H NMR δ ppm: 1.13–1.35 (5H, m, Cy-H), 1.56–1.59 (1H, m, Cy-H), 1.70–1.73 (2H, m, Cy-H), 1.85–1.88 (2H, m, Cy-H), 3.66–3.80 (5H, m, SCH_2, $\underline{CH_2}OH$, Cy-H), 5.03 (1H, t, $J = 4.8$ Hz, OH), 7.94 (1H, s, C_3-H), 8.00 (2H, s, SO_2NH_2), 8.05 (1H, s, C_6-H), 8.71 (1H, d, $J = 7.6$ Hz, NH).^{13}C NMR δ ppm: 24.9, 25.6, 32.3, 48.9, 55.4, 59.4, 129.5, 131.5, 133.2, 137.1, 142.0, 145.2, 165.4. HRMS calcd. for $C_{15}H_{21}ClN_2O_6S_2$ [(M + H)$^+$]: 425.0602, found: 425.0603.

*3.1.4.7. 4-Bromo-2-cyclohexylsulfonyl-N-(2-hydroxyethyl)-5-sulfamoyl-benzamide (**23b**, LJ15-22o).* Yield: 178 mg, 76%, mp 235–237 °C. ^{1}H NMR δ ppm: 1.16–1.24 (3H, m, Cy-H), 1.37–1.45 (2H, m, Cy-H), 1.60–1.65 (1H, m, Cy-H), 1.80–1.82 (4H, m, Cy-H), 3.30 (2H, q, $J = 6.0$ Hz, $NH\underline{CH_2}$), 3.52 (2H, q, $J = 5.6$ Hz, $HO\underline{CH_2}$), 3.75–3.81 (1H, m, Cy-H), 4.70 (1H, t, $J = 5.2$ Hz, OH), 7.94 (2H, s, SO_2NH_2), 8.07 (1H, s, C_6-H), 8.13 (1H, s, C_3-H), 8.81 (1H, t, $J = 5.6$ Hz, NH).^{13}C NMR δ ppm: 24.8, 24.9, 25.2, 42.6, 59.8, 63.0, 120.1, 130.0, 136.8, 138.1, 139.0, 147.3, 166.3. HRMS calcd. for $C_{15}H_{21}BrN_2O_6S_2$[(M + H)$^+$]: 471.0077 (100%), found: 471.0081 (100%).

*3.1.4.8. 2-Benzylsulfonyl-4-bromo-N-(2-hydroxyethyl)-5-sulfamoyl-benzamide (**23c**, LJ15-23o).* Yield: 168 mg, 78%, mp 139–141 °C. ^{1}H NMR δ ppm: 3.36–3.42 (2H, m, $NH\underline{CH_2}$), 3.56–3.59 (2H, m, $HO\underline{CH_2}$), 4.77 (1H, br. s, OH), 4.98 (2H, s, $S\underline{CH_2}$), 7.23–7.36 (5H, m, Ph-H), 7.75 (1H, s, C_6-H), 7.96 (2H, s, SO_2NH_2), 8.09 (1H, s, C_3-H), 8.94 (1H, t, $J = 5.6$ Hz, NH).^{13}C NMR δ ppm: 42.7, 59.9, 62.2, 119.9, 128.2, 129.0, 129.2, 129.7, 131.5, 136.7, 137.7, 139.7, 147.3, 166.6.HRMS calcd. for

$C_{16}H_{17}BrN_2O_6S_2$[(M + H)$^+$]: 478.9764 (100%), found: 478.9769 (100%).

3.1.5. General procedure for the syntheses of ***15d, 18(a-b), 19(a-b), 20(b-c), 21(a-c), 22(a-b), 24(a-b)***

The 30% H_2O_2(aq) (1.50 mmol, 0.148 mL) was added to a solution of appropriate sulfanyl-compound (**3d**, **6(a-b)**, **7(a-b)**, **8(b-c)**, **10(a-c)**, **11(a-b)**, **13(a-b)**) (0.500 mmol) in AcOH (2 mL) at 70 °C and allowed stirring for 2−3h. The solvent was removed under reduced pressure and the resultant precipitate was washed with H_2O.

*3.1.5.1. 4-Chloro-2-(2-phenylethylsulfonyl)-5-sulfamoyl-benzamide (**15d**, EA1A-5o).* Yield: 165 mg, 82%, mp 267−270 °C. ^{1}H NMR δ ppm: 2.99 (2H, t, J = 8.0 Hz, C<u>H</u>$_2$Ph), 4.04 (2H, t, J = 8.0 Hz, CH_2SO_2), 7.18−7.27 (5H, m, Ph-H), 7.92 (1H, s, $CONH_2$), 7.93 (1H, s, C_3-H), 8.00 (2H, s, SO_2NH_2), 8.02 (1H, s, C_6-H), 8.32 (1H, s, $CONH_2$).^{13}C NMR δ ppm: 28.2, 57.0, 127.1, 128.85, 128.87, 129.4, 131.8, 132.3, 137.2, 137.9, 140.7, 145.4, 168.2. HRMS calcd. for $C_{15}H_{15}ClN_2O_5S_2$ [(M + H)$^+$]: 403.0184 found 403.0188.

*3.1.5.2. 2-(benzenesulfonyl)-N-butyl-4-chloro-5-sulfamoyl-benzamide (**18a**, EA5-2o).* Yield: 198 mg, 92%, mp 182−184 °C. ^{1}H NMR δ ppm: 0.93 (3H, t, J = 7.2 Hz, CH_3), 1.39 (2H, sext, J = 7.2 Hz, CH_2),1.54 (2H, quint, J = 7.2 Hz, CH_2), 3.26 (2H, q, J = 6.8 Hz, NHC<u>H</u>$_2$), 7.65 (2H, t, J = 7.2 Hz, $C_{3',5'}$-H), 7.74 (1H, t, J = 7.2 Hz, $C_{4''}$-H), 7.89 (1H, s, C_3-H), 7.98 (2H, s, SO_2NH_2), 8.11 (2H, d, J = 7.6 Hz, $C_{2',6'}$-H), 8.35 (1H, s, C_6-H), 8.69 (1H, t, J = 5.6 Hz, NH).^{13}C NMR δ ppm: 14.2, 20.1, 31.2, 39.5, 129.0, 129.7, 129.8, 132.1, 132.7, 134.7, 137.0, 140.4, 142.1, 145.4, 165.6. HRMS calcd. for $C_{17}H_{19}ClN_2O_5S_2$ [(M + H)$^+$]: 431.0497, found: 431.0494.

*3.1.5.3. N-butyl-4-chloro-2-cyclohexylsulfonyl-5-sulfamoyl-benzamide (**18b**, EA5-3o).* Yield: 175 mg, 80%, mp 213−214 °C. ^{1}H NMR δ ppm: 0.91 (3H, t, J = 7.6 Hz, CH_3), 1.14−1.24 (3H, m, Cy-H), 1.32−1.54 (6H, m, Cy-H, $(CH_2)_2$), 1.64 (1H, br s, Cy-H), 1.80−1.83 (4H, m, Cy-H), 3.24 (2H, q, J = 6.8 Hz, NHC<u>H</u>$_2$), 3.80 (1H, t, J = 12.0 Hz, Cy-H), 8.00 (4H, s, SO_2NH_2, $C_{3,6}$-H), 8.81 (1H, t, J = 5.6 Hz, NH).^{13}C NMR δ ppm: 14.1, 20.0, 24.9 (2C), 25.2, 31.2, 39.4, 63.0, 130.0, 131.7, 133.6, 137.7, 139.4, 145.5, 165.9. HRMS calcd. for $C_{17}H_{25}ClN_2O_5S_2$ [(M + H)$^+$]: 437.0966, found: 437.0966.

*3.1.5.4. 2-(benzenesulfonyl)-4-chloro-N-(2-methoxyethyl)-5-sulfamoyl-benzamide (**19a**, EA8-2o).* Yield: 186 mg, 86%, mp 208−211 °C. ^{1}H NMR δ ppm: 3.31 (3H, s, CH_3), 3.42 (2H, q, J = 5.2 Hz, NHC<u>H</u>$_2$), 3.51 (2H, t, J = 5.6 Hz, OCH_2), 7.65 (2H, t, J = 7.6 Hz, $C_{3',5'}$-H), 7.74 (1H, t, J = 7.2 Hz, $C_{4''}$-H), 7.89 (1H, s, C_3-H), 7.96 (2H, s, SO_2NH_2), 8.12 (2H, d, J = 7.6 Hz, $C_{2',6'}$-H), 8.34 (1H, s, C_6-H), 8.82 (1H, t, J = 5.6 Hz, NH).^{13}C NMR δ ppm: 39.7, 58.5, 70.6, 129.0, 129.8, 129.9, 132.1, 132.7, 134.7, 136.7, 140.4, 142.1, 145.4, 165.9.HRMS calcd. for $C_{16}H_{17}ClN_2O_6S_2$[(M + H)$^+$]: 433.0289, found: 433.0293.

*3.1.5.5. 4-Chloro-2-cyclohexylsulfonyl-N-(2-methoxyethyl)-5-sulfamoyl-benzamide (**19b**, EA8-3o).* Yield: 178 mg, 81%, mp 207−209 °C. ^{1}H NMR δ ppm: 1.13−1.24 (3H, m, Cy-H), 1.38−1.46 (2H, m, Cy-H), 1.64 (1H, br s, Cy-H), 1.81−1.83 (4H, m, Cy-H), 3.29 (3H, s, CH_3), 3.40 (2H, q, J = 5.2 Hz, NHC<u>H</u>$_2$), 3.47 (2H, t, J = 5.2 Hz, OCH_2), 3.78 (1H, t, J = 12.0 Hz, Cy-H), 8.00 (2H, s, $C_{3,6}$-H), 8.01 (2H, s, SO_2NH_2), 8.93 (1H, t, J = 5.2 Hz, NH).^{13}C NMR δ ppm: 24.9 (2C), 25.2, 39.6, 58.4, 63.1, 70.6, 130.1, 131.8, 133.6, 137.5, 139.4, 145.4, 166.2. HRMS calcd. for $C_{16}H_{23}ClN_2O_6S_2$ [(M + H)$^+$]: 439.0759, found: 439.0757.

*3.1.5.6. Methyl 4-[(4-chloro-2-cyclohexylsulfonyl-5-sulfamoyl-benzoyl)amino]butanoate (**20b**, EA11-3o).* The product was purified by chromatography on a column of silica gel with $CHCl_3$:EtOAc (1:1), R_f = 0.41. Yield: 123 mg, 51%, mp 150−152 °C. ^{1}H NMR δ ppm: 1.10−1.24 (3H, m, Cy-H), 1.38−1.46 (2H, m, Cy-H), 1.63 (1H, br s, Cy-H), 1.73−1.82 (6H, m, Cy-H, CH_2), 2.41 (2H, t, J = 7.2 Hz, $COCH_2$), 3.27 (2H, q, J = 6.4 Hz, NHC<u>H</u>$_2$), 3.61 (3H, s, CH_3), 3.78 (1H, m, Cy-H), 8.00 (3H, s, C_3-H, SO_2NH_2), 8.02 (1H, s, C_6-H), 8.86 (1H, t, J = 5.6 Hz, NH).^{13}C NMR δ ppm: 24.5, 24.9 (2C), 25.2, 31.0, 39.0, 51.7, 63.1, 129.9, 131.8, 133.6, 137.6, 139.4, 145.5, 166.1, 173.6. HRMS calcd. for $C_{18}H_{25}ClN_2O_7S_2$ [(M + H)$^+$]: 481.0864, found: 481.0867.

*3.1.5.7. Methyl 4-[(2-benzylsulfonyl-4-chloro-5-sulfamoyl-benzoyl)amino]butanoate (**20c**, EA11-4o).* The product was purified by chromatography on a column of silica gel with $CHCl_3$:EtOAc (1:1), R_f = 0.48. Yield: 215 mg, 88%, mp 108−110 °C. ^{1}H NMR δ ppm: 1.82 (2H, quint, J = 7.2 Hz, CH_2), 2.47 (2H, t, J = 7.6 Hz, $COCH_2$), 3.31−3.35 (2H, m, NHC<u>H</u>$_2$, superposed with H_2O), 3.62 (3H, s, CH_3), 4.99 (2H, s, C<u>H</u>$_2$Ph), 7.24−7.26 (2H, m, Ph-H), 7.32−7.39 (3H, m, Ph-H), 7.61 (1H, s, C_3-H), 8.02 (2H, s, SO_2NH_2), 8.04 (1H, s, C_6-H), 8.98 (1H, t, J = 5.6 Hz, NH).^{13}C NMR δ ppm: 24.5, 31.1, 39.1, 51.8, 62.1, 128.2, 129.0, 129.3, 129.6, 131.5, 131.6, 133.3, 137.2, 140.1, 145.6, 166.4, 173.6. HRMS calcd. for $C_{19}H_{21}ClN_2O_7S_2$ [(M + H)$^+$]: 489.0551, found: 489.0553.

*3.1.5.8. 2-(benzenesulfonyl)-4-chloro-N-cyclohexyl-5-sulfamoyl-benzamide (**21a**, EA9-2o).* Recrystallization was accomplished from MeOH. Yield: 128 mg 56%, mp 259−261 °C. ^{1}H NMR δ ppm: 1.13−1.22 (1H, m, Cy-H), 1.23−1.39 (4H, m, Cy-H), 1.58−1.61 (1H, m, Cy-H), 1.73−1.76 (2H, m, Cy-H), 1.91−1.94 (2H, m, Cy-H), 3.71−3.78 (1H, m, Cy-H),7.64 (2H, t, J = 8.0 Hz, $C_{3',5'}$-H), 7.73 (1H, t, J = 7.6 Hz, $C_{4''}$-H), 7.86 (1H, s, C_3-H), 7.96 (2H, s, SO_2NH_2), 8.11 (2H, d, J = 7.2 Hz, $C_{2',6'}$-H), 8.33 (1H, s, C_6-H), 8.61 (1H, d, J = 7.6 Hz, NH).^{13}C NMR δ ppm: 24.9, 25.7, 32.3, 48.9, 129.0, 129.7, 129.8, 131.9, 132.7, 134.7, 137.1, 140.5, 142.0, 145.4, 164.9. HRMS calcd. for $C_{19}H_{21}ClN_2O_5S_2$[(M + H)$^+$]: 457.0653, found: 457.0656.

*3.1.5.9. 4-Chloro-N-cyclohexyl-2-cyclohexylsulfonyl-5-sulfamoyl-benzamide (**21b**, EA9-3o).* Yield: 201 mg, 87%, mp 264−266 °C. ^{1}H NMR δ ppm: 1.11−1.46 (10H, m, Cy-H), 1.56−1.64 (2H, m, Cy-H), 1.71−1.74 (2H, m, Cy-H), 1.80−1.92 (6H, m, Cy-H), 3.68−3.80 (2H, m, Cy-H), 7.97 (1H, s, C_3-H), 7.99 (1H, s, C_6-H), 8.00 (2H, s, SO_2NH_2), 8.71 (1H, d, J = 7.6 Hz, NH).^{13}C NMR δ ppm: 24.9 (3C), 25.2, 25.7, 32.3, 48.8, 63.0, 130.0, 131.6, 133.5, 137.8, 139.3, 145.4, 165.1. HRMS calcd. for $C_{19}H_{27}ClN_2O_5S_2$ [(M + H)$^+$]: 463.1123, found: 463.1123.

*3.1.5.10. 2-Benzylsulfonyl-4-chloro-N-cyclohexyl-5-sulfamoyl-benzamide (**21c**, EA9-4o).* Yield: 186 mg, 79%, mp 248−251 °C. ^{1}H NMR δ ppm: 1.12−1.40 (5H, m, Cy-H), 1.58−1.61 (1H, m, Cy-H), 1.73−1.76 (2H, m, Cy-H), 1.91−1.93 (2H, m, Cy-H), 3.74−3.83 (1H, m, Cy-H), 4.98 (2H, s, C<u>H</u>$_2$Ph), 7.23−7.25 (2H, m, Ph-H), 7.31−7.37 (3H, m, Ph-H), 7.57 (1H, s, C_3-H), 7.99 (1H, s, C_6-H), 8.02 (2H, s, SO_2NH_2), 8.83 (1H, d, J = 8.0 Hz, NH).^{13}C NMR δ ppm: 24.9, 25.7, 32.3, 49.0, 62.2, 128.3, 129.0, 129.2, 129.6, 131.4, 131.5, 133.2, 137.4, 140.0, 145.5, 165.4. HRMS calcd. for $C_{20}H_{23}ClN_2O_5S_2$ [(M + H)$^+$]: 471.0810, found: 471.0810.

*3.1.5.11. 2-(benzenesulfonyl)-N-benzyl-4-chloro-5-sulfamoyl-benzamide (**22a**, EA10-2o).* Yield: 212 mg, 91%, mp 250−253 °C. ^{1}H NMR δ ppm: 4.51 (2H, d, J = 5.6 Hz, CH_2), 7.29 (1H, t, J = 7.2 Hz, $C_{4''}$-H), 7.38 (2H, t, J = 7.2 Hz, $C_{3'',5''}$-H), 7.43 (2H, d, J = 7.2 Hz, $C_{2'',6''}$-H), 7.63 (2H, t, J = 7.6 Hz, $C_{3',5'}$-H), 7.73 (1H, t, J = 7.6 Hz, $C_{4''}$-H), 7.94 (1H, s, C_3-H), 7.98 (2H, s, SO_2NH_2), 8.11 (2H, d, J = 7.6 Hz, $C_{2',6'}$-H), 8.38 (1H, s, C_6-H), 9.22 (1H, t, J = 5.6 Hz, NH).^{13}C NMR δ ppm: 43.4, 127.5, 128.1, 128.8, 129.0, 129.8 (2C), 132.3, 132.8, 134.8, 136.6, 139.0, 140.4, 142.2, 145.5, 165.8. HRMS calcd. for $C_{20}H_{17}ClN_2O_5S_2$ [(M + H)$^+$]: 465.0340, found: 465.0338.

*3.1.5.12. N-benzyl-4-chloro-2-cyclohexylsulfonyl-5-sulfamoyl-benzamide (**22b**, EA10-3o).* Recrystallization was accomplished from 1-butanol:toluene (8:1). Yield: 113 mg, 48%, mp 270–272 °C. ^{1}H NMR δ ppm: 1.17 (3H, br s, Cy-H), 1.42–1.45 (2H, m, Cy-H), 1.62 (1H, br s, Cy-H), 1.81 (4H, br s, Cy-H), 3.80 (1H, t, J = 11.2 Hz, Cy-H), 4.49 (2H, d, J = 4.8 Hz, CH_2), 7.28–7.39 (5H, m, Ph-H), 8.01 (2H, s, SO_2NH_2), 8.03 (1H, s, C_3-H), 8.07 (1H, s, C_6-H), 9.35 (1H, br s, NH).^{13}C NMR δ ppm: 24.8 (2C), 25.2, 43.3, 63.1, 127.5, 127.9, 128.8, 130.1, 132.0, 133.7, 137.3, 139.0, 139.5, 145.5, 166.0. HRMS calcd. for $C_{20}H_{23}ClN_2O_5S_2$ [(M + H)$^+$]: 471.0810, found: 471.0811.

*3.1.5.13. 2-(benzenesulfonyl)-4-bromo-N-butyl-5-sulfamoyl-benzamide (**24a**, LJ15-31o).* Yield: 155 mg, 65%, mp 212–214 °C. ^{1}H NMR δ ppm: 0.93 (3H, t, J = 7.2 Hz, CH_3), 1.39 (2H, sext, J = 7.2 Hz, $CH_3\underline{CH_2}$), 1.53 (2H, quint, J = 7.2 Hz, $CH_3CH_2\underline{CH_2}$), 3.25 (2H, q, J = 6.8 Hz, $NH\underline{CH_2}$), 7.62–7.75 (3H, m, Ph-H), 7.90 (1H, s, C_6-H), 7.93 (2H, s, SO_2NH_2), 8.08–8.10 (2H, m, Ph-H), 8.45 (1H, s, C_3-H), 8.66 (1H, t, J = 5.6 Hz, NH).^{13}C NMR δ ppm: 14.2, 20.0, 31.1, 39.5, 120.3, 128.9, 129.7, 129.8, 134.7, 135.9, 137.5, 140.4, 141.7, 147.3, 165.7. HRMS calcd. for $C_{17}H_{19}BrN_2O_5S_2$[(M + H)$^+$]: 476.9971 (100%), found: 476.9972 (100%).

*3.1.5.14. 4-Bromo-N-butyl-2-cyclohexylsulfonyl-5-sulfamoyl-benzamide (**24b**, LJ15-32o).* Yield: 205 mg, 85%, mp 222–224 °C. ^{1}H NMR δ ppm: 0.91 (3H, t, J = 7.2, Hz, CH_3), 1.16-1,24 (3H, m, Cy-H), 1.32–1.53 (2H, m, $CH_3\underline{CH_2}$, 2H, m, $CH_3CH_2\underline{CH_2}$ ir 2H, m, Cy-H), 1.63 (1H, m, Cy-H), 1.80–1.82 (4H, m, Cy-H), 3.23 (2H, q, J = 6.8 Hz, $NH\underline{CH_2}$), 3.75–3.81 (1H, m, Cy-H), 7.96 (2H, s, SO_2NH_2), 8.02 (1H, s, C_3-H), 8.14 (1H, s, C_6-H), 8.78 (1H, t, J = 5.6 Hz, NH).^{13}C NMR δ ppm: 14.1, 20.0, 24.8, 24.9, 25.2, 31.2, 39.4, 63.0, 120.0, 130.0, 136.8, 138.2, 139.0, 147.3, 166.0. HRMS calcd. for $C_{17}H_{25}BrN_2O_5S_2$[(M + H)$^+$]: 483.0441 (100%), found: 483.0435 (100%).

*3.1.6. Procedure for the syntheses of **25c, 26a***

The ~38% AcOOH (0.748 mmol) solution in AcOH (0.130 mL) was added dropwise to a solution of 2-benzylsulfanyl-4-chloro-*N*-cyclohexyl-5-sulfamoyl-benzamide (compound **10c**) or 4-bromo-*N*-(2-hydroxyethyl)-2-phenylsulfanyl-5-sulfamoyl-benzamide (compound **12a)** (0.500 mmol) in AcOH (2 mL) at 50 °C and allows stirring for 2–3h. The progress of reaction was monitored by TLC. The solvent was removed under reduced pressure and the resultant precipitate was filtered, washed with H_2O.

*3.1.6.1. 2-Benzylsulfinyl-4-chloro-N-cyclohexyl-5-sulfamoyl-benzamide (**25c**, EA9-4o1).* Product was purified by chromatography on a column of silica gel with EtOAc:$CHCl_3$ (1:1), R_f = 0.35. Yield: 150 mg, 66%, mp 240–243 °C.^{1}H NMR δ ppm: 1.11–1.39 (5H, m, Cy-H), 1.61–1.64 (1H, m, Cy-H), 1.76 (2H, br s, Cy-H), 1.83–1.92 (2H, m, Cy-H), 3.76–3.85 (1H, m, Cy-H), 4.05 (1H_A, d, J = 12.4 Hz, $\underline{CH_2}$Ph), 4.51 (1H_B, d, J = 12.4 Hz, $\underline{CH_2}$Ph), 7.06–7.09 (2H, m, Ph-H), 7.28–7.32 (3H, m, Ph-H), 7.57 (1H, s, C_3-H), 7.81 (2H, s, SO_2NH_2), 8.40 (1H, s, C_6-H), 9.05 (1H, d, J = 8.0 Hz, NH).^{13}C NMR δ ppm: 25.3, 25.6, 32.7, 49.3, 62.2, 128.2, 128.4, 128.5, 128.6, 130.9, 131.2, 131.5, 133.9, 142.7, 151.2, 163.8. HRMS calcd. for $C_{20}H_{23}ClN_2O_4S_2$ [(M + H)$^+$]: 455.0861, found: 455.0856.

*3.1.6.2. 2-(benzenesulfinyl)-4-bromo-N-(2-hydroxyethyl)-5-sulfamoyl-benzamide (**26a**. LJ14-10).* Yield: 127 mg, 57%, mp 138–142 °C (dec). ^{1}H NMR δ ppm: 3.28 (2H, q, J = 5.6 Hz, $NH\underline{CH_2}$), 3.45 (2H, br s, $\underline{CH_2}$OH), 4.78 (1H, s, OH), 7.48–7.49 (3H, m, $C_{3',4',5'}$-H), 7.71–7.73 (2H, m, $C_{2'6'}$-H), 7.77 (2H, s, SO_2NH_2), 8.34 (1H, s, C_3-H), 8.38 (1H, s, C_6-H), 9.03 (1H, t, J = 5.2 Hz, NH).^{13}C NMR δ ppm: 42.8, 59.8, 123.0, 126.2, 129.1, 129.7, 130.5, 131.6, 132.5, 144.6, 146.4, 152.0, 164.5. HRMS calcd. for $C_{15}H_{15}BrN_2O_5S_2$[(M + H)$^+$]: 448.9658 (100%), found: 448.9663 (100%).

*3.1.7. General procedure for the syntheses of **1(b, d), 27, 27(b, d)***

Apropriate compound (**3**(**b, d**), **8, 8b, 20c**) (0.500 mmol) was refluxed in methanol (2 mL), H_2O (1 mL), and concentrated HCl (aq) (1 mL) solution for 12–24 h. The progress of reaction was monitored by TLC. The reaction mixture was concentrated under reduced pressure.

*3.1.7.1. 4-Chloro-2-cyclohexylsulfanyl-5-sulfamoyl-benzoic acid (**1b**, EA1-3).* Recrystallization was accomplished from H_2O:MeOH (5:1). Yield: 134 mg, 77%, mp 243–245 °C. ^{1}H NMR δ ppm: 1.20–1.53 (5H, m, Cy-H), 1.59–1.67 (1H, m, Cy-H), 1.69–1.78 (2H, m, Cy-H), 1.94–2.04 (2H, m, Cy-H), 3.55–3.65 (1H, m, S-Cy-H), 7.59 (1H, s, C_3-H), 7.69 (1H, s, SO_2NH_2), 8.40 (1H, s, C_6-H), 13.58 (1H, s, COOH). ^{13}C NMR δ ppm: 25.7 (2C), 35.5, 42.7, 127.2, 128.6, 131.8, 134.5, 136.6, 147.0, 166.3. HRMS calcd. for $C_{13}H_{16}ClNO_4S_2$ [(M + H)$^+$]: 350.0282, found 350.0278.

*3.1.7.2. 4-Chloro-2-(2-phenylethylsulfanyl)-5-sulfamoyl-benzoic acid (**1d**, EA1-5).* Recrystallization was accomplished from H_2O:MeOH (5:1). Yield: 130 mg, 70%, mp 215–216 °C.^{1}H NMR δ ppm: 2.95 (2H, t, J = 7.6 Hz, $\underline{CH_2}$Ph), 3.32 (2H, t, J = 7.6 Hz, CH_2S), 7.20–7.38 (5H, m, Ph-H), 7.56 (1H, s, C_3-H), 7.68 (3H, s, SO_2NH_2), 8.44 (1H, s, C_6-H), 13.66 (1H, br s, COOH).^{13}C NMR δ ppm: 32.7, 33.8, 126.9, 127.8, 128.9 (2C), 129.0, 131.7, 134.4, 136.4, 140.2, 148.2, 166.5. HRMS calcd. for $C_{15}H_{14}ClNO_4S_2$ [(M + H)$^+$]: 372.0126, found 372.0129.

*3.1.7.3. 4-[(2,4-Dichloro-5-sulfamoyl-benzoyl)amino]butanoic acid (**27**, EA12-1).* Recrystallization was accomplished from NaOAc (20.6 mg, 0.251 mmol) solution in H_2O. Yield: 107 mg, 60%, mp 136–139 °C.^{1}H NMR δ ppm: 1.74 (2H, quint, J = 7.2 Hz, CH_2), 2.31 (2H, t, J = 7.2 Hz, $COCH_2$), 3.27 (2H, q, J = 6.8 Hz, $NH\underline{CH_2}$), 7.82 (2H, s, SO_2NH_2), 7.92 (1H, s, C_3-H), 7.95 (1H, s, C_6-H), 8.69 (1H, t, J = 5.6 Hz, NH), 12.11 (1H, br s, COOH).^{13}C NMR δ ppm: 24.8, 31.4, 39.0, 129.1, 132.2, 132.5, 134.4, 136.4, 140.4, 164.9, 174.6. HRMS calcd. for $C_{11}H_{12}Cl_2N_2O_5S$ [(M + H)$^+$]: 354.9917, found: 354.9918.

*3.1.7.4. 4-[(4-Chloro-2-cyclohexylsulfanyl-5-sulfamoyl-benzoyl) amino]butanoic acid (**27b**, EA12-3).* Recrystallization was accomplished from NaOAc (20.6 mg, 0.251 mmol) solution in H_2O. Yield: 142 mg, 65%, mp 163–165 °C.^{1}H NMR δ ppm: 1.18–1.45 (5H, m, Cy-H), 1.57–1.60 (1H, m, Cy-H), 1.69–1.71 (2H, m, Cy-H), 1.73 (2H, quint, J = 7.2 Hz, CH_2), 1.90–1.92 (2H, m, Cy-H), 2.32 (2H, t, J = 7.2 Hz, $COCH_2$), 3.23 (2H, q, J = 6.4 Hz, $NH\underline{CH_2}$), 3.53–3.58 (1H, m, Cy-H), 7.64 (1H, s, C_3-H), 7.66 (2H, br s, SO_2NH_2), 7.82 (1H, s, C_6-H), 8.56 (1H, t, J = 5.6 Hz, NH), 12.17 (1H, br s, COOH).^{13}C NMR δ ppm: 24.9, 25.5, 25.7, 31.6, 32.7, 38.9, 44.3, 128.2, 130.7, 131.7, 136.9, 137.8, 141.2, 166.4, 174.7. HRMS calcd. for $C_{17}H_{23}ClN_2O_5S_2$[(M + H)$^+$]: 435.0810, found: 435.0809.

*3.1.7.5. 4-[(2-Benzylsulfonyl-4-chloro-5-sulfamoyl-benzoyl)amino] butanoic acid (**28c**, EA12-4o).* Recrystallization was accomplished from NaOAc (20.6 mg, 0.251 mmol) solution in H_2O. Yield: 164 mg, 69%, mp 252–254 °C.^{1}H NMR δ ppm: 1.79 (2H, quint, J = 7.2 Hz, CH_2), 2.37 (2H, t, J = 7.2 Hz, $COCH_2$), 3.30–3.35 (2H, m, $NH\underline{CH_2}$, superposed with H_2O), 4.99 (2H, s, $\underline{CH_2}$Ph), 7.24–7.26 (2H, m, Ph-H), 7.32–7.39 (3H, m, Ph-H), 7.61 (1H, s, C_3-H), 8.03 (2H, s, SO_2NH_2), 8.04 (1H, s, C_6-H), 8.98 (1H, t, J = 6.0 Hz, NH), 12.10 (1H, s, COOH).^{13}C NMR δ ppm: 24.6, 31.4, 39.2, 62.1, 128.2, 129.0, 129.2, 129.6, 131.5 (2C), 133.3, 137.2, 140.1, 145.6, 166.3, 174.7.HRMS calcd. for $C_{18}H_{19}ClN_2O_7S_2$ [(M + H)$^+$]: 475.0395, found: 475.0394.

*3.1.8. General procedure for the syntheses of **27(a-c)***

Apropriate ester (compounds **8**(**a-c**))(0.500 mmol) was stirred

in methanol (5 mL) and 10% NaOH (aq) (0.8 mL, 2.000 mmol) solution for 12–36 h. The progress of reaction was monitored by TLC. The reaction mixture was acidified with acetic acid and concentrated under reduced pressure. Recrystallization was accomplished from 0.1 N HCl(aq).

*3.1.8.1. 4-[(4-Chloro-2-phenylsulfanyl-5-sulfamoyl-benzoyl)amino] butanoic acid (**27a**, VR16-4).* Yield: 174 mg, 81%, mp 176–177 °C.^{1}H NMR δ ppm: 1.77 (2H, quint, $J = 7.2$ Hz, $NHCH_2\underline{CH_2}$), 2.33 (2H, t, $J = 7.2$Hz, $\underline{CH_2}CO$), 3.29 (2H, q, $J = 6.4$ Hz, $NH\underline{CH_2}$), 6.80 (1H, s, C_3-H), 7.53–7.59 (5H, m, C_{Ar}-H), 7.65 (2H, s, NH_2), 8.00 (1H, s, C_6-H), 8.80 (1H, t, $J = 5.2$ Hz, NH), 12.12 (1H, s, COOH).^{13}C NMR δ ppm: 24.9, 31.5, 39.6, 113.6, 128.6, 129.6, 130.4, 130.8, 131.4, 132.3, 133.7, 136.2, 137.9, 144.5, 165.9, 174.6. HRMS calcd. for $C_{17}H_{17}ClN_2O_5S_2$ [$(M + H)^+$]: 429.0340, found: 429.0336.

*3.1.8.2. 4-[(4-Chloro-2-cyclohexylsulfanyl-5-sulfamoyl-benzoyl) amino]butanoic acid (**27b**, EA12-3).* Yield: 167 mg, 77%, mp 163–165 °C.

*3.1.8.3. 4-[(2-Benzylsulfanyl-4-chloro-5-sulfamoyl-benzoyl)amino] butanoic acid (**27c**, EA12-4).* Yield: 144 mg, 65%, mp 125–127 °C.^{1}H NMR δ ppm: 1.72 (2H, quint, $J = 7.2$ Hz, CH_2), 2.29 (2H, t, $J = 7.2$ Hz, $COCH_2$), 3.22 (2H, q, $J = 6.4$ Hz, $NH\underline{CH_2}$), 4.36 (2H, s, $\underline{CH_2}$Ph), 7.25–7.36 (3H, m, Ph-H), 7.40–7.43 (2H, m, Ph-H), 7.62 (2H, s, SO_2NH_2), 7.63 (1H, s, C_3-H), 7.87 (1H, s, C_6-H), 8.63 (1H, t, $J = 5.6$ Hz, NH), 12.11 (1H, br s, COOH).^{13}C NMR δ ppm: 24.8, 31.5, 36.2, 39.0, 51.8, 127.8, 128.1, 128.9, 129.0, 129.5, 132.1, 134.2, 136.6, 137.2, 143.4, 166.2, 174.6. HRMS calcd. for $C_{18}H_{19}ClN_2O_5S_2$ [$(M + H)^+$]: 443.0497, found: 443.0501.

3.2. Protein preparation

We used recombinant human CAs, which were expressed in *E. coli*, except CA IX was expressed in mammalian cells. All CAs were chromatographically purified as described previously: CA I - [31], CA II - [32], CA III, CA IV, CA VA, CA VB, CA VI, CA IX, and CA XIV - [13], CA VII, and CA XIII- [33], CA XII - [34]. The purity of CAs was analyzed by SDS-PAGE, and molecular weights were confirmed by mass spectrometry. Concentrations were determined spectrophotometrically at a wavelength of 280 nm.

3.3. Determination of binding parameters

3.3.1. Fluorescent thermal shift assay (FTSA)

Observed binding affinities (dissociation constant or the change in standard Gibbs energy upon binding) of the compounds to CAs were measured by the fluorescent thermal shift assay, also termed differential scanning fluorimetry, DSF, using a "Corbett Rotor-gene 6000" instrument. Typical data is shown in Fig. 7 while all dissociation constants are listed in Table S1. Protein − compound solutions at various ratios were heated from 25 to 90 °C at the rate of 1 °C/min. Curve-fitting procedure has been explained previously [35] and the dissociation constants are listed for 37 °C.

Protein denaturation was monitored by determining the fluorescence of 8-anilino-1-naphthalene sulfonate (ANS) as a function of temperature. The excitation and emission wavelengths were 365 ± 20 and 460 ± 15 nm. ANS fluorescence increases when it hides from aqueous quenching by binding to exposed hydrophobic parts of the denatured protein. The melting temperature (T_m) of the protein was calculated as the midpoint of the transition. Interaction between protein and compound usually increases the thermal stability (T_m) of proteins. All samples contained 5 μM CA (expect 10 μM CA IV), and 0 μM–200 μM compound, 50 μM 8-anilino-1-naphthalene sulfonate (solvatochromic dye), 50 mM sodium phosphate buffer at pH 7.0, 100 mM sodium chloride and 2.0% (v/v) dimethyl sulfoxide.

3.3.2. Isothermal titration calorimetry (ITC)

All compound dissociation constants were determined for all 12 catalytically active CA isoforms by the FTSA, but only for a selected set of compounds were determined by ITC, because ITC is significantly slower technique and consumes significantly more protein. However, ITC yields information not only on the binding affinity, but also on the changes of binding enthalpy and entropy. Typical ITC data are shown in Fig. 8. The *observed* enthalpies of binding are listed in Table S2. However, these enthalpy values are highly dependent on the buffer and pH due to linked protonation events. Therefore, the *intrinsic* enthalpies of binding were calculated and are listed in Table 2. Both the FTSA and ITC techniques yielded similar affinity values when the affinities were in the range between 1 μM and 10 nM. However, approaching the limit of ITC near the 10 nM K_d, the ITC tended to show a slightly decreased affinity as shown in Fig. S5. This decrease is due to ITC limit to detect

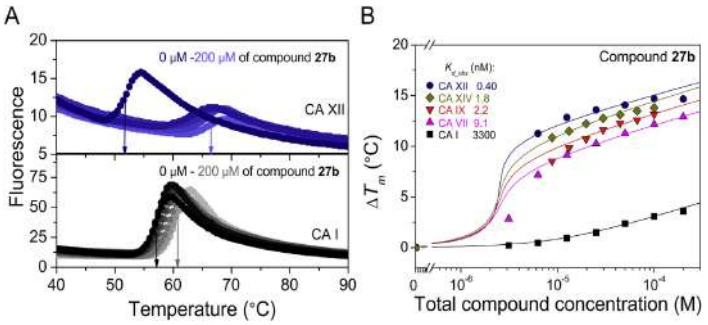

Fig. 7. Determination of compound binding to human carbonic anhydrase (CA) isoforms by the fluorescent thermal shift assay (FTSA). **A**, An example of thermal denaturation curves of CA XII (upper panel, strong binding) and CA I (lower panel, weak binding) in the presence of increasing concentrations of compound **27b**. The protein unfolding curves were registered by following the fluorescence of 8-anilino-1-naphthalene sulfonate [50] in the buffer containing 50 mM sodium phosphate (pH 7.0), 100 mM sodium chloride and 2.0% (v/v) DMSO. The midpoint temperature of the unfolding transition is equal to melting temperature (T_m): high-affinity ligand increases T_m of the protein to a much greater extent as the concentrations of ligand increase than the low-affinity ligand. **B**, Represents the melting temperatures from panels **A** plotted as a function of added compound concentration (data points), and fitted to a model for 37 °C (solid lines) used to determine the dissociation constants. Protein melting temperatures without ligand are zero controls to make it easier to compare the thermal shift of the same ligand on proteins possessing different melting temperatures.

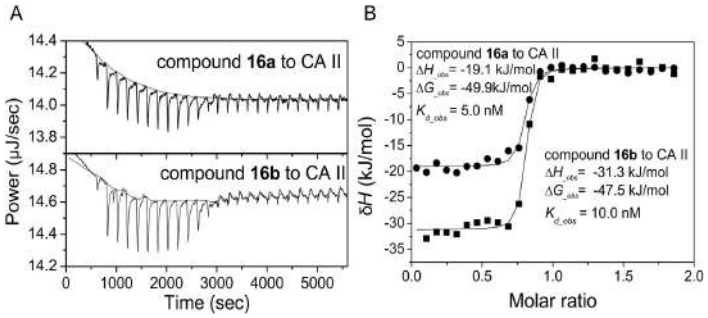

Fig. 8. Examples of the determination of compound affinity and enthalpy change upon binding to CAs by isothermal titration calorimetry (ITC). **A**, Raw ITC data obtained by injecting syringe solution containing 100 μM compound **16a** (top panel) or **16b** (bottom panel) into the cell containing 10 μM CA II, both solutions contained sodium phosphate buffer at pH 7.0 and the experiment was performed isothermally at 37 °C. **B**, Integrated data (after correction for the heat of dilution) plotted against the molar ratio between compound **16a** or compound **16b** and the protein CA II. Lines show the fits to a single-site model. The *observed* fit parameters for both curves are listed. The stoichiometry of these binding reactions is 1:1 as shown by the saturation point occurring at the molar ratio approaching 1.0.

approximately 10 nM K_d, because the curves become too steep at higher affinity. Instead, displacement ITC could be performed to verify stronger affinities.

ITC experiments were carried out using a MicroCal VP-ITC calorimeter (Northampton, MA, USA). Protein solution in the cell contained a constant concentration of CA (4–10 μM), while the concentration of compound loaded in the ITC syringe was ten times higher than the protein concentration (40–100 μM). Both cell and syringe solutions were diluted in buffer: 50 mM sodium phosphate or 50 mM TRIS at pH 7.0 and containing 100 mM sodium chloride and 2.0% (v/v) of dimethyl sulfoxide. A typical experiment consisted of 25 injections with 200 s spacing between injections, volume of the first injection was 1–5 μL and 10 μL for the remaining injections. All ITC experiments were performed at 37 °C.

3.4. Calculation of intrinsic binding parameters

FTSA, ITC, and other experiments allow determination of the *observed* binding parameters. These parameters depend on buffer and pH, because sulfonamide binding to CAs is linked to several reactions (i) Zn^{2+}-bound hydroxide ion protonation into water molecule in the active site of CA; (ii) Sulfonamide amino group deprotonation; (iii) Buffer molecule protonation or deprotonation. (iv) After the protonation reactions, the negatively charged sulfonamide replaces Zn^{2+}-bound water molecule in the active site of CA and binds to the protein in its position [36]. The sum of these four reactions is the *observed* binding affinity (or the *observed* binding enthalpy). However, only the fourth reaction represents the actual binding reaction, which is called *intrinsic* [29]. Observed binding parameters are important in order to see what will be the affinity of the compound under certain conditions, for example, in the human body. Nevertheless, these parameters are less important in the drug design to estimate the energy for binding affinity of each substituent. However, contribution of protonation reactions can be subtracted. Equations of intrinsic dissociation constant (K_{d_intr}) or standard Gibbs energy (ΔG_{intr}) and enthalpy change (ΔH_{intr}) are listed in Supplementary materials (eqs. S1, S4, S5).

3.5. Determination of protonation parameters

3.5.1. Determination of protonation enthalpy

The enthalpy changes of sulfonamide amino group (RSO_2NH_2) protonation, $\Delta_{p\_RSO_2NH_2}H$, were determined by titration of 0.25 mM sulfonamide and 0.375 mM sodium hydroxide with 5 mM nitric acid using a MicroCal VP-ITC calorimeter (Northampton, MA, USA) (Fig. 9A and Fig. S6). Dimethyl sulfoxide concentrations in the

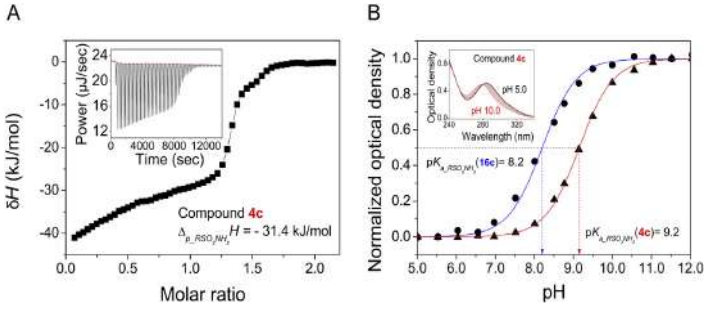

Fig. 9. Experimental determination of the protonation thermodynamics of the sulfonamide group of compounds. **A**, Calorimetric determination of the enthalpy change of sulfonamide group protonation ($\Delta_{p\_RSO_2NH_2}H$) of the compound **4c** obtained by ITC. The insert shows the raw ITC curve of protonating compound **4c**. **B**, Spectrophotometric determination of the pK_a of the sulfonamide group. Insert shows absorbance spectra of compound **4c** in various buffers of different pH values ranging from pH 5.0 to 10.0. The substituent groups of benzenesulfonamides affect the pK_a value of the amino group, e.g., the pK_a of **16c** is one pH unit lower than the pK_a of **4c** due to the second SO_2 group that withdraws electrons from the sulfonamide group.

syringe and the sample cell were 2.5% (v/v).

Experimental parameters: total number of injections – 56, volume of each injection – 5 μL, spacing between injections – 200 s, temperature – 37 °C.

$\Delta_{p_CAZn^{2+}H_2O}H$values were taken from Ref. [37].

3.5.2. Determination of pK_a values

The pK_a values of water molecule bound to Zn^{2+} in the active site of CAs, $pk_{a\_CAZn^{2+}H_2O}$ (Table S1.), were taken from Ref. [37] and of compounds, (Table S1.), were determined as described in Ref. [38].

We used a constant concentration of sulfonamide (100 μM or 200 μM) and 2.0% (v/v) of dimethyl sulfoxide in universal buffer (50 mM sodium acetate, 25 mM sodium borate and 50 mM sodium phosphate) at different pH values (from pH 5.5 to pH 12.5 at every half pH unit). UV/VIS spectra of compound solution were recorded at 37 °C using the spectrophotometer "Agilent 89090A". To determine $pk_{a\_RSO_2NH_2}$, a plot of normalized ratio of two absorbancies (approximately 10 nm above and 10 nm below the isosbestic point) vs. buffer pH and fitted Henderson–Hasselbach curve using least-square method. The midpoint of this fitted curve is equal to $pk_{a\_RSO_2NH_2}$ (Fig. 9B, Figs. S7 and S8).

3.6. Crystallography

3.6.1. Crystallization

The proteins were concentrated by ultrafiltration to 17–37 mg/mL. Crystallization conditions (buffers) are listed in Table S4. The ligand solutions for crystal soaking were made by mixing of 50 μL of corresponding reservoir solution and 0.5 μL of 50 mM ligand solution (in DMSO).

3.6.2. Data collection and structure determination

Datasets of CA XII-**6d,** CA XII-**8b**, CA IX-**5a**, and CA IX-**8b** were collected at BESSY II (Berlin, Germany) beamline 14.1. The CA IX-**6d** dataset was collected at MAX IV (Lund, Sweden) beamline BioMAX. The datasets were processed by MOSFLM [39] and scaled with SCALA [40]. Molecular replacement was made by MOLREP [41], as an initial model using coordinates of CA IX (PDB code 6FE2, [42]) and CA XII (PDB code 1JD0, [43]). Model refinement was made by REFMAC [44] and the structures were visualized with COOT [45]. The ligand parameter files were created using LIBCHECK [46] and the ligand was fitted in the electron density map manually using COOT. Coordinates and structure factors have been deposited to PDB. PDB access codes together with data collection and refinement statistics are shown in table Table S5.

Two datasets of X-ray diffraction (CA II–**4b** and CA XII–**4b**) were collected at the EMBL beamline P14. The CA II-**16a** and CA XII-**16a** datasets were collected at the beamline I911-3 (MaxLAB, Lund). The datasets of CA II–**16a** and CA XII–**4b** were processed using XDS [47] program, whereas datasets CA II–**4b** and CA XII-**16a** – by MOSFLM [39]. The molecular replacement was made by MOLREP [41] program using the following initial models: 3HLJ for CA II and 1JD0 for CA XII. The 3D models of compounds were created using AVOGADRO [48] program. The library files which contain complete chemical and geometric descriptions of compounds were created using LIBCHECK program [49]. The models were prepared using COOT [45] and refined by REFMAC [44]. All represented graphics were made using Pymol programs (PyMOL, version 1.8.x). Coordinates and structure factors have been deposited to the RCSB.

4. Conclusions

We have synthesized a series of di-substituted 2-chloro or 2-bromo-benzensulfonamides, performed their binding analysis to catalytically active human carbonic anhydrases and determined intrinsic Gibbs energy and enthalpy changes of binding. Correlation analysis between these intrinsic binding parameters and the chemical structures of compounds together with the crystal structures of several compound-CA complexes showed the importance and contributions of two tails for the affinity and selectivity of each compound towards a particular CA isoform. A series of compounds exhibited subnanomolar observed affinity and pM intrinsic affinity to CA VII, CA IX, CA XII, or CA XIV.

Declaration of competing interest

The authors declare that they have no known competing financial interests or personal relationships that could have appeared to influence the work reported in this paper.

The authors declare the following financial interests/personal relationships which may be considered as potential competing interests: DM, EC, VL and AZ declare that they have patents and patent applications on benzenesulfonamides as CA inhibitors.

Acknowledgments

This research was supported by the grant S-MIP-17-87 from the Research Council of Lithuania. Authors thank Gleb Bourenkov for the help with data collection at P14 EMBL beamline at PETRA III ring of the DESY synchrotron. (Access to the DESY sinchrotron EMBL beam lines P14) This work has been supported by iNEXT, grant number 653706, funded by the Horizon 2020 program of the European Commission". Authors thank Marjolein Thunnissen in Lund, at I911-3 beamline of the MaxLABIVsynchrotron (Lund, Sweden) for the help with data collection. Access to beamline I911-3 (MaxLAB, Lund, Sweden) was in part funded from the European Community's Seventh Framework Programme [FP7/2007-2013] under BioStruct-X [grant agreement N°283570BioStruct].

Appendix A. Supplementary data

Supplementary data to this article can be found online at https://doi.org/10.1016/j.ejmech.2019.111825.

Appendix A. List of supplementary data

Supplementary data includes:

- The figures of
  - correlation map between intrinsic binding thermodynamics and chemical structures of compounds (Fig. S1);
  - electron densities of inhibitors **4b**, **16a**, **5a**, **6d**, **8b** in CA II, CA XII or CA IX (Fig. S2 and Fig. S3);
  - crystal structure of compound **5a** in complex with CA IX (Fig. S4);
  - correlation between observed affinities by FTSA and ITC (Fig. S5);
  - determination of the pK_a and protonation enthalpy values of the sulfonamide group (Figs. S6, S7, S8);
- The tables of
  - the observed and intrinsic dissociation constants (Table S1);
  - the observed enthalpy changes (Table S2);
  - x-ray data collection and refinement statistics (Table S3, Table S5);
  - crystallization conditions (Table S4);
- Examples of NMR spectra
- Equations

References

[1] R.G. Khalifah, Carbon dioxide hydration activity of carbonic anhydrase: paradoxical consequences of the unusually rapid catalysis, Proc. Natl. Acad. Sci. U.S.A 70 (7) (1973) 1986–1989.

[2] V.M. Krishnamurthy, G.K. Kaufman, A.R. Urbach, I. Gitlin, K.L. Gudiksen, D.B. Weibel, G.M. Whitesides, Carbonic anhydrase as a model for biophysical and physical-organic studies of proteins and Protein–Ligand binding, Chem. Rev. 108 (3) (2008) 946–1051, https://doi.org/10.1021/cr050262p.

[3] M. Aggarwal, C.D. Boone, B. Kondeti, R. McKenna, Structural annotation of human carbonic anhydrases, J. Enzym. Inhib. Med. Chem. 28 (2) (2013) 267–277, https://doi.org/10.3109/14756366.2012.737323.

[4] C.T. Supuran, Carbonic anhydrases–an overview, Curr. Pharmaceut. Des. 14 (7) (2008) 603–614.

[5] B.-B. Gao, A. Clermont, S. Rook, S.J. Fonda, V.J. Srinivasan, M. Wojtkowski, J.G. Fujimoto, R.L. Avery, P.G. Arrigg, S.-E. Bursell, et al., Extracellular carbonic anhydrase mediates hemorrhagic retinal and cerebral vascular permeability through prekallikrein activation, Nat. Med. 13 (2) (2007) 181–188, https://doi.org/10.1038/nm1534.

[6] O.O. Guler, G.D. Simone, C.T. Supuran, Drug design studies of the novel anti-tumor targets carbonic anhydrase IX and XII, Curr. Med. Chem. 17 (15) (2010) 1516–1526.

[7] N. Hen, M. Bialer, B. Yagen, A. Maresca, M. Aggarwal, A.H. Robbins, R. McKenna, A. Scozzafava, C.T. Supuran, Anticonvulsant 4-aminobenzenesulfonamide derivatives with branched-alkylamide moieties: X-ray crystallography and inhibition studies of human carbonic anhydrase isoforms I, II, VII, and XIV, J. Med. Chem. 54 (11) (2011) 3977–3981, https://doi.org/10.1021/jm200209n.

[8] A. Scozzafava, C.T. Supuran, F. Carta, Antiobesity carbonic anhydrase inhibitors: a literature and patent review, Expert Opin. Ther. Pat. 23 (6) (2013) 725–735, https://doi.org/10.1517/13543776.2013.790957.

[9] D. Keilin, T. Mann, Carbonic anhydrase. Purification and nature of the enzyme, Biochem. J. 34 (8–9) (1940) 1163–1176.

[10] V. Alterio, A.D. Fiore, K. D'Ambrosio, C.T. Supuran, G.D. Simone, Multiple binding modes of inhibitors to carbonic anhydrases: how to design specific drugs targeting 15 different isoforms? Chem. Rev. 112 (8) (2012) 4421–4468, https://doi.org/10.1021/cr200176r.

[11] J.Y. Winum, A. Scozzafava, J.L. Montero, C.T. Supuran, New zinc binding motifs in the design of selective carbonic anhydrase inhibitors, Mini Rev. Med. Chem. 6 (8) (2006) 921–936.

[12] C. Congiu, V. Onnis, G. Balboni, C.T. Supuran, Synthesis and carbonic anhydrase I, II, IX and XII inhibition studies of 4-N,N-disubstituted sulfanilamides incorporating 4,4,4-Trifluoro-3-Oxo-but-1-Enyl, phenacylthiourea and imidazole-2(3H)-One/Thione moieties, Bioorg. Med. Chem. Lett 24 (7) (2014) 1776–1779, https://doi.org/10.1016/j.bmcl.2014.02.030.

[13] V. Dudutienė, J. Matulienė, A. Smirnov, D.D. Timm, A. Zubrienė, L. Baranauskienė, V. Morkūnaite, J. Smirnovienė, V. Michailovienė, V. Juozapaitienė, et al., Discovery and characterization of novel selective inhibitors of carbonic anhydrase IX, J. Med. Chem. 57 (22) (2014) 9435–9446, https://doi.org/10.1021/jm501003k.

[14] Z. Hou, B. Lin, Y. Bao, H. Yan, M. Zhang, X. Chang, X. Zhang, Z. Wang, G. Wei, M. Cheng, et al., Dual-tail approach to discovery of novel carbonic anhydrase IX inhibitors by simultaneously matching the hydrophobic and hydrophilic halves of the active site, Eur. J. Med. Chem. 132 (2017) 1–10, https://doi.org/10.1016/j.ejmech.2017.03.023.

[15] C.T. Supuran, S. Kalinin, M. Tanç, P. Sarnpitak, P. Mujumdar, S.-A. Poulsen, M. Krasavin, Isoform-selective inhibitory profile of 2-imidazoline-substituted benzene sulfonamides against a panel of human carbonic anhydrases, J. Enzym. Inhib. Med. Chem. 31 (sup1) (2016) 197–202, https://doi.org/10.1080/14756366.2016.1178248.

[16] R.P. Tanpure, B. Ren, T.S. Peat, L.F. Bornaghi, D. Vullo, C.T. Supuran, S.-A. Poulsen, Carbonic anhydrase inhibitors with dual-tail moieties to match the hydrophobic and hydrophilic halves of the carbonic anhydrase active site, J. Med. Chem. 58 (3) (2015) 1494–1501, https://doi.org/10.1021/jm501798g.

[17] I. Vaškevičienė, V. Paketurytė, A. Zubrienė, K. Kantminienė, V. Mickevičius, D. N-Sulfamoylphenyl- Matulis, N-Sulfamoylphenyl-, N-Thiazolyl-β-Alanines and their derivatives as inhibitors of human carbonic anhydrases, Bioorg. Chem. 75 (2017) 16–29, https://doi.org/10.1016/j.bioorg.2017.08.017.

[18] W. Vernier, W. Chong, D. Rewolinski, S. Greasley, T. Pauly, M. Shaw, D. Dinh, R.A. Ferre, S. Nukui, M. Ornelas, et al., Thioether benzenesulfonamide inhibitors of carbonic anhydrases II and IV: structure-based drug design, synthesis, and biological evaluation, Bioorg. Med. Chem. 18 (9) (2010) 3307–3319, https://doi.org/10.1016/j.bmc.2010.03.014.

[19] A. Zakšauskas, E. Čapkauskaitė, L. Jezepčikas, V. Linkuvienė, M. Kišonaitė, A. Smirnov, E. Manakova, S. Gražulis, D. Matulis, Design of two-tail compounds with rotationally fixed benzenesulfonamide ring as inhibitors of carbonic anhydrases, Eur. J. Med. Chem. 156 (2018) 61–78, https://doi.org/10.1016/j.ejmech.2018.06.059.

[20] B.V. Shetty, L.A. Campanella, T.L. Thomas, M. Fedorchuk, T.A. Davidson, L. Michelson, H. Volz, S.E. Zimmerman, E.J. Belair, A.P. Truant, Synthesis and activity of some 3-aryl- and 3-aralkyl-1,2,3,4-tetrahydro-4-oxo-6-quinazolinesulfonamides, J. Med. Chem. 13 (5) (1970) 886–895, https://doi.org/10.1021/jm00299a022.

[21] K. Sturm, W. Siedel, R. Weyer, H. Ruschig, Zur Chemie Des Furosemids, I. Synthesen von 5-Sulfamoyl-anthranilsäure-Derivaten, Eur. J. Inorg. Chem. 99 (1) (1966) 328–344, https://doi.org/10.1002/cber.19660990150.

[22] M. Nishio, Nuclear magnetic resonance studies of sulfur compounds. II. The substituent effect on geminal coupling constants and on magnetic nonequivalence of the methylene protons of sulfoxides, Chem. Pharm. Bull. (Tokyo) 15 (11) (1967) 1669–1676, https://doi.org/10.1248/cpb.15.1669.

[23] F.H. Niesen, H. Berglund, M. Vedadi, The use of differential scanning fluorimetry to detect ligand interactions that promote protein stability, Nat. Protoc. 2 (9) (2007) 2212–2221, https://doi.org/10.1038/nprot.2007.321.

[24] V. Petrauskas, L. Baranauskienė, A. Zubrienė, D. Matulis, Isothermal titration calorimetry and fluorescent thermal and pressure shift assays in Protein? Ligand interactions, in: Biocalorimetry, CRC Press, 2016, pp. 261–280.

[25] V. Petrauskas, A. Zubrienė, M.J. Todd, D. Matulis, Inhibitor binding to carbonic anhydrases by fluorescent thermal shift assay, in: D. Matulis (Ed.), Carbonic Anhydrase as Drug Target: Thermodynamics and Structure of Inhibitor Binding, Springer International Publishing, Cham, 2019, pp. 63–78.

[26] J. Smirnovienė, V. Smirnovas, D. Matulis, Picomolar inhibitors of carbonic anhydrase: importance of inhibition and binding assays, Anal. Biochem. 522 (2017) 61–72, https://doi.org/10.1016/j.ab.2017.01.022.

[27] L.D. Hansen, G.W. Fellingham, D.J. Russell, Simultaneous determination of equilibrium constants and enthalpy changes by titration calorimetry: methods, instruments, and uncertainties, Anal. Biochem. 409 (2) (2011) 220–229, https://doi.org/10.1016/j.ab.2010.11.002.

[28] V. Paketurytė, A. Zubrienė, W.-Y. Chen, S. Keller, M. Bastos, M.J. Todd, J.E. Ladbury, D. Matulis, Inhibitor binding to carbonic anhydrases by isothermal titration calorimetry, in: D. Matulis (Ed.), Carbonic Anhydrase as Drug Target: Thermodynamics and Structure of Inhibitor Binding, Springer International Publishing, Cham, 2019, pp. 79–95.

[29] A. Zubrienė, D. Matulis, Observed versus intrinsic thermodynamics of inhibitor binding to carbonic anhydrases, in: D. Matulis (Ed.), Carbonic Anhydrase as Drug Target: Thermodynamics and Structure of Inhibitor Binding, Springer International Publishing, Cham, 2019, pp. 107–123.

[30] A. Mickevičiūtė, D.D. Timm, M. Gedgaudas, V. Linkuvienė, Z. Chen, A. Waheed, V. Michailovienė, A. Zubrienė, A. Smirnov, E. Čapkauskaitė, et al., Intrinsic thermodynamics of high affinity inhibitor binding to recombinant human carbonic anhydrase IV, Eur. Biophys. J. 47 (3) (2017) 271–290, https://doi.org/10.1007/s00249-017-1256-0.

[31] E. Čapkauskaitė, A. Zubrienė, A. Smirnov, J. Torresan, M. Kišonaitė, J. Kazokaitė, J. Gylytė, V. Michailovienė, V. Jogaitė, E. Manakova, et al., Benzenesulfonamides with pyrimidine moiety as inhibitors of human carbonic anhydrases I, II, VI, VII, XII, and XIII, Bioorg. Med. Chem. 21 (22) (2013) 6937–6947, https://doi.org/10.1016/j.bmc.2013.09.029.

[32] P. Cimmperman, L. Baranauskienė, S. Jachimovičiūtė, J. Jachno, J. Torresan, V. Michailovienė, J. Matulienė, J. Sereikaitė, V. Bumelis, D. Matulis, A quantitative model of thermal stabilization and destabilization of proteins by ligands, Biophys. J. 95 (7) (2008) 3222–3231, https://doi.org/10.1529/biophysj.108.134973.

[33] J. Sūdžius, L. Baranauskienė, D. Golovenko, J. Matulienė, V. Michailovienė, J. Torresan, J. Jachno, R. Sukackaitė, E. Manakova, S. Gražulis, et al., 4-[N-(Substituted 4-Pyrimidinyl)Amino]Benzenesulfonamides as inhibitors of carbonic anhydrase isozymes I, II, VII, and XIII, Bioorg. Med. Chem. 18 (21) (2010) 7413–7421, https://doi.org/10.1016/j.bmc.2010.09.011.

[34] V. Jogaitė, A. Zubrienė, V. Michailovienė, J. Gylytė, V. Morkūnaitė, D. Matulis, Characterization of human carbonic anhydrase XII stability and inhibitor binding, Bioorg. Med. Chem. 21 (6) (2013) 1431–1436, https://doi.org/10.1016/j.bmc.2012.10.016.

[35] L. Baranauskienė, M. Hilvo, J. Matulienė, D. Golovenko, E. Manakova, V. Dudutienė, V. Michailovienė, J. Torresan, J. Jachno, S. Parkkila, et al., Inhibition and binding studies of carbonic anhydrase isozymes I, II and IX with benzimidazo[1,2-c][1,2,3]thiadiazole-7-sulphonamides, J. Enzym. Inhib. Med. Chem. 25 (6) (2010) 863–870, https://doi.org/10.3109/14756360903571685.

[36] S.Z. Fisher, M. Aggarwal, A.Y. Kovalevsky, D.N. Silverman, R. McKenna, Neutron diffraction of acetazolamide-bound human carbonic anhydrase II reveals atomic details of drug binding, J. Am. Chem. Soc. 134 (36) (2012) 14726–14729, https://doi.org/10.1021/ja3068098.

[37] V. Linkuvienė, A. Zubrienė, E. Manakova, V. Petrauskas, L. Baranauskienė, A. Zakšauskas, A. Smirnov, S. Gražulis, J.E. Ladbury, D. Matulis, Thermodynamic, kinetic, and structural parameterization of human carbonic anhydrase interactions toward enhanced inhibitor design, Q. Rev. Biophys. 51 (2018), https://doi.org/10.1017/S0033583518000082.

[38] P.W. Snyder, J. Mecinović, D.T. Moustakas, S.W. Thomas, M. Harder, E.T. Mack, M.R. Lockett, A. Héroux, W. Sherman, G.M. Whitesides, Mechanism of the hydrophobic effect in the biomolecular recognition of arylsulfonamides by carbonic anhydrase, Proc. Natl. Acad. Sci. U.S.A. 108 (44) (2011) 17889–17894, https://doi.org/10.1073/pnas.1114107108.

[39] T.G.G. Battye, L. Kontogiannis, O. Johnson, H.R. Powell, A.G.W. Leslie, IMOSFLM: a new graphical interface for diffraction-image processing with MOSFLM, Acta Crystallogr. D Biol. Crystallogr. 67 (Pt 4) (2011) 271–281, https://doi.org/10.1107/S0907444910048675.

[40] P. Evans, Scaling and assessment of data quality, Acta Crystallogr. D Biol. Crystallogr. 62 (Pt 1) (2006) 72–82, https://doi.org/10.1107/S0907444905036693.

[41] A. Vagin, A. Teplyakov, Molecular replacement with MOLREP, Acta Crystallogr. D Biol. Crystallogr. 66 (Pt 1) (2010) 22–25, https://doi.org/10.1107/S0907444909042589.

[42] J. Leitans, A. Kazaks, A. Balode, J. Ivanova, R. Zalubovskis, C.T. Supuran, K. Tars, Efficient expression and crystallization system of cancer-associated carbonic anhydrase isoform IX, J. Med. Chem. 58 (22) (2015) 9004–9009, https://doi.org/10.1021/acs.jmedchem.5b01343.
[43] D.A. Whittington, A. Waheed, B. Ulmasov, G.N. Shah, J.H. Grubb, W.S. Sly, D.W. Christianson, Crystal structure of the dimeric extracellular domain of human carbonic anhydrase XII, a bitopic membrane protein overexpressed in certain cancer tumor cells, Proc. Natl. Acad. Sci. U.S.A. 98 (17) (2001) 9545–9550, https://doi.org/10.1073/pnas.161301298.
[44] G.N. Murshudov, P. Skubák, A.A. Lebedev, N.S. Pannu, R.A. Steiner, R.A. Nicholls, M.D. Winn, F. Long, A.A. Vagin, REFMAC5 for the refinement of macromolecular crystal structures, Acta Crystallogr. D Biol. Crystallogr. 67 (Pt 4) (2011) 355–367, https://doi.org/10.1107/S0907444911001314.
[45] P. Emsley, B. Lohkamp, W.G. Scott, K. Cowtan, Features and development of it coot, Acta Crystallogr. D 66 (2010) 486–501, https://doi.org/10.1107/S0907444910007493.
[46] A.A. Lebedev, P. Young, M.N. Isupov, O.V. Moroz, A.A. Vagin, G.N. Murshudov, JLigand: a graphical tool for the CCP4 template-restraint library, Acta Crystallogr. D Biol. Crystallogr. 68 (Pt 4) (2012) 431–440, https://doi.org/10.1107/S090744491200251X.
[47] W.X.D.S. Kabsch, Acta Crystallogr. D D66 (2010) 125–132, https://doi.org/10.1107/S0907444909047337.
[48] M.D. Hanwell, D.E. Curtis, D.C. Lonie, T. Vandermeersch, E. Zurek, G.R. Hutchison, Avogadro: an advanced semantic chemical editor, visualization, and analysis platform, J. Cheminf. 4 (1) (2012) 17, https://doi.org/10.1186/1758-2946-4-17.
[49] A.A. Vagin, R.A. Steiner, A.A. Lebedev, L. Potterton, S. McNicholas, F. Long, G.N. Murshudov, REFMAC5 dictionary: organization of prior chemical knowledge and guidelines for its use, Acta Crystallogr. Biol. Crystallogr. 60 (Pt 12 Pt 1) (2004) 2184–2195.
[50] D. Matulis, C.G. Baumann, V.A. Bloomfield, R.E. Lovrien, 1-Anilino-8-Naphthalene sulfonate as a protein conformational tightening agent, Biopolymers 49 (6) (1999) 451–458, https://doi.org/10.1002/(SICI)1097-0282(199905)49:6<451::AID-BIP3>3.0.CO;2-6.

Bioorganic & Medicinal Chemistry 26 (2018) 675–687

Contents lists available at ScienceDirect

Bioorganic & Medicinal Chemistry

journal homepage: www.elsevier.com/locate/bmc

Benzimidazole design, synthesis, and docking to build selective carbonic anhydrase VA inhibitors

Edita Čapkauskaitė [a], Audrius Zakšauskas [a], Virginijus Ruibys [b], Vaida Linkuvienė [a], Vaida Paketurytė [a], Marius Gedgaudas [a], Visvaldas Kairys [c], Daumantas Matulis [a,*]

[a] Department of Biothermodynamics and Drug Design, Institute of Biotechnology, Vilnius University, Saulėtekio al. 7, Vilnius LT-10257, Lithuania
[b] Department of Organic Chemistry, Faculty of Chemistry and Geosciences, Vilnius University, Naugarduko 24, Vilnius LT-03225, Lithuania
[c] Department of Bioinformatics, Institute of Biotechnology, Vilnius University, Saulėtekio al. 7, Vilnius LT-10257, Lithuania

ARTICLE INFO

Article history:
Received 15 November 2017
Revised 15 December 2017
Accepted 22 December 2017
Available online 24 December 2017

Keywords:
Carbonic anhydrase isozyme I, II, III, IV, VA, VB, VI, VII, IX, XII, XIII, and XIV
Fluorescent thermal shift assay
ThermoFluor®
Sulfonamide
N-Alkylated benzimidazole
Imidazole
Indoline
3,4-Dihydro-*2H*-quinoline
CA inhibitor
Docking

ABSTRACT

The similarity of human carbonic anhydrase (CA) active sites makes it difficult to design selective inhibitors for one or several CA isoforms that are drug targets. Here we synthesize a series of compounds that are based on 5-[2-(benzimidazol-1-yl)acetyl]-2-chloro-benzenesulfonamide (**1a**) which demonstrated picomolar binding affinity and significant selectivity for CA isoform five A (VA), and explain the structural influence of inhibitor functional groups to the binding affinity and selectivity. A series of chloro-substituted benzenesulfonamides bearing a heterocyclic tail, together with molecular docking, was used to build inhibitors that explore substituent influence on the binding affinity to the CA VA isoform.

1. Introduction

Carbonic anhydrases (CAs, EC 4.2.1.1) are zinc-containing metalloenzymes that catalyze the reversible hydration of carbon dioxide to bicarbonate and a proton. This simple reaction is essential for many physiological processes including pH regulation, respiration, electrolyte secretion, bone resorption, calcification, tumorigenesis, and biosynthetic reactions, which require bicarbonate as a substrate. Consequently, malfunction of these enzymes is often related to various diseases, and CA isozymes are interesting therapeutic targets whose inhibition could be used to treat a range of disorders including glaucoma, anemia, oxidative stress, cancer, epilepsy, edema, sterility, osteoporosis, obesity, etc.[1–5]

There are 12 catalytically active human CA isoforms, which differ in their kinetic properties, tissue distribution, and cellular localization.[3,6] In the design of CA inhibitors as drugs it is of crucial importance to inhibit only the target isoform with as little as possible effect on remaining CAs to avoid possible side effects. However, it is difficult to achieve desired selectivity due to high similarity of the active sites in CA isoforms.[1,4,7]

Two CA isoforms in human, CA VA and CA VB, are expressed only in the mitochondria.[8] The CA VA and CA VB are involved in ureagenesis[9], gluconeogenesis[10], and lipogenesis.[11–14] Recently it was demonstrated by using an electrochemical method of wiring mitochondria that the mitochondrial CA VA and CA VB play an important role in the metabolism regulation.[15]

The main class of CA inhibitors contain the primary sulfonamide group, or isosteres of this moiety, such as the sulfamate and the sulfamide.[1] Clinical use of sulfonamides such as an antiepileptic drug Topiramate (TPM)[16] exhibited a significant loss of body weight as a side effect in obese patients. A study of Topiramate showed the reduction of body weight gain in both lean and obese rats[17] and similar results were observed with Zonisamide (ZNS).[18] Subsequently TPM was shown as an effective inhibitor of several CA isoforms[19,20], also for the mitochondrial CAs.[21,22] It has been demonstrated that ZNS is a more potent inhibitor of CA VA than CA II.[23,24]

* Corresponding author.
E-mail address: matulis@ibt.lt (D. Matulis).

https://doi.org/10.1016/j.bmc.2017.12.035
0968-0896/

Numerous CA V inhibitors have been synthesized and their inhibitory activity against CAs has been determined. Below is shown a brief overview of the compounds synthesized and demonstrated as selective CA VA and CA VB inhibitors. In this short review, we have not included anionic inhibitors. The CA VA and CA VB inhibitory activities of compounds have been measured of Supuran group by the stopped-flow CO_2 hydration assay. The examples of some selective CA VA and CA VB inhibitors are shown in Fig. 1.

Daniela Vullo et al.[22] reported first inhibition study of the murine CA V with a series of aromatic and heterocyclic sulfonamides. Acylated sulfanilamides and ureido benzenesulfonamides (example **I**) showed higher affinity for CA V than for the other investigated isozymes (CA I, CA II and bCA IV).

Özlen Güzelet al.[25] prepared a series of aromatic/heterocyclic sulfonamides incorporating phenacetyl, pyridylacetyl, and thienylacetyl tails. All compounds were selective CA VA and CA VB inhibitors over CA I and CA II. The authors distinguish three of the most selective CA VA and CA VB inhibitors (*N*-(2-fluoro-4-sulfamoyl-phenyl)-2-(2-thienyl)acetamide (**II**), 2-phenyl-*N*-(4-sulfamoylphenyl)acetamide (**III**), and *N*-(2-bromo-4-sulfamoyl-phenyl)-2-phenyl-acetamide (**IV**)) over CA II. Unfortunately, later studies showed that compound **III** is not selective to CAs V.[26–29]

Isao Nishimori et al.[21] focused on CA VB inhibition with a library of sulfonamides/sulfamates, that are clinically used (acetazolamide (AZM), methazolamide, ethoxzolamide (EZA), dichlorophenamide, dorzolamide, brinzolamide, benzolamide, TPM, sulpiride, and indisulam). None of these compounds showed better inhibitory activity towards CA VA than CA II but several compounds exhibited selectivity towards CA VB (for example, **SLP** and **V**).

Sally-Ann Poulsen et al.[30] synthesized and investigated 4-(4-phenyltriazole-1-yl)-benzenesulfonamide derivatives as inhibitors of CA VA and CA VB. Several of them possessed selectivity towards CA VA or CA VB. The best of them is represented by example **VI**.

Jean-Yves Winum et al.[31] synthesized and assayed a series of aromatic/heterocyclic sulfonamides incorporating fructopyranose–thioureido tails showing excellent CA VII inhibitory activity, distinguishing compound **VII**, which shows selectivity to CA VA.

Fatma-Zohra Smaine et al.[32] synthesized a small series of 2-substituted-1,3,4-thiadiazole-5-sulfamides. All compounds are selective to CA VA and CA VB over CA I, CA II, and CA IV. Several examples (**VIII** and **IX**) that possessed the best selectivity ratio K_i(CA II)/K_i(CA VA) are shown in Fig. 1.

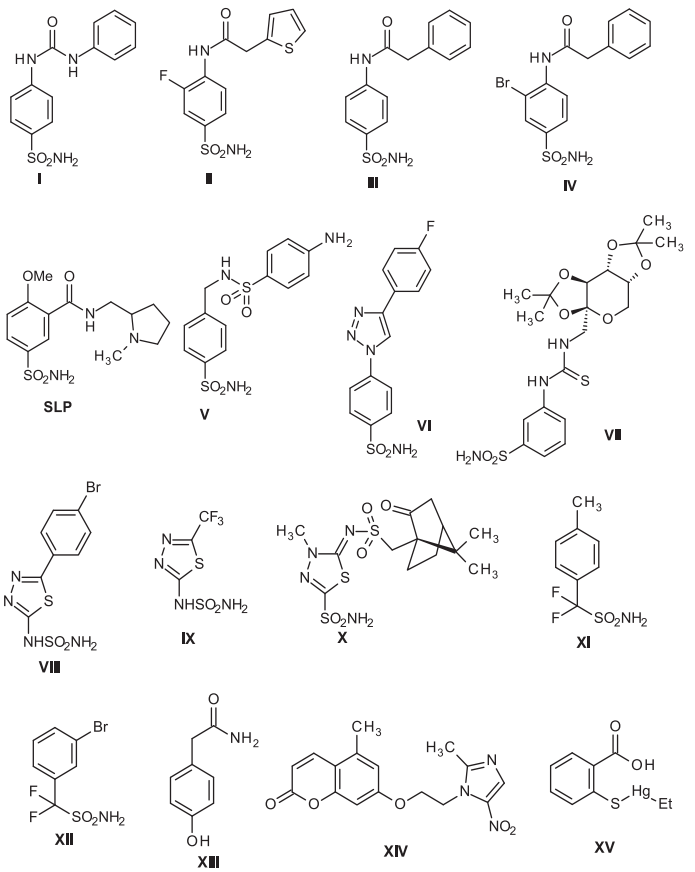

Fig. 1. Literature examples of the chemical structures of compounds that exhibit selectivity by inhibiting CA VA or CA VB stronger than CA I and CA II.

Alfonso Maresca et al.[33] prepared a series of (*R*)-/(*S*)-10-camphorsulfonyl-substituted aromatic/heterocyclic sulfonamides. All compounds are selective to CA VA and CA VB over CA I, CA II but one the best is thiadiazolesulfonamide **X**.

Alessandro Cecchi et al.[34] assayed a series of aromatic/heteroaromatic/polycyclic difluoromethanesulfonamides as inhibitors of CA I, CA II, CA VA, and CA IX. Several derivatives (examples **XI** and **XII**) showed selectivity for CA VA.

Rohan A. Davis et al.[35] investigated the enzyme inhibition characteristics of a natural product based phenolic library against a CA I, CA II, CA VA, and CAVB. Most of these compounds are selective to CA VA and CA VB over CA I and CA II with selectivity ratios in the range of 120–3800. Authors identified 2-(4-hydroxyphenyl)acetamide (**XIII**) as one of the best CA VA and CA VB selective inhibitors.

Adeline Bonneauet al.[36] reported the synthesis of two coumarin derivatives incorporating a nitroazole moiety. These compounds and 3-cyano-7-hydroxy-coumarin were assessed for their ability to inhibit the enzymatic activity of all human CAs. The mitochondrial isoforms CA VA and CA VB were inhibited efficiently with K_Is in the range of 0.38–2.63 μM whereas CA I, CA II, CA IV, and CA XIII were not inhibited significantly. The best inhibitor is represented as example **XIV** shown in Fig. 1.

Fabrizio Carta et al.[37] investigated a series of non-sulfonamide inhibitors of human CAs consisting of pyridine-*N*-oxide-2-thiophenol, thiobenzoic acid, thimerosal, two oxime derivatives, 2-hydroxyquinoline, and coumaphos. The majority of compounds possessed no inhibitory activity to off-target isoform CA II, but inhibited the two mitochondrial isoforms CA VA and CA VB. Unfortunately, significant selectivity to these isoforms was not observed (example **XV**).

In our previous work, the synthesis and binding to human CAs of *N*-alkylated benzimidazoles[38–40] has been described. Several compounds were highly selective for CA VA, especially 5-[2-(benzimidazol-1-yl)acetyl]-2-chloro-benzenesulfonamide (**1a**). This compound exhibited 0.25 nM *observed* affinity to CA VA and bound from 1200 to 800,000 times stronger than to the remaining off-target CAs (K_ds were 200,000–303 nM). This was highly unexpected because, for example, 2-chloro-5-[(2-methyl-1*H*-benzimidazol-1-yl)acetyl]benzenesulfonamide (**1i**) that is different from **1a** by only one methyl group showed more than 1000 times lower binding affinity to CA VA than to **1a**. Therefore, here we explore the influence of substituents for binding affinity to CA VA and synthesized a number of **1a** analogs, a series of chloro-substituted benzene sulfonamides, bearing heterocyclic tail. Furthermore, molecular modeling was used in order to understand how such small changes in the inhibitor structure so significantly influences the binding affinity to CA VA.

2. Results and discussion

2.1. Chemistry

A series of 2-chloro- and 2,4-dichlorobenzenesulfonamides bearing different heterocyclic moieties were designed and synthesized. As shown in Scheme 1, the synthesis of target *N*-alkylated heterocycle derivatives **1**(**a**–**h**) and **2**(**a**–**c**) was achieved by alkylation of appropriate heterocycle with 5-(bromoacetyl)-2-chlorobenzenesulfonamide (**1**) and 5-(bromoacetyl)-2,4-dichlorobenzenesulfonamide (**2**). *N*-alkylation was carried out in the presence of NaOAc in THF at room temperature. It should be noted that the dialkylation of the benzimidazole/imidazole ring can be avoided by using of slight excess of heterocycle. An excess of 1,2,3,4-tetrahydroquinoline and indoline was used in several cases instead of mentioned base for the synthesis of **1g** and **1h**.

First attempt to obtain amide **7** by direct acylation of 1-aminobenzimidazole with acyl chloride (2,4-dichloro-5-sulfamoyl-benzoyl chloride) was unsatisfactory. Using pyridine as a base and performing the reaction in boiling THF led to formation of an inseparable mixture of products. It is presumable that the acylation of sulfonamide group occurred. Therefore it was decided to protect sulfonamide group with an *N*,*N*-dimethylaminomethylidene residue. The protection let us to avoid the formation of byproducts and to enhance the ability of compound **5** to acylation reaction. The treatment of 2,4-dichloro-5-sulfamoyl-benzoic acid (**3**) with dimethylformamide and $SOCl_2$ resulted methylidene **4**. The protected sulfonamide **4** was converted to acyl chloride **5** followed by successful amide **6** formation using pyridine in THF at 80°C and removal of the sulfonamide-protecting group using NaOH (aq) as shown in Scheme 2.

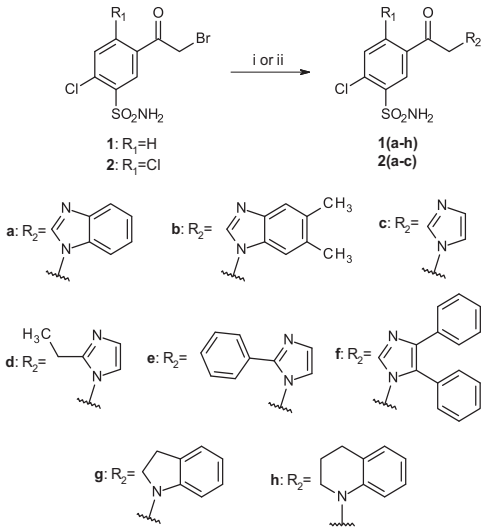

Scheme 1. Synthesis of compounds **1**(**a**–**h**) and **2**(**a**–**c**). Reagents and conditions: (i) benzimidazole or imidazole (1.5 eq), NaOAc, THF, room temperature, 24 h (for **1**(**a**-**f**) and **2**(**a**–**c**)); (ii) 1,2,3,4-tetrahydroquinoline or indoline (2 eq), THF, room temperature, 48 h (for **1g** and **1h**).

2-Chloro-4,5-disubstituted benzenesulfonamides (compounds **8**–**11**) were obtained from compounds **2a**, **2b**, and **7** by using appropriate thiol in methanol or DMSO in the presence of Et_3N as depicted in Scheme 3.

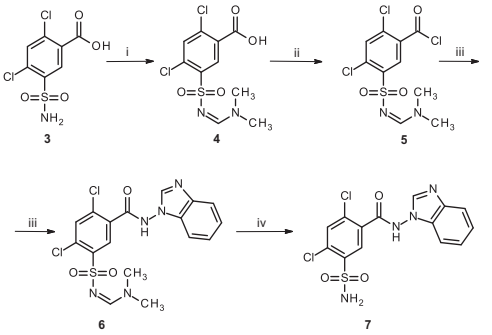

Scheme 2. Synthesis of compound **7**. Reagents and conditions: (i) DMF, $SOCl_2$, −10 °C, then r.t., 2 h; (ii) $SOCl_2$, toluene, reflux, 2 h; (iii) 1-aminobenzimidazole, pyridine, THF 80 °C, 3 h, then overnight at r.t.; (iv) 2 M NaOH(aq), r.t, 48 h, then 2 M HCl(aq).

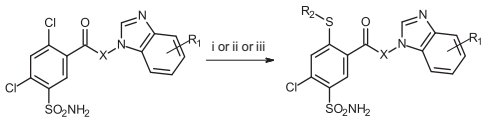

2a: X=CH_2, R_1=H
2b: X=CH_2, R_1=CH_3
7: X=NH, R_1=H

8: X=CH_2, R_1=H, R_2=$(CH_2)_2$Ph
9: X=CH_2, R_1=CH_3, R_2=Ph
10: X=NH, R_1=H, R_2=Ph
11: X=NH, R_1=H, R_2=cyclohexyl

Scheme 3. Synthesis of 2-chloro-4,5-disubstituted benzenesulfonamides (compounds **8**–**11**). Reagents and conditions: (i) 2-phenylethanethiol, Et_3N, DMSO, r.t., 24 h; (ii) thiophenol, Et_3N, MeOH, reflux, 3 h; (iii) thiophenol or cyclohexanethiol, Et_3N, DMSO, r.t., 7 days.

2.2. Binding studies

Compound binding affinities towards all 12 human CAs were determined by the fluorescent thermal shift assay (FTSA). All observed K_d values are listed in Table 1. Several examples of affinity determination by FTSA are shown in Fig. 2.

It has been previously shown that **1a** exhibited exceptional affinity and selectivity towards CA VA and therefore we investigated the binding mode of **1a** analogs by changing substituents in the 4th and 5th position of the benzene ring bearing the sulfonamide group. The *N*-alkylated benzimidazoles **1i** and **1j** (Fig. 3) bearing methyl or ethyl substituent in the 2nd position of the benzimidazole ring have a also been previously reported.[38–40]

2.3. The influence of the substituent in 5th position on CA binding affinity

It was discovered that certain small modifications of the compound structure cause large changes to the CA binding, while most small structural changes did not significantly affect the CA affinity. Newly synthesized compound **1b**, containing benzimidazole moiety with two methyl groups, bound to CA VA with K_d = 0.769 nM, similar to **1a**, and maintained high selectivity against other CA isoforms.

The replacement of the benzimidazole moiety in **1a** with imidazole in **1c** significantly reduced the binding potency to CA VA (53.3 times). The affinity to the other CAs compared to **1a** remained similar, except the increased binding to CA IV (8.63 times) and the decreased binding to CA I and CA VB (10 and 3 times, respectively). Introduction of the methyl substituent in the 2nd position of the benzimidazole ring (compound **1i**) strongly reduced affinity to CA VA (333 nM, 1330 times) while the affinity to other CAs remained similar or slightly lower (200,000–260 nM).

The insertion of the ethyl group (**1j**) reduced the binding potency to CA VA 2670 times, whereas affinity to the other CAs remained similar. The same trend is observed with compounds containing imidazole fragment (**1c** and **1d**). 2-ethyl substituted imidazole (**1d**) compared to unsubstituted (**1c**) showed 34.1 times lower affinity to CA VA, while changes between affinities to remaining CAs were similar with exception of CA IV (affinity diminished 133 times). The introduction of the phenyl substituent in the 2nd position of the imidazole ring (compound **1e**) reduced the binding potency to CA VA 107 times. A strong decrease in all CA affinities (K_d = 15,400 nM–200,000 nM) was observed when the imidazole ring was enriched with phenyl groups in 4th and 5th positions (**1f**).

The selectivity to CA VA disappeared when the benzimidazole moiety was replaced with structurally similar indoline (**1g** and **IND**) or 3,4-dihydro-*2H*-quinoline (**1h**) fragment. In **1g**, it may be noted that selectivity to CA IV (K_d = 154 nM) increased (other CAs were inhibited from 4.06 to 1300 times less).

2.4. The influence of substituent in the 4th position on CA binding affinity

It was known that a ligand's binding affinity depends on the acidity of the sulfonamide group.[2] Therefore, electron-withdrawing groups that increase the sulfonamide acidity, such as chlorine and carbonyl groups, also increase the binding affinity.

Comparison of three pairs of compounds, unsubstituted and substituted with chlorine in the 4th position of benzenesulfonamide (**1c**/**2c**, **1a**/**2a**, **1b**/**2b**) showed that the introduction of chlorine substituent increased the binding affinities to many CAs, especially to the CA III (from 3.6 to 20 times). The largest gain in the binding affinity was observed in compound pairs bearing imi-

Table 1
The observed dissociation constants of compound binding to human recombinant CA isoforms I, II, III, IV, VA, VB, VI, VII, IX, XII, XIII, and XIV as determined by the fluorescent thermal shift assay (values listed for 37 °C, experiments performed at pH 7.0).

Cpd	Dissociation constants K_d (nM) for CA isoforms CA											
	CA I	CA II	CA III	CA IV	CA VA	CA VB	CA VI	CA VII	CA IX	CA XII	CA XIII	CA XIV
1a	11,100	1560	200,000	719	0.25	3330	714	1000	772	2080	667	303
1b	7140	588	80,000	3330	0.77	500	2000	1670	625	313	769	192
1c	111,000	1540	200,000	83.3	13.3	10,000	1250	1180	2040	3030	1280	588
1d	26,300	1720	200,000	11,100	454	3700	4350	2630	1250	2860	625	526
1e	50,000	833	50,000	2220	1430	313	6670	2220	667	9520	454	154
1f	200,000	20,000	200,000	200,000	200,000	200,000	200,000	200,000	15,400	200,000	34,500	16,700
1g	5000	1000	200,000	154	1250	833	3850	4170	1000	1670	625	250
1h	2700	1250	200,000	3330	400	222	10,000	3330	400	2500	526	333
1i	10,000	2000	200,000	952	333	4000	5000	2500	1020	6060	400	260
1j	7140	556	125,000	1330	667	1670	2500	1670	571	1820	400	213
2a	5000	303	16,700	1110	1.82	1000	1410	143	370	3330	714	125
2b	7690	526	22,200	2860	4.54	2500	4000	714	1110	4000	1090	833
2c	28,600	417	10,000	1560	27.8	2630	2000	125	400	1050	263	125
7	200,000	200	5000	500	20.8	66.7	200,000	125	286	3330	1000	111
8	1920	500	90,900	2500	7.14	2000	11,100	1670	26.3	286	294	20.0
9	20,000	2860	200,000	200,000	45.4	25,000	58,800	10,000	714	14,300	6670	625
10	23,800	385	33,300	33.3	76.9	100	200,000	286	10.5	500	1670	10.0
11	2220	133	16,700	250	2.04	22.2	50,000	34.5	4.00	50.0	400	0.83
IND	18,000	530	28,000	77.0	670	59.0	710	250	430	2000	290	63.0
AZM	1400	38.0	200,000	100	1000	310	310	17.0	20.0	130	50.0	11.0

The standard deviation of the FTSA measurements is ±1.6-fold in K_d. The K_d for compounds **1a**, **1i**, and **1j** binding to CAs are taken from our previously published data[38–40] indapamide (**IND**) and acetazolamide (**AZM**) from.[40] The values of 200,000 mean that no binding has been detected and the K_d is equal or above 200,000.

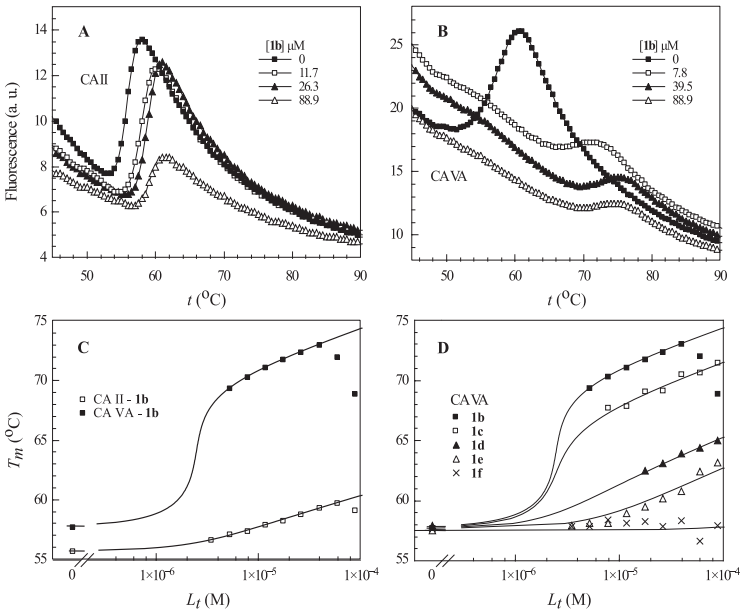

Fig. 2. Thermal shift assay (differential scanning fluorimetry) data where top panels show protein melting curves observed via fluorescence of extrinsic probe (compound **1b** with CA II, Panel A, and CA VA, Panel B) and bottom panels show the melting temperature (T_m) dependence inhibitor dosing curves. Panel C shows selective binding of **1b** towards CA VA over CA II while Panel D compares the dosing curves of **1b**, **1c**, **1d**, **1e**, and **1f**. Lines were fit according to the model.[66] Measurements were performed at pH7.0 in 50 mM sodium phosphate buffer containing 100 mM NaCl.

dazole fragment (**1c**/**2c**), while the smallest – in compound pairs bearing 5,6-dimethylbenzimidazole moiety (**1b**/**2b**). However, an inverse effect was observed for CA VA. 4-chloro substituted compounds (**2**(**a**–**c**)) possessed from 2.08 to 7.27 times diminished binding affinity as compared to chloro unsubstituted compounds (**1**(**a**–**c**)). The selectivity towards CA VA remained.

It was interesting to investigate the influence of larger substituents that should interact with the hydrophobic active site amino acids to improve binding. The introduction of 4-phenethylsulfanyl substituent (**8**) enhanced the binding to many CAs, especially to CA I, CA IX, CA XII, and CA XIV (5.78, 29.3, 7.29, and 15.2, respectively) as compared to the parent compound **1a**. The binding to CA VA decreased 28.6 times, to CA VI – 15.6 times. It should be mentioned that insertion of 4-chloro substituent (**2a**) enhanced binding affinities to other CAs (CA II, CA III, and CA VII - 26.5, 12 and 7 times respectively). The introduction of 4-phenylsulfanyl substituent (**9**) led to a decrease of the binding affinity to all CAs as compared to the parent compound **1a**. The largest decrease in affinity was observed to CA IV, CA VA, CA VB, and CA VI (60.0, 59.1, 50.0, and 29.4 times, respectively). Although the introduction of the substituents reduced selectivity of **8** and **9** towards CA VA, but it still remained.

*2.5. The influence of the linker (NH instead of CH_2) in compounds **7**, **10**, and **11***

When linker carbon atom (**2a**) was replaced with the nitrogen atom (**7**) the affinities to CA VA, CA I, and CA VI decreased (11.5, 40.0, and 142 times, respectively), whereas binding to other CAs remained unchanged. The NH linker-containing compound **10** possessed slightly decreased binding affinity to CA VA (1.69 times) as compared to the structurally related compound **9** bearing CH_2 linker, whereas the binding affinity to the majority of CAs increased from 4 to 35 times, especially towards CA IV – 6000 times.

The replacement of the chlorine substituent in the 4th position (compound **7**) with cyclohexylsulfanyl substituent (compound **11**) increased the affinity to CA VA 10.2 times, while the replacement with phenylsulfanyl substituent (compound **10**) exhibited an opposite effect where the binding to CA VA decreased 3.7 times compared to **7**. Moreover, the introduction of the cyclohexylsulfanyl substituent (**11**), improved the binding to CA I and CA XII (90 and 66.7 times, respectively) more than of the phenylsulfanyl substituent (**10**) (8.4 and 6.7 times, respectively) as compared to the parent compound **7**.

2.6. Compound selectivity towards CA VA

Many of the newly synthesized **1a** analogs (**1b**, **1c**, **2a**, **2b**, **2c**, **8**, **9**, **7**, and **11**) retained high or moderate selectivity towards CA VA (Fig. 2, Panels A, B, and C). Substituents in the 2nd position of the benzimidazole/imidazole ring were not suitable to achieve selectivity to CA VA (**1d**, **1e**, and previously synthesized **1i** and **1j**) (Fig. 2, Panel D). The bulky 4,5-diphenyl imidazole derivative **1f**, and compounds with indoline (**1g**) or 3,4-dihydro-*2H*-quinoline (**1h**) fragments instead of the benzimidazole ring also are not suitable for selective binders to CA VA. The compound **10** affinity to CA VA is smaller than to CA IV. Affinities of all studied compounds to CA isoforms were compared to conventionally used acetazolamide and indapamide as control inhibitors.

2.7. Intrinsic binding affinities

In the design of selective inhibitors of a specific CA isoform, the structure-activity relationship requires the characterization of *intrinsic* thermodynamics, which often is significantly different

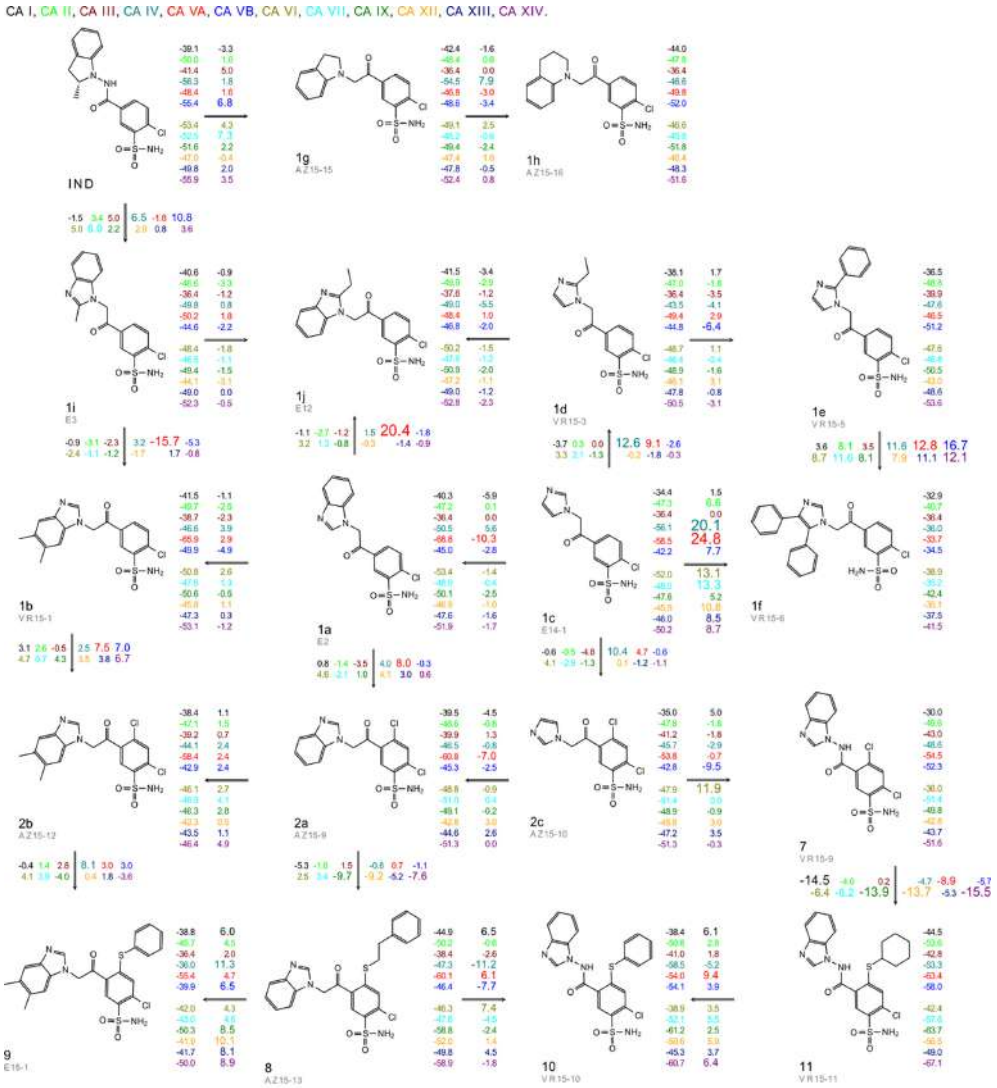

Fig. 3. A map is shown with the inhibitor chemical structures and the intrinsic Gibbs energies of binding (Δ_bGintr) to all 12 recombinant human CA isoforms in different colors listed above the map. The Δ_bGintr are shown on the right side of compound and the differences in binding energies (Δ_bGintr) between compounds of similar chemical structure are shown above and below the arrow connecting the neighboring structures.

from the *observed* (Fig. 4). In this series of compounds, the intrinsic binding affinity is significantly greater than the observed, but the tendency remains essentially the same. The CA VA interaction with **1b** (K_d = 0.8 nM) is a little stronger than compound **11** binding to CA XIV (K_d = 0.83 nM), but intrinsic K_d for CA VA and **1b** binding becomes weaker (K_d = 0.008 nM) than CA XIV with **11** (K_d = 0.005 nM) (Table 2).

Intrinsic parameters describe the binding energy without the influence of protonation. It is known that CA can bind sulfonamide only when Zn^{2+}-bound hydroxide in the active site of CA is protonated and the sulfonamide of the compound is deprotonated. In these experimental conditions only a small fraction of CA and compound can interact (the pK_a values of CA isoforms and sulfonamide groups of every compound are shown in Table 2 in the brackets near each isozyme and compound number). The fractions differ due to different pK_as. For example, the difference between Δ_bG_{obs}s of compound **1h** and **2a** binding to CA I is 1.85, while the difference of Δ_bG_{intr} values is 5.7. Thus, only the intrinsic parameters should be used in drug design when the influence of every functional group of the ligand is being evaluated. Moreover, compound **2a**

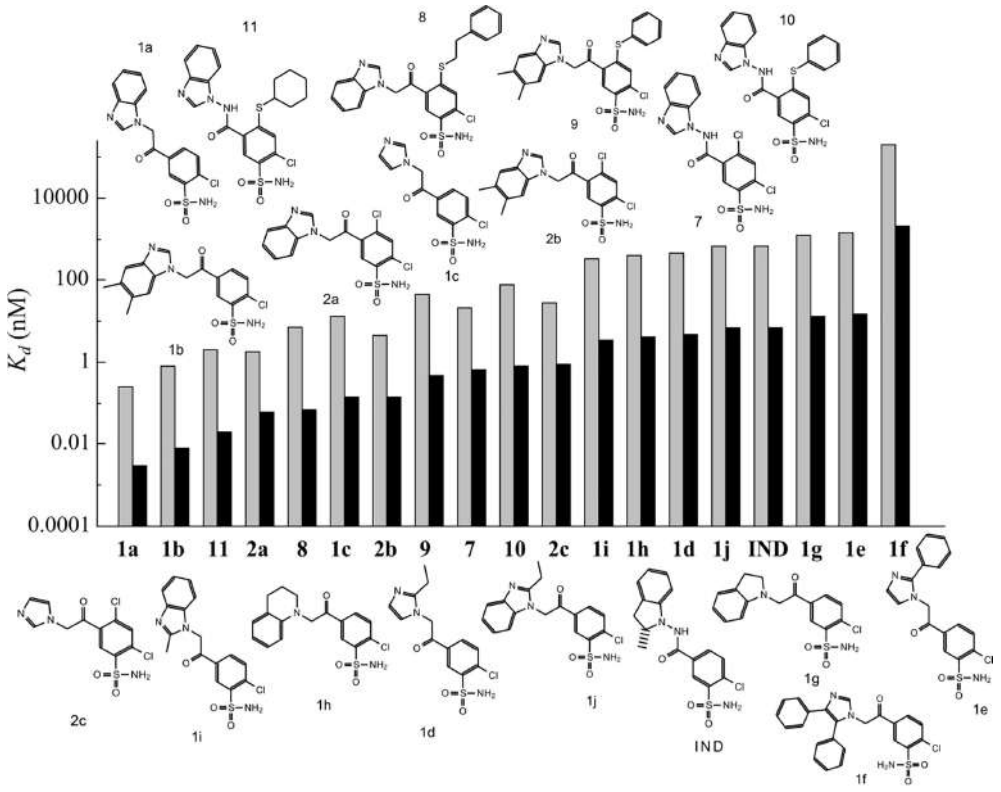

Fig. 4. Comparison of the observed (grey) and intrinsic (black) dissociation constants of the compound binding to CA VA, shown by arranging the compounds in the order of decreasing intrinsic affinity. Intrinsic affinities are approximately 100 fold stronger than the observed ones, but the order of compounds would change if only the observed constants would be compared. The data are listed in Tables 1 and 2.

binds to CA II with affinity Δ_bG_{obs} = −38.7 kJ/mol, while **1b** with Δ_bG_{obs} = −37.0 kJ/mol. The intrinsic parameters showed that the compound **1b** is more potent than **2a** (Δ_bG_{intr} are −49.7 kJ/mol and −48.6 kJ/mol, respectively). The same discrepancies between the observed and intrinsic parameters can be seen for **2a** and **8** binding to CA II, **9** and **7** binding to CA IX, etc.

Fig. 3 shows the map of benzenesulfonamide analogs and the correlation of structural changes with the intrinsic Gibbs energies of binding. Similar compounds are arranged near each other that small structural changes could be compared. The values near the compounds show Gibbs energies of binding, and values near the arrows show Δ_bG differences between compounds. The larger numbers show larger differences. Colors describe CA isoforms.

The largest difference was found between compound **1c** and **1f** binding to CA VA. Bulky hydrophobic group added to tail moiety significantly diminished the binding affinity. These two compounds have the same influence to CA IV. However, small hydrophobic group also highly reduced compound's binding affinity to CA VA as we can see in comparison of compounds **1a** and **1j** interaction to this isoform. It was interesting finding that the functional group added to the *para* position strongly diminished the binding affinity and the chlorine atom (compound **2a**) reduced the affinity similarly to the long 4-phenethylsulfanyl substituent (compound **8**).

Fig. 4 shows the differences of intrinsic and observed dissociation constants when studied compounds bind to CA VA. The affinity decreases when substituent in *para* position is added. However, the potency of binding becomes even lower when tail in *meta* position changes. Bars are grouped from highest to lowest affinity of studied ligand binding to CAs (intrinsic parameters). The observed parameters fluctuated slightly. It means that the protonation effects influence binding. Thus, only intrinsic parameters should be used when thermodynamics of binding are compared.

2.8. Docking studies

Superposition of **1a** conformation in complex with CA II on the homology model of CA VA does not clearly explain the **1a** selectivity towards CA VA. For this reason, it is reasonable to assume that **1a** may bind to CA VA in a different binding mode compared to CA II. One possible reason for the observed binding mode in CA II is that **1a** forms a hydrogen bond, and also an edge-to-face interaction between the ligand's aromatic ring and one of alternative conformations of His64. This conformation of His64 side chain, labeled as B in the PDB file, is pointing towards the ligand. It is impossible to form the same interactions in CA VA since in CA VA the histidine is replaced by a much larger tyrosine. A docking experiment should give insights into the

Table 2
Intrinsic dissociation constants of compound binding to human recombinant CA isoforms determined by FTSA (values listed for 37 °C). The pK_as of the water molecule bound to catalytically active Zn in the active center of CA are listed below CA isoform and the pK_as of compound sulfonamide group are listed next to the compound number.

Cpd (pK_a)	Dissociation constants K_{d_intr} (nM) for CA isoforms CA (pK_a)											
	CA I (8.1)	CA II (6.9)	CA III (6.5)	CA IV (6.6)	CA VA (7.3)	CA VB (7.0)	CA VI (6.0)	CA VII (6.8)	CA IX (6.6)	CA XII (6.8)	CA XIII (8.0)	CA XIV (6.8)
1a (8.8)	161	11.1	750	3.07	0.003	25.9	1.01	5.84	3.64	12.8	9.46	1.83
1b (8.8)	104	4.19	300	14.2	0.008	3.89	2.84	9.73	2.95	19.1	10.9	1.16
1c (8.8)	1612	11.0	750	0.36	0.14	77.7	1.77	6.87	9.63	18.6	18.2	3.55
1d (8.8)	382	12.3	750	47.5	4.72	28.8	6.17	15.4	5.90	17.5	8.87	3.18
1e (8.8)	725	5.93	187	9.49	14.8	2.43	9.46	13.0	3.15	58.3	6.45	0.93
1f (8.8)	2901	142	750	854	2079	1554	284	1167	72.6	1225	489	101
1g (8.8)	72.5	7.12	750	0.66	13.0	6.48	5.46	24.3	4.72	10.2	8.87	1.51
1h (8.8)	39.2	8.90	750	14.2	4.16	1.73	14.2	19.5	1.89	15.3	7.47	2.01
1i (8.8)	145	14.2	750	4.07	3.46	31.1	7.09	14.6	4.79	37.1	5.68	1.57
1j (8.8)	104	3.96	469	5.68	6.93	13.0	3.55	9.75	2.70	11.1	5.68	1.29
2a (8.3)	222	6.60	191	14.5	0.06	23.8	6.11	2.55	5.35	62.4	31.0	2.31
2b (8.3)	341	11.5	255	37.3	0.14	59.4	17.4	12.8	16.0	74.9	47.2	15.4
2c (8.3)	1268	9.07	115	20.4	0.88	62.6	8.68	2.23	5.78	19.7	11.4	2.31
7 (8.3)	8875	4.36	57.3	6.53	0.66	1.58	868	2.23	4.13	62.4	43.4	2.05
8 (8.8)	27.9	3.56	341	10.7	0.07	15.5	15.8	9.73	0.12	1.75	4.17	0.12
9 (8.8)	290	20.3	750	854	0.47	194	83.4	58.4	3.37	87.5	94.6	3.77
10 (8.8)	345	2.74	125	0.14	0.80	0.78	284	1.67	0.05	3.06	23.6	0.06
11 (8.8)	32.2	0.95	62.5	1.07	0.02	0.17	70.9	0.20	0.02	0.31	5.68	0.005
IND (8.8)	261	3.77	105	0.33	6.96	0.46	1.01	1.46	2.03	12.2	4.11	0.38
AZM (7.0)	651	8.67	24,025	13.7	333	77.2	14.1	3.18	3.03	25.5	22.7	2.13

putative binding mode in CA VA. We performed a docking of **1a** ligand into CA VA active site, in order (1) to observe if the docking indeed yields the binding mode which is different from the **1a**/CA II complex and if so, (2) to verify if the trends seen in the binding affinities of various ligands to CA VA can be explained by the putative binding mode.

The **1a** docked to CA VA is shown in Fig. 5. The best docked conformation exhibits two hydrogen bonds between the ligand and the receptor: between the benzimidazole nitrogen and hydroxyl of Thr62, and between the carbonyl of the ligand and the side chain of Gln67. Indeed, this conformation corresponds to a different benzenesulfonamide-CO bond rotamer compared to the **1a**/CA II complex (PDB ID: 3M98) (Fig. 5). Importantly, the carbonyl of the ligand is in a *cis* and *trans* position with respect to the sulfonamide group in **1a**/CA II and **1a**/CA VA, respectively. The carbonyl in **1a**/CA II complex does make hydrogen bonds with Thr200 and with one of His64 alternative conformations visible in the 1.5 Å resolution X-ray structure (not shown). However, the benzimidazole nitrogen apparently is not making hydrogen bonds with the CA II (the nearest Asn62 nitrogen is at a 3.44 Å distance and at an unfavorable angle). Notably, in the **1a**/CA complex, the benzimidazole is likely to benefit from the edge-to-face aromatic-aromatic interaction with Tyr64 (in CA VA), and in CA II (His64), but with a very different geometry (the side chain pointing towards the Zn in CA II and away from Zn in CA VA).

Because of a larger number of hydrogen bonds formed, notably the extra H-bond with the benzimidazole nitrogen in CA VA, the docking offers an explanation of selectivity of the **1a** ligand towards CA VA. Since there are no experimental **1a**/CA VA structures available, the proposed binding conformation could be additionally verified by theoretically exploring the interactions between the receptor and the substituted compounds.

For example, removal of the nitrogen atom from the benzimidazole substituent when going from **1a** to **1g** and **1h** would lead to losing of the hydrogen bond to Thr62 in CA VA. This is consistent with a significant decrease of the binding affinity towards CA VA for the **1g** and **1h**. Since the above-mentioned hydrogen bond is absent in the **1a**/CA II complex, the binding affinity towards CA II is essentially similar for all three ligands (Table 1).

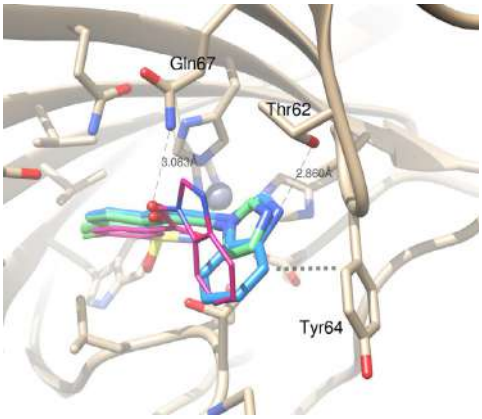

Fig. 5. The docking of compounds **1a** (blue) and **1c** (green) into the CA VA homology model (beige). The side chains of the residues within 4 Å from the ligand are shown. Compound **1a** forms two hydrogen bonds (thin dashed lines) with Thr62 and Gln67 (the residues are numbered according to the homologous CA II). A thick dashed line shows a possible aromatic-aromatic interaction between the benzene ring of the benzimidazole fragment of **1a** and the Tyr64 benzene ring. The superposed **1a** from the complex with CA II is shown as thin purple sticks.

Replacement of the benzimidazole in **1a** with imidazole in **1c** should lead to the loss of aromatic-aromatic interaction with Tyr64 in CA VA (Fig. 3). This is essentially consistent with the observed 50-fold decrease of the binding affinity towards CA VA for **1c** compared to **1a**. In CA II, since the benzimidazole in **1a** does not participate in many aromatic-aromatic interactions, the binding affinity stays essentially the same.

According to the model in Fig. 5, addition of reasonably small groups attached to the benzimidazole in **1b** neither creates clashes with the CA VA receptor, nor adds any new important, hence their binding affinities do not significantly change compared to **1a**. A similar rationale can be applied for the CA II receptor. However,

substitution of the fused benzene ring in benzimidazole by two phenyl rings in **1f** would cause large clashes with the receptor in both CA VA and CA II, strongly negatively affecting the binding affinities.

Inspection of interactions in Fig. 3 also suggests that the introduction of the methyl or ethyl substituent in the 2nd position of benzimidazole moiety in **1i** and **1j** causes sterical clashes in both binding modes, leading to a decrease of the binding affinity towards CA II and CA VA.

The clashes are apparently more easily avoided by some side chain adjustment in **1i**(**1j**)/CA II because the additional alkyl group in **1a** is close to the bulk solvent, and in **1i**(**1j**)/CA VA it is pointing inside the protein, hence it more significantly lowers the binding to CA VA compared to CA II (Table 1).

An important consideration is the fact that **1a** binding modes towards CA II and CA VA correspond to the different rotamers of the COR group with respect to the scaffold consisting of the benzene ring and the sulfonamide group. If new substitutions were introduced into the benzene ring in the *ortho*-position with respect to the COR group, this would cause different stability between the different rotamers.

For example, compound **2a** differs from **1a** by only one atom: the former has a chlorine atom on the benzene ring next to the -COR substituent, while the latter contains hydrogen. It has been shown that the *trans* rotamer is predominant compared to *cis* in *ortho*-chlorobenzaldehyde and *ortho*-chloroacetophenone.[41,42] Hence, we might expect that the conformer where the chlorine atom and the carbonyl oxygen are in the *trans* position is more stable (and therefore binds better) compared to the *cis* position. The **2a** compound is likely to have the same conformation as with **1a** in the complex with CA II. Therefore, the chlorine atom that replaces the hydrogen atom in **2a** will be in the *trans* position with respect to the carbonyl group, and this will not negatively impact the binding to the receptor. The actual 5-fold increase of the binding affinity to CA II when going from **1a** to **2a** can be explained by the increase of the acidity of sulfonamide group due to the electron-withdrawing effect of the chlorine substituent, therefore indirectly improving the binding affinity. In the complex with CA VA, the decrease of the binding affinity from 0.25 nM (**1a**) to 1.82 nM (**2a**) (Table 1) is consistent with the chlorine substituent in the 4th position in **2a** being in the less stable *cis* geometry, predicted by docking (consistent with the conformation of **1a** in Fig. 5). It is also feasible that adding the chlorine substituent in the 4th position of benzene ring with respect to sulfonamide group could cause the conformation of the ligand bound to the CA VA receptor to flip from *cis* to *trans*. Forcing a ligand into the *trans* conformation would lead to the loss of the hydrogen bond as well as the aromatic-aromatic interaction, therefore causing a decrease of the binding affinity.

3. Conclusions

A series of selective CA VA inhibitors, based on a library of new 5-[2-(benzimidazol-1-yl)acetyl]-2-chloro-benzenesulfonamide (**1a**) analogs, a series of chloro substituted benzene sulfonamides, bearing a heterocycle tail were synthesized. The influence of substituents on the binding affinity to the CA VA was investigated. The computational modeling of the **1a** bound to the CA VA suggested a different binding mode from the one observed in the **1a**/CA II complex. The ligand in the proposed binding mode forms several new interactions the CA VA receptor, which are not present in CA II, allowing to interpret CA II/CA selectivity of **1a**, and to predict the effect of modifications of **1a** scaffold. Benzimidazole ring is more favorable than the imidazole due to aromatic-aromatic interaction with Tyr64 of CA VA. The nitrogen atom of the benzimidazole/imidazole ring is also important and it forms hydrogen bonds between the nitrogen atom and the hydroxyl of Thr62 in CA VA. When the nitrogen atom is absent, for example, in the case of indoline or the 3,4-dihydro-*2H*-quinoline substituents (compounds **1g**, **1h**, **IND**), the selectivity towards CA VA disappears. Substituent in the 2nd position of the benzimidazole moiety is not desirable due to the sterical clashes that significantly diminish binding affinity to CA VA. The introduction of a substituent in the 4th position slightly reduces the selectivity towards CA VA due to the less stable *cis* rotamer in CA VA, as predicted by the computational modeling. An introduction of small group to benzimidazole (except in the 2nd position) does not substantially affect the binding affinity to CA VA, as the modification of the linker than CH_2 replaced with NH.

4. Experimental

4.1. Syntheses

Compounds 5-(2-bromoacetyl)-2-chloro-benzenesulfonamide (**1**) and 5-(2-bromoacetyl)-2,4-dichloro-benzenesulfonamide (**2**) were prepared by reduction of a nitro group of appropriate 1-(4-chloro-3-nitro-phenyl)ethanone[43] and 1-(2,4-dichloro-5-nitro-phenyl)ethanone[44] according procedure reported in.[43] An amino group was converted via diazonium salt to sulfonamide group and alfa bromination was carried out as described in[45] to afford corresponding 5-(2-bromoacetyl)-2-chloro-benzenesulfonamide (**1**)[45] and 5-(2-bromoacetyl)-2,4-dichloro-benzenesulfonamide (**2**).[44] Starting compound 1-(4-chloro-3-nitrophenyl)ethanone is commercially available and 1-(2,4-dichloro-5-nitro-phenyl)ethanone was prepared by introducing of a nitro group into commercially available 1-(2,4-dichlorophenyl)ethanone according method reported in.[46]

All starting materials and reagents were commercial products and were used without further purification. Melting points of the compounds were determined in open capillaries on a Thermo Scientific 9100 Series and are uncorrected. ^{1}H and ^{13}C NMR spectra were recorded on a (400 and 100 MHz, respectively) spectrometer in DMSO d_6 using residual DMSO signals (2.52 ppm and 40.21 ppm for ^{1}H and ^{13}C NMR spectra, respectively) as the internal standard. TLC was performed with silica gel 60 F_{254} aluminum plates (Merck) and visualized with UV light. High-resolution mass spectra (HRMS) were recorded on a Dual-ESI Q-TOF 6520 mass spectrometer (Agilent Technologies). The purity of final compounds was verified by HPLC to be >95% using the Agilent 1290 Infinity instrument with a Poroshell 120 SB-C18 (2.1 mm × 100 mm, 2.7 μm) reversed-phase column. Analytes were eluted using a linear gradient of water/methanol (20 mM ammonium formate in both phases) from 60:40 to 30:70 over 12 min, then from 30:70 to 20:80 over 1 min, and then 20:80 over 5 min at a flow rate of 0.2 ml/min. UV detection was at 254 nm.

4.2. General procedure for the synthesis of *1*(*a*–*f*), *2*(*a*–*c*)

A mixture of the appropriate bromoacetophenone **1** or **2** (0.500 mmol), appropriate benzimidazole or imidazole (0.750 mmol), and sodium acetate (49.2 mg, 0.600 mmol) in tetrahydrofuran (3 ml) was stirred at room temperature for 24 h. The reaction mixture was poured into water. The precipitate was filtered off, washed with water, and then with diethyl ether.

5-[2-(Benzimidazol-1-yl)acetyl]-2-chloro-benzenesulfonamide (***1a***) was synthesized as previously described.[38]

2-Chloro-5-[2-(5,6-dimethylbenzimidazol-1-yl)acetyl]benzenesulfonamide (***1b***). The product was purified by flash chromatography over silica gel with EtOAc then EtOAc:MeOH (2:1), R_f = 0.80. Yield

41%, mp 247–249 °C. ^{1}H NMR δ ppm: 2.29 (3H, s, CH_3), 2.31 (3H, s, CH_3), 6.01 (2H, s, CH_2CO), 7.33 (1H, s, $C_{7'}$-H), 7.45 (1H, s, $C_{4'}$-H), 7.89 (2H, s, SO_2NH_2), 7.95 (2H, d, J = 8.4 Hz, C_3-H), 8.03 (1H, s, $C_{2'}$-H), 8.35 (1H, dd, J = 8.4 Hz, J = 2.0 Hz, C_4-H), 8.55 (1H, d, J = 2.0 Hz, C_6-H). ^{13}C NMR δ ppm: 20.3, 20.5, 51.3, 111.1, 119.8, 128.6, 130.3, 131.4, 132.8, 133.2, 133.6, 133.8, 136.2, 142.1, 142.2, 144.4, 192.7. HRMS calcd. for $C_{17}H_{16}ClN_3O_3S$ [(M+H)$^+$]: 378.0674, found: 378.0679.

*2-Chloro-5-(2-imidazol-1-ylacetyl)benzenesulfonamide (**1c**).* The product was purified by chromatography on a column of silica gel with EtOAc:MeOH (2:1), R_f = 0.52. Yield 54%, mp 228–230 °C. ^{1}H NMR δ ppm: 5.78 (2H, s, CH_2CO), 6.94 (1H, s, $C_{4'}$-H), 7.13 (1H, s, $C_{5'}$-H), 7.60 (1H, s, $C_{2'}$-H), 7.87 (2H, s, SO_2NH_2), 7.91 (1H, d, J = 8.0 Hz, C_3-H), 8.26 (1H, dd, J = 8.4 Hz, J = 2.0 Hz, C_4-H), 8.50 (1H, d, J = 2.0 Hz, C_6-H). ^{13}C NMR δ ppm: 53.2, 121.3, 128.4 (2C), 132.8, 133.0, 133.8, 136.1, 138.8, 142.2, 192.8. HRMS calcd. for $C_{11}H_{10}ClN_3O_3S$ [(M+H)$^+$]: 300.0204, found: 300.0200.

*2-Chloro-5-[2-(2-ethylimidazol-1-yl)acetyl]benzenesulfonamide (**1d**).* The product was purified by flash chromatography over silica gel with EtOAc then EtOAc:MeOH (2:1), R_f = 0.70. Yield 32%, mp 223–225 °C. ^{1}H NMR δ ppm: 1.14 (3H, d, J = 7.2 Hz, CH_3), 2.48–2.53 (2H, m, CH_2, superposed with DMSO), 5.74 (2H, s, CH_2CO), 6.81 (1H, d, J = 1.2 Hz, $C_{4'}$-H), 7.00 (1H, d, J = 1.2 Hz, $C_{5'}$-H), 7.86 (2H, s, SO_2NH_2), 7.92 (2H, d, J = 8.0 Hz, C_3-H), 8.29 (1H, dd, J = 8.4 Hz, J = 2.0 Hz, C_4-H), 8.52 (1H, d, J = 2.0 Hz, C_6-H). ^{13}C NMR δ ppm: 12.5, 19.5, 52.4, 121.4, 126.4, 128.5, 132.7, 133.2, 133.7, 136.2, 142.2, 149.8, 192.9. HRMS calcd. for $C_{13}H_{14}ClN_3O_3S$ [(M+H)$^+$]: 328.0517, found: 328.0518.

*2-Chloro-5-[2-(2-phenylimidazol-1-yl)acetyl]benzenesulfonamide (**1e**).* The product was purified by chromatography on a column of silica gel with EtOAc, R_f = 0.39. Yield 29%, mp 131–132 °C. ^{1}H NMR δ ppm: 5.87 (2H, s, CH_2CO), 7.07 (1H, d, J = 0.8 Hz, $C_{4'}$-H), 7.28 (1H, d, J = 1.2 Hz, $C_{5'}$-H), 7.37–7.44 (3H, m, Ph-H), 7.45–7.51 (2H, m, Ph-H), 7.85 (2H, s, SO_2NH_2), 7.89 (2H, d, J = 8.4 Hz, C_3-H), 8.26 (1H, dd, J = 8.4 Hz, J = 2.0 Hz, C_4-H), 8.48 (1H, d, J = 2.0 Hz, C_6-H). ^{13}C NMR δ ppm: 54.0, 123.9, 128.2, 128.4(2C), 129.0, 129.1, 131.1, 132.8, 133.2, 133.4, 136.5, 142.2, 147.7, 192.8. HRMS calcd. for $C_{17}H_{14}ClN_3O_3S$ [(M+H)$^+$]: 376.0517, found: 376.0522.

*2-Chloro-5-[2-(4,5-diphenylimidazol-1-yl)acetyl]benzenesulfonamide (**1f**).* The product was washed with 2 M HCl(aq), dried and then recrystallization was accomplished from toluene:MeOH (1:1). Yield 40%, mp 111–112 °C. ^{1}H NMR δ ppm: 5.96 (2H, s, CH_2-CO), 7.37–7.53 (10*H*, m, Ph-H), 7.87 (2H, d, J = 8.4 Hz, C_3-H), 7.89 (2H, s, SO_2NH_2), 8.17 (1H, dd, J = 8.4 Hz, J = 2.0 Hz, C_4-H), 8.43 (1H, d, J = 2.0 Hz, C_6-H), 8.36 (1H, s, $C_{2'}$-H). ^{13}C NMR δ ppm: 53.6, 126.0, 127.6, 127.7, 128.6, 129.4, 129.6, 129.9, 130.2, 130.5, 131.0, 131.3, 132.6, 132.9, 133.2, 137.0, 137.4, 142.3, 190.9. HRMS calcd. for $C_{23}H_{18}ClN_3O_3S$ [(M+H)$^+$]: 452.0830, found: 452.0836.

*5-[2-(Benzimidazol-1-yl)acetyl]-2,4-dichloro-benzenesulfonamide (**2a**).* Recrystallization was accomplished from MeOH:H_2O (2:1) (twice). Yield 66%, mp 245–250 °C (dec). ^{1}H NMR δ ppm: 5.95 (2H, s, CH_2), 7.20–7.32 (2H, m, $C_{5',6}$-H), 7.56 (1H, dd, J = 6.8 Hz, J = 1.6 Hz, $C_{7'}$-H), 7.70 (1H, dd, J = 6.8 Hz, J = 1.6 Hz, $C_{4'}$-H), 7.92 (2H, s, SO_2NH_2), 8.11 (1H, s, C_3-H), 8.23 (1H, s,$C_{2'}$-H), 8.53 (1H, s, C_6-H). ^{13}C NMR δ ppm: 53.7, 111.1, 119.8, 122.2, 123.0, 130.3, 133.7, 134.8 (2C), 134.9, 135.3, 140.7, 143.4, 145.2, 194.6. HRMS calcd. for $C_{15}H_{11}Cl_2N_3O_3S$ [(M+H)$^+$]: 383.9971, found: 383.9973.

*2,4-Dichloro-5-[2-(5,6-dimethylbenzimidazol-1-yl)acetyl]benzenesulfonamide (**2b**).* Recrystallization was accomplished from MeOH:H_2O (2:1) (twice). Yield 64%, mp 248–251 °C. ^{1}H NMR δ ppm: 2.31 (3H, s, CH_3), 2.32 (3H, s, CH_3), 5.86 (2H, s, CH_2CO), 7.31 (1H, s, $C_{7'}$-H), 7.45 (1H, s, $C_{4'}$-H), 7.91 (2H, s, SO_2NH_2), 8.05 (1H, s, $C_{2'}$-H), 8.10 (1H, s, C_3-H), 8.51 (1H, s, C_6-H). ^{13}C NMR δ ppm: 20.3, 20.6, 53.6, 111.0, 119.9, 130.3, 130.4, 131.5, 133.4, 133.7, 134.7, 134.9, 135.3, 140.7, 142.1, 144.3, 194.7. HRMS calcd. for $C_{17}H_{15}Cl_2N_3O_3S$ [(M+H)$^+$]: 412.0284, found: 412.0279.

*2,4-Dichloro-5-(2-imidazol-1-ylacetyl)benzenesulfonamide (**2c**).* Recrystallization was accomplished from MeOH:EtOAc (1:1). Yield 16%, mp 208–210 °C. ^{1}H NMR δ ppm: 5.62 (2H, s, CH_2CO), 6.93 (1H, s, $C_{4'}$-H), 7.15 (1H, s, $C_{5'}$-H), 7.63 (1H, s, $C_{2'}$-H), 7.88 (2H, s, SO_2NH_2), 8.07 (1H, s, C_3-H), 8.43 (1H, s, C_6-H). ^{13}C NMR δ ppm: 55.4, 121.1, 128.5, 130.2, 133.6, 134.7, 135.0, 135.1, 138.7, 140.6, 194.9. HRMS calcd. for $C_{11}H_9Cl_2N_3O_3S$ [(M+H)$^+$]: 333.9814, found: 333.9818.

4.3. General procedure for the synthesis of (**1g**) and (**1h**).

A mixture of 5-(2-bromoacetyl)-2-chlorobenzene-1-sulfonamide **1**(200 mg, 0.640 mmol) and the appropriate amine (1.30 mmol) in THF (4 ml) was stirred at room temperature for 48 h. The resulting mixture was filtered and the filtrate was evaporated under reduced pressure.

*2-Chloro-5-(2-indolin-1-ylacetyl)benzenesulfonamide (**1g**).* Recrystallization was accomplished from 2-PrOH:H_2O (5:1). Yield 51%, mp 195–198 °C. ^{1}H NMR δ ppm: 2.96 (2H, t, J = 8.4 Hz, CH_2), 3.47 (2H, t, J = 8.4 Hz, CH_2), 4.76 (2H, s, CH_2CO), 6.48 (1H, d, J = 8.0 Hz, $C_{7'}$-H), 6.58 (1H, t, J = 7.6 Hz, $C_{5'}$-H), 6.95 (1H, t, J = 7,6 Hz, $C_{6'}$-H), 7.05 (1H, d, J = 7.2 Hz, $C_{4'}$-H), 7.80 (2H, s, SO_2NH_2), 7.85 (1H, d, J = 8.4 Hz, C_3-H), 8.24 (1H, dd, J = 8.0 Hz, J = 2.0 Hz, C_4-H), 8.50 (1H, d, J = 2.0 Hz, C_6-H). ^{13}C NMR δ ppm: 28.6, 53.4, 55.2, 107.0, 117.7, 124.7, 127.5, 128.4, 129.6, 132.6, 133.1, 134.6, 135.7, 142.0, 152.3, 195.6. HRMS calcd. for $C_{16}H_{15}ClN_2O_3S$ [(M+H)$^+$]: 351.0565, found: 351.0569.

*2-Chloro-5-[2-(3,4-dihydro-2H-quinolin-1-yl)acetyl]benzenesulfonamide (**1h**).* Recrystallization was accomplished from 2-PrOH:H_2O (5:1). Yield 84%, mp 210–213 °C. ^{1}H NMR δ ppm: 1.91 (2H, quint, J = 6.4 Hz, CH_2), 2.74 (2H, t, J = 6.4 Hz, CH_2), 3.34 (2H, t, J = 5.6 Hz, CH_2), 4.93 (2H, s, CH_2CO), 6.34 (1H, d, J = 7.6 Hz, $C_{8'}$-H), 6.48 (1H, td, J = 7.2 Hz, J = 1.2 Hz, $C_{6'}$-H), 6.85 (1H, td, J = 7,6 Hz, J = 1.6 Hz, $C_{7'}$-H), 6.90 (1H, dd, J = 7.2 Hz, J = 1.2 Hz, $C_{5'}$-H), 7.80 (2H, s, SO_2NH_2), 7.87 (2H, d, J = 8.4 Hz, C_3-H), 8.26 (1H, dd, J = 8.4 Hz, J = 2.0 Hz, C_4-H), 8.48 (1H, d, J = 2.0 Hz, C_6-H). ^{13}C NMR δ ppm: 22.3, 28.0, 50.1, 57.7, 110.8, 116.2, 122.3, 127.2, 128.3, 129.3, 132.6, 132.9, 134.5, 135.8, 142.0, 145.6, 196.3. HRMS calcd. for $C_{17}H_{17}ClN_2O_3S$ [(M+H)$^+$]: 365.0721, found: 365.0718.

*Synthesis of 5-[2-(benzimidazol-1-yl)acetyl]-2-chloro-4-phenethylsulfanyl-benzenesulfonamide (**8**).* The mixture of 5-[2-(benzimidazol-1-yl)acetyl]-2,4-dichloro-benzenesulfonamide (**2a**) (65.0 mg, 0.168 mmol), DMSO (1 ml), 2-phenylethanethiol(24.0 mg, 0.168 mmol) and Et_3N (17.6 mg, 0.175 mmol) was stirred at room temperature for 24 h. The brine was added to the mixture and product was extracted with EtOAc (3 × 5 mL). The organic layer was washed with H_2O, dried over anhydrous $MgSO_4$, filtered and concentrated. Recrystallization was accomplished from EtOAc: MeOH (5:1). Yield 31%, mp 205–207 °C. ^{1}H NMR δ ppm: 2.92 (2H, t, J = 7.2 Hz, $\underline{CH_2}$Ph), 3.33–3.40 (2H, m, CH_2S), 6.00 (2H, s, CH_2CO), 7.19–7.32 (7H, m, Ph-H, $C_{5',6}$-H), 7.50 (1H, dd, J = 6.0 Hz, J = 2.8 Hz, $C_{7'}$-H), 7.69 (1H, dd, J = 5.6 Hz, J = 2.8 Hz, $C_{4'}$-H), 7.72 (1H, s, C_3-H), 7.83 (2H, s, SO_2NH_2), 8.15 (1H, s, $C_{2'}$-H), 8.66 (1H, s, C_6-H). ^{13}C NMR δ ppm: 33.0, 33.7, 52.0, 111.1, 119.8, 122.0, 122.8, 126.9, 128.8, 128.9, 129.0, 129.1, 130.1, 135.1, 135.4, 136.8, 140.0, 143.6, 145.3, 147.7, 193.3. HRMS calcd. for $C_{23}H_{20}ClN_3O_3S_2$ [(M+H)$^+$]: 486.0707, found: 486.0709.

*Synthesis of 2-chloro-5-[2-(5,6-dimethylbenzimidazol-1-yl)acetyl]-4-phenylsulfanyl-benzenesulfonamide (**9**).* The mixture of 2,4-dichloro-5-[2-(5,6-dimethylbenzimidazol-1-yl)acetyl]benzenesulfonamide (compound **2b**),MeOH (5 ml), thiophenol (121 mg, 1.10 mmol) and Et_3N (121 mg, 1.20 mmol) was refluxed for 3 h. MeOH was evaporated under reduced pressure and the resultant precipitate was washed with H_2O. Recrystallization was accomplished from acetone:MeOH (1:1). Yield 30%, mp 229–231 °C. ^{1}H NMR δ ppm: 2.30 (3H, s, CH_3), 2.32 (3H, s, CH_3), 6.01 (2H, s, CH_2CO),

6.78 (1H, s, C_3-H), 7.36 (1H, s, $C_{7'}$-H), 7.46 (1H, s, $C_{4'}$-H), 7.60 (5H, br s, Ph-H), 7.81 (2H, s, SO_2NH_2), 8.04 (1H, s, $C_{2'}$-H), 8.72 (1H, s, C_6-H). ^{13}C NMR δ ppm: 20.3, 20.6, 51.8, 111.2, 119.8, 129.1, 129.2, 130.3, 130.6, 131.0, 131.1, 131.3, 131.4, 133.7, 135.3, 135.8, 137.5, 142.3, 144.5, 149.0, 193.2. HRMS calcd. for $C_{23}H_{20}ClN_3O_3S_2$ [$(M+H)^+$]: 486.0707, found: 486.0701.

*Synthesis of 2,4-dichloro-5-[(dimethylamino)methyleneamino]sulfonyl-benzoic acid (**4**).* $SOCl_2$ (2.0 ml 28 mmol) was added dropwise to a solution of 2,4-dichloro-5-sulfamoyl-benzoic acid **3** (1.50 g 5.56 mmol) in DMF (4.3 ml) at −10 °C. The reaction mixture was stirred at room temperature for 2 h and then poured on ice; the resulted precipitate was filtered off and washed with water until pH 7 was reached. Yield 77%, mp 254–255 °C. ^{1}H NMR δ ppm: 2.94 (3H, s, CH_3N), 3.19 (3H, s, CH_3N), 7.92 (1H, s,C_3-H), 8.27 (1H, s,NC-H), 8.41 (1H, s,C_6-H). ^{13}C NMR δ ppm: 35.8, 41.5, 130.2, 132.1, 133.9, 134.6, 136.9, 139.1, 161.3, 165.2. HRMS calcd. for $C_{10}H_{10}Cl_2N_2O_4S$ [$(M+H)^+$]: 324.9811, found: 324.9814.

*Synthesis of N-(benzimidazol-1-yl)-2,4-dichloro-5-[dimethylaminomethyleneamino]sulfonyl-benzamide (**6**).* Mixture of 2,4-dichloro-5-[(dimethylamino)methyleneamino]sulfonyl-benzoic acid (**4**) (326 mg, 1.00 mmol), toluene (0.6 ml) and $SOCl_2$ (1.20 ml, 16.7 mmol) was refluxed for 2 h. Excess $SOCl_2$ and toluene were removed under reduced pressure and the crude acid chloride **5** was used directly in the next step. The obtained 2,4-dichloro-5-[dimethylaminomethyleneamino]sulfonyl-benzoyl chloride (**5**) was added to mixture of 1-aminobenzimidazole (134 mg 1.01 mmol), pyridine (1 ml), and THF (1 ml). The reaction mixture was stirred at 80 °C for 3 h and obtained solution was stirred overnight at room temperature. Then water (15 ml) was added and reaction mixture stirred additionally for some minutes. Precipitate was filtered off, washed with water, dried and recrystallized from large volume of acetic acid. Yield 66%, mp 157–158 °C. ^{1}H NMR δ ppm: 2.97 (3H, s, CH_3N), 3.23 (3H, s, CH_3N), 7.31 (1H, t, J = 8.0 Hz, $C_{5'}$-H), 7.38 (1H, t, J = 7.6 Hz, $C_{6'}$-H), 7.51 (1H, d, J = 8.0 Hz, $C_{4'}$-H), 7.75 (1H, d, J = 8.0 Hz, $C_{7'}$-H), 8.08 (1H, s, C_3-H), 8.33 (1H, s, NC-H), 8.44 (1H, s, C_6-H), 8.49 (1H, s, $C_{2'}$-H), 12.32 (1H, s, NHCO). ^{13}C NMR δ ppm: 35.8, 41.6, 109.8, 120.5, 122.9, 124.1, 130.5, 132.8, 133.1, 133.5, 134.2, 135.4, 139.5, 141.5, 144.3, 161.3, 164.5. HRMS calcd. for $C_{17}H_{15}Cl_2N_5O_3S$[$(M+H)^+$]: 440.0345, found: 440.0349.

*Synthesis of N-(benzimidazol-1-yl)-2,4-dichloro-5-sulfamoyl-benzamide (**7**).* The mixture of *N*-(benzimidazol-1-yl)-2,4-dichloro-5-[dimethylaminomethyleneamino]sulfonyl-benzamide (6) (660 mg, 1.49 mmol) and 2 M NaOH(aq) (5 ml) was stirred at room temperature for 48 h. To obtained solution 2 M HCl(aq) was added until pH 7 was reached. The resulted precipitate was filtered, washed with water, dried and recrystallized from aqueous ethanol. Yield 76%, mp 258–259 °C. ^{1}H NMR δ ppm: 7.31 (1H, t, J = 8.0 Hz, $C_{5'}$-H), 7.38 (1H, t, J = 8.0 Hz, $C_{6'}$-H), 7.51 (1H, d, J = 7.6 Hz, $C_{4'}$-H), 7.75 (1H, d, J = 8.0 Hz, $C_{7'}$-H), 7.92 (2H, s, NH_2SO_2), 8.14 (1H, s, C_3-H), 8.37 (1H, s, C_6-H), 8.49 (1H, s, $C_{2'}$-H), 12.36 (1H, s, NHCO). ^{13}C NMR δ ppm: 109.8, 120.5, 122.9, 124.1, 130.0, 133.0 133.1, 133.5, 133.8, 135.1, 140.8, 141.4, 144.2, 164.5. HRMS calcd. for $C_{14}H_{10}Cl_2N_4O_3S$ [$(M+H)^+$]: 384.9923, found: 384.9920.

*General procedure for the synthesis of **10** and **11**.* The mixture of *N*-(benzimidazol-1-yl)-2,4-dichloro-5-sulfamoyl-benzamide (7) (150 mg, 0.390 mmol), DMSO (1 ml), appropriate thiophenol (47.2 mg, 0.429 mmol) or cyclohexanethiol (49.8 mg, 0.429 mmol) and Et_3N (59.1 mg, 0.585 mmol) was stirred at room temperature under argon for a week. The brine was added to the mixture and product was extracted with EtOAc (3 × 5 mL). The organic layer was washed with H_2O, dried over anhydrous $MgSO_4$, filtered and concentrated.

*N-(benzimidazol-1-yl)-4-chloro-2-phenylsulfanyl-5-sulfamoyl-benzamide (**10**).* The product was purified by flash chromatography over silica gel with $CHCl_3$:MeOH (10:1). Yield 51%, mp 272–274 °C. ^{1}H NMR δ ppm: 6.98 (1H, s, C_3-H), 7.30 (1H, t, J = 7.2 Hz, $C_{5'}$-H), 7.36 (1H, t, J = 7.2 Hz, $C_{6'}$-H), 7.50 (1H, d, J = 8.0 Hz, $C_{4'}$-H), 7.57–7.60 (3H, m, $C_{2'',4'',6''}$-H), 7.63–7.67 (2H, m, $C_{3'',5''}$-H), 7.75 (1H, d, J = 8.0 Hz, $C_{7'}$-H), 7.78 (2H, s, SO_2NH_2), 8.44 (1H, s, C_6-H), 8.48 (1H, s, $C_{2'}$-H), 12.44 (1H, s, CONH). ^{13}C NMR δ ppm: 109.9, 120.5, 122.9, 124.0, 129.5, 130.4, 130.6, 131.0 (2C), 133.6, 133.9, 135.1 (2C), 138.5, 144.3 (2C), 145.2, 165.6. HRMS calcd. for $C_{20}H_{15}ClN_4O_3S_2$ [$(M+H)^+$]: 459.0347, found: 459.0351.

*N-(benzimidazol-1-yl)-4-chloro-2-cyclohexylsulfanyl-5-sulfamoyl-benzamide (**11**).* The product was purified by flash chromatography over silica gel with $CHCl_3$:MeOH (10:1). Yield 22%, mp 231–233 °C. ^{1}H NMR δ ppm: 1.25–1.34 (1H, m, Cy-H), 1.38–1.48 (4H, m, Cy-H), 1.59–1.62 (1H, m, Cy-H), 1.72–1.78 (2H, m, Cy-H), 1.96–2.00 (2H, m, Cy-H), 2.09 (1H, s, Cy-H), 3.71 (1H, br s, Cy-H), 7.31 (1H, t, J = 7.6 Hz, $C_{5'}$-H), 7.37 (1H, t, J = 7.6 Hz, $C_{6'}$-H), 7.55 (1H, d, J = 8.0 Hz, $C_{4'}$-H), 7.75 (1H, d, J = 8.0 Hz, $C_{7'}$-H), 7.77 (2H, s, SO_2NH_2), 7.85 (1H, s, C_3-H), 8.25 (1H, s, C_6-H), 8.45 (1H, s, $C_{2'}$-H), 12.20 (1H, s, CONH). ^{13}C NMR δ ppm: 25.5, 25.7, 32.7, 45.0, 109.9, 120.5, 122.9, 123.9, 129.0, 131.6, 133.3, 133.5, 133.7, 138.4, 141.5, 141.9, 144.3, 166.0. HRMS calcd. for $C_{20}H_{21}ClN_4O_3S_2$ [$(M+H)^+$]: 465.0816, found: 465.0809.

4.4. Protein preparation

Expression and purification of CA III, IV, VA, VB, IX, and XIV has been previously described in[47], of CA I and CA VI in[48], CA II-[49], CA VII and CA XIII-[50], CA XII-[51].

4.5. Determination of compound binding to CAs

4.5.1. Fluorescent thermal shift assay

The fluorescent thermal shift assay (FTSA, ThermoFluor®) measurements were performed by following the temperature shift of protein denaturation curve as a function of the added ligand concentration in a Corbett Rotor-Gene 6000 (QIAGEN Rotor-Gene Q) instrument using the blue channel (excitation 365 ± 20, detection 460 ± 15 nm). The fluorescence of a protein unfolding was followed as a function of temperature due to reporting probe 8-anilino-1-naphthalene sulfonate (ANS), which binds to hydrophobic parts of a protein that expose when protein unfolds. The samples contained a constant concentration of protein, different concentrations of compound, 50 μM ANS in 50 mM phosphate buffer (pH 7.0) containing 100 mM NaCl and 2% (v/v) of DMSO. The applied heating rate was 1 °C/min. Data analysis was performed as previously described.[52]

4.5.2. The pK_as of CAs and sulfonamide group of the compounds

The pK_a values of proteins and compounds **1a** and **1j** were taken from.[40] The pK_as of the other compounds could not be observed by low solubility, thus we stated that ionization constants for structurally similar compounds are the same. For the compounds **2a**, **2b**, **2c** and **7** pK_as were determined according to the NMR chemical shift.[53] Values were compared with pK_as calculated by Marvin, and differ only 0,02–0,1 units.

4.5.3. Intrinsic binding parameters

Sulfonamide binding to CA is linked to protonation reactions. It is known that the binding reaction occurs when sulfonamide group of compound is deprotonated and Zn^{2+}-bound hydroxide is protonated (water molecule is produced).[2,54] The intrinsic Gibbs energy change of this binding is:

$$\Delta_b G_{intr} = -RT \ln K_{b\_intr} = RT \ln K_{d\_intr} \quad (1)$$

where R is the universal ideal gas constant, T– temperature, K_{b_intr} and K_{d_intr}– intrinsic binding and dissociation constants, respectively. The intrinsic binding constant (K_{b_intr}) is related to the observed binding constant (K_b) and the fractions of the protonated

zinc hydroxy anion in active center of carbonic anhydrase (f_{CAZnH_2O}) and the deprotonated sulfonamide ($f_{RSO_2NH^-}$):

$$K_{b\_intr} = \frac{K_b}{f_{RSO_2NH^-} \times f_{CAZnH_2O}} \quad (2)$$

$$f_{RSO_2NH^-} = \frac{10^{pH-pK_{a\_RSO_2NH_2}}}{1+10^{pH-pK_{a\_RSO_2NH2}}} \quad (3)$$

$$f_{CAZnH_2O} = 1 - \frac{10^{pH-pK_{a\_CAZnH_2O}}}{1+10^{pH-pK_{a\_CAZnH_2O}}} \quad (4)$$

The pK_as of the carbonic anhydrases (H_2O bound to the Zn^{2+} in the active center), sulfonamides and K_{d_intr} are listed in Table 2 and the intrinsic Gibbs energies of binding in Fig. 4.

4.6. Computational docking details

The homology model for human CA VA was taken from SWISS-MODEL repository[55], based on the murine CA V template (PDB ID: 1dmx). The ligand-receptor complex was prepared for docking using UCSF Chimera, v. 1.10.[56] The protein atoms were assigned CHARMM22[57] parameters. The ligand atoms were typed by Discovery Studio Visualizer 3.5 (Accelrys Software Inc., San Diego, CA) using CHARMm[58] parameters. Vdock program was used for docking.[59,60] The coordinates of the ligand atoms for **1a** were taken directly from PDB ID: 3M98 without reoptimization, unless otherwise noted. For the derivative ligands, necessary changes were made in the substituent, and the substituent was afterwards optimized with MMFF94s force field[61] using Avogadro program, v. 1.2.0.[62] The influence of the solvent was approximated using the 4*r* distance-dependent dielectric approximation.[63] As in our previous study[64], the position of the sulfonamide nitrogen was fixed in space, and the dihedral angle between the chlorophenyl group and the sulfonamide group was fixed as well. Because of the presence of the alternative conformations of the His64 residue in CA II bound to **1a**, we permitted the side chain of the homologous Tyr64 in CA VA receptor to remain flexible during docking. This allowed a formation of aromatic-aromatic interactions between the receptor and the ligand (see Discussion for more details). To validate the used docking approach, we also performed a docking of **1a** into CA II receptor (PDB ID: 3M98) using similar protocol as with CA VA, resulting in reasonable 1.67 and 1.65 Å ligand heavy atom RMSDs from the X-ray structure, if the ligand coordinates were taken straight from the PDB file, or optimized using MMFF94s force field, correspondingly. Some deviation from the experimental structure was mostly due to the relatively poor ability of the force field to model a possibly strong histidine-aromatic interaction.[65] However, when docking into the CA VA receptor this was not essential, because the docking in CA VA was able to discover aromatic-aromatic interaction, differently from the CA II.

Acknowledgment

This research was funded by grant no. S-MIP-17-87 from the Research Council of Lithuania.

References

1. Alterio V, Fiore AD, D'Ambrosio K, Supuran CT, Simone GD. Multiple binding modes of inhibitors to carbonic anhydrases: how to design specific drugs targeting 15 different isoforms? *Chem Rev*. 2012;112:4421–4468.
2. Krishnamurthy VM, Kaufman GK, Urbach AR, et al. Carbonic anhydrase as a model for biophysical and physical-organic studies of proteins and protein-ligand binding. *Chem Rev*. 2008;108:946–1051.
3. Supuran CT. Carbonic anhydrases: novel therapeutic applications for inhibitors and activators. *Nat Rev Drug Discov*. 2008;7:168–181.
4. Aggarwal M, Boone CD, Kondeti B, McKenna R. Structural annotation of human carbonic anhydrases. *J Enz Inh Med Chem*. 2013;28:267.
5. Supuran C. Carbonic anhydrases as drug targets - an overview. *Curr Top Med Chem*. 2007;7:825–833.
6. Frost SC. Physiological functions of the alpha class of carbonic anhydrases. *Subcell Biochem*. 2014;75:9–30.
7. Pinard MA, Mahon B, McKenna R. Probing the surface of human carbonic anhydrase for clues towards the design of isoform specific inhibitors. *Biomed Res Int*. 2015;2015:1–15.
8. Shah GN, Hewett-Emmett D, Grubb JH, et al. Mitochondrial carbonic anhydrase CA VB: differences in tissue distribution and pattern of evolution from those of CA VA suggest distinct physiological roles. *Proc Natl Acad Sci USA*. 2000;97:1677–1682.
9. Dodgson SJ. Inhibition of mitochondrial carbonic anhydrase and ureagenesis: a discrepancy examined. *J Appl Physiol*. 1987;63:2134–2141.
10. Dodgson SJ, Cherian K. Mitochondrial carbonic anhydrase is involved in rat renal glucose synthesis. *Am J Physiol*. 1989;257:E791–E796.
11. Chegwidden WR, Spencer IM. Carbonic anhydrase provides bicarbonate for de novo lipogenesis in the locust. *Comp Biochem Physiol B: Biochem Mol Biol*. 1996;115:247–254.
12. Hazen SA, Waheed A, Sly WS, LaNoue KF, Lynch CJ. Differentiation-dependent expression of CA V and the role of carbonic anhydrase isozymes in pyruvate carboxylation in adipocytes. *FASEB J*. 1996;10:481–490.
13. Lynch CJ, Fox H, Hazen SA, Stanley BA, Dodgson S, Lanoue KF. Role of hepatic carbonic anhydrase in de novo lipogenesis. *Biochem J*. 1995;310:197–202.
14. Spencer IM, Hargreaves I, Chegwidden WR. Effect of the carbonic anhydrase inhibitor acetazolamide on lipid synthesis in the locust. *Biochem Soc Trans*. 1988;1988:973–974.
15. Arechederra RL, Waheed A, Sly WS, Supuran CT, Minteer SD. Effect of sulfonamides as carbonic anhydrase VA and VB inhibitors on mitochondrial metabolic energy conversion. *Bioorg Med Chem*. 2013;21:1544–1548.
16. Gordon A, Price LH. Mood stabilization and weight loss with topiramate. *Am J Psychiatry*. 1999;156:968–969.
17. Picard F, Deshaies Y, Lalonde J, Samson P, Richard D. Topiramate reduces energy and fat gains in lean (Fa/?) and obese (fa/fa) Zucker rats. *Obes Res*. 2000;8:656–663.
18. Zareba G. Zonisamide review of its use in epilepsy therapy. *Drugs Today (Barc)*. 2005;41:589–597.
19. Casini A, Antel J, Abbate F, et al. Carbonic anhydrase inhibitors: SAR and X-ray crystallographic study for the interaction of sugar sulfamates/sulfamides with isozymes I, II and IV. *Bioorg Med Chem Lett*. 2003;13:841–845.
20. Dodgson SJ, Shank RP, Maryanoff BE. Topiramate as an inhibitor of carbonic anhydrase isoenzymes. *Epilepsia*. 2000;41:S35–S39.
21. Nishimori I, Vullo D, Innocenti A, Scozzafava A, Mastrolorenzo A, Supuran CT. Carbonic anhydrase inhibitors. The mitochondrial isozyme VB as a new target for sulfonamide and sulfamate inhibitors. *J Med Chem*. 2005;48:7860–7866.
22. Vullo D, Franchi M, Gallori E, Antel J, Scozzafava A, Supuran CT. Carbonic anhydrase inhibitors. Inhibition of mitochondrial isozyme V with aromatic and heterocyclic sulfonamides. *J Med Chem*. 2004;47:1272–1279.
23. Simone GD, Fiore AD, Menchise V, et al. Carbonic anhydrase inhibitors. Zonisamide is an effective inhibitor of the cytosolic isozyme II and mitochondrial isozyme V: solution and X-ray crystallographic studies. *Bioorg Med Chem Lett*. 2005;15:2315–2320.
24. Vitale RM, Pedone C, Amodeo P, et al. Molecular modeling study for the binding of zonisamide and topiramate to the human mitochondrial carbonic anhydrase isoform VA. *Bioorg Med Chem*. 2007;15:4152–4158.
25. Güzel Ö, Innocenti A, Scozzafava A, Salman A, Supuran CT. Carbonic anhydrase inhibitors. Aromatic/heterocyclic sulfonamides incorporating phenacetyl, pyridylacetyl and thienylacetyl tails act as potent inhibitors of human mitochondrial isoforms VA and VB. *Bioorg Med Chem*. 2009;17:4894–4899.
26. Biswas S, McKenna R, Supuran CT. Effect of incorporating a thiophene tail in the scaffold of acetazolamide on the inhibition of human carbonic anhydrase isoforms I, II, IX and XII. *Bioorg Med Chem Lett*. 2013;2013:5646–5649.
27. Güzel Ö, Innocenti A, Scozzafava A, Salman A, Supuran CT. Carbonic anhydrase inhibitors. Phenacetyl-, pyridylacetyl- and thienylacetyl-substituted aromatic sulfonamides act as potent and selective isoform VII inhibitors. *Bioorg Med Chem Lett*. 2009;19:3170–3173.
28. Güzel-Akdemir Ö, Biswas S, Lastra K, McKenna R, Supuran CT. Structural study of the location of the phenyl tail of benzene sulfonamides and the effect on human carbonic anhydrase inhibition. *Bioorg Med Chem*. 2013;21:6674–6680.
29. Hen N, Bialer M, Yagen B, et al. Anticonvulsant 4-aminobenzenesulfonamide derivatives with branched-alkylamide moieties: X-ray crystallography and inhibition studies of human carbonic anhydrase isoforms I, II, VII, and XIV. *J Med Chem*. 2011;54:3977–3981.
30. Poulsen S-A, Wilkinson BL, Innocenti A, Vullo D, Supuran CT. Inhibition of human mitochondrial carbonic anhydrases VA and VB with para-(4-phenyltriazole-1-yl)-benzenesulfonamide derivatives. *Bioorg Med Chem Lett*. 2008;18:4624–4627.
31. Winum J-Y, Thiry A, Cheikh KE, et al. Carbonic anhydrase inhibitors. Inhibition of isoforms I, II, IV, VA, VII, IX, and XIV with sulfonamides incorporating fructopyranose-thioureido tails. *Bioorg Med Chem Lett*. 2007;17:2685–2691.
32. Smaine F-Z, Pacchiano F, Rami M, et al. Carbonic anhydrase inhibitors: 2-substituted-1,3,4-thiadiazole-5-sulfamides act as powerful and selective inhibitors of the mitochondrial isozymes VA and VB over the cytosolic and membrane-associated carbonic anhydrases I, II and IV. *Bioorg Med Chem Lett*. 2008;18:6332–6335.

33. Maresca A, Supuran CT. (R)-/(S)-10-camphorsulfonyl-substituted aromatic/heterocyclic sulfonamides selectively inhibit mitochondrial over cytosolic carbonic anhydrases. *Bioorg Med Chem Lett*. 2011;21:1334–1337.
34. Cecchi A, Taylor SD, Liu Y, et al. Carbonic anhydrase inhibitors: inhibition of the human isozymes I, II, VA, and IX with a library of substituted difluoromethanesulfonamides. *Bioorg Med Chem Lett*. 2005;15:5192–5196.
35. Davis RA, Innocenti A, Poulsen S-A, Supuran CT. Carbonic anhydrase inhibitors. Identification of selective inhibitors of the human mitochondrial isozymes VA and VB over the cytosolic isozymes I and II from a natural product-based phenolic library. *Bioorg Med Chem*. 2010;18:14–18.
36. Bonneau A, Maresca A, Winum J-Y, Supuran CT. Metronidazole-coumarin conjugates and 3-cyano-7-hydroxy-coumarin act as isoform-selective carbonic anhydrase inhibitors. *J Enz Inhib Med Chem*. 2013;28:397–401.
37. Carta F, Vullo D, Maresca A, Scozzafava A, Supuran CT. New chemotypes acting as isozyme-selective carbonic anhydrase inhibitors with low affinity for the offtarget cytosolic isoform II. *Bioorg Med Chem Lett*. 2012;22:2182–2185.
38. Čapkauskaitė E, Baranauskienė L, Golovenko D, et al. Indapamide-like benzenesulfonamides as inhibitors of carbonic anhydrases I, II, VII, and XIII. *Bioorg Med Chem*. 2010;18:7357–7364.
39. Zubrienė A, Čapkauskaitė E, Gylytė J, Kišonaitė M, Tumkevičius S, Matulis D. Benzenesulfonamides with benzimidazole moieties as inhibitors of carbonic anhydrases I, II, VII, XII and XIII. *J Enz Inhib Med Chem*. 2014;29:124–131.
40. Čapkauskaitė E, Linkuvienė V, Smirnov A, et al. Combinatorial approach to build selective inhibitors of carbonic anhydrases: N-alkylated benzimidazoles, their affinities to all 12 human CA isoforms. *Chem Select*. 2017;2:5360–5371.
41. Mirarchi D, Ritchie GLD. Solution-state conformations of 2-fluoro-, 2-chloro- and 2-bromo-acetophenone: a dipole moment and kerr effect study. *J Mol Struct*. 1984;118:303–310.
42. Bednarek P, Bally T, Gebicki J. Characterization of rotameric mixtures in o- and m-substituted benzaldehydes by matrix isolation IR spectroscopy. *J Org Chem*. 2002;67:1319–1322.
43. Oelschlager H. 3-Alkyl-6-Halogen-Aniline Aus p-Halogenierten Fettaromatischen Ketonen. *Justus Liebigs Ann Chem*. 1961;641:81–94.
44. Lang HJDCD., Muschaweck RD. Thiazolidinderivate und verfahren zu ihrer herstellung. Patent DE 2533821 A1; 1977.
45. Fujikura T, Miigata K, Hashimoto S, Imai K, Takenaka T. Studies on benzenesulfonamide derivatives with alpha- and beta-adrenergic antagonistic and antihypertensive activities. *Chem Pharm Bull*. 1982;30:4092–4101.
46. Habicht, E.D., Ferrini, P.G.D. and Sallmann, A.D. Verfahren zur herstellung von acylierten heterocyclylcarbonsaeuren A process for preparing acylated heterocyclylcarbonsaeuren. Patent DE 2737462 A1, 1978.
47. Dudutienė V, Matulienė J, Smirnov A, et al. Discovery and characterization of novel selective inhibitors of carbonic anhydrase IX. *J Med Chem*. 2014;57:9435–9446.
48. Čapkauskaitė E, Zubrienė A, Smirnov A, et al. Benzenesulfonamides with pyrimidine moiety as inhibitors of human carbonic anhydrases I, II, VI, VII, XII, and XIII. *Bioorg Med Chem*. 2013;21:6937–6947.
49. Cimmperman P, Baranauskiene L, Jachimoviciute S, et al. A quantitative model of thermal stabilization and destabilization of proteins by ligands. *Biophys J*. 2008;95:3222–3231.
50. Südžius J, Baranauskienė L, Golovenko D, et al. 4-[*N*-(substituted 4-pyrimidinyl) amino]benzenesulfonamides as inhibitors of carbonic anhydrase isozymes I, II, VII, and XIII. *Bioorg Med Chem*. 2010;18:7413–7421.
51. Jogaitė V, Zubrienė A, Michailovienė V, Gylytė J, Morkūnaitė V, Matulis D. Characterization of human carbonic anhydrase XII stability and inhibitor binding. *Bioorg Med Chem*. 2013;21:1431–1436.
52. Baranauskienė L, Hilvo M, Matulienė J, et al. Inhibition and binding studies of carbonic anhydrase isozymes I, II and IX with benzimidazo[1,2-c][1,2,3] thiadiazole-7-sulphonamides. *J Enz Inhib Med Chem*. 2010;25:863–870.
53. Zubrienė A, Smirnovienė J, Smirnov A, et al. Intrinsic thermodynamics of 4-substituted-2,3,5,6-tetrafluorobenzenesulfonamide binding to carbonic anhydrases by isothermal titration calorimetry. *Biophys Chem*. 2015;205:51–65.
54. Khalifah RG, Zhang F, Parr JS, Rowe ES. Thermodynamics of binding of the carbon dioxide-competitive inhibitor imidazole and related compounds to human carbonic anhydrase I: an isothermal titration calorimetry approach to studying weak binding by displacement with strong inhibitors. *Biochemistry*. 1993;32:3058–3066.
55. Kiefer F, Arnold K, Künzli M, Bordoli L, Schwede T. The SWISS-MODEL Repository and associated resources. *Nucleic Acids Res*. 2009;37:D387–D392.
56. Pettersen EF, Goddard TD, Huang CC, et al. UCSF Chimera? A visualization system for exploratory research and analysis. *J Comput Chem*. 2004;25:1605–1612.
57. MacKerell AD, Bashford D, Bellott M, et al. All-atom empirical potential for molecular modeling and dynamics studies of proteins. *J Phys Chem B*. 1998;102:3586–3616.
58. Momany FA, Rone R. Validation of the general purpose QUANTA ®3.2/CHARMm® force field. *J Comput Chem*. 1992;13:888–900.
59. Kairys V, Gilson MK. Enhanced docking with the mining minima optimizer: acceleration and side-chain flexibility. *J Comput Chem*. 2002;23:1656–1670.
60. David L, Luo R, Gilson MK. Ligand-receptor docking with the Mining Minima optimizer. *J Computer-Aided Mol Des*. 2001;15:157–171.
61. Halgren TA. MMFF VI. MMFF94s option for energy minimization studies. *J Comput Chem*. 1999;20:720–729.
62. Hanwell MD, Curtis DE, Lonie DC, Vandermeersch T, Zurek E, Hutchison GR. Avogadro: an advanced semantic chemical editor, visualization, and analysis platform. *J Cheminf*. 2012;4:17.
63. Gelin BR, Karplus M. Side-chain torsional potentials: effect of dipeptide, protein, and solvent environment. *Biochemistry*. 1979;18:1256–1268.
64. Čapkauskaitė E, Zubrienė A, Baranauskienė L, et al. Design of [(2-pyrimidinylthio)acetyl]benzenesulfonamides as inhibitors of human carbonic anhydrases. *Eur J Med Chem*. 2012;51:259–270.
65. Cauët E, Rooman M, Wintjens R, Liévin J, Biot C. Histidine–aromatic interactions in proteins and protein–ligand complexes: quantum chemical study of X-ray and model structures. *J Chem Theory Comput*. 2005;2005:472–483.
66. Kazlauskas E, Petrikaitė V, Michailovienė V, et al. Thermodynamics of aryl-dihydroxyphenyl-thiadiazole binding to human Hsp90. *PLoS ONE*. 2012;7:e36899.

International Journal of
Molecular Sciences

MDPI

Article

Methyl 2-Halo-4-Substituted-5-Sulfamoyl-Benzoates as High Affinity and Selective Inhibitors of Carbonic Anhydrase IX

Audrius Zakšauskas [1], Edita Čapkauskaitė [1], Vaida Paketurytė-Latvė [1], Alexey Smirnov [1], Janis Leitans [2], Andris Kazaks [2], Elviss Dvinskis [2], Laimonas Stančaitis [1], Aurelija Mickevičiūtė [1], Jelena Jachno [1], Linas Jezepčikas [1], Vaida Linkuvienė [1], Andrius Sakalauskas [1], Elena Manakova [3], Saulius Gražulis [3], Jurgita Matulienė [1], Kaspars Tars [2] and Daumantas Matulis [1,*]

[1] Department of Biothermodynamics and Drug Design, Institute of Biotechnology, Life Sciences Center, Vilnius University, Saulėtekio al. 7, LT-10257 Vilnius, Lithuania; audrius.zaksauskas@bti.vu.lt (A.Z.); edita.capkauskaite@bti.vu.lt (E.Č.); vaida.paketuryte@gmc.vu.lt (V.P.-L.); alexeyus1@gmail.com (A.S.); laimonas.stancaitis@gmc.vu.lt (L.S.); aurelija.mickeviciute@bti.vu.lt (A.M.); jelena.jachno@bti.vu.lt (J.J.); linasje@gmail.com (L.J.); linkuviene.vaida@gmail.com (V.L.); andrius.sakalauskas@gmc.vu.lt (A.S.); jurgita.matuliene@bti.vu.lt (J.M.)

[2] Latvian Biomedical Research and Study Centre, Ratsupites 1 k-1, LV-1067 Riga, Latvia; janis.leitans@biomed.lu.lv (J.L.); andris@biomed.lu.lv (A.K.); elviss.dvinskis@protonmail.com (E.D.); kaspars@biomed.lu.lv (K.T.)

[3] Department of Protein—DNA Interactions, Institute of Biotechnology, Life Sciences Center, Vilnius University, Saulėtekio al. 7, LT-10257 Vilnius, Lithuania; elena.manakova@bti.vu.lt (E.M.); saulius.grazulis@bti.vu.lt (S.G.)

* Correspondence: daumantas.matulis@bti.vu.lt

check for updates

Citation: Zakšauskas, A.; Čapkauskaitė, E.; Paketurytė-Latvė, V.; Smirnov, A.; Leitans, J.; Kazaks, A.; Dvinskis, E.; Stančaitis, L.; Mickevičiūtė, A.; Jachno, J.; et al. Methyl 2-Halo-4-Substituted-5-Sulfamoyl-Benzoates as High Affinity and Selective Inhibitors of Carbonic Anhydrase IX. *Int. J. Mol. Sci.* **2022**, *23*, 130. https://doi.org/10.3390/ijms23010130

Academic Editor: Christophe Morisseau

Received: 24 November 2021
Accepted: 18 December 2021
Published: 23 December 2021

Publisher's Note: MDPI stays neutral with regard to jurisdictional claims in published maps and institutional affiliations.

Abstract: Among the twelve catalytically active carbonic anhydrase isozymes present in the human body, the CAIX is highly overexpressed in various solid tumors. The enzyme acidifies the tumor microenvironment enabling invasion and metastatic processes. Therefore, many attempts have been made to design chemical compounds that would exhibit high affinity and selective binding to CAIX over the remaining eleven catalytically active CA isozymes to limit undesired side effects. It has been postulated that such drugs may have anticancer properties and could be used in tumor treatment. Here we have designed a series of compounds, methyl 5-sulfamoyl-benzoates, which bear a primary sulfonamide group, a well-known marker of CA inhibitors, and determined their affinities for all twelve CA isozymes. Variations of substituents on the benzenesulfonamide ring led to compound **4b**, which exhibited an extremely high *observed* binding affinity to CAIX; the K_d was 0.12 nM. The *intrinsic* dissociation constant, where the binding-linked protonation reactions have been subtracted, reached 0.08 pM. The compound also exhibited more than 100-fold selectivity over the remaining CA isozymes. The X-ray crystallographic structure of compound **3b** bound to CAIX showed the structural position, while several structures of compounds bound to other CA isozymes showed structural reasons for compound selectivity towards CAIX. Since this series of compounds possess physicochemical properties suitable for drugs, they may be developed for anticancer therapeutic purposes.

Keywords: methyl 5-sulfamoyl-benzoate; human carbonic anhydrase; *intrinsic* binding thermodynamics; enzyme inhibitor; X-ray crystallography; fluorescent thermal shift assay

1. Introduction

Low-molecular-weight compounds that strongly interact and inhibit the disease target enzymes may be developed as therapeutic drugs. The carbonic anhydrase (CA) family (CA, EC 4.2.1.1), consisting of twelve catalytically active human isozymes, performs the catalysis of reversible hydration of CO_2 into bicarbonate and acid protons. These enzymes participate in numerous physiological processes such as pH regulation and carbon metabolism and are also related to various diseases and conditions such as glaucoma, epilepsy, cancer, edema, osteoporosis, and obesity [1,2]. Since it has been observed that CAIX isozyme is highly

overexpressed in numerous cancers, it has been postulated that compounds inhibiting CAIX may possess the anticancer activity and may be used in tumor treatment [3–5].

Many CA inhibitors have been synthesized bearing flexible tails capable of finding an energetically favorable position in several CA isozymes, thus losing selectivity [6,7]. We have attempted to design inhibitors with a restrained position of the ring and two functional groups attached to the benzenesulfonamide [8–10]. This approach helped design inhibitors selective for CAVII, CAIX, CAXII, and CAXIV.

The introduction of a halogen in the *ortho*- position relative to sulfonamide constrained the benzenesulfonamide ring in a stable position in the CA active site. Additional substituents in the *meta*- and *para*-positions provided additional leverage for increased affinity and selectivity [11–13]. However, these compounds did not fully exploit differences in the CA active site and did not reach sufficient selectivity.

The isozymes CAIX and CAXII exhibit slightly more opened active site entrance than CAI and CAII because, at the entrance of the binding pocket, CAIX has Val131, and CAXII has Ala131, while CAI and CAII have bulky Tyr204 and Phe131 at isostructural positions [14]. Substituents in the *ortho*-position would be expected to interact with the narrower entrance to the active site closer to the Zn(II) and, therefore, would result in greater selectivity for CAIX and CAXII. We attempted to exploit these differences by designing inhibitors selective for CAIX and CAXII—*ortho*-substituted benzenesulfonamides. Two such compounds were designed to bear bulky groups in *ortho*- or *para*-positions to study the effect of substituent's position, size, and flexibility. The compounds were synthesized, and binding affinities and selectivities were determined for the entire set of 12 recombinant human CA isozymes. Key compounds were crystallized with several CA isozymes demonstrating their exact structural positions when bound to CAIX and other isozymes that lead to significant changes in affinity and selectivity for a particular isozyme. Several inhibitors possessed subnanomolar affinities for CAIX and greater than 100-fold selectivities over the remaining human CA isozymes. Thus, such compounds could be further developed for therapeutic purposes.

2. Results and Discussion

2.1. Organic Synthesis of Designed Compounds

Based on substituted halogenated benzenesulfonamide, a series of compounds were designed as potentially high-affinity and selective inhibitors of particular CA isozymes. Starting from methyl 2,4-dichloro-5-sulfamoyl-benzoate **1** and methyl 2,4-dibromo-5-sulfamoyl-benzoate **2**, the designed methyl halo 2- and 4-substituted-5-sulfamoyl-benzoates were synthesized (Scheme 1). Reaction conditions were first chosen according to our previous series where sulfur-containing nucleophiles reacted with dihalosulfamoylbenzamides [9]. The reactions of 2,4-dihalo-5-sulfamoyl-benzoates **1**, **2** with thiols were performed in boiling methanol with triethylamine. However, the reaction was successful only with aromatic thiols (benzenethiol and naphthalene-1-thiol), yielding the *para*-substituted benzenesulfonamides **5**(**a**,**f**) and **6a**. The reaction was very slow or absent, with thiols bearing aliphatic CH_2 or CH group next to the sulfur atom.

To improve the synthesis and based on the reaction of dihalobenzamide with cyclohexanethiol [9], the polar protic solvent MeOH was replaced with a polar aprotic solvent DMSO. This replacement enabled the synthesis of *ortho*-substituted benzenesulfonamides (**3b**–**e**), **4b** as the main product. However, by-products also formed, including *para*-substituted or even-disubstituted benzenesulfonamides.

The regioselectivity of the nucleophilic aromatic substitution of a halogen in methyl 2,4-dihalo-5-sulfamoyl-benzoates **1**, **2** was investigated. All reactions were repeatedly performed in DMSO with triethylamine at 60 °C temperature for 72 h. Determination of conversion yield, product ratio, and structure identification has been performed by NMR and HPLC/UV/MS (Table 1, and Supplementary material).

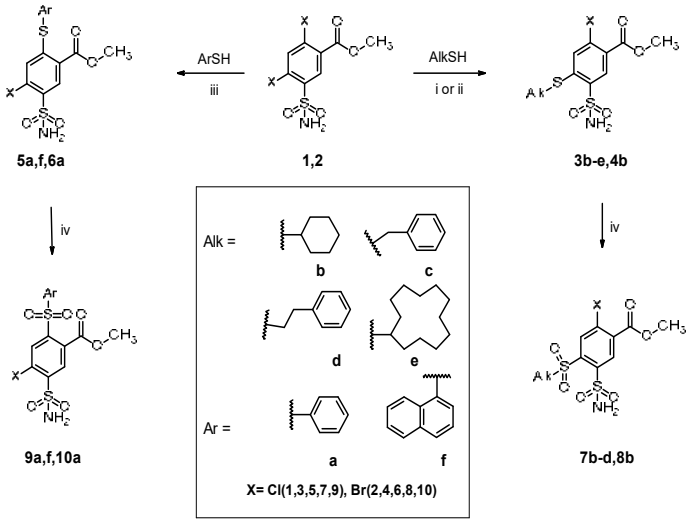

Scheme 1. The synthesis of methyl halo 2- and 4-substituted-5-sulfamoyl-benzoates: (i) TEA, DMSO, 60 °C; (ii) K_2CO_3, DMSO, 60 °C; (iii) TEA, MeOH, Δ; (iv) H_2O_2, AcOH, 75 °C. The legend in the middle explains the structures of alkyl (Ak; **b**, **c**, **d**, **e**) and aromatic (Ar; **a**, **f**) substituents and halogen atoms (Cl—compounds **1**, **3**, **5**, **7**, **9** or Br—**2**, **4**, **6**, **8**, **10**).

Table 1. The reaction of 2,4-dihalo-5-sulfamoyl-benzoates **1**, **2** with thiols and the ratios of the products as determined by NMR spectroscopy and HPLC/UV/MS system data (*italic*). * The separation of the 2- and 4-substituted isomers formed in the reaction of compounds **1** and **2** with phenylthiol using HPLC was unsuccessful.

Starting Compound	Thiol	Conversion (%)	2-Substituted (%)	4-Substituted (%)	2,4-Disubstituted (%)
1		30.07 *28.77*	18.70 *17.38*	81.30 *82.62*	-
2		15.71 *13.92*	9.09 *14.11*	90.91 *85.89*	-
1		89.47 *96.67*	58.82 *88.78 **	35.29	5.88 *11.22*
2		95.07 *96.92*	51.81 *85.55 **	40.42	*7.77* *14.45*
1		72.73 *71.55*	23.53 *22.91*	73.53 *72.79*	2.94 *4.30*
1		72.15 *73.60*	12.28 *12.05*	87.72 *87.95*	-
1		90.97 *95.25*	76.34 *78.84*	19.08 *15.72*	4.58 *5.44*
1		13.70 *18.19*	-	100.00 *100.00*	-

Thiols could be arranged in descending order by their reactivity: phenyl ≥ naphthyl > benzyl ≥ ethylphenyl > cyclohexyl ≥ cyclododecyl. The formation of a disubstituted product was observed in the reaction with phenyl-, naphthyl-, and benzyl- thiols. The 2-substituted product was mainly formed in the reactions with aromatic thiols (naphthyl- and phenylthiol), while in the remaining cases, the formation of the 4-substituted product was dominant. In the case of bulky dodecylthiol, only the formation of the 4-substituted isomer was observed.

A group of 2-substituted methyl benzoates **5**(**a**–**d**,**f**) was synthesized via 2,4-dichloro-5-sulfamoyl-benzamide (**11**) (Scheme 2) [9]. The nucleophilic substitution of chlorine occurred only in the *para*- position relative to the sulfonamide group. The amide group of the substituted products **12**(**a**–**d**,**f**) was converted to the ester group using thionyl chloride and MeOH to yield the 2-substituted benzenesulfonamide methyl esters **5**(**a**–**d**,**f**). Oxidation of sulfanyl derivatives **3**(**b**–**d**), **4b**, **5**(**a**–**d**,**f**), **6a** to sulfonyl derivatives **7**(**b**–**d**), **8b**, **9**(**a**–**d**,**f**), **10a** (Schemes 1 and 2) was carried out using in situ generated peracetic acid.

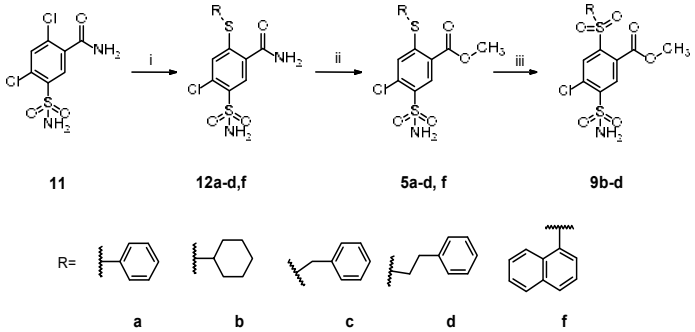

Scheme 2. Synthesis of 2-halo-4,5-disubstitutedbenzenesulfonamides: (i) TEA, DMSO, 60 °C; (ii) $SOCl_2$, MeOH, Δ; (iii) H_2O_2, AcOH, 75 °C.

2.2. Thermodynamics of Compound Binding to CA Isozymes

The chemical structures of 21 compounds used in this study are summarized in Figure 1A. The main goal was to determine the influence of the type and position of the sulfanyl or sulfonyl substituent on the affinity for human CA isozymes. The compounds were divided into four groups with different sulfanyl (-S-) or sulfonyl (-SO_2-) substituents in *para*- or *ortho*-positions with respect to the sulfonamide group. All compounds had the same ester group in the *meta*-position. The influence of the diversity of the *meta* group on the binding affinity to CAs has been investigated and described in greater detail in a previous publication [9]. We found no significant difference in binding for compounds with chlorine or bromine atoms in that study. Therefore, there is only one analogous brominated compound for comparison (**4b**, **6a**, **8b**, **10a**) in each of the four groups.

Dissociation constants (Table 2) of every compound for each of the 12 catalytically active human CA isozymes were measured using the fluorescent thermal shift assay (FTSA). Some experimental data of selected compounds are provided in Figures S1 and S2 in the Supplementary material. The observed constants (K_{d_obs}) were converted to the observed standard change in the Gibbs energy of binding ($\Delta G_{obs} = RT\ln K_{d\_obs}$, where R *is* the universal ideal gas constant and T *is* the temperature), shown in Figure 1B, upper panel, and Table S1. For visual simplicity, the affinity is averaged for all compounds belonging to one of the four groups and shown in the Figure by coloring the groups: **3**(**b**–**e**), **4b** are blue rhombs, **5**(**a**–**d**,**f**), **6a** are orange squares, **7**(**b**–**d**), **8b** are cyan triangles, and **9**(**a**–**d**,**f**), **10a** are yellow circles (Figure 1B). The bars show the range from the strongest to the weakest affinity for each CA isozyme in that group of compounds (not the error bars).

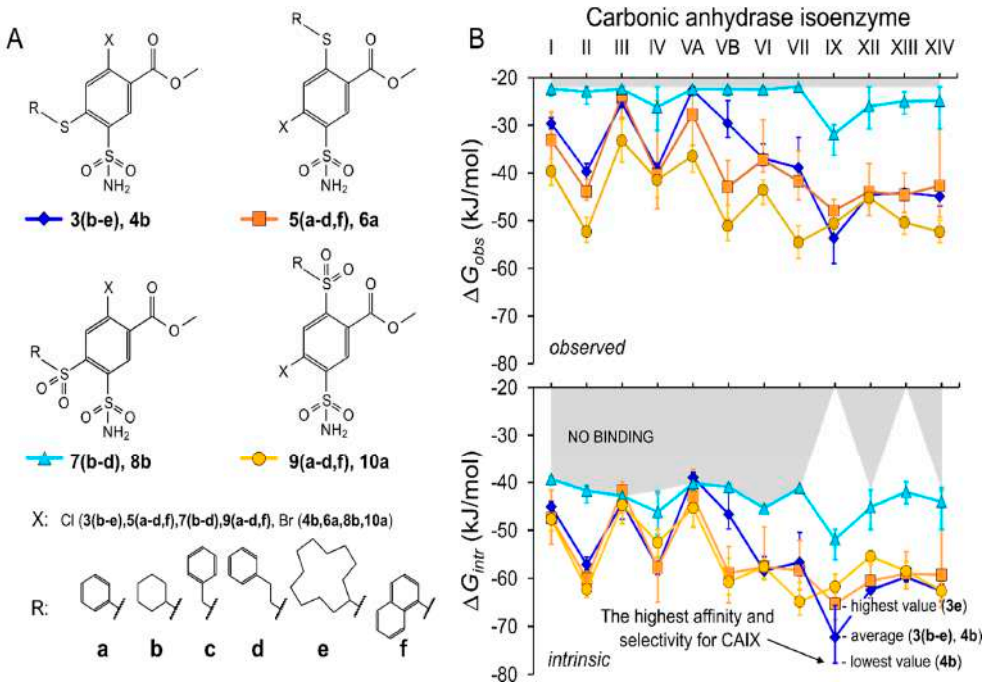

Figure 1. (**A**) Chemical structures of the four groups of compounds—methyl halo 2- or 4-substituted-5-sulfamoyl-benzoates containing chlorine or bromine and substituents listed at the bottom of the panel. (**B**) Averaged change in the standard *observed* (upper panel) or *intrinsic* (lower panel) Gibbs energy for compounds belonging to one of the four groups: **3**(**b**–**e**), **4b**—blue rhombs, **5**(**a**–**d**,**f**), **6a**—orange squares, **7**(**b**–**d**), **8b**—cyan triangles, and **9**(**a**–**d**,**f**), **10a**—yellow circles. The bars show the margin between the strongest and weakest affinity of compounds in that group for the indicated CA isozyme. The *intrinsic* binding affinity of compounds **3**(**b**–**e**), **4b** to CAIX is highlighted: the blue rhombus is the average of all five interactions, the bar above shows the weakest CAIX interaction with **3e**, and below is the strongest with **4b**. Compounds in this group have the highest selectivity and affinity for CAIX.

Interaction of CA with any primary sulfonamide is pH-dependent in identical shape. The affinity is greatest in the near-neutral range and decreases by exactly 10-fold with every pH unit in the acidic and alkaline pH regions. This is explained by the binding mechanism where the deprotonated sulfonamide compound replaces a water molecule (but not a hydroxide ion) coordinated by the Zn(II) in the active site of CA. The deprotonated state of the sulfonamide amino group bound to CA is directly observed by the neutron diffraction structures [15]. However, the sulfonamide state in the solution is predominantly in the protonated form because sulfonamide pK_a is usually in the region of 9–10. Both the compound and the protein have to undergo protonation–deprotonation reactions to be able to bind. These binding-linked reactions significantly reduce the affinity. Interaction energies of the binding-able states of the protein and ligand are termed *intrinsic*. However, since the protonation reactions occur indistinguishably from protein-ligand binding, we experimentally observe diminished energies, termed *observed*.

Table 2. *Intrinsic* (K_{d_intr}), calculated according to the model, and *observed* (K_{d_obs} at pH = 7.0), determined by the fluorescent thermal shift assay, dissociation constants, K_d (nM), of investigated compounds binding to all catalytically active human carbonic anhydrases (CAs) at 37 °C. pK_a values of the sulfonamide group were calculated from spectra at various pH as described in Methods and are listed to all compounds. Some compounds exhibited poorer solubility, which was observed visually and prompted in absorption spectra. Therefore, for such compounds, the pK_a value was assigned based on the average value of the other compounds in that group and is marked with *.

Compound (Lab. Name)	Chemical Structure	*ortho* Substituent	*para* Substituent	pK_a	K_d (nM)	CAI	CAII	CAIII	CAIV	CAVA	CAVB	CAVI	CAVII	CA IX	CAXII	CAXIII	CAXIV
1	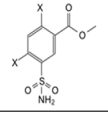	Cl	Cl	8.9	*Observed*	14,000	71	50,000	180	6700	310	170	67	59	560	83	72
(*EA2-1*)					*Intrinsic*	160	0.39	150	0.65	55	1.9	0.19	0.32	0.21	2.7	0.94	0.35
2		Br	Br	8.8	*Observed*	20,000	91	$\geq 2 \times 10^5$	140	3700	33	290	56	120	330	63	40
(*LJ14-4*)					*Intrinsic*	290	0.63	≥750	0.63	38	0.26	0.41	0.34	0.52	2	0.89	0.24
3b		*cyclohexyl*	Cl	9.6	*Observed*	17,000	250	40,000	400	100,000	11,000	330	150	0.33	33	50	13
(*EA2-3*)					*Intrinsic*	39	0.28	24	0.29	170	14	0.080	0.15	0.00020	0.030	0.11	0.010
3c		*benzyl*	Cl	9.5	*Observed*	6900	110	80,000	120	$\geq 2 \times 10^5$	5000	360	150	2.9	22	38	40
(*EA2-4*)					*Intrinsic*	20	0.16	61	0.11	≥420	7.9	0.10	0.19	0.0030	0.030	0.11	0.050
3d		*2-phenylethyl*	Cl	9.6	*Observed*	13,000	170	15,000	430	110,000	10,000	630	100	13	53	38	43
(*EA2-5*)					*Intrinsic*	30	0.18	9.3	0.30	190	13	0.14	0.10	0.0090	0.050	0.090	0.040
3e		*cyclododecyl*	Cl		*Observed*	12,000	400	$\geq 2 \times 10^5$	200	$\geq 2 \times 10^5$	67,000	2000	3300	0.44	41	27	37
(*EA2-12*)					*Intrinsic*	27	0.44	≥120	0.14	≥330	84	0.46	3.2	0.00030	0.040	0.060	0.040
4b		*cyclohexyl*	Br	9.6 *	*Observed*	6700	200	48,000	330	$\geq 2 \times 10^5$	3300	560	220	0.12	16	33	20
(*LJ15-12*)					*Intrinsic*	15	0.22	29	0.24	≥330	4.2	0.13	0.22	0.000080	0.020	0.080	0.020
5a		Cl	*phenyl*	9.4 * LS	*Observed*	3300	36	17,000	14	$\geq 2 \times 10^5$	250	200	50	2.5	5.7	20	19
(*EA2-2*)					*Intrinsic*	12	0.060	16	0.020	≥530	0.50	0.070	0.080	0.0030	0.0090	0.070	0.030
5b		Cl	*cyclohexyl*	9.4	*Observed*	330	20	$\geq 2 \times 10^5$	67	4000	5.7	210	21	7.5	13	10	5.1
(*EA1-3N*)					*Intrinsic*	1.2	0.040	≥190	0.080	11	0.010	0.070	0.030	0.0080	0.020	0.040	0.0080
5c		Cl	*benzyl*	9.4 * LS	*Observed*	2000	33	$\geq 2 \times 10^5$	120	1800	470	290	130	14	400	100	47
(*EA1-4N*)					*Intrinsic*	7.3	0.060	≥190	0.13	4.8	0.92	0.10	0.19	0.020	0.61	0.36	0.070
5d		Cl	*2-phenylethyl*	9.3	*Observed*	3400	27	89,000	1000	3800	4.4	850	24	12	180	7.4	17
(EA1-5N)					*Intrinsic*	16	0.060	110	1.5	13	0.010	0.38	0.050	0.020	0.34	0.030	0.030
5f		Cl	1-naphthyl	9.4 * LS	*Observed*	27,000	110	$\geq 2 \times 10^5$	66,000	96,000	510	14,000	1100	22	66	57	63,000
(EA2-NF)					*Intrinsic*	98	0.20	≥190	75	250	1.0	5.0	1.7	0.020	0.10	0.21	97
6a		Br	phenyl	9.4 * LS	*Observed*	2500	80	$\geq 2 \times 10^5$	40	86,000	31	420	210	9.8	20	16	13
(LJ15-11)					*Intrinsic*	9.2	0.14	≥190	0.050	230	0.060	0.15	0.32	0.010	0.030	0.060	0.020

Table 2. *Cont.*

Compound (Lab. Name)	Chemical Structure	*ortho* Substituent	*para* Substituent	pK_a	K_d (nM)	CA I	CA II	CA III	CA IV	CA VA	CA VB	CA VI	CA VII	CA IX	CA XII	CA XIII	CA XIV
7b	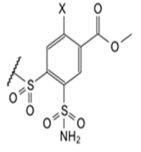	cyclohexyl	Cl	9.8	*Observed*	100,000	50,000	100,000	41,000	100,000	100,000	190,000	$\geq 2 \times 10^5$	9200	67,000	69,000	69,000
(EA2-3o)					*Intrinsic*	150	35	38	19	110	79	28	≥120	4.2	41	99	42
7c		benzyl	Cl	9.8* LS	*Observed*	$\geq 2 \times 10^5$	190,000	$\geq 2 \times 10^5$	5900	$\geq 2 \times 10^5$	$\geq 2 \times 10^5$	130,000	$\geq 2 \times 10^5$	790	6700	140,000	6700
(EA2-4o)					*Intrinsic*	≥290	130	≥76	2.7	≥210	≥160	19	≥120	0.36	4.1	200	4.1
7d		2-phenylethyl	Cl	9.8 * LS	*Observed*	$\geq 2 \times 10^5$	$\geq 2 \times 10^5$	$\geq 2 \times 10^5$	$\geq 2 \times 10^5$	$\geq 2 \times 10^5$	$\geq 2 \times 10^5$	130,000	$\geq 2 \times 10^5$	6700	34,000	22,000	$\geq 2 \times 10^5$
(EA2-5o)					*Intrinsic*	≥300	≥140	≥76	≥90	≥210	≥160	19	≥120	3.0	21	32	≥120
8b		cyclohexyl	Br	9.9	*Observed*	$\geq 2 \times 10^5$	$\geq 2 \times 10^5$	$\geq 2 \times 10^5$	$\geq 2 \times 10^5$	$\geq 2 \times 10^5$	$\geq 2 \times 10^5$	$\geq 2 \times 10^5$	$\geq 2 \times 10^5$	6700	$\geq 2 \times 10^5$	71,000	$\geq 2 \times 10^5$
(LJ15-12o)					*Intrinsic*	≥230	≥110	≥60	≥16	≥170	≥130	≥23	≥97	2.4	≥97	82	≥97
9a	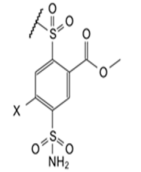	Cl	phenyl	8.2	*Observed*	140	0.91	3300	25	770	13	56	0.45	3.3	22	5.6	0.83
(EA2-2o)					*Intrinsic*	7.9	0.020	48	0.42	30	0.40	0.30	0.010	0.060	0.51	0.30	0.020
9b		Cl	cyclohexyl	8.2	*Observed*	67	0.67	2800	200	500	0.75	42	0.18	1	14	2.7	0.64
(EA1-3No)					*Intrinsic*	3.7	0.020	40	3.4	20	0.020	0.22	0.0040	0.020	0.33	0.15	0.010
9c		Cl	benzyl	8.2	*Observed*	560	5	450	100	830	1.1	14	2.5	2.5	20	5	2.6
(EA1-4No)					*Intrinsic*	31	0.13	6.5	1.7	33	0.030	0.080	0.060	0.040	0.46	0.27	0.060
9d		Cl	2-phenylethyl	8.4	*Observed*	330	1.7	920	140	200	1.1	26	0.85	2.5	48	3	1.3
(EA1-5No)					*Intrinsic*	12	0.030	8.5	1.6	5.1	0.020	0.090	0.010	0.030	0.72	0.10	0.020
9f		Cl	1-naphthyl	8.4	*Observed*	140	1.3	14,000	50	1400	3.4	100	0.67	10	50	1.3	4
(EA2-Nfo)					*Intrinsic*	5.1	0.020	130	0.55	36	0.060	0.35	0.010	0.11	0.74	0.040	0.060
10a		Br	phenyl	8.4	*Observed*	330	2.3	4800	370	1600	5.3	110	0.67	3.3	16	4.3	2
(LJ15-11o)					*Intrinsic*	12	0.040	44	4.0	41	0.10	0.37	0.010	0.040	0.24	0.15	0.030
Acetazolamide	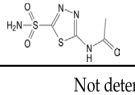			7.0	*Observed*	2400	46	40,000	87	840	140	220	13	21	130	120	63
					Intrinsic	1100	9.8	4600	12	270	34	9.8	2.4	2.9	24	53	12

Not determined, ND; low solubility, LS. * pK_a value was assigned based on the average value of the other compounds in that group. The measurement limit is $\geq 2 \times 10^5$. The highest used ligand concentration was 200 µM. *Intrinsic* values are calculated according to the model described in the Methods section.

The *intrinsic* dissociation constants were calculated according to the model described in the Methods section and Supplementary material using measured pK_a values of the sulfonamide group of the compounds (Table 2). It is more appropriate to use the *intrinsic* parameters in interpreting the interactions, as they help separate the linked protonation reactions that can lead to erroneous conclusions [16]. The *intrinsic* standard change in the Gibbs energy of binding is shown in Figure 1B, lower panel, and Table S2. These parameters were also used in the analysis of crystal structures.

2.3. X-ray Crystal Structures and Correlations with Compound Binding Thermodynamics to CA Isozymes

Eight crystal structures of CA complexes with compounds are presented in this study: **9a** bound to CAI and CAII, **3b**, **3d**, **5b**, and **9a** bound to CAXII, **3b** bound to CAIX and mimic-CAIX (mutant of CAII containing amino acids in the active site as in CAIX: A65S, N67Q, I91L, F130V, V134L, and L203A). The electron density maps of the ligands bound in the active site of CA are shown in Figure S3. The data collection and refinement statistics are presented in Table S3. The crystal structures of CAI, CAII (and mimic-CAIX), CAIX, and CAXII complexes in the asymmetric unit contained 2, 1, 4, and 4 protein subunits, respectively.

The structure–thermodynamics correlations that determine the recognition between the CA active site and the ligand will be analyzed in three sections:

(i) methyl 2-halo-4-substituted-5-sulfamoyl-benzoates, abbreviated *ortho*- by substituent at the *ortho*- position relative to sulfonamide group;
(ii) methyl 4-halo-2-substituted-5-sulfamoyl-benzoates, abbreviated as *para*-,
(iii) the position of the substituent in benzenesulfonamide is compared in these two groups of compounds.

2.3.1. Methyl 2-Halo-4-Substituted-5-Sulfamoyl-Benzoates Binding to CA Isozymes

In the group of *ortho*- sulfanyl– **3**(**b**–**e**), **4b**, and sulfonyl– **7**(**b**–**d**), **8b** substituted benzenesulfonamides, the chlorinated **3b**, and brominated **4b** bound similarly. Their K_d differed by less than 3-fold; not a significant difference within the error limits (Table 2). Compounds **7** bound most isozymes with barely detectable affinity, except CAIX, where chlorinated and brominated bound similarly (K_{d_obs} (**7b**) = 9200 nM and K_{d_obs} (**8b**) = 6700 nM). Sulfonyl (-SO_2-, **7**(**b**–**d**), **8b**) compounds bound CA significantly weaker than the parent compound **1** or analogous sulfanyl compounds **3b**–**e**. The strongest interaction with CAIX was likely due to its wider active site than in other CAs [10]. The sulfonyl compounds likely were in an unfavorable conformation for binding and prevented an optimal formation of the sulfonamide group-nitrogen and protein-Zn(II) coordination bond due to steric hindrance.

The pK_a values of the sulfonamide amino group of a series of these compounds were determined. Although the compounds showed limited solubility, the absorption spectra of **7b** and **8b** at different pH were used to determine their pK_a values, 9.8 and 9.9, respectively (Supplementary material, Figure S5). The same, 9.8, value was assigned to other compounds (**7c** and **7d**) in the same group. *Para*-substituted sulfonyl (-SO_2-) compounds **9**(**a**–**d**,**f**), and **10a** (pK_a = 8.2–8.4) had lower pK_a values than sulfanyl (-S-) compounds **5**(**a**–**d**,**f**), and **6a** (pK_a = 9.3–9.4), while *ortho*-substituted compounds showed the opposite (Figure 1B, upper panel and Table 2). The pK_a values were 9.9 for sulfonyl (-SO_2-) compounds **7**(**b**–**d**,**f**), **8b**, and 9.5-9.6 for sulfanyl (-S-) compounds **3**(**b**–**e**), **4b**. Therefore, oxidation did not reduce the pK_a of the sulfonamide group in all cases. The pK_a values were well correlated with chemical shifts determined by NMR (Supplementary material, Figure S6). Chemical shifts show the same trend: values of *ortho*-sulfonyl compounds were lower than sulfanyl, and, in contrast, *para*-sulfonyl compounds had higher values than sulfanyl.

Sulfanyl- compounds **3b**–**e** and **4b** bound weakly to CAI, CAIII (narrow entrance to the active site due to Phe198), CAVA, and CAVB. However, compounds had μM affinity to CAII, CAIV, CAVI, CAVII and even approximately 10-fold stronger (K_{d_obs} is 13–53 μM) to CAXII, CAXIII, and CAXIV (the measured affinity to CAIX is up to 0.12 μM (Table 2 and Figure 1B).

Comparison between parent compound **1** and the *ortho*-substituted sulfanyl compounds showed that the hydrophobic substituent had a significant effect (Figure 2). The intrinsic affinity for CAXII (−11.4 kJ/mol), CAXIII (−5.4 kJ/mol), CAXIV (−8.6 kJ/mol), and especially for CAIX (−17.5 kJ/mol or about 1000-fold) significantly increased, and CAVA (2.9 kJ/mol) and CAVB (5.1 kJ/mol) decreased (**1**→**3b**). The affinity strongly depended on the flexibility of the substituent and shorter substituents in compounds **3b** and **3e** had higher affinity to CAIX than longer and more flexible substituents in compounds **3c** and **3d**: the difference was at least about 6 kJ/mol or about 10-fold (ΔG_{intr} (**3b**) = −75.0 kJ/mol, ΔG_{intr} (**3c**) = −68.8 kJ/mol, ΔG_{intr} (**3d**) = −65.6 kJ/mol, ΔG_{intr} (**3e**) = −74.2 kJ/mol). The affinity for CAVII decreased significantly (9.0 kJ/mol) from compound **3d** to compound **3e**, possibly due to the size of the substituent. In other cases, the differences were within the error margin.

We compared the crystal structures of several compounds in two different CA isozymes (Figure 2B–D). Figure 2B shows the binding mode of **3b** and **3d** in the active site of CAXII. These compounds are structurally similar and differ only in the size of large hydrophobic *ortho* substituents; compound **3b** has the octyl, while **3d** has the 2-phenylethyl moiety. The binding modes of both ligands in the active site of CAXII were the same: *ortho* groups were directed to the hydrophobic part of the active site, while *meta* substituents were orientated to the hydrophilic part. The binding affinities and enthalpy changes to CAXII were almost identical (ΔG_{intr} = −62.3 kJ/mol, ΔH_{intr} = −48.0 kJ/mol (**3b**) vs. ΔG_{intr} = −61.1 kJ/mol, ΔH_{intr} = −50.1 kJ/mol (**3d**), Figure 2B). Experimental data of the ΔH_{obs} are shown in the Supplementary material in Figure S8.

Figure 2C shows the superposition of **3b** in the active sites of CAIX and CAXII. The positions of the compounds were similar. However, the binding affinities of **3b** to CAIX and CAXII differed significantly and were 150 times stronger to CAIX than CAXII (K_{d_intr} = 0.030 nM or ΔG_{intr} = −62.3 kJ/mol to CAXII and K_{d_intr} 0.20 pM or ΔG_{intr} = −75.0 kJ/mol to CAIX, Table 2 and Table S2). Again, the side chains interacting with **3b** in CAIX and CAXII were different. They were more hydrophobic in CAIX (A203, L135, V131, L91, and Q67) and more hydrophilic in CAXII (N204, S135, V131, T91, and K68). Thus, these differences could be related to the solvation entropy because binding to CAIX was much more entropy-driven than to CAXII (ΔH_{intr} = −29.9 kJ/mol, $-T\Delta S_{intr}$ = −45.1 kJ/mol to CAIX and ΔH_{intr} = −48.0 kJ/mol, $-T\Delta S_{intr}$ = −14.3 kJ/mol to CAXII).

The binding of **3b** to CAIX and mimic-CAIX is compared in Figure 2D. Mimic-CAIX is CAII with multiple point mutations that replace the side chains of the active site of CAII with the corresponding residues of CAIX. It has been shown that six-point mutations (A65S, N67Q, I91L, F130V, V134L, and L203A) are sufficient to switch the binding mode of the selective ligand [17–19] (mutations slightly different A65S, N67Q, E69T, I91L, F131V, K170E, and L204A). The ligand positions were similar except for the shift of the *ortho* cyclooctyl group. Nevertheless, the native CAIX bound **3b** 10-fold more strongly than the mimic-CAIX (Supplementary material Figure S1). The crystal structure could not answer this question with certainty, but the differences in binding affinities between CAIX and CAII were even greater: ΔG_{intr} = −56.7 kJ/mol to CAII, ΔG_{intr} = −67.4 kJ/mol to mimic-CAIX and ΔG_{intr} = −75.0 kJ/mol to CAIX. The mutations introduced in CAII mimicked the active site of CAIX. The binding affinities were more similar to CAIX than CAII, and very similar enthalpy changes between CAIX and mimic-CAIX were observed: ΔH_{intr} = −29.9 kJ/mol to CAIX and ΔH_{intr} = −31.2 kJ/mol to mimic-CAIX).

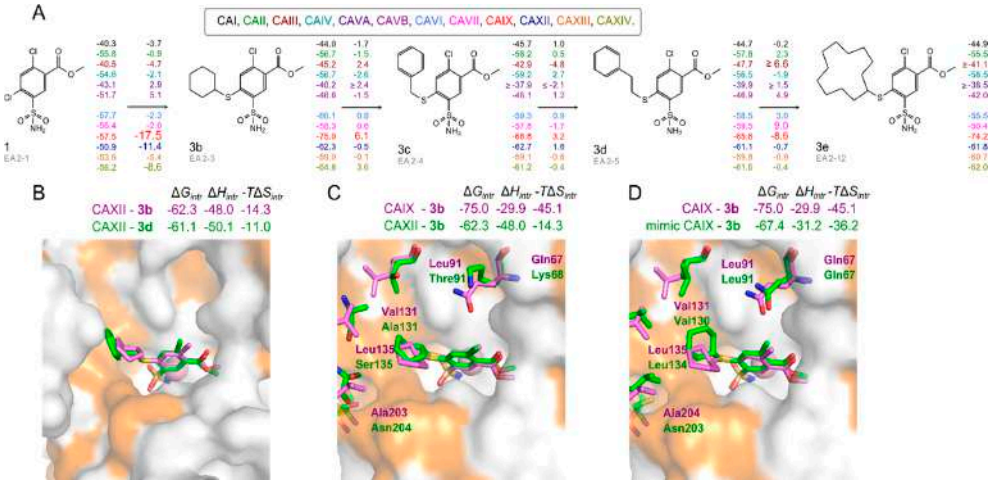

Figure 2. Correlation of compound chemical structures with the changes in standard intrinsic Gibbs energy upon binding and the comparison of the crystal structures between CA isozymes. (**A**) Differences of ΔG_{intr} between neighboring compounds are listed on the connecting arrows. All values have units of kJ/mol. Colors represent CA isozymes. (**B**) Compounds **3b** (magenta, PDB ID: 7PP9) and **3d** (green, PDB ID: 7PUW) bound to CAXII. (**C**) Compound **3b** bound to CAXII (green, PDB ID: 7PP9) and CAIX (magenta, PDB ID: 7POM). (**D**) Compound **3b** bound to CAIX (magenta, PDB ID: 7POM) and mimic-CAIX (green, PDB ID: 7Q0C). Zinc ion is shown as a pink sphere. The notable nonconservative residues between active sites are shown in the "stick" mode. The protein surface of the CA active site is colored orange for hydrophobic residues (V, I, L, F, M, A, G, and P) and gray for the residues with charged and polar side chains (R, D, N, E, Q, H, K, S, T, Y, W, and C).

2.3.2. Methyl 4-Halo-2-Substituted-5-Sulfamoyl-Benzoates Binding CA Isozymes

The compounds that contain *para*- and *ortho*- substituents are similar in the weak binding affinity to CAI, CAIII, and CAVA. The binding of *ortho* **3b**–**f**, **4b**, and *para* **5a**–**f**, **6a**, **9a**–**f**, and **10a** was similar to CAII, CAVI, and CAXIII. The affinity of **5a**–**f** (*para*-sulfanyl) to CAVB was even 10-fold higher than of *ortho*-substituted **3b**–**e**, but no significant differences between *para*-substituted sulfanyl (-S-), **5a**–**f**, **6a**, and sulfonyl (-SO_2-), **9a**–**f**, **10a**, compounds was observed while comparing the intrinsic constants. Thus, only in some cases the oxidation of the sulfanyl group in the *para*- position had an effect on the affinity for several isozymes, namely, CAVII, CAIX, CAXII, and CAXIV (Figure 1B, lower graph). The binding affinity was quite similar for CAII, CAXII, and other isozymes, containing similar amino acids in the active site.

Comparing the influence of chlorine and bromine, the binding affinities to all CA isozymes were practically identical between compounds **5a** and **6a**, **9a** and **10a** (Table 2). The influence of the R substituent could not be clearly compared, but compounds with more hydrophobic substituents were weaker binders, e.g., **5d** and **5f**. This was possibly due to solubility issues that were visually apparent at the highest concentrations used in the experiment. There was a slight trend that the compounds bearing less flexible substituents, **5a** and **5b** or **9a** and **9b**, often had higher affinity than **5c**, **5d**, **5f**, and **9c**, **9d**, **9f**. The greater effect was seen for CAVB going from phenyl to cyclohexyl (**5a** → **5b** −9.7 kJ/mol and **9a** →**9b** −7.4 kJ/mol) in Figure 3A. The affinity similarly decreased in vertical transition for CAIV (**5a** → **9a** 8.4 kJ/mol, **5b** → **9b** 9.8 kJ/mol, **5c** → **9c** 6.5 kJ/mol), CAIX (**5b** → **9b** 1.8 kJ/mol, **5c** → **9c** 2.5 kJ/mol, **5d** → **9d** 1.2 kJ/mol).

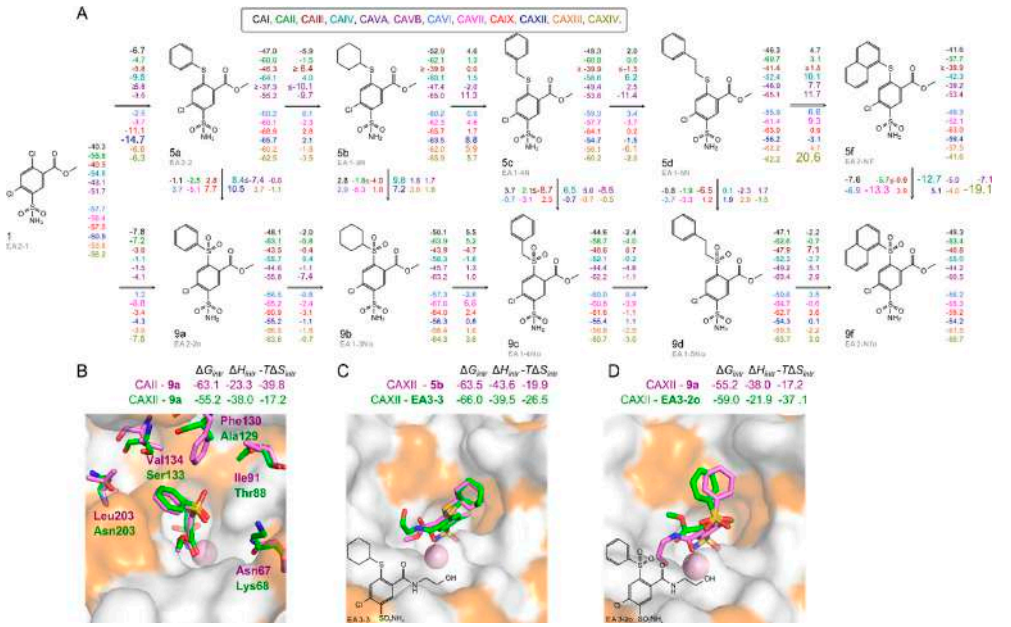

Figure 3. Correlations of compound chemical structures with the changes in the standard intrinsic Gibbs energies of binding and the crystal structures of CAII and CAXII isozymes. (**A**) Differences of ΔG_{intr} (kJ/mol) between neighboring compounds are listed on the connecting arrows. Colors represent CA isozymes. (**B**) Compound **9a** bound to CAII (PDB ID: 7Q0E) and CAXII (PDB ID: 7PUV). Protein side chains and ligands bound to CAII are colored magenta, CAXII green. The notable nonconservative residues between active sites are shown in the "stick" mode. (**C**) Compounds **5b** (magenta, PDB ID: 7PUU) and **EA3-3** (green, previously studied, PDB ID: 6R6Y) in the active site of CAXII. (**D**) Compounds **9a** (green, PDB ID: 7PUV) and **EA3-2o** (magenta, previously described, PDB ID: 6R71) in the active site of CAXII. Zinc ion is shown as a pink sphere. The protein surface of the CA active site is colored orange for hydrophobic residues (V, I, L, F, M, A, G, and P) and gray for the residues with charged and polar side chains (R, D, N, E, Q, H, K, S, T, Y, W, and C).

The X-ray crystal structures showed the energetically best pose of the compound when bound to a CA isozyme. Compound **9a** was found at an identical position in the active sites of CAII and CAXII (Figure 3B). On the other hand, the binding affinity for CAXII differed from CAII by a factor of 26 (K_{d_intr} = 0.020 nM or ΔG_{intr} = −63.1 kJ/mol for CAII vs. K_{d_intr} = 0.51 nM or ΔG_{intr} = −55.2 kJ/mol for CAXII, Table 2 and Figure 3B). The same binding mode of **9a** in CAII and CAXII could be explained by the same interactions between the compound and conservative residues of these active sites. The active site of CAII is more hydrophobic than CAXII (see residues in "stick" mode shown in Figure 3B). For this reason, the binding of this compound to CAII was 26-fold stronger than for CAXII. The interaction of the phenyl group with the hydrophobic side chains was more favorable. The solvation of the ligand during the dissociation process in the presence of a more hydrophobic environment is more difficult. In this case, the stronger interaction was characterized by a lower enthalpy contribution (ΔH_{intr} = −23.3 kJ/mol to CAII, ΔH_{intr} = −38.0 kJ/mol to CAXII, Figure 3B). The structure of **9a** was also determined in the active site of CAI and compared with the positions determined in CAII and CAXII (Figure S4). In this case, the results were somewhat inconclusive because two alternative positions of the compound were found in CAI. One position is partially similar to the positions determined in CAII

and CAXII, and the alternative is rotated (Figure S4). The **9a** is unlikely to occupy a well-defined position and had a weak binding to CAI (ΔG_{intr} = −48.1 kJ/mol). Still, it showed a significant change in the enthalpy of binding (ΔH_{intr} = −39.7 kJ/mol).

We divided the compounds bound to CAXII into pairs according to their similar binding affinity (Figure 3C,D). Compounds **5b** and **EA3-3** in the active site of CAXII were compared in Figure 3C. Compound **EA3-3** was described in our previous study [9] and was named "4b". The **5b** is well defined in the crystal structure (Figure S3D). The binding affinities of the two compounds for CAXII differed by a factor of 2.5, which is insignificant: K_{d_intr} = 0.020 nM, ΔG_{intr} = −63.5 kJ/mol (**5b**) and K_{d_intr} = 0.0080 nM, ΔG_{intr} = −66.0 kJ/mol (**EA3-3**). These compounds differ structurally by *meta*-substituents; **EA3-3** has a longer and more flexible substituent (-$NH(CH_2)_2OH$), but both *meta*- groups were mostly exposed to the solvent, so they did not contribute much to the positioning in the active site. Both compounds are chlorinated at the *ortho*- position of the benzenesulfonamide, and chlorine is known to restrict the position of the ligand in the active site [11,20]. In addition, the *para*-cyclooctyl groups of both compounds occupied the same position. Since the chlorinated compounds had less freedom in the active site, the differences in entropy and enthalpy of the slightly different binding of the *meta*- groups compensated each other: ΔH_{intr} = −43.6 kJ/mol, $-T\Delta S_{intr}$ = −19.9 kJ/mol (**5b**) ΔH_{intr} = −39.5 kJ/mol, $-T\Delta S_{intr}$ = −26.5 kJ/mol (**EA3-3**).

The comparison of **9a** and **EA3-2o** bound to CAXII (described in [9] and named "16a") is shown in Figure 3D. Like the previous pair, these compounds differ only by their *meta*- groups: compound **EA3-2o** contains -$NH(CH_2)_2OH$, while **9a** contains -OCH_3. The positions of both compounds were not similar in CAXII; the *para*-benzene rings had slightly different orientations, and they were directed into the center of the active site cavity. Their orientation was defined by the bulky SO_2 group of the linker, which was in contact with the protein surface. The **EA3-2o** bound to CAXII with 3.4-fold greater affinity than **9a** (K_{d_intr} = 0.12 nM, ΔG_{intr} = −59.0 kJ/mol vs. K_{d_intr} = 0.51 nM ΔG_{intr} = −55.2 kJ/mol). The differences of binding modes between compounds were found in the position of both *meta*- and *para*- groups, but the different terms of the binding reaction mutually compensated each other: ΔH_{intr} = −38.0 kJ/mol, $-T\Delta S_{intr}$ = −17.2 kJ/mol (**9a**) ΔH_{intr} = −21.9 kJ/mol, $-T\Delta S_{intr}$ = −37.1 kJ/mol (**EA3-2o**).

The pairs of compounds bound to the same CA isozyme analyzed in Figures 2D and 3C,D had the following common features: the positions and the binding affinities of the compounds in the pairs were the same or similar. Analogous observations were made previously [21], and such pairs were called "similar" binders. In pairs of "similar" binders, the additional hydrophobic surface did not produce additional interactions with the active site of CA. The possible origin of the entropy–enthalpy compensation was the changes in the solvation–desolvation processes of ligands and the active sites.

Comparison of compound binding to different isozymes when the differences of binding affinities were experimentally significant (Figure 2C,D and Figure 3A) showed some similarities. The compound occupied a similar position in the active site of different isozymes, and the binding of the ligand to a more hydrophobic site was stronger.

2.3.3. Comparison of Methyl Halo 2- and 4-Substituted-5-Sulfamoyl-Benzoates Binding to CA Isozymes

The crystal structures discussed below suggested that the binding interactions between *ortho*- and *para*-sulfanyl/sulfonyl compounds with several CA were quite different. Various *ortho*- and *para*-substituted compounds had different affinities for CA isozymes. Figure 4A compares the affinity of analogous sulfanyl compounds for CA isozymes, and panels B and C compare the positions of these compounds in different crystal structures. The transition from **1** to **3b** and **5b** shows different changes in affinity and selectivity; compound **3b** bound distinctly more strongly to CAIX (−17.5 kJ/mol), CAXII (-11.4 kJ/mol), whereas compound **5b** bound more strongly to CAI (−12.6 kJ/mol), CAVB (−13.3 kJ/mol) and CAXII (−12.6 kJ/mol). The influence of the hydrophobic R substituent in the same group

(transition from left to right (→) has already been discussed above, but in some cases, the transition from *para*- to *ortho*-positions (↑) showed similar trends and was in all cases favorable only for binding to CAIX. However, a change in the position of more flexible substituents (**5c**→**3c**: 2.6 kJ/mol and **5d**→**3d**: 1.6 kJ/mol) had a lower negative effect on the binding affinity to CAI than a rigid cyclohexyl (**5b**→**3b**: 8.9 kJ/mol).

Figure 4B upper part shows 5 superimposed structures: CAXII—**EA3-3** (PDB ID: 6R6Y), CAXII—**EA3-2o** (PDB ID: 6R71), CAXII—**5b** (PDB ID: 7PUU), CAXII—**9a** (PDB ID: 7PUV), CAII—**9a** (PDB ID: 7Q0E); and 4 structures in the lower part: CAXII—**3b** (PDB ID: 7PP9), CAXII—**3d** (PDB ID: 7PUW), CAIX—**3b** (PDB ID: 7POM), mimic CAIX—**3b** (PDB ID: 7Q0C). Therefore, regardless of the compound, all *ortho*-compounds occupied a similar position in CAIX and CAXII, and *para*- occupied another but similar position to each other in CAII and CAXII (Figure 4C,D, respectively). Despite all the differences in the substituents and amino acids in the active sites, the main frame of the compound depicted in the scheme in Figure 4D maintained a similar position. The position of hydrophobic substituents varied, but in the optimal conformation, it was close to the hydrophobic part of the active site. The *meta* substituents were not analyzed in this study, but a comparison with previously published compounds shows that the hydrophilic substituents in these cases did not result in a different binding mode and were flexible. Thus, the hydrophobic effect plays a key role in enabling the compounds to be in the optimal position.

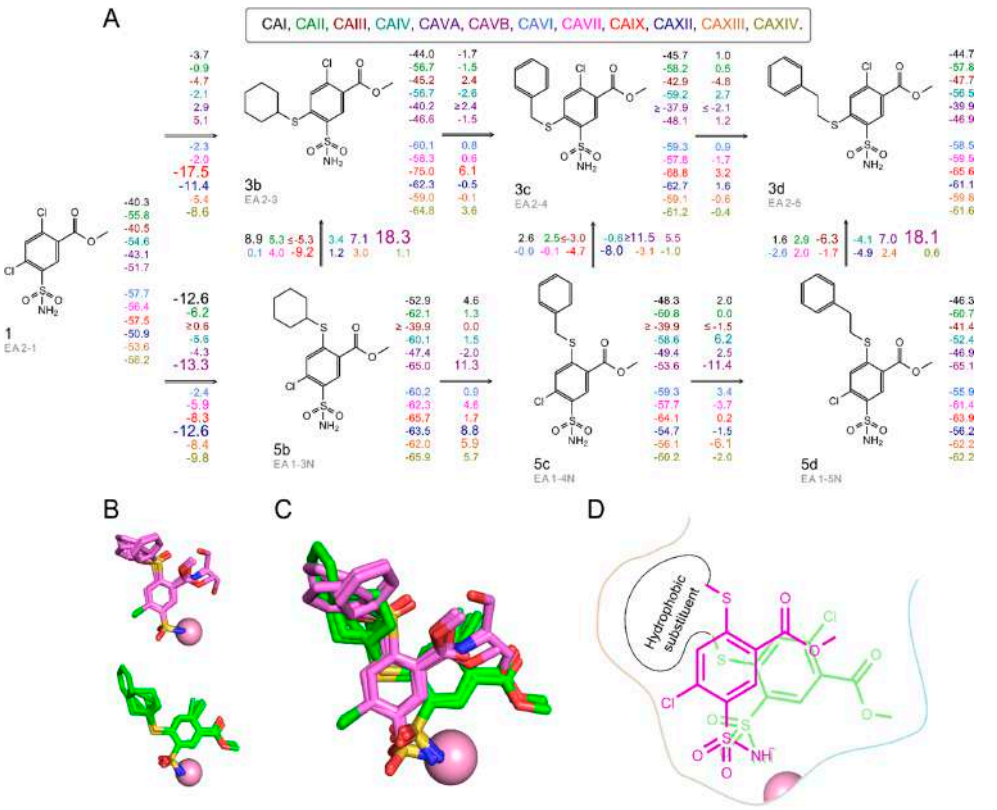

Figure 4. Correlation of compound chemical structures with the changes in standard intrinsic Gibbs energy upon binding and comparison of the crystal structures between CA isozymes. (**A**) Differences of ΔG_{intr} (kJ/mol) between neighboring compounds are listed on the connecting arrows. Colors represent CA isozymes. (**B**) Superimposed ligands of these crystal structures: (upper panel) *para*-substituted ligands are colored magenta: CAXII—**3b** (PDB ID: 7PP9), CAXII—**3d** (PDB ID: 7PUW), CAIX—**3b** (PDB ID: 7POM), mimic-CAIX—**3b** (PDB ID: 7Q0C), (lower panel) *ortho*-substituted ligands are colored green: CAXII—**EA3-3** (PDB ID: 6R6F), CAXII—**EA3-2o** (PDB ID: 6R71), CAXII—**5b** (PDB ID: 7PUU), CAXII—**9a** (PDB ID: 7PUV), CAII—**9a** (PDB ID: 7Q0E). (**C**) The abovementioned superimposed structures are shown for comparison. (**D**) Scheme representing compound position shown in panel C. Orange line represents more hydrophobic side of the active site. Zinc ion is shown as a pink sphere.

3. Conclusions

We have designed a series of compounds and investigated the effect of substituents and their positions in methyl halo 2- and 4-substituted-5-sulfamoyl-benzoate binding to human CA isozymes. The sulfanyl (-S) and sulfonyl (-SO_2-) substituents of different sizes and hydrophobicity were examined in greater detail. We provided a crystallographic position of these two groups of compounds bound in the active sites of CA. Although there were differences in the orientation of the substituents and the thermodynamic parameters, the positions in the same group of compounds remained similar among CA isozymes.

The strongest binding *ortho*-sulfanyl-substituted benzenesulfonamides, especially compounds **3b** and **4b**, showed extremely high femtomolar *intrinsic* affinity (80 fM, cor-

responding to very high, 120 pM *observed* affinity) and selectivity for tumor-associated CAIX. Meanwhile, analogous sulfonyl compounds bound weakly. Other *para*-substituted compounds had completely different binding profiles and bound similarly to several CA isozymes not demonstrating such selectivity.

The crystal structures of the complexes containing compounds bound to CAI, CAII, mimic-CAIX (mutant of CAII$^{A65S, N67Q, I91L, F130V, V134L, L203A}$), CAIX, and CAXII provided a broader understanding of the differences and similarities in the thermodynamic parameters of binding. We observed a tendency that interaction, where there was a higher contribution of the hydrophobic effect and higher entropy contribution, usually also had a higher affinity. This may be explained by the fact that (i) the hydrophobic side chains and bulky hydrophobic substituents of the ligand prevented water molecules from entering the cavity, leading to stronger interaction, and (ii) the water molecules could penetrate between the ligand and the active site cavity through the hydrophilic surface part of the active site. Water molecules in the deeper part of the active site could compete with the compound and cause weaker interaction than in the first case.

4. Materials and Methods

4.1. Organic Synthesis

All starting materials and reagents were commercial products and were used without further purification. Melting points of the compounds were determined in open capillaries on a Thermo Scientific 9100 Series and are uncorrected. ^{1}H and ^{13}C NMR spectra were recorded on a (400 and 100 MHz, respectively) spectrometer in DMSO-d_6 using residual DMSO signals (2.52 ppm and 40.21 ppm for ^{1}H and ^{13}C NMR spectra, respectively) as the internal standard. TLC was performed with silica gel 60 F254 aluminum plates (Merck) and visualized with UV light. Column chromatography was performed using silica gel 60 (0.040–0.063 mm, Merck). High-resolution mass spectra (HRMS) were recorded on a Dual-ESI Q-TOF 6520 mass spectrometer (Agilent Technologies). The purity of final compounds was verified by HPLC to be >95% using the Agilent 1290 Infinity instrument with a Poroshell 120 SB-C18 (2.1 mm × 100 mm, 2.7 µm) reversed-phase column. Analytes were eluted using a linear gradient of water/methanol (20 mM ammonium formate in both phases) from 60:40 to 30:70 over 12 min, then from 30:70 to 20:80 over 1 min, and then 20:80 over 5 min at a flow rate of 0.2 mL/min. UV detection was at 254 nm.

4.2. General Procedure for the Syntheses of **1**, **2**

The appropriate 2,4-dichloro-5-sulfamoylbenzoic acid or 2,4-dibromo-5-sulfamoylbenzoic acid [8] (10.0 mmol) was refluxed in MeOH (100 mL) with concentrated H_2SO_4 (1 mL) for 20 h. The reaction mixture was concentrated under reduced pressure.

*Methyl 2,4-dichloro-5-sulfamoyl-benzoate (***1**, *EA2-1).* Recrystallization was accomplished from MeOH. Yield: 2.70 g, 95%, mp 202 °C. ^{1}H NMR δ ppm: 3.91 (3H, s, CH_3), 7.87 (2H, s, SO_2NH_2), 8.04 (1H, s, C_3-H), 8.40 (1H, s, C_6-H). ^{13}C NMR δ ppm: 53.5, 128.8, 131.7, 134.0, 135.0, 136.8, 140.5, 164.1. HRMS calculated for $C_8H_7Cl_2NO_4S$ [$(M+H)^+$]: 283.9546, found: 283.9546.

*Methyl 2,4-dibromo-5-sulfamoyl-benzoate (***2**, *LJ14-4).* Recrystallization was accomplished from MeOH. Yield: 2.35 g, 63%, mp 201–203 °C. ^{1}H NMR δ ppm: 3.90 (3H, s, CH_3), 7.84 (2H, s, SO_2NH_2), 8.33 (1H, s, C_6-H), 8.35 (1H, s, C_3-H). ^{13}C NMR δ ppm: 53.6, 123.6, 125.2, 131.3, 131.6, 140.2, 142.8, 164.9. HRMS calculated for $C_8H_7Br_2NO_4S$[$(M+H)^+$]: 373.8515 (100%), found: 373.8514 (100%).

4.3. General Procedure for the Syntheses of **3b**, **3e**, *and* **4b**

The mixture of appropriate methyl 2,4-dihalogeno-5-sulfamoylbenzoate (compounds **1**,**2**) (1.00 mmol), DMSO (2 mL), appropriate cyclohexanethiol or cyclododecanethiol (1.10 mmol), and K_2CO_3 (553 mg, 4.00 mmol) was heated at 60 °C temperature for 4–6 h. The mixture was cooled to room temperature, and brine was added. The product was

extracted with EtOAc (3 × 7 mL). The organic layer was washed with H_2O, dried over anhydrous $MgSO_4$, filtered, and concentrated.

*Methyl 2-chloro-4-(cyclohexylsulfanyl)-5-sulfamoylbenzoate (***3b**, *EA2-3).* The product was purified by chromatography on a column of silica gel with $CHCl_3$:EtOAc (10:1), R_f = 0.40. Yield: 131 mg, 36%, mp 112–114 °C. ^{1}H NMR δ ppm: 1.21–1.31 (1H, m, Cy-H), 1.38–1.50 (4H, m, Cy-H), 1.60–1.63 (1H, m, Cy-H), 1.70–1.77 (2H, m, Cy-H), 1.93–2.01 (2H, m, Cy-H), 3.71–3.77 (1H, m, Cy-H), 3.88 (3H, s, CH_3), 7.56 (2H, s, SO_2NH_2), 7,71 (1H, s, C_3-H), 8.33 (1H, s, C_6-H).^{13}C NMR δ ppm: 25.6, 25.7, 32.4, 44.3, 53.2, 125.1, 130.3, 131.5, 136.4, 140.2, 142.9, 164.4. HRMS calculated. for $C_{14}H_{18}ClNO_4S_2$[(M+H)$^+$]: 364.0439, found: 364.0440.

*Methyl 2-chloro-4-(cyclododecylsulfanyl)-5-sulfamoylbenzoate (***3e**, *EA2-12).* The product was purified by chromatography on a column of silica gel with $CHCl_3$:EtOAc (5:1), R_f = 0.65, then recrystallization was accomplished from toluene:EtOAc (8:1). Yield: 210 mg, 47%, mp 185–187 °C. ^{1}H NMR δ ppm: 1.25–1.64 (20H, m, cyclododecyl-H), 1.71–1.83 (2H, m, cyclododecyl-H), 3.71–3.79 (1H, m, cyclododecyl-H), 3.88 (3H, s, CH_3), 7.56 (2H, s, SO_2NH_2), 7.67 (1H, s, C_3-H), 8.33 (1H, s, C_6-H). ^{13}C NMR δ ppm: 22.1, 23.3, 23.4, 23.8, 24.1, 29.2, 43.2, 53.2, 124.9, 130.3, 131.4, 136.3, 140.3, 143.5, 164.4. HRMS calculated for $C_{20}H_{30}ClNO_4S_2$[(M+H)$^+$]: 448.1378, found: 448.1370.

*Methyl 2-bromo-4-(cyclohexylsulfanyl)-5-sulfamoylbenzoate (***4b**, *LJ15-12).* The product was purified by chromatography on a column of silica gel with $CHCl_3$:EtOAc (15:1), R_f = 0.29. Yield: 180 mg, 44%, mp123–125 °C. ^{1}H NMR δ ppm: 1.24–1.31 (1H, m, Cy-H), 1.38–1.50 (4H, m, Cy-H), 1.60–1.63 (1H, m, Cy-H), 1.70–1.75 (2H, m, Cy-H), 1.95–1.97 (2H, m, Cy-H), 3.72–3.77 (1H, m, Cy-H), 3.88 (3H, s, CH_3), 7.54 (2H, s, SO_2NH_2), 7.85 (1H, s, C_6-H), 8.27 (1H, s, C_3-H). ^{13}C NMR δ ppm: 25.6, 25.7, 32.4, 44.5, 53.2, 125.1, 127.5, 131.0, 133.6, 140.1, 142.5, 165.0. HRMS calculated for $C_{14}H_{18}BrNO_4S_2$[(M+H)$^+$]: 409.9913 (100%), found: 409.9915 (100%).

4.4. General Procedure for the Syntheses of **3c** *and* **3d**

The mixture of methyl 2,4-dichloro-5-sulfamoylbenzoate (**1**) (284 mg, 1.00 mmol), DMSO (2 mL), appropriate phenylmethanethiol or 2-phenylethanethiol (1.10 mmol), and TEA (121 mg, 1.20 mmol) was heated at 50 °C temperature for 6–12 h. The progress of the reaction was monitored by TLC. The mixture was cooled to room temperature, and brine was added. The product was extracted with EtOAc (3 × 7 mL). The organic layer was washed with H_2O, dried over anhydrous $MgSO_4$, filtered, and concentrated.

*Methyl 4-(benzylsulfanyl)-2-chloro-5-sulfamoylbenzoate (***3c**, *EA2-4).* The product was purified by chromatography on a column of silica gel with $CHCl_3$:EtOAc (4:1), R_f = 0.48. Yield: 119 mg, 32%, mp 125–126 °C. ^{1}H NMR δ ppm: 3.87 (3H, s, CH_3), 4.50 (2H, s, CH_2), 7.29 (1H, t, *J* = 7.2 Hz, Ph-H), 7.36 (2H, t, *J* = 7.2 Hz, Ph-H), 7.51 (2H, d, *J* = 7.2 Hz, Ph-H), 7.64 (2H, s, SO_2NH_2), 7.69 (1H, s, C_3-H), 8.31 (1H, s, C_6-H). ^{13}C NMR δ ppm: 36.3, 53.2, 124.9, 128.0, 129.1, 129.2, 129.8, 131.3, 135.8, 136.4, 139.1, 143.7, 164.3. HRMS calculated for $C_{15}H_{14}ClNO_4S_2$ [(M+H)$^+$]: 372.0126, found: 372.0125.

*Methyl 2-chloro-4-[(2-phenylethyl)sulfanyl]-5-sulfamoylbenzoate (***3d**, *EA2-5).* The product was purified by chromatography on a column of silica gel with $CHCl_3$:EtOAc (5:1), R_f = 0.67. Yield: 97 mg, 25%, mp 111–112 °C. ^{1}H NMR δ ppm: 2.97 (2H, t, *J* = 7.6 Hz, $\underline{CH_2}$Ph), 3.46 (2H, t, *J* = 7.6 Hz, CH_2S), 3.88 (3H, s, CH_3), 7.23 (1H, m, Ph-H), 7.29–7.33 (4H, m, Ph-H), 7.59 (2H, s, SO_2NH_2), 7.65 (1H, s, C_3-H), 8.31 (1H, s, C_6-H). ^{13}C NMR δ ppm: 33.3, 34.1, 53.2, 124.8, 126.9, 128.9, 129.1, 129.2, 131.2, 136.5, 139.4, 140.0, 143.9, 164.4. HRMS calculated for $C_{16}H_{16}ClNO_4S_2$ [(M+H)$^+$]: 386.0282, found: 386.0282.

4.5. General Procedure for the Syntheses of **5a**, **5f**, *and* **6a**

The mixture of appropriate 2,4-dihalogeno-5-sulfamoylbenzoate (compounds **1**,**2**) (1.00 mmol), MeOH (5 mL), thiophenol or 1-thionaphthol (1.10 mmol,) and TEA (121 mg, 1.20 mmol) was refluxed for 2–6 h. MeOH was evaporated under reduced pressure, and the resultant precipitate was washed with H_2O.

*Methyl 4-chloro-2-(phenylsulfanyl)-5-sulfamoylbenzoate (***5a**, *EA2-2).* The product was purified by chromatography on a column of silica gel with $CHCl_3$:EtOAc (10:1), R_f = 0.32. Yield: 161 mg, 45%, mp 223–226 °C. ^{1}H NMR δ ppm: 3.94 (3H, s, CH_3), 6.68 (1H, s, C_3-H), 7.62–7.67 (5H, m, Ph-H), 7.74 (2H, s, SO_2NH_2), 8.50 (1H, s, C_6-H). ^{13}C NMR δ ppm: 53.3, 124.3, 128.7, 130.1, 131.2 (2C), 131.8, 135.2, 136.2, 137.5, 149.6, 164.8. HRMS calculated for $C_{14}H_{12}ClNO_4S_2$ [(M+H)$^+$]: 357.9969, found: 357.9970.

*Methyl 4-chloro-2-(1-naphthylsulfanyl)-5-sulfamoyl-benzoate (***5f**, *EA2-NF).* The product was purified by chromatography on a column of silica gel with $CHCl_3$:EtOAc (5:1), R_f = 0.77. Yield: 265 mg, 65%, mp 235–237 °C. ^{1}H NMR δ ppm: 3.99 (3H, s, CH_3), 6.34 (1H, s, C_3-H), 7.61–7.68 (2H, m, Naph-H), 7.70 (2H, s, SO_2NH_2), 7.71–7.74 (1H, m, Naph-H), 8.04 (1H, dd, *J* =7.2 Hz, *J* =1.2 Hz, Naph-H), 8.08–8.15 (2H, m, Naph-H), 8.26 (1H, d, *J* = 8.4 Hz, Naph-H), 8.54 (1H, s, C_6-H). ^{13}C NMR δ ppm: 53.4, 124.3, 125.0, 126.7, 127.2, 127.6, 128.5, 128.8, 129.8, 132.0, 132.6, 133.8, 134.6, 135.1, 136.9, 137.5, 148.9, 164.9. HRMS calculated for $C_{18}H_{14}ClNO_4S_2$ [(M+H)$^+$]: 408.0126, found: 408.0131.

*Methyl 4-bromo-2-(phenylsulfanyl)-5-sulfamoylbenzoate (***6a**, *LJ15-11).* The product was purified by chromatography on a column of silica gel with $CHCl_3$:EtOAc (15:1), R_f = 0.20, then recrystallization was accomplished from toluene. Yield: 145 mg, 36%, mp 202–204 °C. ^{1}H NMR δ ppm: 3.93 (3H, s, CH_3), 6.89 (1H, s, C_3-H), 7.58–7,63 (5H, m, Ph-H), 7.71 (2H, s, SO_2NH_2), 8.52 (1H, s, C_6-H). ^{13}C NMR δ ppm: 53.3, 124.3, 124.8, 130.2, 131.1(2C), 131.7, 132.3, 136.1, 139.3, 149.2, 165.0. HRMS calculated for $C_{14}H_{12}BrNO_4S_2$[(M+H)$^+$]: 403.9443 (100%), found: 403.9437 (100%).

4.6. General Procedure for the Syntheses of **7b**–**d**, **8b**, **9a**–**d**, **9f**, **10a**

The 30% H_2O_2(aq) (1.50 mmol, 0.148 mL) was added to a solution of appropriate benzenesulfonamide (compounds **3b**–**d**,**4b**,**5a**–**d**,**f**,**6a**) (0.500 mmol) in AcOH (1.7 mL) at 70 °C and allowed stirring for 2–3h. The solvent was removed under reduced pressure, and the resultant precipitate was washed with H_2O.

*Methyl 2-chloro-4-cyclohexylsulfonyl-5-sulfamoylbenzoate (***7b**, *EA2-3o).* Yield: 164 mg, 83%, mp 184–187 °C. ^{1}H NMR δ ppm: 1.14–1.21 (3H, m, Cy-H), 1.42–1.50 (2H, m, Cy-H), 1.63 (1H, br s, Cy-H), 1.81–1.87 (4H, m, Cy-H), 3.89–3.92 (1H, m, Cy-H), 3.96 (3H, s, CH_3), 7.48 (2H, s, SO_2NH_2), 8.11 (1H, s, C_3-H), 8.57 (1H, s, C_6-H). ^{13}C NMR δ ppm: 24.9 (2C), 25.1, 53.9, 62.2, 133.3, 135.1, 135.5, 136.7, 138.6, 142.1, 163.9. HRMS calculated for $C_{14}H_{18}ClNO_6S_2$ [(M+H)$^+$]: 396.0337, found: 396.0336.

*Methyl 4-benzylsulfonyl-2-chloro-5-sulfamoylbenzoate (***7c**, *EA2-4o).* Recrystallization was accomplished from MeOH. Yield: 123 mg, 61%, mp 154–156 °C. ^{1}H NMR δ ppm: 3.95 (3H, s, CH_3), 5.04 (2H, s, CH_2), 7.24–7.26 (2H, m, Ph-H), 7.33–7.40 (3H, m, Ph-H), 7.58 (2H, s, SO_2NH_2), 7.77 (1H, s, C_3-H), 8.57 (1H, s, C_6-H).^{13}C NMR δ ppm: 53.9, 60.9, 127.5, 129.1, 129.5, 131.7, 132.9, 135.0, 135.4, 136.3, 139.2, 142.0, 163.8. HRMS calculated for $C_{15}H_{14}ClNO_6S_2$ [(M+H)$^+$]: 404.0024, found: 404.0023.

*Methyl 2-chloro-4-(2-phenylethylsulfonyl)-5-sulfamoylbenzoate (***7d**, *EA2-5o).* Recrystallization was accomplished from MeOH. Yield: 161 mg, 77%, mp 132–134 °C. ^{1}H NMR δ ppm: 3.03 (2H, t, *J* = 7.8 Hz, CH_2), 3.95 (3H, s, CH_3), 4.08 (2H, t, *J* = 7.8 Hz, CH_2), 7.13–7.27 (5H, m, Ph-H), 7.50 (2H, s, SO_2NH_2), 8.07 (1H, s, C_3-H), 8.49 (1H, s, C_6-H). ^{13}C NMR δ ppm: 28.0, 53.9, 55.8, 127.1, 128.9(2C), 132.8, 135.0, 135.3, 136.7, 137.7, 140.0, 141.6, 163.9. HRMS calculated for $C_{16}H_{16}ClNO_6S_2$ [(M+H)$^+$]: 418.0180, found: 418.0175.

*Methyl 2-bromo-4-cyclohexylsulfonyl-5-sulfamoylbenzoate (***8b**, *LJ15-12o).* Yield: 172 mg, 78%, mp 217–219 °C. ^{1}H NMR δ ppm: 1.16–1.24 (3H, m, Cy-H), 1.42–1.50 (2H, m, Cy-H), 1.57–1.63 (1H, m, Cy-H), 1.79–1.86 (4H, m, Cy-H), 3.89–3.92 (1H, m, Cy-H), 3.95 (3H, s, CH_3), 7.47 (2H, s, SO_2NH_2), 8.25 (1H, s, C_3-H), 8.50 (1H, s, C_6-H). ^{13}C NMR δ ppm: 24.9(2C), 25.1, 53.9, 62.2, 125.3, 132.8, 137.7, 138.1, 138.4, 142.6, 164.6. HRMS calculated for $C_{14}H_{18}BrNO_6S_2$[(M+H)$^+$]: 441.9811 (100%), found: 441.9806 (100%).

*Methyl 2-(benzenesulfonyl)-4-chloro-5-sulfamoylbenzoate (***9a**, *EA2-2No).* The product was purified by chromatography on a column of silica gel with $CHCl_3$:EtOAc (4:1), R_f = 0.33. Yield: 158 mg, 81%, mp 166–168 °C. ^{1}H NMR δ ppm: 3.86 (3H, s, CH_3), 7.68 (2H, t, *J* = 7.6 Hz,

Ph-H), 7.78 (1H, t, *J* = 7.6 Hz, Ph-H), 8.03 (2H, s, SO_2NH_2), 8.07 (2H, d, *J* = 7.6 Hz, Ph-H), 8.23 (1H, s, C_3-H), 8.51 (1H, s, C_6-H). ^{13}C NMR δ ppm: 53.8, 128.5, 130.1, 130.3, 131.7, 133.5, 134.2, 134.9, 140.0, 142.3, 146.0, 165.7. HRMS calculated for $C_{14}H_{12}ClNO_6S_2$ [$(M+H)^+$]: 389.9867, found: 389.9869.

*Methyl 4-chloro-2-cyclohexylsulfonyl-5-sulfamoyl-benzoate (***9b**, *EA1-3No).* Yield: 150 mg, 76%, mp 181–183 °C. ^{1}H NMR δ ppm: 1.18–1.30 (3H, m, Cy-H), 1.41–1.50 (2H, m, Cy-H), 1.62–1.66 (1H, m, Cy-H), 1.80–1.91 (4H, m, Cy-H), 3.64–3.70 (1H, m, Cy-H), 3.90 (3H, s, CH_3), 8.06 (2H, s, SO_2NH_2), 8.12 (1H, s, C_3-H), 8.30 (1H, s, C_6-H). ^{13}C NMR δ ppm: 24.8, 25.0, 25.1, 54.0, 62.9, 130.5, 132.6, 133.8, 134.1, 140.1, 145.9, 165.9. HRMS calculated for $C_{14}H_{18}ClNO_6S_2$ [$(M+H)^+$]: 396.0337, found: 396.0341.

*Methyl 2-benzylsulfonyl-4-chloro-5-sulfamoylbenzoate (***9c**, *EA1-4No).* Yield: 162 mg, 80%, mp 224–225 °C. ^{1}H NMR δ ppm: 3.97 (3H, s, CH_3), 4.97 (2H, s, CH_2), 7.27–7.30 (2H, m, Ph-H), 7.37–7.42 (3H, m, Ph-H), 7.79 (1H, s, C_3-H), 8.07 (2H, s, SO_2NH_2), 8.31 (1H, s, C_6-H). ^{13}C NMR δ ppm: 54.2, 61.7, 127.7, 129.1, 129.4, 130.4, 131.7, 132.1, 133.6, 133.9, 140.9, 145.9, 166.0. HRMS calculated for $C_{15}H_{14}ClNO_6S_2$ [$(M+H)^+$]: 404.0024, found: 404.0018.

*Methyl 4-chloro-2-(2-phenylethylsulfonyl)-5-sulfamoylbenzoate (***9d**, *EA1-5o).* Recrystallization was accomplished from MeOH. Yield: 142 mg, 68%, mp 156–158 °C. ^{1}H NMR δ ppm: 3.06 (2H, t, *J* = 7.6 Hz, CH_2), 3.91 (3H, s, CH_3), 4.00 (2H, t, *J* = 8.0 Hz, CH_2), 7.16–7.20 (1H, m, Ph-H) 7.21–7.27 (4H, m, Ph-H), 8.03 (1H, s, C_3-H), 8.04 (2H, s, SO_2NH_2), 8.26 (1H, s, C_6-H). ^{13}C NMR δ ppm: 28.2, 54.1, 56.5, 127.2, 128.89, 128.92, 130.3, 131.8, 133.8, 133.9, 137.8, 141.5, 145.8, 165.9. HRMS calculated for $C_{16}H_{16}ClNO_6S_2$ [$(M+H)^+$]: 418.0180, found: 418.0178.

*Methyl 4-chloro-2-(1-naphthylsulfonyl)-5-sulfamoylbenzoate (***9f**, *EA2-NFo).* Yield: 180 mg, 82%, mp 244–245 °C. ^{1}H NMR δ ppm: 3.72 (3H, s, CH_3), 7.66–7.75 (2H, m, Naph-H), 7.81 (1H, t, *J* = 7.6 Hz, Naph-H), 8.00 (2H, s, SO_2NH_2), 8.17 (1H, d, *J* = 8.0 Hz, Naph-H), 8.23 (1H, s, C_3-H), 8.35 (1H, s, C_6-H), 8.36 (2H, t, *J* = 8.0 Hz, Naph-H), 8.41 (1H, d, *J* = 8.4 Hz, Naph-H).^{13}C NMR δ ppm: 53.8, 123.5, 125.2, 127.7, 127.8, 129.5, 130.1, 130.6, 131.5, 131.6, 132.4, 133.9, 134.0, 134.2, 136.4, 142.4, 145.8, 165.4. HRMS calculated for $C_{18}H_{14}ClNO_6S_2$ [$(M+H)^+$]: 440.0024,found: 440.0020.

*Methyl 2-(benzenesulfonyl)-4-bromo-5-sulfamoylbenzoate (***10a**, *LJ15-11o).* Yield: 189 mg, 87%, mp 191–193 °C. ^{1}H NMR δ ppm: 3.86 (3H, s, CH_3), 7.67-7.79 (3H, m, Ph-H), 7.98 (2H, s, SO_2NH_2), 8.04–8.07 (2H, m, Ph-H), 8.22 (1H, s, C_6-H), 8.62 (1H, s, C_3-H). ^{13}C NMR δ ppm: 53.8, 122.7, 128.5, 130.1, 130.2, 132.2, 134.9, 136.7, 140.0, 141.9, 147.8, 165.8. HRMS calculated for $C_{14}H_{12}BrNO_6S_2$[$(M+H)^+$]: 435.9342 (100%), found: 435.9345 (100%).

4.7. General Procedure for the Syntheses of **12a**–**d**,**f**

The mixture of methyl 2,4-dichloro-5-sulfamoylbenzamide (**11**) [8] (269 mg, 1.00 mmol), DMSO (1.5 mL), appropriate thiol(1.10 mmol), and TEA (121 mg, 1.20 mmol) was heated at 60 °C temperature for 12 h. The mixture was cooled to room temperature, and brine (15 mL) was added. The product was extracted with EtOAc (3 × 15 mL). The organic layer was washed with H_2O, dried over anhydrous $MgSO_4$, filtered, and concentrated.

*4-chloro-2-(1-naphthylsulfanyl)-5-sulfamoylbenzamide (***12f**, *EA1A-NF).* The product was crystallized from toluene:MeOH (7:1).Yield: 277 mg, 70%, mp 277–280 °C.^{1}H NMR δ ppm: 6.38 (1H, s, C_3-H), 7.59 (2H, s, SO_2NH_2), 7.61–7.66 (2H, m, Naph-H), 7.67–7.71(1H, m, Naph-H), 7.85 (1H, s, $CONH_2$), 8.00 (1H, dd, *J* = 7.2 Hz, *J* =1.2 Hz, Naph-H), 8.10 (1H, s, C_6-H), 8.10–8.14 (2H, m, Naph-H), 8.21 (1H, d, *J* = 8.4 Hz, Naph-H), 8.34 (1H, s, $CONH_2$). ^{13}C NMR δ ppm: 125.2, 127.0, 127.5, 127.7, 128.5 128.6, 128.9, 129.7, 131.1, 132.1, 132.3, 133.7, 134.6, 135.0, 136.6, 137.5, 168.0. HRMS calculated for $C_{17}H_{13}ClN_2O_3S_2$ [$(M+H)^+$]: 393.0129, found: 393.0133.

*4-chloro-2-phenylsulfanyl-5-sulfamoylbenzamide (***12a**, *EA1A-2)* [9].

*4-chloro-2-cyclohexylsulfanyl-5-sulfamoylbenzamide (***12b**, *EA1A-3)* [9].

*2-benzylsulfanyl-4-chloro-5-sulfamoylbenzamide (***12c**, *EA1A-4)* [9].

*4-chloro-2-(2-phenylethylsulfanyl)-5-sulfamoylbenzamide (***12d**, *EA1A-5)* [9].

4.8. General Procedure for the Syntheses of **5a**–**d**,**f**

The mixture of appropriate 2-substituted 4-chloro-5-sulfamoylbenzamide (compounds **12a–d,f**) (0.500 mmol), methanol (5 mL), and thionyl chloride (0.200 mL, 2.76 mmol) was heated at 50 °C temperature for 48–96 h. The progress of the reaction was monitored by TLC. The mixture was concentrated under reduced pressure.

Methyl 4-chloro-2-phenylsulfanyl-5-sulfamoylbenzoate (**5a**, *EA2-2).* The product was recrystallized from H_2O. Yield: 122 mg, 68%, mp 223-226 °C.

Methyl 4-chloro-2-cyclohexylsulfanyl-5-sulfamoylbenzoate (**5b**, *EA1-3N).* The product was recrystallized from H_2O. Yield: 120 mg, 66%, mp 150–151 °C. ^{1}H NMR δ ppm: 1.20–1.51 (5H, m, Cy-H), 1.58–1.66 (1H, m, Cy-H), 1.69–1.77 (2H, m, Cy-H), 1.93–2.02 (2H, m, Cy-H), 3.60–3.69 (1H, m, Cy-H), 3.86 (3H, s, CH_3), 7,65 (1H, s, C_3-H), 7.71 (2H, s, SO_2NH_2), 8.39 (1H, s, C_6-H). ^{13}C NMR δ ppm: 25.6, 25.7, 32.5, 42.9, 53.1, 126.3, 129.0, 131.6, 135.0, 136.9, 146.9, 165.0. HRMS calculated for $C_{14}H_{18}ClNO_4S_2$[(M+H)$^+$]: 364.0439, found: 364.0444.

Methyl 2-benzylsulfanyl-4-chloro-5-sulfamoylbenzoate (**5c**, *EA1-4N).* The product was recrystallized from H_2O. Yield: 145 mg, 78%, mp 211–212 °C. ^{1}H NMR δ ppm: 3.86 (3H, s, CH_3), 4.42 (2H, s, CH_2), 7.30 (1H, t, *J* = 7.2 Hz, Ph-H), 7.37 (2H, t, *J* = 7.2 Hz, Ph-H), 7.47 (2H, d, *J* = 6.8 Hz, Ph-H) 7.70 (1H, s, C_3-H), 7.73 (2H, s, SO_2NH_2), 8.44 (1H, s, C_6-H). ^{13}C NMR δ ppm: 36.0, 53.1, 124.7, 128.0, 128.5, 129.1, 129.7, 131.6, 135.2, 136.0, 136.8, 148.4, 164.9. HRMS calculated for $C_{15}H_{14}ClNO_4S_2$ [(M+H)$^+$]: 372.0126, found: 372.0129.

Methyl 4-chloro-2-(2-phenylethylsulfanyl)-5-sulfamoylbenzoate (**5d**, *EA1-5N).* The product was recrystallized from H_2O:acetone (3:1). Yield: 166 mg, 85%, mp 135–137 °C. ^{1}H NMR δ ppm: 2.96 (2H, t, *J* = 7.6 Hz, $\underline{CH_2}$Ph), 3.39 (2H, t, *J* = 7.6 Hz, CH_2S), 3.87 (3H, s, CH_3), 7.24 (1H, m, Ph-H), 7.29–7.33 (4H, m, Ph-H), 7.63 (1H, s, C_3-H), 7.73 (2H, s, SO_2NH_2), 8.44 (1H, s, C_6-H). ^{13}C NMR δ ppm: 33.7, 33.8, 53.1, 125.1, 126.9, 128.3, 128.9, 129.0, 131.6, 135.3, 136.7, 140.1, 148.5, 164.9. HRMS calculated for $C_{16}H_{16}ClNO_4S_2$ [(M+H)$^+$]: 386.0282, found: 386.0286.

Methyl 4-chloro-2-(1-naphthylsulfanyl)-5-sulfamoylbenzoate (**5f**, *EA2-NF).* The product was recrystallized from H_2O:MeOH (4:1). Yield: 143 mg, 70%, mp 235–237 °C.

4.9. Protein Preparation

Recombinant human carbonic anhydrases (CAs) were expressed in *E. coli* (CAI, CAII, mutant CAII$^{A65S, N67Q, I91L, F130V, V134L, L203A}$, CAIII, CAIV, CAVA, CAVB, CAVII, CAXII, CAXIII, CAXIV), yeast (CAIX used to obtain only PDB ID: 7POM crystal structure) or mammalian cells (CAVI and CAIX used for all remaining experiments). Proteins were chromatographically purified following published protocols: CAI [22], CAII [23], CAII$^{A65S, N67Q, I91L, F130V, V134L, L203A}$ (mimic-CAIX), CAIII, CAIV, CAVA, CAVB, CAVI, CAIX (except CAIX (PDB ID: 7POM) crystal was obtained using yeast-expressed protein [24], and [17], CAVII, CAXIII- [25], CAXII [26]. The protein stock solutions were stored at −80 °C. The protein concentration was determined by UV absorption at 280 nm using Beer-Lambert law and extinction coefficient determined by amino acid analysis. Proteins used for crystallization were additionally purified by affinity chromatography and concentrated.

4.10. Determination of Binding Parameters

4.10.1. Fluorescent Thermal Shift Assay (FTSA)

Observed affinities (dissociation constant, $K_{d,obs}$, proportional to the change in standard Gibbs energy upon binding, $\Delta G = RT\ln K_d$) of the compounds binding to CAs were determined by the fluorescent thermal shift assay [27,28], using a QIAGEN's real-time PCR cycler the "Rotor-Gene Q" and Rotor-Gene® Style 4-strip tubes from STARLAB. Ligands were dissolved in DMSO stock solutions to concentrations of 10 mM or 20 mM and used for the serial dilution in DMSO of the dilution factor 2. These samples were diluted with buffer solution and mixed with a prepared protein solution, consisting of protein stock, buffer solution, and 8-anilino-1-naphthalene sulfonate (ANS; solvatochromic dye). All final samples typically contained up to 10 μM CA, compound solutions of serial dilution from 0 μM to 200 μM at 8 different concentrations differing by two times, 50 μM ANS,

50 mM sodium phosphate buffer at pH 7.0, 100 mM sodium chloride, and 2.0% (*v/v*) DMSO. Samples preparation is explained in detail in [28]. Protein denaturation was monitored by determining the fluorescence of ANS as a function of temperature[29]. The excitation and emission wavelengths of ANS are 365 ± 20 and 460 ± 15 nm. Samples were heated from 25 °C to 99 °C at the rate of 1 °C/min. The curve-fitting procedure has been explained previously [30] and was performed at 37 °C.

The dissociation constants of each compound with all 12 catalytically active human CAs are listed in Table 2, and some experimental data are provided in Supplementary material in Figures S1 and S2.

4.10.2. Isothermal Titration Calorimetry (ITC)

Additionally, a selected set of compounds binding to CAs were tested by ITC [31,32] to determine changes in binding enthalpies. ITC experiments were carried out using a MicroCal PEAQ-ITC calorimeter (Northampton, MA, USA). The protein solution in the cell contained a constant concentration of CA (10–20 μM), while the concentration of compound loaded in the ITC syringe was ten times higher than the protein concentration (100–200 μM). Both cell and syringe solutions were diluted in the buffer: 50 mM sodium phosphate at pH 7.0 and containing 100 mM sodium chloride and 2.0 % (*v/v*) of DMSO. Samples were centrifuged prior to the experiment to improve quality. A typical experiment consisted of 19 injections with 150 s spacing between injections; the volume of the first injection was 0.4 μL (duration 0.8s) and 2.0 μL (duration 4.0 s) for the remaining injections. All experiments were performed at 37 °C with reference power 4.0 μcal/s.

The enthalpy changes of binding are listed in Table S8, and experimental data are provided in Supplementary material in Figure S6. A comparison of the affinity determined by FTSA and ITC is shown in Supplementary material in Figure S9. ITC shows weaker affinity than FTSA for strong interactions. Thus, the affinity determined by the FTSA was used due to the ITC detection limit as the more reliable.

4.10.3. Calculation of Intrinsic Binding Parameters

All experiments allow the determination of the *observed* binding parameters of the sulfonamide binding to CA. However, the change in standard Gibbs energy (or dissociation constant), enthalpy, and entropy upon binding depend on buffer and pH because sulfonamide binding to CAs is linked to several reactions: (i) Zn^{2+}-bound hydroxide ion protonate into water molecule in the active site of CA; (ii) Sulfonamide amino group ($R\text{-}SO_2NH_2$) deprotonate ($R\text{-}SO_2NH^-$); (iii) Buffer molecule protonate or deprotonate depending on the protons' balance; (iv) After these reactions, the negatively charged sulfonamide ($R\text{-}SO_2NH^-$) replaces the Zn^{2+}-bound water molecule in the active site of CA and binds to the protein in its position [15]. The sum of these reactions is the *observed* binding. However, only the fourth reaction represents the actual binding reaction, called *intrinsic* [16]. Observed binding parameters are important to obtain the compound's affinity under certain conditions, for example, in the human body. Nevertheless, these parameters are less important in the drug design to estimate the energy for the binding affinity of each substituent. However, the contribution of protonation reactions can be subtracted. Equations of intrinsic dissociation constant (K_{d_intr}) or standard Gibbs energy (ΔG_{intr}) and enthalpy change (ΔH_{intr}) are listed in Table 2 and Table S7 in Supplementary materials.

4.11. Determination of Protonation Parameters

4.11.1. Determination of pK_a Values

The pK_a values of water molecules bound to Zn^{2+} in the active site of CAs, p$K_{a_CAZn(II)H2O}$, were taken from [33] and of compounds, p$K_{a_RSO2NH2}$, were determined as described in [34]. Figure 2D shows the intrinsic parameters of the binding of mimic-CAIX (mutant $CAII^{A65S, N67Q, I91L, F130V, V134L, L203A}$) and compound **3b**, which were calculated using the p$K_{a_CAZn(II)H2O}$ of CAII.

We used a constant concentration of sulfonamide (25–400 μM) and 2.0% (*v*/*v*) of DMSO in universal buffer (50 mM sodium acetate, 25 mM sodium borate, and 50 mM sodium phosphate) at different pH values (in the range from pH 6 to 12 at every half pH unit). UV–VIS spectra of compound solution were recorded at 37 °C using the spectrophotometer "Agilent 89090A". To determine $pK_{a\_RSO2NH2}$, a plot of the normalized ratio of two absorbancies (approximately 10 nm above and 10 nm below the isosbestic point) vs. buffer pH and fitted Henderson–Hasselbach curve using the least-square method. The midpoint of this fitted curve is equal to $pK_{a\_RSO2NH2}$. Experimental data are provided in Supplementary material in Figure S5 and Table 2.

4.11.2. Determination of Protonation Enthalpy

The enthalpy changes of sulfonamide amino group (RSO_2NH_2) protonation, $\Delta_{p\_RSO2NH2}H$, were determined by titration of 0.25 mM sulfonamide and 0.375 mM sodium hydroxide with 2.75 mM nitric acid using a MicroCal PEAQ-ITC calorimeter (Northampton, MA, USA). DMSO concentrations in the syringe and the sample cell were 2% (*v*/*v*). Experimental parameters: total number of injections was 40, the volume of each injection was 0.9 μL, spacing between injections was 120 s, the temperature was 37 °C. $\Delta_{p\_CAZn(II)H2O}H$ values of the water molecule in the active site CAs were taken from [33]. Figure 2D shows the change in binding enthalpy of mimic-CAIX (mutant $CAII^{A65S, N67Q, I91L, F130V, V134L, L203A}$) and compound **3b**, which was calculated using the $\Delta_{p\_CAZn(II)H2O}H$ of CAII. Experimental data are provided in Supplementary material in Figure S7 and Table S5.

4.12. X-ray Crystallography: Crystallization, Data Collection, and Structure Determination

The proteins were ultrafiltered to the indicated concentration in Table S4. The same table lists the crystallization conditions and solutions. Crystals of CAIX (PDB ID: 7POM) and CAXII (PDB ID: 7PP9) were achieved by co-crystallization and others by soaking. The crystal soaking ligand solutions were produced by combining 50 μL of matching reservoir solution with 1 μL of 50 mM ligand solution in DMSO. The data were processed and scaled using XDS [35], MOSFLM [36], and SCALA [37]. Except CAXII dataset was processed and scaled using SAINT [38] and SADABS [39]. MOLREP [40] was used for molecular replacement with an initial model of 1CAB for CAI, 4HT0 for CAII, 3HLJ for mimic-CAIX, 6FE2 for CAIX, and 6QNL for CAXII. The model was refined with REFMAC [41] and fitted in the electron density map using COOT [42]. The 3D models of compounds were constructed by AVOGADRO [43] program, and ligand parameter files were created using LIBCHECK [44,45]. Coordinates and structure factors have been deposited to PDB. The PDB IDs, data collection, and refinement statistics are shown in Supplementary material in Table S3. The PyMOL program was used to create graphics.

Supplementary Materials: The following are available online at https://www.mdpi.com/article/10.3390/ijms23010130/s1.

Author Contributions: Conceptualization, A.Z. and E.Č.; methodology, A.Z. and E.Č.; investigation, A.Z., V.P.-L., A.S. (Alexey Smirnov), J.L., A.K., E.D., L.S., A.M., J.J., L.J., V.L., A.S. (Andrius Sakalauskas) and J.M.; resources, E.M. and S.G.; writing—original draft preparation, V.P.-L.; writing—review and editing, A.Z.; supervision, K.T., D.M.; project administration, D.M.; funding acquisition, J.L., J.M. and D.M. All authors have read and agreed to the published version of the manuscript.

Funding: This work was supported by the grant S-SEN-20-10 from the Research Council of Lithuania. J.L. was supported by the European Regional Development Fund (ERDF) grant No. 1.1.1.2/VIAA/3/19/464 'Structural and kinetic studies of human carbonic anhydrases as multiple drug targets'. Access to EMBL beamlines was in part supported by the European Community's Seventh Framework Programme (FP7/2007–2013) under grant agreement number 283570 and by iNEXT funded by the Horizon 2020 program of the European Commission [grant number 653706].

Data Availability Statement: The data that support the findings of this study are available from the corresponding author upon reasonable request.

Conflicts of Interest: The authors declare that they may have authored patent applications on carbonic anhydrase inhibitors.

Abbreviations

CA	carbonic anhydrase
FTSA	fluorescent thermal shift assay (or differential scanning fluorimetry, DSF)
intr	intrinsic
ITC	isothermal titration calorimetry
obs	observed
VARIABLES	
ΔG_{intr}	change of the intrinsic standard Gibbs energy upon binding
ΔG_{obs}	change of the observed standard Gibbs energy upon binding
ΔH_{intr}	change of the intrinsic standard enthalpy upon binding
ΔH_{obs}	change of the observed standard enthalpy upon binding
K_{d_intr}	the intrinsic equilibrium dissociation constant
K_{d_obs}	the observed equilibrium dissociation constant
T_m	melting temperature (midpoint of the unfolding transition)
$T\Delta S_{intr}$	change of the intrinsic standard entropy upon binding multiplied by absolute temperature

References

1. Dodgson, S.J.; Tashian, R.E.; Gros, G.; Carter, N.D. (Eds.) *The Carbonic Anhydrases*; Springer: Boston, MA, USA, 1991.
2. Chegwidden, W.R.; Carter, N.D.; Edwards, Y.H. (Eds.) *The Carbonic Anhydrases*; Birkhäuser: Basel, Switzerland, 2000.
3. Oosterwijk, E.; Ruiter, D.J.; Hoedemaeker, P.J.; Pauwels, E.K.; Jonas, U.; Zwartendijk, J.; Warnaar, S.O. Monoclonal antibody G 250 recognizes a determinant present in renal-cell carcinoma and absent from normal kidney. *Int. J. Cancer* **1986**, *38*, 489–494. [CrossRef] [PubMed]
4. Pastorek, J.; Pastoreková, S.; Callebaut, I.; Mornon, J.P.; Zelník, V.; Opavský, R.; Zat'ovicová, M.; Liao, S.; Portetelle, D.; Stanbridge, E.J. Cloning and characterization of MN, a human tumor-associated protein with a domain homologous to carbonic anhydrase and a putative helix-loop-helix DNA binding segment. *Oncogene* **1994**, *9*, 2877–2888.
5. Saarnio, J.; Parkkila, S.; Parkkila, A.-K.; Haukipuro, K.; Pastoreková, S.; Pastorek, J.; Kairaluoma, M.I.; Karttunen, T.J. Immunohistochemical Study of Colorectal Tumors for Expression of a Novel Transmembrane Carbonic Anhydrase, MN/CA IX, with Potential Value as a Marker of Cell Proliferation. *Am. J. Pathol.* **1998**, *153*, 279–285. [CrossRef]
6. Krishnamurthy, V.M.; Kaufman, G.K.; Urbach, A.R.; Gitlin, I.; Gudiksen, K.L.; Weibel, D.B.; Whitesides, G.M. Carbonic Anhydrase as a Model for Biophysical and Physical-Organic Studies of Proteins and Protein−Ligand Binding. *Chem. Rev.* **2008**, *108*, 946–1051. [CrossRef]
7. Lomelino, C.L.; Andring, J.T.; McKenna, R. Crystallography and Its Impact on Carbonic Anhydrase Research. *Int. J. Med. Chem.* **2018**, *2018*, 9419521. [CrossRef] [PubMed]
8. Zakšauskas, A.; Čapkauskaitė, E.; Jezepčikas, L.; Linkuvienė, V.; Kišonaitė, M.; Smirnov, A.; Manakova, E.; Gražulis, S.; Matulis, D. Design of two-tail compounds with rotationally fixed benzenesulfonamide ring as inhibitors of carbonic anhydrases. *Eur. J. Med. Chem.* **2018**, *156*, 61–78. [CrossRef]
9. Zakšauskas, A.; Čapkauskaitė, E.; Jezepčikas, L.; Linkuvienė, V.; Paketurytė, V.; Smirnov, A.; Leitans, J.; Kazaks, A.; Dvinskis, E.; Manakova, E.; et al. Halogenated and di-substituted benzenesulfonamides as selective inhibitors of carbonic anhydrase isoforms. *Eur. J. Med. Chem.* **2020**, *185*, 111825. [CrossRef]
10. Dudutienė, V.; Zubrienė, A.; Kairys, V.; Smirnov, A.; Smirnovienė, J.; Leitans, J.; Kazaks, A.; Tars, K.; Manakova, L.; Gražulis, S.; et al. Isoform-Selective Enzyme Inhibitors by Exploring Pocket Size According to the Lock-and-Key Principle. *Biophys. J.* **2020**, *119*, 1513–1524. [CrossRef]
11. Scott, A.D.; Phillips, C.; Alex, A.; Flocco, M.; Bent, A.; Randall, A.; O'Brien, R.; Damian, L.; Jones, L.H. Thermodynamic Optimisation in Drug Discovery: A Case Study using Carbonic Anhydrase Inhibitors. *ChemMedChem* **2009**, *4*, 1985–1989. [CrossRef]
12. Čapkauskaitė, E.; Zubrienė, A.; Baranauskienė, L.; Tamulaitienė, G.; Manakova, E.; Kairys, V.; Gražulis, S.; Tumkevičius, S.; Matulis, D. Design of [(2-pyrimidinylthio)acetyl]benzenesulfonamides as inhibitors of human carbonic anhydrases. *Eur. J. Med. Chem.* **2012**, *51*, 259–270. [CrossRef] [PubMed]
13. Čapkauskaitė, E.; Zubrienė, A.; Smirnov, A.; Torresan, J.; Kišonaitė, M.; Kazokaitė, J.; Gylytė, J.; Michailovienė, V.; Jogaitė, V.; Manakova, E.; et al. Benzenesulfonamides with pyrimidine moiety as inhibitors of human carbonic anhydrases I, II, VI, VII, XII, and XIII. *Bioorg. Med. Chem.* **2013**, *21*, 6937–6947. [CrossRef]
14. Singh, S.; Lomelino, C.; Mboge, M.; Frost, S.; McKenna, R. Cancer Drug Development of Carbonic Anhydrase Inhibitors beyond the Active Site. *Molecules* **2018**, *23*, 1045. [CrossRef] [PubMed]

15. Fisher, S.Z.; Aggarwal, M.; Kovalevsky, A.Y.; Silverman, D.N.; McKenna, R. Neutron Diffraction of Acetazolamide-Bound Human Carbonic Anhydrase II Reveals Atomic Details of Drug Binding. *J. Am. Chem. Soc.* **2012**, *134*, 14726–14729. [CrossRef] [PubMed]
16. Zubrienė, A.; Matulis, D. Observed Versus Intrinsic Thermodynamics of Inhibitor Binding to Carbonic Anhydrases. In *Carbonic Anhydrase as Drug Target: Thermodynamics and Structure of Inhibitor Binding*; Matulis, D., Ed.; Springer International Publishing: Cham, Switzerland, 2019; pp. 107–123.
17. Dudutienė, V.; Matulienė, J.; Smirnov, A.; Timm, D.D.; Zubrienė, A.; Baranauskienė, L.; Morkūnaite, V.; Smirnovienė, J.; Michailovienė, V.; Juozapaitienė, V.; et al. Discovery and characterization of novel selective inhibitors of carbonic anhydrase IX. *J. Med. Chem.* **2014**, *57*, 9435–9446. [CrossRef] [PubMed]
18. Genis, C.; Sippel, K.H.; Case, N.; Wengang Cao Avvaru, B.S.; Tartaglia, L.J.; Lakshmanan Govindasamy Tu, C.; Agbandje-McKenna, M.; Silverman, D.N.; Rosser, C.J.; McKenna, R. Design of a carbonic anhydrase IX active-site mimic to screen inhibitors for possible anticancer properties. *Biochemistry* **2009**, *48*, 1322–1331. [CrossRef]
19. Pinard, M.A.; Boone, C.D.; Rife, B.D.; Supuran, C.T.; McKenna, R. Structural study of interaction between brinzolamide and dorzolamide inhibition of human carbonic anhydrases. *Bioorg. Med. Chem.* **2013**, *21*, 7210–7215. [CrossRef]
20. Čapkauskaitė, E.; Linkuvienė, V.; Smirnov, A.; Milinavičiūtė, G.; Timm, D.D.; Kasiliauskaitė, A.; Manakova, E.; Gražulis, S.; Matulis, D. Combinatorial Design of Isoform-Selective N-Alkylated Benzimidazole-Based Inhibitors of Carbonic Anhydrases. *ChemistrySelect* **2017**, *2*, 5360–5371. [CrossRef]
21. Smirnov, A.; Zubrienė, A.; Manakova, E.; Gražulis, S.; Matulis, D. Crystal structure correlations with the intrinsic thermodynamics of human carbonic anhydrase inhibitor binding. *PeerJ* **2018**, *6*, e4412. [CrossRef]
22. Matulis, D. Thermodynamics of the hydrophobic effect. III. Condensation and aggregation of alkanes, alcohols, and alkylamines. *Biophys. Chem.* **2001**, *93*, 67–82. [CrossRef]
23. Cimmperman, P.; Baranauskienė, L.; Jachimovičiūtė, S.; Jachno, J.; Torresan, J.; Michailovienė, V.; Matulienė, J.; Sereikaitė, J.; Bumelis, V.; Matulis, D. A Quantitative Model of Thermal Stabilization and Destabilization of Proteins by Ligands. *Biophys. J.* **2008**, *95*, 3222–3231. [CrossRef]
24. Leitans, J.; Kazaks, A.; Balode, A.; Ivanova, J.; Zalubovskis, R.; Supuran, C.T.; Tars, K. Efficient Expression and Crystallization System of Cancer-Associated Carbonic Anhydrase Isoform IX. *J. Med. Chem.* **2015**, *58*, 9004–9009. [CrossRef] [PubMed]
25. Sūdžius, J.; Baranauskienė, L.; Golovenko, D.; Matulienė, J.; Michailovienė, V.; Torresan, J.; Jachno, J.; Sukackaitė, R.; Manakova, E.; Gražulis, S.; et al. 4-[N-(Substituted 4-pyrimidinyl)amino]benzenesulfonamides as inhibitors of carbonic anhydrase isozymes I, II, VII, and XIII. *Bioorg. Med. Chem.* **2010**, *18*, 7413–7421. [CrossRef]
26. Jogaitė, V.; Zubrienė, A.; Michailovienė, V.; Gylytė, J.; Morkūnaitė, V.; Matulis, D. Characterization of human carbonic anhydrase XII stability and inhibitor binding. *Bioorg. Med. Chem.* **2013**, *21*, 1431–1436. [CrossRef]
27. Pantoliano, M.W.; Petrella, E.C.; Kwasnoski, J.D.; Lobanov, V.S.; Myslik, J.; Graf, E.; Carver, T.; Asel, E.; Springer, B.A.; Lane, P.; et al. High-density miniaturized thermal shift assays as a general strategy for drug discovery. *J. Biomol. Screen* **2001**, *6*, 429–440. [CrossRef]
28. Kazlauskas, E.; Petrauskas, V.; Paketurytė, V.; Matulis, D. Standard operating procedure for fluorescent thermal shift assay (FTSA) for determination of protein-ligand binding and protein stability. *Eur. Biophys. J.* **2021**, *50*, 373–379. [CrossRef] [PubMed]
29. Matulis, D.; Baumann, C.G.; Bloomfield, V.A.; Lovrien, R.E. 1-Anilino-8-naphthalene sulfonate as a protein conformational tightening agent. *Biopolymers* **1999**, *49*, 451–458. [CrossRef]
30. Baranauskienė, L.; Hilvo, M.; Matulienė, J.; Golovenko, D.; Manakova, E.; Dudutienė, V.; Michailovienė, V.; Torresan, J.; Jachno, J.; Parkkila, S.; et al. Inhibition and binding studies of carbonic anhydrase isozymes I, II and IX with benzimidazo[1,2-c][1,2,3]thiadiazole-7-sulphonamides. *J. Enzyme Inhib. Med. Chem.* **2010**, *25*, 863–870. [CrossRef]
31. Falconer, R.J. Applications of isothermal titration calorimetry—The research and technical developments from 2011 to 2015: Review of Isothermal Titration Calorimetry from 2011 to 2015. *J. Mol. Recognit.* **2016**, *29*, 504–515. [CrossRef]
32. Callies, O.; Daranas, A.H. Application of isothermal titration calorimetry as a tool to study natural product interactions. *Nat. Prod. Rep.* **2016**, *33*, 881–904. [CrossRef]
33. Linkuvienė, V.; Zubrienė, A.; Manakova, E.; Petrauskas, V.; Baranauskienė, L.; Zakšauskas, A.; Smirnov, A.; Gražulis, S.; Ladbury, J.E.; Matulis, D. Thermodynamic, kinetic, and structural parameterization of human carbonic anhydrase interactions toward enhanced inhibitor design. *Q. Rev. Biophys.* **2018**, *51*, 1–48. [CrossRef] [PubMed]
34. Snyder, P.W.; Mecinović, J.; Moustakas, D.T.; Thomas, S.W.; Harder, M.; Mack, E.T.; Lockett, M.R.; Héroux, A.; Sherman, W.; Whitesides, G.M. Mechanism of the hydrophobic effect in the biomolecular recognition of arylsulfonamides by carbonic anhydrase. *Proc. Natl. Acad. Sci. USA* **2011**, *108*, 17889–17894. [CrossRef]
35. Kabsch, W. XDS. *Acta Crystallogr. Sect. D* **2010**, *66*, 125–132. [CrossRef]
36. Battye, T.G.G.; Kontogiannis, L.; Johnson, O.; Powell, H.R.; Leslie, A.G.W. iMOSFLM: A new graphical interface for diffraction-image processing with MOSFLM. *Acta Crystallogr. D Biol. Crystallogr.* **2011**, *67*, 271–281. [CrossRef]
37. Evans, P. Scaling and assta quality. *Acta Crystallogr. D Biol. Crystallogr.* **2006**, *62*, 72–82. [CrossRef] [PubMed]
38. Bruker. SAINT (Version 8.18c). In *Bruker Advanced X-ray Solutions*; Bruker AXS: Madison, WI, USA, 2012.
39. Bruker. SADABS (Version 2.11). In *Bruker Advanced X-ray Solutions*; Bruker AXS: Madison, WI, USA, 2012.
40. Vagin, A.; Teplyakov, A. Molecular replacement with MOLREP. *Acta Crystallogr. D Biol. Crystallogr.* **2010**, *66*, 22–25. [CrossRef]

41. Murshudov, G.N.; Skubák, P.; Lebedev, A.A.; Pannu, N.S.; Steiner, R.A.; Nicholls, R.A.; Winn, M.D.; Long, F.; Vagin, A.A. REFMAC5 for the refinement of macromolecular crystal structures. *Acta Crystallogr. D Biol. Crystallogr.* **2011**, *67*, 355–367. [CrossRef] [PubMed]
42. Emsley, P.; Lohkamp, B.; Scott, W.G.; Cowtan, K. Features and development of ıt Coot. *Acta Crystallogr. Sect. D* **2010**, *66*, 486–501. [CrossRef] [PubMed]
43. Hanwell, M.D.; Curtis, D.E.; Lonie, D.C.; Vandermeersch, T.; Zurek, E.; Hutchison, G.R. Avogadro: An advanced semantic chemical editor, visualization, and analysis platform. *J. Cheminform.* **2012**, *4*, 17. [CrossRef] [PubMed]
44. Lebedev, A.A.; Young, P.; Isupov, M.N.; Moroz, O.V.; Vagin, A.A.; Murshudov, G.N. JLigand: A graphical tool for the CCP4 template-restraint library. *Acta Crystallogr. D Biol. Crystallogr.* **2012**, *68*, 431–440. [CrossRef] [PubMed]
45. Vagin, A.A.; Steiner, R.A.; Lebedev, A.A.; Potterton, L.; McNicholas, S.; Long, F.; Murshudov, G.N. REFMAC5 dictionary: Organization of prior chemical knowledge and guidelines for its use. *Acta Crystallogr. D Biol. Crystallogr.* **2004**, *60*, 2184–2195. [CrossRef]

Journal of Medicinal Chemistry

pubs.acs.org/jmc

Article

Affinity and Selectivity of Protein−Ligand Recognition: A Minor Chemical Modification Changes Carbonic Anhydrase Binding Profile

Audrius Zakšauskas, Vaida Paketurytė-Latvė, Alberta Jankūnaitė, Edita Čapkauskaitė, Yann Becart, Alexey Smirnov, Klára Pospíšilová, Janis Leitans, Jiří Brynda, Andris Kazaks, Lina Baranauskienė, Elena Manakova, Saulius Gražulis, Visvaldas Kairys, Kaspars Tars, Pavlína Řezáčová, and Daumantas Matulis*

Cite This: https://doi.org/10.1021/acs.jmedchem.5c01421

Read Online

ACCESS | Metrics & More | Article Recommendations | Supporting Information

ABSTRACT: Discovery of small-molecule drugs relies on their strong binding affinity compared to nontarget proteins, thus possessing selectivity. Minor chemical structure changes usually exhibit little change in the compound efficacy, with rare exceptions. We developed a series of nearly 50 *ortho*-substituted benzenesulfonamides and experimentally measured their interactions with the 12 catalytically active human carbonic anhydrase (CA) isozymes. Inhibitors were designed using seven different substituent groups, including 4-*sulfanyl*-substituted 3-sulfamoyl benzoates and benzamides, 4-*sulfinyl*-substituted 3-sulfamoyl benzoates and benzamides, 4-*sulfonyl*-substituted 3-sulfamoyl benzoates and benzamides, and 4-amino-substituted benzamides. The oxidation state of sulfur at the *ortho* position significantly influenced the compound's affinity for CAIX, a target for anticancer drugs, demonstrating affinities hundreds of thousands of times stronger than related compounds. Coupled with X-ray crystal structures and molecular docking, the relationship between structure and thermodynamics offers insights into how small changes in the structure lead to significant changes in affinity for drug design.

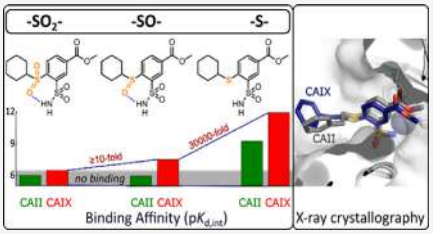

INTRODUCTION

A detailed understanding of protein−ligand recognition is an essential goal in small-molecule drug discovery.[1] Any drug-like chemical compound should bind the disease-related target protein with sufficiently high affinity. Furthermore, the compound must bind with high selectivity and thus not interact strongly with other nontarget proteins whose inhibition or binding could cause undesired side effects.[2] Rational design of such compounds is complex because of the limited understanding of the underlying energies of binding and how a compound recognizes and binds to the target protein.

As a model system, we study sulfonamide compound binding to human carbonic anhydrases (CA), zinc-containing enzymes.[3] Humans have 12 catalytically active CA isozymes (EC 4.2.1.1).[4−6] The enzyme catalyzes the reversible hydration of carbon dioxide and has many essential physiological functions. Since these enzymes function in pH and electrolyte homeostasis and regulation, many drugs target CA isozymes to treat diseases like glaucoma, edema, obesity, epilepsy, infertility, and cancer.[7−9] Primary sulfonamides are the most investigated CA inhibitors.[10−12] Their amino group binds directly to the catalytic zinc in the active site by forming a coordination bond and inhibits the activity of all CA isozymes. However, the binding affinity may be low or high and depends on small details of each compound arrangement on the protein surface, possible steric hindrances, or attraction due to hydrogen bonds or hydrophobic interactions.[13]

The 12 catalytically active human CA isozymes have nearly identical beta-sheet folds. Their active sites are highly similar in shape, but several amino acids in the active site vary among the isozymes.[14−16] Because the differences in the active site amino acid composition are small, it is difficult to design compounds that would bind one isozyme with high affinity while all other isozymes with low affinity, thus leading toward high selectivity for only one isozyme. The active site of CAs is funnel-shaped and has hydrophobic and hydrophilic sides for some isozymes. Differences in a few amino acids determine the selectivity of inhibitors for particular isozymes. Introducing various scaffolds on the aromatic sulfonamide ring targets unique residues in the active site.[17] In most studies, the tails are relatively distant from

Received: May 26, 2025
Revised: June 27, 2025
Accepted: July 8, 2025

Scheme 1. Synthesis of Methyl 4-Substituted-3-Sulfamoylbenzoates 4a−d, f−m, 4-Substituted 3-Sulfamoylbenzamides 5a−d, f, g, j−m, and 4-Amino-Substituted Benzamides 6b, c, e[a]

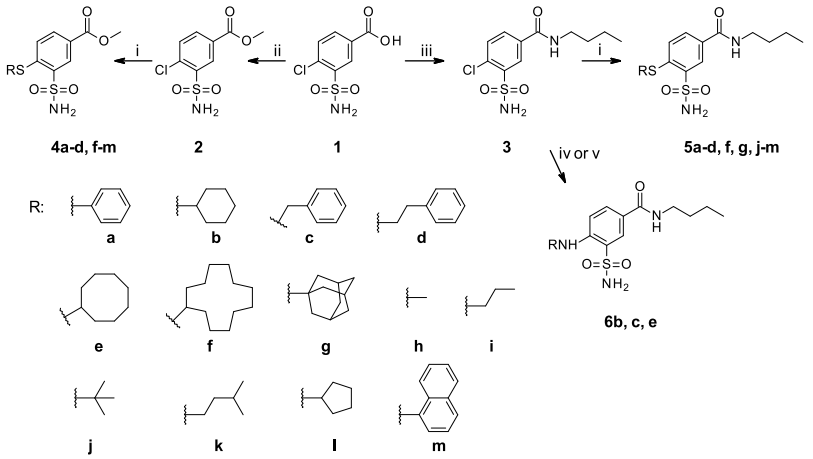

[a]Reagents and conditions: (i) RSH, K_2CO_3, DMF, 80 °C; (ii) H_2SO_4, MeOH, Δ; (iii) (a) $SOCl_2$, toluene, Δ, (b) RNH_2, THF, 0 °C; (iv) RNH_2, 130 °C; (v) RNH_2, TEA, toluene, Δ.

the sulfonamide group, resulting in weak interactions with peripheral amino acids. The affinity profile depended mostly on the substituents located close to the sulfonamide headgroup.[18−20] This is also dependent on the flexibility of the substituents, which help adjust to the protein shape.

Depending on the variation of the substituents while investigating doubly substituted compounds,[20−22] several high-affinity compounds exhibiting picomolar K_d were obtained for CAVII, CAIX, CAXII, and CAXIV. A significant achievement was a *LJ15-12* compound that exhibited 0.08 pM intrinsic K_d for CAIX.[20] In this study, we investigate the functional groups in the *ortho* position by varying 13 substituents from small methyl to bulky adamantyl. Sulfinyl and amino substituents were also synthesized to examine the influence of the linking atoms. Interestingly, the substitution of only one atom, an addition of an oxygen atom in the *ortho* position, decreased compound affinity for nontarget isozymes by a million-fold, significantly improving the selectivity, which is one of the main goals in small-molecule drug discovery.

RESULTS

Organic Synthesis of Designed Compounds. The synthesis of 2,5-disubstituted benzenesulfonamides was performed starting from 4-chloro-3-sulfamoylbenzoic acid **1** (Scheme 1). Methyl ester **2** was obtained from 4-chloro-3-sulfamoylbenzoic acid **1** by reflux in methanol in the presence of a catalytic amount of sulfuric acid. Amide **3** was synthesized by refluxing acid **1** with thionyl chloride in toluene and subsequent treatment, the resulting anhydride with an appropriate amine, using as the base excess of amine according to the procedure reported in ref 21.

The synthesis of 4-substituted sulfamoylbenzoic acid derivatives **4a−d, f−m** was achieved by aromatic nucleophilic substitution of the chlorine substituent with various thiols under an inert atmosphere in dimethylformamide using potassium carbonate as the base (Scheme 1). All thiols were commercially available except cyclododecylthiol, which was synthesized by subjecting cyclododecanone to reaction with 1,2-ethanedithiol and subsequent reduction of intermediate dithiolane with *n*-butyllithium.[23]

The 4-substituted 3-sulfamoylbenzamides **5a−d, f, g, j−m** were synthesized using the same reaction conditions as 4-sulfanyl-substituted esters **4a−d, f−m**. Substitution of the chlorine group with amines required harsher reaction conditions than thiols. Therefore, 4-amino-substituted benzamides **6b** and **c** were synthesized by heating amide **3** over the appropriate amine at 130 °C. Compound **6e** was synthesized by boiling amide **3** in toluene with 2 equiv of cyclooctylamine and 2 equiv of triethylamine.

The oxidation of esters **4a−d, h, i, k−m** and benzamides **5a, b, k−m** to the sulfinyl and sulfonyl compounds was performed using in situ generated peracetic acid (Scheme 2). The reaction was carried out at room temperature and produced 4-sulfinyl compounds **7a, b, h, i, k−m**, **8a, b, k−m**, and heating the reaction mixture at 70 °C yielded the corresponding 4-sulfonyl compounds **9a−d, h, i, l, m**, **10b,** and **k−m**.

Compound Binding to CA Isozymes. All synthesized compounds were divided into 7 groups: **4(a−d, f−m)**, **5(a−d, f, g, j−m)**, **6(b, c, e)**, **7(a, b, h, i, k−m)**, **8(a, k−m)**, **9(a−d, h, i, l, m)**, and **10(b, k−m)** (Figure 1). Compounds that started with numbers **4**, **7**, and **9** were 4-sulfanyl-, 4-sulfinyl, and 4-sulfonyl-substituted esters, respectively. Compounds starting with the numbers **5**, **8**, and **10** were 4-sulfanyl-, 4-sulfinyl, and 4-sulfonyl-substituted benzamides analogous to the previous series. Compounds starting with the number **6** were 4-amino-substituted benzamides. Various linear, branched, and cyclic aliphatic and aromatic substituents at the *ortho* position were tested to assess whether size, flexibility, and hydrophobicity affect affinity. Compound affinities for the 12 catalytically active human CA isozymes are listed in Table 1.

As one of the important findings in this manuscript, Figure 2 arranges the compounds in the order of their affinity for CAIX

https://doi.org/10.1021/acs.jmedchem.5c01421
J. Med. Chem. XXXX, XXX, XXX−XXX

Scheme 2. Synthesis of Methyl 4-Sulfinyl-Substituted-3-Sulfamoyl Benzoates 7a, b, h, i, k−m, *N*-Butyl-4-sulfinyl-Substituted-3-Sulfamoylbenzamides 8a, b, k−m, Methyl 4-Sulfonyl-Substituted-3-Sulfamoylbenzoates 9a-d, h, i, l, m, and *N*-Butyl-4-sulfonyl-Substituted-3-Sulfamoylbenzamides 10b, k−m[a]

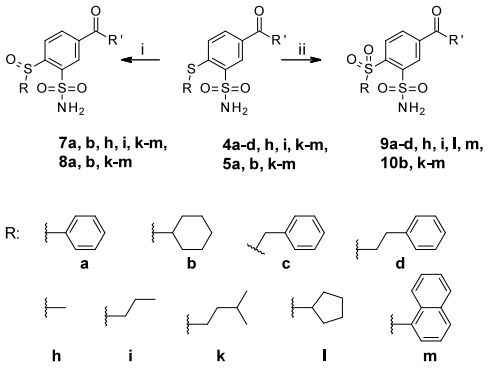

[a]Reagents and conditions: (i) 30% H_2O_2, AcOH, r. t.; (ii) 30% H_2O_2, AcOH, 70 °C.

and compared to undesired target CAII. A high affinity for CAIX is desired, because CAIX is implicated in various types of cancer.[24] However, CAII is abundant in erythrocytes, thus an off-target for anticancer inhibitors.

Compound affinities for human CA isozymes were analyzed using fluorescence-based thermal shift assay (FTSA) and the enzymatic activity stopped-flow-based inhibition assay (SFA) (Figure 3). The FTSA determined the observed dissociation constants for all compounds with all 12 CA isozymes (Table 1 and Supplementary Figure S1). From these experimentally determined $K_{d,obs}$, the *intrinsic* dissociation constants $K_{d,int}$ were calculated, and the results are primarily focused on them. Figure 3B,C shows two compounds with strong and weak affinity for CAII and CAIX by FTSA. A single oxygen atom strongly diminished affinity for both isozymes. The stopped-flow assay of CO_2 hydration enzymatic activity inhibition confirmed that the compounds inhibited CAIX and CAII (Figure 3D,E). Inhibition K_i values are presented in Table 2 and Figure S2. The FTSA is a convenient technique covering a significantly wider K_d range than the SFA.[25]

The experimental conditions slightly differed between FTSA and SFA, and it is therefore not appropriate to directly compare the $K_{d,obs}$ and K_i. However, the measured affinities were similar in both techniques. Further analysis is based on FTSA data due to its wider limits in identifying strong binders. Note that the enzyme concentration limits the SFA's ability to determine high-affinity binders. For example, if we use a 10 nM concentration of a CA isozyme, the lowest IC_{50} is 5 nM, half of the protein concentration. Any compound with an IC_{50} stronger than 5 nM would exhibit a dosing curve that appears as an IC_{50} of 5 nM. Thus, compounds that possess single-digit nM or picomolar K_d, cannot be distinguished by SFA.

Sulfonamide binding of CA is a pH-dependent reaction.[6,26,27] The water molecule bound to the CA zinc ion is replaced by the deprotonated form of sulfonamide upon binding.[28,29] The protonation forms required for the interaction exist at different pHs: the CA-Zn(II)-H_2O has the largest fraction at acidic pH and the deprotonated sulfonamide has the largest fraction at alkaline pH. Therefore, the measured affinity is always lower than the intrinsic affinity. The intrinsic parameters are calculated (see equations in the Experimental section) by knowing the pK_a of the CA zinc-bound water and the pK_a of the sulfonamide group (Table 1 and Figure S3). Experimental data of the sulfonamide group pK_a determination for compound **4b** are shown in Figure 4. Figure S3 shows the graphs of pK_a determination for the remaining compounds.

Intrinsic affinities are especially important in rational drug design. It is not rare when a stronger affinity is observed not because of the formed bonds but because of the substitutions that lower the pK_a of the sulfonamide group and thus increase the fraction of the ready-to-bind form.[30] Intrinsic parameters are used to avoid misleading conclusions when comparing the affinity of compounds for CAs.

Esters vs Benzamides. 4-sulfanyl-substituted esters **4a−d, f−m** were the largest (12 compounds) studied group of compounds with the same framework. Compounds of this group, even almost independently of the substituent, interacted strongly and selectively with several CAs. $K_{d,int}$ of **4b** for CAIX was 0.0010 nM and it was the strongest interaction measured in this study, CAXIII—0.090 nM and CAXIV—0.020 nM, with others interacting much weaker. The size of the substituent was critical in this interaction. CAIX has a larger active site than the rest of the CAs.[31] It was interesting that compound **4g** (*adamantyl*), which has a similar affinity for CAIX ($K_{d,int}$ =

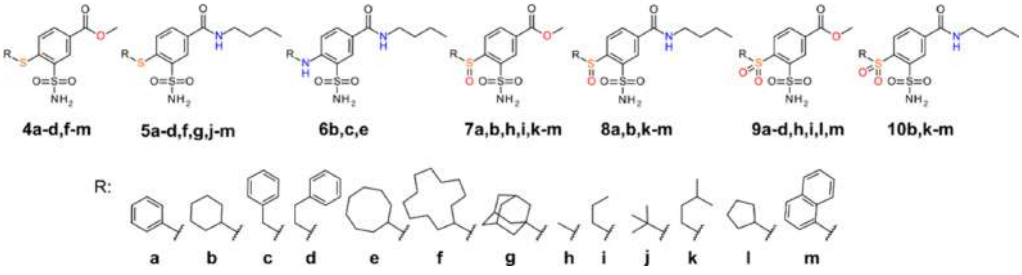

Figure 1. Chemical structures of the compounds synthesized and investigated in this study. Compounds **1**, **2**, and **3** are the starting compounds of the synthesis shown in Scheme 1.

https://doi.org/10.1021/acs.jmedchem.5c01421
J. Med. Chem. XXXX, XXX, XXX−XXX

Table 1. ***Observed*** **and** ***Intrinsic*** **($K_{d,obs}$ and $K_{d,int}$) Dissociation Constants (in nM Units) of Investigated Compounds to All Catalytically Active Human CAs at 37 °C Obtained by Fluorescent Thermal Shift Assay (FTSA)**[a]

					CAI	CAII	CAIII	CAIV	CAVA	CAVB	CAVI	CAVII	CAIX	CAXII	CAXIII	CAXIV
				$pK_{a,SA}$	8.1	6.9	6.5	6.6	7.3	7.0	6.0	6.8	6.6	6.8	8.0	6.8
Compound *lab. name*	A framework of the structure	$pK_{a,SA}$	fraction at pH 7.0		92.6%	44.3%	24.0%	28.5%	66.6%	50.0%	9.1%	38.7%	28.5%	38.7%	90.9%	38.7%
2 *JA17-1*		9.2	0.63%	$K_{d,obs}$	21000	460	≥200000	500	770	42	300	240	240	92	220	170
				$K_{d,int}$	120	1.3	≥300	0.90	3.2	0.13	0.17	0.58	0.43	0.22	1.3	0.41
3 *JA17-3*	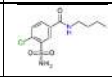	9.1	0.79%	$K_{d,obs}$	36000	140	44000	99	1800	70	340	94	190	10	880	290
				$K_{d,int}$	260	0.50	83	0.22	10	0.28	0.24	0.29	0.43	0.030	6.3	0.89
4a *JA17-1-1*		9.8	0.16%	$K_{d,obs}$	≥200000	87	≥200000	460	≥200000	120	430	140	4.0	260	12	10
				$K_{d,int}$	≥290	0.060	≥76	0.21	≥210	0.10	0.060	0.090	0.0020	0.16	0.020	0.0060
4b *JA17-1-2*		9.7	0.20%	$K_{d,obs}$	≥200000	560	≥200000	810	≥200000	440	710	680	1.8	280	52	22
				$K_{d,int}$	≥370	0.49	≥96	0.46	≥270	0.44	0.13	0.52	0.0010	0.22	0.090	0.020
4c *JA17-1-3*		9.8	0.16%	$K_{d,obs}$	≥200000	590	≥200000	110	140000	930	660	960	10	350	52	90
				$K_{d,int}$	≥290	0.42	≥76	0.050	150	0.70	0.10	0.60	0.0050	0.21	0.080	0.050
4d *JA17-1-4*		9.6	0.25%	$K_{d,obs}$	160000	580	≥200000	1100	97000	190	1300	360	19	450	27	20
				$K_{d,int}$	380	0.64	≥120	0.79	160	0.23	0.29	0.34	0.010	0.43	0.060	0.020
4f *JA18-29*		9.7[a]	0.20%	$K_{d,obs}$	≥200000	1000	≥200000	2100	≥200000	1800	6500	18000	11	68	100	100
				$K_{d,int}$	≥370	0.90	≥96	1.2	≥270	1.8	1.2	14	0.0060	0.050	0.18	0.080
4g *E19-3*		9.7[b]	0.20%	$K_{d,obs}$	≥200000	3300	≥200000	100000	≥200000	≥200000	13000	96000	4.8	1500	1200	1200
				$K_{d,int}$	≥370	2.9	≥96	57	≥270	≥200	2.3	74	0.0030	1.1	2.2	1.0
4h *JA19-17*		9.8	0.16%	$K_{d,obs}$	≥200000	2200	≥200000	960	120000	680	500	1000	650	6500	570	440
				$K_{d,int}$	≥290	1.6	≥76	0.43	130	0.54	0.070	0.61	0.29	4.0	0.80	0.27
4i *JA18-30*		9.6	0.25%	$K_{d,obs}$	≥200000	1000	≥200000	400	91000	990	700	490	23	1800	98	70
				$K_{d,int}$	≥460	1.1	≥120	0.28	150	1.2	0.16	0.48	0.020	1.7	0.22	0.070
4j *JA18-33*		9.6	0.25%	$K_{d,obs}$	≥200000	2400	≥200000	10000	≥200000	4900	4600	15000	290	120	220	370
				$K_{d,int}$	≥460	2.7	≥120	7.4	≥330	6.1	1.0	14	0.21	0.12	0.51	0.36
4k *JA18-32*		9.8	0.16%	$K_{d,obs}$	40000	370	≥200000	160	85000	310	300	210	2.7	190	40	33
				$K_{d,int}$	58	0.26	≥76	0.070	89	0.25	0.040	0.13	0.0010	0.11	0.060	0.020
4l *E19-1*		9.6	0.25%	$K_{d,obs}$	≥200000	670	≥200000	1000	180000	6700	560	180	3.3	670	110	20
				$K_{d,int}$	≥460	0.74	≥120	0.71	300	8.4	0.13	0.18	0.0020	0.65	0.25	0.020
4m *E19-2*		9.7	0.20%	$K_{d,obs}$	≥200000	50	11000	2000	≥200000	1300	500	8.7	2.5	500	1.4	25
				$K_{d,int}$	≥370	0.040	5.3	1.1	≥270	1.2	0.090	0.0070	0.0010	0.39	0.0030	0.020
5a *JA17-3-1*		9.7	0.20%	$K_{d,obs}$	≥200000	16000	≥200000	≥200000	120000	9000	19000	53000	360	17000	17000	60000
				$K_{d,int}$	≥370	14	≥96	≥110	160	9	3.5	41	0.20	13	30	46
5b *JA17-3-2*		9.8	0.16%	$K_{d,obs}$	≥200000	180000	100000	≥200000	≥200000	33000	≥200000	≥200000	450	140000	150000	≥200000
				$K_{d,int}$	≥290	120	38	≥90	≥210	26	≥29	≥120	0.20	83	220	≥120
5c *JA17-3-3*		9.8	0.16%	$K_{d,obs}$	≥200000	12000	≥200000	40000	68000	33000	43000	77000	2100	8600	43000	50000
				$K_{d,int}$	≥290	8.1	≥76	18	72	26	6.2	47	0.93	5.3	62	31
5d *JA17-3-4*		9.9	0.13%	$K_{d,obs}$	≥200000	58000	≥200000	≥200000	110000	17000	98000	≥200000	3200	46000	110000	≥200000
				$K_{d,int}$	≥230	32	≥60	≥72	95	10	11	≥97	1.2	22	130	≥97
5f *JA19-16*	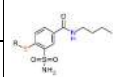	9.8[b]	0.16%	$K_{d,obs}$	≥200000	100000	≥200000	≥200000	≥200000	≥200000	≥200000	≥200000	840	≥200000	≥200000	62000
				$K_{d,int}$	≥290	70	≥76	≥90	≥210	≥160	≥29	≥120	0.38	≥120	≥290	38
5g *YB19-4*		9.8[b]	0.16%	$K_{d,obs}$	≥200000	≥200000	≥200000	≥200000	≥200000	≥200000	≥200000	≥200000	2000	≥200000	≥200000	≥200000
				$K_{d,int}$	≥290	≥140	≥76	≥90	≥210	≥160	≥29	≥120	0.90	≥120	≥290	≥120
5j *YB19-3*		9.8	0.16%	$K_{d,obs}$	≥200000	≥200000	≥200000	≥200000	≥200000	≥200000	≥200000	≥200000	25000	≥200000	≥200000	≥200000
				$K_{d,int}$	≥290	≥140	≥76	≥90	≥210	≥160	≥29	≥120	11	≥120	≥290	≥120

https://doi.org/10.1021/acs.jmedchem.5c01421
J. Med. Chem. XXXX, XXX, XXX−XXX

Table 1. continued

Compound lab. name	A framework of the structure	$pK_{a,SA}$	fraction at pH 7.0		CAI	CAII	CAIII	CAIV	CAVA	CAVB	CAVI	CAVII	CAIX	CAXII	CAXIII	CAXIV
				$pK_{a,CA}$	8.1	6.9	6.5	6.6	7.3	7.0	6.0	6.8	6.6	6.8	8.0	6.8
					92.6%	44.3%	24.0%	28.5%	66.6%	50.0%	9.1%	38.7%	28.5%	38.7%	90.9%	38.7%
5k *YB19-2*	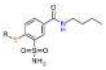	9.7	0.20%	$K_{a,obs}$	≥200000	≥200000	≥200000	≥200000	≥200000	≥200000	≥200000	≥200000	670	≥200000	≥200000	≥200000
				$K_{a,int}$	≥370	≥180	≥96	≥110	≥270	≥200	≥36	≥150	0.38	≥150	≥360	≥150
5l *YB19-5*		9.8	0.16%	$K_{a,obs}$	≥200000	≥200000	≥200000	≥200000	≥200000	≥200000	≥200000	≥200000	800	≥200000	≥200000	≥200000
				$K_{a,int}$	≥290	≥140	≥76	≥90	≥210	≥160	≥29	≥120	0.36	≥120	≥290	≥120
5m *YB19-1*		9.9	0.13%	$K_{a,obs}$	≥200000	≥200000	≥200000	≥200000	≥200000	≥200000	≥200000	≥200000	500	≥200000	10000	≥200000
				$K_{a,int}$	≥230	≥110	≥60	≥72	≥170	≥130	≥23	≥97	0.18	≥97	11	≥97
6b *IA17-3-11*	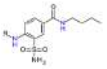	9.8	0.16%	$K_{a,obs}$	180000	20000	≥200000	68000	80000	6500	26000	62000	420	27000	44000	46000
				$K_{a,int}$	260	14	≥76	31	84	5.2	3.7	38	0.19	16	64	28
6c *IA17-3-9*		9.8	0.16%	$K_{a,obs}$	≥200000	22000	≥200000	63000	83000	10000	25000	62000	1500	6500	32000	33000
				$K_{a,int}$	≥290	16	≥76	29	88	8.0	3.6	38	0.66	4.0	47	20
6e *IA17-3-10*		9.8	0.16%	$K_{a,obs}$	≥200000	110000	≥200000	≥200000	190000	≥200000	≥200000	≥200000	1200	64000	150000	20000
				$K_{a,int}$	≥290	79	≥76	≥90	200	≥160	≥29	≥120	0.53	39	220	12
7a *IA19-11*	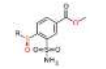	8.9[a]	1.24%	$K_{a,obs}$	≥200000	340	93000	900	≥200000	910	970	79	130	2900	120	99
				$K_{a,int}$	≥2300	1.8	280	3.2	≥1700	5.6	1.1	0.38	0.45	14	1.3	0.48
7b *IA19-10*		8.9	1.24%	$K_{a,obs}$	≥200000	≥200000	≥200000	≥200000	≥200000	≥200000	≥200000	≥200000	7800	≥200000	≥200000	≥200000
				$K_{a,int}$	≥2300	≥1100	≥600	≥710	≥1700	≥1200	≥230	≥960	28	≥960	≥2300	≥960
7h *IA19-19*		8.9	1.24%	$K_{a,obs}$	≥200000	4300	≥200000	5500	≥200000	33000	1200	18000	5200	15000	720	3300
				$K_{a,int}$	≥2300	24	≥600	19	≥1700	200	1.3	87	18	74	8.1	16
7i *IA19-3*		8.9	1.24%	$K_{a,obs}$	≥200000	≥200000	≥200000	≥200000	100000	≥200000	111000	≥200000	43000	≥200000	26100	45000
				$K_{a,int}$	≥2300	≥1100	≥600	≥710	830	≥1200	130	≥960	150	≥960	290	220
7k *IA19-8*		8.8	1.56%	$K_{a,obs}$	≥200000	2400	≥200000	9000	≥200000	14000	13000	9300	140	7600	400	2000
				$K_{a,int}$	≥2900	16	≥750	40	≥2100	110	18	56	0.63	46	5.6	12
7l *E19-6*		8.9	1.24%	$K_{a,obs}$	27000	3600	≥200000	12000	≥200000	130000	9800	68000	200	18000	1600	510
				$K_{a,int}$	310	20	≥600	42	≥1700	780	11	330	0.72	86	18	2.5
7m *E19-7*		9.1	0.79%	$K_{a,obs}$	52000	2900	≥200000	1200	≥200000	58000	65000	5400	110	2600	700	180
				$K_{a,int}$	380	10	≥380	2.8	≥1000	230	47	16	0.24	8.1	5.0	0.54
8a *IA19-15*		9.0	0.99%	$K_{a,obs}$	180000	13000	≥200000	50000	≥200000	13000	≥200000	100000	14000	≥200000	50000	≥200000
				$K_{a,int}$	1600	55	≥480	140	≥1300	62	≥180	380	40	≥770	450	≥770
8k *YB19-10*		9.0	0.99%	$K_{a,obs}$	≥200000	160000	≥200000	≥200000	≥200000	≥200000	≥200000	≥200000	3300	≥200000	180000	≥200000
				$K_{a,int}$	≥1800	710	≥480	≥560	≥1300	≥990	≥180	≥770	9	≥770	1600	≥770
8l *YB19-11*		9.0[b]	0.99%	$K_{a,obs}$	33000	14000	≥200000	≥200000	≥200000	≥200000	≥200000	≥200000	13000	≥200000	≥200000	10000
				$K_{a,int}$	310	63	≥480	≥560	≥1300	≥990	≥180	≥770	35	≥770	≥1800	38
8m *YB19-7*		8.9	1.24%	$K_{a,obs}$	≥200000	141800	≥200000	≥200000	≥200000	≥200000	≥200000	≥200000	4600	≥200000	146300	≥200000
				$K_{a,int}$	≥2300	780	≥600	≥710	≥1700	≥1200	≥230	≥960	16.0	≥960	1700	≥960
9a *IA17-1-5*	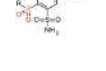	9.0	0.99%	$K_{a,obs}$	≥200000	56000	≥200000	≥200000	≥200000	≥200000	110000	57000	76000	≥200000	16000	42000
				$K_{a,int}$	≥1800	250	≥480	≥560	≥1300	≥990	94	220	220	≥770	140	160
9b *IA17-1-7*		8.9	1.24%	$K_{a,obs}$	≥200000	≥200000	≥200000	≥200000	≥200000	≥200000	≥200000	28000	90000	≥200000	100000	140000
				$K_{a,int}$	≥2300	≥1100	≥600	≥710	≥1700	≥1200	≥230	130	320	≥960	1100	680
9c *IA17-1-8*		8.9	1.24%	$K_{a,obs}$	≥200000	≥200000	≥200000	68000	≥200000	≥200000	≥200000	70000	11000	≥200000	56000	29000
				$K_{a,int}$	≥2300	≥1100	≥600	240	≥1700	≥1200	≥230	340	37	≥960	640	140
9d *IA17-1-6*		9.0	0.99%	$K_{a,obs}$	≥200000	≥200000	≥200000	140000	≥200000	≥200000	160000	≥200000	≥200000	≥200000	25000	54000
				$K_{a,int}$	≥1800	≥880	≥480	390	≥1300	≥990	150	≥770	≥560	≥770	220	210
9h *IA19-20*		8.8	1.56%	$K_{a,obs}$	≥200000	82000	≥200000	89000	140000	≥200000	64000	160000	73000	170000	22000	59000
				$K_{a,int}$	≥2900	570	≥750	400	1400	≥1600	91	960	320	1100	310	350

https://doi.org/10.1021/acs.jmedchem.5c01421
J. Med. Chem. XXXX, XXX, XXX−XXX

Table 1. continued

Compound lab. name	A framework of the structure	$pK_{a,SA}$	fraction at pH 7.0		CAI	CAII	CAIII	CAIV	CAVA	CAVB	CAVI	CAVII	CAIX	CAXII	CAXIII	CAXIV
				$pK_{a,CA}$	8.1	6.9	6.5	6.6	7.3	7.0	6.0	6.8	6.6	6.8	8.0	6.8
					92.6%	44.3%	24.0%	28.5%	66.6%	50.0%	9.1%	38.7%	28.5%	38.7%	90.9%	38.7%
9i *IA19-2*		8.9	1.24%	$K_{d,obs}$	≥200000	1700	≥200000	6200	≥200000	9000	1500	≥200000	900	16000	250	920
				$K_{d,int}$	≥2300	10	≥600	22	≥1700	56	1.7	≥960	3.2	76	2.8	4.4
9l *E19-4*		9.0	0.99%	$K_{d,obs}$	≥200000	71000	≥200000	190000	≥200000	≥200000	≥200000	≥200000	9100	≥200000	22000	20000
				$K_{d,int}$	≥1800	310	≥480	540	≥1300	≥990	≥180	≥770	26	≥770	200	78
9m *E19-5*		9.0	0.99%	$K_{d,obs}$	≥200000	5900	≥200000	≥200000	≥200000	≥200000	35000	6800	4000	≥200000	630	6300
				$K_{d,int}$	≥1800	26	≥480	≥560	≥1300	≥990	31	26	11	≥770	5.6	24
10b *IA19-14*	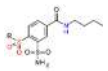	9.0	0.99%	$K_{d,obs}$	≥200000	≥200000	≥200000	≥200000	≥200000	≥200000	≥200000	≥200000	≥200000	≥200000	≥200000	≥200000
				$K_{d,int}$	≥1800	≥880	≥480	≥560	≥1300	≥990	≥180	≥770	≥560	≥770	≥1800	≥770
10k *YB19-8*		9.0	0.99%	$K_{d,obs}$	≥200000	≥200000	≥200000	≥200000	≥200000	≥200000	≥200000	≥200000	≥200000	≥200000	≥200000	160000
				$K_{d,int}$	≥1800	≥880	≥480	≥560	≥1300	≥990	≥180	≥770	≥560	≥770	≥1800	620
10l *YB19-9*		9.1	0.79%	$K_{d,obs}$	≥200000	≥200000	≥200000	≥200000	≥200000	150000	≥200000	≥200000	≥200000	≥200000	≥200000	≥200000
				$K_{d,int}$	≥1500	≥700	≥380	≥450	≥1000	610	≥140	≥610	≥450	≥610	≥1400	≥610
10m *YB19-6*		8.9	1.24%	$K_{d,obs}$	≥200000	≥200000	≥200000	≥200000	≥200000	≥200000	≥200000	≥200000	≥200000	≥200000	≥200000	≥200000
				$K_{d,int}$	≥2300	≥1100	≥600	≥710	≥1700	≥1200	≥230	≥960	≥710	≥960	≥2300	≥960
AZM	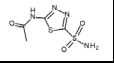	7.0	50%	$K_{d,obs}$	2400	46	40000	87	840	140	220	13	21	130	79	63
				$K_{d,int}$	1100	9.8	4600	12	270	34	9.8	2.4	2.9	24	35	12

[a]Observed values were determined using 50 mM sodium phosphate buffer at pH 7.0 containing 100 mM sodium chloride, 50 μM ANS dye, and 2% (v/v) DMSO. $K_{d,int}$s were calculated according to eq 1 (see the Experimental Section). Values with a "≥" sign show that they are at the detection limit of ≥200 000 nM of $K_{d,obs}$ according to the highest used ligand concentration. The intrinsic value limits vary for different CAs and compounds due to differences in pK_a. $pK_{a,SA} - pK_a$ of the sulfonamide group; $pK_{a,CA} - pK_a$ value of water molecule bound to Zn(II) in the active site of CA; AZM, acetazolamide (a standard inhibitor). [b]Not determined due to solubility issues or low intensity of the spectrum curves. The $pK_{a,SA}$ value was assigned based on similarities in chemical structure.

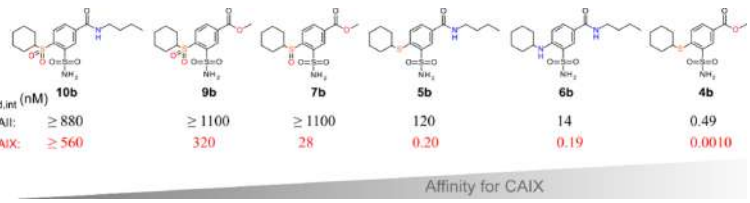

Figure 2. Compounds are arranged in the order of increasing affinity for CAIX. Compound **4b** had the highest affinity and selectivity for CAIX. The intrinsic dissociation constants (in nM units) are compared for CAII and CAIX, while values for the remaining CAs are listed in Table 1.

0.0030 nM) to most of the compounds in this group, is a few hundred times more selective for CAIX, whereas, for example, **4b** (*cyclohexyl*) is only a few tens of times more selective for CAIX and can be considered a strong binder to several undesired CAs. On the other hand, the 4-methylsulfanyl- substituted compound **4h** is no longer selective. Thus, the hydrophobic interaction made a significant contribution to affinity for CAIX, and selectivity was mainly obtained by the size of the substituent when the binding to CAIX was optimal and binding to other CAs was limited by steric interference. Analogous benzamides were much weaker binders of CAs. Most benzamides exhibited no interaction with CAs. Nevertheless, all compounds in this series bound to CAIX and were, in most cases, at least several dozen times more selective for it than for other CAs.

Sulfanyl vs Sulfinyl vs Sulfonyl Compounds. Different forms of sulfur oxidation led to drastically different affinities for CAs. A higher degree of oxidation in these compounds weakened the affinity. However, in our opinion, it was not the oxidation itself that had the main influence, but rather the conformation of the compound. The affinity of all sulfinyl- compounds with all CAs was significantly weaker than analogous sulfanyl- compounds. The decrease in affinity varied depending on the CA isozyme and the substituents. Therefore, no generalized observations could be made. For example, compound **7a** did not bind to CAI and CAVA, but the weak affinity was determined for CAIII, with all other CAs the interactions were similar and did not exceed more than 10-fold in most cases and there was no selectivity for CAIX. Compounds **7b**, **7h**, and **7i** did not bind or bind weakly and nonselectively to all CAs. Except for **7b**, it is bound only to CAIX with 28 nM. The $K_{d,int}$ of compounds **7k**, **7l**, and **7m** were 0.63, 0.72, and 0.24 nM, respectively. Also, there was a similar affinity for CAXIII and CAXIV and weaker for the other CAs. From compounds **5(a–d, f, g, j–m)** to **8(a, k–m)** decreased affinity for all CAs.

https://doi.org/10.1021/acs.jmedchem.5c01421
J. Med. Chem. XXXX, XXX, XXX−XXX

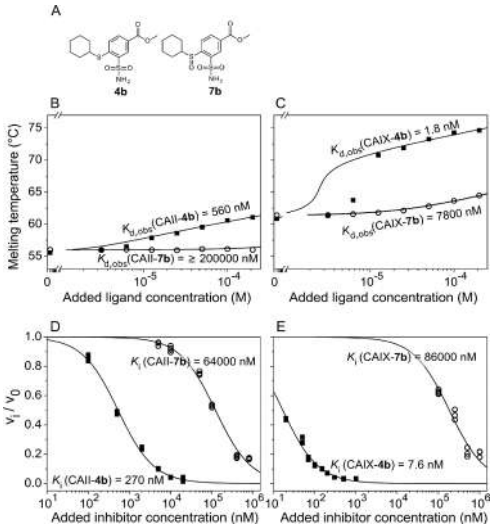

Figure 3. Compound affinity was determined by two assays in this study. (A) Chemical structures of two compounds whose binding data are shown below. (B) and (C) Fluorescent thermal shift assay data (FTSA) of compounds **4b** (closed squares) and **7b** (open circles) binding to CAII and CAIX, respectively. (D) and (E) Stopped-flow carbon dioxide hydration assay (SFA) data of compounds **4b** (closed squares) and **7b** (open circles) inhibition of CAII and CAIX, respectively. The dissociation constants (K_d) or inhibition constants (K_i) are given next to the corresponding curves. It is important to note that the experimental conditions of the methods were slightly different: FTSA, pH 7.0, 37 °C, while for SFA, pH 7.5, 25 °C.

Switching to sulfonyl compounds reduced the affinity and abolished the selectivity for CAIX. **9b** only bound to CAVII, CAIX, CAXIII, and CAXIV with $K_{d,int}$ 130, 320, 1100, and 680 nM, respectively. The most strongly interacting compound in this series was **9i**, e.g., $K_{d,int}$ of CAVI—1.7 nM, CAIX—3.2 nM but also bound to other CAs quite similarly. Meanwhile, compounds **10(b, k−m)** did not bind to any isozymes, only a couple of measurements showed a weak interaction.

4-Sulfanyl- vs 4-Amino-Substituted. Comparing **5b** vs. **6b** and **5c** vs. **6c**, in most cases, the dissociation constants differed

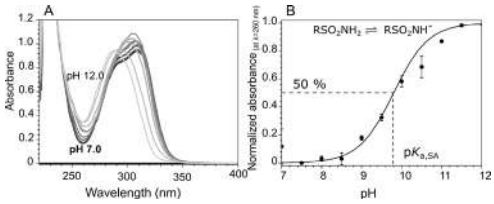

Figure 4. Spectrophotometric determination of the sulfonamide group deprotonation pK_a for compound **4b**. (A) Absorption spectra of compound **4b** in solutions at various pH at intervals of 0.5 pH units at 37 °C. (B) Normalized absorbance at 260 nm was plotted as a function of pH, and the pK_a value was determined as a midpoint of the curve. The data points are the mean points of two repeats ((A) shows one repeat for simplicity), with standard deviations. The pK_a value of compound **4b** was 9.74 ± 0.13 (±1.3%) with a confidence interval [9.62−9.87] of 95%.

only a few times, and the constants for CAIX did not exceed the margin of error. The S or N atom in the same position of the compound almost did not change the affinity for all isozymes. Compound **6e** (cyclooctyl-substituted) selectively interacted with CAIX, $K_{d,int}$ of CAIX—0.53 nM, CAXII—39 nM, and CAXIV—12 nM. It did not bind to other CAs. Most likely the selectivity was due to the size of the active site pocket.

X-ray Crystal Structures of Compound Binding to CAII and CAXIII. Nine crystal structures were determined by X-ray crystallography, the complexes of CAII with compounds **2**, **3**, **4c**, **4d**, **4h**, CAIX with **4d** and **5b**, and CAXIII with **4c** and **4d**. Table 3 lists the data collection and refinement statistics. Figure 5 shows the electron density maps of these compounds in the active site of CAs. Two molecules of compound **4h** were identified in the active site of CAII, one conventionally formed a coordination bond between the sulfonamide group and zinc, and the other was independently located near the periphery of the active site. The localization of both separated molecules relative to the same zinc is shown in Figure 5E,F. The main highlights of the identified protein−ligand interactions are described below and illustrated in Figure 6.

*Structures of **2** vs **3** Bound to CAII.* Starting compounds **2** and **3** used in the synthesis differed by one substitution at the *meta* position relative to the sulfonamide group, ester vs. amide. Figure 6A,B shows the position of these compounds in the active site of CAII. Both compounds retained the same position of the sulfonamide group and the chlorine atom in the active site of

Table 2. Inhibition Constants and IC_{50} (in nM Units) of CAII and CAIX with Compounds Obtained by Stopped-Flow Carbon Dioxide Hydration Assay (SFA) at 25 °C[a]

	K_i (nM)		IC_{50} (nM)	
compound	CAII	CAIX	CAII	CAIX
4a	25 ± 1.3	5.4 ± 0.5	47 ± 2.6	12 ± 0.5
4b	270 ± 20	7.6 ± 0.5	530 ± 40	16 ± 1.3
4c	210 ± 30	37 ± 3.5	400 ± 50	79 ± 7
4d	120 ± 10	51 ± 6	230 ± 20	110 ± 12
4h	9200 ± 500	1300 ± 200	18,000 ± 1000	2700 ± 400
7a	63 ± 6	360 ± 30	120 ± 12	760 ± 60
7b	64,000 ± 7500	86,000 ± 16,000	100,000 ± 10,000	200,000 ± 30,000
7h	3400 ± 200	7600 ± 700	6500 ± 300	16,000 ± 1600
9a	34,000 ± 4000	3700 ± 600	65,000 ± 7000	7800 ± 1300

[a]Experiments were performed using 20 mM HEPES Na at pH 7.5, 20 mM Na_2SO_4, and 0.2 mM Phenol Red.

https://doi.org/10.1021/acs.jmedchem.5c01421
J. Med. Chem. XXXX, XXX, XXX−XXX

Table 3. X-ray Diffraction Data Collection and Refinement Statistics

isozyme—ligand	CAII—**2**	CAII—**3**	CAII—**4c**	CAII—**4d**	CAII—**4h**	CAIX—**4d**	CAIX—**5b**	CAXIII—**4c**	CAXIII—**4d**
PDB ID	9FPT	9FPU	9FPQ	9FPR	9FPS	9R8X	9R8Y	9FPV	9FPW
				Data Collection Statistics					
space group	$P12_11$	$P12_11$	$P12_11$	$P12_11$	$P12_11$	H3	H3	$P2_12_12_1$	$P2_12_12_1$
unit-cell parameters (a, b, c (Å); α, β, γ (°))	a = 42.1, b = 40.9, c = 71.7, $\alpha = \gamma$ = 90, β = 104.0	a = 42.0, b = 41.1, c = 71.9, $\alpha = \gamma$ = 90, β = 104.2	a = 42.3, b = 41.3, c = 72.2, $\alpha = \gamma$ = 90, β = 104.2	a = 42.3, b = 41.3, c = 72.1, $\alpha = \gamma$ = 90, β = 104.5	a = 42.3, b = 41.2, c = 72.0, $\alpha = \gamma$ = 90, β = 104.4	$a = b$ = 152.5, c = 172.4, $\alpha = \beta$ = 90, γ = 120	$a = b$ = 151.9, c = 173.7, $\alpha = \beta$ = 90, γ = 120	a = 55.1, b = 58.0, c = 160.2, $\alpha = \beta = \gamma$ = 90	a = 55.5, b = 58.4, c = 160.7, $\alpha = \beta = \gamma$ = 90
resolution range (Å)	69.6−1.2	40.7−1.1	70.0−1.5	40.0−1.5	39.9−1.4	47.95−2.0	47.8−1.95	80.1−1.7	40.2−1.9
unique reflections number	75321	87594	38824	41447	47284	101012	108927	57402	42102
R_{merge}, overall (outer shell)	0.04 (0.38)	0.05 (0.31)	0.05 (0.25)	0.05 (0.39)	0.04 (0.38)	0.08 (1.18)	0.21 (1.30)	0.09 (0.32)	0.12 (0.31)
I/σ overall (outer shell)	16.9 (3.5)	13.7 (3.8)	15.9 (4.9)	19.6 (4.6)	24.2 (4.7)	21.1 (2.3)	7.1 (1.5)	16.8 (7.4)	13.0 (7.6)
multiplicity overall (outer shell)	6.8 (6.7)	6.6 (6.0)	6.6 (6.4)	7.0 (6.9)	7.0 (6.8)	10.4 (10.5)	10.4 (9.9)	13.2 (13.1)	13.1 (13.4)
completeness (%) overall (outer shell)	96.7 (94.0)	96.0 (91.3)	99.6 (99.2)	98.7 (97.7)	97.6 (94.9)	100.0 (100.0)	100.0 (100.0)	100 (100)	100 (100)
Wilson B-factor	12.8	11.4	17.8	15.5	17.0	28.0	22.4	16.9	22.5
				Refinement Statistics					
R_{work}	0.14	0.15	0.17	0.14	0.14	0.17	0.21	0.16	0.19
R_{free}	0.18	0.17	0.20	0.21	0.19	0.21	0.25	0.19	0.23
RMSD bond lengths (Å)/ angles (°)	0.02/2.13	0.02/2.26	0.01/1.80	0.01/2.04	0.01/2.02	0.01/1.81	0.01/1.73	0.01/1.90	0.01/1.57
average B factors (Å^2): all atoms/inhibitors	22.7/17.2	19.6/16.9	21.6/21.9	20.1/15.7	21.8/21.7	31.9/50.4	30.7/39.4	21.6/32.5	25.9/35.6
Ramachandran statistics (%): favored/allowed/outliers	97/3/ 0	97/3/ 0	97/3/ 0	96/4/ 0	96/4/ 0	96/4/ 0.11	94/5/ 0.32	chain A: 98/2/ 0 chain B: 97/3/ 0	chain A: 97/3/ 0 chain B: 97/3/ 0

https://doi.org/10.1021/acs.jmedchem.5c01421
J. Med. Chem. XXXX, XXX, XXX−XXX

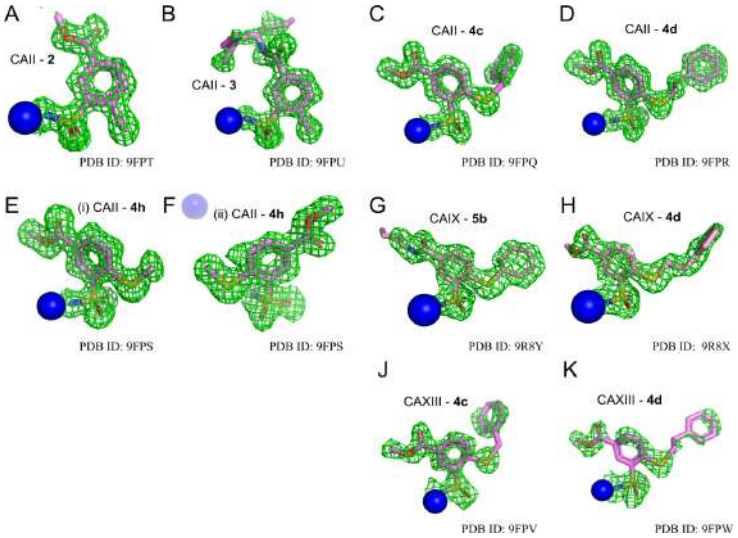

Figure 5. $|F(o) - F(c)|$ omit maps at 3σ in green for the investigated ligands in the active site of CAs. (A) CAII—**2** (PDB ID: 9FPT), (B) CAII—**3** (PDB ID: 9FPU), (C) CAII—**4c** (PDB ID: 9FPQ), (D) CAII—**4d** (PDB ID: 9FPR), (E) and (F) CAII—**4h** (PDB ID: 9FPS; two ligand molecules were identified, one bound directly to Zn in a conventional position, while the second was seen located nearby toward the edge of the active site), (G) CAIX—**5b** (PDB ID: 9R8Y), (H) CAIX—**4d** (PDB ID: 9R8X), (**J**) CAXIII—**4c** (PDB ID: 9FPV), (**K**) CAXIII—**4d** (PDB ID: 9FPW). Omit maps were taken from a refinement run of the final model without the ligand. Zinc is shown in blue.

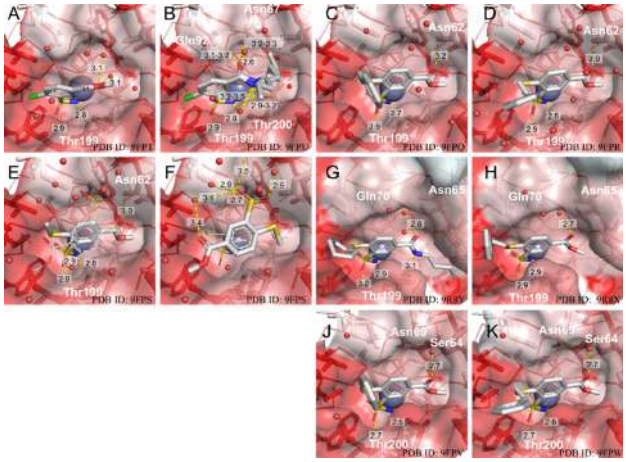

Figure 6. X-ray crystal structures of (A) CAII—**2** (PDB ID: 9FPT), (B) CAII—**3** (PDB ID: 9FPU), (C) CAII—**4c** (PDB ID: 9FPQ), (D) CAII—**4d** (PDB ID: 9FPR), (E) and (F) CAII—**4h** (PDB ID: 9FPS; two ligand molecules were identified, one bound directly (E) to Zn in a conventional position, while the second is seen located nearby toward the edge (F) of the active site), (G) CAIX—**5b** (PDB ID: 9R8Y), (H) CAIX—**4d** (PDB ID: 9R8X), (**J**) CAXIII—**4c** (PDB ID: 9FPV), (**K**) CAXIII—**4d** (PDB ID: 9FPW). The yellow dashed line represents the hydrogen bond; the distances are given in angstroms. The amino acids directly involved in hydrogen bond formation are labeled. Amino acids are colored according to hydrophobicity:[52] the most intense red color represents the most hydrophobic amino acids.

CAII. The amide substituent formed multiple hydrogen bonds with the amino acid side groups, while the ester was stabilized by a network of hydrogen bonds through water molecules. Presumably, a different network of hydrogen bonds pulled the entire molecule slightly, so a partially rotated benzene ring was observed in the crystal structure. No significant conformational changes were observed in the amino acid chains of the active site of CAII. However, the amide substituent of the compound was

https://doi.org/10.1021/acs.jmedchem.5c01421
J. Med. Chem. XXXX, XXX, XXX−XXX

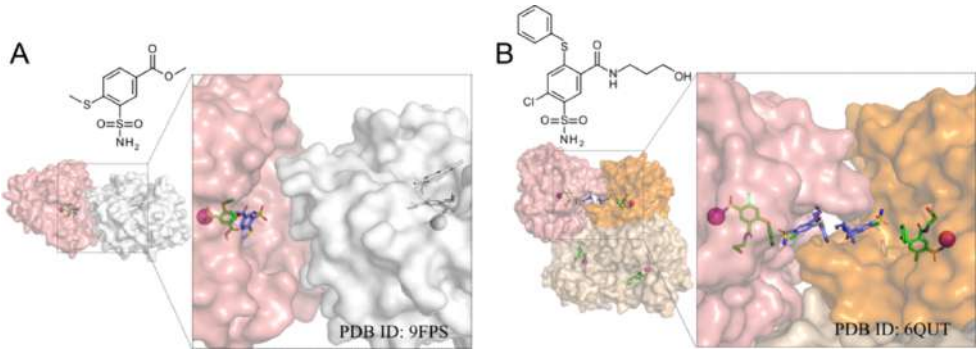

Figure 7. Unusual ligand positions in crystal structures of CAII (PDB ID: 9FPS) and CAIX (PDB ID: 6QUT, published previously[2]). The chemical structures of the ligands are shown above the crystal structures. The crystal structures represent a view of the monomers and a zoomed-in view of the active site. Zn(II) is shown as a pink sphere. Bound to Zn(II) inhibitor molecules are green and others are blue. (A) Monomer of CAII is shown in surface mode and colored salmon. The symmetric chain is colored white. (B) In the case of CAIX, only the asymmetric unit is represented. Six inhibitor molecules are bound to 4 CA IX chains. Chain C (orange) and chain D (salmon) have two inhibitor molecules, and chains A and B (beige) have one molecule. In this case, the interaction of ligands between separate chains is visible.

not in one fixed position. Instead, 3 alternative conformations of the substituent were identified in the structure. However, it should be noted that this substituent has a poor electron density, likely due to its high flexibility. Consequently, its exact arrangement cannot be determined.

*Structures of CAII with Chlorine-Substituted (**2**, **3**) vs Sulfanyl-Substituted (**4c**, **4d**, and **4h**).* The position of *ortho-sulfanyl* and chlorine-substituted compounds in the CAII active site differed significantly. The entire sulfanyl-substituted molecule was shifted to avoid steric interference but maintained a similar distance between the sulfonamide group's nitrogen and the enzyme's zinc compared to the chlorine-substituted compound. Meanwhile, the studied *ortho*-substituted compounds occupied similar positions, and the ester groups of all three compounds formed a hydrogen bond with Asn62. Notably, the electron density of all inhibitor molecules is well-defined.

*Structures of CAII vs CAIX and CAXIII with Bound Sulfanyl-Substituted (**4c** and **4d** or **5b**).* Figure 6 shows the interactions between CAII with compounds **4c** and **4d** (Figure 6C,D), CAIX with **4d** (Figure 6H), and CAXIII with compounds **4c** and **4d** (Figure 6J,K). One of the main differences was in the formed hydrogen bonds. The oxygen of the ester group of the compound formed a direct hydrogen bond with Asn62 in the active site of CAII. Meanwhile, a hydrogen bond is formed in the active site of CAIX and CAXIII through a water molecule with Gln70 and Asn65 or Ser64 and Asn69, respectively. Asn62 in CAII, Asn65 in CAIX, and Asn69 in CAXIII differ only by the numbering but correspond to the same position.

Incidentally, compound **5b** CAIX also forms the same hydrogen bond through a water molecule, and the entire molecule adopts a similar conformation. Notably, the electron density of the 17 amino acids at the N-terminus of both X-ray crystal structures of CAIX is not defined as expected. These amino acids fold in their 3D structure to form the active site of the protein. This side of the active site is called the hydrophilic part. This suggests that the bound ligand pushes these amino acids to fit fully into the active site. When comparing these structures (PDB ID: 9R8X and 9R8Y) with those existing in the PDB (e.g., PDB ID: 3iai), the clash between ligand and Tyr7 is seen without changing their arrangement.

It is important to emphasize that both **4c** and **4d** have very poor electron density in the CAXIII active center, so the arrangement of the compound should be evaluated more cautiously. On the other hand, a comparison of the structures shows that compound **4d** is more similarly located in the active sites of CAII and CAXIII, while in CAIX, it is shifted toward the hydrophilic side, which, as mentioned, is not fully visible in the X-ray structure.

Atypical Binding Position. The structure 9FPS was unique because two ligand molecules were identified as bound in the active site. One molecule was bound classically and formed a coordination bond with the zinc ion. The second formed a hydrophobic interaction with the first molecule, and hydrogen bonds with water molecules located toward the edge of the active site. This could be a crystallographic artifact or a secondary interaction with the protein.[33] A previous publication[2] identified a similar case with CAIX (PDB ID: 6QUT) (Figure 7). In that case, the molecules interacted in the active site and among themselves between the chains in an asymmetric unit. This case with CAII was different because the two chains had no interaction between ligand molecules. The active sites of symmetric chains were not oriented face-to-face. The atoms of the second nonclassical ligand were further than 5Å from the amino acids of the symmetric chain.

Molecular Docking. To understand the differences in the binding affinities of series **4**, **7**, and **9** ligands, they were docked into CAII, except for **4e** and **4f**, containing large, flexible rings that are challenging to dock. Series **4** ligands were also docked into CAIX and CAXIII, to compare with crystal structures and thus assess the docking accuracy. To reduce bias, different receptors (PDB IDs – CAII: 3HS4; CAIX: 6G9U, chain A; CAXIII: 4KNN, chain A) were chosen instead of the new X-ray structures presented in this paper.

To mimic the donor–acceptor bond between the zinc ion and the sulfonamide nitrogen of the ligand, we employed constrained docking using the Smina program.[34] The constraint forced the sulfonamide nitrogen to maintain its original position in the X-ray structure. The generated poses were afterward

https://doi.org/10.1021/acs.jmedchem.5c01421
J. Med. Chem. XXXX, XXX, XXX–XXX

rescored using the Vinardo scoring function.[35] Vina[36] and GNINA[37] Machine-learning-based scoring functions were found to be inferior to Vinardo for this system, and therefore only the latter was employed for further analysis. The pose with the best rescored affinity that matched the X-ray conformation of the benzenesulfonamide moiety was then chosen as the representative best docked structure (in all cases, for ligand **4** series, it was ranked 1 by Vinardo, except for **4j**, where the correct benzenesulfonamide conformation was ranked 3). The best docked poses for CAII are shown in Figure 8A. The Pearson correlation coefficient R with the experimental *intrinsic* binding affinities to CAII for the best docked poses was 0.87. Figure 8B plots the corresponding computed and experimental binding affinities for CAII and CAIX (values listed in Table S1 in the Supporting Information). Notably, for CAII, the scoring function correctly predicts the best binder, **4m**, and the four worst binders (**4g**–**j**). The panel also shows the correspondence between the experimental and predicted binding affinities for CAIX, with R = 0.66.

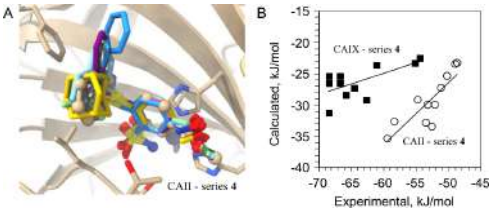

Figure 8. (A) Docked series **4** ligands (see main text for details) superposed onto the X-ray structure of **4c** (PDB ID: 9FPQ; rendered using ball-and-stick representation) in a complex with CAII. Note that hydrophobic substituents stack against the Phe131 side chain. (B) Computed ligand binding affinities to CAII (circles) and CAIX (squares) using Vinardo scoring function plotted against the experimental binding affinities—intrinsic Gibbs energy changes. The Pearson correlations R of the plotted points are 0.87 for CAII and 0.66 for CAIX. The large difference between the computed and experimental binding affinities is because the Vinardo scoring function does not take into account the interaction with zinc. However, it can be assumed to be approximately equal for all ligands.

Validation of the Docking Protocol via Comparison with the X-ray Structures. The proposed docking and scoring protocol was further validated by comparing the predicted docked poses of some of the ligands with their conformations in the newly reported X-ray structures. Figure S4A–C shows the ranked poses of ligands **4c**, **4d**, and **4h** compared against their X-ray conformations in the complex with CAII. The heavy atom Root Mean Square Deviation (RMSD) between the docked and X-ray conformation is 2.03, 3.13, and 0.46 Å, respectively. For the first two ligands, however, the rank 2 conformations are close to the X-ray conformation (**4c**: 0.61 Å; **4d**: 0.67 Å, see Figure S4A,B).

To further validate the chosen docking protocol, **4d** and **5b** were docked into CAIX (PDB ID: 6G9U, chain A). The best-scored poses after reranking using Vinardo are shown in Figure S5. The corresponding heavy atom RMSDs for **4d** and **5b** are 2.18 and 0.92 Å, respectively, and despite the RMSD for **4d** being above 2 Å, the binding mode is captured by the docking reasonably well, especially since the receptor used for docking was originally bound to a ligand from a chemically different series.

Compounds **4c** and **4d** were also docked into the CAXIII receptor (PDB ID: 4KNN, chain A). Similarly to CAIX, the docking protocol picked the docked pose with the approximately correct binding mode (with RMSDs equal to 1.90 and 0.95 Å, respectively) (Figure S6).

Docking of Series 7 and 9 Compounds. Since series **4** compounds using the docking protocol described above can reproduce the scaffold rather well and generally seem to stack the hydrophobic substituents reasonably, we applied a similar procedure by docking series **9** ligands into CAII as a model protein, in hopes that it will help to explain a difference between the binding affinities of series **4** and **9**. Docking using the same protocol led to comparable binding affinities between the two series (not shown). However, experiments indicate that **9** binds worse by several orders of magnitude, and rescored constrained pose affinities for this series exhibit practically no correlation with the experiment ($R \cong 0.12$). A careful examination of the docking results for series **9** revealed the source of the poor binding affinities and the poor performance of the docking score. Figure 9A displays the best ranking pose of **9a**. While the phenyl substituent of **9a** stacks well with Phe131 side chain, the two sulfonyl moieties exhibit an apparent clash against each other.

To further explore this clash, we ran simulations of a simple compound 2-(methylsulfonyl)benzenesulfonamide containing sulfonamide and methylsulfonyl groups at the *ortho*-positions on a benzene ring. The lowest energy conformer for this compound was generated using CREST software[38] using semiempirical GFN2-xTB wave function,[39] and afterward reoptimized in the implicit solvent using the Density Functional Theory (DFT) approach with the GAMESS-US program.[40] In the lowest energy conformer, sulfonamide nitrogen forms a hydrogen bond with the sulfonyl oxygen at the *ortho* position (Figure 9B, bottom). The approximate conformational energy of the docked conformation was also computed using DFT, keeping frozen the sulfonamide S–N and methylsulfonyl S–C bond torsional angles for the benzene ring, and optimizing the rest of the 2-methylsulfonylbenzenesulfonamide molecule (Figure 9B, top). The freezing of the select torsions was necessary because the DFT calculation lacks the protein environment that keeps them at certain values seen in docking. The energy difference between the lowest energy and the docked conformers in Figure 9B was 53.8 kJ/mol. It became clear that the used scoring function did not report a correct binding energy of the conformation in Figure 9A because the Vinardo scoring function neither takes into account the change of the ligand conformation when going from the solution into the receptor, nor the ligand intramolecular energy (in fact, none of the several built-in scoring functions in Smina do). This means that in the conformation shown in Figure 9A the 2-methylsulfonyl group must rotate to avoid the rather severe clash with the sulfonamide oxygens (Figure 9B, top), and by doing so the hydrophobic substituent rotates away from Phe131, potentially yielding other clashes with the protein and leading to the poor binding energies.

Series **7** compounds are more complex to investigate because two enantiomers of the S atom of sulfinyl exist (Figure 9C,D). We will explore the behavior of sulfinyl-containing series **7** using compound **7a** as an example. One of its docked enantiomers, (*S*)-**7a** forms sulfonyl-sulfinyl clash (Figure 9C and the top left part of Figure 9D) similar to what we found for **9a**. The docked (*R*)-**7a** enantiomer is about 1.7 times more stable compared to the (*S*)- enantiomer because of the lack of the clash (Figure 9D,F). Calculations also show that in the absence of the protein,

https://doi.org/10.1021/acs.jmedchem.5c01421
J. Med. Chem. XXXX, XXX, XXX–XXX

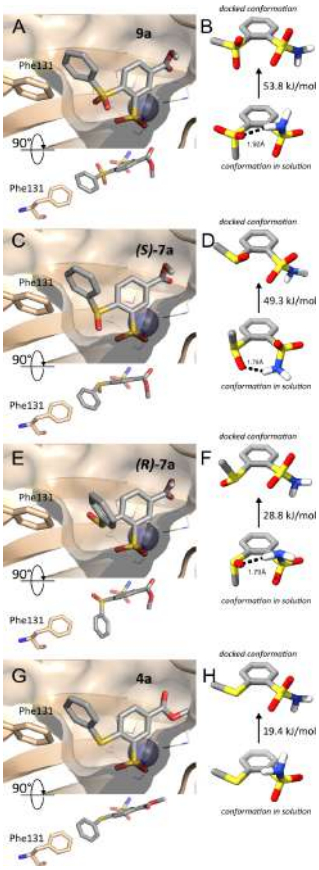

Figure 9. Best ranking docked pose of **9a**, (S)-**7a**, (R)-**7a**, and **4a** in the active site of CAII as a model protein. (A) Best-ranking docked pose of **9a**. While the phenyl substituent stacks well with the Phe131 side chain, the two SO_2 moieties presumably clash. (B) Two conformations of 2-(methylsulfonyl)benzenesulfonamide: Top: conformation with two benzene-to-S bond dihedrals constrained so that it is similar to the docked conformation in (A); bottom: lowest energy conformation with an intramolecular H-bond that is likely to be found in solution. The energy difference between the two rotamers computed using density functional theory is 53.8 kJ/mol. The fact that the used scoring function does not take into account this difference explains why the calculated affinities (not shown) do not match the experimental values. (C), (E) Best-ranked docked conformations of *(S)*- and *(R)*-**7a**, correspondingly. (D), (F) Top: the conformations 2-(methylsulfinyl)-benzenesulfonamide, matching the docked geometries in (C) and (E). Bottom: The lowest energy conformer with an intramolecular H-bond, presumably existing in solution. The docked *(R)*- enantiomer is much more stable due to the lack of clashes present in the docked *(S)*-enantiomer. (G) Best-ranking docked pose of **4a**. (H) Two conformations of 2-methylsulfanylbenzenesulfonamide: Top: the optimized with constraints conformation matching the docked conformation; bottom: The lowest energy conformer. Compared with the sulfinyl- and sulfonyl-forms, the docked conformation for the sulfanyl analog is the most stable, which is also reflected in the binding affinities.

the preferred conformation **7a** (of either chirality) has an intramolecular H-bond (Figure 9D,F, bottom).

For comparison, we also used DFT calculations of the 2-methylsulfanylbenzenesulfonamide molecule to estimate the stability of the docked **4a** (Figure 9G), which does not seem to exhibit clashes. Comparison of Figure 9B,D,F,H shows that the docked conformer **4a** is ∼1.5 times more stable than the most stable docked conformer of **7a** and nearly 3 times more stable than docked **9a**, corresponding to the experimentally determined binding affinities that are best in series **4**, followed by **7** and **9**. Interestingly, calculations suggest that one reason for the relative stability of docked **4** is the lack of the intramolecular hydrogen bond in solution (Figure 9H, bottom), and this observation could be potentially used in designing better binders for carbonic anhydrases, or even other receptors.

DISCUSSION

Recognition of the pockets on the protein surface by small-molecule ligands is still rather poorly understood, and it is not possible to accurately calculate the thermodynamic binding parameters.[41] Primary sulfonamide compounds are known to inhibit CA isozymes by binding to the catalytic Zn(II). Chemical variation of the remaining molecule often has a limited influence on binding affinity and selectivity. However, some chemical changes made near the sulfonamide group have a significant impact and may change the behavior from strong binder to completely undetectable binding. To investigate this phenomenon, we synthesized *ortho*-substituted benzenesulfonamides, determined their binding affinity to all catalytically active isoforms of human carbonic anhydrases, obtained crystal structures with CAII, CAIX, and CAXIII, and performed molecular docking. Different oxidation forms of the linker at the *ortho* position were used: −S−, −SO−, and $-SO_2-$. Compounds with −SO− or $-SO_2-$ linker were much weaker binders to any CA isozyme than compounds with the −S− linker. Several reasons could cause this. First, a substituent with a higher oxidation state exhibits a stronger electron-withdrawing effect, thus lowering the pK_a of the amine of the sulfonamide group and causing stronger binding. Second, the linker oxygen atoms may prevent the easier rotation of the ligand molecule bonds and prevent conformational changes needed for the ligand to adapt to the protein surface. Third, the oxygen atoms take additional space, and the steric hindrance could be an essential factor in diminishing the binding affinity.

To test the electron-withdrawing effect, the pK_a values of compounds were determined experimentally. The pK_a of compounds containing −S− linker was almost an entire pH unit higher than compounds with linkers −SO− or $-SO_2-$. Sulfonamides bind to CA in their negatively charged deprotonated form.[42] Therefore, the lowering of sulfonamide pK_a increases the fraction of the binding-ready deprotonated sulfonamide and thus increases the observed affinity. This effect is simply the effect of compound availability in the proper form. To eliminate this misleading increase in affinity, we subtract the fraction effects and calculate the *intrinsic* affinity. The intrinsic dissociation constants of all compounds are provided next to the observed values in the table. In all cases, the intrinsic affinities are higher than the observed ones. The intrinsic values show the 'real' affinities between the binding components in the binding-ready protonation state. These values should be used in drug design to explain the structure−function relationship of the compound effects and not the experimentally observed ones. However, the experimentally observed affinity values show the

https://doi.org/10.1021/acs.jmedchem.5c01421
J. Med. Chem. XXXX, XXX, XXX−XXX

affinities observed by any experimental technique, and the values are biologically relevant. They should be used to calculate the bound fractions and drug effect at particular conditions.

Furthermore, the compounds with a higher oxidation state (**7a, b, h, i, k−m** and **9a−d, h, i, l, m**) did not bind or bind with lower affinity than compounds **4a−d, f−m**. Even the compounds **7h** and **9h** with the smallest methyl substituent did not match the sulfanyl compound **4h** in affinity. The main reason for this was the allowed conformations of the compounds, which were calculated using quantum Density Functional Theory (DFT). The oxygen atoms limited both the flexibility of the molecule in finding the optimal position and acted as a steric hindrance. The present study shows that the *ortho* modifications had a more significant effect than the *para* variations.[21]

The highest affinity for CAIX in this study was exhibited by compound **4b** (methyl 4-cyclohexylsulfanyl-3-sulfamoylbenzoate). Previously we have designed similar compounds bearing 2-chloro or 2-bromo substituents that exhibited slightly higher affinity for CAIX.[20] Here, we have intentionally omitted the halogen atoms to synthesize the *ortho*-substituted compounds more easily and explore the binding without halogens. It was also easier to synthesize compounds with an amide substituent in the *meta* position. The length of these amide-substituted compounds was of limited importance in the previous study but had a significant influence on this study, likely due to reasons of steric hindrance.

Sulfonamide compounds usually bind to CA isozymes by forming a coordination bond between the Zn(II) and sulfonamide amino groups. This bond significantly increases the affinity, but is not necessary for binding to occur.[43] Removal of the metal or change of the metal with another demonstrated that the coordination bond contribution is additive and metal-dependent. Strongly binding compounds like brinzolamide to CAII also bind to the Zn-free apoCAII. The energy contribution of the coordination bond could be determined by using a metal-exchange approach.

In the crystal structure of compound **4h** bound to CAII, two well-resolved compound molecules were bound in the active site. The first was bound in a conventional way forming a coordination bond with the Zn(II), but the second was bound to the protein residues without forming a coordination bond with the Zn(II). This second compound molecule did not bind solely due to crystal-forming effects because it did not bind to the second protein molecule. Therefore, the binding of the second molecule is likely not an artifact. However, the presence of the second molecule in the crystal structure does not mean that it is bound as strongly, nor that we can measure its binding affinity experimentally. Binding assays showed that the stoichiometry here was 1:1, and the affinity of the second molecule was likely weak compared to the first one. Compound concentration in the crystallization experiments was relatively high, millimolar, thus the second molecule could be seen in the crystal structure even if the K_d was in the millimolar range and therefore not interfering in any binding assays. This also means that the second molecule is biologically irrelevant and would not play an essential role in drug design.

CONCLUSIONS

The strategy to acidify the pK_a of *ortho* sulfanyl-substituted benzenesulfonamides by oxidation, with the goal of increased affinity to CA, yielded an unexpected drop of affinity in the order of hundreds of thousands of times. Small changes in chemical structures influenced the flexibility of the molecule's substituents and steric restrictions on interactions with proteins. Furthermore, some minor changes led to the discovery of novel CAIX inhibitors with high affinity and selectivity.

EXPERIMENTAL SECTION

Organic Synthesis. All starting materials and reagents were commercial products used without further purification. Melting points of the compounds were determined in open capillaries on a Thermo Scientific 9100 Series and are uncorrected. ^{1}H and ^{13}C NMR spectra (Figure S7) were recorded on a (400 and 100 MHz, respectively) spectrometer in DMSO-d_6 using residual DMSO signals (2.52 and 40.21 ppm for ^{1}H and ^{13}C NMR spectra, respectively) as the internal standard. TLC was performed with silica gel 60 F254 aluminum plates (Merck) and visualized with UV light. Column chromatography used silica gel 60 (0.040−0.063 mm, Merck). High-resolution mass spectra (HRMS) were recorded by an Agilent TOF 6230 equipped with an Agilent Infinity 1260 HPLC system (Agilent Technologies). HPLC verified the purity of final compounds to be >95% (Figure S8) using the Agilent Infinity 1260 instrument with a ZORBAX Eclipse Plus C18 Rapid Resolution 4.6 × 100 mm 3.5 μm column, ZORBAX Eclipse Plus-C18 4.6 × 12.5 mm 5.0 μm analytical guard column, eluents A − 20 mM ammonium acetate (pH = 6.9 of unadjusted solution) and B − 100% MeOH was used. HPLC gradient elution with a flow rate of 0.80 mL/min was used, B gradient: 0−10 min 55−95%, 10−14 min 95%. UV detection was recorded at 254 nm. Figure S9 contains ESI-MS spectra of representative compounds.

*Methyl 4-Chloro-3-sulfamoyl-benzoate (**2**).* 4-chloro-3-sulfamoyl-benzoic acid **1** (1.78 g, 7.55 mmol, Sigma-Aldrich) was refluxed in MeOH (30 mL) with concentrated H_2SO_4 (0.3 mL) for 8 h. The reaction mixture was concentrated under reduced pressure. Residue was filtered, washed with H_2O and crystallized from H_2O:MeOH(4:1). Yield: 1.70 g, 91%, mp 129−130 °C (Literature[44] mp 124−125 °C).

^{1}H NMR (400 MHz, DMSO-d_6) δ ppm: 3.91 (s, 3H, C**H**$_3$O), 7.80 (d, J = 8.4 Hz, 1H, Ar**H**), 7.84 (s, 2H, $SO_2N\mathbf{H}_2$), 8.14 (dd, J = 8.4 Hz, J = 2.1 Hz, 1H, Ar**H**), 8.52 (d, J = 2.1 Hz, 1H, Ar**H**).

*N-Butyl-4-chloro-3-sulfamoyl-benzamide (**3**).* The mixture of 4-chloro-3-sulfamoylbenzoic acid **1** (500 mg, 2.12 mmol), $SOCl_2$ (0.616 mL, 8.48 mmol), and one drop DMF in toluene (6.0 mL) was refluxed for four h. Excess $SOCl_2$ and toluene were removed by distillation under reduced pressure. The crude acid chloride was dissolved in THF (20 mL) and added dropwise to a solution of *N*-butylamine (0.591 mL, 6.0 mmol) in THF (20 mL) at 0 °C and allowed stirring for one h. The mixture was warmed to room temperature and stirred for another 4 h. THF was removed under reduced pressure. The crude product was crystallized from H_2O. Yield: 492 mg, 80%, mp 172−173 °C (lit.[45] mp 171−172 °C).

^{1}H NMR (400 MHz, DMSO-d_6) δ ppm: 0.92 (t, J = 7.3 Hz, 3H, C**H**$_3$CH$_2$), 1.37 (sextet, J = 7.3 Hz, 2H, C**H**$_2$CH$_3$), 1.54 (quint, J = 7.3 Hz, 2H, CH$_2$C**H**$_2$CH$_2$), 3.29 (q, J = 6.8 Hz, 2H, C**H**$_2$NH), 7.72 (s, 2H, $SO_2N\mathbf{H}_2$), 7.77 (d, J = 8.2 Hz, 1H, Ar**H**), 8.04 (dd, J = 8.2 Hz, J = 2.0 Hz, 1H, Ar**H**), 8.45 (d, J = 2.0 Hz, 1H, Ar**H**), 8.77 (t, J = 5.5 Hz, 1H, N**H**).

*General Procedure for the syntheses of **4a−d, f, g, i−m**.* The mixture of methyl 4-chloro-3-sulfamoylbenzoate **2** (285 mg, 1,14 mmol), DMF (4.0 mL), appropriate thiol (1.25 mmol), and K_2CO_3 (630 mg, 4,56 mmol) was heated at 80 °C for 4−6 h in an inert atmosphere (argon). The mixture was cooled to room temperature, and 10 mL of H_2O was added. The product was extracted with EtOAc (3 × 8 mL). The organic layer was washed with H_2O, dried over anhydrous $MgSO_4$, filtered, and concentrated under reduced pressure.

*Methyl 4-Phenylsulfanyl-3-sulfamoyl-benzoate (**4a**).* The product was purified by flash chromatography on silica gel ($CHCl_3$:EtOAc, 6:1). Yield: 303 mg, 82%, mp 155−156 °C. (lit.[46] mp 154−157).

^{1}H NMR (400 MHz, DMSO-d_6) δ ppm: 3.86 (s, 3H, C**H**$_3$O), 7.00 (d, J = 8.4 Hz, 1H, Ar**H**), 7.55−7.62 (m, 5H, Ar**H**), 7.74 (s, 2H, $SO_2N\mathbf{H}_2$), 7.93 (dd, J = 8.4 Hz, J = 1.9 Hz, 1H, Ar**H**), 8.46 (t, J = 1.9 Hz, 1H, Ar**H**).

https://doi.org/10.1021/acs.jmedchem.5c01421
J. Med. Chem. XXXX, XXX, XXX−XXX

^{13}C NMR (100 MHz, DMSO-d_6) δ ppm: 52.9, 126.8, 129.0, 129.2, 130.5, 130.8, 131.0, 132.6, 135.5, 140.8, 144.2, 165.4.

HRMS calcd for $C_{14}H_{13}NO_4S_2$ [(M+H)$^+$]: 324.0359, found: 324.0354.

*Methyl 4-Cyclohexylsulfanyl-3-sulfamoyl-benzoate (**4b**).* The product was purified by flash chromatography on silica gel ($CHCl_3$:EtOAc, 7:1). Yield: 315 mg, 84%, mp 119−120 °C.

^{1}H NMR (400 MHz, DMSO-d_6) δ ppm: 1.26−1.99 (m, 10H, C**H** cyclohexyl), 3.61 (m, 1H, C**H**S), 3.88 (s, 3H, CH_3O), 7.47 (s, 2H, SO_2NH_2), 7.74 (d, J = 8.4 Hz, 1H, Ar**H**), 8.04 (dd, J = 8.3 Hz, J = 1.9 Hz, 1H, Ar**H**), 8.43 (d, J = 1.9 Hz, 1H, Ar**H**).

^{13}C NMR (100 MHz, DMSO-d_6) δ ppm: 25.7, 25.8, 32.5, 44.4, 52.9, 100.0, 125.9, 129.1, 132.3, 141.7, 142.8, 165.6.

HRMS calcd for $C_{14}H_{19}NO_4S_2$ [(M+H)$^+$]: 330.0828, found: 330.0833.

*Methyl 4-Benzylsulfanyl-3-sulfamoyl-benzoate (**4c**).* The product was purified by flash chromatography on silica gel ($CHCl_3$:EtOAc, 6:1). Yield: 211 mg, 55%, mp 135−136 °C.

^{1}H NMR (400 MHz, DMSO-d_6) δ ppm: 3.88 (s, 3H, CH_3O), 4.43 (s, 2H, CH_2S), 7.29−7.37 (m, 3H, Ar**H**), 7.51−7.53 (m, 2H, Ar**H**), 7.58 (s, 2H, SO_2NH_2), 7.74 (d, J = 8.3 Hz, 1H, Ar**H**), 8.02 (dt, J = 8.3 Hz, J = 1.7 Hz, 1H, Ar**H**), 8.42 (t, J = 2.2 Hz, 1H, Ar**H**).

^{13}C NMR (100 MHz, DMSO-d_6) δ ppm: 36.4, 52.9, 125.9, 127.7, 128.0, 128.9, 129.0, 129.8, 132.2, 136.0, 140.7, 143.7, 165.6.

HRMS calcd for $C_{15}H_{15}NO_4S_2$ [(M+H)$^+$]: 338.0515, found: 338.0517.

*Methyl 4-(2-Phenylethylsulfanyl)-3-sulfamoyl-benzoate (**4d**).* The product was purified by flash chromatography on silica gel ($CHCl_3$:EtOAc, 5:1). Yield: 332 mg, 83%, mp 146−147 °C.

^{1}H NMR (400 MHz, DMSO-d_6) δ ppm: 2.99 (t, J = 7.5 Hz, 2H, CH_2Ph), 3.41 (t, J = 7.5 Hz, 2H, CH_2S), 3.88 (s, 3H, CH_3O), 7.23−7.34 (m, 5H, Ar**H**), 7.51 (s, 2H, SO_2NH_2), 7.73 (d, J = 8.4 Hz, 1H, Ar**H**), 8.05 (dd, J = 8.4 Hz, J = 1.8 Hz, 1H, Ar**H**), 8.43 (d, J = 1.8 Hz, 1H, Ar**H**).

^{13}C NMR (100 MHz, DMSO-d_6) δ ppm: 33.4, 34.3, 52.9, 125.8, 126.9, 127.8, 128.8, 128.9, 129.1, 132.4, 140.2, 141.,0, 143.6, 165.6.

HRMS calcd for $C_{16}H_{17}NO_4S_2$ [(M+H)$^+$]: 352.0672, found: 352.0675.

*Methyl 4-Cyclododecylsulfanyl-3-sulfamoyl-benzoate (**4f**).* The product was purified by flash chromatography on silica gel ($CHCl_3$:EtOAc, 10:1). Yield: 203 mg, 43%, mp 167−168 °C.

^{1}H NMR (400 MHz, DMSO-d_6) δ ppm: 1.32−1.59 (m, 20H, C**H** cyclododecyl), 1.76 (m, 2H, C**H** cyclododecyl), 3.66 (m, 1H, C**H**S), 3.88 (s, 3H, CH_3O), 7.47 (s, 2H, SO_2NH_2), 7.70 (d, J = 8.4 Hz, 1H, Ar**H**), 8.07 (dd, J = 8.4 Hz, J = 2.0 Hz, 1H, Ar**H**), 8.44 (d, J = 2.0 Hz, 1H, Ar**H**).

^{13}C NMR (100 MHz, DMSO-d_6) δ ppm: 22.0, 23.2, 23.3, 24.0, 24.2, 29.2, 43.5, 52.9, 125.9, 129.0, 129.2, 132.3, 142.0, 143.2, 165.6.

HRMS calcd for $C_{20}H_{31}NO_4S_2$ [(M+H)$^+$]: 414.1767, found: 414.1773.

*Methyl 4-(1-Adamantylsulfanyl)-3-sulfamoyl-benzoate (**4g**).* The product was purified by flash chromatography on silica gel ($CHCl_3$:EtOAc, 10:1). Yield: 173 mg, 40%, mp 189−190 °C.

^{1}H NMR (400 MHz, DMSO-d_6) δ ppm: 1.63 (br s, 6H, C**H** adamantanyl), 1.98 (br s, 6H, C**H** adamantanyl), 2.00 (br s, 3H, C**H** adamantanyl), 3.90 (s, 3H, OCH_3), 7.40 (s, 2H, SO_2NH_2), 7.87 (d, J = 8.0 Hz, 1H, Ar**H**), 8.08 (dd, J = 8.0 Hz, J = 2.0 Hz, 1H, Ar**H**), 8.53 (d, J = 2.0 Hz, 1H, Ar**H**).

^{13}C NMR (100 MHz, DMSO-d_6) δ ppm: 30.1, 35.9, 43.8, 52.2, 53.0, 128.8, 128.9, 131.8, 137.7, 137.9, 147.0, 165.5.

HRMS calcd for $C_{18}H_{23}NO_4S_2$ [(M+H)$^+$]: 382.1141, found: 382.1144.

*Methyl 4-Propylsulfanyl-3-sulfamoyl-benzoate (**4i**).* The product was purified by flash chromatography on silica gel ($CHCl_3$:EtOAc, 5:1). Yield: 202 mg, 61%, mp 111−112 °C.

^{1}H NMR (400 MHz, DMSO-d_6) δ ppm: 1.05 (t, J = 7.3 Hz, 3H, CH_3CH_2), 1.71 (quint, J = 7.3 Hz, 2H, CH_3CH_2), 3.11 (t, J = 7.3 Hz, 2H, CH_2S), 3.88 (s, 3H, CH_3O), 7.54 (s, 2H, SO_2NH_2), 7.65 (d, J = 8.3 Hz, 1H, Ar**H**), 8.04 (dd, J = 8.3 Hz, J = 1.9 Hz, 1H, Ar**H**), 8.43 (d, J = 1.9 Hz, 1H, Ar**H**).

^{13}C NMR (100 MHz, DMSO-d_6) δ ppm: 13.8, 21.7, 33.9, 52.8, 125.6, 127.5, 128.9, 132.3, 140.9, 144.1, 165.6.

HRMS calcd for $C_{11}H_{15}NO_4S_2$ [(M+H)$^+$]: 290.0515, found: 290.0519.

*Methyl 4-tert-Butylsulfanyl-3-sulfamoyl-benzoate (**4j**).* The product was purified by flash chromatography on silica gel ($CHCl_3$:EtOAc, 5:1). Yield: 214 mg, 62%, mp 124−125 °C.

^{1}H NMR (400 MHz, DMSO-d_6) δ ppm: 1.43 (s, 9H, CH_3), 3.90 (s, 3H, CH_3O), 7.43 (s, 2H, SO_2NH_2), 7.91 (d, J = 8.2 Hz, 1H, Ar**H**), 8.11 (dd, J = 8.2 Hz, J = 2.0 Hz, 1H, Ar**H**), 8.52 (d, J = 2.0 Hz, 1H, Ar**H**).

^{13}C NMR (100 MHz, DMSO-d_6) δ ppm: 31.6, 49.6, 53.0, 128.4, 128.9, 132.0, 136.2, 140.0, 146.1, 165.5.

HRMS calcd for $C_{12}H_{17}NO_4S_2$ [(M+H)$^+$]: 304.0672, found: 304.0671.

*Methyl 4-Isopentylsulfanyl-3-sulfamoyl-benzoate (**4k**).* The product was purified by flash chromatography on silica gel ($CHCl_3$:EtOAc, 5:1). Yield: 265 mg, 74%, mp 92−93 °C.

^{1}H NMR (400 MHz, DMSO-d_6) δ ppm: 0.94 (d, J = 6.6 Hz, 6H, CH_3), 1.57 (td, J = 7.8 Hz, J = 6.8 Hz, 2H, CH_2CH), 1.76 (m, 1H, C**H**), 3.11 (t, J = 7.8 Hz, 2H, CH_2S), 3.88 (s, 3H, CH_3O), 7.52 (s, 2H, SO_2NH_2), 7.67 (d, J = 8.4 Hz, Ar**H**), 8.05 (dd, J = 8.4 Hz, J = 2.0 Hz, 1H, Ar**H**), 8.42 (d, J = 2.0 Hz, 1H, Ar**H**).

^{13}C NMR (100 MHz, DMSO-d_6) δ ppm: 22.6, 27.5, 30.2, 36.9, 52.8, 125.6, 127.5, 128.9, 132.3, 140.9, 144.1, 165.6.

HRMS calcd for $C_{13}H_{19}NO_4S_2$ [(M+H)$^+$]: 318.0828, found: 318.0833.

*Methyl 4-Cyclopentylsulfanyl-3-sulfamoyl-benzoate (**4l**).* The product was purified by flash chromatography on silica gel ($CHCl_3$:EtOAc, 8:1). Yield: 259 mg, 72%, mp 106−107 °C.

^{1}H NMR (400 MHz, DMSO-d_6) δ ppm: 1.55−1.65 (m, 4H, C**H** cyclopentyl), 1.73−1.78 (m, 2H, C**H** cyclopentyl), 2.18−2.23 (m, 2H, C**H** cyclopentyl), 3.84−3.92 (m, 4H, CH_3O and C**H**S), 7.50 (s, 2H, SO_2NH_2), 7.72 (d, J = 8.4 Hz, 1H, Ar**H**), 8,.04 (dd, J = 8.4 Hz, J = 2.0 Hz, 1H, Ar**H**), 8.42 (d, J = 2.0 Hz, 1H, Ar**H**).

^{13}C NMR (100 MHz, DMSO-d_6) δ ppm: 25.1, 33.3, 43.9, 52.8, 125.5, 128.4, 128.9, 132.3, 140.8, 144.7, 165.6.

HRMS calcd for $C_{13}H_{17}NO_4S_2$ [(M+H)$^+$]: 316.0672, found: 316.0677.

*Methyl 4-(1-Naphthylsulfanyl)-3-sulfamoyl-benzoate (**4m**).* The product was purified by flash chromatography on silica gel ($CHCl_3$:EtOAc, 8:1). Yield: 281 mg, 66%, mp 187−188 °C.

^{1}H NMR (400 MHz, DMSO-d_6) δ ppm: 3.83 (s, 3H, CH_3O), 6.64 (d, J = 8.4 Hz, 1H, Ar**H**), 7.54−7.64 (m, 2H, Ar**H**), 7.69 (m, 1H, Ar**H**), 7.74 (dd, J = 8.4 Hz, J = 2.0 Hz, 1H, Ar**H**), 7.93 (s, 2H, SO_2NH_2), 8.04−8.15 (m, 3H, Ar**H**), 8.22 (d, J = 8.3 Hz, 1H, Ar**H**), 8.49 (d, J = 2.,0 Hz, 1H, Ar**H**).

^{13}C NMR (100 MHz, DMSO-d_6) δ ppm: 52.9, 125.6, 126.7, 126.9, 127.3, 127.5, 128.4, 128.5, 129.1, 129.6, 132.2, 132.5, 133.8, 134.8, 136.8, 140.4, 143.9, 165.4.

HRMS calcd for $C_{18}H_{15}NO_4S_2$ [(M+H)$^+$]: 374.0515, found: 374.0511.

*Methyl 4-Methylsulfanyl-3-sulfamoyl-benzoate (**4h**).* The mixture of methyl 4-chloro-3-sulfamoylbenzoate **2** (308 mg, 1,23 mmol), DMSO (4.0 mL), sodium methanethiolate (259 mg, 3.69 mmol), and K_2CO_3 (509 mg, 3.69 mmol) was heated at 80 °C temperature for 12 h in inert atmosphere(argon). The mixture was cooled to room temperature and 20 mL brine was added. The product was extracted with EtOAc (3 × 10 mL). The organic layer was washed with H_2O, dried over anhydrous $MgSO_4$, filtered, and concentrated under reduced pressure. The product was crystallized from H_2O:MeOH(4:1). Yield: 203 mg, 64%, mp 157−158 °C.

^{1}H NMR (400 MHz, DMSO-d_6) δ ppm: 2.59 (s, 3H, CH_3S), 3.89 (s, 3H, CH_3O), 7.54 (s, 2H, SO_2NH_2), 7.61 (d, J = 8.3 Hz, 1H, Ar**H**), 8.07 (dd, J = 8.3 Hz, J = 1.4 Hz, 1H, Ar**H**), 8.42 (d, J = 1.4 Hz, 1H, Ar**H**).

^{13}C NMR (100 MHz, DMSO-d_6) δ ppm: 15.5, 52.9, 125.4, 126.6, 128.8, 132.4, 140.4, 145.1, 165.7.

HRMS calcd for $C_9H_{11}NO_4S_2$ [(M+H)$^+$]: 262.0202, found: 262.0199.

*General Procedure for the Syntheses of **5a−d, f−g, j−m**.* The mixture of *N*-butyl-4-chloro-3-sulfamoyl-benzamide **3** (111 mg, 0.381

https://doi.org/10.1021/acs.jmedchem.5c01421
J. Med. Chem. XXXX, XXX, XXX−XXX

mmol), DMF (4.0 mL), appropriate thiol (0.572 mmol), and K_2CO_3 (210 mg, 1.52 mmol) was heated at 80 °C temperature for 12 h in an inert atmosphere(argon). The mixture was cooled to room temperature and 20 mL H_2O was added. The product was extracted with EtOAc (3 × 8 mL). The organic layer was washed with H_2O, dried over anhydrous $MgSO_4$, filtered, and concentrated under reduced pressure.

*N-Butyl-4-phenylsulfanyl-3-sulfamoyl-benzamide (**5a**).* The product was purified by flash chromatography on silica gel ($CHCl_3$:EtOAc, 1:1). Yield: 71 mg, 51%, mp 109−110 °C.

^{1}H NMR (400 MHz, DMSO-d_6) δ ppm: 0.90 (t, J = 7.3 Hz, 3H, CH_3), 1.33 (sext, J = 7.3 Hz, 2H, $CH_2CH_2CH_3$), 1.52 (quint, J = 7.3 Hz, 2H, $CH_2CH_2CH_2$), 3.27 (dt, J = 6.9 Hz, J = 5.7 Hz, 2H, CH_2NH), 6.99 (d, J = 8.3 Hz, 1H, ArH), 7.51−7.58 (m, 5H, ArH), 7.60 (s, 2H, SO_2NH_2), 7.82 (dd, J = 8.3 Hz, J = 2.0 Hz, 1H, ArH), 8.38 (d, J = 2.0 Hz, 1H, ArH), 8.59 (t, J = 5.7 Hz, 1H, NH).

^{13}C NMR (100 MHz, DMSO-d_6) δ ppm: 14.2, 20.1, 31.6, 39.4, 127.5, 129.6, 129.9, 130.5, 130.6, 132.3, 132.4, 134.9, 140.7, 141.2, 164.9.

HRMS calcd for $C_{17}H_{20}N_2O_3S_2$ [(M+H)$^+$]: 365.0988, found: 365.0985.

*N-Butyl-4-cyclohexylsulfanyl-3-sulfamoyl-benzamide (**5b**).* The product was purified by flash chromatography on silica gel ($CHCl_3$:EtOAc, 1:1). Yield: 70 mg, 50%, mp 114−115 °C.

^{1}H NMR (400 MHz, DMSO-d_6) δ ppm: 0.92 (t, J = 7.3 Hz, 3H, CH_3), 1.23−1.63 (m, 10H, CH cyclohexyl and butyl), 1.72 (m, 2H, CH cyclohexyl), 1.90−1.96 (m, 2H, CH cyclohexyl), 3.29 (q, J = 6.6 Hz, 2H, CH_2NH), 3.55−3.60 (m, 1H, CHS), 7.34 (s, 2H, SO_2NH_2), 7.70 (d, J = 8.2 Hz, 1H, ArH), 7.96 (dd, J = 8.2 Hz, J = 1.2 Hz, 1H, ArH), 8.36 (d, J = 1.2 Hz, 1H, ArH), 8.64 (t, J = 5.3 Hz, 1H, NH).

^{13}C NMR (100 MHz, DMSO-d_6) δ ppm: 14.2, 20.1, 25.7, 25.8, 31.6, 32.5, 39.4, 44.8, 127.6, 129.7, 130.3, 131.6, 139.0, 142.1, 165.1

HRMS calcd for $C_{17}H_{26}N_2O_3S_2$ [(M+H)$^+$]: 371.1458, found: 371.1463.

*4-Benzylsulfanyl-N-butyl-3-sulfamoyl-benzamide (**5c**).* The product was purified by flash chromatography on silica gel ($CHCl_3$:EtOAc, 1:1). Yield: 65 mg, 45%, mp 185−186 °C.

^{1}H NMR (400 MHz, DMSO-d_6) δ ppm: 0.91 (t, J = 7.2 Hz, 3H, CH_3), 1.36 (sext, J = 7.2 Hz, 2H, CH_2CH_3), 1.53 (quint, J = 7.2 Hz, 2H, $CH_2CH_2CH_2$), 3.28 (q, J = 6.9 Hz, 2H, CH_2NH), 4.40 (s, 2H, CH_2S), 7.29 (t, J = 7.1 Hz, 1H, ArH), 7.36 (t, J = 7.1 Hz, 2H, ArH), 7.44 (s, 2H, SO_2NH_2), 7.52 (d, J = 7.1 Hz, 2H, ArH), 7.66 (d, J = 8.3 Hz, 1H, ArH), 7.94 (dd, J = 8.3 Hz, J = 1.9 Hz, 1H, ArH), 8.36 (d, J = 1.9 Hz, 1H, ArH), 8.62 (t, J = 5.6 Hz, 1H, NH).

^{13}C NMR (100 MHz, DMSO-d_6) δ ppm: 14.2, 20.1, 31.6, 36.5, 39.4, 127.6, 127.7, 127.8, 128.9, 129.7, 130.2, 131.2, 136.5, 140.2, 140.7, 165.0.

HRMS calcd for $C_{18}H_{22}N_2O_3S_2$ [(M+H)$^+$]: 379.1145, found: 379.1140.

*N-Butyl-4-(2-phenylethylsulfanyl)-3-sulfamoyl-benzamide (**5d**).* The product was purified by flash chromatography on silica gel ($CHCl_3$:EtOAc, 1:1). Yield: 95 mg, 63%, mp 116−117 °C.

^{1}H NMR (400 MHz, DMSO-d_6) δ ppm: 0.92 (t, J = 7.3 Hz, 3H, CH_3), 1.37 (sext, J = 7.3 Hz, 2H, CH_2CH_3), 1.55 (quint, J = 7.3 Hz, 2H, $CH_2CH_2CH_2$), 2.98 (t, J = 7.3 Hz, 2H, CH_2Ar), 3.28 (q, J = 6.6 Hz, 2H, CH_2NH), 3.34−3.38 (m, 2H, CH_2S), 7.25−7.27 (m, 1H, ArH), 7.31−7.33 (m, 4H, ArH), 7.35 (s, 2H, SO_2NH_2), 7.69 (d, J = 8.3 Hz, 1H, ArH), 7.99 (d, J = 8.3 Hz, 1H, ArH), 8.38 (s, 1H, ArH), 8.65 (t, J = 5.4 Hz, 1H, NH).

^{13}C NMR (100 MHz, DMSO-d_6) δ ppm: 14.2, 20.1, 31.6, 33.7, 34.4, 39.4, 126.9, 127.5, 127.9, 128.9, 129.0, 130.4, 131.3, 140.1, 140.3, 141.2, 165.1.

HRMS calcd for $C_{19}H_{24}N_2O_3S_2$ [(M+H)$^+$]: 393.1301, found: 393.1297.

*N-Butyl-4-cyclododecylsulfanyl-3-sulfamoyl-benzamide (**5f**).* The product was purified by flash chromatography on silica gel ($CHCl_3$:EtOAc, 3:1). Yield: 76 mg, 44%, mp 166−168 °C.

^{1}H NMR (400 MHz, DMSO-d_6) δ ppm: 0.93 (t, J = 7.3 Hz, 3H, CH_3), 1.24−1.59 (m, 24H, $CH_2CH_2CH_3$ and CH cyclododecyl), 1.72−1.75 (m, 2H, CH cyclododecyl), 3.29 (dt, J = 6.8 Hz, J = 5.6 Hz, 2H, CH_2NH), 3.68 (s, 1H, CHS), 7.33 (s, 2H, SO_2NH_2), 7.66 (d, J = 8.3 Hz, 1H, ArH), 7.99 (dd, J = 8.3 Hz, J = 2.0 Hz, 1H, ArH), 8.37 (d, J = 2.0 Hz, 1H, ArH), 8.64 (t, J = 5.6 Hz, 1H, NH).

^{13}C NMR (100 MHz, DMSO-d_6) δ ppm: 14.2, 20.1, 22.1, 23.4, 23.8, 23.9, 24.2, 29.4, 31.6, 39.4, 43.7, 127.6, 129.5, 130.3, 131.6, 139.7, 142.3, 165.1.

HRMS calcd for $C_{23}H_{38}N_2O_3S_2$ [(M+H)$^+$]: 455.2397, found: 455.2399.

*4-(1-Adamantylsulfanyl)-N-butyl-3-sulfamoyl-benzamide (**5g**).* The product was purified by flash chromatography on silica gel ($CHCl_3$:EtOAc, 1:1). Yield: 64 mg, 40%, mp 187−189 °C.

^{1}H NMR (400 MHz, DMSO-d_6) δ ppm: 0.91 (t, J = 6.8 Hz, 3H, CH_3), 1.34 (sext, J = 7.2 Hz, 2H, CH_2CH_3), 1.52 (quint, J = 7.2 Hz, 2H, $NHCH_2CH_2$), 1.63 (br s, 6H, CH adamantanyl), 1.95 (br s, 6H, CH adamantanyl), 2.01 (br s, 3H, CH adamantanyl), 3.28 (q, J = 6.8 Hz, 2H, $NHCH_2$), 7.28 (s, 2H, SO_2NH_2), 7.78 (d, J = 8.0 Hz, 1H, ArH), 7.98 (dd, J = 8.0 Hz, J = 2.0 Hz, 1H, ArH), 8.44 (d, J = 2.0 Hz, 1H, ArH), 8.71 (t, J = 5.6 Hz, 1H, NH).

^{13}C NMR (100 MHz, DMSO-d_6) δ ppm: 14.2, 20.1, 30.1, 31.6, 36.0, 39.5, 43.9, 51.8, 127.4, 129.8, 134.0, 134.5, 138.2, 147.3, 165.2.

HRMS calcd for $C_{21}H_{30}N_2O_3S_2$ [(M+H)$^+$]: 423.1771, found: 423.1777.

*N-Butyl-4-tert-butylsulfanyl-3-sulfamoyl-benzamide (**5j**).* The product was purified by flash chromatography on silica gel ($CHCl_3$:EtOAc, 1:1). Yield: 55 mg, 42%, mp 150−152 °C.

^{1}H NMR (400 MHz, DMSO-d_6) δ ppm: 0.91 (t, J = 7.6 Hz, 3H, CH_3), 1.30−1.37 (m, 2H, $CH_2CH_2CH_3$), 1.41 (s, 9H, $C(CH_3)_3$), 1.52 (quint, J = 7.2 Hz, 2H, $NHCH_2CH_2$), 3.28 (q, J = 6.0 Hz, 2H, $NHCH_2$), 7.31 (s, 2H, SO_2NH_2), 7.82 (d, J = 7.6 Hz, 1H, ArH), 7.99 (dd, J = 8.0 Hz, J = 1.6 Hz, 1H, ArH), 8.44 (d, J = 2.0 Hz, 1H, ArH), 8.71 (t, J = 5.8 Hz, 1H, NH).

^{13}C NMR (100 MHz, DMSO-d_6) δ ppm: 14.2, 20.1, 31.6, 31.7, 39.5, 49.4, 127.5, 130.1, 134.3, 136.2, 137.0, 146.7, 165.2.

HRMS calcd for $C_{15}H_{24}N_2O_3S_2$ [(M+H)$^+$]: 345.1301, found: 345.1295.

*N-Butyl-4-isopentylsulfanyl-3-sulfamoyl-benzamide (**5k**).* The product was purified by flash chromatography on silica gel ($CHCl_3$:EtOAc, 1:1). Yield: 98 mg, 72%, mp 130−132 °C.

^{1}H NMR (400 MHz, DMSO-d_6) δ ppm: 0.89−0.94 (m, 9H, CH_3), 1.33 (sext, J = 7.2 Hz, 2H, $CH_2CH_2CH_3$), 1.48−1.57 (m, 4H, $NHCH_2CH_2$ and SCH_2CH_2), 1.75 (hept, J = 7.6 Hz, 1H, $CH(CH_3)_2$), 3.09 (t, J = 7.8 Hz, 2H, SCH_2), 3.30 (q, J = 6.4 Hz, 2H, $NHCH_2$), 7.38 (s, 2H, SO_2NH_2), 7.61 (d, J = 8.4 Hz, 1H, ArH), 7.97 (dd, J = 8.3 Hz, J = 1.6 Hz, 1H, ArH), 8.36 (d, J = 1.7 Hz, 1H, ArH), 8.62 (t, J = 5.3 Hz, 1H, NH).

^{13}C NMR (100 MHz, DMSO-d_6) δ ppm: 14.2, 20.1, 22.6, 27.5, 30.4, 31.7, 37.2, 39.4, 127.6(2C), 130.4, 131.1, 140.6, 141.0, 165.1.

HRMS calcd for $C_{16}H_{26}N_2O_3S_2$ [(M+H)$^+$]: 359.1458, found: 359.1464.

*N-Butyl-4-cyclopentylsulfanyl-3-sulfamoyl-benzamide (**5l**).* The product was purified by flash chromatography on silica gel ($CHCl_3$:EtOAc, 1:1). Yield: 84 mg, 62%, mp 122−124 °C.

^{1}H NMR (400 MHz, DMSO-d_6) δ ppm: 0.91 (t, J = 7.2 Hz, 3H, CH_3), 1.33 (sext, J = 7.2 Hz, 2H, $CH_2CH_2CH_3$), 1.48−1.67 (m, 6H, $NHCH_2CH_2$ and CH cyclopentyl), 1.71−1.81 (m, 2H, CH cyclopentyl), 2.12−2.21 (m, 2H, CH cyclopentyl), 3.28 (q, J = 6.4 Hz, 2H, $NHCH_2$), 3.92 (quint, J = 6.0 Hz, 1H, SCH), 7.36 (s, 2H, SO_2NH_2), 7.66 (d, J = 8.4 Hz, 1H, ArH), 7.96 (d, J = 7.6 Hz, 1H, ArH), 8.36 (s, 1H, ArH), 8.61 (t, J = 5.2 Hz, 1H, NH).

^{13}C NMR (100 MHz, DMSO-d_6) δ ppm: 14.2, 20.1, 25.1, 31.7, 33.3, 39.4, 44.2, 127.6, 128.5, 130.3, 131.0, 141.0, 141.2, 165.1.

HRMS calcd for $C_{16}H_{24}N_2O_3S_2$ [(M+H)$^+$]: 357.1301, found: 357.1307.

*N-Butyl-4-(1-naphthylsulfanyl)-3-sulfamoyl-benzamide (**5m**).* The product was purified by flash chromatography on silica gel ($CHCl_3$:EtOAc, 1:1). Yield: 96 mg, 61%, mp 216−218 °C.

^{1}H NMR (400 MHz, DMSO-d_6) δ ppm: (DMSO−D_6): 0.86 (t, J = 7.6 Hz, 3H, CH_3), 1.28 (sext, J = 7.6 Hz, 2H, $CH_2CH_2CH_3$), 1.45 (quint, J = 7.2 Hz, 2H, $NHCH_2CH_2$), 3.21 (q, J = 6.8 Hz, 2H, $NHCH_2$), 6.57 (d, J = 8.4 Hz, 1H, ArH), 7.53−7.63 (m, 3H, ArH and, naphthyl-H), 7.68 (t, J = 8.0 Hz, 1H, naphthyl-H), 7.83 (s, 2H,

https://doi.org/10.1021/acs.jmedchem.5c01421
J. Med. Chem. XXXX, XXX, XXX−XXX

SO_2NH_2), 8.03 (d, J = 6.8 Hz, 1H, naphthyl-**H**), 8.08 (d, J = 8.0 Hz, 1H, naphthyl-**H**), 8.15 (d, J = 8.4 Hz, 1H, naphthyl-**H**), 8.19 (d, J = 8.4 Hz, 1H, naphthyl-**H**), 8.41 (d, J = 2.0 Hz, 1H, Ar**H**), 8.50 (t, J = 5.6 Hz, 1H, N**H**).

^{13}C NMR (100 MHz, DMSO-d_6) δ ppm: 14.1, 20.0, 31.6, 39.4, 125.8, 126.9, 127.4, 127.7, 128.1, 128.2(2C), 129.5, 130.4, 131.8, 132.1, 133.7, 134.8, 136.5, 140.4, 140.7, 165.1.

HRMS calcd for $C_{21}H_{22}N_2O_3S_2$ [(M+H)$^+$]: 415.1145, found: 415.1151.

*General Procedure for the Syntheses of **6b, c, e**.* The mixture of *N*-butyl-4-chloro-3-sulfamoyl-benzamide **3** (100 mg, 0.344 mmol) and appropriate amine (2.0 mL) was heated at 130 °C for 24 h in an inert atmosphere. The mixture was cooled to room temperature and 2 N HCl(aq) (5 mL) was added. The product was extracted with EtOAc (3 × 5 mL). The organic layer was washed with H_2O, dried over anhydrous $MgSO_4$, filtered, and concentrated under reduced pressure.

*N-Butyl-4-(cyclohexylamino)-3-sulfamoyl-benzamide (**6b**).* The product was purified by flash chromatography on silica gel ($CHCl_3$:EtOAc, 1:1). Yield: 64 mg, 53%, mp 89−91 °C.

^{1}H NMR (400 MHz, DMSO-d_6) δ ppm: 0.91 (t, J = 7.3 Hz, 3H, CH_3), 1.23−1.60 (m, 10H, $CH_2CH_2CH_3$ and C**H** cyclohexyl), 1.66−1.69 (m, 2H, C**H** cyclohexyl), 1.90−1.93 (m, 2H, C**H** cyclohexyl), 3.25 (dt, J = 6.8 Hz, J = 5.7 Hz, 2H, CH_2NH), 3.49−3.52 (m, 1H, C**H**NH), 6,17 (d, J = 7.6 Hz, 1H, N**H**-cyclohexyl), 6.84 (d, J = 8.8 Hz, 1H, Ar**H**), 7.43 (s, 2H, SO_2NH_2), 7.85 (dd, J = 8.8 Hz, J = 2.1 Hz, 1H, Ar**H**), 8.21 (d, J = 2.1 Hz, 1H, Ar**H**), 8.25 (t, J = 5.7 Hz, 1H, N**H**).

^{13}C NMR (100 MHz, DMSO-d_6) δ ppm: 14.2, 20.1, 24.4, 25.8, 31.9, 32.3, 39.2, 50.5, 111.8, 120.9, 124.5, 129.2, 132.3, 146.3, 165.4.

HRMS calcd for $C_{17}H_{27}N_3O_3S$ [(M+H)$^+$]: 354.1846, found: 354.1840.

*4-(Benzylamino)-N-butyl-3-sulfamoyl-benzamide (**6c**).* The product was purified by flash chromatography on silica gel ($CHCl_3$:EtOAc, 1:1). Yield: 40 mg, 32%, mp 132−133 °C.

^{1}H NMR (400 MHz, DMSO-d_6) δ ppm: 0.88 (t, J = 7.2 Hz, 3H, CH_3), 1.35 (sext, J = 7.2 Hz, 2H, CH_2CH_3), 1.49 (quint, J = 7.2 Hz, 2H, $CH_2CH_2CH_2$), 3.23 (dt, J = 6.8 Hz, J = 5.9 Hz, 2H, CH_2NH), 4.55 (d, J = 5.8 Hz, 2H, $PhCH_2NH$), 6.69 (d, J = 8.8 Hz, 1H, Ar**H**), 6.82 (t, J = 5.8 Hz, 1H, N**H**-benzyl), 7.23−7.39 (m, 5H, Ar**H**), 7.49 (s, 2H, SO_2NH_2), 7.77 (dd, J = 8.8 Hz, J = 2.0 Hz, 1H, Ar**H**), 8.23 (m, 2H, Ar**H** and N**H**).

^{13}C NMR (100 MHz, DMSO-d_6) δ ppm: 14.2, 20.1, 31.8, 39.2, 46.5, 111.9, 121.5, 125.1, 127.4, 128.9, 128.9, 132.1, 139.2, 146.8, 165.4.

HRMS calcd for $C_{18}H_{23}N_3O_3S$ [(M+H)$^+$]: 362.1533, found: 362.1539.

*N-Butyl-4-(cyclooctylamino)-3-sulfamoyl-benzamide (**6e**).* The product was purified by flash chromatography on silica gel ($CHCl_3$:EtOAc, 1:1). Yield: 55 mg, 42%, brownish oily residue.

^{1}H NMR (400 MHz, DMSO-d_6) δ ppm: 0.91 (t, J = 7.3 Hz, 3H, CH_3), 1.35 (sext, J = 7.3 Hz, 2H, CH_2CH_3), 1.44−1.73 (m, 14H, C**H** cyclooctyl and $CH_2CH_2CH_2$), 1.81−1.86 (m, 2H, C**H** cyclooctyl), 3.25 (dt, J = 6.9 Hz, J = 5.9 Hz, 2H, CH_2NH), 3.70−3.73 (m, 1H, C**H**NH cyclooctyl), 6.19 (d, J = 7.6 Hz, 1H, N**H**-cyclooctyl), 6.75 (d, J = 8.8 Hz, 1H, Ar**H**), 7.43 (s, 2H, SO_2NH_2), 7,.86 (dd, J = 8.8 Hz, J = 2.1 Hz, 1H, Ar**H**), 8.19 (d, J = 2.1 Hz, 1H, Ar**H**), 8.24 (t, J = 5.9 Hz, 1H, N**H**).

^{13}C NMR (100 MHz, DMSO-d_6) δ ppm: 14.2, 20.1, 23.6, 25.5, 27.2, 31.7, 31.9, 39.2, 51.9, 111.9, 120.8, 124.6, 129.3, 132.4, 146.1, 165.5.

HRMS calcd for $C_{19}H_{31}N_3O_3S$ [(M+H)$^+$]: 382.2159, found: 382.2155.

*General Procedure for the Syntheses of **7(a, b, h, i, k−m), 8(a, b, k−m)**.* The mixture of appropriate methyl 4-sulfanilsubstituted-3-sulfamoyl-benzoate (**4a, b, h, i, k−m**) or appropriate *N*-butyl-4-sulfanilsubstituted-3-sulfamoyl-benzamide (**8a, b, k−m**) (0.200 mmol), acetic acid (2.0 mL) and 30% H_2O_2 (0.090 mL, 1.15 mmol) was stirred for 12 h. Then 1% Na_2SO_3(aq) (6.0 mL) was added to the mixture and the product was extracted with EtOAc (3 × 5 mL). The organic layer was washed with H_2O, dried over anhydrous $MgSO_4$, filtered, and concentrated under reduced pressure.

*Methyl 4-(Benzenesulfinyl)-3-sulfamoyl-benzoate (**7a**).* The product was purified by flash chromatography on silica gel ($CHCl_3$:EtOAc, 3:1). Yield: 56 mg, 82%, mp 107−108 °C.

^{1}H NMR (400 MHz, DMSO-d_6) δ ppm: 3,91 (s, 3H, CH_3O), 7.48−7.53 (m, 3H, Ar**H**), 7.75−7.78 (m, 2H, Ar**H**), 8.09 (s, 2H, SO_2NH_2), 8.32 (d, J = 8.2 Hz, 1H, Ar**H**), 8.37 (dd, J = 8.2 Hz, J = 1.7 Hz, 1H, Ar**H**), 8.47 (d, J = 1.7 Hz, 1H, Ar**H**).

^{13}C NMR (100 MHz, DMSO-d_6) δ ppm: 53.3, 125.6, 126.9, 128.5, 129.9, 131.6, 132.8, 133.9, 142.3, 145.9, 149.7, 164.9.

HRMS calcd for $C_{14}H_{13}NO_5S_2$ [(M+H)$^+$]: 340.0308, found: 340.0311.

*Methyl 4-Cyclohexylsulfinyl-3-sulfamoyl-benzoate (**7b**).* The product was purified by flash chromatography on silica gel ($CHCl_3$:EtOAc, 3:1). Yield: 52 mg, 75%, mp 188−189 °C.

^{1}H NMR (400 MHz, DMSO-d_6) δ ppm: 1.14−2.07 (m, 10H, CH_2 cyclohexyl), 2.96−3.04 (m, 1H, CHSO), 3.94 (s, 3H, CH_3O), 7.97 (s, 2H, SO_2NH_2), 8.11 (d, J = 8.2 Hz, 1H, Ar**H**), 8.38 (dd, J = 8.2 Hz, J = 1.7 Hz, 1H, Ar**H**), 8.51 (d, J = 1.7 Hz, 1H, Ar**H**).

^{13}C NMR (100 MHz, DMSO-d_6) δ ppm: 20.9, 25.1, 25.4, 26.1, 28.6, 53.3, 60.9, 127.3, 129.1, 132.5, 132.6, 142.1, 146.5, 165.1.

HRMS calcd for $C_{14}H_{19}NO_5S_2$ [(M+H)$^+$]: 346.0777, found: 346.0783.

*Methyl 4-Methylsulfinyl-3-sulfamoyl-benzoate (**7h**).* The product was purified by flash chromatography on silica gel ($CHCl_3$:EtOAc, 5:1). Yield: 50 mg, 90%, mp 258−259 °C.

^{1}H NMR (400 MHz, DMSO-d_6) δ ppm: 2.81 (s, 3H, CH_3SO), 3.95 (s, 3H, CH_3O), 7.97 (s, 2H, SO_2NH_2), 8.34 (d, J = 8.2 Hz, 1H, Ar**H**), 8.43 (dd, J = 8.2 Hz, J = 1.6 Hz, 1H, Ar**H**), 8.47 (d, J = 1.6 Hz, 1H, Ar**H**).

^{13}C NMR (100 MHz, DMSO-d_6) δ ppm: 44.6, 53.3, 125.7, 128.5, 132.6, 133.8, 141.5, 151.2, 165.1.

HRMS calcd for $C_9H_{11}NO_5S_2$ [(M+H)$^+$]: 278.0151, found: 278.0155.

*Methyl 4-Propylsulfinyl-3-sulfamoyl-benzoate (**7i**).* The product was purified by flash chromatography on silica gel ($CHCl_3$:EtOAc, 3:1). Yield: 40 mg, 66%, mp 144−145 °C.

^{1}H NMR (400 MHz, DMSO-d_6) δ ppm: 0.99 (t, J = 7.4 Hz, 3H, CH_3CH_2), 1.59−1.62 (m, 1H, $CH_AH_BCH_3$); 1,77−1.81 (m, 1H, $CH_AH_BCH_3$), 2.66−2.69 (m, 1H, CH_AH_BSO), 3.10−3.13 (m, 1H, CH_AH_BSO), 3.93 (s, 3H, CH_3O), 7.97 (s, 2H, SO_2NH_2), 8.26 (d, J = 8.2 Hz, 1H, Ar**H**), 8.41 (dd, J = 8.2 Hz, J = 1.7 Hz, 1H, Ar**H**), 8.48 (d, J = 1.7 Hz, 1H Ar**H**).

^{13}C NMR (100 MHz, DMSO-d_6) δ ppm: 13.2, 16.5, 53.3, 58.9, 126.3, 128.7, 132.5, 133.4, 141.7, 149.2, 165.1.

HRMS calcd for $C_{11}H_{15}NO_5S_2$ [(M+H)$^+$]: 306.0464, found: 306.0470.

*Methyl 4-Isopentylsulfinyl-3-sulfamoyl-benzoate (**7k**).* The product was purified by flash chromatography on silica gel ($CHCl_3$:EtOAc, 5:1). Yield: 37 mg, 55%, mp 98−99 °C.

^{1}H NMR (400 MHz, DMSO-d_6) δ ppm: 0.86 (d, J = 6.5 Hz, 3H, CH_3), 0.89 (d, J = 6.5 Hz, 3H, CH_3), 1.40−1.45 (m, 1H, CH_AH_BCH), 1.63−1.68 (m, 2H, $CHCH_3$ and CH_AH_BCH), 2.66−2.69 (m, 1H, CH_AH_BSO), 3.15−3.19 (m, 1H, CH_AH_BSO), 3.94 (s, 3H, CH_3O), 7.97 (s, 2H, SO_2NH_2), 8.26 (d, J = 8.2 Hz, 1H, Ar**H**), 8.41 (dd, J = 8.2 Hz, J = 1.7 Hz, 1H, Ar**H**), 8.49 (d, J = 1.7 Hz, 1H, Ar**H**).

^{13}C NMR (100 MHz, DMSO-d_6) δ ppm: 22.4, 22.8, 27.2, 31.4, 53.3, 55.1, 126.4, 128.7, 132.5, 133.4, 141.7, 149.1, 165.1.

HRMS calcd for $C_{13}H_{19}NO_5S_2$ [(M+H)$^+$]: 334.0777, found: 334.0771.

*Methyl 4-Cyclopentylsulfinyl-3-sulfamoyl-benzoate (**7l**).* The product was purified by flash chromatography on silica gel ($CHCl_3$:EtOAc, 4:1). Yield: 51 mg, 77%, mp 109−111 °C.

^{1}H NMR (400 MHz, DMSO-d_6) δ ppm: 1.08−1.18 (m, 1H, C**H** cyclopentyl), 1.43−1.53 (m, 1H, C**H** cyclopentyl), 1.54−1.66 (m, 3H, C**H** cyclopentyl), 1.80−1.94 (m, 2H, C**H** cyclopentyl), 2.00−2.11 (m, 1H, C**H** cyclopentyl), 3.53 (quint, J = 7.6 Hz, 1H, C**H** cyclopentyl), 3.94 (s, 3H, OCH_3), 7.97 (s, 2H, SO_2NH_2), 8.16 (d, J = 8.4 Hz, 1H, Ar**H**), 8.36 (dd, J = 8.0 Hz, J = 1.6 Hz, 1H, Ar**H**), 8.49 (d, J = 1.3 Hz, 1H, Ar**H**).

^{13}C NMR (100 MHz, DMSO-d_6) δ ppm: 21.3, 25.7, 26.3, 29.6, 53.3, 61.7, 126.6, 128.9, 132.4, 132.9, 141.7, 148.0, 165.1.

HRMS calcd for $C_{13}H_{17}NO_5S_2$ [(M+H)$^+$]: 332.0621, found: 332.0615.

https://doi.org/10.1021/acs.jmedchem.5c01421
J. Med. Chem. XXXX, XXX, XXX−XXX

*Methyl 4-(1-Naphthylsulfinyl)-3-sulfamoyl-benzoate (**7m**).* The product was purified by flash chromatography on silica gel ($CHCl_3$:EtOAc, 1:1). Yield: 47 mg, 60%, mp 125−127 °C.

^{1}H NMR (400 MHz, DMSO-d_6) δ ppm: 3.93 (s, 3H, CH_3), 7.61−7.68 (m, 4H, naphthyl-**H**), 8.04−8.08 (m, 1H, naphthyl-**H**), 8.11 (s, 2H, SO_2NH_2), 8.14 (d, J = 7.6 Hz, 1H, naphthyl-**H**), 8.22 (d, J = 8.0 Hz, 1H, Ar**H**), 8.39 (dd, J = 1.6 Hz, J = 8.0 Hz, 1H, Ar**H**), 8.49−8.52 (m, 1H, naphthyl-**H**), 8.54 (d, 1H, J = 1.6 Hz, Ar**H**).

^{13}C NMR (100 MHz, DMSO-d_6) δ ppm: 53.4, 123.5, 125.5, 126.3, 127.5, 128.0, 128.7, 128.8, 129.2, 129.8, 132.5, 133.2, 133.8 (2C), 141.9, 143.1, 146.7, 165.0.

HRMS calcd for $C_{18}H_{15}NO_5S_2$ [(M+H)$^+$]: 390.0464, found: 390.0460.

*4-(Benzenesulfinyl)-N-butyl-3-sulfamoyl-benzamide (**8a**).* The product was purified by flash chromatography on silica gel ($CHCl_3$:EtOAc, 1:1). Yield: 61 mg, 80%, mp 168−171 °C.

^{1}H NMR (400 MHz, DMSO-d_6) δ ppm: 0.89 (t, J = 7.4 Hz, 3H, CH_3),), 1.32 (sext, J = 7.8 Hz, 2H, NH(CH_2)$_2$$CH_2CH_3$), 1.50 (quint, J = 7.2 Hz, 2H, $NHCH_2CH_2$), 3.27 (q, J = 7.2 Hz, 2H, $NHCH_2$), 7.47−7.53 (m, 3H, Ar**H**), 7.75 (d, J = 6.4 Hz, 2H, Ar**H**), 7.97 (s, 2H, SO_2NH_2), 8.20 (s, 2H, Ar**H**), 8.35 (s, 1H, Ar**H**), 8.77 (t, J = 5.4 Hz, 1H, N**H**).

^{13}C NMR (100 MHz, DMSO-d_6) δ ppm: 14.1, 20.1, 31.5, 39.6, 125.5, 126.4, 127.2, 129.8, 131.5, 131.7, 138.0, 142.0, 146.3, 147.3, 164.8.

HRMS calcd for $C_{17}H_{20}N_2O_4S_2$ [(M+H)$^+$]: 381.0937, found: 381.0933.

*N-Butyl-4-cyclohexylsulfinyl-3-sulfamoyl-benzamide (**8b**).* The product was purified by flash chromatography on silica gel ($CHCl_3$:EtOAc, 1:1). Yield: 63 mg, 82%, mp 195−196 °C.

^{1}H NMR (400 MHz, DMSO-d_6) δ ppm: 0.93 (t, J = 7.3 Hz, 3H, CH_3), 1.07−1.18 (m, 3H, C**H** cyclohexyl), 1.29−1.43 (m, 4H, C**H** cyclohexyl and CH_2CH_3), 1.49−1.60 (m, 4H, C**H** cyclohexyl and $CH_2CH_2CH_2$), 1.71−1.74 (m, 1H, C**H** cyclohexyl), 1.81−1.87 (m, 1H, C**H** cyclohexyl), 2.01−2.05 (m, 1H, C**H** cyclohexyl), 3.01 (tt, J = 12.3 Hz, J = 3.6 Hz, 1H, C**H**SO), 3.24−3.29 (m, 2H, CH_2NH), 7.84 (s, 2H, SO_2NH_2), 8.02 (d, J = 8.2 Hz, 1H, Ar**H**), 8.24 (dd, J = 8.2 Hz, J = 1.7 Hz, 1H, Ar**H**), 8.41 (d, J = 1.7 Hz, 1H, Ar**H**), 8.82 (t, J = 5.7 Hz, 1H, N**H**).

^{13}C NMR (100 MHz, DMSO-d_6) δ ppm: 14.2, 20.1, 21.0, 25.1, 25.4, 26.1, 28.5, 31.6, 39.5, 60.9, 126.6, 127.9, 130.3, 137.7, 141.7, 143.8, 164.9.

HRMS calcd for $C_{17}H_{26}N_2O_4S_2$ [(M+H)$^+$]: 387.1407, found: 387.1401.

*N-Butyl-4-isopentylsulfinyl-3-sulfamoyl-benzamide (**8k**).* The product was purified by flash chromatography on silica gel ($CHCl_3$:EtOAc, 1:1). Yield: 55 mg, 74%, mp 121−124 °C.

^{1}H NMR (400 MHz, DMSO-d_6) δ ppm: 0.83 (d, J = 6.4 Hz, 6H, S(CH_2)$_2$CH(CH_3)$_2$), 0.92 (t, J = 7.2 Hz, 3H, NH(CH_2)$_3$$CH_3$), 1.35 (sext, J = 7.2 Hz, 2H, $NHCH_2CH_2CH_2$), 1.45−1.66 (m, 5H, $NHCH_2CH_2$, SCH_2CH_2CH), 3.31 (q, J = 6.8 Hz, 2H, $NHCH_2$), 3.66−3.70 (m, 2H, SCH_2), 7.33 (s, 2H, SO_2NH_2), 8.25 (d, J = 8.0 Hz, 1H, Ar**H**), 8.30 (dd, J = 8.0 Hz, J = 1.6 Hz, 1H, Ar**H**), 8.60 (d, J = 1.6 Hz, 1H, Ar**H**), 8.96 (t, J = 5.6 Hz, 1H, N**H**).

^{13}C NMR (100 MHz, DMSO-d_6) δ ppm: 14.2, 20.1, 22.3, 27.0, 30.7, 31.5, 39.6, 53.4, 129.6, 131.5, 133.8, 138.1, 140.4, 143.1, 164.2.

HRMS calcd for $C_{16}H_{26}N_2O_4S_2$ [(M+H)$^+$]: 375.1407, found: 375.1411.

*N-Butyl-4-cyclopentylsulfinyl-3-sulfamoyl-benzamide (**8l**).* The product was purified by flash chromatography on silica gel ($CHCl_3$:EtOAc, 1:1). Yield: 47 mg, 63%, mp 103−107 °C.

^{1}H NMR (400 MHz, DMSO-d_6) δ ppm: 0.92 (t, J = 7.2 Hz, 3H, CH_3), 1.09−1.17 (m, 1H, C**H** cyclopentyl), 1.35 (sext, J = 7.2 Hz, 2H, NH(CH_2)$_2$$CH_2CH_3$), 1.45−1.63 (m, 6H, $NHCH_2CH_2$, C**H** cyclopentyl), 1.82−1.94 (m, 2H, C**H** cyclopentyl), 2.01−2.10 (m, 1H, C**H** cyclopentyl), 3.26−3.33 (m, 2H, $NHCH_2$), 3.52 (quint, J = 7.6 Hz, 1H, C**H** cyclopentyl), 7.85 (s, 2H, SO_2NH_2), 8.07 (d, J = 8.4 Hz, 1H, Ar**H**), 8.23 (dd, J = 8.0 Hz, J = 1.6 Hz, 1H, Ar**H**), 8.39 (d, J = 1.6 Hz, 1H, Ar**H**), 8.80 (t, J = 5.6 Hz, 1H, N**H**).

^{13}C NMR (100 MHz, DMSO-d_6) δ ppm: 14.2, 20.1, 21.4, 25.8, 26.3, 29.6, 31.5, 39.6, 61.7, 125.9, 127.7, 130.6, 137.7, 141.3, 145.4, 164.9.

HRMS calcd for $C_{16}H_{24}N_2O_4S_2$ [(M+H)$^+$]: 373.1250, found: 373.1255.

*N-Butyl-4-(1-naphthylsulfinyl)-3-sulfamoyl-benzamide (**8m**).* The product was purified by flash chromatography on silica gel ($CHCl_3$:EtOAc, 1:1). Yield: 28 mg, 33%, mp 232−235 °C.

^{1}H NMR (400 MHz, DMSO-d_6) δ ppm: 0.95 (t, J = 7.2 Hz, 3H, CH_3), 1.38 (sext, J = 7.2 Hz, 2H, NH(CH_2)$_2$$CH_2CH_3$), 1.56 (quint, J = 7.2 Hz, 2H, $NHCH_2CH_2$), 3.28−3.37 (m, 2H, $NHCH_2$), 7.63−7.73 (m, 4H, naphthyl-**H**), 8.08 (s, 2H, SO_2NH_2), 8.11−8.13 (m, 2H, naphthyl-**H**, Ar**H**), 8.18−8.22 (m, 1H, naphthyl-**H**), 8.26 (dd, J = 1.6 Hz, J = 8.0 Hz, 1H, Ar**H**), 8.47 (d, 1H, J = 1.6 Hz, Ar**H**), 8.52−8.54 (m, 1H, naphthyl-**H**), 8.86 (t, J = 5.6 Hz, 1H, N**H**).

^{13}C NMR (100 MHz, DMSO-d_6) δ ppm: 14.2, 20.1, 31.5, 39.6, 123.5, 125.3, 126.2, 127.4, 127.5, 128.0, 128.3, 129.2, 129.7, 131.5, 132.3, 133.8, 138.4, 142.0, 142.8, 144.3, 164.8.

HRMS calcd for $C_{21}H_{22}N_2O_4S_2$ [(M+H)$^+$]: 431.1094, found: 431.1088.

*General Procedure for the Syntheses of **9(a−d, h, i, l, m)** and **10(b, k−m)**.* The 30% H_2O_2(aq) (1.08 mmol, 0.110 mL) was added in small portions over 3 h to a solution of appropriate methyl 4-sulfanilsubstituted-3-sulfamoyl-benzoate (**4a−d, h, i, l, m**) or appropriate *N*-butyl-4-sulfanilsubstituted-3-sulfamoyl-benzamide (**10b, k−m**) (0.200 mmol) and acetic acid (2.0 mL) at 70 °C and allowed stirring for 6−8h. The solvent was removed under reduced pressure and the resultant precipitate was filtered, and washed with H_2O.

*Methyl 4-(Benzenesulfonyl)-3-sulfamoyl-benzoate (**9a**).* The product was purified by flash chromatography on silica gel ($CHCl_3$:EtOAc, 5:1). Yield: 57 mg, 80%, mp 212−213 °C.

^{1}H NMR (400 MHz, DMSO-d_6) δ ppm: 3.94 (s, 3H, CH_3O), 7.55 (s, 2H, SO_2NH_2), 7.61 (t, J = 7.4 Hz, 2H, Ar**H**), 7.70 (t, J = 7.4 Hz, 1H, Ar**H**), 7.95 (d, J = 7.4 Hz, 2H, Ar**H**), 8.43 (dd, J = 8.2 Hz, J = 1.7 Hz, 1H, Ar**H**), 8.61 (d, J = 8.2 Hz, 1H, Ar**H**), 8,64 (d, J = 1.7 Hz, 1H, Ar**H**).

^{13}C NMR (100 MHz, DMSO-d_6) δ ppm: 53.6, 128.4, 129.6, 130.7, 133.9, 134.3, 134.4, 135.1, 140.6, 141.6, 143.4, 164.5.

HRMS calcd for $C_{14}H_{13}NO_6S_2$ [(M+H)$^+$]: 356.0257, found: 356.0266.

*Methyl 4-Cyclohexylsulfonyl-3-sulfamoyl-benzoate (**9b**).* The product was purified by flash chromatography on silica gel ($CHCl_3$:EtOAc, 5:1). Yield: 61 mg, 85%, mp 155−156 °C.

^{1}H NMR (400 MHz, DMSO-d_6) δ ppm: 1.17−1.81 (m, 10H, CH_2 cyclohexyl), 3.86−3.91 (m, 1H, C**H**SO_2), 3.95 (s, 3H, CH_3O), 7.42 (s, 2H, SO_2NH_2), 8.25 (d, J = 8.1 Hz, 1H, Ar**H**), 8.42 (dd, J = 8.1 Hz, J = 1.7 Hz, 1H, Ar**H**), 8.70 (d, J = 1.7 Hz, 1H, Ar**H**).

^{13}C NMR (100 MHz, DMSO-d_6) δ ppm: 24.8, 24.9, 25.1, 53.6, 61.8, 130.9, 133.6, 134.9, 135.2, 138.6, 143.8, 164.6.

HRMS calcd for $C_{14}H_{19}NO_6S_2$ [(M+H)$^+$]: 362.0727, found: 362.0721.

*Methyl 4-Benzylsulfonyl-3-sulfamoyl-benzoate (**9c**).* The product was purified by flash chromatography on silica gel ($CHCl_3$:EtOAc, 5:1). Yield: 66 mg, 89%, mp 189−190 °C.

^{1}H NMR (400 MHz, DMSO-d_6) δ ppm: 3.94 (s, 3H, CH_3O), 5.03 (s, 2H, CH_2SO_2), 7.19−7.21 (m, 2H, Ar**H**), 7.30−7.34 (m, 3H, Ar**H**), 7.53 (s, 2H, SO_2NH_2), 7.88 (d, J = 8.0 Hz, 1H, Ar**H**), 8.25 (dd, J = 8.0 Hz, J = 1.8 Hz, 1H, Ar**H**), 8.70 (d, J = 1.8 Hz, Ar**H**).

^{13}C NMR (100 MHz, DMSO-d_6) δ ppm: 53.6, 60.9, 127.9, 129.0, 129.3, 130.6, 131.2, 133.4, 134.5, 135.1, 139.4, 143.7, 164.5.

HRMS calcd for $C_{15}H_{15}NO_6S_2$ [(M+H)$^+$]: 370.0414, found: 370.0419.

*Methyl 4-(2-Phenylethylsulfonyl)-3-sulfamoyl-benzoate (**9d**).* The product was purified by flash chromatography on silica gel ($CHCl_3$:EtOAc, 5:1). Yield: 64 mg, 83%, mp 186−187 °C.

^{1}H NMR (400 MHz, DMSO-d_6) δ ppm: 2.98 (t, J = 8.0 Hz, 2H, CH_2Ph), 3.94 (s, 3H, CH_3O), 4.02 (t, J = 8.0 Hz, 2H,CH_2SO_2), 7.18−7.27 (m, 5H, Ar**H**), 7.44 (s, 2H, SO_2NH_2), 8.30 (d, J = 8.0 Hz, 1H, Ar**H**), 8.40 (d, J = 8.0 Hz, 1H, Ar**H**), 8.67 (s, 1H, Ar**H**).

^{13}C NMR (100 MHz, DMSO-d_6) δ ppm: 28.1, 53.6, 55.9, 127.1, 128.9, 129.0, 130.7, 133.9, 134.3, 135.1, 137.9, 140.0, 143.5, 164.5.

https://doi.org/10.1021/acs.jmedchem.5c01421
J. Med. Chem. XXXX, XXX, XXX−XXX

HRMS calcd for $C_{16}H_{17}NO_6S_2$ [(M+H)$^+$]: 384.0570, found: 384.0578.

*Methyl 4-Methylsulfonyl-3-sulfamoyl-benzoate (**9h**).* The product was purified by flash chromatography on silica gel ($CHCl_3$:EtOAc, 5:1). Yield: 55 mg, 95%, mp 187−188 °C.

^{1}H NMR (400 MHz, DMSO-d_6) δ ppm: 3.51 (s, 3H, CH_3SO_2), 3.96 (s, 3H, CH_3O), 7.42 (s, 2H, SO_2NH_2), 8.36 (d, J = 8.2 Hz, 1H, Ar**H**), 8.45 (dd, J = 8.2 Hz, J = 1.6 Hz, 1H, Ar**H**), 8.67 (d, J = 1.6 Hz, 1H, Ar**H**).

^{13}C NMR (100 MHz, DMSO-d_6) δ ppm: 44.1, 53.6, 130.5, 133.4, 134.1, 135.1, 141.6, 143.2, 164.6.

HRMS calcd for $C_9H_{11}NO_6S_2$ [(M+H)$^+$]: 294.0101, found: 294.0106.

*Methyl 4-Propylsulfonyl-3-sulfamoyl-benzoate (**9i**).* The product was purified by flash chromatography on silica gel ($CHCl_3$:EtOAc, 5:1). Yield: 57 mg, 88%, mp 169−170 °C.

^{1}H NMR (400 MHz, DMSO-d_6) δ ppm: 0.94 (t, J = 7.4 Hz, 3H, CH_3CH_2), 1.63−1.66 (m, 2H, CH_2CH_3), 3.66 (t, J = 7.7 Hz, 2H, CH_2SO_2), 3.96 (s, 3H, CH_3O), 7.43 (s, 2H, SO_2NH_2), 8.33 (d, J = 8.1 Hz, 1H, Ar**H**), 8.44 (dd, J = 8.1 Hz, J = 1.6 Hz, 1H, Ar**H**), 8.69 (d, J = 1.6 Hz, 1H, Ar**H**).

^{13}C NMR (100 MHz, DMSO-d_6) δ ppm: 13.1, 16.2, 53.6, 56.7, 130.7, 133.9, 134.2, 135.2, 140.2, 143.5, 164.6.

HRMS calcd for $C_{11}H_{15}NO_6S_2$ [(M+H)$^+$]: 322.0414, found: 322.0422.

*Methyl 4-Cyclopentylsulfonyl-3-sulfamoyl-benzoate (**9l**).* The product was purified by flash chromatography on silica gel ($CHCl_3$:EtOAc, 5:1). Yield: 63 mg, 90%, mp 199−200 °C.

^{1}H NMR (400 MHz, DMSO-d_6) δ ppm: 1.55−1.65 (m, 2H, C**H** cyclopentyl), 1.68−1.76 (m, 2H, C**H** cyclopentyl), 1.77−1.86 (m, 2H, C**H** cyclopentyl), 1.88−1.96 (m, 2H, C**H** cyclopentyl), 3.96 (s, 3H, OCH_3), 4.44 (quint, J = 7.2 Hz, 1H, C**H** cyclopentyl), 7.41 (s, 2H, SO_2NH_2), 8.34 (d, J = 8.0 Hz, 1H, Ar**H**), 8.42 (dd, J = 8.0 Hz, J = 1.6 Hz, 1H, Ar**H**), 8.70 (d, J = 1.6 Hz, 1H, Ar**H**).

^{13}C NMR (100 MHz, DMSO-d_6) δ ppm: 26.0, 27.0, 53.6, 62.7, 130.9, 133.8, 134.6, 135.1, 139.7, 143.6, 164.6.

HRMS calcd for $C_{13}H_{17}NO_6S_2$ [(M+H)$^+$]: 348.0570, found: 348.0560.

*Methyl 4-(1-Naphthylsulfonyl)-3-sulfamoyl-benzoate (**9m**).* The product was purified by flash chromatography on silica gel ($CHCl_3$:EtOAc, 8:1). Yield: 63 mg, 78%, mp 223−224 °C.

^{1}H NMR (400 MHz, DMSO-d_6) δ ppm: 3.92 (s, 3H, OCH_3), 7.63−7.67 (m, 4H, naphthyl**H** and SO_2NH_2), 7.74 (t, J = 8.0 Hz, 1H, Ar**H**), 8.12−8.14 (m, 1H, naphthyl**H**), 8.25 (d, J = 8.0 Hz, 1H, Ar**H**), 8.31−8.37 (m, 4H, naphthyl**H**), 8.70 (s, 1H, Ar**H**).

^{13}C NMR (100 MHz, DMSO-d_6) δ ppm: 53.6, 123.9, 125.0, 127.5, 127.8, 129.1, 129.9, 130.8, 131.0, 133.0, 133.8, 134.2, 134.9, 135.2, 135.9, 141.8, 143.5, 164.5.

HRMS calcd for $C_{18}H_{15}NO_6S_2$ [(M+H)$^+$]: 406.0414, found: 406.0423.

*N-Butyl-4-cyclohexylsulfonyl-3-sulfamoyl-benzamide (**10b**).* The product was purified by flash chromatography on silica gel ($CHCl_3$:EtOAc, 3:1). Yield: 68 mg, 84%, mp 155−156 °C.

^{1}H NMR (400 MHz, DMSO-d_6) δ ppm: 0.93 (t, J = 7.3 Hz, 3H, CH_3), 1.17−1.81 (m, 14H, $CH_2CH_2CH_3$ and C**H** cyclohexyl), 3.30−3.32 (m, 2H, CH_2NH), 3.90−3.93 (m, 1H, $CHSO_2$), 7.33 (s, 2H, SO_2NH_2), 8.19 (d, J = 8.1 Hz, 1H, Ar**H**), 8.29 (d, J = 8.1 Hz, 1H, Ar**H**), 8.61 (s, 1H, Ar**H**), 8.96 (t, J = 5.3 Hz, 1H, N**H**).

^{13}C NMR (100 MHz, DMSO-d_6) δ ppm: 14.1, 20.1, 24.9, 24.9, 25.1, 31.5, 39.6, 61.8, 129.8, 131.2, 134.4, 136.5, 140.4, 143.4, 164.2.

HRMS calcd for $C_{17}H_{26}N_2O_5S_2$ [(M+H)$^+$]: 403.1356, found: 403.1351.

*N-Butyl-4-isopentylsulfonyl-3-sulfamoyl-benzamide (**10k**).* The product was purified by flash chromatography on silica gel ($CHCl_3$:EtOAc, 1:1). Yield: 53 mg, 68%, mp 160−162 °C.

^{1}H NMR (400 MHz, DMSO-d_6) δ ppm: 0.83 (d, J = 6.4 Hz, 6H, $S(CH_2)_2CH(CH_3)_2$), 0.92 (t, J = 7.6 Hz, 3H, $NH(CH_2)_3CH_3$), 1.35 (sext, J = 7.2 Hz, 2H, $NHCH_2CH_2CH_2$), 1.46−1.66 (m, 5H, $NHCH_2CH_2$, SCH_2CH_2CH), 3.31 (q, J = 6.8 Hz, 2H, $NHCH_2$), 3.66−3.70 (m, 2H, SCH_2), 7.33 (s, 2H, SO_2NH_2), 8.25 (d, J = 8.0 Hz, 1H, Ar**H**), 8.30 (dd, J = 8.0 Hz, J = 1.6 Hz, 1H, Ar**H**), 8.60 (s, 1H, Ar**H**), 8.97 (t, J = 5.2 Hz, 1H, N**H**).

^{13}C NMR (100 MHz, DMSO-d_6) δ ppm: 14.2, 20.1, 22.3, 27.0, 30.7, 31.5, 39.7, 53.4, 129.6, 131.5, 133.8, 138.1, 140.4, 143.1, 164.2.

HRMS calcd for $C_{16}H_{26}N_2O_5S_2$ [(M+H)$^+$]: 391.1356, found: 391.1359.

*N-Butyl-4-cyclopentylsulfonyl-3-sulfamoyl-benzamide (**10l**).* The product was purified by flash chromatography on silica gel ($CHCl_3$:EtOAc, 1:1). Yield: 57 mg, 73%, mp 143−145 °C.

^{1}H NMR (400 MHz, DMSO-d_6) δ ppm: 0.92 (t, J = 7.6 Hz, 3H, CH_2CH_3), 1.35 (sext, J = 7.6 Hz, 2H, $CH_2CH_2CH_3$), 1.54 (quint, J = 7.2 Hz, 2H, $NHCH_2CH_2$), 1.57−1.65 (m, 2H, C**H** cyclopentyl), 1.68−1.85 (m, 4H, C**H** cyclopentyl), 1.88−1.96 (m, 2H, C**H** cyclopentyl), 3.31 (q, J = 6.8 Hz, 2H, $NHCH_2$), 4.44 (quint, J = 7.2 Hz, 1H, SO_2CH cyclopentyl), 7.32 (br. s, 2H, SO_2NH_2), 8.26−8.31 (m, 2H, Ar**H**), 8.62 (s, 1H, Ar**H**), 8.96 (t, J = 5.6 Hz, 1H, N**H**).

^{13}C NMR (100 MHz, DMSO-d_6) δ ppm: 14.2, 20.1, 26.0, 27.0, 31.5, 39.6, 62.6, 129.7, 131.4, 134.1, 137.7, 140.3, 143.2, 164.2.

HRMS calcd for $C_{16}H_{24}N_2O_5S_2$ [(M+H)$^+$]: 389.1199, found: 389.1205.

*N-Butyl-4-(1-naphthylsulfonyl)-3-sulfamoyl-benzamide (**10m**).* The product was purified by flash chromatography on silica gel ($CHCl_3$:EtOAc, 1:1). Yield: 22 mg, 24%, mp 266−268 °C.

^{1}H NMR (400 MHz, DMSO-d_6) δ ppm: 0.89 (t, J = 7.6 Hz, 3H, CH_2CH_3), 1.32 (sext, J = 7.2 Hz, 2H, $CH_2CH_2CH_3$), 1.51 (quint, J = 7.2 Hz, 2H, $NHCH_2CH_2$), 3.29 (q, J = 6.4 Hz, 2H, $NHCH_2$), 7.52 (s, 2H, SO_2NH_2), 7.62−7.68 (m, 2H, naphthyl**H**), 7.74 (t, J = 8.0 Hz, 1H, naphthyl**H**), 8.13−8.15 (m, 1H, naphthyl**H**), 8.19−8.23 (m, 2H, Ar**H**), 8.30 (d, J = 8.4 Hz, 1H, naphthyl**H**), 8.34−8.39 (m, 2H, naphthyl**H**), 8.60 (d, J = 1.6 Hz, 1H, Ar**H**), 8.92 (t, J = 5.2 Hz, 1H, N**H**).

^{13}C NMR (100 MHz, DMSO-d_6) δ ppm: 14.1, 20.1, 31.4, 39.6, 124.0, 125.0, 127.5, 127.8, 129.0, 129.8, 129.9, 130.7, 131.4, 132.7, 134.2, 135.5, 135.8, 139.8, 140.2, 143.1, 164.3.

HRMS calcd for $C_{21}H_{22}N_2O_5S_2$ [(M+H)$^+$]: 447.1043, found: 447.1048.

Protein Preparation. Recombinant human carbonic anhydrases (CAI, CAII, CAIII, CAIV, CAVA, CAVB, CAVI, CAVII, CAIX, CAXII, CAXIII, CAXIV) were expressed and chromatographically purified according to previously published protocols[47] and were used for FTSA experiments. Proteins (CAII and CAXIII) used for crystallization were additionally purified by affinity chromatography and concentrated. CAIX used for crystallization were expressed and purified according to this protocol.[48] Production of recombinant CAII and the extracellular part of CAIX comprising PG and CA domains (residues 38−391) used in SFA experiments is described in ref 49.

Determination of Observed Binding Parameters. *Fluorescent Thermal Shift Assay (FTSA).* Dissociation constants, $K_{d,obs}$, (listed in Table 1) of the compounds binding to CAs were determined by the fluorescent thermal shift assay using a QIAGEN's real-time PCR cycler the "Rotor-Gene Q" and Rotor-Gene Style 4-strip tubes from STARLAB. Ligands were dissolved in DMSO stock solutions to concentrations of 10 mM or 20 mM and used for the serial dilution of the dilution factor 2 in DMSO. These samples were diluted with buffer solution and mixed with a prepared protein solution, consisting of protein stock, buffer solution, and solvatochromic dye 8-anilino-1-naphthalenesulfonate (ANS). All final samples typically contained up to 10 μM CA, compound solutions of serial dilution from 0 μM to 200 μM at 8 different concentrations differing by 2 times, 50 μM ANS, 50 mM sodium phosphate buffer at pH 7.0, 100 mM sodium chloride, and 2.0% (v/v) DMSO. Samples preparation is explained in detail in.[50] The excitation and emission wavelengths of ANS were 365 ± 20 and 460 ± 15 nm. Samples were heated from 25 to 99 °C at the rate of 1 °C/min. The curve-fitting procedure was performed by Thermott[51] at 37 °C. Data are deposited in the public database: Protein−Ligand Binding Database[52] (Database URL: https://plbd.org/).

Stopped-Flow Carbon Dioxide Hydration Assay. Recombinant CAII and the extracellular part of CAIX comprising PG and CA domains (residues 38−391) were used in inhibition assays. A stopped-flow instrument (BioLogic) was used for measuring the CA-catalyzed CO_2 hydration activity in the presence of inhibitors.[53] The assay buffer

https://doi.org/10.1021/acs.jmedchem.5c01421
J. Med. Chem. XXXX, XXX, XXX−XXX

Table 4. Crystallization Conditions Used to Grow Protein Crystals in This Study

PDB ID	isozyme—compound	cystallization buffer	sitting drop
9FPT	CAII—**2**	0.1 M sodium bicine (pH 9.0) and 2 M sodium malonate (pH 7.0)	2 μL of 41 mg/mL CAII solution and 2 μL of crystallization buffer
9FPU	CAII—**3**	0.1 M sodium bicine (pH 9.0) and 2 M sodium malonate (pH 7.0)	2 μL of 41 mg/mL CAII solution and 2 μL of crystallization buffer
9FPQ	CAII—**4c**	0.1 M sodium bicine (pH 9.0), 0.2 M ammonium sulfate, and 2 M sodium malonate (pH 7.0)	2 μL of 41 mg/mL CAII solution and 2.5 μL of crystallization buffer
9FPR	CAII—**4d**	0.1 M sodium bicine (pH 9.0), 0.2 M ammonium sulfate, and 2 M sodium malonate (pH 7.0)	3 μL of 12 mg/mL CAII solution and 3 μL of crystallization buffer
9FPS	CAII—**4h**	0.1 M sodium bicine (pH 9.0) and 2 M sodium malonate (pH 7.0)	3 μL of 12 mg/mL CAII solution and 3 μL of crystallization buffer
9R8X	CAIX—**4d**	1.0 M diammonium hydrogen phosphate and 0.1 M sodium acetate (pH 4.5)	10 mg/mL CAIX solution
9R8Y	CAIX—**5b**	1.0 M diammonium hydrogen phosphate and 0.1 M sodium acetate (pH 4.5)	10 mg/mL CAIX solution
9FPV	CAXIII—**4c**	0.1 M sodium citrate (pH 5.5), 0.1 M sodium acetate (pH 4.5), and 26% of PEG4000	1 μL of 23 mg/mL CAXIII solution and 0.4 μL of crystallization buffer
9FPW	CAXIII—**4d**	0.1 M sodium citrate (pH 5.5), 0.1 M sodium acetate (pH 4.5), and 26% of PEG4000	1 μL of 23 mg/mL CAXIII solution and 0.4 μL of crystallization buffer

consisted of 0.2 mM Phenol Red (pH indicator used in absorbance maximum of 557 nm), 20 mM HEPES Na (pH 7.5), and 20 mM Na_2SO_4. The concentration of CAII and CAIX in the enzyme assay was 4 nM and 1 nM, respectively. To stabilize CAIX during the measurements, 0.0025% dodecyl-β-D-maltopyranoside (DDM, Anatrace, and Anagrade purity) was included in the reaction mixture.

The substrate (CO_2) concentration in the reaction was 8.5 mM. Rates of the CA-catalyzed CO_2 hydration reaction were followed for 30 s at 25 °C. Four traces of substrate conversion in the reaction were fitted by the exponential function to determine the rate for each inhibitor concentration. The uncatalyzed rates were determined in the same manner and subtracted from the total observed rates. Stock solutions of inhibitors (100 mM) were prepared in dimethyl sulfoxide, and dilutions of up to 100 nM were made thereafter in DMSO. Apparent K_i' values were obtained from dose−response curves recorded for at least six different concentrations of the test compound by the nonlinear least-squares method using an Excel spreadsheet fitting the Williams-Morrison equation.[54] K_i values were then derived using the Cheng-Prusoff equation.[55] The K_m values used in the Cheng−Prusoff equation were 9.3 mM for CAII and 7.5 mM for CAIX. Inhibition data are provided in Figure S2.

Calculation of the Intrinsic Binding Parameters. The detailed description of the importance and calculation of the intrinsic values have been previously described.[27] For the calculation of the *intrinsic* dissociation constants, the experimentally measured *observed* dissociation constants determined by the FTSA, the pK_a of the sulfonamide group of the compound, and the pK_a of the water molecule bound to the zinc cation by the CA were used.

The intrinsic dissociation constant, $K_{d,int}$, is equal to

$$K_{d,int} = K_{d,obs} \times f_{RSO_2NH^-} \times f_{CAZnH_2O} \quad (1)$$

The fraction of deprotonated sulfonamide:

$$f_{RSO_2NH^-} = \frac{10^{pH-pK_{a,SA}}}{1 + 10^{pH-pK_{a,SA}}} \quad (2)$$

The fraction of Zn(II)-bound water form of CA:

$$f_{CAZnH_2O} = \frac{10^{pK_{a,CA}-pH}}{1 + 10^{pK_{a,CA}-pH}} \quad (3)$$

- $K_{d,obs}$ − observed dissociation constant;
- $f_{RSO_2NH^-}$ and f_{CAZnH_2O} − fractions of deprotonated sulfonamide and Zn(II)-bound water molecule;
- $pK_{a,SA}$ − pK_a of the sulfonamide group;
- $pK_{a,CA}$ − pK_a value of water molecule bound to Zn(II) in the active site of CA.

In this study, the pH value was equal to 7.0.

Determination of pK_a Values of the Compound Sulfonamide Group. The pK_a values of the water molecule bound to Zn^{2+} in the active site of CAs, $pK_{a,CA}$, were taken from ref 42 and of compounds, $pK_{a,SA}$, (Figure S3) were experimentally determined as described in ref S6.

We used a constant concentration of sulfonamide (25−400 μM) and 2.0% (v/v) or 20% (v/v; but only for very poorly soluble ones) of DMSO in universal buffer (50 mM sodium acetate, 25 mM sodium borate, and 50 mM sodium phosphate) at different pH values (in the range from pH 6.0 to 12.0 with 0.5 pH increment). UV/vis spectra of the compound solution were recorded at 37 °C using BMG Labtech CLARIOstarPlus plate reading spectrophotometer. The pK_a values were calculated by normalizing the absorbance and plotting it as a function of pH, then fitting it to the Henderson−Hasselbalch equation using the least-square method. The midpoint of this fitted curve is equal to the sulfonamide group $pK_{a,SA}$.

X-ray Crystallography. *Crystallization.* Crystals of CAII, CAIX, and CAXIII were obtained using the sitting-drop vapor diffusion method at room temperature. Table 4 lists the concentrations of proteins and buffers used for crystallization.

Ligand Soaking. The crystal structures of CAII and CAXIII with ligands were obtained by soaking. A 50 mM solution of each ligand was prepared in dimethyl sulfoxide. One μL of this solution was then diluted using 50 μL of matching reservoir solution corresponding to the conditions under which the crystal was formed. Crystals were incubated for up to 1 week in the soaking solution.

Cocrystallization. The crystal structures of CAIX with ligands were obtained by cocrystallization. Table 4 lists crystallization conditions. The ligand used for cocrystallization was in 5−10 mM concentration, while the stock solution contained 100 mM ligand dissolved in dimethyl sulfoxide.

Data Collection and Structure Determination. Data for CAII and CAXII were collected at PETRA III BEAMLINE P13 (MX1) and for CAIX at BESSY II beamline 14.1.

The data were processed and scaled using XDS,[58] MOSFLM,[59,60] and SCALA.[61] The crystal structures were solved by molecular replacement using MOLREP.[62] The initial model for molecular replacement−CAII: 3HLJ; CAIX: 8Q18,[63] CAXIII: 2NNO. The structure was refined by REFMAC[64] and remodeled using COOT.[57] The 3D models of compounds were constructed by the AVOGADRO[65] program and ligand parameter files were created using LIBCHECK.[66,67]

The data diffraction and final model refinement statistics and PDB IDs are summarized in Table 3. All graphics were created using PyMOL Molecular Graphics System. Authors will release the atomic coordinates upon article publication.

Molecular Docking. The following receptors PDB IDs were chosen for docking: CAII: 3HS4; CAIX: 6G9U, chain A; CAXIII: 4KNN, chain A. The receptors selected from the Protein Data Bank

https://doi.org/10.1021/acs.jmedchem.5c01421
J. Med. Chem. XXXX, XXX, XXX−XXX

differed from the new X-ray structures presented in this Paper to decrease bias. The proteins were prepared for docking using ChimeraX (version 1.9).[68−70] The ligands were optimized using the MMFF94s force field[71−76] within Avogadro molecular viewer (version 1.2.0).[65] For series 7 ligands, two enantiomers of the chiral sulfur were created and docked separately. The format conversions were performed using OpenBabel (The Open Babel Package, version 3.1.1, http://openbabel.org).[77] The docking was performed using the Smina program (version master:dc3dfab+).[34] Smina is based on Autodock Vina.[36] The constrained optimization was done using Smina, using a custom scoring function with a quadratic bias function with weight w=−10 added to the default Vina scoring function.[36] The quadratic constraint forced sulfonamide nitrogen to adhere to its position in the X-ray structure. A cubic docking box of size (24 Å),[3] exhaustiveness 100, and energy range 10 kcal/mol was set as docking parameters. The resulting poses were rescored with Smina using the Vinardo scoring function[35] without the constraint. Only one of the symmetry equivalent poses (e.g., phenyl ring flip) was included when evaluating pose ranking after docking. Heavy atom Root Mean Square Deviations (RMSD) were calculated using DockRMSD software (version 1.1).[78]

The quantum Density Functional Theory (DFT) optimizations were performed using GAMESS-US (version 2019.R2)[40] using DFT functional ωB97X-D[79] with the cc-pVDZ basis set[80,81] and the C-PCM implicit solvation model for water.[82] The conformational search was performed using CREST software (version 3.0.2)[38] using xTB (version 6.7.1)[83] computational engine, employing the GFN2-xTB semiempirical tight binding method[39] and the ALPB implicit solvation model for water.[84]

■ ASSOCIATED CONTENT

Supporting Information

The Supporting Information is available free of charge at https://pubs.acs.org/doi/10.1021/acs.jmedchem.5c01421.

FTSA data of compound binding to CA isozymes; SFA data of CA isozyme inhibition by compounds; determination of pK_a values of compound − RSO_2NH_2; NMR spectra of compounds; HPLC chromatograms of representative compounds; ESI-MS spectra of representative compounds; and comparison of docking and crystallographic binding poses (PDF)

SMILE strings of the synthesized compound and corresponding biological activity: *observed* and *intrinsic* ($K_{d,obs}$ and $K_{d,int}$) dissociation constants (in nM units) of investigated compounds to all catalytically active human CAs at 37 °C obtained by FTSA (CSV)

■ AUTHOR INFORMATION

Corresponding Author

Daumantas Matulis − *Department of Biothermodynamics and Drug Design, Institute of Biotechnology, Life Sciences Center, Vilnius University, Vilnius LT-10257, Lithuania;* orcid.org/0000-0002-6178-6276; Email: daumantas.matulis@bti.vu.lt

Authors

Audrius Zakšauskas − *Department of Biothermodynamics and Drug Design, Institute of Biotechnology, Life Sciences Center, Vilnius University, Vilnius LT-10257, Lithuania*

Vaida Paketurytė-Latvė − *Department of Biothermodynamics and Drug Design, Institute of Biotechnology, Life Sciences Center, Vilnius University, Vilnius LT-10257, Lithuania;* orcid.org/0000-0003-0919-7826

Alberta Jankūnaitė − *Department of Biothermodynamics and Drug Design, Institute of Biotechnology, Life Sciences Center, Vilnius University, Vilnius LT-10257, Lithuania*

Edita Čapkauskaitė − *Department of Biothermodynamics and Drug Design, Institute of Biotechnology, Life Sciences Center, Vilnius University, Vilnius LT-10257, Lithuania*

Yann Becart − *Department of Biothermodynamics and Drug Design, Institute of Biotechnology, Life Sciences Center, Vilnius University, Vilnius LT-10257, Lithuania*

Alexey Smirnov − *Department of Biothermodynamics and Drug Design, Institute of Biotechnology, Life Sciences Center, Vilnius University, Vilnius LT-10257, Lithuania*

Klára Pospíšilová − *Institute of Organic Chemistry and Biochemistry of the Czech Academy of Sciences, Prague 6 16610, Czech Republic*

Janis Leitans − *Latvian Biomedical Research and Study Centre, Riga LV-1067, Latvia*

Jiří Brynda − *Institute of Organic Chemistry and Biochemistry of the Czech Academy of Sciences, Prague 6 16610, Czech Republic*

Andris Kazaks − *Latvian Biomedical Research and Study Centre, Riga LV-1067, Latvia*

Lina Baranauskienė − *Department of Biothermodynamics and Drug Design, Institute of Biotechnology, Life Sciences Center, Vilnius University, Vilnius LT-10257, Lithuania;* orcid.org/0000-0002-9924-9177

Elena Manakova − *Department of Protein−DNA Interactions, Institute of Biotechnology, Life Sciences Center, Vilnius University, Vilnius LT-10257, Lithuania*

Saulius Gražulis − *Sector of Crystallography and Cheminformatics, Institute of Biotechnology, Life Sciences Center, Vilnius University, Vilnius LT-10257, Lithuania*

Visvaldas Kairys − *Department of Bioinformatics, Institute of Biotechnology, Life Sciences Center, Vilnius University, Vilnius LT-10257, Lithuania;* orcid.org/0000-0002-5427-0175

Kaspars Tars − *Latvian Biomedical Research and Study Centre, Riga LV-1067, Latvia;* orcid.org/0000-0001-8421-9023

Pavlína Řezáčová − *Institute of Organic Chemistry and Biochemistry of the Czech Academy of Sciences, Prague 6 16610, Czech Republic*

Complete contact information is available at: https://pubs.acs.org/10.1021/acs.jmedchem.5c01421

Author Contributions

A.Z. and V.P.-L. contributed equally to this paper.

Notes

The authors declare the following competing financial interest(s): Authors declare that they have patents and patent applications pending on CA inhibitors.

■ ACKNOWLEDGMENTS

This research was supported by (i) a grant from the Research Council of Lithuania (No. S-MIP-22-35); (ii) the National Institute for Cancer Research (Programme EXCELES, ID Project No. LX22NPO5102), Funded by the European Union, Next Generation EU awarded to PR; and (iii) the European Union's Recovery and Resilience Mechanism project (No.5.2.1.1.i.0/2/24/I/CFLA/001) "Consolidation of the Latvian Institute of Organic Synthesis and the Latvian Biomedical Research and Study Centre". The authors also thank Martynas Malikėnas for performing HPLC analysis of compounds. We thank Vilma Michailovienė†, who died in 2022, for performing numerous protein affinity purification procedures.

■ ABBREVIATIONS

CA, human carbonic anhydrase; FTSA, fluorescent thermal shift assay (or differential scanning fluorimetry DSF); int, intrinsic; $K_{d,int}$, intrinsic equilibrium dissociation constant; $K_{d,obs}$, observed equilibrium dissociation constant; obs, observed; $pK_{a,CA}$, pK_a value of water molecule bound to Zn(II) in the active site of CA; $pK_{a,SA}$, pK_a of the sulfonamide group; SFA, stopped-flow carbon dioxide hydration assay

■ REFERENCES

(1) Whitesides, G. M.; Krishnamurthy, V. M. Designing ligands to bind proteins. *Q. Rev. Biophys.* **2005**, *38*, 385−395.
(2) Maren, T. H. Use of inhibitors in physiological studies of carbonic anhydrase. *Am. J. Physiol.-Ren. Physiol.* **1977**, *232*, F291−F297.
(3) Meldrum, N. U.; Roughton, F. J. Some properties of carbonic anhydrase, the CO2 enzyme present in blood. *J. Physiol* **1932**, *75*, 15P−16P.
(4) *The Carbonic Anhydrases*; Springer US: Boston, MA, 1991.
(5) *The Carbonic Anhydrases*; Birkhäuser Basel: Basel, 2000.
(6) Krishnamurthy, V. M.; et al. Carbonic Anhydrase as a Model for Biophysical and Physical-Organic Studies of Proteins and Protein−Ligand Binding. *Chem. Rev.* **2008**, *108*, 946−1051.
(7) *The Carbonic Anhydrases: Current and Emerging Therapeutic Targets*; Springer International Publishing: Cham, 2021; Vol. 75.
(8) Zamanova, S.; Shabana, A. M.; Mondal, U. K.; Ilies, M. A. Carbonic anhydrases as disease markers. *Expert Opin. Ther. Pat.* **2019**, *29*, 509−533.
(9) *Carbonic Anhydrase: Mechanism, Regulation, Links to Disease, and Industrial Applications*; Springer: Netherlands, Dordrecht, 2014; Vol. 75.
(10) Abbate, F.; et al. Nonaromatic sulfonamide group as an ideal anchor for potent human carbonic anhydrase inhibitors: role of hydrogen-bonding networks in ligand binding and drug design. *J. Med. Chem.* **2002**, *45*, 3583−3587.
(11) Martin, D. P.; Hann, Z. S.; Cohen, S. M. Metalloprotein−Inhibitor Binding: Human Carbonic Anhydrase II as a Model for Probing Metal−Ligand Interactions in a Metalloprotein Active Site. *Inorg. Chem.* **2013**, *52*, 12207−12215.
(12) Carta, F.; Supuran, C. T.; Scozzafava, A. Sulfonamides and their isosters as carbonic anhydrase inhibitors. *Future Med. Chem.* **2014**, *6*, 1149−1165.
(13) Fox, J. M.; Zhao, M.; Fink, M. J.; Kang, K.; Whitesides, G. M. The Molecular Origin of Enthalpy/Entropy Compensation in Biomolecular Recognition. *Annu. Rev. Biophys.* **2018**, *47*, 223−250.
(14) Aggarwal, M.; Boone, C. D.; Kondeti, B.; McKenna, R. Structural annotation of human carbonic anhydrases. *J. Enzyme Inhib Med. Chem.* **2013**, *28*, 267−277.
(15) Supuran, C. T. Structure and function of carbonic anhydrases. *Biochem. J.* **2016**, *473*, 2023−2032.
(16) Lomelino, C. L.; Andring, J. T.; McKenna, R. Crystallography and Its Impact on Carbonic Anhydrase Research. *Int. J. Med. Chem.* **2018**, *2018*, No. 9419521.
(17) Smirnovienė, J.; et al. Switching the Inhibitor-Enzyme Recognition Profile via Chimeric Carbonic Anhydrase XII. *ChemistryOpen* **2021**, *10*, 567−580.
(18) Scott, A. D.; et al. Thermodynamic Optimisation in Drug Discovery: A Case Study using Carbonic Anhydrase Inhibitors. *ChemMedChem.* **2009**, *4*, 1985−1989.
(19) Glöckner, S.; Ngo, K.; Wagner, B.; Heine, A.; Klebe, G. The Influence of Varying Fluorination Patterns on the Thermodynamics and Kinetics of Benzenesulfonamide Binding to Human Carbonic Anhydrase II. *Biomolecules* **2020**, *10*, 509.
(20) Zakšauskas, A.; et al. Methyl 2-Halo-4-Substituted-5-Sulfamoyl-Benzoates as High Affinity and Selective Inhibitors of Carbonic Anhydrase IX. *Int. J. Mol. Sci.* **2021**, *23*, 130.
(21) Zakšauskas, A.; et al. Design of two-tail compounds with rotationally fixed benzenesulfonamide ring as inhibitors of carbonic anhydrases. *Eur. J. Med. Chem.* **2018**, *156*, 61−78.
(22) Zakšauskas, A.; et al. Halogenated and di-substituted benzenesulfonamides as selective inhibitors of carbonic anhydrase isoforms. *Eur. J. Med. Chem.* **2020**, *185*, No. 111825.
(23) MERCAPTANS FROM THIOKETALS: CYCLODODECYL MERCAPTAN. *Org. Synth. 61*, 74 (**1983**).
(24) Mahalingam, S. M.; Chu, H.; Liu, X.; Leamon, C. P.; Low, P. S. Carbonic Anhydrase IX-Targeted Near-Infrared Dye for Fluorescence Imaging of Hypoxic Tumors. *Bioconjugate Chem.* **2018**, *29*, 3320−3331.
(25) Smirnovienė, J.; Smirnovas, V.; Matulis, D. Picomolar inhibitors of carbonic anhydrase: Importance of inhibition and binding assays. *Anal. Biochem.* **2017**, *522*, 61−72.
(26) Taylor, P. W.; King, R. W.; Burgen, A. S. V. Influence of pH on the kinetics of complex formation between aromatic sulfonamides and human carbonic anhydrase. *Biochemistry* **1970**, *9*, 3894−3902.
(27) Zubrienė, A.; Matulis, D. Observed Versus Intrinsic Thermodynamics of Inhibitor Binding to Carbonic Anhydrases. In *Carbonic Anhydrase as Drug Target: Thermodynamics and Structure of Inhibitor Binding*; Matulis, D., Ed.; Springer International Publishing: Cham, 2019; pp 107−123.
(28) Fisher, S. Z.; Aggarwal, M.; Kovalevsky, A. Y.; Silverman, D. N.; McKenna, R. Neutron Diffraction of Acetazolamide-Bound Human Carbonic Anhydrase II Reveals Atomic Details of Drug Binding. *J. Am. Chem. Soc.* **2012**, *134*, 14726−14729.
(29) Aggarwal, M.; et al. Neutron structure of human carbonic anhydrase II in complex with methazolamide: mapping the solvent and hydrogen-bonding patterns of an effective clinical drug. *IUCrJ.* **2016**, *3*, 319−325.
(30) Zubrienė, A.; et al. Intrinsic thermodynamics of 4-substituted-2,3,5,6-tetrafluorobenzenesulfonamide binding to carbonic anhydrases by isothermal titration calorimetry. *Biophys Chem.* **2015**, *205*, 51−65.
(31) Dudutienė, V.; et al. Isoform-Selective Enzyme Inhibitors by Exploring Pocket Size According to the Lock-and-Key Principle. *Biophys. J.* **2020**, *119*, 1513−1524.
(32) Eisenberg, D.; Schwarz, E.; Komaromy, M.; Wall, R. Analysis of membrane and surface protein sequences with the hydrophobic moment plot. *J. Mol. Biol.* **1984**, *179*, 125−142.
(33) Supuran, C. T. How many carbonic anhydrase inhibition mechanisms exist? *J. Enzyme Inhib. Med. Chem.* **2016**, *31*, 345−360.
(34) Koes, D. R.; Baumgartner, M. P.; Camacho, C. J. Lessons Learned in Empirical Scoring with smina from the CSAR 2011 Benchmarking Exercise. *J. Chem. Inf. Model.* **2013**, *53*, 1893−1904.
(35) Quiroga, R.; Villarreal, M. A. Vinardo: A Scoring Function Based on Autodock Vina Improves Scoring, Docking, and Virtual Screening. *PLoS One* **2016**, *11*, No. e0155183.
(36) Trott, O.; Olson, A. J. AutoDock Vina: Improving the speed and accuracy of docking with a new scoring function, efficient optimization, and multithreading. *J. Comput. Chem.* **2010**, *31*, 455−461.
(37) McNutt, A. T.; et al. GNINA 1.0: molecular docking with deep learning. *J. Cheminf.* **2021**, *13*, 43.
(38) Pracht, P.; et al. CREST-A program for the exploration of low-energy molecular chemical space. *J. Chem. Phys.* **2024**, *160*, 114110.
(39) Bannwarth, C.; Ehlert, S.; Grimme, S. GFN2-xTB—An Accurate and Broadly Parametrized Self-Consistent Tight-Binding Quantum Chemical Method with Multipole Electrostatics and Density-Dependent Dispersion Contributions. *J. Chem. Theory Comput.* **2019**, *15*, 1652−1671.
(40) Schmidt, M. W.; et al. General atomic and molecular electronic structure system. *J. Comput. Chem.* **1993**, *14*, 1347−1363.
(41) Summa, C. M.; Langford, D. P.; Dinshaw, S. H.; Webb, J.; Rick, S. W. Calculations of Absolute Free Energies, Enthalpies, and Entropies for Drug Binding. *J. Chem. Theory Comput.* **2024**, *20*, 2812−2819.
(42) Linkuvienė, V.; et al. Thermodynamic, kinetic, and structural parameterization of human carbonic anhydrase interactions toward enhanced inhibitor design. *Q. Rev. Biophys.* **2018**, *51*, No. e10.
(43) Baronas, D.; et al. Inhibitor binding to metal-substituted metalloenzyme: Sulfonamide affinity for carbonic anhydrase IX. *J. Inorg. Biochem.* **2024**, *256*, No. 112547.

https://doi.org/10.1021/acs.jmedchem.5c01421
J. Med. Chem. XXXX, XXX, XXX−XXX

(44) Jackman, G. B.; Petrow, V.; Stephenson, O.; Wild, A. M. Studies in the Field of Diuretic Agents. Part VI Some Sulphamoylbenzoic Acids. *J. Pharm. Pharmacol.* **1962**, *14*, 679−686.
(45) Jackman, G. B.; Petrow, V.; Stephenson, O.; Wild, A. M. Studies in the Field of Diuretic Agents. *J. Pharm. Pharmacol.* **1963**, *15*, 202−211.
(46) Englert, H. C.; Lang, H.-J.; Linz, W.; Schoelkens, B.; Scholz, W. *Benzoylguanidines, a Process for Their Preparation, Their Use as Medicaments and Medicaments Containing Them*; 1992.
(47) Mickevičiūtė, A.et al.Recombinant Production of 12 Catalytically Active Human CA Isoforms. In *Carbonic Anhydrase as Drug Target: Thermodynamics and Structure of Inhibitor Binding*; Matulis, D., Ed.; Springer International Publishing: Cham, 2019; pp 15−37.
(48) Leitans, J.; et al. Efficient Expression and Crystallization System of Cancer-Associated Carbonic Anhydrase Isoform IX. *J. Med. Chem.* **2015**, *58*, 9004−9009.
(49) Grüner, B.; et al. Metallacarborane Sulfamides: Unconventional, Specific, and Highly Selective Inhibitors of Carbonic Anhydrase IX. *J. Med. Chem.* **2019**, *62*, 9560−9575.
(50) Kazlauskas, E.; Petrauskas, V.; Paketurytė, V.; Matulis, D. Standard operating procedure for fluorescent thermal shift assay (FTSA) for determination of protein−ligand binding and protein stability. *Eur. Biophys. J.* **2021**, *50*, 373−379.
(51) Gedgaudas, M.; Baronas, D.; Kazlauskas, E.; Petrauskas, V.; Matulis, D. Thermott: A comprehensive online tool for protein−ligand binding constant determination. *Drug Discovery Today* **2022**, *27*, 2076−2079.
(52) Lingė, D.; et al. PLBD: protein−ligand binding database of thermodynamic and kinetic intrinsic parameters. *Database* **2023**, *2023*, baad040.
(53) Khalifah, R. G. The carbon dioxide hydration activity of carbonic anhydrase. I. Stop-flow kinetic studies on the native human isoenzymes B and C. *J. Biol. Chem.* **1971**, *246*, 2561−2573.
(54) Williams, J. W.; Morrison, J. F. The kinetics of reversible tight-binding inhibition. In *Methods in Enzymology*; Academic Press: 1979; Vol. *63*, pp 437−467.
(55) Cheng, Y.-C.; Prusoff, W. H. Relationship between the inhibition constant (Ki) and the concentration of inhibitor which causes 50% inhibition (I50) of an enzymatic reaction. *Biochem. Pharmacol.* **1973**, *22*, 3099−3108.
(56) Snyder, P. W.; et al. Mechanism of the hydrophobic effect in the biomolecular recognition of arylsulfonamides by carbonic anhydrase. *Proc. Natl. Acad. Sci. U. S. A.* **2011**, *108*, 17889−17894.
(57) Emsley, P.; Cowtan, K. Coot: model-building tools for molecular graphics. *Acta Crystallogr. Biol. Crystallogr.* **2004**, *60*, 2126−2132.
(58) Kabsch, W. XDS. *Acta Crystallogr. Sect. D* **2010**, *D66*, 125−132.
(59) Battye, T. G. G.; Kontogiannis, L.; Johnson, O.; Powell, H. R.; Leslie, A. G. W. iMOSFLM: a new graphical interface for diffraction-image processing with MOSFLM. *Acta Crystallogr. D Biol. Crystallogr.* **2011**, *67*, 271−281.
(60) Leslie, A. G. W. The integration of macromolecular diffraction data. *Acta Crystallogr. Biol. Crystallogr.* **2006**, *62*, 48−57.
(61) Evans, P. Scaling and assessment of data quality. *Acta Crystallogr. D Biol. Crystallogr.* **2006**, *62*, 72−82.
(62) Vagin, A.; Teplyakov, A. MOLREP: an Automated Program for Molecular Replacement. *J. Appl. Crystallogr.* **1997**, *30*, 1022−1025.
(63) Leitans, J.; et al. Structural Basis of Saccharin Derivative Inhibition of Carbonic Anhydrase IX. *ChemMedChem* **2023**, *18*, No. e202300454.
(64) Murshudov, G. N.; Vagin, A. A.; Dodson, E. J. Refinement of macromolecular structures by the maximum-likelihood method. *Acta Crystallogr. Biol. Crystallogr.* **1997**, *53*, 240−255.
(65) Hanwell, M. D.; et al. Avogadro: An advanced semantic chemical editor, visualization, and analysis platform. *J. Cheminf.* **2012**, *4*, 17.
(66) Vagin, A. A.; et al. REFMAC5 dictionary: organization of prior chemical knowledge and guidelines for its use. *Acta Crystallogr. Biol. Crystallogr.* **2004**, *60*, 2184−2195.
(67) Lebedev, A. A.; et al. JLigand: a graphical tool for the CCP4 template-restraint library. *Acta Crystallogr. D Biol. Crystallogr.* **2012**, *68*, 431−440.
(68) Meng, E. C.; et al. UCSF ChimeraX: Tools for structure building and analysis. *Protein Sci.* **2023**, *32*, No. e4792.
(69) Pettersen, E. F.; et al. UCSF ChimeraX: Structure visualization for researchers, educators, and developers. *Protein Sci. Publ. Protein Soc.* **2021**, *30*, 70−82.
(70) Goddard, T. D.; et al. UCSF ChimeraX: Meeting modern challenges in visualization and analysis. *Protein Sci. Publ. Protein Soc.* **2018**, *27*, 14−25.
(71) Halgren, T. A. Merck molecular force field. I. Basis, form, scope, parameterization, and performance of MMFF94. *J. Comput. Chem.* **1996**, *17*, 490−519.
(72) Halgren, T. A. Merck molecular force field. II. MMFF94 van der Waals and electrostatic parameters for intermolecular interactions. *J. Comput. Chem.* **1996**, *17*, 520−552.
(73) Halgren, T. A. Merck molecular force field. III. Molecular geometries and vibrational frequencies for MMFF94. *J. Comput. Chem.* **1996**, *17*, 553−586.
(74) Halgren, T. A.; Nachbar, R. B. Merck molecular force field. IV. conformational energies and geometries for MMFF94. *J. Comput. Chem.* **1996**, *17*, 587−615.
(75) Halgren, T. A. Merck molecular force field. V. Extension of MMFF94 using experimental data, additional computational data, and empirical rules. *J. Comput. Chem.* **1996**, *17*, 616−641.
(76) Halgren, T. A. MMFF VI. MMFF94s option for energy minimization studies. *J. Comput. Chem.* **1999**, *20*, 720−729.
(77) O'Boyle, N. M.; et al. Open Babel: An open chemical toolbox. *J. Cheminf.* **2011**, *3*, 33.
(78) Bell, E. W.; Zhang, Y. DockRMSD: an open-source tool for atom mapping and RMSD calculation of symmetric molecules through graph isomorphism. *J. Cheminf.* **2019**, *11*, 40.
(79) Chai, J.-D.; Head-Gordon, M. Long-range corrected hybrid density functionals with damped atom−atom dispersion corrections. *Phys. Chem. Chem. Phys.* **2008**, *10*, 6615−6620.
(80) Dunning, T. H. Gaussian basis sets for use in correlated molecular calculations. I. The atoms boron through neon and hydrogen. *J. Chem. Phys.* **1989**, *90*, 1007−1023.
(81) Woon, D. E.; Dunning, T. H., Jr. Gaussian basis sets for use in correlated molecular calculations. III. The atoms aluminum through argon. *J. Chem. Phys.* **1993**, *98*, 1358−1371.
(82) Barone, V.; Cossi, M. Quantum Calculation of Molecular Energies and Energy Gradients in Solution by a Conductor Solvent Model. *J. Phys. Chem. A* **1998**, *102*, 1995−2001.
(83) Bannwarth, C.; et al. Extended tight-binding quantum chemistry methods. *Wiley Interdiscip. Rev.: Comput. Mol. Sci.* **2021**, *11*, No. e1493.
(84) Ehlert, S.; Stahn, M.; Spicher, S.; Grimme, S. Robust and Efficient Implicit Solvation Model for Fast Semiempirical Methods. *J. Chem. Theory Comput.* **2021**, *17*, 4250−4261.

https://doi.org/10.1021/acs.jmedchem.5c01421
J. Med. Chem. XXXX, XXX, XXX−XXX

GYVENIMO APRAŠYMAS

Vardas Pavardė Audrius Zakšauskas

Išsilavinimas

1995-1997 Vilniaus Universitetas, Chemijos fakultetas, magistro studijos. Suteiktas chemijos magistro kvalifikacinis laipsnis. Magistro darbo tema: „Pakeistų titanilo ftalocianinų sintezė“

1991-1995 Vilniaus Universitetas, Chemijos fakultetas, bakalauro studijos. Suteiktas chemijos bakalauro kvalifikacinis laipsnis. Bakalauro baigiamojo darbo tema: “Biciklo[3.3.1]nonan-2,6-diono oksidacija talio(III) druskomis

Pagrindinės mokslinės veiklos kryptys

2013-iki dabar Vilniaus universitetas, Biotechnologijos Institutas, Biotermodinamikos ir vaistų tyrimo skyrius. Fermentų slopiklių sintezė.

2002-2013 Vilniaus universitetas, Taikomųjų mokslų institutas, Skystųjų kristalų laboratorija. Organinių junginių sintezė.

1994-2001 Vilniaus universitetas, Chemijos fakultetas, Organinės chemijos katedra. Organinių junginių sintezė. Darbo vadovai doc. P.Kadziauskas, prof. A.Undzėnas.

Mokymo patirtis

1997-1999 Vilniaus universitetas, Chemijos fakultetas, Organinės chemijos katedra. Magistro baigiamojo darbo vadovas

2015-2016 Vilniaus universitetas, Biotechnologijos Institutas, Biotermodinamikos ir vaistų tyrimo skyrius. Bakalauro baigiamojo darbo vadovas

Darbo patirtis

2013- iki dabar Vilniaus universitetas, Biotechnologijos Institutas, Biotermodinamikos ir vaistų tyrimo skyrius, j.m. darbuotojas

2007-2013 UAB „Tikslioji sintezė“, chemikas.

2002-2013 Vilniaus universitetas, Taikomųjų mokslų institutas, Skystųjų kristalų laboratorija, vyresnysis inžinierius

1994-1998 Vilniaus universitetas, Chemijos fakultetas, Organinės chemijos katedra, laborantas

Dalyvavimas projektuose

1. Junginių efektyvumo slopinant SARS CoV-2 rekombinantinius virusinius fermentus įvertinimo technologijos prototipo sukūrimas (296 127 Eur.,

2021-2023, 3.1.1-LMT-K-718-05-0001. Vadovas J. Matulienė, Vykdytojas VU).

2. Vėžinių auglių išplitimo diagnostikos ir metastazių vaizdinimo operacijos metu sistemų vystymas naudojant CA IX biožymenį.(140 000 Eur., 2020-2021. Sveikas senėjimas Nr. S-SEN-20-10. Vadovas J. Matulienė. Vykdytojas VU)
3. Karboanhidrazių-slopiklių atpažinimo mechanizmas – priešvėžinės terapijos link.(100 000 Eur., 2017-2020. MIP-17-87. Vadovas D. Matulis. Vykdytojas VU)
4. Žmogaus karboanhidrazės IX, kaip vėžinių ląstelių žymens, taikymo onkologinių ligų diagnostikai, vaizdinimui bei prognozei, tyrimas.(Eur., 2015-2017. Sveikas senėjimas Nr. SEN-04/2015. Vadovas J. Matulienė. Vykdytojas VU)
5. Nuo 2014-04 iki 2014-12-31. Karboanhidrazės hCA XII, kaip vėžinių ląstelių žymens, diagnostinio potencialo įvertinimas. (590 500 Lt, 2012 05 02 - 2014 12 31, ES struktūrinių fondų lėšos, Lėtinės neinfekcinės ligos LIG-09/2012 , vadovas D. Matulis. Vykdytojas VU)
6. Nuo 2013-05-24 iki 2013-10-09. Nauji lanksčios struktūros bifluoreno junginiai optoelektronikos pramonei (BiFluorenas). (1 460 000 Lt, 2013-2015, VP1-3.1-ŠMM-10-V-02-023/LSS-23000-933, vykdytojas VU)
7. Inovatyvūs tiofeno junginiai OLED technologijai bei fotovoltainei konversijai (saulės baterijoms). **(**706 090 Lt, 2009-2012, „Intelektas LT“ VP2-1.3-ŪM-02-K-01-011, vykdytojas UAB “Tikslioji sintezė“).
8. Organinės elektronikos medžiagos ir prietaisai energiją taupančioms technologijoms**.** (2007-2009, VMSF remiamas Aukštųjų technologijų plėtros programos projektas, vykdytojas VU).

Mokslinės publikacijos

1. **Zakšauskas, A.,** Paketurytė-Latvė, V., Jankūnaitė, A., Čapkauskaitė, et al. Affinity and Selectivity of Protein–Ligand Recognition: A Minor Chemical Modification Changes Carbonic Anhydrase Binding Profile. *Journal of Medicinal Chemistry*. 2025, 68(16), 17752-17773. doi: 10.1021/acs.jmedchem.5c01421
2. Bagdonas, M., Stančaitis, L., Urniežius, E., **Zakšauskas**, **A**., Mickevičiūtė, A., Kananavičiūtė, R., et al. Design, synthesis, and binding analysis of target-specific covalent inhibitors of SARS-CoV-2 papain-like protease. *European Journal of Medicinal Chemistry Reports*. 2025, 15, 100306. doi.org/10.1016/j.ejmcr.2025.100306
3. Petrosiute, A., **Zakšauskas, A**., Lučiūnaitė, A., Petrauskas, V., Baranauskienė, L., Kvietkauskaitė, A., et al. Carbonic anhydrase IX

inhibition as a path to treat neuroblastoma. *British Journal of Pharmacology*, 2025, 182(7), 1610-1629. doi.org/10.1111/bph.17429

4. Paketurytė-Latvė, V., Smirnov, A., Manakova,E., Baranauskiene, L., Petrauskas, V., Zubrienė, A., Matulienė, J., Dudutienė, V., Čapkauskaitė, E., **Zakšauskas, A**., et al. From X-ray crystallographic structure to intrinsic thermodynamics of protein–ligand binding using carbonic anhydrase isozymes as a model system. *IUCrJ*, 2024, 11|, 4, 556-569. doi.org/10.1107/S2052252524004627
5. Žvinys, G., Petrosiute, A., **Zakšauskas, A**., Zubrienė, A., et al. High-Affinity NIR-Fluorescent Inhibitors for Tumor Imaging via Carbonic Anhydrase IX. *Bioconjugate Chem*, 2024, 35, 6, 790–803. doi.org/10.1021/acs.bioconjchem.4c00144
6. Lingė, D., Gedgaudas, M., Merkys, A., Petrauskas, V., Vaitkus, A., Grybauskas, A., Paketurytė, V., Zubrienė, A., **Zakšauskas, A**., et al. PLBD: protein–ligand binding database of thermodynamic and kinetic intrinsic parameters, *Database*, Volume 2023, 2023, baad040.doi.org/10.1093/database/baad040
7. Matulienė, J., Žvinys, G., Petrauskas, V., Kvietkauskaitė, A., **Zakšauskas, A**., et al. Picomolar fluorescent probes for compound affinity determination to carbonic anhydrase IX expressed in live cancer cells. *Scientific Reports,* 2022**,** 12, 17644. doi.org/10.1038/s41598-022-22436-1
8. **Zakšauskas, A.,** Čapkauskaitė, E., Paketurytė-Latvė, V., Smirnov, A., Leitans, J., Kazaks, A., Dvinskis, E., Stančaitis, L., Mickevičiūtė, A., Jachno, J., Jezepčikas, L., Linkuvienė, V., Sakalauskas, A., Manakova, E., Gražulis, S., Matulienė, J., Tars, K., Matulis, D. Methyl 2-Halo-4-Substituted-5-Sulfamoyl-Benzoates as High Affinity and Selective Inhibitors of Carbonic Anhydrase IX. *Int. J. Mol. Sci*. 2022, 23, 130. doi.org/10.3390/ijms23010130
9. Smirnovienė, J., Smirnov, A., **Zakšauskas, A**., Zubrienė, A., Petrauskas, V., Mickevičiūtė, A., Michailovienė, V., Čapkauskaitė, E., Manakova, E., Gražulis, S., Baranauskienė, L., Wen-Yih Chen, Ladbury, J.E., Matulis, D. Switching the Inhibitor-Enzyme Recognition Profile via Chimeric Carbonic Anhydrase XII. *ChemistryOpen*, 2021, 10(5), 567-580. doi:10.1002/open.202100042
10. **Zakšauskas, A**., Čapkauskaitė, E., Jezepčikas, L., Linkuvienė, V., Paketurytė, V., Smirnov, A., Leitans, J., Kazaks, A., Dvinskis, E., Manakova, E., Gražulis, S., Tars, K., Matulis, D. Halogenated and Di-Substituted Benzenesulfonamides as Selective Inhibitors of Carbonic Anhydrase Isoforms. *European Journal of Medicinal Chemistry*, 2020, 185, 111825. Doi:org/10.1016/j.ejmech.2019.111825.

11. Linkuvienė, V., Zubrienė, A., Manakova, E., Petrauskas, V., Baranauskienė, L., **Zakšauskas, A**., Smirnov, A., Gražulis, S., Ladbury, J.E., Matulis, D. Thermodynamic, kinetic, and structural parameterization of human carbonic anhydrase interactions toward enhanced inhibitor design. *Q Rev Biophys*., Published online: 26 November 2018, e10. doi: 10.1017/S0033583518000082
12. **Zakšauskas, A.**, Čapkauskaitė, E., Jezepčikas, L., Linkuvienė, V., Kišonaitė, M., Smirnov, A., Manakova, E., Gražulis, S., Matulis, D. Design of two-tail compounds with rotationally fixed benzenesulfonamide ring as inhibitors of carbonic anhydrases. *European Journal of Medicinal Chemistry,* 2018, 156, 61-78. doi: 10.1016/j.ejmech.2018.06.059
13. Čapkauskaitė, E., **Zakšauskas, A**., Ruibys, V., Linkuvienė, V., Paketurytė, V., Gedgaudas, M., Kairys, V., Matulis. D. Benzimidazole design, synthesis, and docking to build selective carbonic anhydrase VA inhibitors. *Bioorganic & Medicinal Chemistry*. 2018, 26(3), 675-687. DOI: 10.1016/j.bmc.2017.12.035.
14. Zubrienė, A., Smirnov, A., Dudutienė, V., Timm, D. D., Matulienė, J., Michailovienė, V., **Zakšauskas, A**., Manakova, E., Gražulis, S., Matulis, D. Intrinsic Thermodynamics and Structures of 2,4- and 3,4-Substituted Fluorinated Benzenesulfonamides Binding to Carbonic Anhydrases. *ChemMedChem*, 2017, 12 (2), 161-176. DOI: 10.1002/cmdc.201600509.
15. Juozapaitienė, V., Bartkutė, B., Michailovienė, V., **Zakšauskas, A**., Baranauskienė, L., Satkūnė, S., Matulis, D. 2016. Purification, enzymatic activity and inhibitor discovery for recombinant human carbonic anhydrase XIV. *Journal of Biotechnology*. 2016, 240, 31-42. DOI: 10.1016/j.jbiotec.2016.10.018
16. V. Dudutienė, A. Zubrienė, A. Smirnov, D. D. Timm, J. Smirnovienė, J. Kazokaitė, V. Michailovienė, **A. Zakšauskas**, E. Manakova, S. Gražulis and D. Matulis. Functionalization of Fluorinated Benzenesulfonamides and Their Inhibitory Properties toward Carbonic Anhydrases. *ChemMedChem*, 2015, 10 (4), 662–687. DOI: 10.1002/cmdc.201402490
17. Dudutienė, V., Matulienė, J., Smirnov, A., Timm, D., Zubrienė, A., Baranauskienė, L., Morkūnaitė, V., Smirnovienė, J., Michailovienė, V., Juozapaitienė, V., Mickevičiūtė, A., Kazokaitė, J., Bakšytė, S., Kasiliauskaitė, A., Jachno, J., Revuckienė, J., Kišonaitė, M., Pilipuitytė, V., Ivanauskaitė, E., Milinavičiūtė, G., Smirnovas, V., Petrikaitė, V., Kairys, V., Petrauskas, V., Norvaišas, P., Lingė, D., Gibieža, P., Čapkauskaitė, E., **Zakšauskas, A**., Kazlauskas, E., Manakova, E., Gražulis, S., Ladbury, J., Matulis, D. Discovery and characterization of

novel selective inhibitors of carbonic anhydrase IX. *Journal of Medicinal Chemistry,* 2014, 57 (22), 9435–9446. DOI**:** 10.1021/jm501003k
18. Gaidelis, V.; Jankauskas, V.; Kadziauskas, P.; Montrimas, E.; Undzėnas, A.; **Zakšauskas, A**. Asymmetric dioxothiapyranes as electron transporting materials. *Environmental and chemical physics*. 2001, Vol. 23, no 2. ISSN 1392-740X p. 64-70
19. **Zakšauskas, A**.; Kadziauskas, P.; Undzėnas, A. Hydroxygallium phthalocyanine and its forms. *Environmental and chemical physics*., 2000, Vol. 22, no 3-4. ISSN 1392-740X p. 145-150

Patentinės paraiškos

1. EP4255886(A1) D. Matulis, **A. Zakšauskas**, A. Zubrienė, L. Baranauskienė, J. Matulienė, V. Dudutienė, E. Čapkauskaitė, V. Paketurytė, J. Smirnovienė. Carbonic anhydrase inhibitors synthesized on interconnecting linker chains
2. US11312682 (B2) E. Čapkauskaitė, **A. Zakšauskas**, V. Morkūnaitė, D. Matulis. Selective inhibitors of carbonic anhydrase.
3. Lietuvos patentas Nr. 5510B Ona Adomėnienė, Povilas Adomėnas, **Audrius Zakšauskas**, Virginija Žvinytė. 2-(4'-fenilbenzoil)benzoinės rūgšties gamybos būdas. Paraiškos numeris 2006 084. Patento paskelbimo data 2008-07-25 Process for preparing of 2-(4'-phenylbenzoyl)benzoic acid.

Vilniaus universiteto leidykla
Saulėtekio al. 9, III rūmai, LT-10222 Vilnius
El. p. info@leidykla.vu.lt, www.leidykla.vu.lt
bookshop.vu.lt, journals.vu.lt
Tiražas 15 egz.